

**MoDOT**

Research, Development and Technology

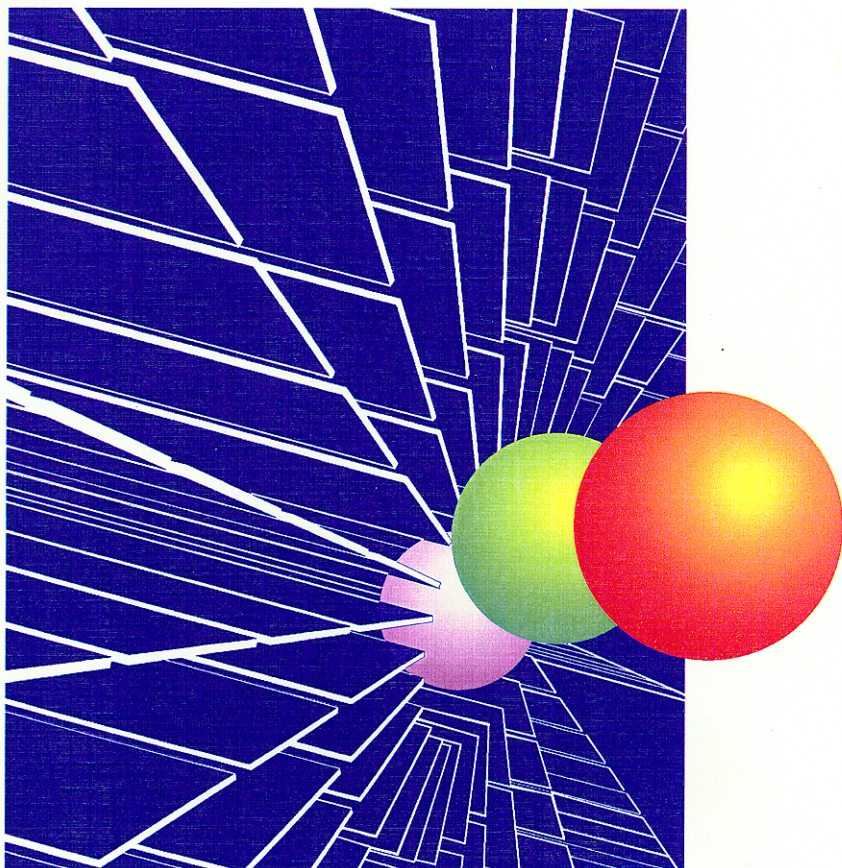
---

University of Missouri-Rolla

RDT 01-009

# **Earthquake Hazard Assessment Along Designated Emergency Vehicle Priority Access Routes**

RI 98-043



November, 2001

# **Final Report**

**RDT REDT01-009**

## **Earthquake Hazard Assessment Along Designated Emergency Vehicle Priority Access Routes**

Neil Anderson, Geology and Geophysics, UMR  
Hal Baker, Geology and Land Survey, MoDNR  
Genda Chen, Civil Engineering, UMR  
Tom Hertell, Geology and Land Survey, MoDNR  
Dave Hoffman, Geology and Land Survey, MoDNR  
Ronaldo Luna, Civil Engineering, UMR  
Yulman Munaf, Civil Engineering, UMR  
Shamsher Prakash, Civil Engineering, UMR  
Paul Santi, Geological Engineering, UMR  
Richard Stephenson, Civil Engineering, UMR

**Prepared For:**

**Missouri Department of Transportation Geotechnical Group  
Research, Development and Technology  
Jefferson City, Missouri  
November 2001**

The opinions, findings, and conclusions expressed in this publication are those of the principal investigators and the Missouri Department of Transportation, Research, Development and Technology.

They are not necessarily those of the U.S. Department of Transportation, Federal Highways Administration. This report does not constitute a standard or regulation.

## TECHNICAL REPORT DOCUMENTATION PAGE

1. Report No. RDT 01-009	2. Government Accession No.	3. Recipient's Catalog No.	
4. Title and Subtitle Earthquake Hazard Assessment Along Designated Emergency Vehicle Priority Access Routes		5. Report Date November, 2001	
		6. Performing Organization Code University of Missouri-Rolla	
7. Author(s) Neil Anderson, Geology and Geophysics, UMR, Hal Baker, Geology and Land Survey, MoDNR, Genda Chen, Civil Engineering, UMR, Tom Hertell, Geology and Land Survey, MoDNR, Dave Hoffman, Geology and Land Survey, MoDNR, Ronaldo Luna, Civil Engineering, UMR, Yulman Munaf, Civil Engineering, UMR, Shamsher Prakash, Civil Engineering, UMR, Paul Santi, Geological Engineering, UMR, Richard Stephenson, Civil Engineering, UMR		8. Performing Organization Report No. RDT 01-009/RI 98-043	
9. Performing Organization Name and Address University of Missouri-Rolla Department of Geology and Geophysics 1870 Miner Circle Rolla, MO 65409		10. Work Unit No.	
		11. Contract or Grant No. R-198-0143	
12. Sponsoring Agency Name and Address Missouri Department of Transportation Research, Development and Technology P. O. Box 270, Jefferson City, MO 65102		13. Type of Report and Period Covered Final Report	
		14. Sponsoring Agency Code MoDOT	
15. Supplementary Notes The investigation was conducted in cooperation with the U. S. Department of Transportation, Federal Highway Administration.			
16. Abstract Because of the compelling need to reopen vehicular access routes into Sikeston, Cape Girardeau and St. Louis following a devastating earthquake, Missouri Department of Transportation initiated a study of those portions of US 60 and MO 100 that have been officially designated as emergency vehicle priority access routes. The primary objectives of this study were twofold. Objective 1 was to establish a current subsurface and earthquake design geographic information systems (GIS) database for areas in proximity to designated portions of US 60 and MO 100 (includes counties of Butler, Stoddard, New Madrid, Franklin and St. Louis). Objective 2 was to conduct detailed earthquake assessments at two sites along designated emergency access route US 60. Databases have been established for current subsurface and earthquake design data for the US 60 corridor in Butler, Stoddard and New Madrid counties and for the MO 100 corridor in Franklin and St. Louis counties. These databases serve as the beginning of a larger regional or statewide database for future development and usage by Missouri Department of Transportation. Detailed earthquake site assessments were conducted for two critical US 60 roadway bridge sites (Wahite Ditch Bridge and St. Francis River Bridge). Liquefaction potential, slope stability, flooding potential, abutment stability, and structure stability analyses were performed at both sites for selected worst case scenario synthetic bedrock ground motions based on New Madrid source zone earthquakes with 2% and 10% probabilities of exceedance in fifty years.			
17. Key Words earthquake, liquefaction, emergency access, GIS, bridges		18. Distribution Statement No restrictions. This document is available to the public through National Technical Information Center, Springfield, Virginia 22161	
19. Security Classification (of this report) Unclassified	20. Security Classification (of this page) Unclassified	21. No. of Pages 390	22. Price

## EXECUTIVE SUMMARY

Southeast Missouri experiences relatively small magnitude earthquakes on a regular basis, and is the site of several of the largest earthquakes to strike North America in recorded history (1811 - 1812). Experts agree that high consequence events are anticipated in the Midwest New Madrid Seismic Zone. Experts also agree that if a very high magnitude earthquake struck southeastern Missouri today the damage to critical lifeline infrastructure would be catastrophic.

Because of the compelling need to reopen vehicular access routes into Sikeston, Cape Girardeau and St. Louis following a devastating earthquake, the Missouri Department of Transportation initiated a study of those portions of US 60 and MO 100 that have been officially designated as emergency vehicle priority access routes.

The goals of this study were twofold. Goal one was to establish a geotechnical database for earthquake design for areas in proximity to designated portions of US 60 and Missouri 100 (includes counties of Butler, Stoddard, New Madrid, Franklin and St. Louis). Goal two was to conduct detailed earthquake assessments at two sites along designated emergency vehicle priority access US 60.

Both goals of the research have been met. Databases have been established for current subsurface and geotechnical data for the US 60 corridor in Butler, Stoddard and New Madrid Counties and for the Missouri 100 corridor in Franklin and St. Louis Counties. These databases serve as the beginning of a larger regional and statewide database for future development and usage by the Missouri Department of Transportation. A discussion of the databases and documentation for their use is contained in *User Instructions for Data Entry and Editing of The Database of Borehole and Geophysical Data for Missouri Highway Structures*.

Detailed earthquake site assessments were conducted for two critical US 60 roadway bridge sites. Both the new and old bridges at the Wahite Ditch and the St. Francis River crossings were analyzed. Liquefaction potential, slope stability, flooding potential, abutment stability, and structure stability analysis were performed at both sites for selected critical synthetic bedrock ground motions based on New Madrid source zone earthquakes with 2% and 10% probabilities of exceedance in fifty years.

The site assessment studies indicate that both the Old Wahite Ditch Bridge and the Old St. Francis River Bridge could be rendered unusable by strong ground motion with a 2% probability of exceedance in the next fifty years. The New St. Francis River Bridge would likely suffer severe damage in the cross frames of the superstructure for a 2% probability of exceedance in the next fifty years earthquake. Studies indicate that the approach structures of all the study bridges would fail as a result of slope instability and liquefaction. Problems could be exacerbated by the localized flooding as a result of levee failure and/or damage to the Wappapello Dam.

## **ACKNOWLEDGEMENTS**

A work of this magnitude requires the assistance of a large number of people. In particular, the principal investigators would like to thank the professionals of the Missouri Department of Transportation for their assistance and encouragement. These people include Thomas Fennessey, Michael Fritz, Dan Camden and Lonnie Blasingame.

Graduate students at the University of Missouri-Rolla carried much of the work on this project out. The dedication of the following graduate students is gratefully acknowledged: Eric Neuner, Kenneth Zur, Huimin Mu and Pamela Thebeau.

## TABLE OF CONTENTS

	<b>Page</b>
<b>EXECUTIVE SUMMARY</b>	iii
<b>ACKNOWLEDGEMENTS</b>	iv
<b>TABLE OF CONTENTS</b>	v
<b>LIST OF ILLUSTRATIONS</b>	xii
<b>LIST OF TABLES</b>	xvi
<b>APPENDICES</b>	xviii

<b>Section</b>	<b>Page</b>
<b>1.0 INTRODUCTION</b>	1
<b>2.0 STATEMENT OF PROBLEM/SCOPE OF WORK</b>	2
<b>3.0 OBJECTIVES</b>	2
<b>3.1 Geotechnical Databases</b>	2
<b>3.2 Site Specific Earthquake Hazards Assessments</b>	3
<b>4.0 MISSOURI DEPARTMENT OF TRANSPORTATION     GEOTECHNICAL DATABASE</b>	3
<b>4.1 Design</b>	3
<b>4.1.1 Design Approach</b>	4
<b>4.1.2 A Geotechnical Generic Example</b>	5
<b>4.1.3 Analysis and Data Structure</b>	6
<b>4.2 Implementation</b>	8
<b>4.3 Link to Spatial Database (GIS)</b>	8
<b>5.0 SITE CHARACTERIZATION PROCEDURES</b>	8
<b>5.1 Field Investigations</b>	8
<b>5.1.1 Drilling and Sampling</b>	9
<b>5.1.2 Test Pits</b>	9
<b>5.1.3 Cone Penetrometer</b>	9

5.1.4	Surface Mapping	9
5.1.5	Interviews with Local Personnel	10
5.2	Laboratory Investigations	10
5.2.1	Missouri Department of Transportation Laboratory Testing	10
5.2.2	University of Missouri-Rolla Laboratory Soil Testing	10
5.2.2.1	Consolidated Undrained (CU) Triaxial Tests	11
5.2.2.2	Cyclic Triaxial Tests	11
5.3	Base Rock Motion Determination	11
5.3.1	Current Peak Ground Acceleration	11
5.3.2	Magnitudes and Distances for the Recommended Acceleration Values	12
5.3.3	Time Histories	12
5.4	Seismic Response of Soil	14
5.4.1	Wave Propagation Analysis	14
5.4.2	Liquefaction Analysis	15
5.5	Slope Stability of Abutment Fills	25
5.5.1	Soil Property Estimation	25
5.5.2	Groundwater Elevation Selection	27
5.5.3	Design Horizontal and Vertical Earthquake Accelerations	28
5.6	Flood Hazard Analysis	29
<b>6.0</b>	<b>PROCEDURES FOR SEISMIC CONDITION ASSESSMENT OF BRIDGES AND ABUTMENTS</b>	<b>30</b>
6.1	Global Performance Goals	30
6.1.1	American Association of State Highway and Transportation Officials Specifications	30
6.1.2	Bridges Along US 60	30
6.2	Engineering Performance Criteria	31
6.2.1	Performance Assessment	31
6.2.2	Seismic Demand	32
6.2.3	Seismic Capacity	33
6.2.4	Acceptable Damage	33
6.3	Analysis Procedures	33
6.3.1	Computer Modeling of Bridges	33
6.3.1.1	Design Ground Motions	33
6.3.1.2	Analysis Procedure	34
6.3.2	Computer Modeling of Abutments	34
<b>7.0</b>	<b>REGIONAL GEOLOGY AND GEOTECHNICAL DATA</b>	<b>38</b>
7.1	Regional Geology	38
7.2	Summary of Field and Laboratory Data	40

<b>8.0</b>	<b>RESULTS OF SITE SPECIFIC STUDIES</b>	41
<b>8.1</b>	<b>St. Francis River Site</b>	41
8.1.1	Site Geology	41
8.1.2	Selected Base Rock Motion	41
8.1.3	Seismic Response of Soil	41
8.1.3.1	Horizontal Seismic Response of Soil	42
8.1.3.2	Resulting Ground Motion Time Histories	43
8.1.3.3	Vertical Seismic Response of Soil	50
8.1.4	Liquefaction Potential Analysis	50
8.1.4.1	Cyclic Stress Ratio (CSR), Cyclic Resistant Ratio (CRR) and Factor of Safety (FOS)	65
8.1.5	Slope Stability of Abutment Fills	65
8.1.6	Flood Hazard Analysis Results	66
8.1.7	Structure Response of Bridges and Abutments	72
8.1.7.1	New St. Francis River Bridge	72
8.1.7.1.1	Bridge Description	72
8.1.7.1.2	Bridge Model and Analysis	72
8.1.7.1.3	Detailed Description of Bridge Evaluation	76
8.1.7.1.3.1	Load Combination Rule	76
8.1.7.1.3.2	Minimum Support Length and C/D Ratio for Bearing	77
8.1.7.1.3.3	C/D Ratios for Shear Force at Bearings	77
8.1.7.1.3.4	C/D Ratios for Columns/Piers	78
8.1.7.1.3.5	C/D Ratios for Hooked Anchorage in Columns	84
8.1.7.1.3.6	C/D Ratios for Splices in Longitudinal Reinforcement	84
8.1.7.1.3.7	C/D Ratio for Transverse Confinement	85
8.1.7.1.3.8	C/D Ratio for Column Shear	85
8.1.7.1.3.9	C/D Ratio for Diaphragm and Cross-Frame Members	87
8.1.7.1.3.10	C/D Ratio for Abutment Displacements	88
8.1.7.1.4	Summary of Problem Areas	89
8.1.7.1.5	Time History Analysis vs: Response Spectrum Analysis	90
8.1.7.1.6	Comparison of AASHTO Response Spectrum vs. Site-Specific Response Spectrum	96
8.1.7.2	Old St. Francis River Bridge	97
8.1.7.2.1	Bridge Description	97
8.1.7.2.2	Bridge Model and Analysis	98
8.1.7.2.3	Bridge Evaluation	99

	8.1.7.2.3.1	Load Combination Rule	102
	8.1.7.2.3.2	Minimum Support Length and C/D Ratio for Bearing	102
	8.1.7.2.3.3	C/D Ratios for Shear Force at Bearings	103
	8.1.7.2.3.4	C/D Ratios for Columns/Piers	103
	8.1.7.2.3.5	C/D Ratios for Reinforcement Anchorage in Columns	104
	8.1.7.2.3.6	C/D Ratios for Splices in Longitudinal Reinforcement	104
	8.1.7.2.3.7	C/D Ratio for Transverse Confinement	104
	8.1.7.2.3.8	C/D Ratio for Column Shear	105
	8.1.7.2.3.9	C/D Ratio for Diaphragm and Cross-Frame Members	105
	8.1.7.2.3.10	C/D Ratio for Abutment Displacements	105
	8.1.7.2.4	Summary of Problem Areas	106
	8.1.7.2.5	Time History Analysis vs. Response Spectrum Analysis	107
	8.1.7.2.6	Structure Response of Abutments	109
	8.1.7.2.6.1	Calculated Time Dependent Displacements of Abutment	109
8.2		Wahite Ditch Site	113
	8.2.1	Site Geology	113
	8.2.2	Selected Base Rock Motion	114
	8.2.3	Seismic Response of Soil	114
	8.2.3.1	Horizontal Seismic Response of Soil	117
	8.2.3.2	Resulting Ground Motion Time Histories	123
	8.2.3.3	Vertical Seismic Response of Soil	124
	8.2.4	Liquefaction Potential Analysis	140
	8.2.4.1	Cyclic Stress Ratio (CSR) and Cyclic Resistant Ratio (CRR) and Factor of Safety (FOS)	140
	8.2.5	Slope Stability of Abutment Fills	140
	8.2.6	Flood Hazard Analysis Results	142
	8.2.7	Structure Response of Wahite Ditch Bridges and Abutments	142
	8.2.7.1	New Wahite Ditch Bridge	142
	8.2.7.1.1	Bridge Description	142
	8.2.7.1.2	Bridge Model and Analysis	144
	8.2.7.1.3	Description of Bridge Evaluation	148
	8.2.7.1.3.1	Load Combination Rule	148
	8.2.7.1.3.2	Minimum Support Length and C/D Ratio for Bearing	148

	8.2.7.1.3.3	C/D Ratios for Shear Force at Bearings	148
	8.2.7.1.3.4	C/D Ratios for Columns/Piers	149
	8.2.7.1.3.5	C/D Ratios for Reinforcement Anchorage in Columns	149
	8.2.7.1.3.6	C/D Ratios for Splices in Longitudinal Reinforcement	150
	8.2.7.1.3.7	C/D Ratio for Transverse Confinement	150
	8.2.7.1.3.8	C/D Ratio for Column Shear	150
	8.2.7.1.3.9	C/D Ratio for Diaphragm Members	150
	8.2.7.1.3.10	C/D Ratio for Abutment Displacements	150
	8.2.7.1.4	Summary of Problem Areas	150
	8.2.7.1.5	Comparison of AASHTO Response Spectrum vs. Site-Specific Response Spectrum	151
8.2.7.2		Old Wahite Ditch Bridge	153
	8.2.7.2.1	Bridge Description	153
	8.2.7.2.2	Bridge Model and Analysis	154
	8.2.7.2.3	Bridge Evaluation	158
	8.2.7.2.3.1	Load Combination Rule	158
	8.2.7.2.3.2	Minimum Support Length and C/D Ratio for Bearing	158
	8.2.7.2.3.3	C/D Ratios for Shear Force at Bearings	158
	8.2.7.2.3.4	C/D Ratios for Columns/Piers	158
	8.2.7.2.3.5	C/D Ratios for Reinforcement Anchorage in Columns	159
	8.2.7.2.3.6	C/D Ratios for Splices in Longitudinal Reinforcement	159
	8.2.7.2.3.7	C/D Ratio for Transverse Confinement	159
	8.2.7.2.3.8	C/D Ratio for Column Shear	160
	8.2.7.2.3.9	C/D Ratio for Diaphragm Members	160
	8.2.7.2.3.10	C/D Ratio for Abutment Displacements	160
	8.2.7.2.4	Summary of Problem Areas	160
	8.2.7.2.5	Time History vs. Response Spectrum Analysis	161
	8.2.7.2.6	Structural Response of Abutments	165
	8.2.7.2.6.1	Calculated Time Dependent Displacements of Abutment	165
9.0		CONCLUSIONS	169
	9.1	Summary	169
	9.2	Geotechnical GIS Databases	169

<b>9.3</b>	<b>Site Specific Earthquake Hazards Assessments</b>	<b>169</b>
<b>9.3.1</b>	<b>St. Francis River Site</b>	<b>170</b>
<b>9.3.1.1</b>	<b>Liquefaction</b>	<b>170</b>
<b>9.3.1.2</b>	<b>Slope Stability</b>	<b>170</b>
<b>9.3.1.3</b>	<b>Flood Hazard</b>	<b>170</b>
<b>9.3.1.4</b>	<b>Structural Response of St. Francis River Bridges</b>	<b>170</b>
<b>9.3.1.4.1</b>	<b>New St. Francis River Bridge</b>	<b>170</b>
<b>9.3.1.4.2</b>	<b>Old St. Francis River Bridge</b>	<b>171</b>
<b>9.3.1.4.3</b>	<b>Old St. Francis River Bridge Abutment</b>	<b>171</b>
<b>9.3.2</b>	<b>Wahite Ditch Site</b>	<b>171</b>
<b>9.3.2.1</b>	<b>Liquefaction</b>	<b>171</b>
<b>9.3.2.2</b>	<b>Slope Stability</b>	<b>171</b>
<b>9.3.2.3</b>	<b>Flood Hazard</b>	<b>171</b>
<b>9.3.2.4</b>	<b>Structure Stability of Wahite Ditch Bridges</b>	<b>172</b>
<b>9.3.2.4.1</b>	<b>New Wahite Ditch Bridge</b>	<b>172</b>
<b>9.3.2.4.2</b>	<b>Old Wahite Ditch Bridge</b>	<b>172</b>
<b>9.3.2.4.3</b>	<b>Old Wahite Ditch Bridge Abutment</b>	<b>172</b>
<b>10.0</b>	<b>RECOMMENDATIONS</b>	<b>172</b>
<b>10.1</b>	<b>Protocol</b>	<b>172</b>
<b>10.1.1</b>	<b>Determination of Site-Specific Strong Rock Motion</b>	<b>173</b>
<b>10.1.2</b>	<b>Determination of Liquefaction Potential</b>	<b>173</b>
<b>10.1.3</b>	<b>Determination of Slope Stability</b>	<b>174</b>
<b>10.1.4</b>	<b>Determination of Potential for Flooding in Response to Strong Ground Motion</b>	<b>174</b>
<b>10.1.5</b>	<b>Evaluation of Flooding Potential</b>	<b>175</b>
<b>10.1.6</b>	<b>Determination of Structural Stability</b>	<b>175</b>
<b>10.1.6.1</b>	<b>Evaluation of Abutment Stability</b>	<b>175</b>
<b>10.1.6.2</b>	<b>Evaluation of Stability of Integrated Bridge Abutments</b>	<b>175</b>
<b>10.1.6.3</b>	<b>Evaluation of Stability of Structural Members</b>	<b>175</b>
<b>10.2</b>	<b>Further Work</b>	<b>176</b>
<b>10.2.1</b>	<b>Proposed Study: Retrofit of Critical Structures Along Designated Emergency Vehicle Priority Access Routes</b>	<b>176</b>
<b>10.2.2</b>	<b>Proposed Study: Site Specific Earthquake Assessments along MO 100</b>	<b>176</b>
<b>10.2.3</b>	<b>Proposed Study: Regional Liquefaction Hazard Analysis</b>	<b>177</b>
<b>10.2.4</b>	<b>Proposed Study: Geo-Referencing of Boring Locations</b>	<b>178</b>
<b>10.2.5</b>	<b>Proposed Study: Regional Prioritization for Future Earthquake Hazards Assessments</b>	<b>178</b>
<b>10.2.6</b>	<b>Proposed Study: Laboratory Testing of Truss-Type Diaphragms or Cross Frames and Effective Retrofitting Techniques</b>	<b>178</b>

<b>10.2.7</b>	<b>Proposed Study: Integration of LOGMAIN Surficial Material Information</b>	<b>178</b>
<b>10.2.8</b>	<b>Proposed Study: Long Term Strategic Plan</b>	<b>178</b>
<b>11.0</b>	<b>BIBLIOGRAPHY</b>	<b>179</b>
<b>12.0</b>	<b>LIST OF SYMBOLS</b>	<b>183</b>

## LIST OF ILLUSTRATIONS

Figure	Page
2.1 Study Site Locations	2
4.1 System Design: Top-Down vs. Bottom-Up	4
4.2 Organization of Missouri Department of Transportation Subsurface Data	5
4.3 Example of an Object-Oriented Geotechnical Database Model (Luna and Frost, 1995)	7
5.1 Seismicity in the 1974-1995 Time Period in the Vicinity of the St. Francis River Site (SF) and the Wahite Ditch Site (WD). (Herrmann, (2000))	13
5.2 The Selected Base Rock Motion for the St. Francis River Bridge Site	
5.2a PE 10% in 50 Years, Magnitude 6.2	16
5.2b PE 10% in 50 Years, Magnitude 7.2	17
5.2c PE 2% in 50 Years, Magnitude 6.4	18
5.2d PE 2% in 50 Years, Magnitude 8.0	19
5.3 The Selected Base Rock Motion for The Wahite Ditch Bridge Site	
5.3a PE 10% in 50 Years, Magnitude 6.4	20
5.3b PE 10% in 50 Years, Magnitude 7.0	21
5.3c PE 2% in 50 Years, Magnitude 7.8	22
5.3d PE 2% in 50 Years, Magnitude 8.0	23
5.4 Simplified Base Curve Recommended for Calculation of CRR From SPT ( $N_1$ ) <sub>60</sub> Data Along With Empirical Liquefaction Data for M=7.5 (Seed <i>et al.</i> , 1971, modified by Youd and Idriss, 1997)	26
5.5 St. Francis River Site Topography, Cross-Sections and Boring Locations	27
5.6 Wahite Ditch Site Topography, Cross-Sections and Boring Locations	28
6.1 Typical Non-Integral Bridge Abutment Supported on Piles	36
6.2 Translation and Rotation Movement of Bridge Abutment Forces Acting on the Non-Integral Bridge Abutment	36
6.3 Forces Acting on the Non-Integral Bridge Abutment	37
7.1 Extent of Mississippi Embayment	39
7.2 Cross-Section of Regional Geology	40
8.1 St. Francis River Site Topography, Cross-Section and Boring Locations	42
8.2 Cross-Section of St. Francis River Site Geology	43
8.3 Soil Profile St. Francis River Site Boring B-1	44
8.4 Acceleration Time Histories for St. Francis River Site	
8.4a PE 10% in 50 Years Magnitude = 6.2	46
8.4b PE 10% in 50 Years Magnitude = 7.2	47
8.4c PE 2% in 50 Years, Magnitude = 6.4	48
8.4d PE 2% in 50 Years, Magnitude = 8.0	49

<b>8.5</b>	<b>Peak Ground Acceleration vs. Depth for PE 10% in 50 Years Magnitudes 6.2 and 7.2 St. Francis River Site</b>	<b>51</b>
<b>8.6</b>	<b>Peak Ground Acceleration vs. Depth for PE 2% in 50 Years Magnitudes 6.4 and 8.0 St. Francis River Site</b>	<b>52</b>
<b>8.7</b>	<b>Ground Acceleration at the Surface of the St. Francis River Site</b>	
<b>8.7a</b>	<b>PE 10% in 50 years, Magnitude = 6.2</b>	<b>53</b>
<b>8.7b</b>	<b>PE 10% in 50 years, Magnitude = 7.2</b>	<b>54</b>
<b>8.7c</b>	<b>PE 2% in 50 years, Magnitude = 6.4</b>	<b>55</b>
<b>8.7d</b>	<b>PE 2% in 50 years, Magnitude = 8.0</b>	<b>56</b>
<b>8.8</b>	<b>Ground Acceleration at the Abutment of the St. Francis River Site</b>	
<b>8.8a.</b>	<b>PE 10% in 50 years, Magnitude = 6.2</b>	<b>57</b>
<b>8.8b</b>	<b>PE 10% in 50 years, Magnitude = 7.2</b>	<b>58</b>
<b>8.8c</b>	<b>PE 2% in 50 years, Magnitude = 6.4</b>	<b>59</b>
<b>8.8d</b>	<b>PE 2% in 50 years, Magnitude = 8.0</b>	<b>60</b>
<b>8.9</b>	<b>Ground Acceleration at the Pier of the St. Francis River Site</b>	
<b>8.9a</b>	<b>PE 10% in 50 years, Magnitude = 6.2</b>	<b>61</b>
<b>8.9b</b>	<b>PE 10% in 50 years, Magnitude = 7.2</b>	<b>62</b>
<b>8.9c</b>	<b>PE 2% in 50 years, Magnitude = 6.4</b>	<b>63</b>
<b>8.9d</b>	<b>PE 2% in 50 years, Magnitude = 8.0</b>	<b>64</b>
<b>8.10</b>	<b>Soil Profile, CSR, CRR and Factor of Safety Against Liquefaction at the St. Francis River Site for PE 10% in 50 years and Magnitude=6.2</b>	<b>67</b>
<b>8.11</b>	<b>Example Slope Stability Results for St. Francis River Site</b>	<b>68</b>
<b>8.12</b>	<b>Estimated Flooding Zone Due to Wappapello Dam Failure</b>	<b>71</b>
<b>8.13</b>	<b>Region of Potential Flooding</b>	<b>71</b>
<b>8.14</b>	<b>Bridge General Elevation (New St. Francis River Bridge)</b>	<b>73</b>
<b>8.15</b>	<b>Mode 1, Period 0.2519 Seconds (New St. Francis River Bridge)</b>	<b>74</b>
<b>8.16</b>	<b>Mode 2, Period 0.2295 Seconds (New St. Francis River Bridge)</b>	<b>74</b>
<b>8.17</b>	<b>Mode 3, Period 0.1421 Seconds (New St. Francis River Bridge)</b>	<b>75</b>
<b>8.18</b>	<b>Mode 4, Period 0.0901 Seconds (New St. Francis River Bridge)</b>	<b>75</b>
<b>8.19</b>	<b>Mode 5, Period 0.0896 Seconds (New St. Francis River Bridge)</b>	<b>76</b>
<b>8.20</b>	<b>Shear Force Calculations</b>	<b>79</b>
<b>8.21</b>	<b>Calculations of Axial Loads and Column Shears</b>	<b>83</b>
<b>8.22</b>	<b>Calculations for Hooked Anchorage in Columns</b>	<b>85</b>
<b>8.23</b>	<b>Calculations for Splices in Longitudinal Reinforcement</b>	<b>86</b>
<b>8.24</b>	<b>Calculations for Transverse Confinement FHWA Manual (1995)</b>	<b>86</b>
<b>8.25</b>	<b>Calculations for Column Shear</b>	<b>88</b>
<b>8.26</b>	<b>Calculations for Diaphragm and Cross-Frame Members</b>	<b>89</b>
<b>8.27</b>	<b>Calculations for Abutment Displacements</b>	<b>90</b>
<b>8.28</b>	<b>Comparison of AASHTO Response Spectrum and Site-Specific Response Spectrum</b>	<b>96</b>
<b>8.29</b>	<b>Bridge General Elevation (Old St. Francis River Bridge)</b>	<b>98</b>

<b>8.30</b>	Mode 1, Period 1.3173 Seconds (Old St. Francis River Bridge)	100
<b>8.31</b>	Mode 2, Period 0.4773 Seconds (Old St. Francis River Bridge)	100
<b>8.32</b>	Mode 3, Period 0.3673 Seconds (Old St. Francis River Bridge)	101
<b>8.33</b>	Mode 4, Period 0.2065 Seconds (Old St. Francis River Bridge)	101
<b>8.34</b>	Mode 5, Period 0.1501 Seconds (Old St. Francis River Bridge)	102
<b>8.35</b>	Old St. Francis River Bridge Plans	113
<b>8.36</b>	Time Histories of Sliding, Rocking and Total Permanent Displacement of the Old St. Francis River Bridge Abutment, PE 10% in 50 Years, Magnitudes 6.2 and 7.2	115
<b>8.37</b>	Time Histories of Sliding, Rocking and Total Permanent Displacement of the Old St. Francis River Bridge Abutment, PE 2% in 50 Years, Magnitudes 6.4 and 8.0	116
<b>8.38</b>	Cross-Section of Wahite Ditch Site Geology	117
<b>8.39</b>	Acceleration Time Histories for the Wahite Ditch Site	
	8.39a PE 2% in 50 Years, Magnitude = 6.4	119
	8.39b PE 10% in 50 Years, Magnitude = 7.0	120
	8.39c PE 2% in 50 Years, Magnitude = 7.8	121
	8.39d PE 2% in 50 Years, Magnitude = 8.0	122
<b>8.40</b>	Wahite Ditch Site Topography, Cross-Section and Boring Locations	123
<b>8.41</b>	Soil Profile Wahite Ditch Bridge Site	125
<b>8.42</b>	Peak Ground Acceleration vs. Depth for PE 10% in 50 Years Magnitudes 6.4 and 7.0 Wahite Ditch Site Boring B-1	126
<b>8.43</b>	Peak Ground Acceleration vs. Depth for PE 2% in 50 Years Magnitudes 7.8 and 8.0 Wahite Ditch Site	127
<b>8.44</b>	Ground Acceleration at the Surface of the Wahite Ditch Site	
	8.44a PE 10% in 50 years, Magnitude = 6.4	128
	8.44b PE 10% in 50 years, Magnitude = 7.0	129
	8.44c PE 2% in 50 years, Magnitude = 7.8	130
	8.44d PE 2% in 50 years, Magnitude = 8.0	131
<b>8.45</b>	Ground Acceleration at the Abutment of the Wahite Ditch Site	
	8.45a PE 10% in 50 years, Magnitude = 6.4	132
	8.45b PE 10% in 50 years, Magnitude = 7.0	133
	8.45c PE 2% in 50 years, Magnitude = 7.8	134
	8.45d PE 2% in 50 years, Magnitude = 8.0	135
<b>8.46</b>	Ground Acceleration at the Wahite Ditch Bridge Pier	
	8.46a PE 10% in 50 years, Magnitude = 6.4	136
	8.46b PE 10% in 50 years, Magnitude = 7.0	137
	8.46c PE 2% in 50 years, Magnitude = 7.8	138
	8.46d PE 2% in 50 years, Magnitude = 8.0	139
<b>8.47</b>	Soil Profile, CSR, CRR and Factor of Safety Against Liquefaction at the Wahite Ditch Bridge Site for PE 10% in 50 Years and Magnitude=6.4	141

<b>8.48</b>	<b>Example Slope Stability Results for the Wahite Ditch Site</b>	<b>144</b>
<b>8.49</b>	<b>Bridge General Elevation (New Wahite Ditch Bridge)</b>	<b>145</b>
<b>8.50</b>	<b>Mode 1, Period 0.2686 Seconds (New Wahite Ditch Bridge)</b>	<b>146</b>
<b>8.51</b>	<b>Mode 2, Period 0.2558 Seconds (New Wahite Ditch Bridge)</b>	<b>146</b>
<b>8.52</b>	<b>Mode 3, Period 0.0915 Seconds (New Wahite Ditch Bridge)</b>	<b>147</b>
<b>8.53</b>	<b>Mode 4, Period 0.0854 Seconds (New Wahite Ditch Bridge)</b>	<b>147</b>
<b>8.54</b>	<b>Mode 5, Period 0.0729 Seconds (New Wahite Ditch Bridge)</b>	<b>148</b>
<b>8.55</b>	<b>Bridge General Elevation (Old Wahite Ditch Bridge)</b>	<b>154</b>
<b>8.56</b>	<b>Mode 1, Period 0.5641 Seconds (Old Wahite Ditch Bridge)</b>	<b>155</b>
<b>8.57</b>	<b>Mode 2, Period 0.3518 Seconds (Old Wahite Ditch Bridge)</b>	<b>156</b>
<b>8.58</b>	<b>Mode 3, Period 0.1809 Seconds (Old Wahite Ditch Bridge)</b>	<b>156</b>
<b>8.59</b>	<b>Mode 4, Period 0.1229 Seconds (Old Wahite Ditch Bridge)</b>	<b>157</b>
<b>8.60</b>	<b>Mode 5, Period 0.1025 Seconds (Old Wahite Ditch Bridge)</b>	<b>157</b>
<b>8.61</b>	<b>Bridge General Elevation (Old Wahite Ditch Bridge)</b>	<b>162</b>
<b>8.62</b>	<b>Plan and Cross-Section of Old Wahite Ditch Bridge Abutment</b>	
	<b>8.62a Plan of Old Wahite Ditch Bridge Abutment</b>	<b>166</b>
	<b>8.62b Cross Section of Old Wahite Ditch Bridge Abutment</b>	<b>166</b>
<b>8.63</b>	<b>Time Histories of Sliding, Rocking and Total Permanent Displacement of the Old Wahite Ditch Bridge Abutment PE 10% in 50 Years, Magnitudes 6.4 and 7.0</b>	<b>167</b>
<b>8.64</b>	<b>Time Histories of Sliding, Rocking and Total Permanent Displacement of the Old Wahite Ditch Bridge Abutment PE 2% in 50 Years, Magnitudes 7.8 and 8.0</b>	<b>168</b>

## LIST OF TABLES

<b>Table</b>	<b>Page</b>
4.1 Example of Data Structure Input to Database	8
5.1 Peak Ground Acceleration (Herrmann, 2000) (Source; USGS 1996 Seismic Hazard Maps)	13
5.2 Magnitudes and Distances for Selected Earthquakes, (Herrmann, 2000)	
5.2a St. Francis River Site	14
5.2b Wahite Ditch Site	14
5.3 Design Horizontal and Vertical Earthquake Accelerations	
5.3a St. Francis River Site	29
5.3b Wahite Ditch Site	29
8.1 Detail of Synthetic Ground Motion at the Rock Base of St. Francis River Site With Corresponding Maximum Peak Horizontal Ground Acceleration	
8.1a PE 10% in 50 Years	45
8.1b PE 2 % in 50 Years	45
8.2 Detail of Peak Ground Motion Used at the St. Francis River Site Rock Base, Ground Surface, Bridge Abutment and Pier	
8.2a PE 10% in 50 Years	65
8.2b PE 2 % in 50 Years	65
8.3 The Different Zones of Soil Liquefaction for Different Factors of Safety, St. Francis River Site	66
8.4 Soil Properties Used for the Slope Stability Analysis, St. Francis River Site	66
8.5 Slope Stability Results for the St. Francis River Site	69
8.6 Natural Periods and Their Corresponding Vibration Modes (New St. Francis River Bridge)	73
8.7 Elastic Moments Due to Transverse Acceleration	81
8.8 Elastic Moments Due to Longitudinal Acceleration	81
8.9 Elastic Moments Due to Vertical Acceleration	82
8.10 Summary of All Moment Demands	82
8.11 Summary of Moment C/D Ratios for Columns	84
8.12 Summary of All C/D Ratios for New St. Francis Bridge Structure -- for One 2% PE Earthquake	91
8.13 Summary of C/D Ratios for All Earthquakes on New St. Francis River Bridge	92
8.14 Comparison of Moments for Time History and Response Spectrum Analysis for Column 2 (New St. Francis River Bridge)	93
8.15 Comparison of Moments for Time History and Response Spectrum Analysis for Column 5 (New St. Francis River Bridge)	94
8.16 Comparison of Displacements for Time History and Response Spectrum Analysis for Maximum Abutment Displacement (New St. Francis River Bridge)	95

<b>8.17</b>	<b>Comparison of AASHTO Response Spectrum vs. Site Specific Response Spectrum (New St. Francis River Bridge)</b>	<b>97</b>
<b>8.18</b>	<b>Natural Periods and their Corresponding Vibration Modes (Old St. Francis River Bridge)</b>	<b>99</b>
<b>8.19</b>	<b>Summary of C/D Ratios for all Earthquakes at Old St. Francis River Bridge for all Earthquakes</b>	<b>108</b>
<b>8.20</b>	<b>Comparison of Moments for Time History and Response Spectrum Analysis for Column 2 (Old St. Francis River Bridge)</b>	<b>110</b>
<b>8.21</b>	<b>Comparison of Moments for Time History and Response Spectrum Analysis for Column 5 (Old St. Francis River Bridge)</b>	<b>111</b>
<b>8.22</b>	<b>Comparison of Displacements for Time History and Response Spectrum Analysis for Maximum Abutment Displacement (Old St. Francis River Bridge)</b>	<b>112</b>
<b>8.23</b>	<b>Displacement at Top of the Old St. Francis Bridge Abutment</b>	<b>114</b>
<b>8.24</b>	<b>Detail of Synthetic Ground Motion at the Rock Base of Wahite Ditch Site, With Corresponding Maximum Peak Horizontal Ground Acceleration</b>	
	<b>8.24a PE 10% in 50 Years</b>	<b>118</b>
	<b>8.24b PE 2% in 50 Years</b>	<b>118</b>
<b>8.25</b>	<b>Detail of Peak Ground Motion Used at the Wahite Ditch Site Rock Base, Ground Surface, Bridge Abutment and Pier</b>	
	<b>8.25a PE 10% in 50 years</b>	<b>124</b>
	<b>8.25b PE 2% in 50 years</b>	<b>124</b>
<b>8.26</b>	<b>The Different Zones of Soil Liquefaction for Different Factors of Safety, Wahite Ditch Site</b>	<b>142</b>
<b>8.27</b>	<b>Soil Properties Used for the Slope Stability Analysis, Wahite Ditch Site</b>	<b>142</b>
<b>8.28</b>	<b>Slope Stability Results, Wahite Ditch Bridge Site</b>	<b>143</b>
<b>8.29</b>	<b>Natural Periods and Their Corresponding Vibration Modes (New Wahite Ditch Bridge)</b>	<b>145</b>
<b>8.30</b>	<b>Summary of all Earthquakes for New Wahite Ditch Bridge</b>	<b>152</b>
<b>8.31</b>	<b>Comparison of AASHTO Response Spectrum vs. Site Specific Response Spectrum (New Wahite)</b>	<b>153</b>
<b>8.32</b>	<b>Natural Periods and Their Corresponding Vibration Modes (Old Wahite Ditch Bridge)</b>	<b>155</b>
<b>8.33</b>	<b>Summary of all Earthquakes for Old Wahite Ditch Bridge</b>	<b>163</b>
<b>8.34</b>	<b>Comparison of Column Moments for Old Wahite Ditch Bridge</b>	<b>164</b>
<b>8.35</b>	<b>Displacement at Top of Old Wahite Ditch Bridge Abutment</b>	<b>165</b>

## APPENDICES

<b>A.</b>	<b>FIELD DATA</b>	A1
<b>A.1</b>	Symbols Used on Boring Information	A1
<b>A.2</b>	St. Francis River Bridge Site Test Pits	A3
<b>A.3</b>	St. Francis River Bridge Site Boring Logs	A6
<b>A.4</b>	St. Francis River Bridge Site Cone Penetrometer Logs	A13
<b>A.5</b>	Wahite Ditch Bridge Site Test Pits	A19
<b>A.6</b>	Wahite Ditch Bridge Site Boring Logs	A24
<b>A.7</b>	Wahite Ditch Bridge Site Cone Penetrometer Logs	A30
<b>B.</b>	<b>LABORATORY DATA</b>	A35
<b>B.1</b>	Cyclic Stress Test Results	A35
<b>B.2</b>	St. Francis River Site Laboratory Results	A37
<b>B.3</b>	Wahite Ditch Bridge Site Laboratory Results	A43
<b>C.</b>	<b>SOFTWARE DESCRIPTION</b>	A48
<b>C.1</b>	<i>SHAKE91</i> and <i>SHAKEDIT</i>	A48
<b>C.1.1</b>	<i>SHAKE91</i>	A48
<b>C.1.2</b>	<i>SHAKEDIT</i> Program	A48
<b>C.2</b>	Modified <i>DDRW2</i> Program	A48
<b>C.3</b>	<i>PCSTABL5</i>	A49
<b>C.4</b>	<i>SAP2000</i>	A49
<b>D.</b>	<b>DETAILS OF SYNTHETIC GROUND MOTION</b>	A51
<b>D.1</b>	Task	A51
<b>D.2</b>	Overview of Problem	A51
<b>D.3</b>	Defining Earthquakes	A51
<b>D.4</b>	Discussion	A56
<b>E.</b>	<b>DATABASE FOR EARTHQUAKE ANALYSIS</b>	A89
<b>F.</b>	<b>BRIDGE ABUTMENT AND PIER SUPPORTED ON A PILE GROUP</b>	A90
<b>F.1</b>	Stiffness and Damping Factors of Single Pile	A90
<b>F.1.1</b>	Vertical Stiffness ( $k_z$ ) and Damping Factors ( $c_z$ )	A90
<b>F.1.2</b>	Torsional Stiffness ( $k_\psi$ ) and Damping Factors ( $c_\psi$ )	A90
<b>F.1.3</b>	Sliding and Rocking Stiffness and Damping Factors	A93
<b>F.2</b>	Group Interaction Factor	A94
<b>F.3</b>	Group Stiffness and Damping Factors	A98
<b>F.3.1</b>	Vertical Group Stiffness( $k_{zg}$ ) and Damping Factors ( $c_{zg}$ )	A98

<b>F.3.2</b>	<b>Torsional Group Stiffness (<math>k_{\psi^g}</math>) and Damping Factors (<math>c_{\psi^g}</math>)</b>	<b>A98</b>
<b>F.3.3</b>	<b>Sliding and Rocking and Cross Coupled Group Stiffness and Damping Factors</b>	<b>A99</b>
<b>F.4</b>	<b>Strain-Displacement Relationships</b>	<b>A100</b>
<b>F.5</b>	<b>Solution Technique for Displacement Dependent k's and c's</b>	<b>A101</b>
<b>F.6</b>	<b>Equations of Motion</b>	<b>A101</b>
<b>G.</b>	<b>LIQUEFACTION ANALYSIS</b>	<b>A156</b>
<b>H.</b>	<b>STRUCTURAL ANALYSIS RESULTS</b>	<b>A180</b>

## 1.0 INTRODUCTION

Southeast Missouri experiences relatively small magnitude earthquakes on a regular basis, and is the site of several of the largest magnitude (estimated 8.0 - 8.3) earthquake events to strike North America in recorded history (1811 - 1812). Experts agree that similar or greater magnitude earthquakes will strike this region again.

Geologic conditions in southeast Missouri make this region one of the most seismically susceptible in the country, based on its damage potential from intrinsically susceptible soil, high ground water levels and vast expanses of flood sensitive ground. If a high magnitude earthquake struck southeast Missouri today, infrastructure in the area would be devastated. Levees and dams could be breached. Bridges across the Mississippi and Missouri rivers could collapse or be rendered unusable. Landslides, floods, soil liquefaction, and the failure of roadway bridges and overpasses would close extended sections of highway. The network of lifeline facilities and services required for commerce and public health in St. Louis, Sikeston, Cape Girardeau and surrounding communities would be devastated. Utilities, including electrical power, communications, oil and gas distribution, sewage disposal and water distribution, would be disabled until emergency repair crews were able to access these communities. Southeast Missouri would be effectively cut-off from the rest of the world and individual towns and communities isolated.

In the event of a major earthquake, the reopening of emergency vehicle priority access routes into St. Louis, Sikeston and Cape Girardeau would be a top priority. To facilitate the rapid, cost-effective reopening of roadways and expedite the transport of aid into affected communities, a study of the earthquake susceptibility of roadways, bridges and overpasses in southeast Missouri is required. The Missouri Department of Transportation has designated the most viable of these routes as emergency vehicle priority access. In order to insure that the designated access routes will remain open post earthquake, the Missouri Department of Transportation needs to confirm that these re-entry routes will not sustain major unacceptable earthquake related damage, and, hence, could be reopened quickly following an earthquake event. In order to determine if the routes are viable, the Missouri Department of Transportation must assess the earthquake susceptibility of existing overpasses, bridges, dams, levees, canals and foundation soils along these routes. Ultimately, the Missouri Department of Transportation may elect to reinforce these features where necessary, thereby minimizing earthquake damage, repair time and costs.

The earthquake hazards assessment of designated emergency vehicle priority access routes, which are mainly National Highway System route in southeast Missouri, will produce tangible economic and humanitarian benefits. The benefits will be realized if the Missouri Department of Transportation is able to reopen designated highways in a timely and cost-effective manner. This effort fully supports the Federal Highway Administration (FHWA) National Strategic Plan's mobility goal related to the strategic objective of returning highways to full service following disasters. The expertise, methodologies and technologies developed during the course of this study will be made available to adjacent states through presentations in appropriate venues and by publications of the study in appropriate journals. In this way, similar site-specific studies of priority access routes in other Midwestern States will have the benefit of the protocols and procedures developed in this work.

## 2.0 STATEMENT OF PROBLEM/SCOPE OF WORK

The designated emergency vehicle priority access route into southeast Missouri includes portions of US 60. This route traverses varied geologic settings and includes or crosses many critical roadway features such as bridges, slopes, box culverts, and retaining walls. The extent of damage and survivability of these critical roadway features in the event of a major earthquake event is not fully known and would impact the ability to use these designated routes to provide emergency vehicular access in a timely manner.

This study involves the assessment of four critical bridges at two sites along US 60 (Figure 2.1) and the development of an initial geotechnical database that will be part of a future regional geotechnical GIS database. The methodologies developed in this study will be used to establish an assessment protocol. The output-interpreted geotechnical data will be used for future prioritization and retrofit of deficiencies noted at the bridge sites studied.

## 3.0 OBJECTIVES

There were two primary objectives for this study. Objective 1 was to establish a geotechnical database for earthquake design and future use in a geographic information system (GIS) for the portions of US 60 and MO 100 in the counties of Butler, Stoddard, New Madrid, Franklin and St. Louis. Objective 2 was to conduct detailed earthquake assessments at two sites along designated emergency vehicle priority access route US 60.

### 3.1 Geotechnical Databases

Databases have been established for current subsurface and earthquake design data for the US 60 corridor in Butler, Stoddard and New Madrid Counties and for the MO 100 corridor in Franklin and St. Louis Counties. The database includes appropriate geotechnical data from Missouri Department of Transportation files. These databases will be integrated into the existing Missouri Department of Transportation GIS system for future access, and serve as the beginning of a larger regional or statewide database for future development and use by the Missouri Department of Transportation.

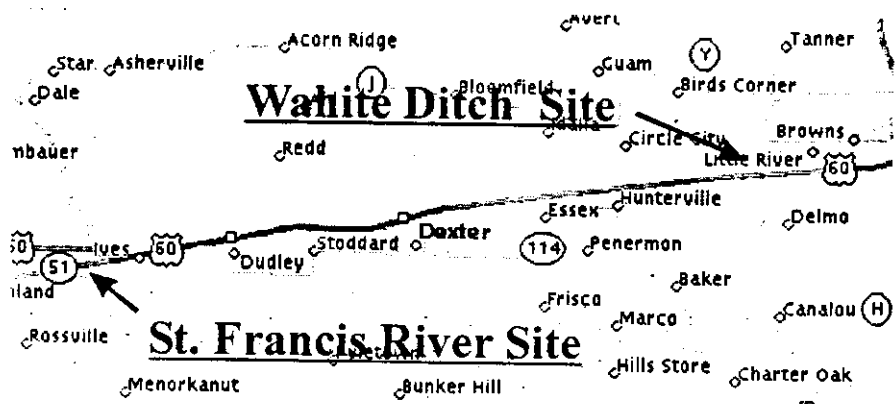


Figure 2.1 Study Site Locations

### **3.2 Site Specific Earthquake Hazards Assessments**

Members of the Missouri Department of Transportation, University of Missouri-Rolla Departments of Geology and Geophysics, Civil Engineering and Geological Engineering and the Missouri Department of Natural Resources research team visited US 60 in Butler, Stoddard and New Madrid Counties. Sites with critical roadway features were visually evaluated and ranked based upon geologic, structural and perceived criticality/risk factors. The top two sites with differing geologic settings and potential high-risk earthquake hazards were selected for detailed site-specific earthquake assessments as part of this study. The sites selected are located in Stoddard County where US 60 crosses Wahite Ditch Number 1 and in Butler County and Stoddard County where US 60 crosses the St. Francis River.

Detailed earthquake site assessments were conducted for the two critical US 60 roadway sites. Site assessments included subsurface exploration and laboratory testing to identify subsurface materials and their engineering properties, evaluation of available seismic records and the characterization of the ground motions associated with various design earthquake events. The responses of the subsurface materials and the existing bridge structures to the estimated ground motions were determined.

The goals of the site assessments at these two locations were to:

1. Estimate peak magnitude and duration of ground surface motion (including amplification and damping) associated with various events at each site.
2. Evaluate the susceptibility of each site to earthquake-induced slope instability and liquefaction.
3. Estimate shaking effects on the two types of existing bridge structures at each site.
4. Compare ground motion and structural response parameters from the site-specific earthquake analysis with those from the American Association of State Highway and Transportation Officials (AASHTO) response spectrum analysis method and provide preliminary guidance regarding selection of the analysis method at future sites.
5. Evaluate modified site assessment techniques and establish a basis for using these modified techniques at other sites along designated emergency access routes.

## **4.0 MISSOURI DEPARTMENT OF TRANSPORTATION GEOTECHNICAL DATABASE**

### **4.1 Design**

The primary goal for this database was to develop a repository of usable geotechnical data for the Missouri Department of Transportation. This section of the report outlines the philosophies behind both the development of the database and the design approach.

### 4.1.1 Design Approach

The approach to the development of the database revolved around the overall goal of designing a Missouri Department of Transportation statewide geotechnical database, customized to the needs of this project. There are two classical approaches to data management design: "top-down" or "bottom-up." A top-down design approach consists of conceptualizing the problem, breaking it into manageable sub-problems, identifying appropriate methodologies and processes, and manipulating the data to achieve a result that will impact the "real" world. This approach is idealistic and generally applicable only when there is no existing data and/or database.

On the other hand, when there are abundant data and information, or an existing database, the development of a system requires the use of a bottom-up approach. This requires the analysis of data format and structure prior to the identification of methodologies and processes. Once methodologies/processes have been identified, a final model can be developed. Figure 4.1 shows a hierarchical schematic of these two alternative system design approaches. The two classical approaches described above represent the extremes of how systems are designed.

For this project, an initial step was to model geologic and geotechnical data using a top-down approach. Topics related to construction of transportation systems and their subsurface characterizations were included in this phase. Data were categorized into different classes (Figure 4.2).

Missouri Department of Transportation investigators provided borehole logs and associated soil-testing data. This necessitated modification to the database design approach. When data became available, the database design shifted to a bottom-up approach. The categories dimmed in Figure 4.2 were not pursued any further. The scope of the database was focused to include only data at highway structure locations provided by Missouri Department of Transportation investigations.

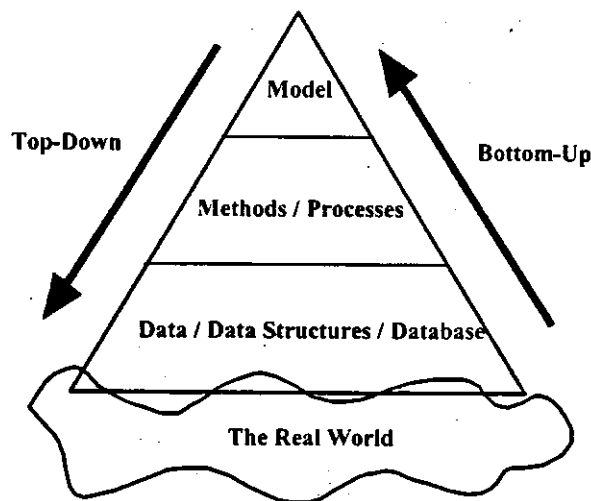
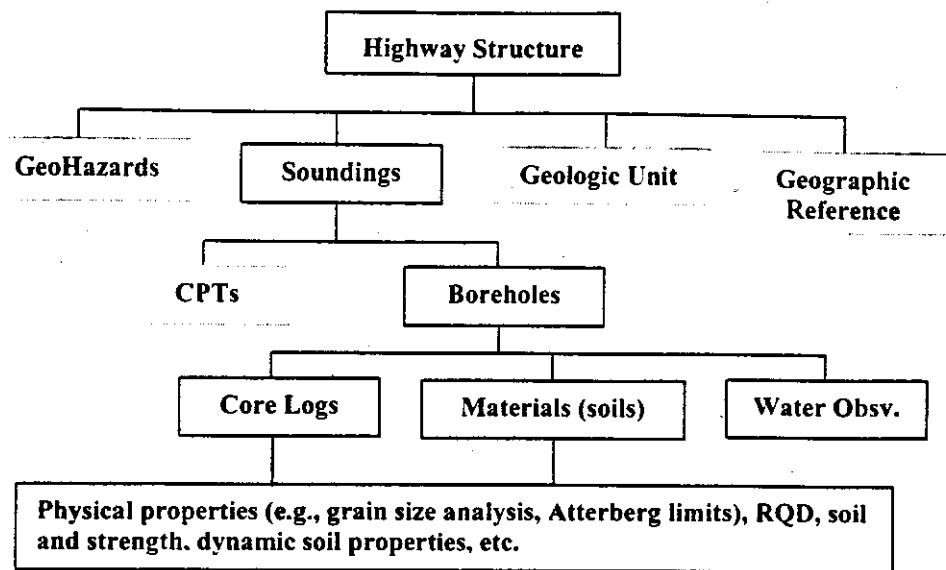


Figure 4.1 System Design: Top-Down vs. Bottom-Up



**Figure 4.2** Organization of Missouri Department of Transportation Subsurface Data

Ultimately, a combination of the top-down and bottom-up approaches was used to design the database. The existing geotechnical data dictated the uniqueness of the application and the model developed. However, the design of the different tables was organized from a hierarchical point of view. In other words, the design was an iterative process of studying the data definitions/form/structure and developing the conceptual model and methods.

#### 4.1.2 A Geotechnical Generic Example

A traditional geotechnical engineering project typically focuses on the subsurface characterization of a specific site and the interaction of man-made structures with the earth mass. However, multi-disciplinary projects usually require the expansion of the focus into other related fields (e.g., bridges, environmental, geology, etc.). In such instances, the engineer may be required to collect a broad range of available information to help solve a problem. The sources of information are the subsurface data recovered by invasive (e.g., boreholes, soundings) and non-invasive (e.g., geophysical, remotely sensed) explorations, the existing surface features, and the future surface and subsurface features planned for the site, if any. The multiple types of information are available in different physical forms and the engineer's expertise and judgment are used to synthesize this information and make decisions and recommendations about how to proceed with the project. When the amount of information that can be effectively collected and manipulated is abundant, the use of an information and database management system can aid in the problem solving process.

Data introduced into a database can serve not only a specific project, but for a continued period of time and for other projects. However, problems involving the legacy and integrity of the data may become an issue. For example, when data is retrieved and used, it may incur changes that alter the database, depending on the read/write permissions allocated to a user. Spatial information uses coordinate systems and map projections that may be modified during the life of the data and a record of these transformations needs to be stored. The date and the units of a value stored

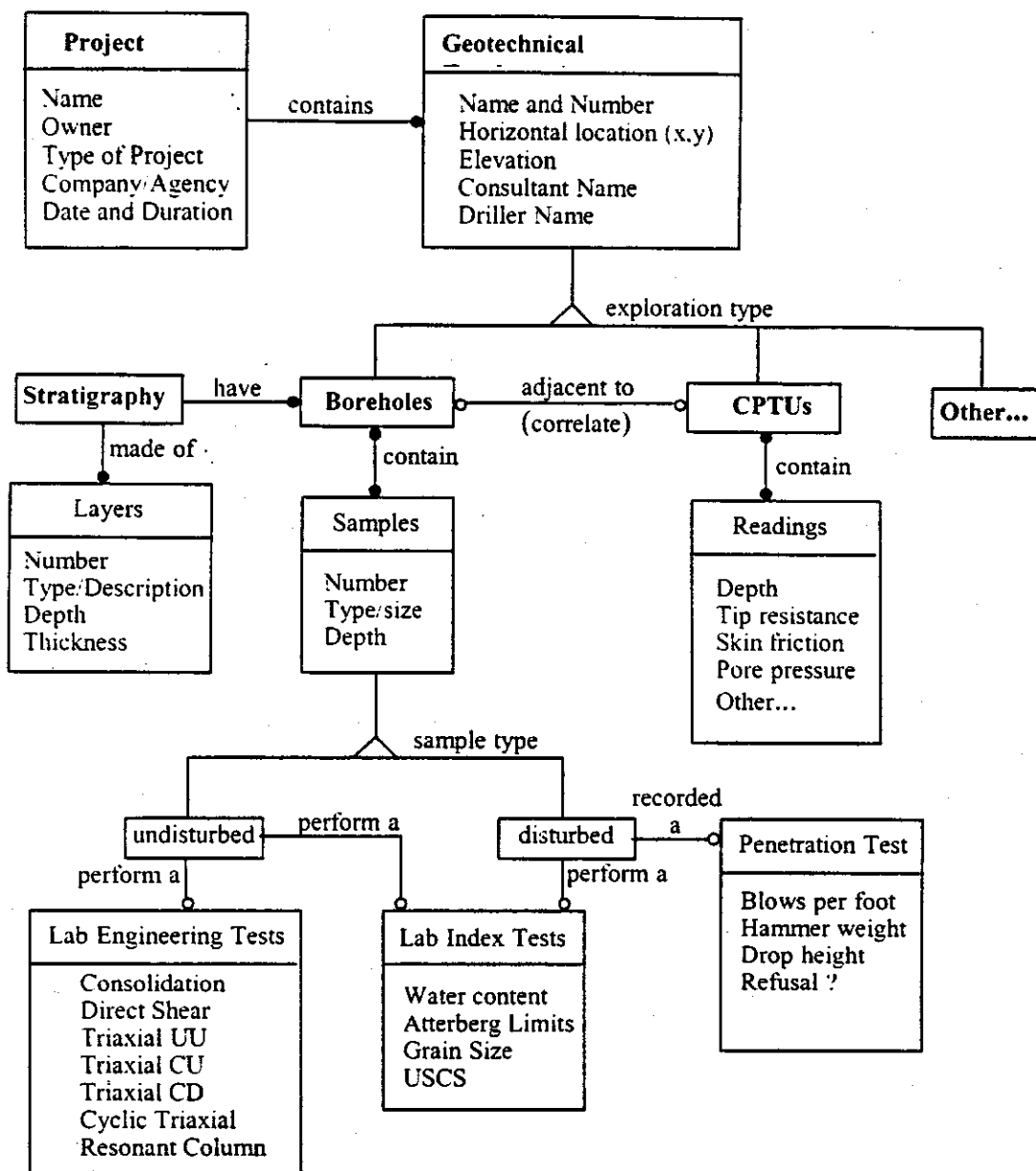
in a field need to be documented. Therefore, a record that keeps track of the data transformation and contents should be used and is usually referred as "data about the data" or metadata. Since a database may be intended to serve information for a continued period of time it is important to identify the data sources, the data requirements, and the data structures (Luna and Frost, 1995).

The general principles of object-oriented modeling and design were followed. However, the diagram included in this section does not necessarily follow a standard notation for reasons of clarity (also not common language in civil engineering). The three models used in the Object Modeling Technique (OMT) are the object model, the dynamic model, and the functional model. They each represent a different aspect of the system: object model - static, structural, "data"; dynamic model - temporal, behavioral, "control"; functional model - transformational, "function" (Rumbaugh et al., 1991). For this Missouri Department of Transportation database, the object model has been adopted to represent subsurface geotechnical data and a generic example is shown in Figure 4.3. These three kinds of models separate a system into three orthogonal views and are not completely independent, but each model can be examined and understood by itself to a large extent. The final architecture of the database was a product of the data structures and the module integration and will be discussed in more detail later.

#### **4.1.3 Analysis and Data Structure**

Probably the most time consuming task in the database aspect of the project was the analysis and definition of the data structure for the database. Missouri Department of Transportation's customized needs were met by focusing on data from borehole explorations and by retaining the terminology consistent with the analog data (paper form) provided, such as soil descriptions, stratigraphy, and testing nomenclature. No digital data were available for inclusion in this database. An extensive reference was developed by The Missouri Department of Natural Resources to perform data entry into database (refer to accompanying User's Manual). Soil descriptions and soil test names were standardized with the assistance of Missouri Department of Transportation.

Additionally, one item that required several iterations was related to the definition of fields and records. To overcome this problem, the Missouri Department of Transportation and project investigators were asked to submit the nomenclature of geotechnical parameters, and to provide typical value units, and maximum and minimum values for each. For example, Table 4.1 shows an example of a more extensive list of geotechnical earthquake engineering parameters with the required information to define the structure of the data. The complete list is provided in User Instructions for Data Entry and Editing Database of Borehole and Other Geotechnical Data for Missouri Highway Structures.



**LEGEND:**

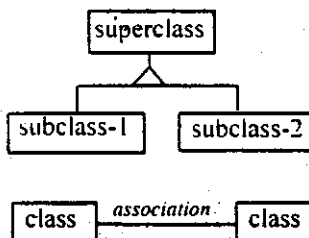
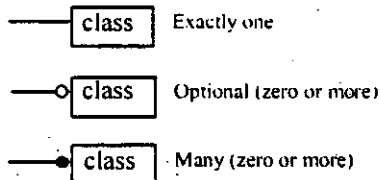
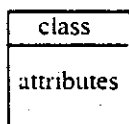


Figure 4.3 Example of An Object-Oriented Geotechnical Database Model (Luna and Frost, 1995)

**Table 4.1 Example of Data Structure Input to Database**

Field Name	Field Description	Field Type <sup>(1)</sup>	Field Size	Decimal Places	Min. Value	Max. Value	Units
Elev	Top of layer elevation	N	6	2	0.00	100.00	m
Soil Type	USCS Soil Classification	A	10				
$\gamma$	Dry Unit Weight	N	5	2	90.00	140.00	Lb/ft <sup>3</sup>
NSPT	Measured Standard Penetration Value	N	3	0	1	50	Blow/ft
Nspt-CPT Corr	Correlation SPT_CPT data (qc/N, qc in kN/m <sup>2</sup> ; N=Nspt)	N	6	2	400.0	1000.00	
Less than 0.075	Percent passing 0.075 mm sieve	N	5	2	0	100.00	%
Vs	Shear wave velocity	N	6	2	110.0	260.00	M/s
G	Shear modulus	N	7	2	50.00	3200.00	Kg/cm <sup>2</sup>

Notes: (1) N= numeric; A = alphanumeric

## 4.2 Implementation

The database design was implemented using the Microsoft Access software package. It is currently operational on a Pentium-based computer using the Windows NT operating system. The database is being populated by means of an interface designed specifically for this project. Refer to the companion document, User Instructions for Data Entry and Editing Database of Borehole and Other Geotechnical Data for Missouri Highway Structures for details about the rationale and usage of these "forms" for data entry into the tables.

## 4.3 Link to a Spatial Database (GIS)

The database was designed to link to a Geographic Information System (GIS). In principle, it can be referred as a spatial database. The data fields with geographic coordinates and referenced coordinate system are field identified as key items in the databases. However, at this time the entries to each borehole are not available. It is essential to link the boreholes to a common geographic reference so they can be related to the other spatial themes.

## 5.0 SITE CHARACTERIZATION: PROCEDURES

### 5.1 Field Investigations

The two study sites were investigated using both surface and subsurface exploration and mapping techniques. The details of the investigation program are discussed below.

### **5.1.1 Drilling and Sampling**

Exploratory boreholes were advanced at each bridge site using mud-rotary techniques with a drill rig and personnel provided by Missouri Department of Transportation. Three 50-foot boreholes, two 100-foot boreholes, and one 200-foot borehole were made at both bridge sites.

The sampling interval varied with depth. The planned intervals were to sample continuously from the ground surface to a depth of 30 feet, to sample at 5-foot intervals from 30 to 80 feet, and to sample at 10-foot intervals thereafter. Several types of samples were collected, depending upon the soil type and depth. Shelby tube and SPT samples were alternated for cohesive soils, and only SPT samples were taken for non-cohesive soils. Shelby tube diameters were varied between 3-inch and 5-inch tubes so samples could be used for a variety of tests. Missouri Department of Transportation personnel logged the borings, retrieved and field-tested the samples. The samples were wrapped and sealed in paraffin for later testing. Field-testing consisted of torvane and pocket penetrometer testing of the cohesive samples. SPT values were recorded for both cohesive and non-cohesive soils.

### **5.1.2 Test Pits**

Shallow exploratory test pits were dug to provide information on fill depths, lateral stratigraphy, and homogeneity of site soils. The local Missouri Department of Transportation maintenance shed near each bridge site provided a backhoe and operator to dig and backfill pits. An engineer from the University of Missouri-Rolla selected trench locations and prepared a log of soil units visible in the test pit walls.

### **5.1.3 Cone Penetrometer**

Six seismic cone penetrometer soundings were completed at the St. Francis River Site and five at the Wahite Ditch Site, with a goal of advancing the soundings as deep as feasible (estimated to be 80 ft or 25 m). Recorded parameters included tip resistance, local friction, pore pressure, and inclination at 0.15 ft (0.05 m) intervals, as well as seismic velocity at 3.3 ft (1 m) intervals. Parameters calculated or correlated from recorded parameters included friction ratio, soil type, and SPT. In many cases, soil resistance exceeded the available capacity of the cone rig (CME 850) and soundings were halted before the target depth was reached.

### **5.1.4 Surface Mapping**

A University of Missouri-Rolla engineer developed site engineering geologic maps showing estimated limits and types of fill material, geometry of site slopes, and other geologic features potentially impacting the roadway, bridges, or abutments. Because both bridge sites proved to be rather simple and homogeneous geologically, information from this field mapping was incorporated into the slope stability cross-sections and the site geology discussion and is not presented separately.

### **5.1.5 Interviews with Local Personnel**

Mr. Dan Camden of the Wappapello Lake Control office, U.S. Army Corps of Engineers was contacted to obtain information regarding potential impacts to the US 60 roadway following catastrophic failure of the Wappapello Dam, on the St. Francis River.

Mr. Lonnie Blasingame, Missouri Department of Transportation Regional Superintendent, provided information on historic maintenance on the portions of US 60 near the St. Francis River Site and Wahite Ditch Site.

## **5.2 Laboratory Investigations**

Soil samples taken from the borings at the two sites were transported initially to the Missouri Department of Transportation Geotechnical Laboratory. The field boring logs were reviewed and soil samples selected for testing. Missouri Department of Transportation personnel conducted basic index tests at the Missouri Department of Transportation Geotechnical Laboratory. Static and cyclic triaxial tests were conducted at the University of Missouri-Rolla Civil Engineering Geotechnical Laboratories.

### **5.2.1 Missouri Department of Transportation Laboratory Testing**

Soil tests conducted by Missouri Department of Transportation personnel include:

- Pocket penetrometer
- Torvane
- Natural water content
- Liquid limit
- Plastic limit
- Unconfined compression
- Sieve and hydrometer

All tests were conducted in general accord with the applicable AASHTO Standards. The results of their testing are given in Appendix B.

### **5.2.2 University of Missouri-Rolla Laboratory Soil Testing**

Upon completion of the classification testing, the soils were transported to the University of Missouri-Rolla for testing in their Geotechnical Engineering Laboratory. The soils were categorized into three general soil types for testing (high plastic clay, low plastic clay and silt). The University of Missouri-Rolla conducted static consolidated-undrained (staged and multi-sample CU) tests and strain controlled cyclic triaxial tests on samples of the cohesive soils. The silt soils were disturbed such that they could not be tested in the laboratory.

### **5.2.2.1 Consolidated-Undrained (CU) Triaxial Tests**

Consolidated-undrained triaxial compression tests were conducted on selected samples of cohesive soils from the borings. All tests were conducted in general agreement with Test Method for Consolidated-Undrained Triaxial Compression Test on Cohesive Soils, ASTM D5567. When there were only limited volumes of soil sample suitable for testing, a staged CU test was conducted. These tests were conducted in general agreement with the procedure developed by Sridharan and Rao (1972). Effective stress and total stress cohesion intercept and friction angles were determined. The results are presented in Appendix B.

### **5.2.2.2 Cyclic Triaxial Tests**

Selected cohesive soil samples were tested for their strain dependent shear modulus and damping. The tests were conducted in general accordance with Test Methods for the Determination of the Modulus and Damping Properties of Soils Using the Cyclic Triaxial Apparatus, ASTM D 3999. All tests were conducted at a frequency of 10 cycles per second (Hz). The tests were staged in that a single sample was tested at three different deformation levels. The resulting moduli and damping were then plotted as a function of the imposed strain. The results are presented in tabular form in Appendix B.

## **5.3 Base Rock Motion Determination**

In a traditional earthquake hazard assessment project, the first step is to select a rock base ground motion at the site. This usually requires a site-specific seismic hazard analysis taking into consideration the characteristics of all the known earthquake sources (faults, zones, epicentral distance, geological condition, and background) that could affect the site. However, in the central United States there is a lack of recorded strong ground motion in the New Madrid area that can be used for such purposes. Therefore investigators in the research community have resorted to procedures that develop synthetic base rock motions at a site.

Dr. Robert Herrmann, Professor of Geophysics at St. Louis University, was requested to provide credible synthetic ground motions at both the St. Francis River Site and the Wahite Ditch Site.

### **5.3.1 Current Peak Ground Acceleration**

The locations of both the bridge sites (St. Francis River Site (SF) and the Wahite Ditch Site (WD)) are shown in Figure 5.1 together with neighboring earthquake locations for the time period 1974-1995. The St. Francis River Site is about 37 - 150 km from possible earthquakes in the active part of the current seismicity zone, while the Wahite Ditch Site is about 15 - 150 km from active seismicity (Herrmann, 2000).

In the preparation of the 1996 National Earthquake Hazards Reduction Program (NEHRP) maps, the United States Geological Survey (USGS) considered other possible locations obtained by moving the 'Z' seismicity pattern westward slightly to the edge of the ancient right and eastward to the eastern boundary. They then assigned weights of 1/3 to each of the three patterns.

The USGS 1996 maps equally weighted two ground motion magnitude – distance relations: one based of the Toro and McGuire model for EPRI and the other a purely USGS model. The 1996 maps were generated for a nationwide NEHRPB-C soil condition boundary so that one could use the methodology in Federal Emergency Management Agency (FEMA) -273, for example, to adjust the mapped values to sites with other than the B-C soil condition in the upper 30 meters.

By entering a latitude and longitude at the USGS - National Seismic Hazard Mapping Project, the peak ground acceleration can be obtained (Table 5.1 Peak Ground Acceleration, Herrmann, 2000). However, Herrmann, (2000) has not used these values in the final recommendations of base rock motions.

### **5.3.2 Magnitudes and Distances for the Recommended Acceleration Values**

The magnitudes and distances for the study sites were selected from a table of ground motion parameters as a function of magnitude and distance (the USGS ground motion model enters into the hazard analysis code by a table lookup). The following acceptable combinations are shown in Table 5.2 (Herrmann, 2000).

### **5.3.3 Time Histories**

Using the band-limited Gaussian white noise technique of Boore (1922), the program *DORVT180* and *TD\_DRVR* were used together with auxiliary programs for display.

The Central United States (CUS) deep soil ground motion model with F96 (USGS96 source scaling) given on the CUS ground motion web page, with a soil thickness of 0 meters was used. Because the CUS model includes 1 km of Paleozoic layers, there is a slight frequency dependent site amplification. The model uses recently determined, CUS specific, crustal wave propagation from the source to the site (Appendix D).

The recommend rock base accelerations for a probability of exceedance (PE) of 10 % in 50 years and a PE of 2 % in 50 years for each site was obtained, i.e. 40-rock base synthetic ground motions (time histories) are available. Half of these were for PE of 10% in 50 years and other half were for PE of 2 % in 50 years.

The details of these rock base motions are shown in Appendix D. Selected sets of time histories of rock base acceleration-time histories are shown in Figures 5.2a, b, c, d and 5.3a, b, c, d. These will be used in all subsequent analysis as explained further.

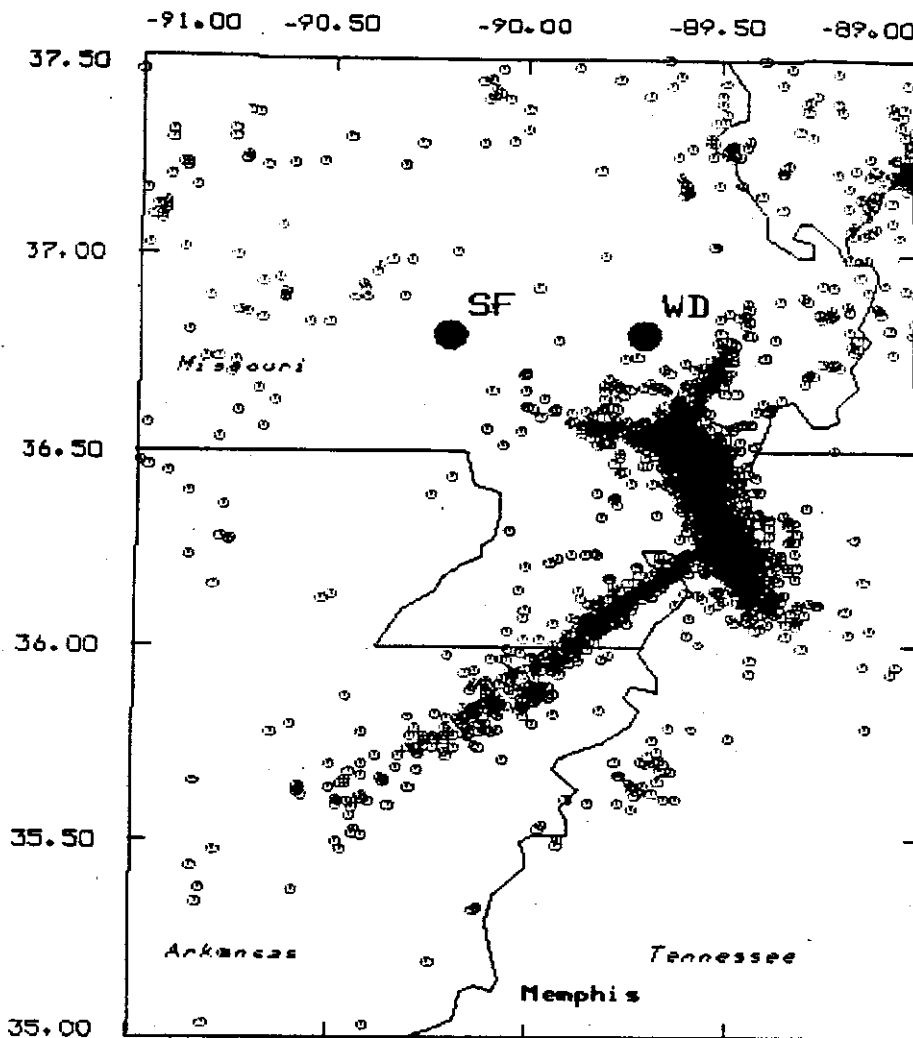


Figure. 5.1 Seismicity in the 1974 - 1995 Time Period in the Vicinity of the St. Francis River Site (SF) and the White Ditch Site (WD). (Herrmann, (2000))

Table 5.1 Peak Ground Acceleration (Herrmann, 2000)  
(Source; USGS 1996 Seismic Hazard Maps)

Site location	Peak Ground Acceleration (g)	
	10 % PE in 50 years	2% PE in 50 years
St. Francis River Site (36.8°N, 90.2°W)	0.158	0.643
White Ditch Site (36.8°N, 89.7°W)	0.196	1.343

**Table 5.2 Magnitudes and Distances for Selected Earthquakes,  
(Herrmann, 2000)**

**a. St. Francis River Site**

Probability of Exceedance	Magnitude	Distance, R
	Mw	(km)
10 % in 50 years	6.2	40
10 % in 50 years	7.2	100
2 % in 50 years	6.4	10
2 % in 50 years	8.0	40

**b. Wahite Ditch Site**

Probability of Exceedance	Magnitude	Distance, R
	Mw	(km)
10 % in 50 years	6.4	40
10 % in 50 years	7	65
2 % in 50 years	7.8	16
2 % in 50 years	8.0	20

For the purpose of establishing procedures for the remainder of this earthquake engineering study, the following rationale was adopted to select what ground motion time history be used in the subsequent analysis.

All of the 20 ground motions were used for one-dimensional wave propagation analysis (using the *SHAKE* program, Schnabel, 1972) for each bridge site. This resulted in a profile of peak accelerations for each soil layer for both bridge sites. The three ground motions with highest peak horizontal ground acceleration (maximum PGA) at the surface were selected for the subsequent analyses.

**5.4 Seismic Response of Soil**

This section describes the procedures used to evaluate the response of the various site features to the selected simulated earthquakes.

**5.4.1 Wave Propagation Analysis**

Several methods for evaluating the effect of local soil conditions on ground response during earthquake are presently available. Most of these assume that the soil response is caused by the upward propagation of shear wave from the rock base. Analytical procedures, considering nonlinear soil behavior, have been used in the *SHAKE* (Schnabel, et. al. 1972) and *SHAKE91* (Idriss and Sun, 1991) computer programs.

The *SHAKE91* procedure generally involves the following steps:

1. Determination of the ground motion at the base rock for use in the analysis. This ground motion is a function of the maximum acceleration, effective duration, magnitude and epicentral-distance.

2. Determination of the dynamic properties of the soil deposit (shear modulus, mass density, shear wave velocity, etc.). Non-linear properties of several soils have been established for use in this and other analyses (Seed and Idriss, 1971, Vucetic and Dobry, 1991).
3. Computation of the response of the soil deposit to the rock-base motions using SHAKE91.

SHAKE91, with its pre- and post-processor SHAKEDIT, were used to propagate the horizontal rock-base motion to the soil layers, and were also used to transfer P-waves from the rock base to the above layers. Brief descriptions of these programs are presented in Appendix C.

#### 5.4.2 Liquefaction Analysis

A universally accepted procedure of liquefaction analysis (Seed and Idriss, 1971 and Youd and Idriss, 1997) is as follows:

1. At a point in the soil mass, compute  $\tau_{av}$  shear stress caused by the earthquake (base rock motion in Figures 5.2 and 5.3) using equation 5.1:

$$\tau_{av} = 0.65 \cdot \left( \frac{a_{max}}{g} \right) \cdot \sigma_o \cdot r_d \quad (5.1)$$

$\tau_{av}$  may be expressed as the Cyclic Stress Ratio (CSR) (equation 5.2),

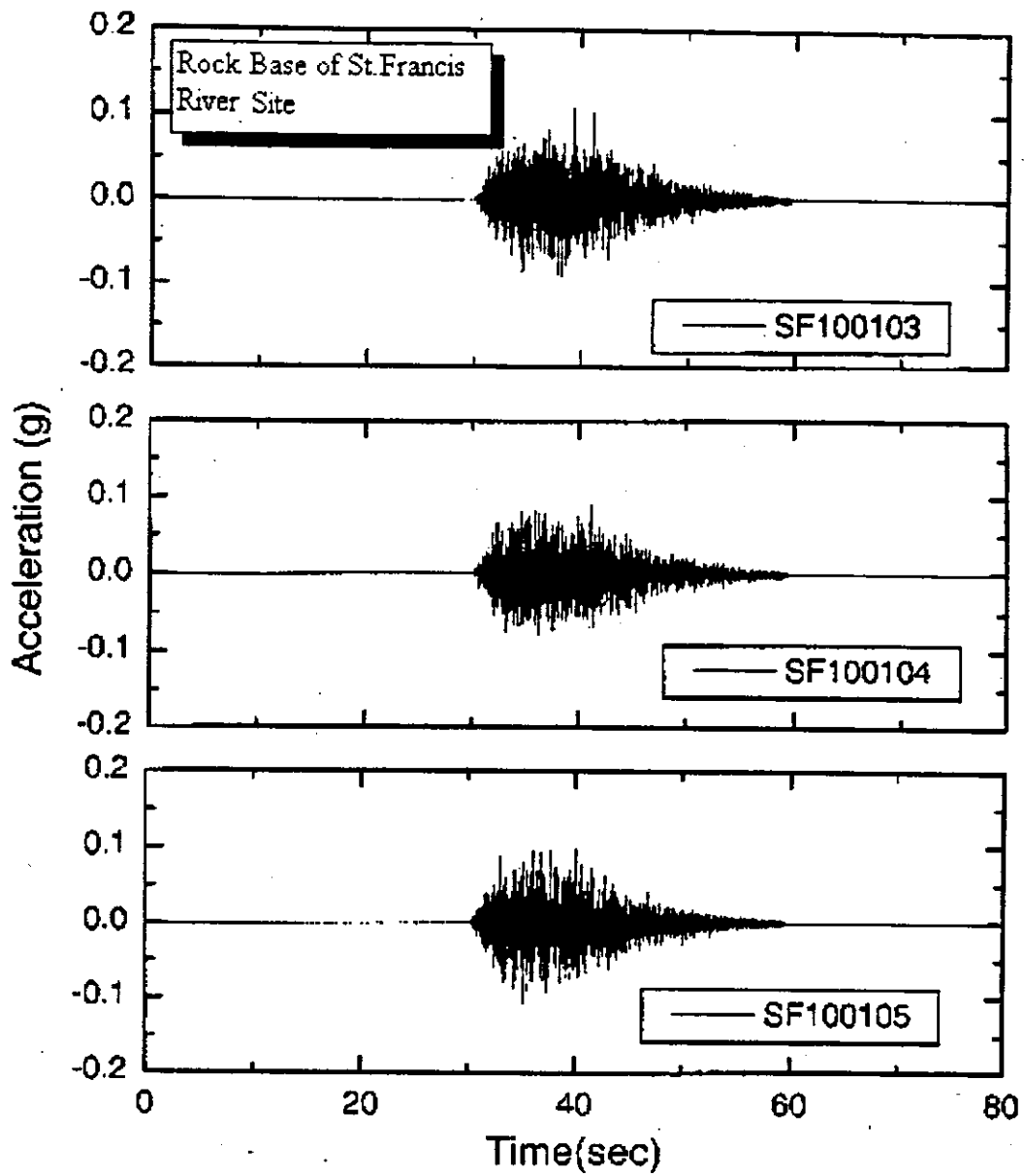
$$CSR = \frac{\tau_{av}}{\sigma_o} = 0.65 \cdot \left( \frac{a_{max}}{g} \right) \cdot \left( \frac{\sigma_o}{\sigma_o} \right) \cdot r_d \quad (5.2)$$

where,

- $a_{max}$  = peak horizontal ground acceleration at that surface.  $a_{max}$  is considered constant throughout the entire depth.
- $g$  = acceleration due to gravity
- $\sigma_o$  = total vertical overburden stress
- $\sigma_o'$  = effective vertical overburden stress
- $r_d$  = stress reduction coefficient

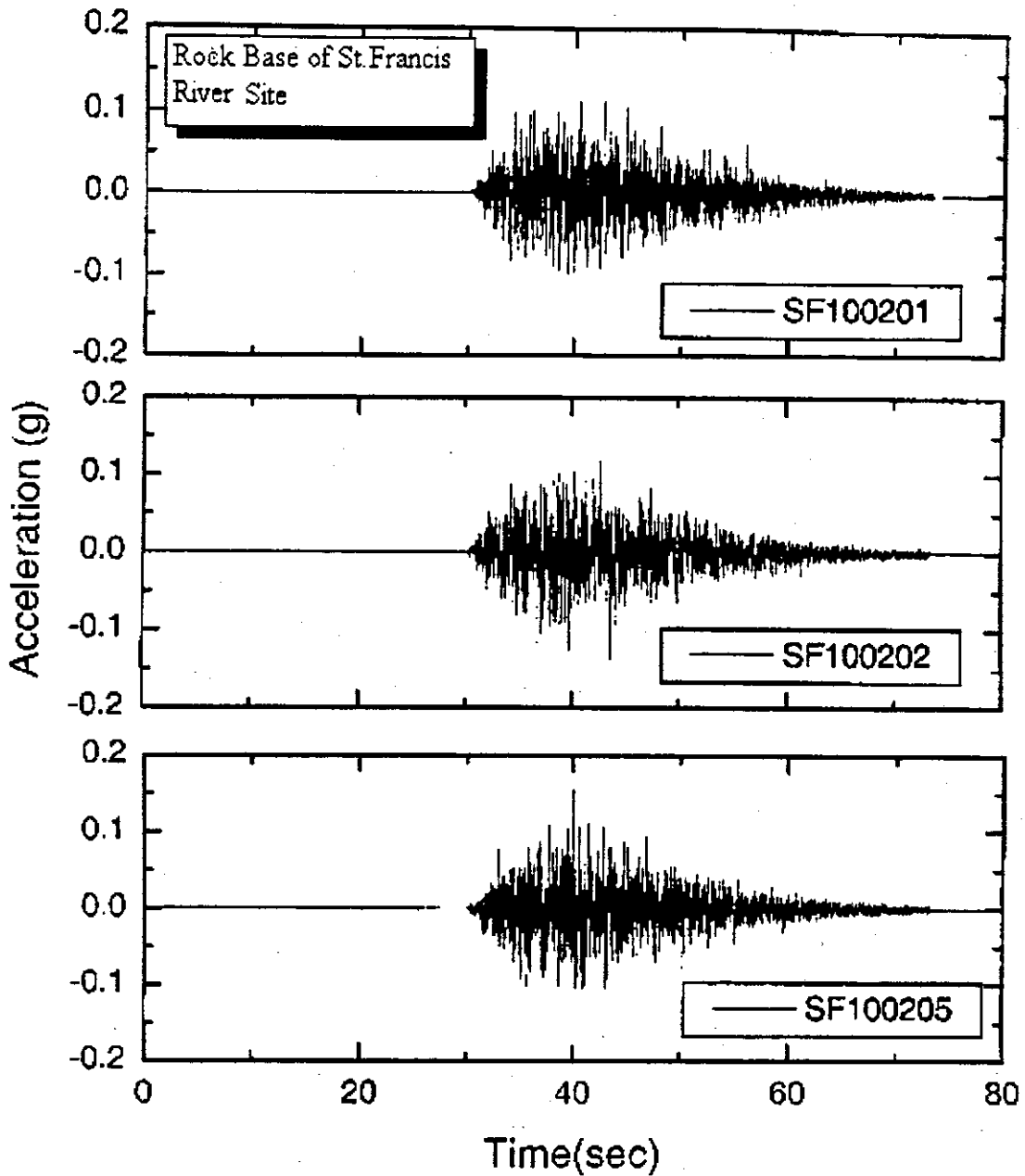
$r_d$  has been expressed as a function of depth below the ground level  $z$ , as (Youd and Idriss, 1997):

$$r_d = \frac{[1 - 0.4113z^{0.5} + 0.04052z + 0.001753z^{1.5}]}{[1 - 0.4117z^{0.5} + 0.05729z - 0.006205z^{1.5} + 0.00121z^2]} \quad (5.3)$$



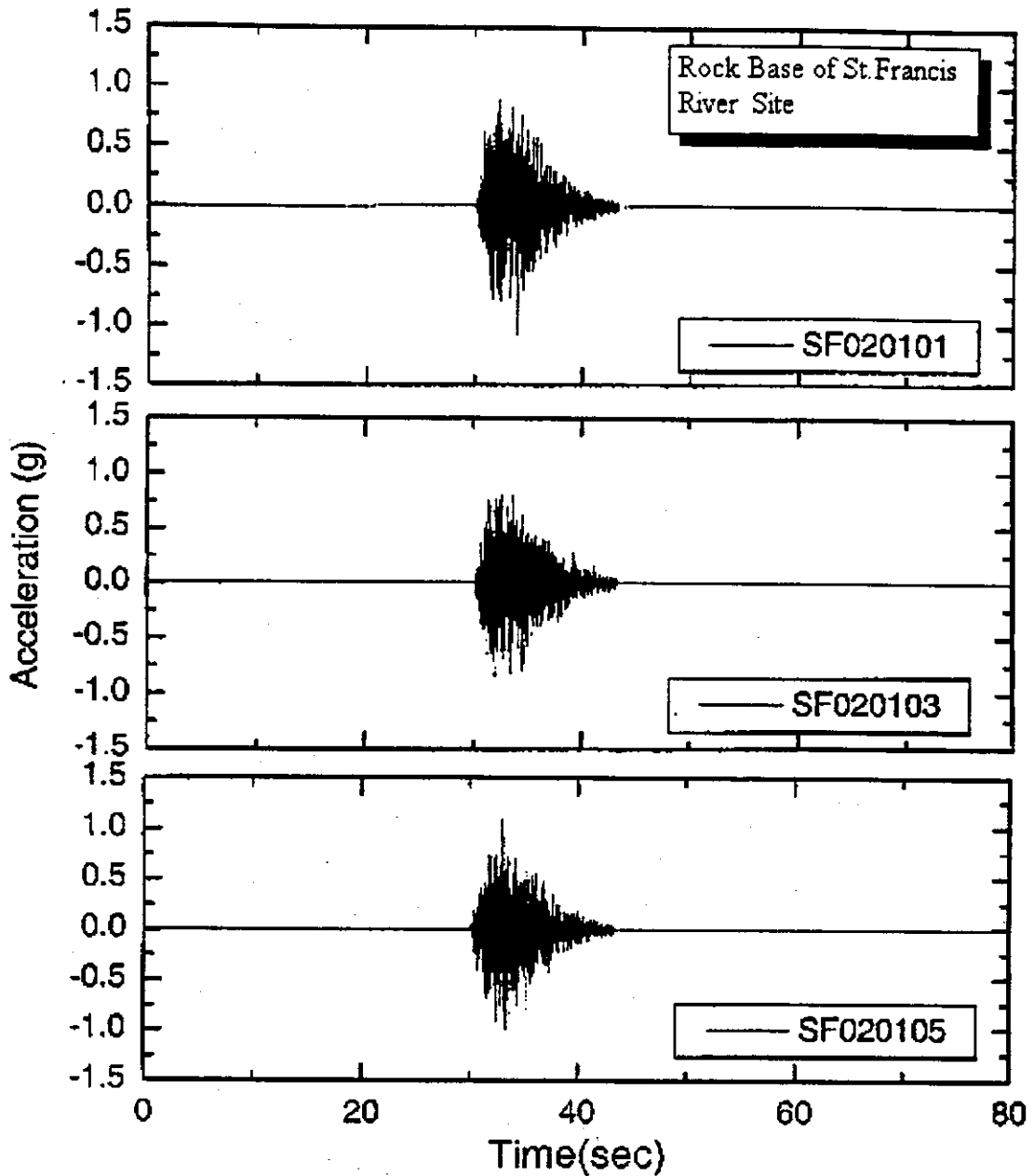
a. PE 10 % in 50 years, Magnitude = 6.2

**Figure 5.2.a** The Selected Base Rock Motion for the St. Francis River Site, PE 10 % in 50 Years, Magnitude 6.2



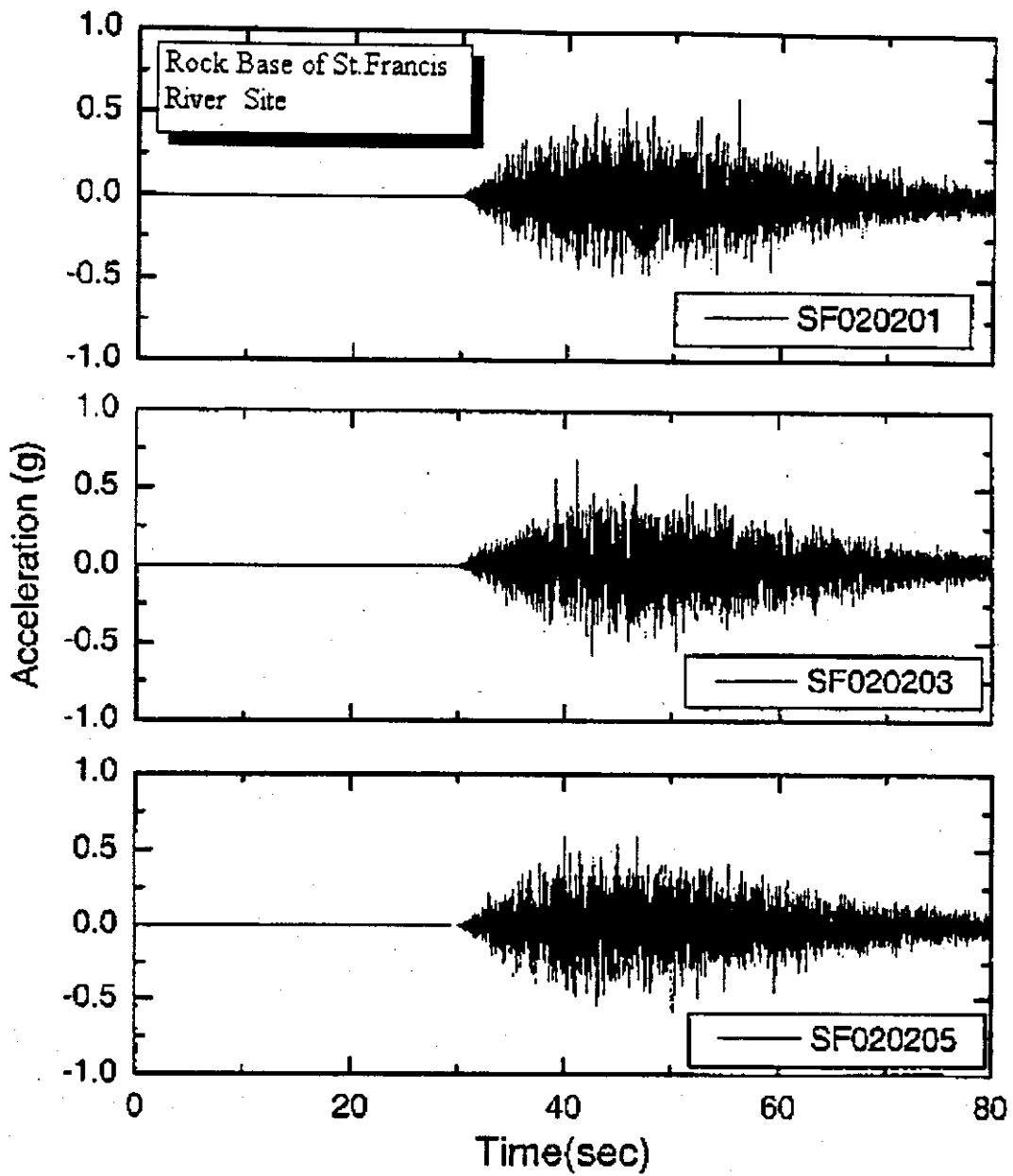
b. PE 10 % in 50 years, Magnitude = 7.2

Figure 5.2.b The Selected Base Rock Motion for the St. Francis River Site, PE 10 % in 50 years, Magnitude 7.2



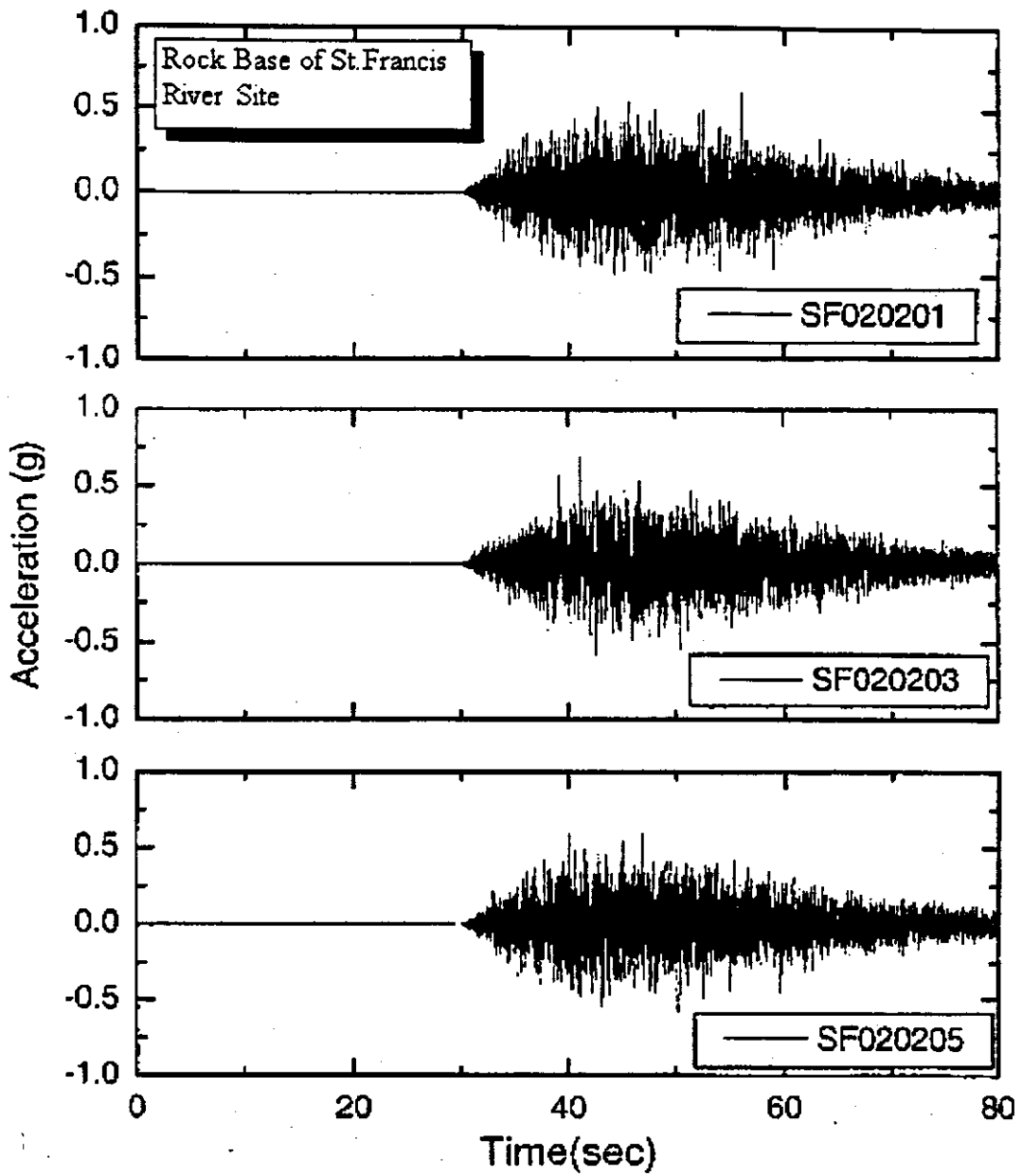
c. PE 2 % in 50 years, Magnitude = 6.4

Figure 5.2.c The Selected Base Rock Motion for the St. Francis River Site, PE 2 % in 50 years, Magnitude 6.4



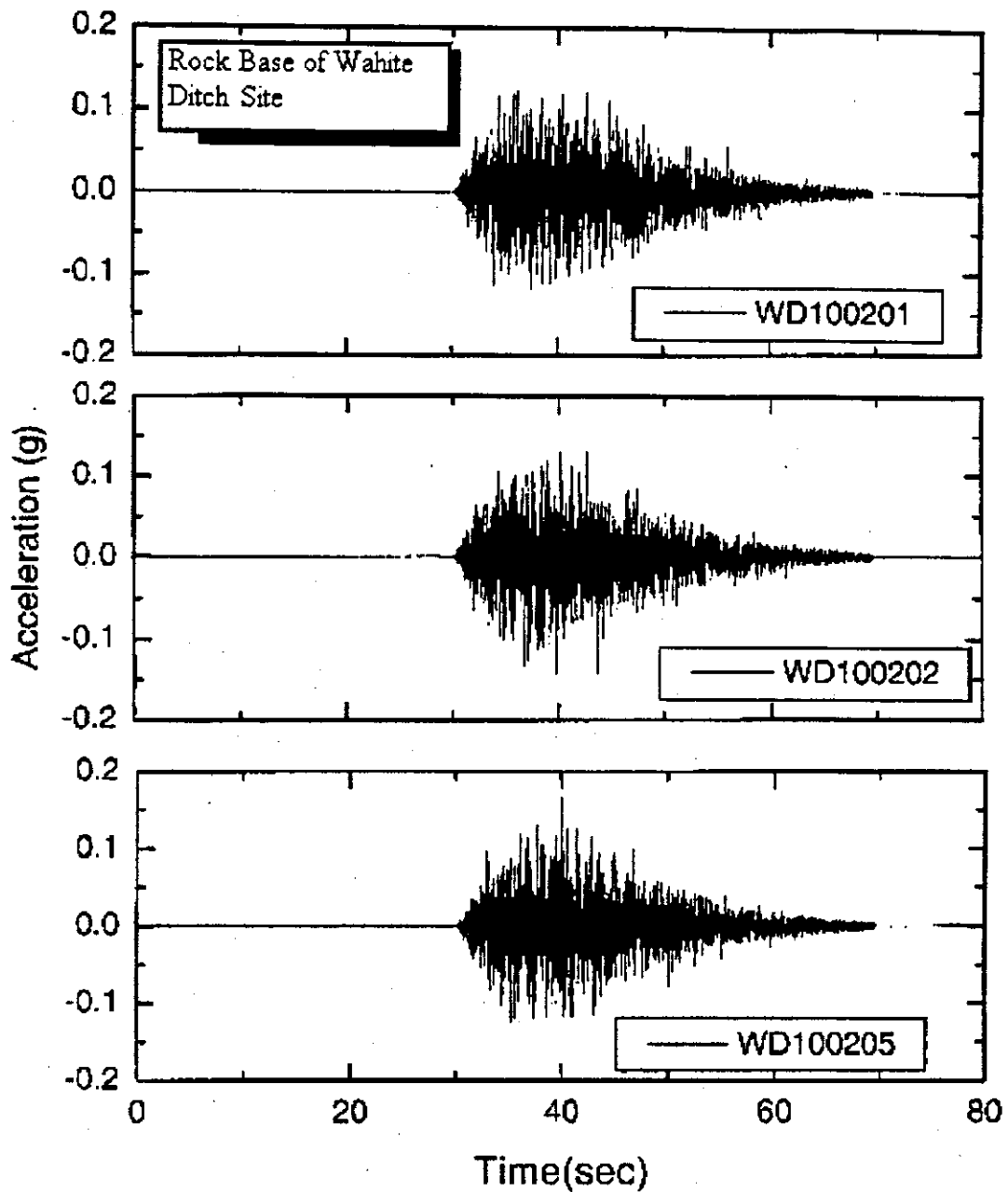
d. PE 2 % in 50 years, Magnitude = 8.0

Figure 5.2.d The Selected Base Rock Motion for the St. Francis River Site, PE 2 % in 50 years, Magnitude 8.0



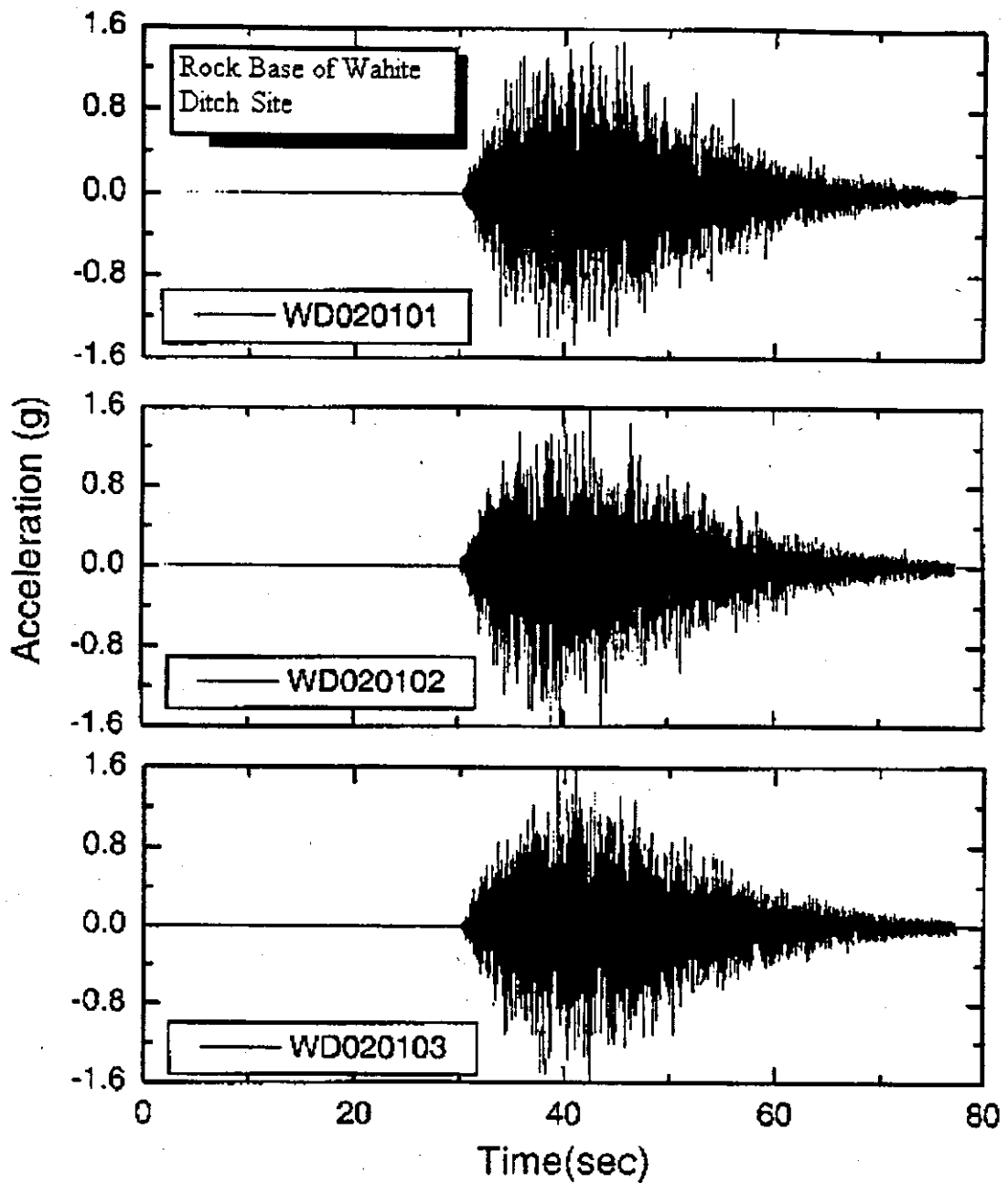
d. PE 2 % in 50 years, Magnitude = 8.0

Figure 5.3.a The Selected Base Rock Motion for the Wahite Ditch Site, PE 10 % in 50 years, Magnitude 6.4



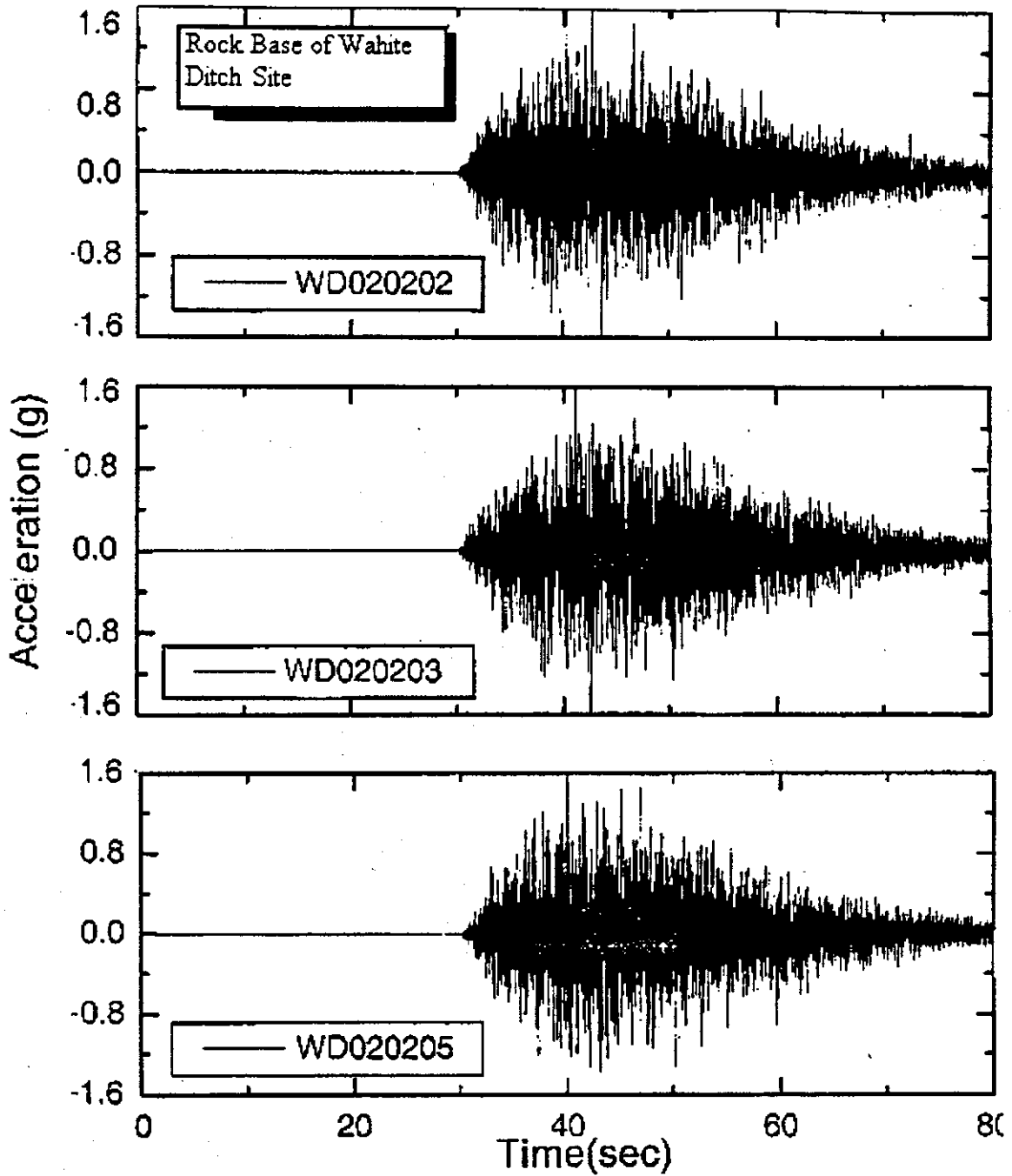
b. PE 10 % In 50 years, Magnitude = 7.0

Figure 5.3.b The Selected Base Rock Motion for the Wahite Ditch Site, PE 10 % in 50 years, Magnitude 7.0



c. PE 2 % in 50 years, Magnitude = 7.8

Figure 5.3.c The Selected Base Rock Motion for the Wahite Ditch Site, PE 2% in 50 years, Magnitude 7.8



d. PE 2 % in 50 years, Magnitude = 8.0

Figure 5.3.d The Selected Base Rock Motion for the Waite Ditch Site, PE 2 % in 50 years, Magnitude 8.0

2. Estimate  $\tau_{liq}$ , the shear strength to cause liquefaction at the above point under the ground motion (Figures 5.2 and 5.3).

$\tau_{liq}$  is also expressed as cyclic resistant ratio (CRR) i.e.  $\tau_{liq}/\sigma'_o$  at the above point. A relationship with  $\tau_{liq}/\sigma'_o$  and corrected  $(N1)_{60}$  for earthquake magnitude 7.5 is in Figure 5.4.

The standard penetration test values NM are converted to  $(N1)_{60}$  by correcting for energy and other factors as below (equation 5.4).

$$(N1)_{60} = NM \cdot CN \cdot CE \cdot CB \cdot CR \cdot CS \quad (5.4)$$

where,

NM = Observed SPT value

CN = factor to correct NM for overburden pressure

CE = Correction for hammer energy ratio

CB = Correction for borehole diameter

CR = Correction for rod length

CS = Correction for samplers with or without liners

3. The factor of safety (FOS) against liquefaction is computed as:

$$FOS = \tau_{liq}/\tau_{av} \quad (5.5a)$$

or

$$FOS = CRR/CSR \quad (5.5b)$$

In this manner,  $\tau_{av}$  (or CSR) and  $\tau_{liq}$  (CRR) are computed along the depth of a profile at several points and the factors of safety of a deposit are evaluated.

#### Modifications to $\tau_{av}$ in the SHAKE Program

1. The SHAKE program is used to analyze the wave propagation from base rock up to surface layer.
2. The output of SHAKE program includes peak acceleration of each soil layer.
3. This peak acceleration ( $a_{max}$ ) is used to compute  $\tau_{av}$ . This may give slightly different value of  $\tau_{av}$  as compared to their result using equation 5.1.

The Seed and Idriss simplified method (1971), as modified by Youd and Idriss (1997) was used in the liquefaction potential analysis of this project.

## 5.5 Slope Stability of Abutment Fills

Seven cross-sections from the St. Francis River Site were selected for slope stability analysis (Figure 5.5), as were seven from the Wahite Ditch Site (Figure 5.6). At both sites, the cross-sections represented the steepest site slopes. The cross-sections were developed from the topographic maps created by Missouri Department of Transportation and from the subsurface information obtained by drilling and cone penetrometer soundings. The cross-section data was then entered into the slope stability program *PCSTABLS* using the pre and post processor *STEDwin*. The slopes were analyzed under static and pseudostatic conditions using the Modified Bishop Method.

### 5.5.1 Soil Property Estimation

The soil properties needed for *PCSTABLS* analysis were estimated using a conservative approach. Wet unit weight, saturated unit weight, cohesion and internal angle of friction were estimated by correlation with SPT values, Cone Penetration Tests (CPT), Missouri Department of Transportation and University of Missouri-Rolla laboratory tests, and several technical references. Specifically, values were estimated as follows:

- The  $(N_1)_{60}$ , CPT, and laboratory data values were matched at various depths and compared for consistency.
- The density condition of the soil was based on correlations with  $(N_1)_{60}$  and CPT (McCarthy, 1998; Meigh, 1987). The relative density ( $D_r$ ) was based on correlations with  $(N_1)_{60}$  and CPT (Hunt, 1984; Meigh, 1987).
- The dry unit weight of granular soils was determined from relative density (McCarthy, 1998). Dry unit weight could not be measured directly in the field or laboratory for granular soils.
- The void ratio of granular soils was calculated from the minimum and maximum dry unit weight of silty sand (Lambe and Whitman, 1969).
- For clays the equation below was used to determine the void ratio:

$$e = \frac{\gamma_{water}}{\gamma_{dry}} - 1 \quad (5.6)$$

The Missouri Department of Transportation assumed  $G_s$  of 2.67, and the dry unit weight of the clay was obtained from Missouri Department of Transportation laboratory tests.

- The wet and saturated unit weight of the soil was determined by using equation 5.7:

$$\gamma = \frac{(G_s + S(e))\gamma_{water}}{(1 + e)} \quad (5.7)$$

The degree of saturation was set equal to 50% ( $S = 0.5$ ) for the wet unit weight of soil and equal to 100% ( $S=1$ ) for the saturated unit weight of soil.

- Internal angle of friction for clays was found from cone resistance and friction ratio (Meigh, 1987).

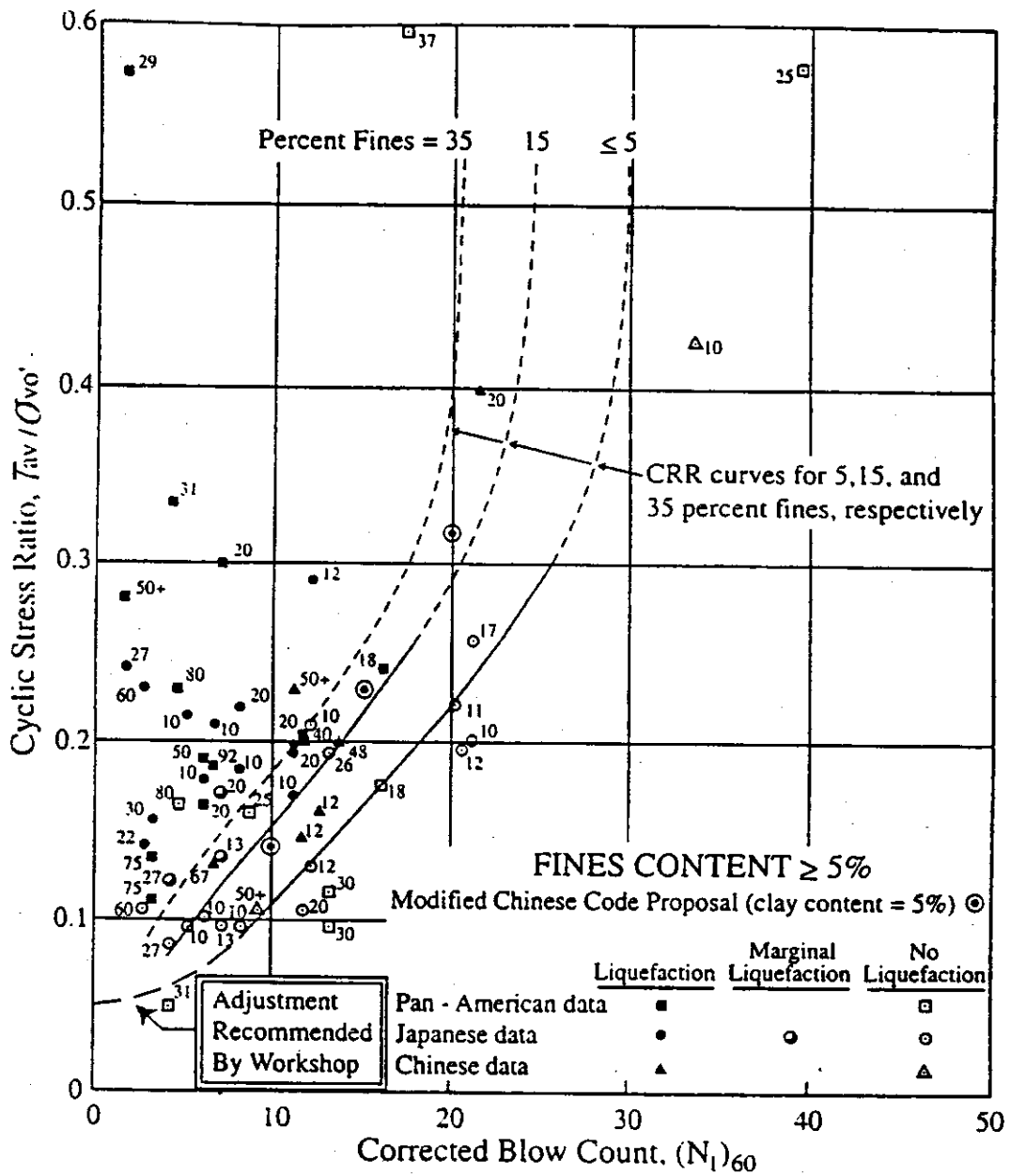
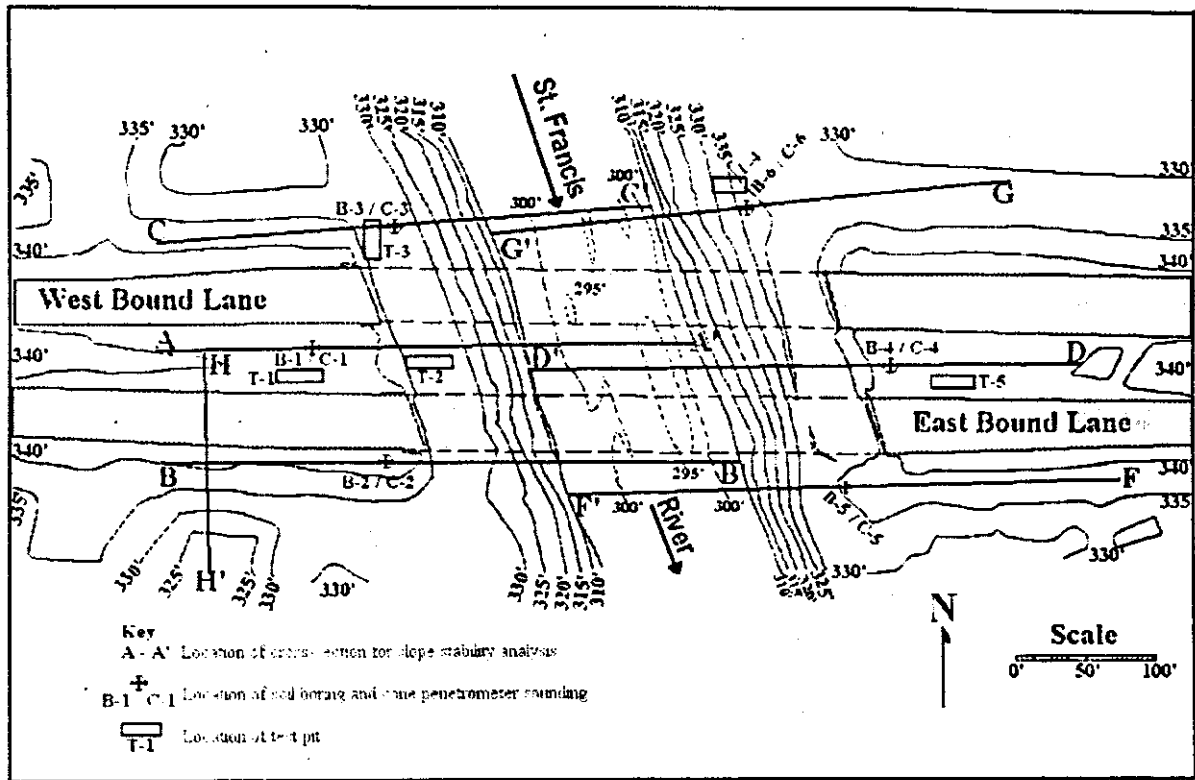


Figure 5.4 Simplified Base Curve Recommended for Calculation of CRR From SPT  $(N_1)_{60}$  Data Along With Empirical Liquefaction Data for  $M=7.5$  (Seed et. al., 1971, modified by Youd and Idriss, 1997)



**Figure 5.5 St. Francis River Site Topography, Cross-Sections and Boring Locations**

- For cohesionless soils,  $(N_1)_{60}$  values were used to determine the internal angle of friction (McCarthy, 1998).
- Cohesion was determined from the torvane and laboratory tests conducted by the Missouri Department of Transportation.

The soil properties obtained through this procedure were then averaged for each stratigraphic unit at the St. Francis River Site and the Wahite Ditch Site

### 5.5.2 Groundwater Elevation Selection

Two groundwater elevations were selected for the stability analysis at each slope: a low water condition and a high water condition. The low water condition was based on the water elevations measured by Missouri Department of Transportation and University of Missouri-Rolla in September and October of 1999. These elevations were anticipated to be lowest reasonable levels due to the lack of rain for the preceding 6-8 weeks. The high water condition was estimated from the height of the water staining on the bridge piers and was expected to be the highest reasonable groundwater elevation, representing levels during a prolonged wet season and flooding event. The two groundwater elevations were then used to conduct the static and dynamic slope stability analysis at the study sites.

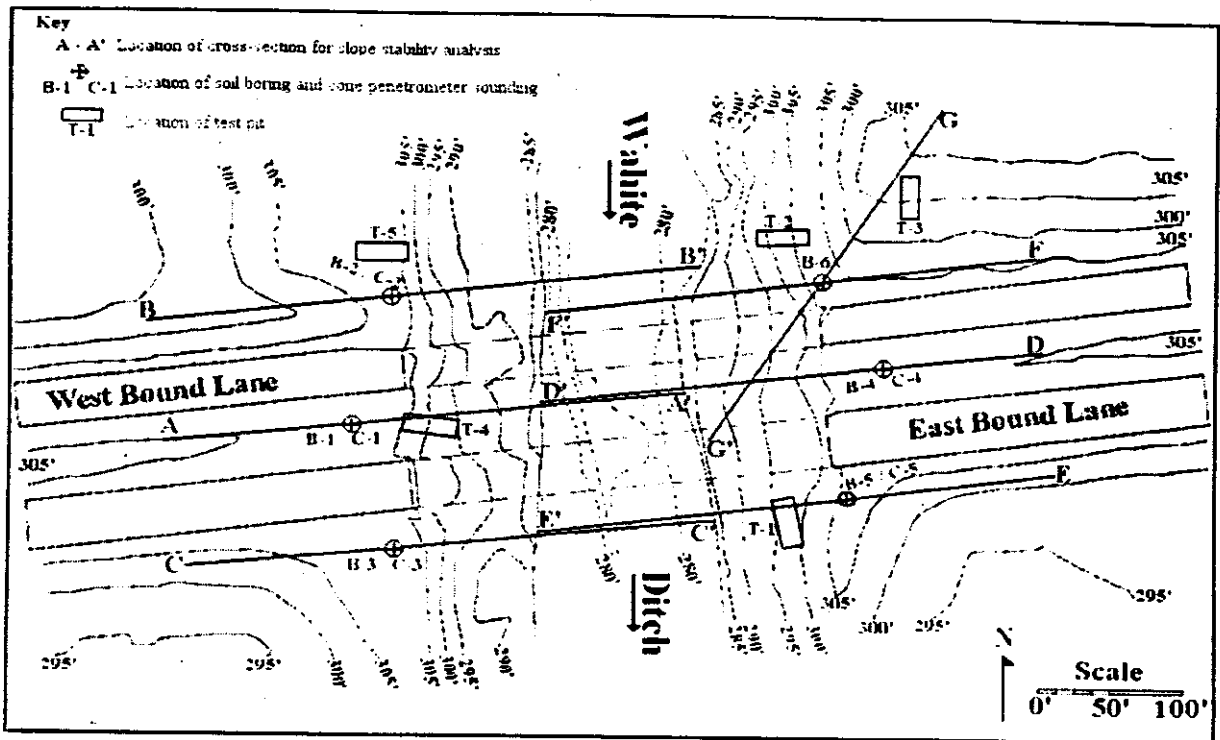


Figure 5.6 Wahite Ditch Site Topography, Cross-Sections and Boring Locations

### 5.5.3 Design Horizontal and Vertical Earthquake Accelerations

Three sets of ground accelerations were selected for the St. Francis River Site and the Wahite Ditch Site based on the *SHAKE91* analysis. The acceleration sets covered the following conditions:

1. Adjusted Peak Horizontal Ground Acceleration (PHGA). PHGA was selected for each bridge site as the maximum horizontal acceleration from the ten synthetic time records. PHGA was adjusted to a level of 66% of the original value. While Kramer (1996) and other researchers recommend using lower values (on the order of 50%), it is prudent to conduct a slightly more conservative analysis, since the effects of transient pore-water pressures are not accounted for in the analysis, and the strength and density values used in the analysis were obtained, in part, from published correlations.
2. Adjusted PHGA with corresponding Adjusted Peak Vertical Ground Acceleration (PVGA). For this set of analyses, the Adjusted PHGA values from set 1 were used along with the corresponding PVGA occurring at the same time as the PHGA in the synthetic time records. The PVGA values were adjusted using the modification factors described in Section 8.1.3.3 and 8.2.3.3 ( $C = 66\% * PHGA/PVGA$ ), and then adjusted to 66% of the modified value. Both positive and negative vertical ground accelerations were analyzed.

- Adjusted PVGA with corresponding Adjusted PHGA. For this set of analyses, the PVGA was selected as the maximum vertical acceleration from the same time record as set 1, used with the corresponding PHGA occurring at the same time. The values were adjusted as described for set 2.

Each set above used acceleration values for earthquakes with 2% and 10% exceedance probabilities in 50 years. The selected design horizontal accelerations were used in *PCSTABL5* to represent pseudo-static earthquake conditions, for both low and high ground water. The adjusted accelerations are summarized below in Table 5.3.

### 5.6 Flood Hazard Analysis

Flood hazards were estimated assuming that an earthquake caused catastrophic failure of waterway levees in the vicinity of US 60 or failure of the Wappapello Dam, located approximately eight miles north of US 60.

Eleven 7.5-minute topographic maps were collected to map the areas that would be affected by flooding if local levees failed during an earthquake. The flooding analysis consisted of the following procedures:

- River, creek, and drainage ditch locations, approximate elevations of water levels, and approximate elevations of both natural and man-made levees flanking the waterways were identified.
- Zones on the topographic maps were subdivided along the roadway by 5-foot contour intervals.
- Areas where the land was below water levels in waterways were marked as zones of potential flooding. Each area was field checked to visually assess the elevation of the roadway compared to surrounding land.

An evaluation of the effects of catastrophic failure of the Wappapello Dam was completed by U.S. Army Corps of Engineers (1985). Flood maps presented in the U.S. Army Corps of Engineers report are summarized in Section 8.1.6

**Table 5.3 Design Horizontal and Vertical Earthquake Accelerations**

**a. St. Francis River Site**

	Set 1		Set 2		Set 3	
Earthquake	HGA	VGA	HGA	VGA	HGA	VGA
10% PE	0.135	0	0.135	±0.048	0.012	±0.090
2% PE	0.331	0	0.331	±0.170	0.014	±0.221

**b. Wahite Ditch Site**

	Set 1		Set 2		Set 3	
Earthquake	HGA	VGA	HGA	VGA	HGA	VGA
10% PE	0.123	0	0.123	±0.006	0.008	±0.082
2% PE	0.350	0	0.350	±0.007	0.060	±0.233

## **6.0 PROCEDURES FOR SEISMIC CONDITION ASSESSMENT OF BRIDGES AND ABUTMENTS**

This section describes the complete procedure used to assess the condition of highway bridges based on the site-specific seismicity. The work delineated in this study includes the setup of computer models of the study bridges assuming rigid abutments and foundations, seismic analysis of the bridges under site specific ground motions, preliminary evaluation of various structural components, and comparison between the AASHTO spectrum and site-specific ground motions.

A set of performance goals, relating to the responses of the bridge to earthquakes of specified hazard level, are established for condition assessment. The performance goals are achieved through computer modeling and analyses using engineering criteria concerning the evaluation procedures of structural components. These criteria include the specification of acceptable levels of damage that meet the global performance goals as defined by AASHTO.

### **6.1 Global Performance Goals**

Global performance goals are generally defined to set the criteria for acceptable performance during an earthquake event. These goals are described below.

#### **6.1.1 American Association Of State Highway and Transportation Officials Specifications**

The performance goals in the current AASHTO Specifications Division I-A, Seismic Design, are as follows:

- Small to moderate earthquake should be resisted within the elastic range of the structural elements without significant damage.
- Severe earthquakes should not cause collapse of all or part of a bridge. Damage that does occur should be readily detectable and accessible for inspection and repair.

Based on the AASHTO Specifications, bridges are designed only for one level of seismic hazard representing a severe event (the 500-year return period event). For that hazard level, damage must be limited, but not necessarily eliminated. The implication of this methodology is that the structure will sustain minimal or no damage for small to moderate earthquakes if the design is performed for a severe earthquake.

#### **6.1.2 Bridges Along US 60**

Many studies have shown that the seismic hazard in the Midwest increases considerably for an earthquake with a return period of 2,500 years instead of 500 years as specified by AASHTO. Bridges along the designated emergency vehicles access routes are needed the most to allow rescue teams and necessary rescue equipment to pass through for saving the lives in the stricken areas in case of a devastating earthquake event.

In principle, it is possible to eliminate any damage occurring from earthquakes, if bridges are upgraded for the maximum credible earthquake. However, the unreasonably high costs of such a

retrofit as well as budgetary constraints often dictate a more realistic approach that would significantly reduce cost, but as a tradeoff would permit some damage under certain conditions.

The recommended performance goals of a bridge that could satisfy the above requirements are:

1. For the low hazard level (10% probability of exceedance in 50 years or approximately 500-year return period), the bridge shall be capable to carry normal traffic almost immediately after the earthquake. Damage shall be minimal and mostly limited to secondary structural elements.
2. For the high hazard level (2% probability of exceedance in 50 years or approximately 2500-year return period), the bridge shall be able to carry limited traffic within days (reduced lanes, light emergency traffic). The goal is to avoid collapse.
3. It is clear that the above-stated goals involve policy issues concerning the desirable level of service after an earthquake as well as the financial expenditures necessary to achieve this service. These issues are of socioeconomic nature and need to be addressed by the Missouri Department of Transportation as a matter of public policy. The present condition assessment provides the background information in terms of vulnerability of the bridge in terms of the expected level of service.

## **6.2 Engineering Performance Criteria**

Earthquakes in the Midwest are characterized as infrequent but high consequence events. Once it occurs, an earthquake often induces larger forces in structural members (especially vertical structural components) than other dead and live loads. Economic considerations dictate that structural components resist earthquake loads using the available capacity in the inelastic range of their response. Thus ductility, or the ability of structural members to deform inelastically without loss of strength, is an important consideration in the response of structural components to seismic loads.

The established engineering performance criteria address a range of issues including the procedures for performance assessment, seismic demand and capacity, and acceptable damage. They are based on the AASHTO Specifications and the FHWA Seismic Retrofitting Manual for Highway Bridges (1995).

### **6.2.1 Performance Assessment**

The seismic performance of the bridge is determined on the basis of the performance of its components. For all critical structural components, a capacity over demand (C/D) ratio is determined for each potential mode of failure. The lowest C/D ratio value of each component indicates the controlling mode of failure. A C/D ratio less than one implies a vulnerable component. Potential damage of groups of components is also considered to reflect the performance of overall structural systems.

The C/D ratio is defined as:

$$C/D = \frac{R_c - \sum Q_i}{Q_{EQ}} \quad (6.1)$$

where  $R_c$  is the ultimate force or deformation capacity of the component for the mode of failure under consideration.  $\sum Q_i$  is the sum of the force or deformation demands for loads other than earthquake loads (dead loads, live loads, etc.).  $Q_{EQ}$  is the earthquake force or deformation demand.

When components such as columns and pile caps resist failure in a ductile mode, the C/D ratios are multiplied by ductility indicators ( $\mu > 1$ ) to enable the use of the elastic analysis results. For non-ductile modes of failure (buckling of bracing members and shear of beams, etc.), the ductility indicators are taken equal to one. For bridge bents with multiple columns, a ductility indicator of 5.0 is used. The ductility indicators of other members can be found in the FHWA Manual (1995).

### 6.2.2 Seismic Demand

Structural analysis was performed using the computer program *SAP2000*. The method of analysis of the bridge is the time-history analysis procedure and response spectrum analysis with uniform support excitations. The soil-structure interaction was taken into account by including several springs, representing soil flexibility. Nonlinear soil properties were accounted for by selecting strain compatible constants of the springs.

The computation of seismic demand was based on three-dimensional computer models of the bridge. These models were developed to the extent that the essential characteristics of the structure were adequately represented and the response of the bridge sufficiently predicted. They describe the as-built condition of the bridge.

The seismic forces to be resisted by the pile caps were determined based on the smaller forces due to the column over-strength capacity and the elastic analysis results. For the purpose of determining the over-strength capacity of columns, the nominal strength of reinforced concrete was increased by a factor of 1.30.

The seismic demands were calculated at two hazard levels for the site specific evaluation. They were also determined under the AASHTO design spectrum for comparison with the site-specific assessment. The well-known Complete Quadratic Combination (CQC) combination rule was applied to combine the effect of all vibration modes. The effect of different earthquake components were combined using the "30 percent rule" specified in AASHTO Specifications for peak responses.

### 6.2.3 Seismic Capacity

The current FHWA Seismic Retrofit Manual for Highway Bridges Guidelines (1995) are used to determine the capacity of concrete structure components.

### 6.2.4 Acceptable Damage

Examples of acceptable damage at low hazard levels for the AASHTO earthquake include:

- Damage to non-structural components.
- Limited cracking and spalling of the concrete columns.
- Some yielding of columns.
- Sign of yielding of member connections.
- Some damage to expansion joints.

Examples of acceptable damage at high hazard levels include:

- Serious damage to non-structural components.
- Cracking and spalling of the concrete columns.
- Yielding of columns.
- Yielding of member connections.
- Damage to bracings.

## 6.3 Analysis Procedures

This study focused on the condition assessment of both the superstructure (deck, girder, bearing, etc.) and the substructure (abutment, cap beam, column, and pile cap) for the selected bridges.

### 6.3.1 Computer Modeling of Bridges

One computer model was prepared for the analysis of each bridge. The concrete deck is simulated using shell elements while the remaining structural components are modeled as frame elements. To match the elevation of the actual bridge (deck and bearing), rigid dummy elements were introduced. Soil flexibility was represented by a set of springs at the centroid of pile caps at both interior bents and abutments. More detailed information on the computer model is discussed in Section 8.1.7.

#### 6.3.1.1 Design Ground Motions

The bedrock motions for the analysis of the bridge were obtained from the procedures described in Section 5.3. They were used to determine the time-history response at the centroid of the pile caps based on one-dimensional seismic wave propagation from the *SHAKE* program as discussed in Section 5.4. The ground motion at one pile cap is considered as input for the entire bridge model.

### 6.3.1.2 Analysis Procedure

After the computer model was checked for connectivity, the seismic demand of structural members was computed based on the following procedure:

- Step 1. The stiffness constants of springs at the pile caps of interior bents and abutments were estimated.
- Step 2. The bridge model was analyzed under a longitudinal, transverse, vertical earthquake excitation, respectively.
- Step 3. The effects of longitudinal, transverse and vertical earthquake excitations were combined.
- Step 4. The compatibility between the load and displacement of the springs at all pile caps were checked. If they were not compatible, the stiffness constants were revised and Steps 1-3 were repeated until compatibility was satisfied.

### 6.3.2 Computer Modeling of Abutments

The abutments of all four bridges are supported on piles. However, only the abutments of the Old St. Francis River Bridge and the Old Wahite Ditch Bridge support the deck in simple support. The decks and the abutments of the two new bridges are constructed integrally with the bridge deck.

Figure 6.1 depicts a typical non-integral bridge abutment supported on piles. Choudhry (1999) and Wu (1999) have proposed methods to calculate displacements of bridge abutment and retaining wall due to earthquake. The bridge abutment in their model was considered as a two degree of freedom model (Figure 6.2). Based on this model, displacements of bridge abutment may occur in translation and rotation. A modification is used in this analysis to predict response of a bridge abutment supported on piles. The stiffness and damping factors due to pile-soil interaction are calculated by Novak's (1974) model (Appendix F).

Figure 6.3 shows the forces acting on the bridge abutment. These forces consists of:

1. The vertical seismic force increment ( $V_1$ ) is

$$V_1 = k_v W \quad (6.2a)$$

where:

- $k_v$  = vertical seismic coefficient
- $W$  = weight of the abutment.

The vertical force may act in the positive (+) or negative (-) direction. The case that gives maximum displacement was adopted.

The point of application of  $V_1$  is the center of gravity of the abutment and the horizontal distance from this point to the heel of the abutment is expressed as  $x_1$  Figure 6.3.

The horizontal force ( $H_1$ ) due to weight ( $W$ ) of the abutment is computed as:

$$H_1 = k_h W \quad (6.2b)$$

where:

$k_h$  = horizontal seismic coefficient

The height of the line of action of  $H_1$  is at the centroid of the abutment,  $z_1$  from the bottom.

2. The vertical seismic force increment,  $V_2$ , applied to the abutment is

$$V_2 = k_v Q \quad (6.3a)$$

where:

$Q$  = Weight of the girder and traffic load acting on the bearing

The vertical force may act in the positive (+) or negative (-) direction. The case that gives the maximum displacement was adopted. The point of application of  $V_2$  is the center of the bearing and the horizontal distance from this point to the heel of the abutment is expressed as  $x_2$ .

The horizontal seismic force  $H_2$  of the girder is:

$$H_2 = k_h Q \quad (6.3b)$$

The height of the line of action of  $H_2$  is assumed to be coincident with the upper surface of the bearing and at a distance  $z_2$  from the bottom of the abutment.

3. The seismic force due to the weight of earth ( $W_s$ ) ABCE (Figure 6.3) is given below with the point of application at the centroid ( $x_3, z_3$ ) of the earth mass:

$$V_3 = k_v W_s \quad (6.4a)$$

$$H_3 = k_h W_s \quad (6.4b)$$

The earth pressure acting on the abutment is the sum of the earth pressure acting on the vertical line DE and the weight of soil mass ABCE and the seismic force. The earth pressure increment acting on the vertical line DE is calculated by the Mononobe-Okabe method. Its point of application is at 1/2 of the height of the line ED and the direction is inclined  $\delta$  (Section 6.3) to normal on ED.

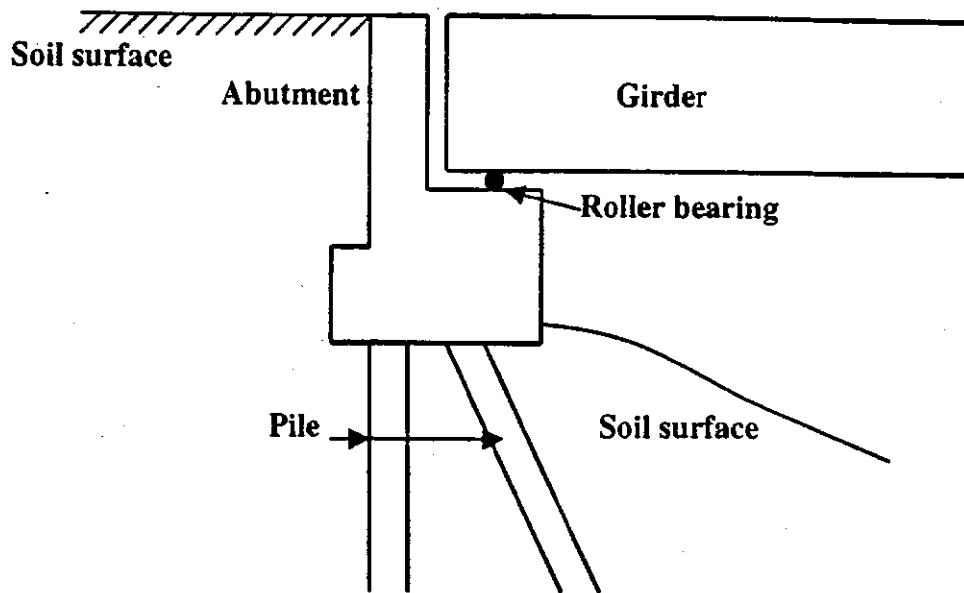


**Figure 6.1** Typical Non-Integral Bridge Abutment Supported on Piles

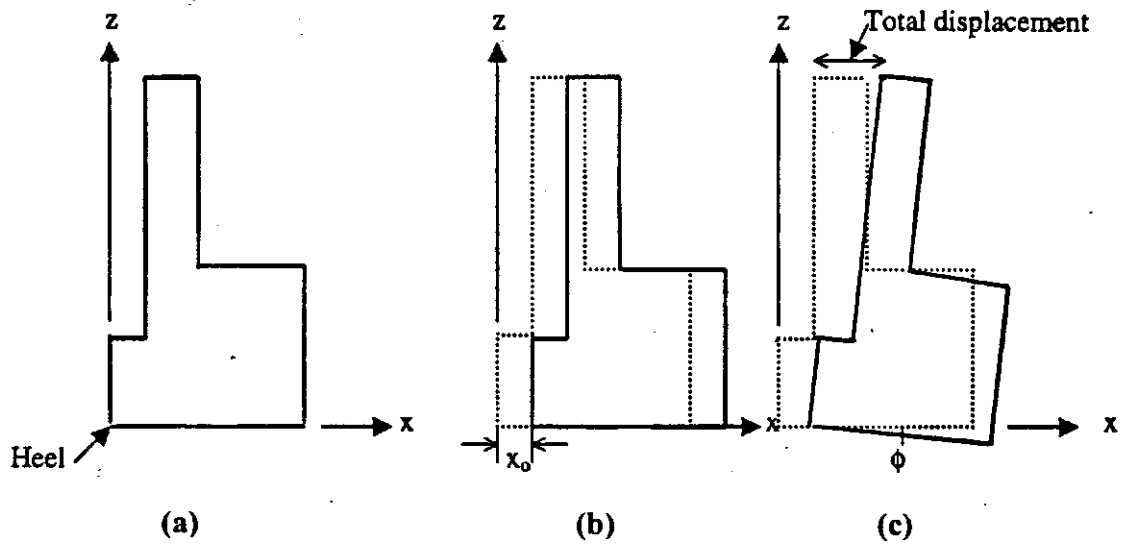


**Figure 6.2** Translation and Rotation Movement of Bridge Abutment Forces Acting on the Non-Integral Bridge Abutment

- a) Initial Condition
- b) Sliding
- c) Sliding and Rotation

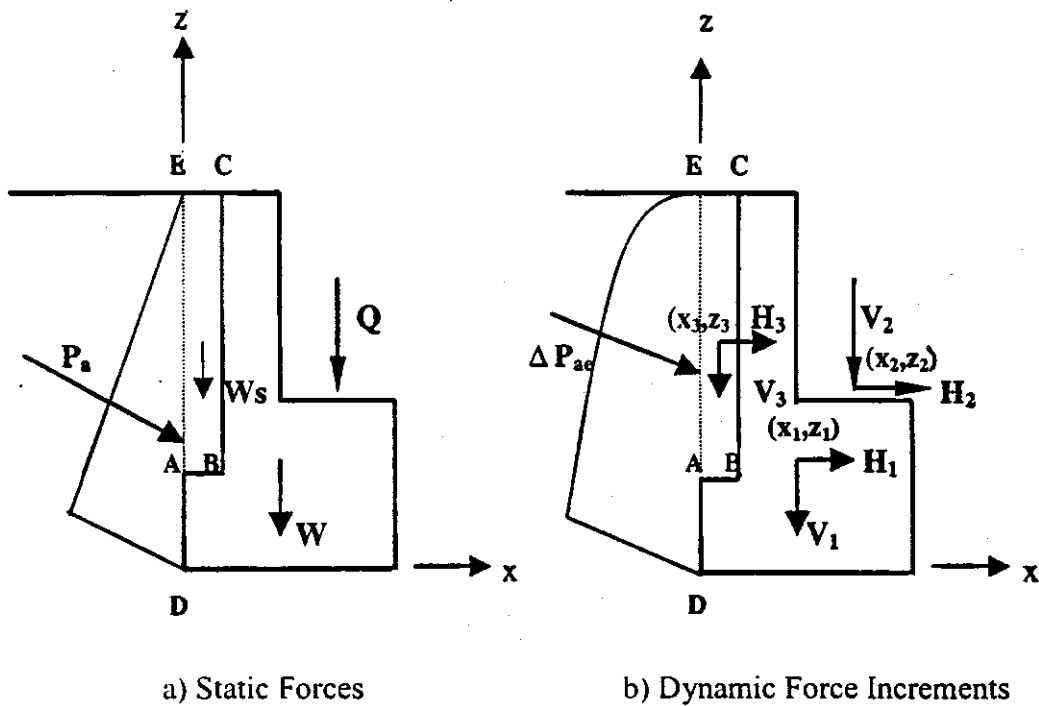


**Figure 6.3** Forces Acting on the Non-Integral Bridge Abutment

The horizontal force ( $P_x$ ) and moment ( $M_\phi$ ) about the heel (D) due to seismic force are:

$$P_x = H_1 + H_2 + H_3 + \Delta P_{ac} \cos(\delta) \quad (6.5a)$$

$$M_\phi = V_1 \cdot x_1 + V_2 \cdot x_2 + V_3 \cdot x_3 + \Delta P_{ac} \cos(\delta) \cdot \frac{1}{2}H + H_1 \cdot z_1 + H_2 \cdot z_2 + H_3 \cdot z_3 \quad (6.5b)$$

The seismic displacement analysis procedure is presented as follow;

1. The bridge abutment supported on piles is shown (Figure 6.1).
2. Two degree of freedom of motion is used to obtain displacement of bridge abutment.
3. Point of rotation was assumed at the heel of bridge abutment (Figure 6.2, Wu, 1999).
4. Seismic response of bridge abutment was calculated based on the time history of acceleration acting on the base of bridge abutment.
5. The pile and soil interaction provided stiffness and damping, and the abutment provides the mass.
6. Stiffness and damping constants of soil-pile interaction were calculated using recommendation of Novak's (1974) and Novak and El-Sharnouby (1983) (Appendix H).
7. The seismic forces are presented based in Figure 6.3.
8. Non-linear soil properties were used to calculate strain-dependent stiffness and damping factors (Appendix B).
9. Displacements were calculated by solving the seismic force equilibrium for the active state condition. This means that the permanent displacement occurred if the acceleration acts towards the fill and the wall moves away from the fill.

10. Total displacements at the top of bridge abutment were calculated by adding the sliding and overturning displacement.

The solution technique to obtain the abutment displacement is presented in Appendix F.

## **7.0 REGIONAL GEOLOGY AND GEOTECHNICAL DATA**

This section describes the regional geology of the study sites and summarizes the pertinent geotechnical data.

### **7.1 Regional Geology**

The regional geology of the US 60 roadway between Poplar Bluff and Sikeston, Missouri is characterized by alluvial sands and gravels deposited by the ancestral Mississippi River, underlain by a dipping sedimentary sequence of limestones, dolomites, shales, and sandstones.

The study section of US 60 is located along the western margin of the Mississippi Embayment, as shown in Figure 7.1. This portion of the Embayment is bounded on the west by the Ozark Escarpment in Poplar Bluff, which consists of Paleozoic Dolomite and Sandstone overlain by thin residual soils. The Embayment extends in other directions beyond the study section. Shallow materials below the study section may be characterized as Wisconsin Braided Stream Terraces, from previous channels of the post-glacial Mississippi River. The terraces are broken into two groups, separated at Dexter by Crowley's Ridge (composed of Wilcox Group sand). The first groups of terrace deposits are older early Wisconsin terraces, located to the west of Crowley's Ridge, spanning from Poplar Bluff to Dexter. The second groups of terraces are younger late Wisconsin terraces, located to the east and extending from Dexter to Sikeston. The relationship of these terraces to Crowley's Ridge may be seen in the cross-section in Figure 7.2.

The early Wisconsin terraces to the west range in thickness up to 200 feet, based on maps by Saucier (1994), and consist of sand with some gravel (Grohskopf, 1955). Near Poplar Bluff, Ozark Escarpment Alluvial Fan deposits overlie the terraces. The terraces also contain the incised channels of the modern Black and St. Francis Rivers (near Poplar Bluff and Fisk, respectively) and an abandoned channel of the St. Francis River (approximately six miles east of Poplar Bluff). A more significant abandoned channel of an unnamed creek just west of Dexter has deposited undifferentiated Holocene Alluvium along approximately three miles of US 60. The slightly elevated Dudley Ridge represents a separate valley train deposit within the early Wisconsin sequence.

The late Wisconsin terraces to the east range in thickness up to 150 feet, an estimate also based Saucier (1994) maps, and are similar in composition to the early Wisconsin terraces.

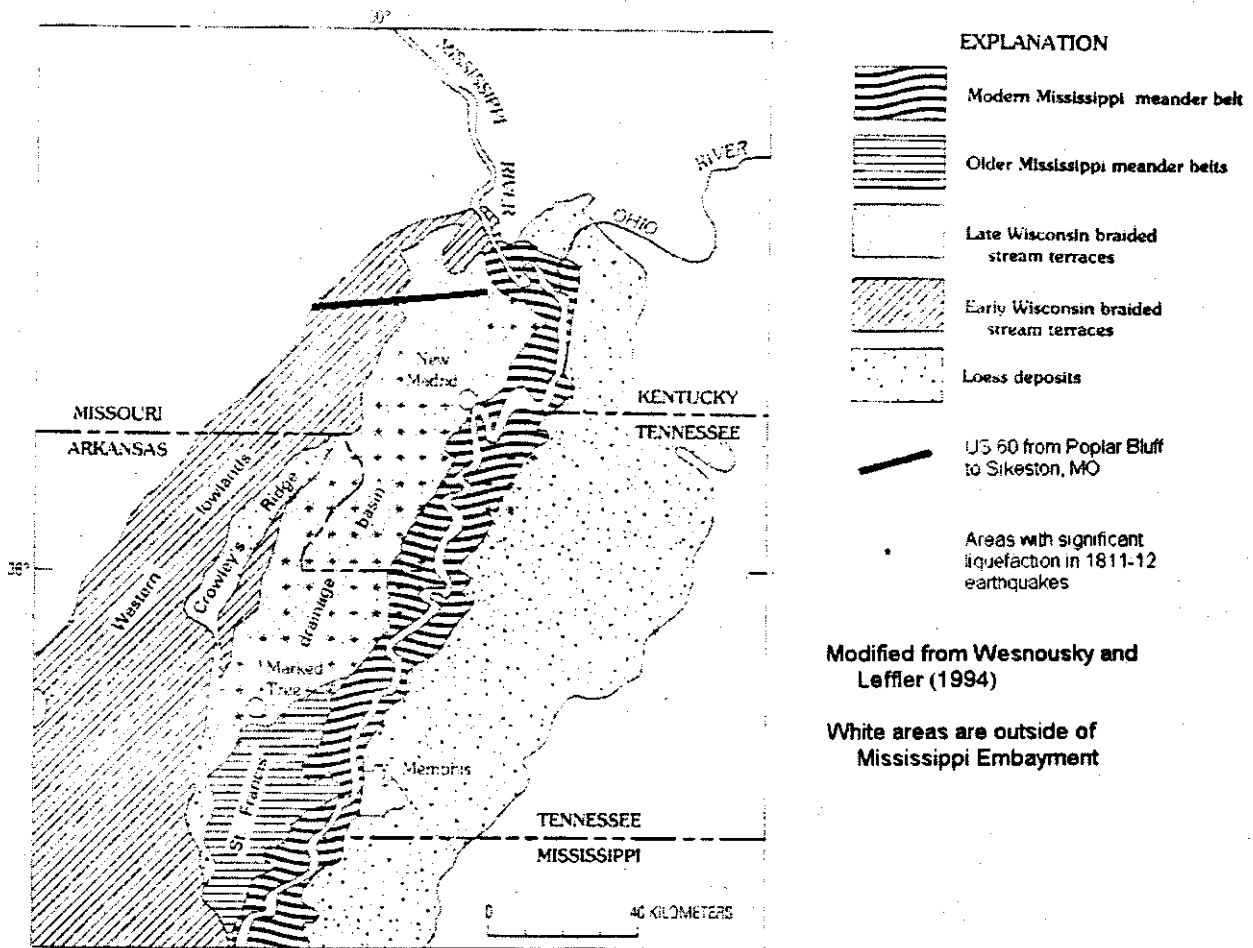


**Figure 7.1** Extent of Mississippi Embayment

Sikeston Ridge is composed of early Wisconsin materials and is the remnant of a stream terrace deposited before the Mississippi occupied the Dexter-to-Sikeston floodplain. East of the Sikeston Ridge, late Wisconsin materials are overlain by sand and aeolian deposits (Saucier, 1994).

Crowley's Ridge is 40-mile long linear feature, trending northeast, which near Dexter is a cuesta of resistant Wilcox and Midway Group materials. The ridge is capped by residual soils and loess.

Bedrock beneath the US 60 alignment dips to the east, and the bedrock sequence from Poplar Bluff to Sikeston progresses from Paleozoic (Powell, Cotter / Jefferson City, Roubidoux and Gasconade Formations), to Cretaceous (McNairy and Owl Creek Formations), to Paleocene (Midway Group) and Eocene (Wilcox Group).

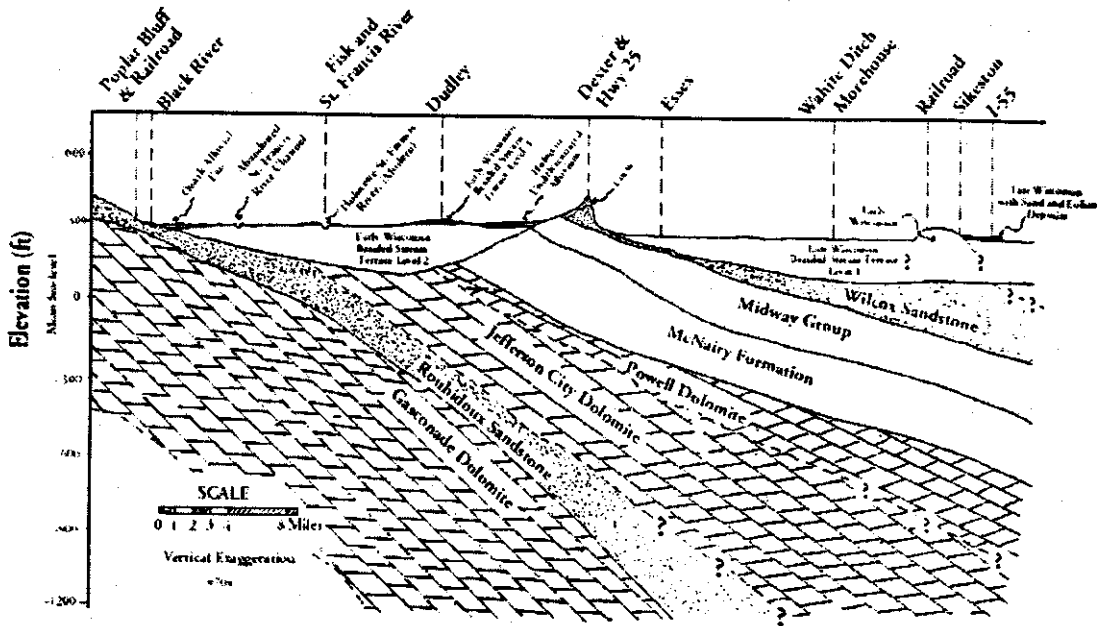


Figure 7.2 Cross-Section of Regional Geology

7.2 Summary of Field and Laboratory Data

The first task of the field investigation involved discussions with local Missouri Department of Transportation personnel regarding general road conditions. Mr. Lonnie Blasingame, the Missouri Department of Transportation Regional Superintendent for this portion of US 60, provided information regarding roadwork related to earthquake, slope stability, or flooding issues. In his experience in the area, which spans the last 14 years, no major roadwork has been required for slope stability, flooding, or seismicity-related damage. In general, work along the roadway has been to fill small potholes, and to cut expansion joints because the summer heat permanently expands the concrete, creating a potential for buckling of the pavement.

The majority of the field investigation involved drilling of exploratory boreholes, advancing CPT soundings, and digging shallow test pits. Boring and test pit logs are attached in Appendix A. The general stratigraphy shown by these logs was summarized in Section 7.2 above.

CPT data summaries are also attached in Appendix A. The stratigraphy indicated by the CPT soundings was used to confirm and enhance the cross-sections developed for slope stability analysis and to provide soil density and gradation information for liquefaction analysis.

## 8.0 RESULTS OF SITE-SPECIFIC STUDIES

The results of the specific studies at each site are discussed separately below.

### 8.1 St. Francis River Site

#### 8.1.1 Site Geology

The topography at the St. Francis River Site is given in Figure 8.1. The following geologic units, listed from the ground surface downward, characterize local geology at the St. Francis River Bridge:

- Approximately 20 feet of low plasticity silty clay,
- Approximately 0-15 feet of clayey silt
- Approximately 5-10 feet of silty sand,
- Approximately 150 feet of coarse sand, containing numerous thin gravel lenses, and,
- Limestone bedrock, assumed to represent either the Lower Jefferson City or Upper Roubidoux Formations.

An example cross-section from the St. Francis River Site is shown on Figure 8.2. Figure 8.3 shows the soil profile from boring B-1 for the St. Francis River Site.

#### 8.1.2 Selected Base Rock Motion

Herrmann, (2000) recommends ten rock base motions for PE 10% in 50 years and the other ten for PE 2% in 50 years for each site. All of the 40 rock motions have been used for one-dimensional wave propagation analysis using the *SHAKE91* program. Based on wave propagation analysis, peak ground accelerations for each rock motion were obtained. A total of 12 ground motions were selected based on these peak ground acceleration values.

Table 8.1a lists 5-ground motion for PE 10% in 50 years with corresponding maximum peak ground accelerations for M6.2 with epicentral distance of 40 km and 5-more ground motions of M7.2 and epicentral-distance of 100 km. Table 8.1b shows listing of ground motion for PE 2 % in 50 years with different M's and epicentral-distance. In these tables columns 1-4 are basic data from Herrmann (2000).

Twelve synthetic ground motions at the rock base (6 for each PE) are selected as representative of the "worst case scenarios". They are given in Table 8.1. The associated acceleration-time histories are shown in Figures 8.4a-8.4d.

#### 8.1.3 Seismic Response of Soil

The *SHAKE* and *SHAKEDIT* programs were used to propagate the design earthquake base rock motions to the ground surface. This resulted in peak ground motions and time histories of acceleration at the soil surface, the base of bridge abutments and the piers

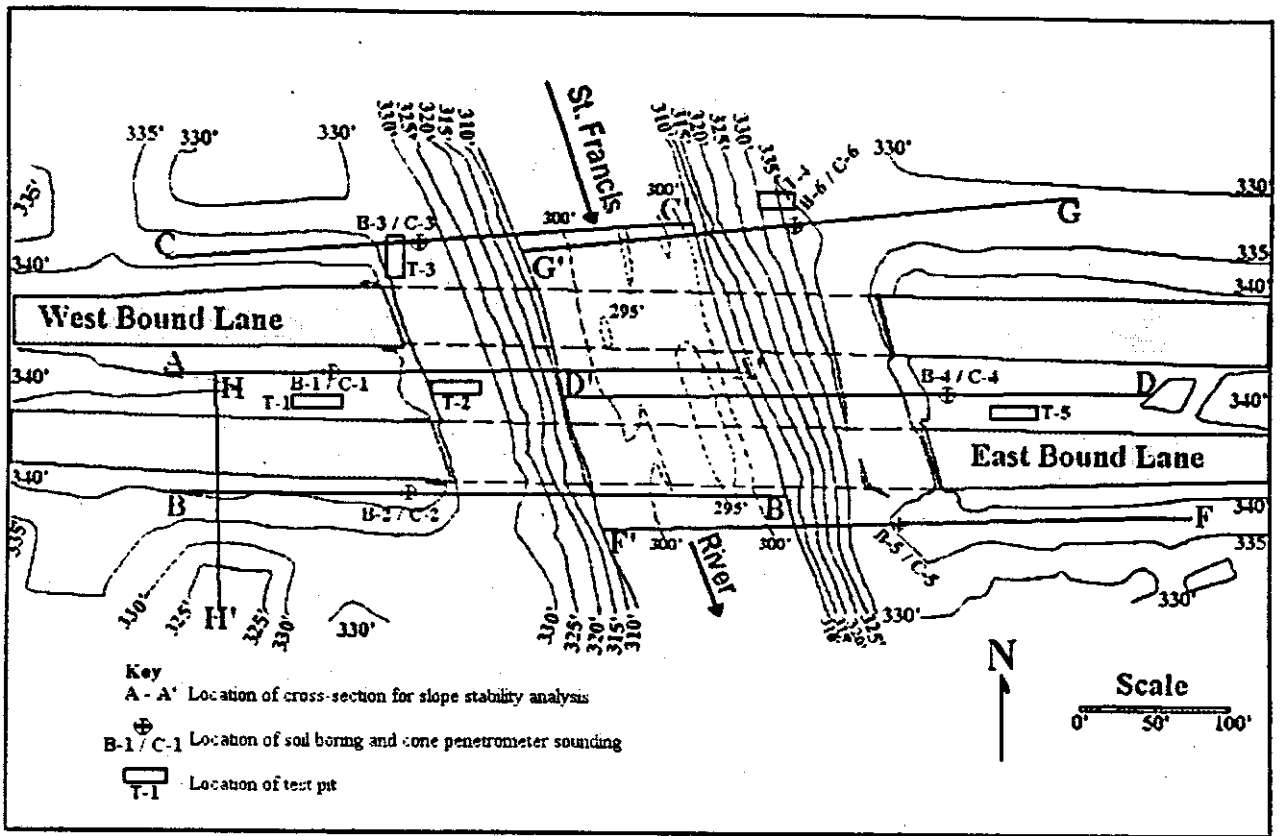
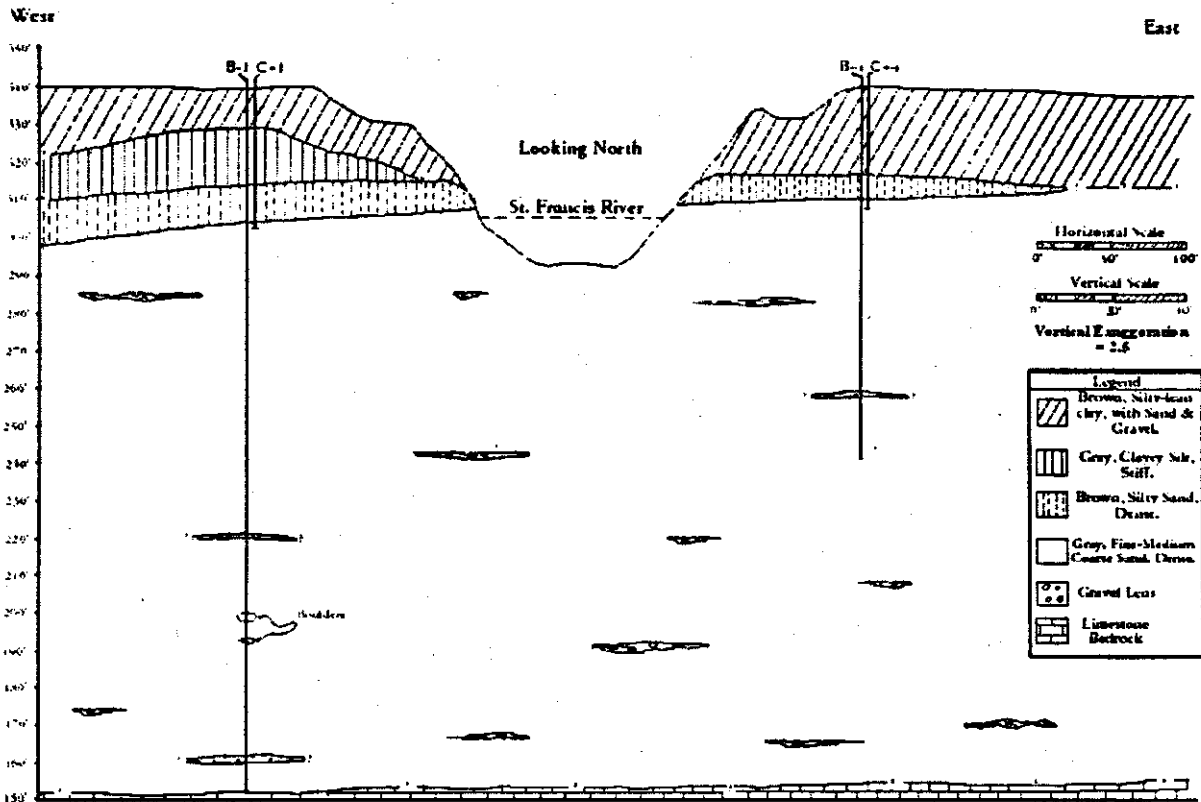


Figure 8.1 St. Francis River Site Topography, Cross-Section and Boring Locations

### 8.1.3.1 Horizontal Seismic Response of Soil

Figure 8.1 shows the location of the St. Francis River Site. A brief description of the soil profile including observed SPT ( $N_{obs}$ ) and corrected ( $N_1$ )<sub>60</sub> values, is shown in Figure 8.3 for borehole B1. The subsurface soil consists of up to 25 feet of medium to stiff clay underlain by about 30 ft of medium dense sand underlain by a dense to very dense sand to a depth of up to 192.0 ft. The soil profile from bore log B1, as shown in Figure 8.3 has been used in the seismic response analysis since B1 is located close to the bridge abutment and there is complete soil information up to rock base.

The initial shear modulus ( $G_0$ ) as well as shear wave velocity, which are needed in the wave propagation analysis, are calculated by direct measurement of shear wave velocity up to 35 feet and by correlation with the measured  $N_{spt}$  value and depths beyond 35 feet. This calculation is performed in the *SHAKEDIT* program itself. The non-linear soil properties such as modulus degradation with shear strain and material damping with shear strain, have been adopted for each soil type.



**Figure 8.2 Cross-Section of St. Francis River Site Geology**

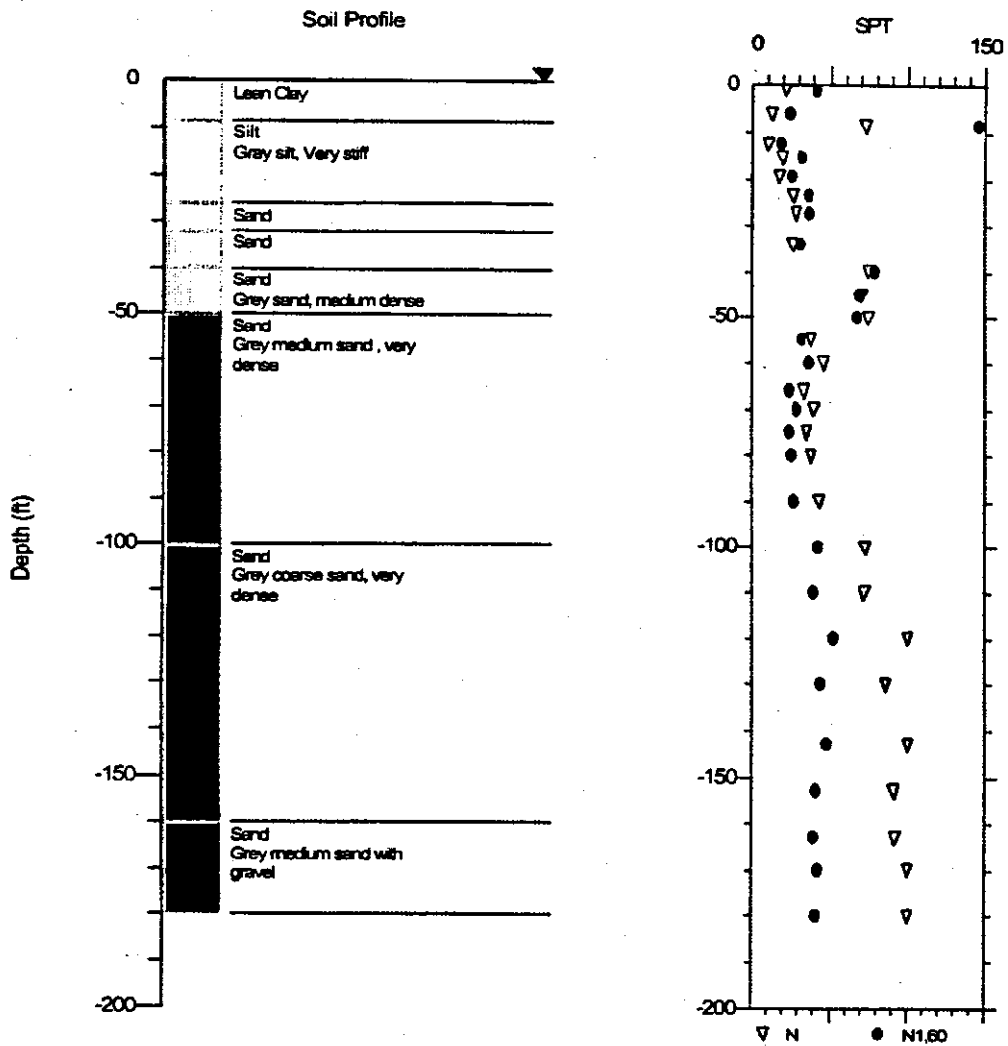
The calculated peak ground accelerations at each soil level from the wave propagation analysis were plotted against depth. Figures 8.5a and b show the peak acceleration for PE 10% in 50 years for M6.2 and M7.2 respectively. Figures 8.6a and b show the peak acceleration for PE 2% in 50 years for M6.4 and M8.0 respectively

For PE 10 % in 50 years and M6.2 and M7.2 respectively, the peak accelerations at the soil surface are higher than those at the base-rock. However, for PE 2 % in 50 years, the peak accelerations at the soil surface of this site are smaller than those at the base rock.

### 8.1.3.2 Resulting Ground Motion Time Histories

Table 8.2a shows the peak horizontal acceleration of design earthquake at the soil surface, bridge abutment and pier respectively for PE 10% in 50 years, Table 8.2b shows similar information for PE 2 % in 50 years.

Figures 8.7a and b contain 6-plots of surface ground acceleration for PE 10 % in 50 years and earthquake magnitude M6.2 and M7.2. Similarly, Figures 8.7c and d



Notes:

- CSR analysis using SHAKE results.
- CSR File: D:\I-O SF Pe10t\SF100103\SF100103.grf
- CRR using SPT Data and Seed et. al. Method in 1997 NCEER Workshop.
- Earthquake File for SHAKE Analysis: D:\SF\SF100103.ACC
- Earthquake Magnitude for CRR Analysis: 6.2
- Magnitude Scaling Factor (MSF): 1.42
- Depth to Water Table for CRR Analysis (ft): 0
- Depth to Water Table for Cn Calculation (ft): 0
- Depth to Base Layer for CSR Analysis (ft): 219.6
- MSF Option: I.W. Idriss (1997)
- Cn Option: Liao & Whitman (1984)
- Ksigma Option: L.F. Harder & R. Boulanger (1997)
- SPT Energy Ratio: USA/Safety/Rope: 0

Figure 8.3 Soil Profile St. Francis River Site Boring B-1

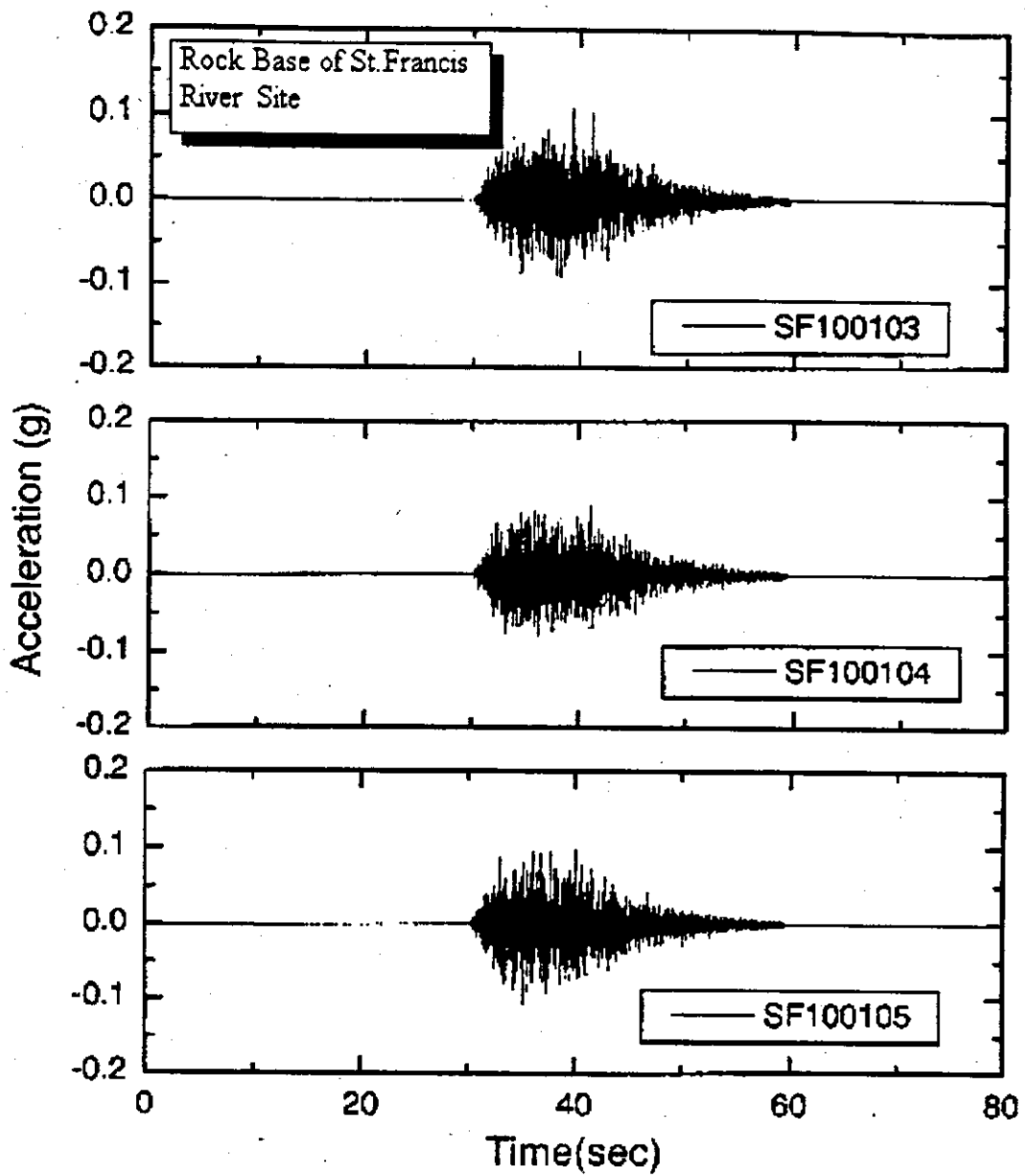
**Table 8.1 Detail of Synthetic Ground Motion at the Rock Base of St. Francis River Site with Corresponding Maximum Peak Horizontal Ground Acceleration**

**a. PE 10% in 50 Years**

<b>Name (1)</b>	<b>Mw (2)</b>	<b>R (km) (3)</b>	<b>Max acc. at rock-base(g) (4)</b>	<b>Max acc. at soil-surface(g) (5)</b>
SF100101	6.2	40	0.105	0.135
SF100102	6.2	40	0.095	0.128
SF100103*	6.2	40	0.106	0.146
SF100104*	6.2	40	0.100	0.146
SF100105*	6.2	40	0.107	0.151
SF100201*	7.2	100	0.113	0.203
SF100202*	7.2	100	0.136	0.196
SF100203	7.2	100	0.154	0.163
SF100204	7.2	100	0.117	0.173
SF100205*	7.2	100	0.153	0.187
Mw = Magnitude                      R = Epicentral distance				
* Used in further analysis				

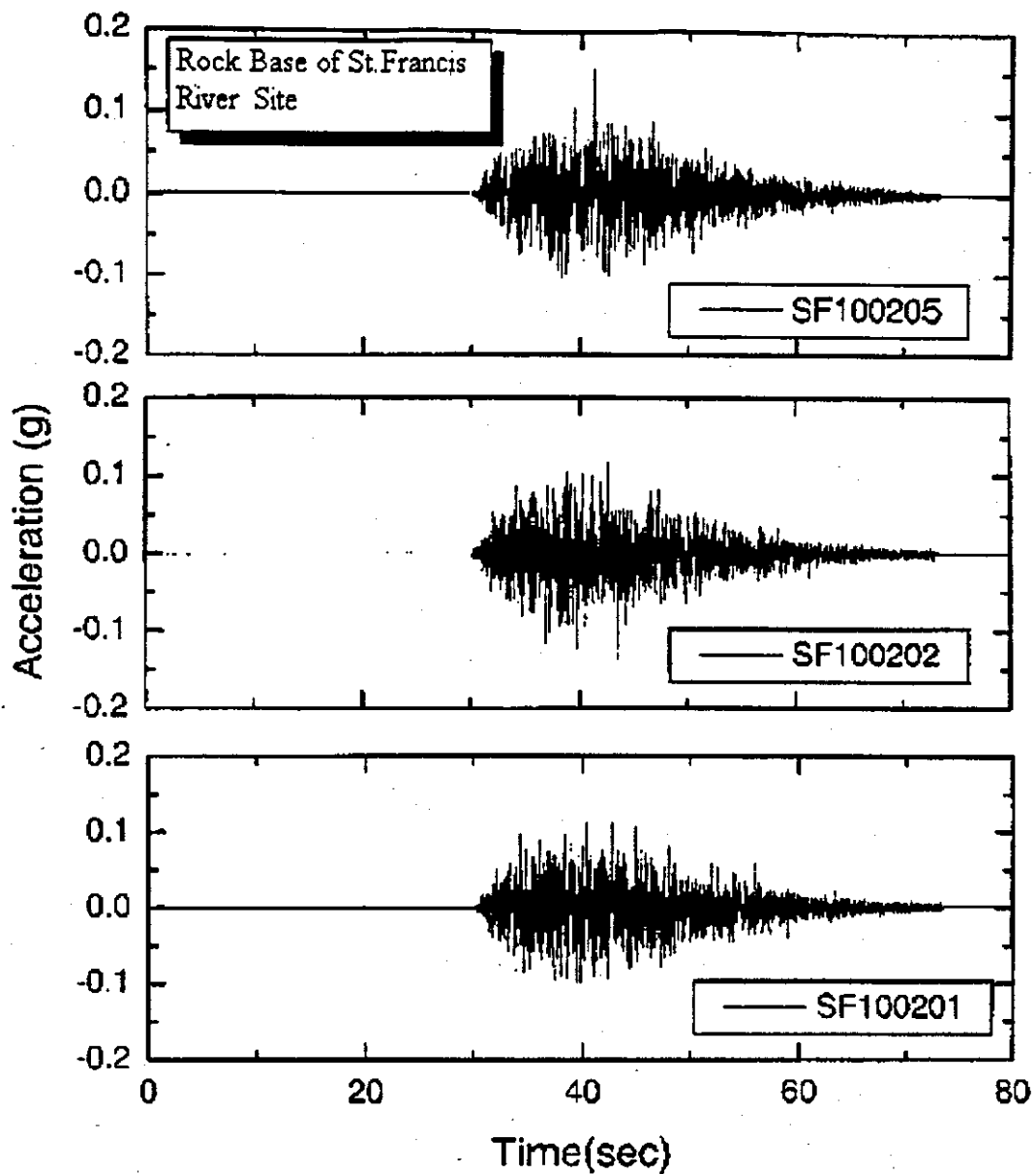
**b. PE 2 % in 50 Years**

<b>Name (1)</b>	<b>Mw (2)</b>	<b>R (km) (3)</b>	<b>Max acc. at rock-base(g) (4)</b>	<b>Max acc. at soil-surface(g) (5)</b>
SF020101*	6.4	10	1.069	0.497
SF020102	6.4	10	1.018	0.399
SF020103*	6.4	10	0.845	0.428
SF020104	6.4	10	1.068	0.376
SF020105*	6.4	10	1.089	0.473
SF020201*	8	40	0.604	0.447
SF020202	8	40	0.655	0.362
SF020203*	8	40	0.693	0.453
SF020204	8	40	0.609	0.378
SF020205*	8	40	0.596	0.391
Mw = Magnitude                      R = Epicentral distance				
* Used in further analysis				



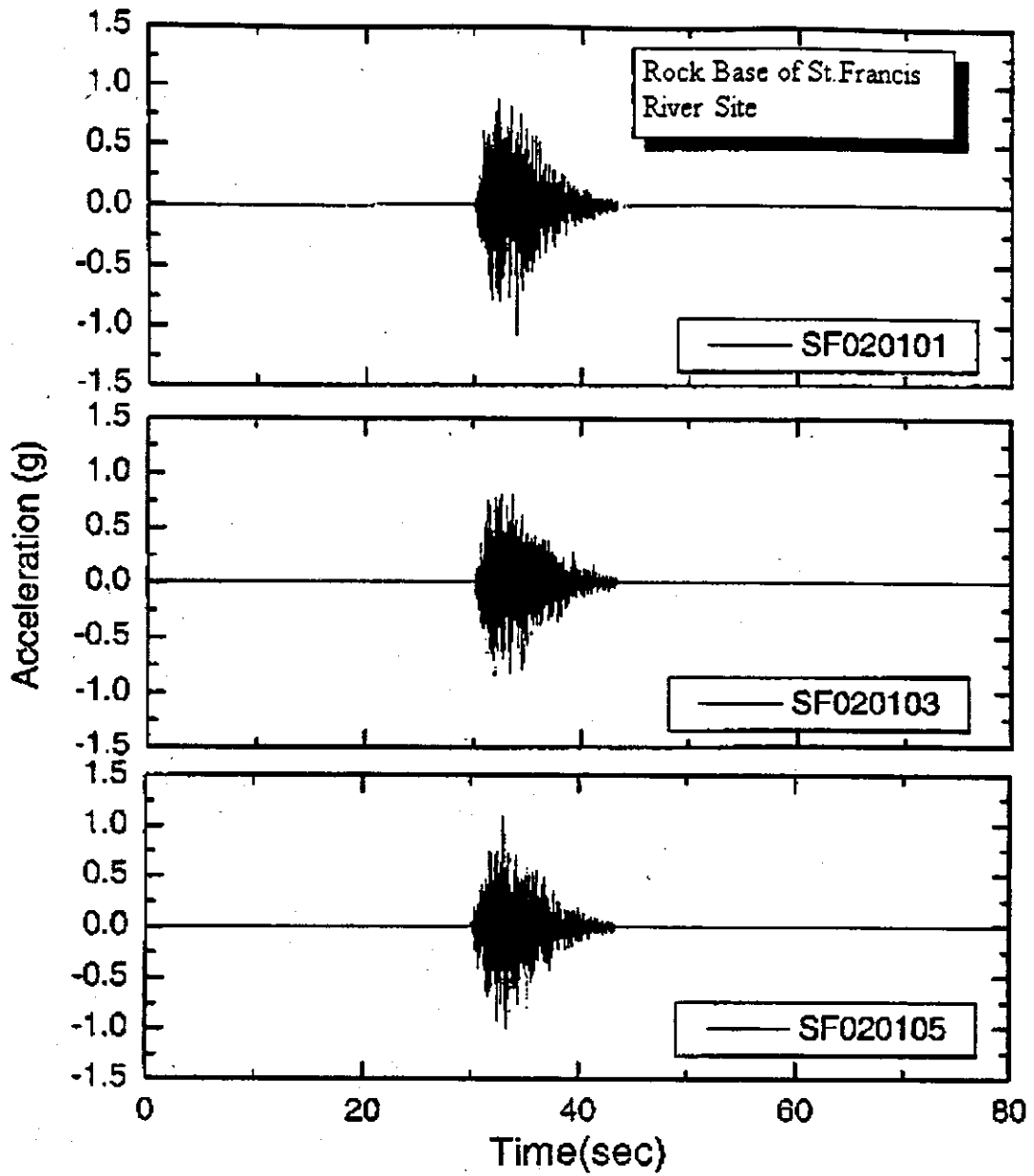
a. PE 10 % in 50 years, Magnitude = 6.2

Figure 8.4a Acceleration Time Histories for St. Francis River Site, PE 10% in 50 Years, Magnitude = 6.2



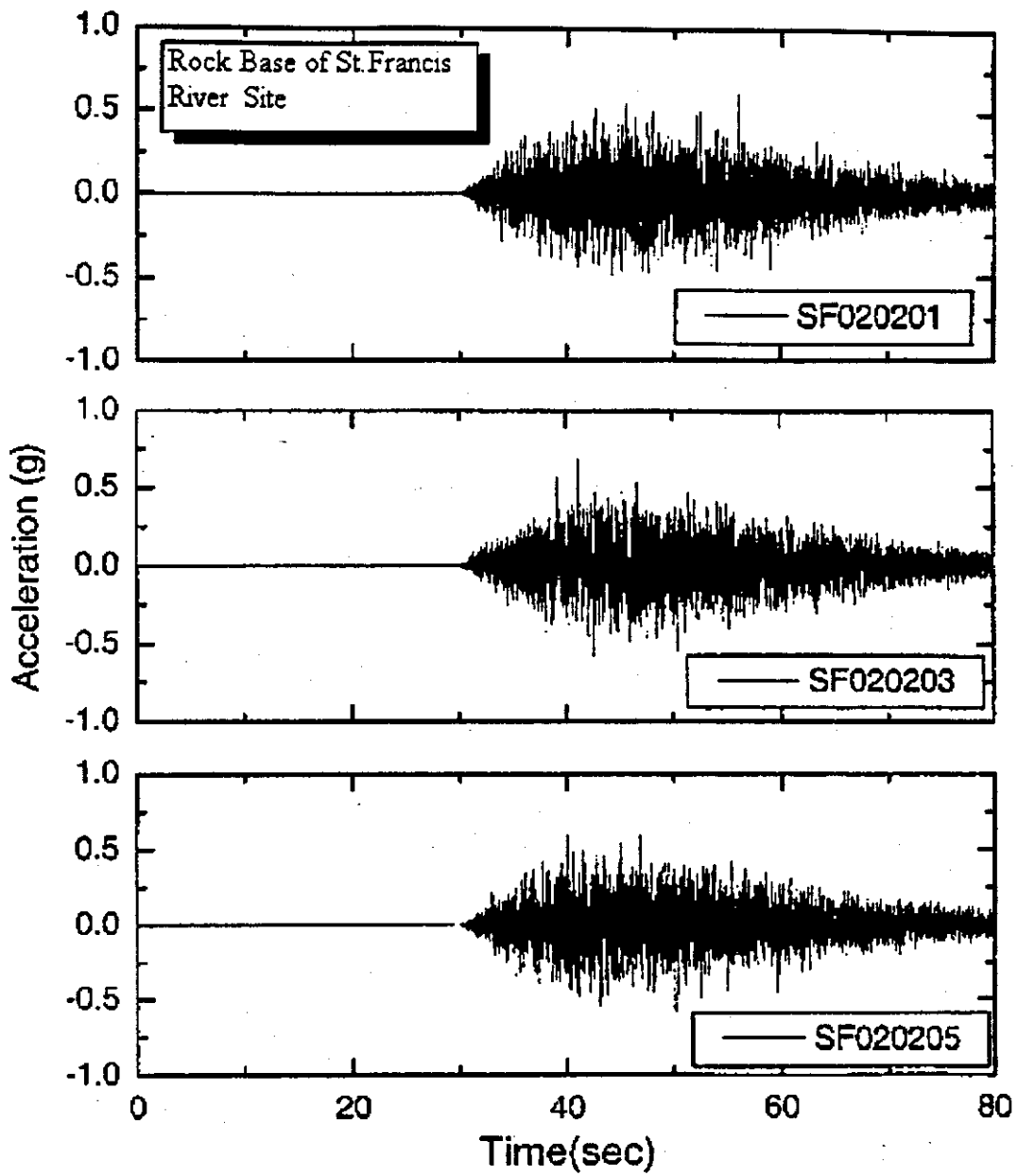
b. PE 10 % in 50 years, Magnitude = 7.2

Figure 8.4b Acceleration Time Histories for St. Francis River Site, PE 10% in 50 Years, Magnitude = 7.2



c. PE 2 % in 50 years, Magnitude = 6.4

Figure 8.4c Acceleration Time Histories for St. Francis River Site, PE 2% in 50 Years, Magnitude = 6.4



d. PE 2 % in 50 years, Magnitude = 8.0

Figure 8.4d Acceleration Time Histories for St. Francis River Site, PE 2% in 50 Years, Magnitude = 8.0

contain plots of surface acceleration for PE 2% in 50 years and M6.4 and M8.0 respectively. Figures 8.8a, b, c, and d show plots of design acceleration time history at the bridge abutment for (a) PE 10 % in 50 years M6.2. (b) PE 10 % in 50 years M7.2, (c) PE 2% in 50 years M6.4 and (d) PE 2% in 50 years M8.0.

Similarly Figures 8.9a, b, c and d contain plots of design acceleration time histories at the bridge pier.

### 8.1.3.3 Vertical Seismic Response of Soil

Herrmann (2000) also recommended that vertical rock motion is of the same order as the horizontal rock motion. *SHAKE91* is used to transmit the horizontal rock motion to the soil surface and/or any other depth. No such solution is available for transmission of vertical motion. Therefore the following procedure was adopted to transfer vertical rock motion to desired elevation.

1. Use *SHAKE* to transfer the P-wave.
2. Adjust peak vertical ground motion to be 2/3 of the peak horizontal ground motion.
3. Adjust the time history to reflect adjustment in (2) above.

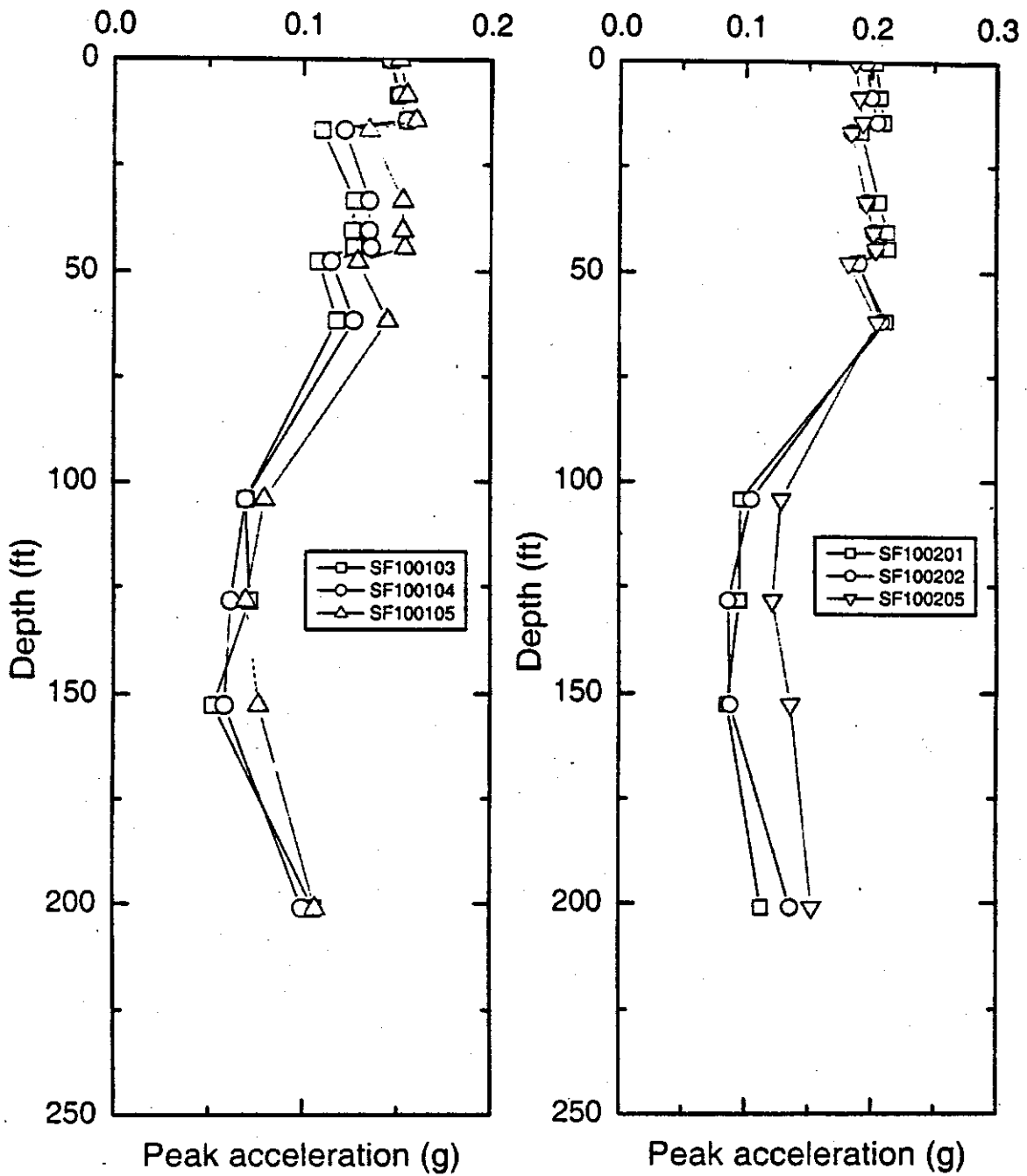
The calculated vertical time histories of acceleration at the soil surface, the base of bridge abutment and at the bridge pier were also modified as above.

The time histories of the modified vertical acceleration at the soil surface, the base of the bridge abutment and the base of the pier of each site are presented in Appendix D. It appears that for the horizontal and vertical time histories of any one event:

1.  $(k_v)_{max}$  and  $(k_h)_{max}$  do not occur at the same instant of time.
2. Frequency contents of these two-motions are quite different.

### 8.1.4 Liquefaction Potential Analysis

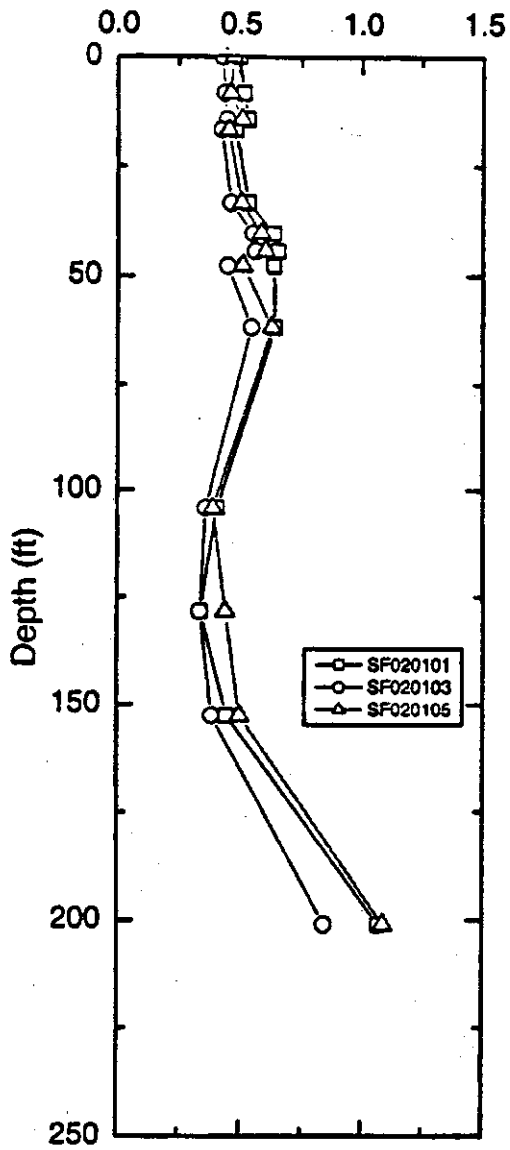
The liquefaction potential of St. Francis sites are evaluated by Seed and Idriss (1971) simplified method as modified by Youd and Idriss (1997). The procedure to obtain liquefaction potential was explained in Section 5.



a. Magnitude = 6.2

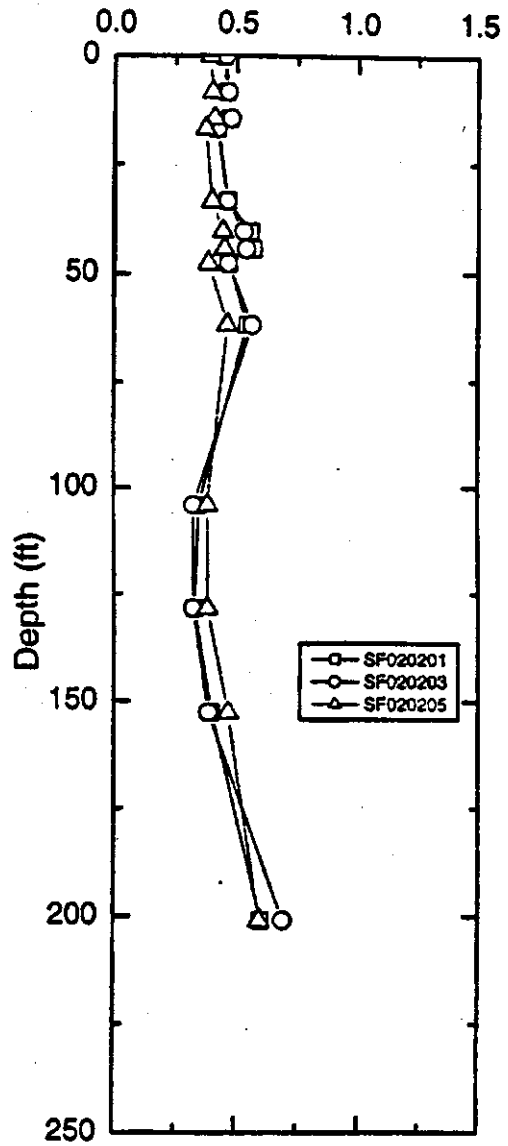
b. Magnitude = 7.2

Figure 8.5 Peak Ground Acceleration vs. Depth for PE 10% in 50 Years Magnitudes 6.2 and 7.2 St. Francis River Site



Peak acceleration (g)

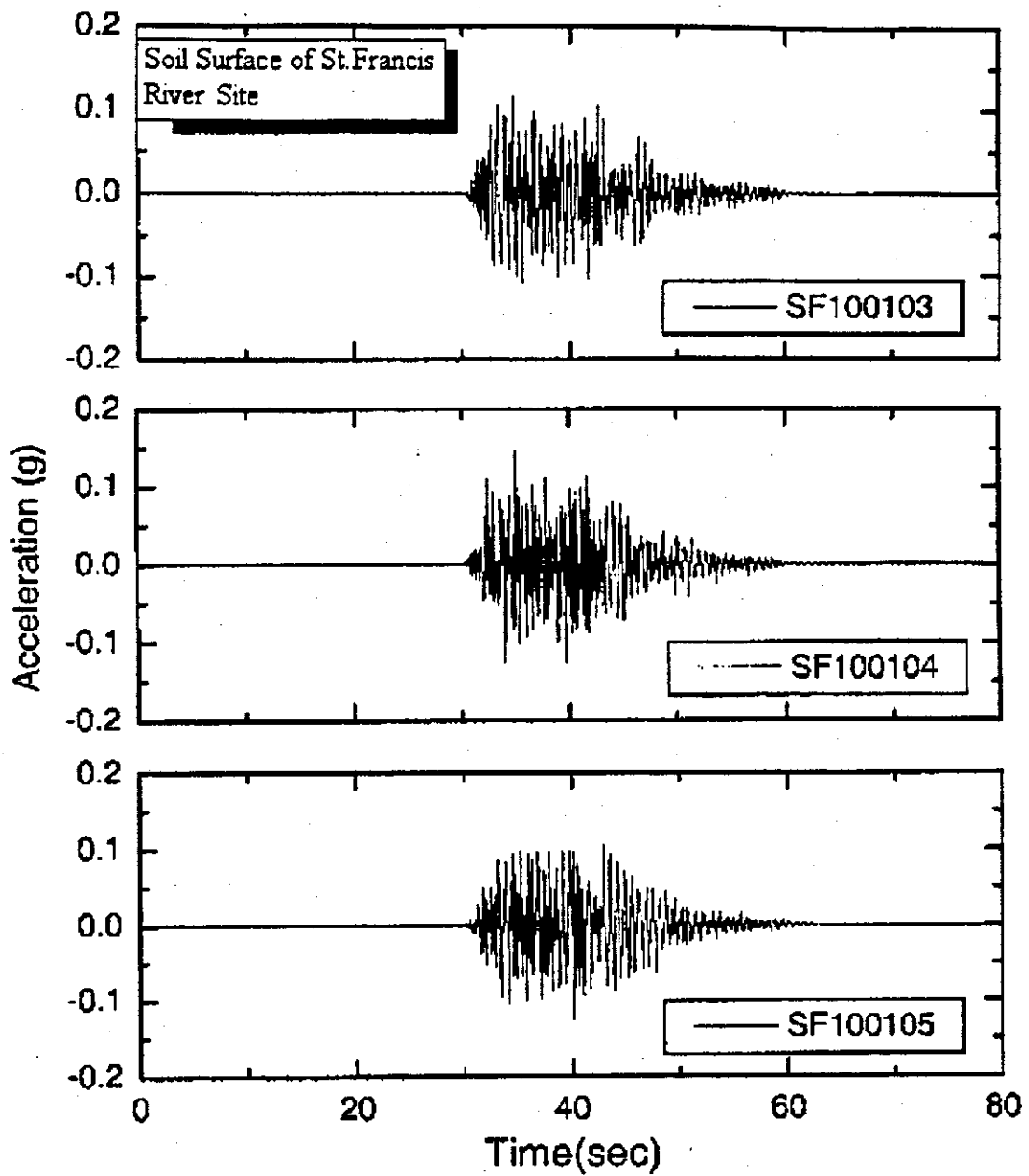
a. Magnitude = 6.4



Peak acceleration (g)

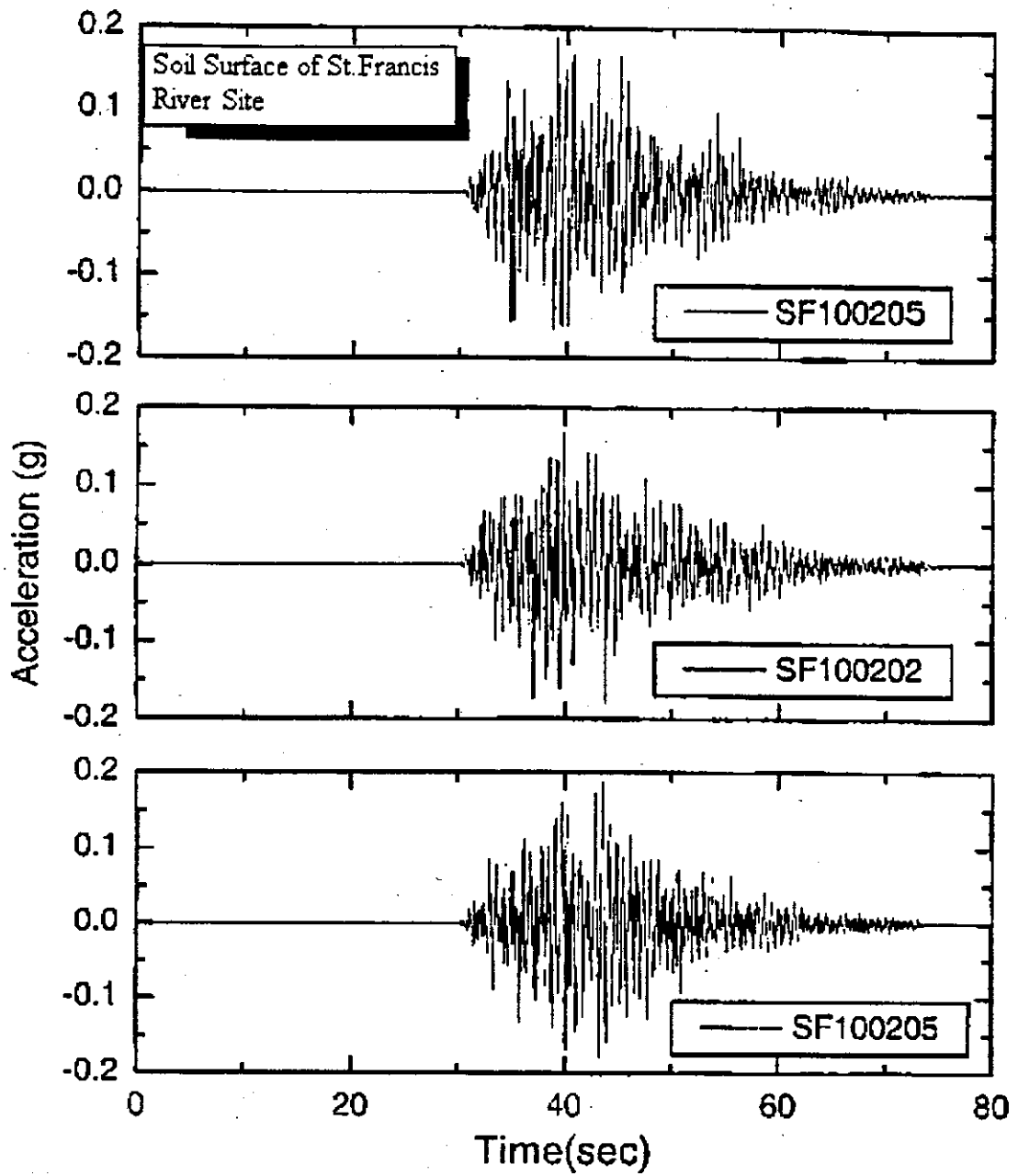
b. Magnitude = 8.0

**Figure 8.6** Peak Ground Acceleration vs. Depth for PE 2% in 50 Years Magnitudes 6.4 and 8.0 St. Francis River Site



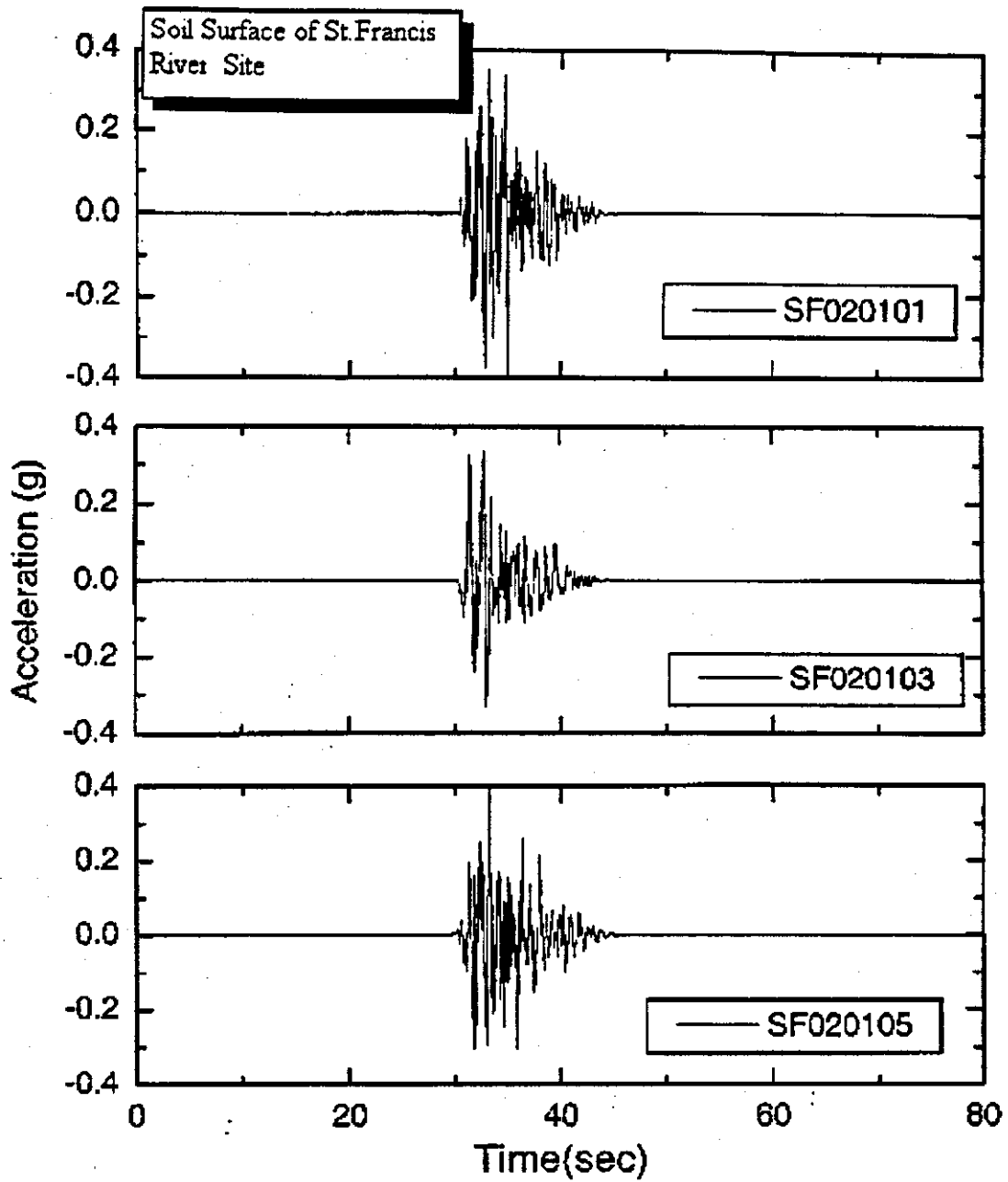
a. PE 10 % in 50 years, Magnitude = 6.2

Figure 8.7a Ground Acceleration at the surface of the St. Francis River Site, PE 10% in 50 years, Magnitude = 6.2



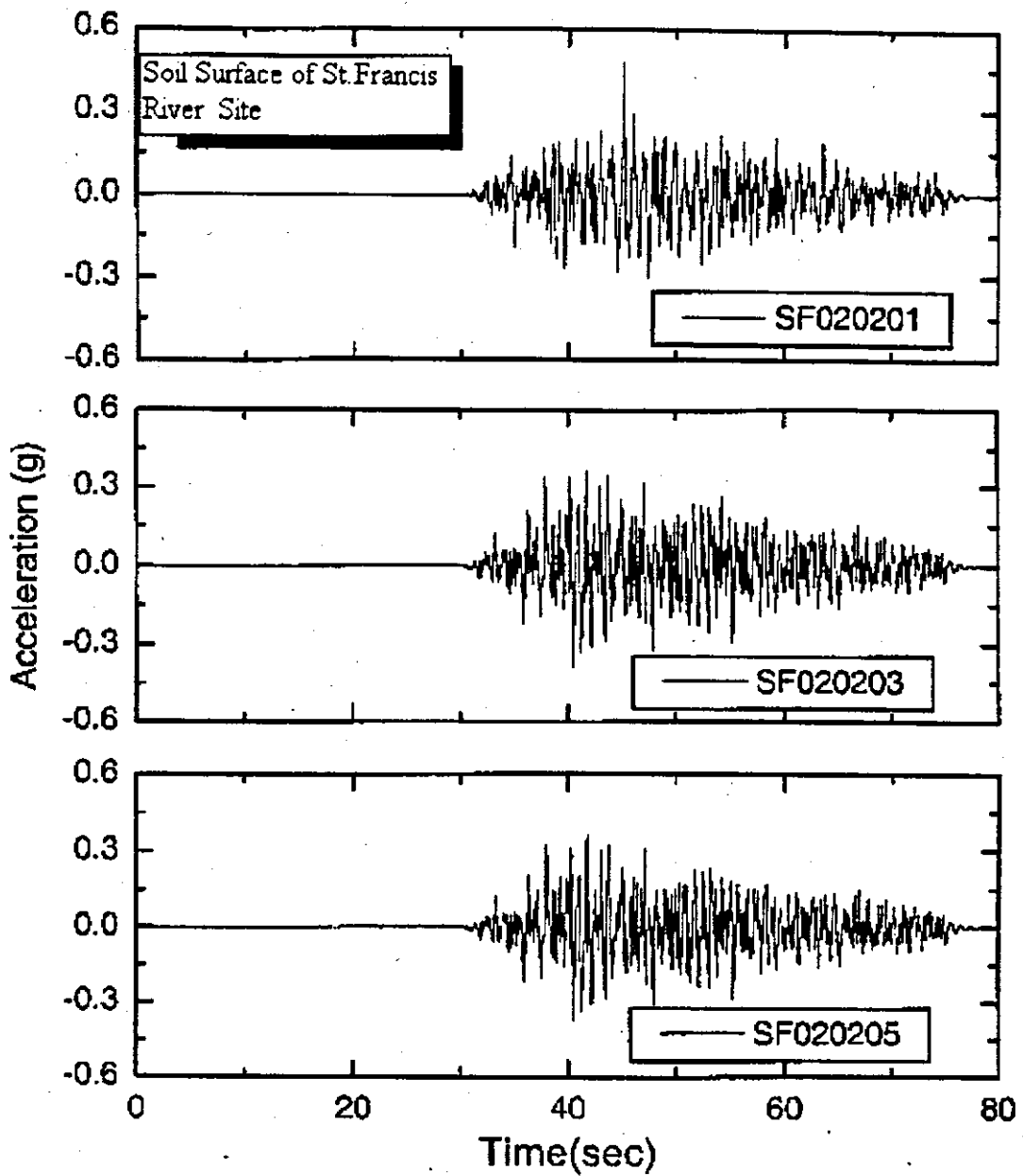
b. PE 10 % in 50 years, Magnitude = 7.2

Figure 8.7b Ground Acceleration at the surface of the St. Francis River Site, PE 10% in 50 years, Magnitude = 7.2



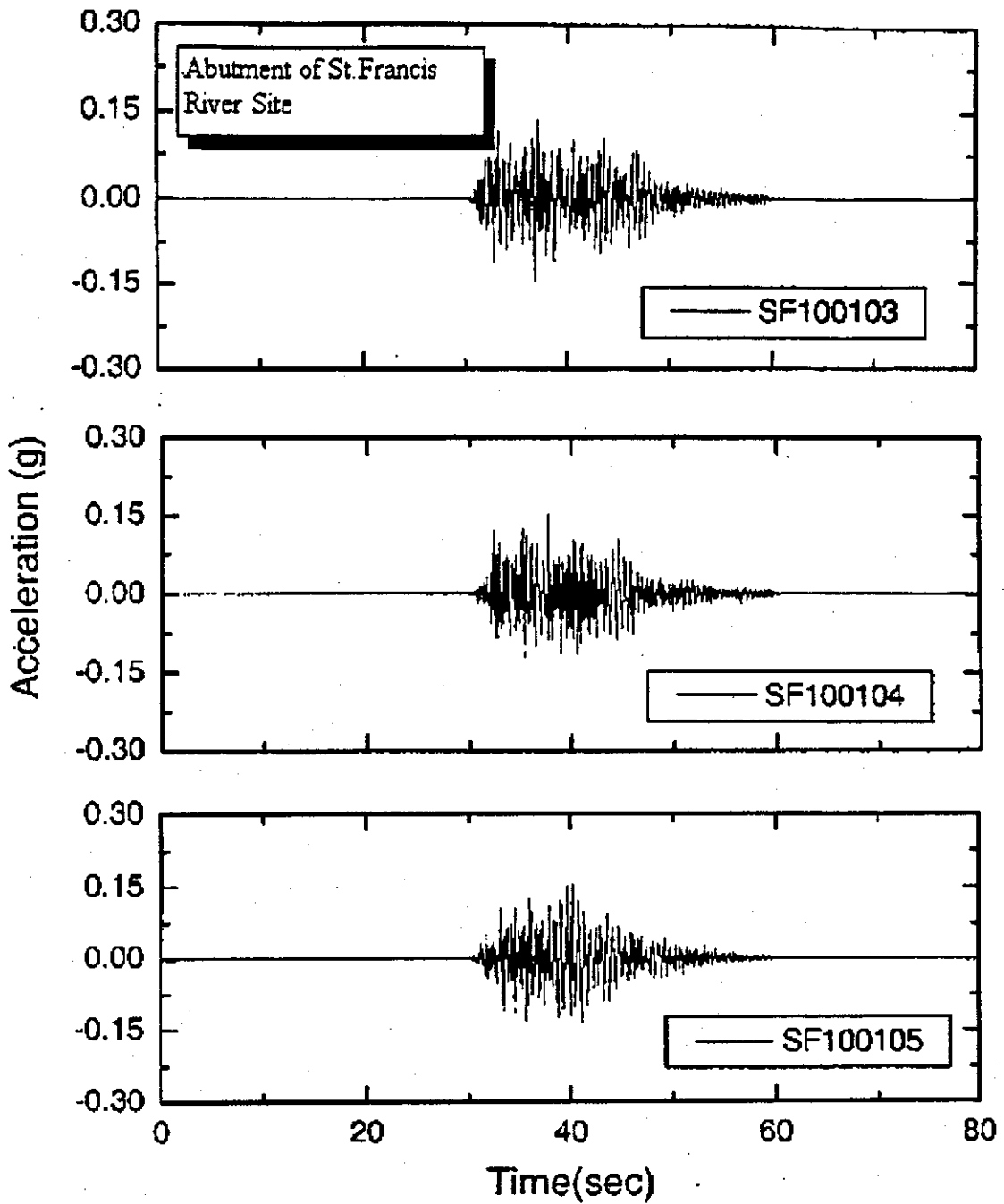
c. PE 2 % in 50 years, Magnitude = 6.4

Figure 8.7c Ground Acceleration at the surface of the St. Francis River Site, PE 2% in 50 years, Magnitude = 6.4



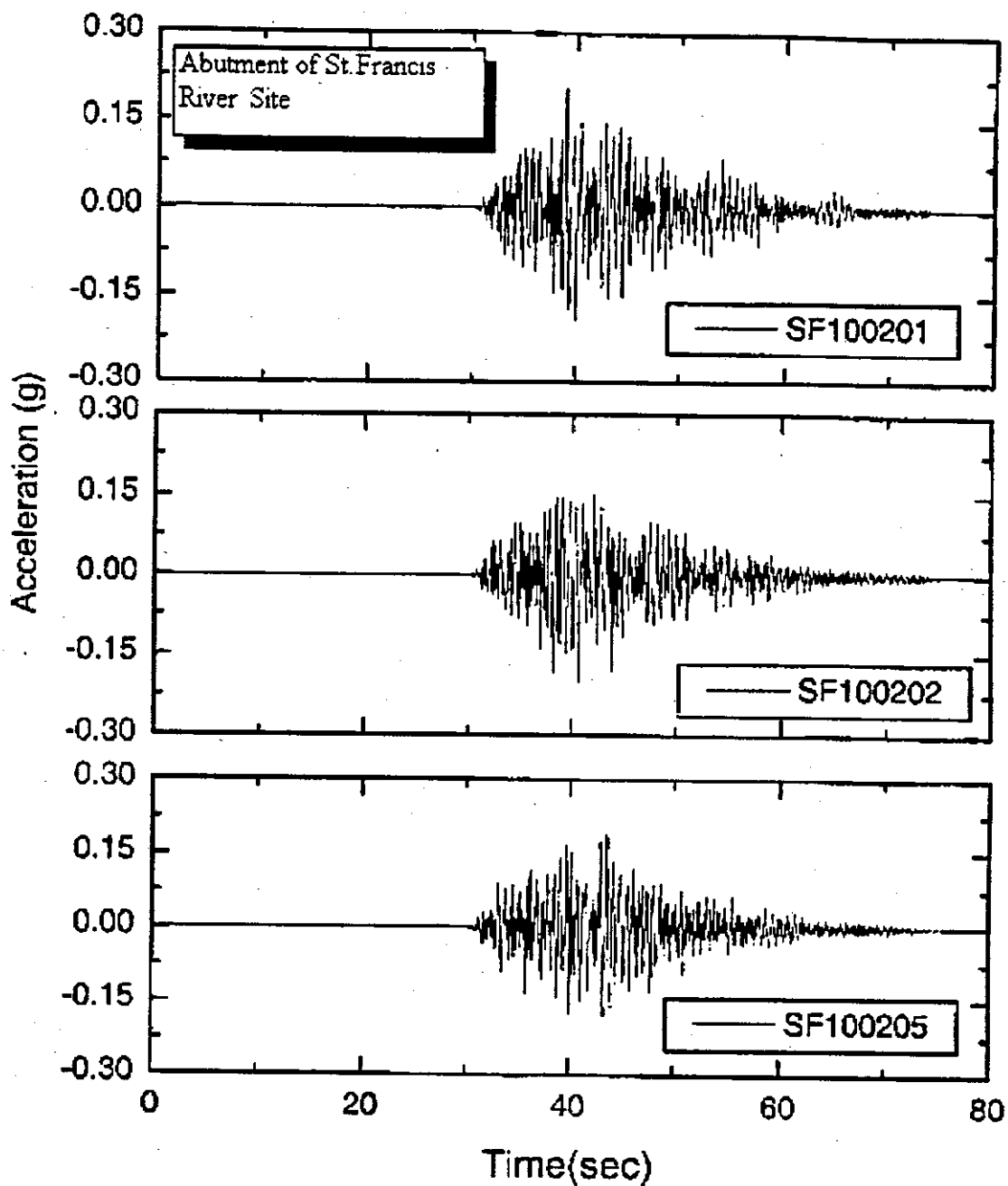
d. PE 2 % in 50 years, Magnitude = 8.0

Figure 8.7d Ground Acceleration at the surface of the St. Francis River Site, PE 2% in 50 years, Magnitude = 8.0



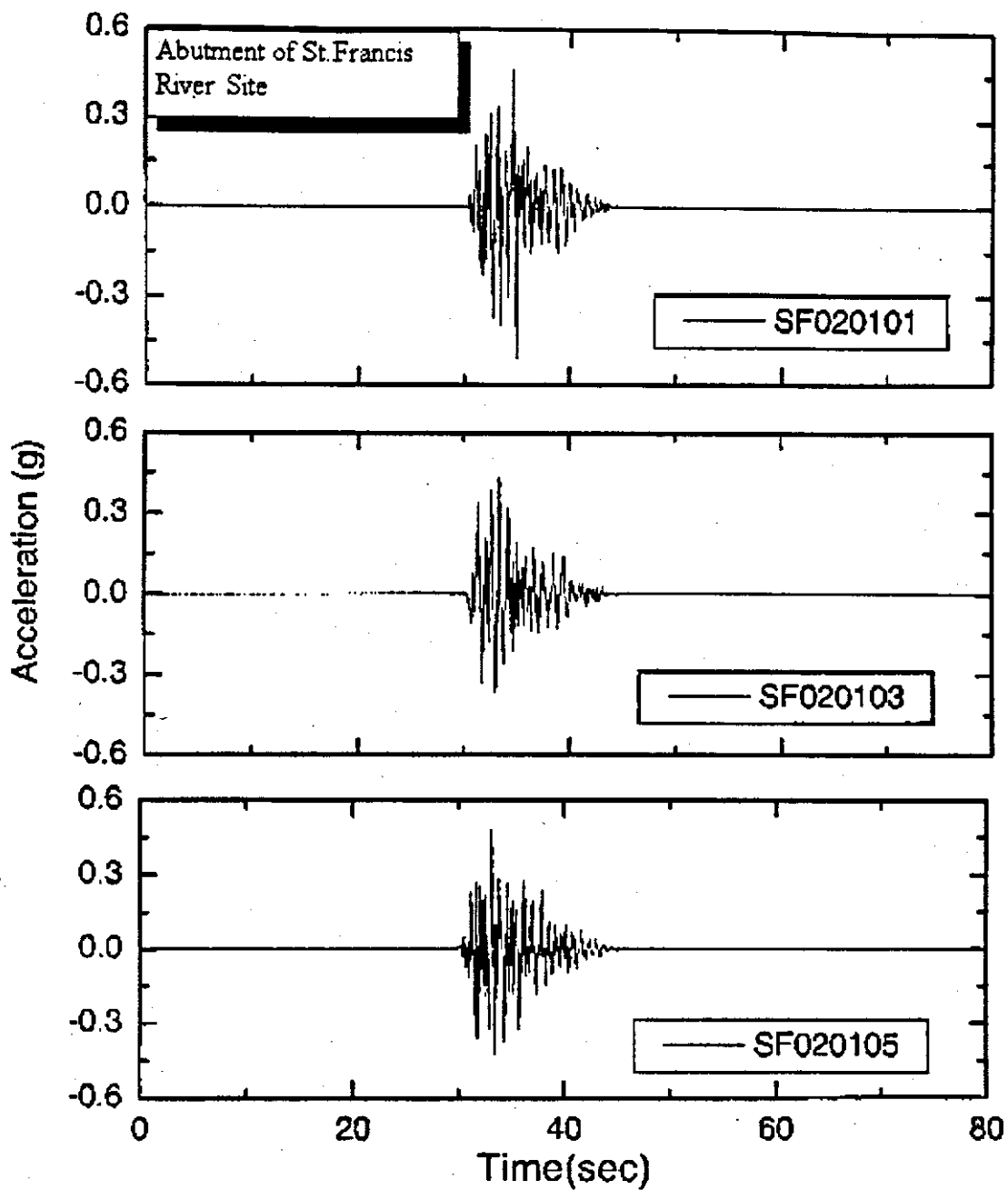
a. PE 10 % in 50 years, Magnitude = 6.2

Figure 8.8a Ground Acceleration at the abutment of the St. Francis River Site, PE 10% in 50 years, Magnitude = 6.2



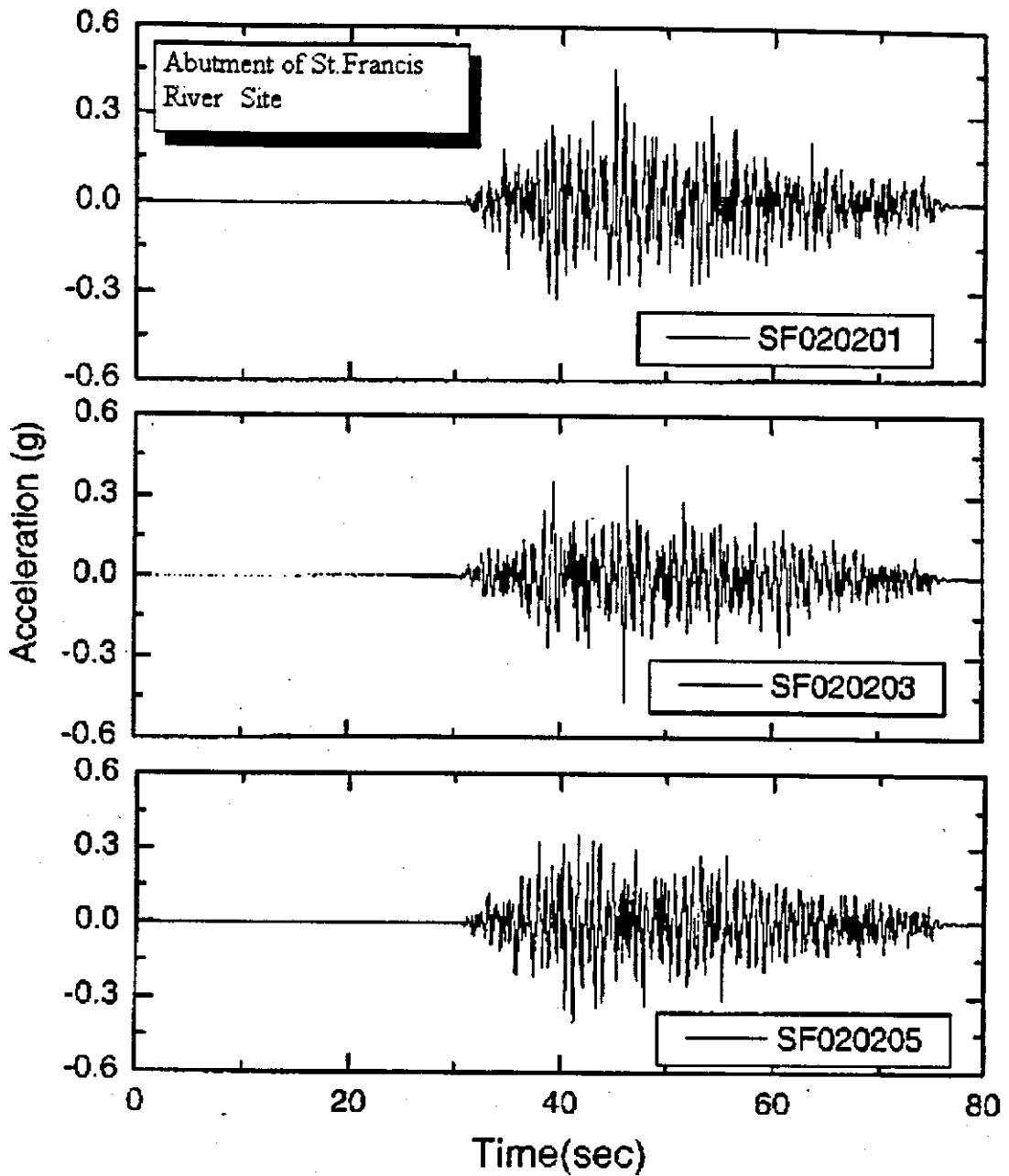
b. PE 10 % in 50 years, Magnitude = 7.2

Figure 8.8b Ground Acceleration at the abutment of the St. Francis River Site, PE 10% in 50 years, Magnitude = 7.2



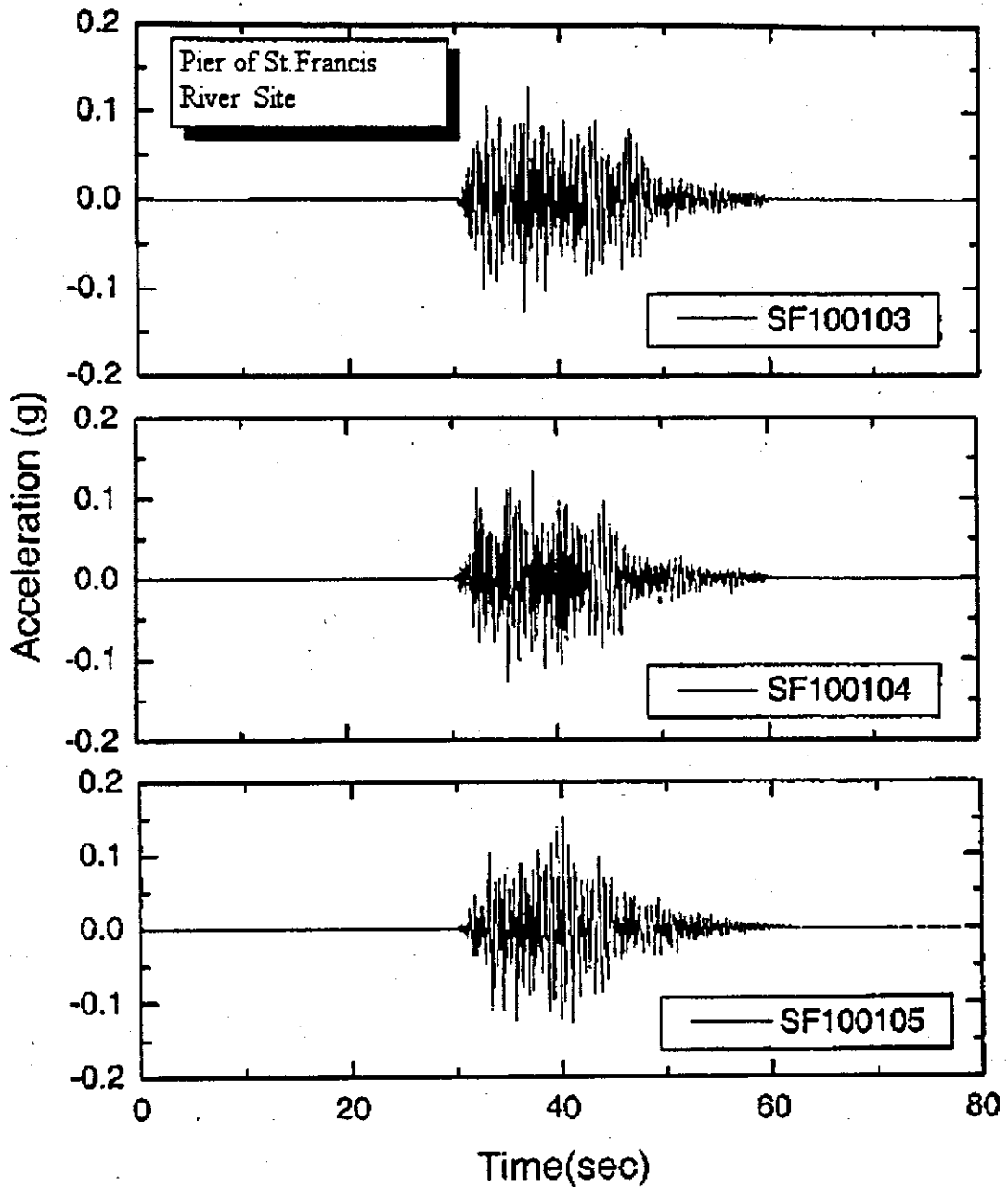
c. PE 2 % in 50 years, Magnitude = 6.4

Figure 8.8c Ground Acceleration at the abutment of the St. Francis River Site, PE 2% in 50 years, Magnitude = 6.4



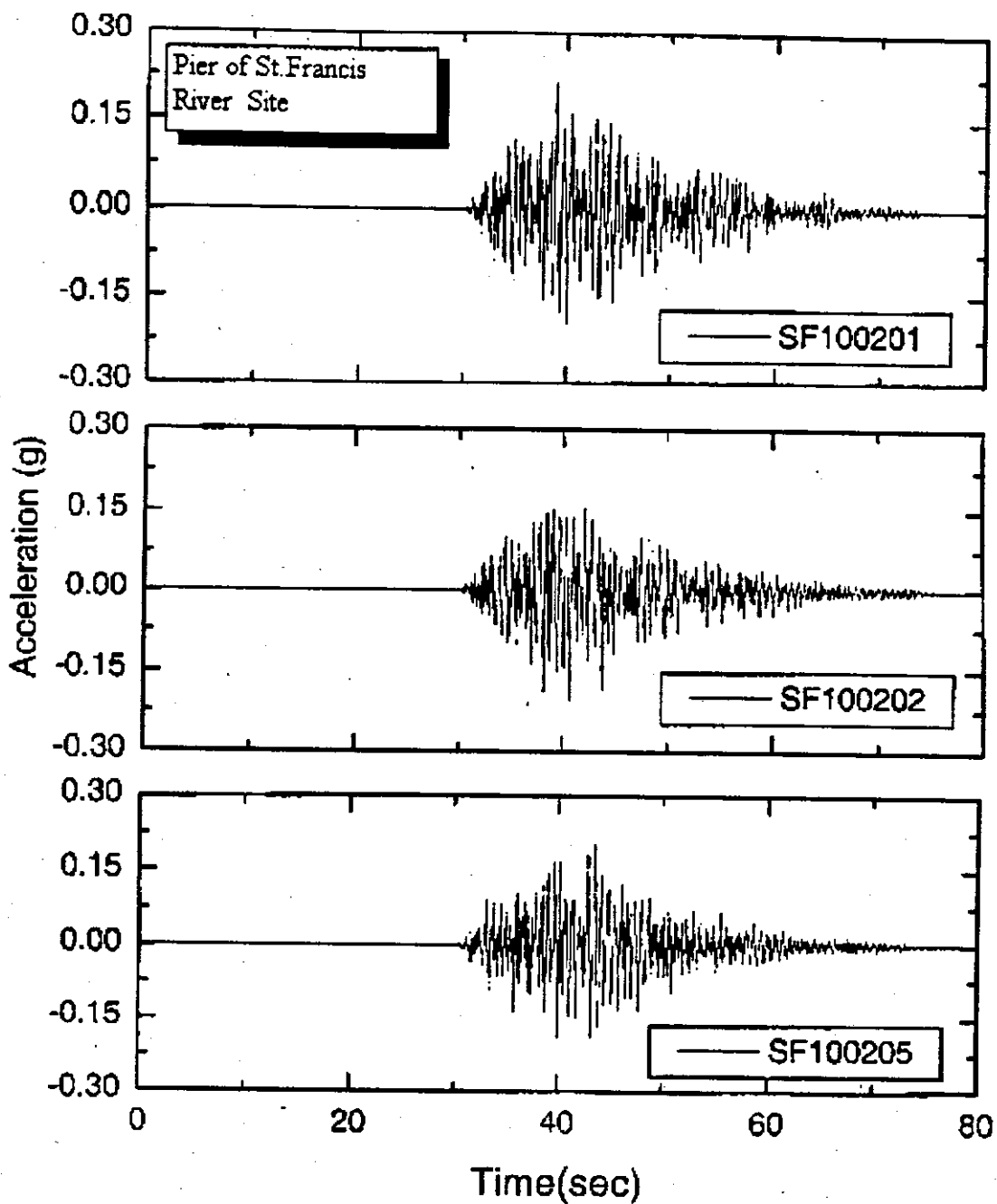
d. PE 2 % in 50 years, Magnitude = 8.0

Figure 8.8d Ground Acceleration at the abutment of the St. Francis River Site, PE 2% in 50 years, Magnitude = 8.0



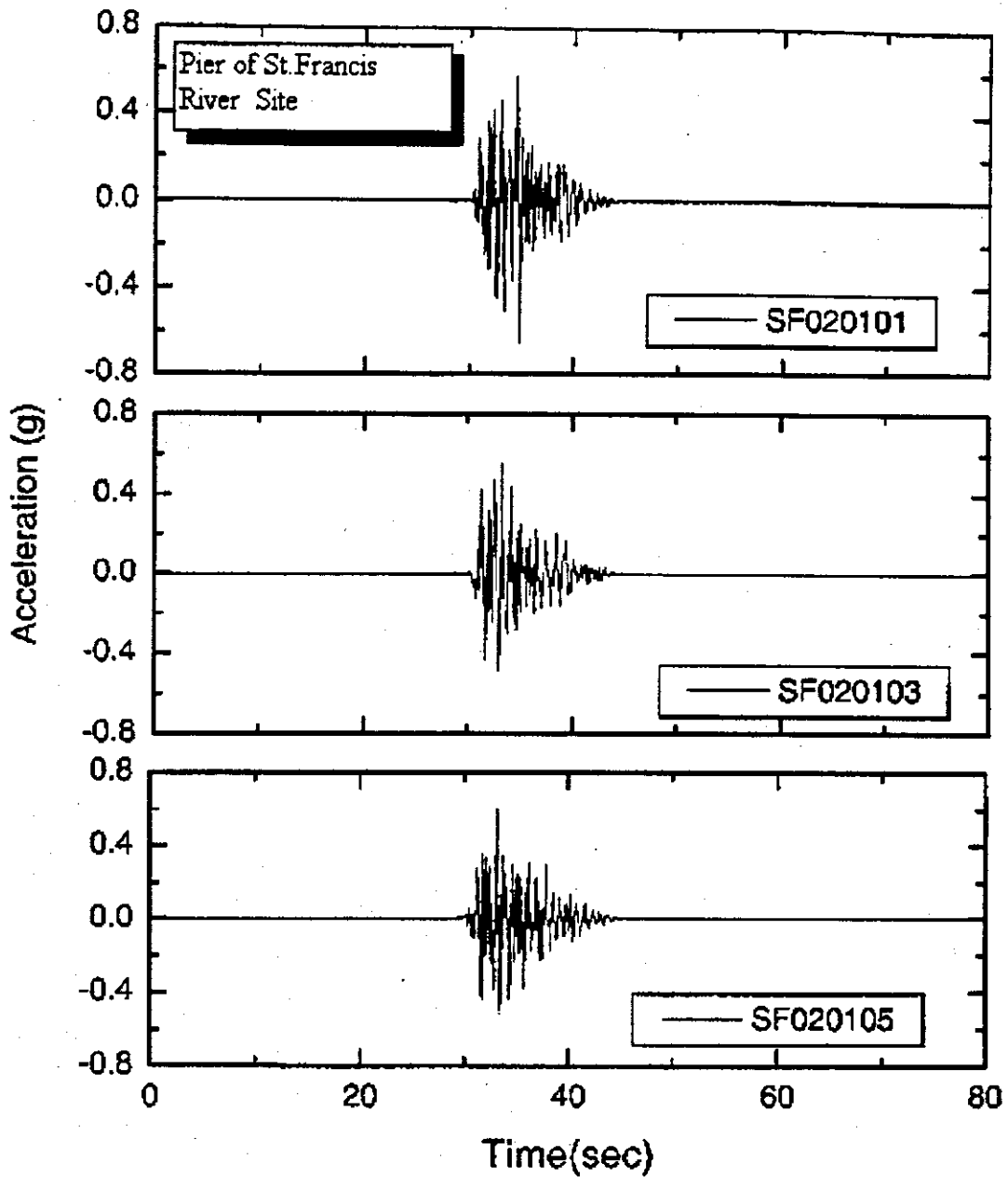
a. PE 10 % in 50 years, Magnitude = 6.2

Figure 8.9a Ground Acceleration at the pier of the St. Francis River Site, PE 10% in 50 years, Magnitude = 6.2



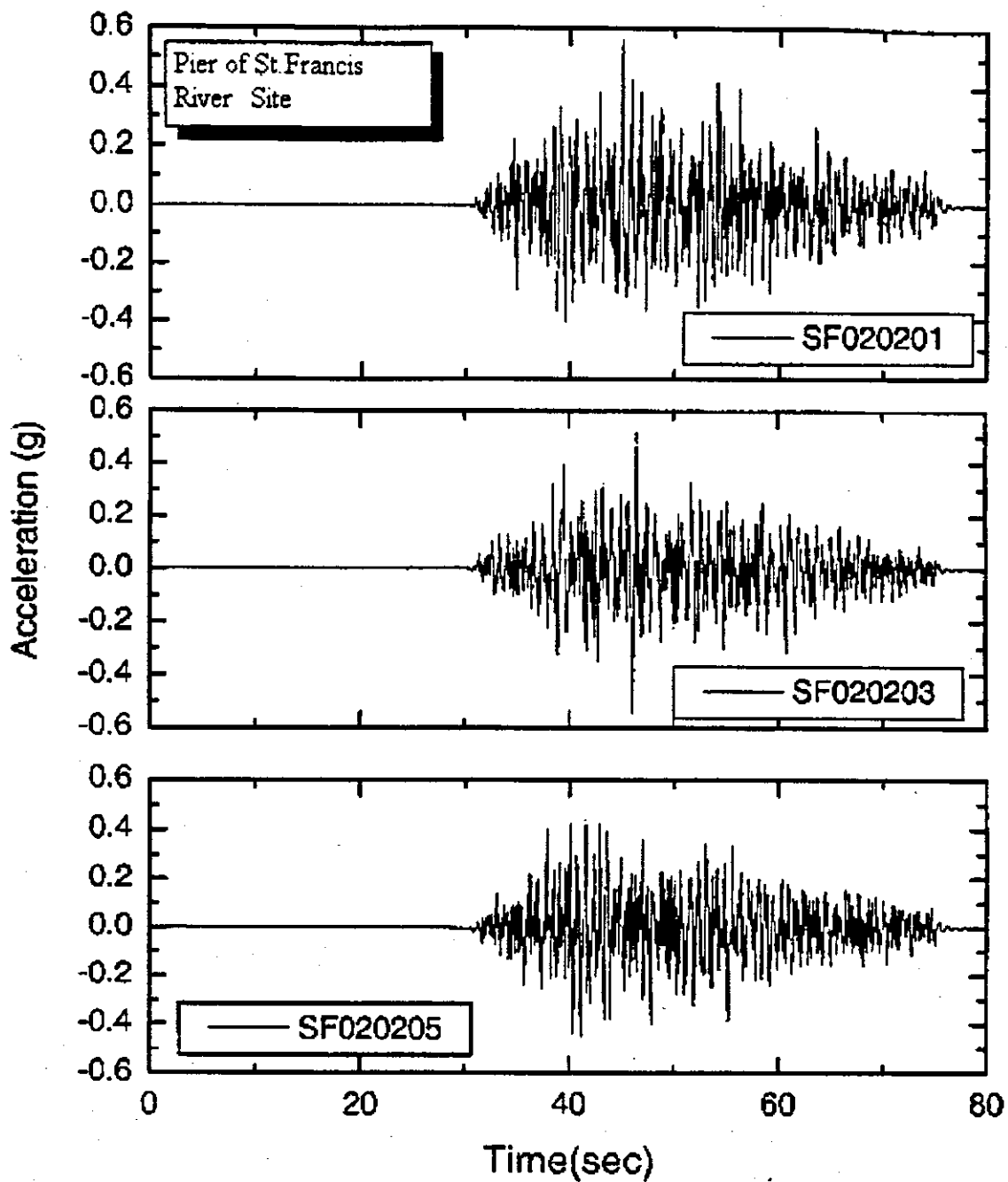
**b. PE 10 % in 50 years, Magnitude = 7.2**

**Figure 8.9b** Ground Acceleration at the pier of the St. Francis River Site, PE 10% in 50 years, Magnitude = 7.2



c. PE 2 % in 50 years, Magnitude = 6.4

Figure 8.9c Ground Acceleration at the pier of the St. Francis River Site, PE 2% in 50 years. Magnitude = 6.4



d. PE 2 % in 50 years. Magnitude = 8.0

Figure 8.9d Ground Acceleration at the Pier of the St. Francis River Site, PE 2% in 50 years, Magnitude = 8.0

**Table 8.2** Detail of Peak Ground Motion Used at the St. Francis River Site Rock Base, Ground Surface, Bridge Abutment and Pier.

**a. PE 10% In 50 Years**

Name	Max. acc. at rock-base EL. 149.8. (g)	Max acc. at soil-surface EL341.8 (g)	Max acc. at bridge abutment EL 333.4 (g)	Max acc. at bridge pier EL 301.4. (g)
SF100103*	0.106	0.146	0.160	0.126
SF100104*	0.100	0.146	0.160	0.134
SF100105*	0.107	0.151	0.155	0.154
SF100201*	0.113	0.203	0.206	0.214
SF100202*	0.136	0.196	0.200	0.204
SF100205*	0.153	0.187	0.190	0.204

**b. PE 2 % In 50 Years**

Name	Max. acc. at rock-base EL. 149.8. (g)	Max acc. at soil-surface EL341.8 (g)	Max acc. at bridge abutment EL 333.4 (g)	Max acc. at bridge pier EL 301.4. (g)
SF020101*	1.069	0.497	0.514	0.655
SF020103*	0.845	0.428	0.437	0.560
SF020105*	1.089	0.473	0.490	0.602
SF020201*	0.604	0.447	0.457	0.571
SF020203*	0.693	0.453	0.465	0.544
SF020205*	0.596	0.391	0.400	0.452

**8.1.4.1 Cyclic Stress Ratio (CSR), Cyclic Resistant Ratio (CRR) and Factor of Safety (FOS)**

Figure 8.10 shows the soil profile and N-values with depth, used for liquefaction analysis. A plot of factor of safety (FOS), CSR and CRR with depth for PE 10% in 50 years and Magnitude 6.2 is plotted as well. It can be seen that the soil does not liquefy for PE 10% in 50 years for Magnitude 6.2. However, for a PE of 10% in 50 years, magnitude 7.2, and for PE 2 % in 50 years and Magnitude 6.4 and 8.0, the soil liquefies to different depths as given in Table 8.4. This table lists the depths of liquefaction for each earthquake magnitude.

**8.1.5 Slope Stability of Abutment Fills**

Slope stability analyses were completed for seven cross-sections for the St. Francis River Site. Each cross-section was analyzed for both low and high ground-water conditions under static analysis and under three sets of pseudo-static earthquake accelerations. Cross-section locations are shown on Figure 8.1. The soil properties used for the analysis are given in Table 8.4.

An example analysis output for Cross-Section C-C' is shown on Figure 8.11. A summary of the St. Francis River Site analyses is included in Table 8.5. In general, the site slopes appear to be

stable under static conditions, with both low and high ground-water tables, with factors of safety ranging from 1.93 to 3.96. When subjected to an earthquake with a 10% exceedance probability in 50 years (10%PE), slopes continue to show stability, with factors of safety ranging from 1.19 to 3.91. When subjected to an earthquake with a 2% PE, factors of safety less than or approximately equal to one are calculated for all cross-sections except G-G' for low water conditions, and all section for high water conditions. The analysis set 2, using adjusted PHGA with corresponding adjusted PVGA showed the lowest factors of safety. Expected failure planes pass through both the roadway and bridge piers.

**Table 8.3 The Different Zones of Soil Liquefaction for Different Factors of Safety, St. Francis River Site**

Factor of Safety	Zones of Soil Liquefaction			
	PE 10% in 50 years		PE 2% in 50 years	
	M6.2	M7.2	M6.4	M8.0
< 1.0	No	10-12.5	8-22, 64-68, 71-85	6-110
< 1.1	No	9-13	8-24, 64-68, 70-91	6-145
< 1.2	No	8-14, 19-20	8-32, 61-93	6-180
< 1.3	No	8-15, 18-20	8-44, 61-94	5-180
< 1.4	No	8-16, 18-20, 64-65, 75-80	8-94	5-180

**Table 8.4 Soil Properties Used for the Slope Stability Analysis, St. Francis River Site**

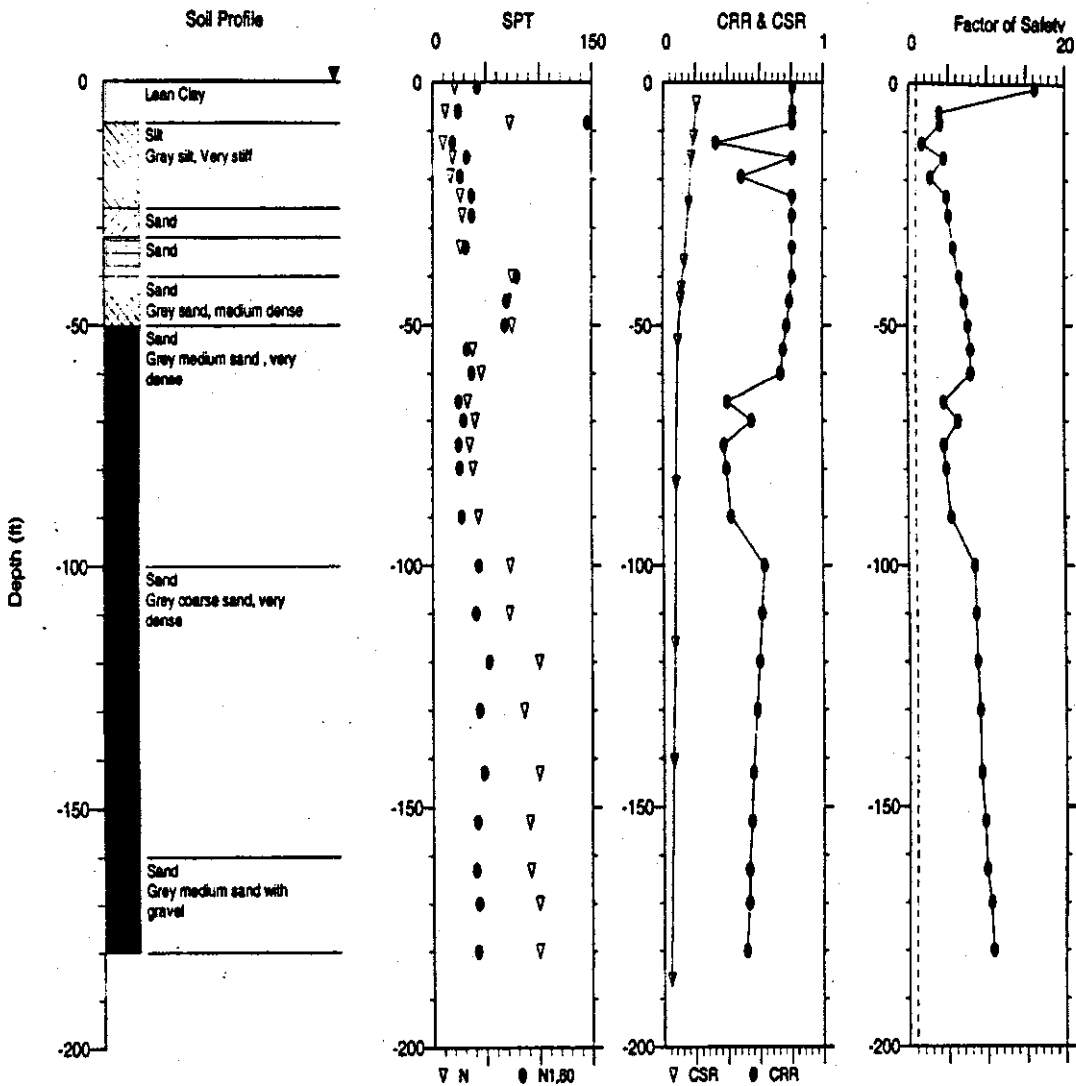
Soil Characteristics*				
Class	$\gamma_{moist}$ (pcf)	$\gamma_{saturated}$ (pcf)	c (psf)	$\phi$ (deg.)
CL	121.3	133.5	860	30
ML	106.0	122.5	450	34
SM	115.0	127.0	50	35
SP	134.9	141.9	0.0	40

\* Soil characteristics obtained from slope stability procedures, Section (5.5.1)

These results indicate that slopes at the St. Francis River Site are expected to be stable under small earthquake shaking (10% PE), and unstable at higher levels of shaking (2% PE), regardless of the ground-water level.

### 8.1.6 Flood Hazard Analysis Results

Flood hazards were estimated assuming that an earthquake caused catastrophic failure of waterway levees in the vicinity of US 60 or failure of the Wappapello Dam, located approximately eight miles north of US 60. Hazards were estimated based solely on relative elevations of land and waterways, assuming complete failure of either levees or of the dam. The likelihood of such failure during an earthquake was not calculated, so the flood hazard analysis is considered a worst-case scenario. However, levee or dam failure was assumed to occur during moderate flow conditions and not during flood or elevated water conditions in the waterways.



Notes:  
 CSR analysis using SHAKE results.  
 CSR File: D:\Y-0 SP Palos\SP100103\SE100103.grf  
 CSR using SPT Data and Seed et. al. Method in 1997 NCEER Workshop.  
 Earthquake File for SHAKE Analysis: D:\SP\SP100103.ACC  
 Earthquake Magnitude for CSR Analysis: 6.2  
 Magnitude Scaling Factor (MSF): 1.62  
 Depth to Water Table for CSR Analysis (ft): 0  
 Depth to Water Table for Cn Calculation (ft): 0  
 Depth to Base Layer for CSR Analysis (ft): 219.6  
 SPT Option: I.M. Idriss (1997)  
 Cn Option: Liao & Whitman (1986)  
 Xsigma Option: L.F. Harder & S. Boulanger (1997)  
 SPT Energy Ratio: USA/Safety/Sope: 0

Figure 8.10 Soil Profile, CSR, CRR and Factor of Safety Against Liquefaction at the St. Francis River Site for PE 10% in 50 years and Magnitude = 6.2

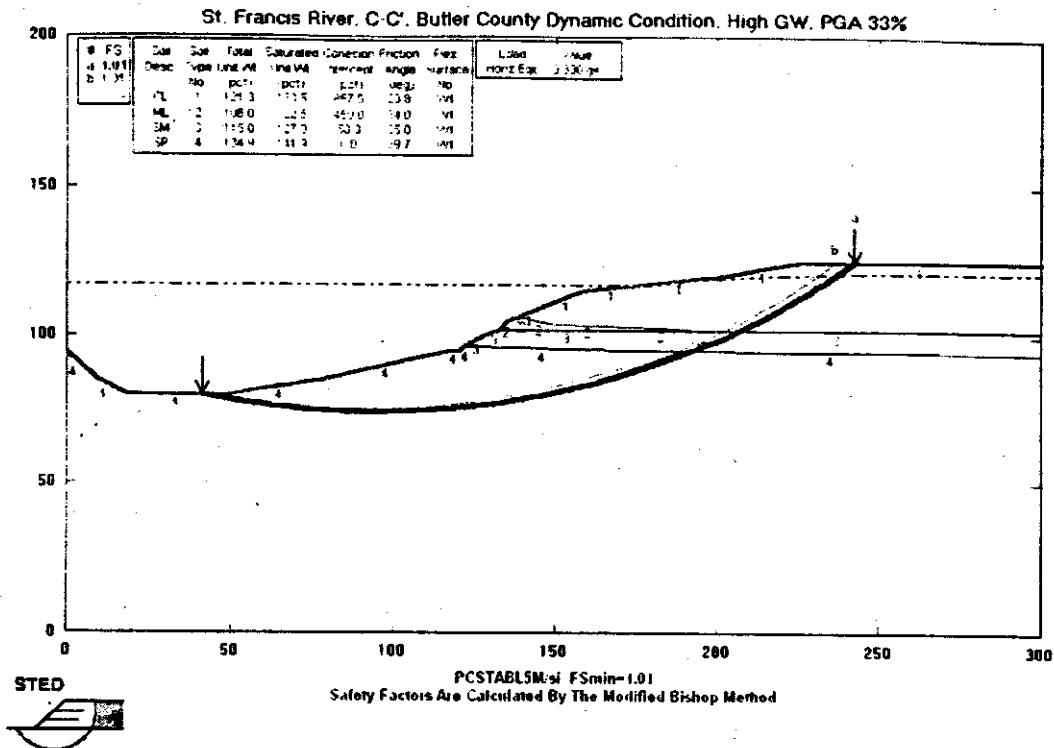


**Figure 8.11 Example Slope Stability Results for St. Francis River Site**

Evaluation of the effects of catastrophic failure of the Wappapello Dam was completed by USACE (1985). In general, they concluded that the peak flooding elevation in the vicinity of US 60 would be 340.0, cresting approximately two hours after failure. The estimated flooded zone is shown on Figure 8.12. This zone includes 5.7 miles of roadway from the St. Francis River eastward to approximately 0.4 miles west of Highway WW/TT (which leads to Dudley), and 3.4 miles of roadway from approximately 0.3 miles east of Highway WW/TT eastward to Highway ZZ. Highway WW/TT runs along the Dudley Ridge, which is slightly higher in elevation than the surrounding land.

Evaluation of the effects of flooding due to failure of levees was based on a series of topographic maps covering the entire study section of US 60 (Figure 8.13). This evaluation was field checked by visual observation of the elevation of the roadway compared to surrounding land. Some of the maps were as old as 1962 vintage without photo revision, so the estimate of the limits of potential flooding should be considered tentative. Furthermore, the roadway elevation was shown only to 5-foot accuracy, and slight elevations or depressions in the roadway could significantly

**Table 8.5 Slope Stability Results for the St. Francis River Site**

<b>Factor of Safety for Most Sensitive Potential Failure Plane</b>							
<b>Cross-Section</b>	<b>A - A'</b>	<b>B - B'</b>	<b>C - C'</b>	<b>D - D'</b>	<b>E - E'</b>	<b>F - F'</b>	<b>G - G'</b>
<b>Static</b>							
Low GW	2.63	2.76	2.88	2.71	2.52	1.93	3.96
High GW	3.06	3.14	3.48	3.23	2.87	2.02	2.67
<b>Pseudo-Static Set 1*</b>							
<b>10% PE in 50 years</b>							
Low GW (0.135)	1.73	1.74	1.82	1.79	1.59	1.41	2.60
High GW (0.135)	1.61	1.68	1.78	1.72	1.64	1.23	1.74
<b>2% PE in 50 years</b>							
Low GW (0.331)	1.31	1.10	1.17	1.18	1.08	0.98	1.71
High GW (0.331)	0.93	0.97	1.01	1.00	0.94	0.74	1.08
<b>Pseudo-Static Set 2</b>							
<b>10% PE (HGA, VGA)</b>							
Low GW (0.135,+0.048)	1.68	1.64	1.76	1.74	1.55	1.39	2.59
Low GW (0.135,-0.048)	1.77	1.75	1.87	1.83	1.62	1.43	2.62
High GW (0.135,+0.048)	1.55	1.61	1.71	1.66	1.54	1.19	1.64
High GW (0.135,-0.048)	1.67	1.73	1.84	1.77	1.63	1.26	1.75
<b>2% PE (HGA, VGA)</b>							
Low GW (0.331,+0.170)	0.95	0.91	0.97	0.99	0.92	0.84	1.58
Low GW (0.331,-0.170)	1.28	1.26	1.33	1.32	1.20	1.08	1.82
High GW (0.331,+0.170)	0.70	0.74	0.78	0.78	0.74	0.57	0.88
High GW (0.331,-0.170)	1.10	1.14	1.20	1.17	1.09	0.86	1.25
<b>Pseudo-Static Set 3</b>							
<b>10% PE (HGA, VGA)</b>							
Low GW (0.012,+0.090)	2.50	2.50	2.71	1.80	2.21	1.89	3.91
Low GW (0.012,-0.090)	2.57	2.61	2.81	1.95	2.24	1.89	3.74
High GW (0.012,+0.090)	2.89	2.98	3.29	3.08	2.74	1.95	2.50
High GW (0.012,-0.090)	2.87	2.94	3.25	3.02	2.70	1.91	2.62
<b>2% PE (HGA, VGA)</b>							
Low GW (0.014,+0.221)	2.39	2.37	2.58	2.49	2.14	1.88	4.06
Low GW (0.014,-0.221)	2.59	2.66	2.86	2.66	2.23	1.89	3.65
High GW (0.014,+0.221)	2.90	2.46	3.28	3.11	2.78	1.95	2.34
High GW (0.014,-0.221)	2.85	2.91	3.21	2.96	2.68	1.88	2.67

\* Peak ground acceleration values calculated with the computer program *SHAKE* Section 5.4.

HGA – Horizontal Ground Acceleration

VGA – Vertical Ground Acceleration

PE – Probability of Exceedance in 50 years

change the degree of anticipated flooding. In general, the following conditions are expected for each waterway along the study section, presented in order from west to east:

1. Blue Spring Slough – Failure of the levee could potential flood a 1-mile section of the roadway flanking the slough and a 0.25 section of the roadway 1 mile west of Highway FF.
2. St. Francis River – The river is entrenched within a levee, and then flanked by a natural floodplain bounded by a second levee to the west and higher ground to the east. Failure of the levees could potentially flood two 0.25-mile sections of roadway near Highway 51 slightly less than a mile east of the river.

1. Mingo, Cypress Creek Lateral, and Prairie Creek Ditches – Failure of the levees for these ditches could potentially flood the same two sections of roadway at risk from the St. Francis River, as well as a 0.25-mile section of roadway located 0.75 miles west of the Cypress Creek Lateral Ditch. Flooding would be limited by levees that did not fail.
2. Lick Creek – The roadway appears to be elevated above the surrounding land in this area, and flooding is not anticipated.
3. Unnamed Creek 1 mile West of Essex – Failure of levees could potentially flood a 0.1-mile section of roadway.
4. Bess Slough – It appears that the roadway is elevated in the vicinity of this waterway, except for a 0.5 mile section located 0.5 to 1 mile west of Highway FF, which may possibly flood in the event of a levee failure.
5. Six Unnamed Ditches Between Bess Slough and the Castor River – The roadway and surrounding fields appear to be elevated between Highways FF and N to the west. Areas to the east which may potentially flood include a 0.5 mile section located 0.5 to 1 mile east of Highway N, 2 sections 100 to 300 feet in length located 1 to 1.25 miles east of Highway N, and a 1 mile section located 1.5 to 2.5 miles east of Highway N.
6. Castor River – The river appears to be separated from the original flow source and is expected to have a limited flowing length and flooding potential.

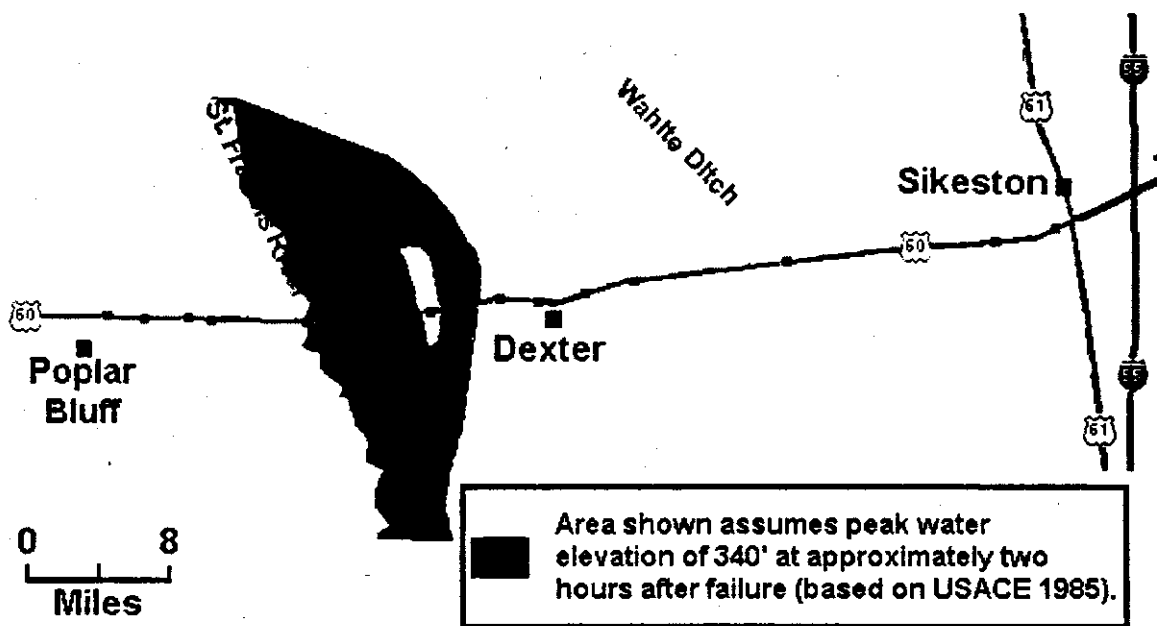


Figure 8.12 Estimated Flooding Zone Due to Wappapello Dam Failure

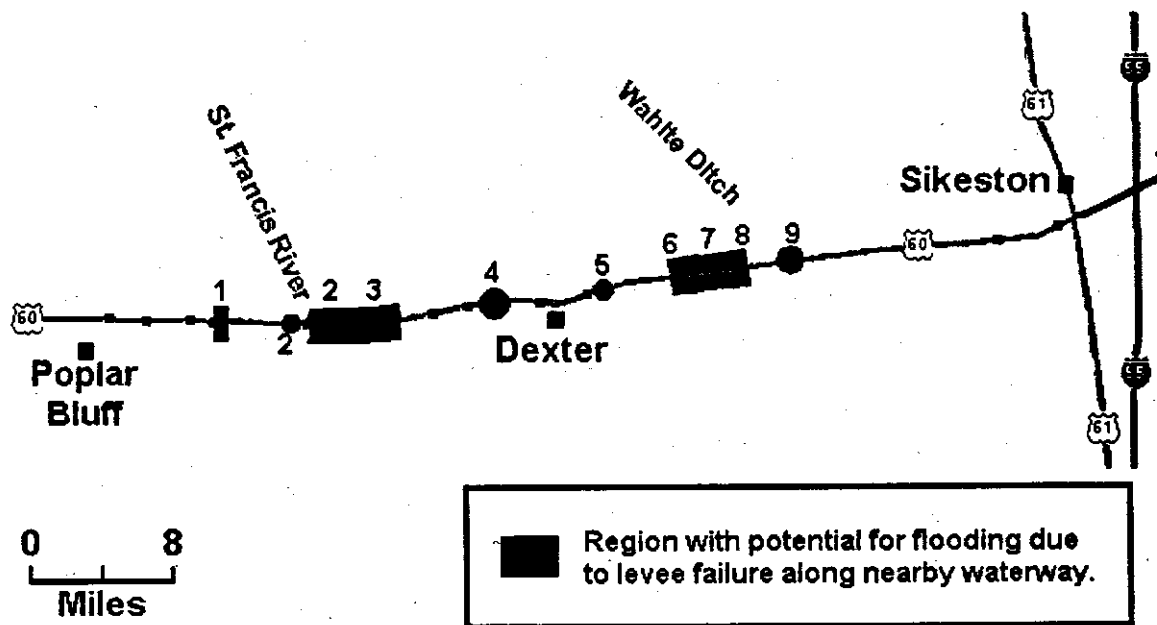


Figure 8.13 Region of Potential Flooding

## **8.1.7 Structure Response of Bridges and Abutments**

### **8.1.7.1 New St. Francis River Bridge**

The bridges of interest for this project are located near the New Madrid seismic zone in southeastern Missouri. These bridges were modeled in order to determine their susceptibility to earthquake damage under various ground motions. They were of particular concern for the Missouri Department of Transportation, as they are located on a key emergency route that must be kept open in the event of an earthquake.

#### **8.1.7.1.1 Bridge Description**

The bridge discussed in this section is denoted as Bridge A-3709, located in Butler-Stoddard County on US 60 where it crosses the St. Francis River. It was designed with seismic considerations according to the 1992 AASHTO Specifications. This 292 foot 8 inch bridge consists of three continuous spans supported by steel plate girders, as shown in Figure 8.14. The dimensions of these plate girders varied slightly within a span depending on the location of the tension flange. The interior diaphragms and the cross-frames each consist of two L 3x3x5/16 crossed over one another. The top and bottom horizontal members on the diaphragms and cross-frames were L 4x4x5/16. All interior diaphragms were placed perpendicular to the girders. The bridge, however, was placed at a 20° skew angle, so the ends of the girders were offset from one another at the ends of the bridge. The cross-frames were constructed differently than the diaphragms in that they were placed parallel to the abutments, and therefore were not perpendicular to the girders.

The bridge superstructure is supported by two intermediate bents through fixed neoprene elastomeric pads and two integral abutments at its ends. Each bent consists of a reinforced concrete cap beam and three reinforced concrete columns. Deep pile foundations support both bents and abutments. There are 20 piles for each column footing and 11 piles for each abutment footing.

#### **8.1.7.1.2 Bridge Model and Analysis**

In order to later analyze this bridge for susceptibility to earthquake damage, the structure was modeled with the finite element method in the *SAP2000* structural analysis program. In this program, the bridge can be modeled in three dimensions, and earthquake input data can be used to simulate how the bridge would respond in the event of an earthquake.

All of the components of the structure were included in the bridge model. These components include the girders, diaphragms, cross-frames, interior bents and columns, and the bridge deck. The deck was represented by 241 shell elements with a thickness of 8.5 inches. All girders, cross-frames, and diaphragms were modeled as 927 frame members. Each frame section was then assigned member properties, such as material type and cross-section dimensions. The model also included 792 nodes.

To further assist in modeling ground soil conditions, springs were used at the base of each column (six columns total, three on each interior bent). Also, springs were placed at the ends of the bridge on each abutment. The stiffness constants of the springs were taken from Appendix F.

Rigid elements were used to model the abutments in *SAP2000*. Because of their presence, the bridge is relatively stiff and is expected to experience small displacements during earthquakes. Therefore, a linear time-history analysis was used for the bridge model. For each analysis with one directional earthquake excitation, 30 Ritz-vectors were considered associated with the earthquake direction. In Table 8.6, a sampling of five of the significant vibration modes are listed with its period in seconds and a brief description of the motion represented within the given mode. It should be noted that the fundamental period of the bridge is 0.2519 seconds. In Figures 8.15-8.19, visual representations of the mode shapes described above are shown.

The bridge was analyzed under a total of twelve earthquake ground motions described in Section 8.1.3. Six of the twelve motions correspond to a 10% PE level while the others to a 2% PE level. At each PE level of earthquakes, three were considered as near-field and the other three as far-field. The internal loads such as shear and moments and the abutment displacements were obtained at various critical locations. They will be presented together with the vulnerability evaluation of structural members in the next section. It is noted that one bridge analysis was conducted for

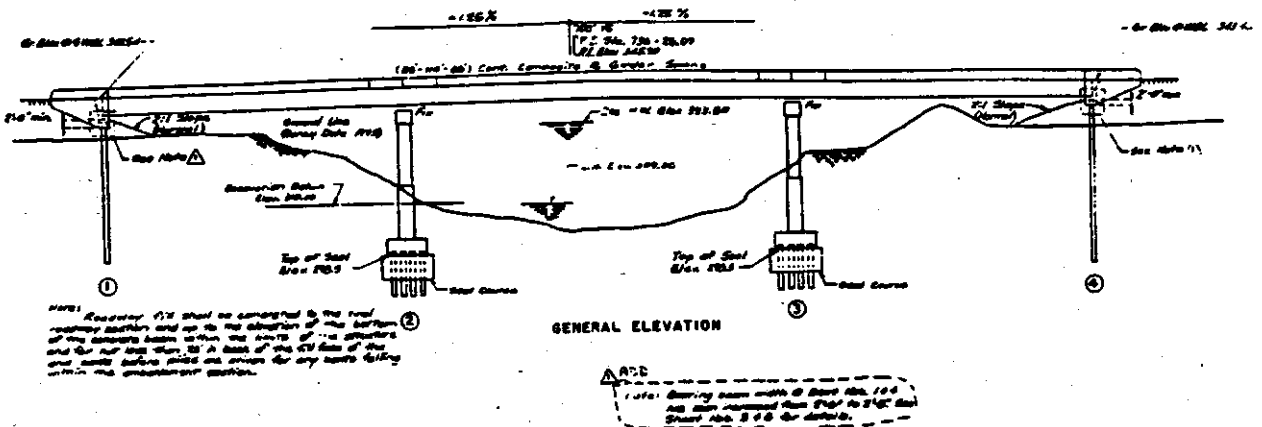
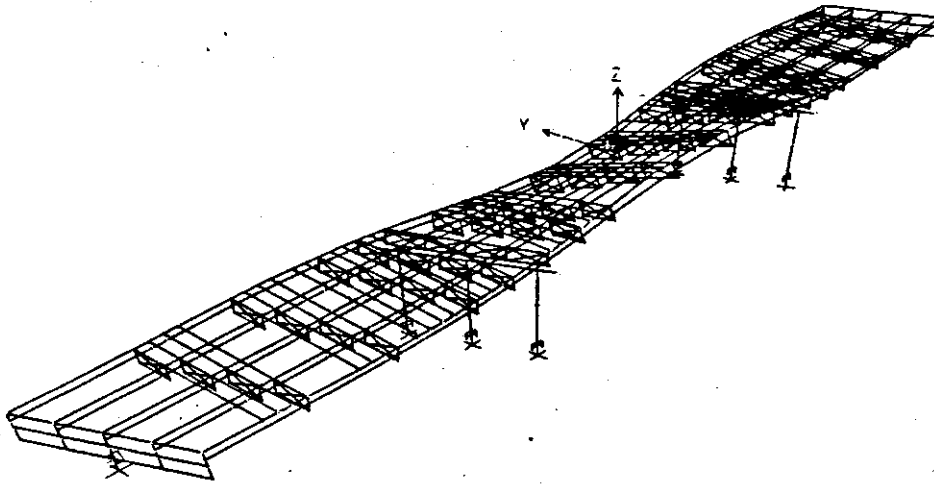


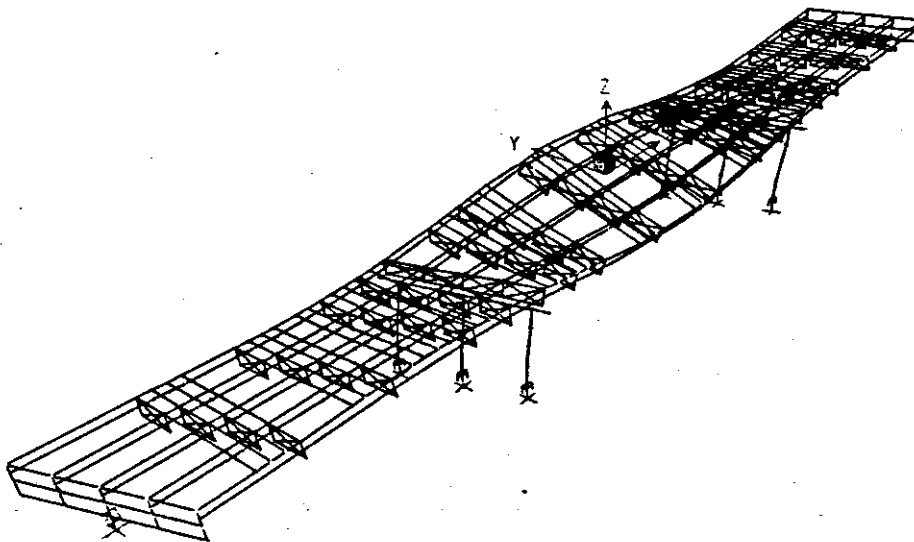
Figure 8.14 Bridge General Elevation (New St. Francis River Bridge)

Table 8.6 Natural Periods and Their Corresponding Vibration Modes (New St. Francis River Bridge)

Mode Number	Period (seconds)	Motion Description
1	0.2519	Transverse
2	0.2295	Transverse
3	0.1421	Vertical
4	0.0901	Longitudinal
5	0.0896	Longitudinal



**Figure 8.15** Mode 1, Period 0.2519 Seconds (New St. Francis River Bridge)



**Figure 8.16** Mode 2, Period 0.2295 Seconds (New St. Francis River Bridge)

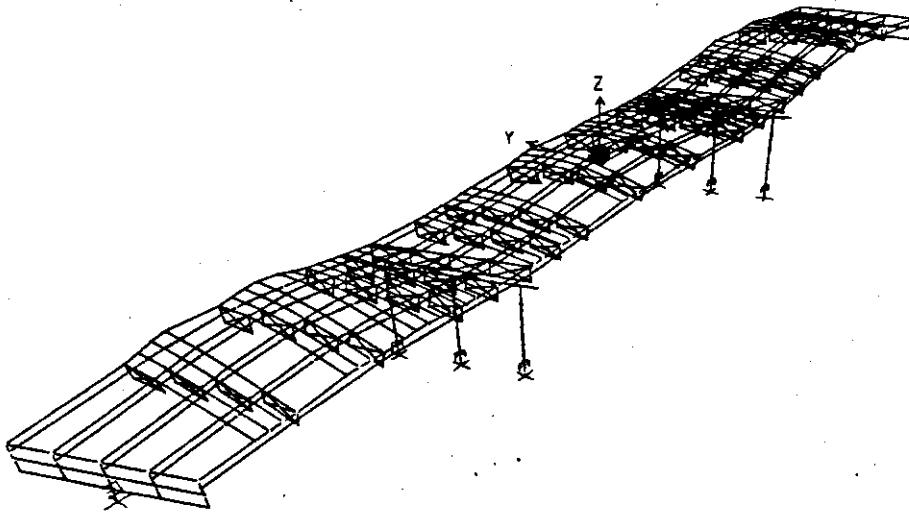


**Figure 8.17** Mode 3, Period 0.1421 Seconds (New St. Francis River Bridge)

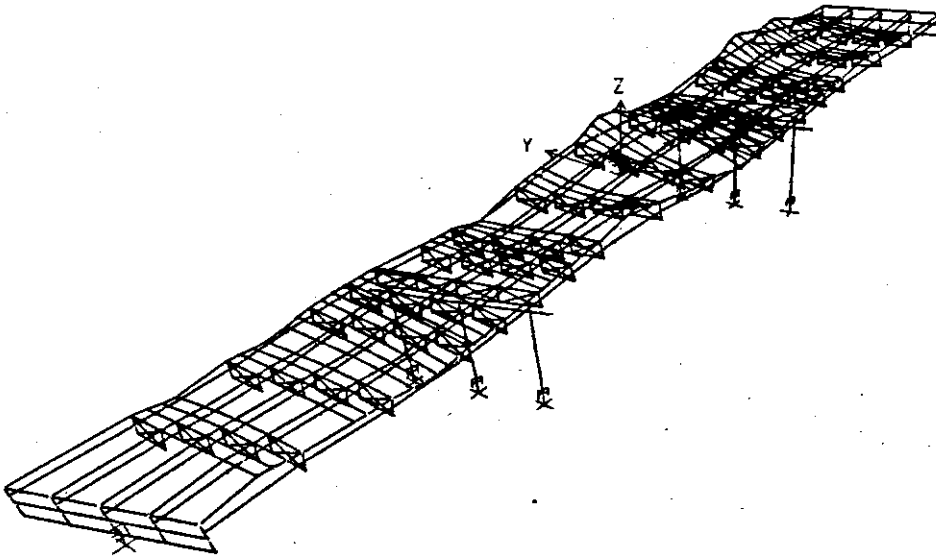


**Figure 8.18** Mode 4, Period 0.0901 Seconds (New St. Francis River Bridge)

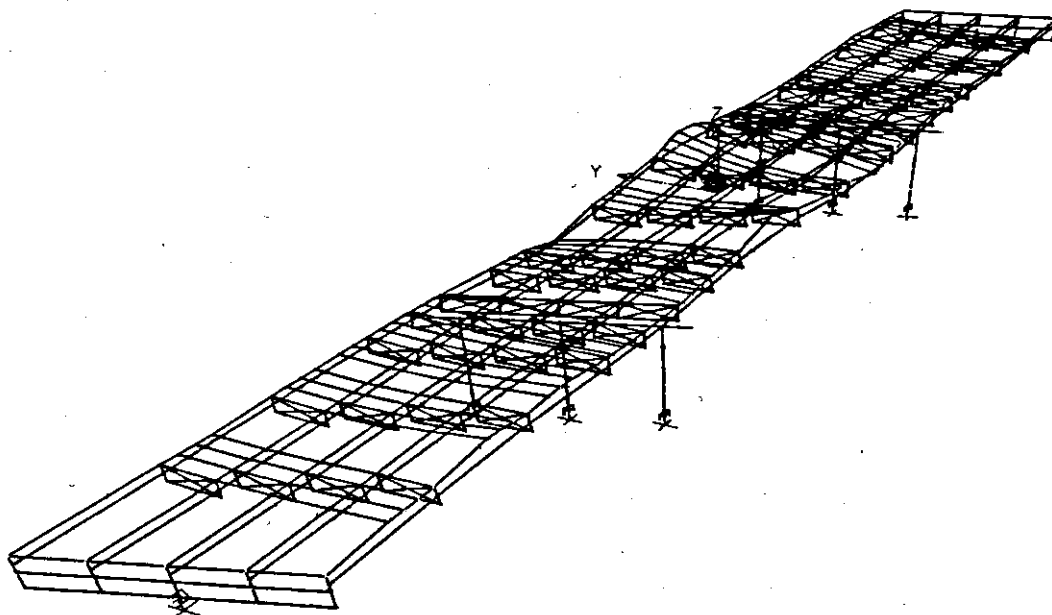


**Figure 8.19 Mode 5, Period 0.0896 Seconds (New St. Francis River Bridge)**

each directional earthquake excitation due to the special directional combination rule specified in the AASHTO Specifications (1996). Consequently, a total of 36 runs were completed.

### **8.1.7.1.3 Detailed Description of Bridge Evaluation**

This section is delineated according to the various sections labeled on the spreadsheet of analysis and results. Each section explains the method and reasoning behind the calculations. The methods outlined here are mainly taken from the FHWA Seismic Retrofitting Manual for Highway Bridges (1995) with necessary modifications based on engineering judgment.

The purpose of the analysis was to form a quantitative summary of which components “pass” and which “fail” due to earthquake motions. To do this, the FHWA Manual outlined a method for determining Capacity / Demand ratios, which will further be referred to as C/D ratios. The concept is relatively simple, with the goal to determine whether a component’s capacity is greater than its demand. If so, the ratio will be greater than one, indicating that there should be no problems associated with that component. If the capacity is less than the demand, the ratio will be less than one, indicating that problems may arise with that component in the event of an earthquake. Although no method is foolproof, these ratios do yield a reasonably accurate measure of the performance of the structure.

#### **8.1.7.1.3.1 Load Combination Rule**

For all force (moment, shear, axial) and displacement C/D ratios in this analysis, the 30% Combination Rule was used (AASHTO Division I-A, Section 3.9, 1996) for the effect of two horizon-

tal ground motions that are perpendicular to each other. This rule states that the forces/displacements due to transverse and longitudinal earthquake motions are added as follows:

CASE I:  $0.3 * (\text{force/displacement}_{\text{due to transverse}}) + 1.0 * \text{force/displacement}_{\text{due to longitudinal}}$

CASE II:  $0.3 * (\text{force/displacement}_{\text{due to longitudinal}}) + 1.0 * \text{force/displacement}_{\text{due to transverse}}$

The above relationship would be used for forces/displacements in both the longitudinal and transverse directions. The larger of CASE I and II would then be combined with the force/displacement due to the vertical earthquake motion, using a square-root-of-the-sum-of-the-squares relationship (SRSS).

This combination rule was used in several instances throughout these calculations for various types of demands on the structure (shear, moment, and axial forces, as well as transverse and longitudinal displacements).

#### **8.1.7.1.3.2 Minimum Support Length and C/D Ratio for Bearing**

Because this bridge has integral abutments, there are no expansion joints, and therefore there is no need to calculate this capacity/demand ratio. This C/D ratio is only applicable for bridges with seat-type abutments, which are susceptible to the dropping of exterior spans during earthquake motion.

#### **8.1.7.1.3.3 C/D Ratios for Shear Force at Bearings**

The first C/D ratios calculated in this section define the behavior of the bolts located at the neoprene elastomeric pads on the cap beams at the interior bents. In both the transverse and the longitudinal directions, there are two bolts for capacity. From the bridge analysis the shear demand at each of these points was determined and the maximum demand among these points was used to compute the C/D ratio for the "worst case". Before these shear values were used in determining the C/D ratios, the values were compared to 20% of the axial dead load at that location (FHWA, 1995). The greater of these two values were used in the subsequent calculations.

The second set of C/D ratios in this section involves the embedment length and edge distance requirements for the bolts discussed in the previous paragraph. First, the required embedment length was found from Table 8-26 of the LRFD AISC Manual (1998). This length, for the 2.5-inch diameter rods that were used on this bridge, is 42.5 inches. From the plans, it is noted that the rods only extend 25 inches into the concrete. With the check, this results in a C/D ratio less than one, which would indicate a possible failure due to axial forces acting on the bolts.

Finally, the edge distance was checked using another C/D ratio. From the same AISC table that provided the embedment lengths, allowable edge distances were also provided. For the rods used here, the required distance is 17.5 inches. The actual edge distance was estimated from the

plans to be approximately 20 inches. This indicates that there should be no problems with the edge distance provided for the bolts.

Figure 8.20 shows that the combination rule in Section 8.1.7.1.3.1 was used to combine the shear demands from all directions.

#### 8.1.7.1.3.4 C/D Ratios for Columns/Piers

In this section, the C/D ratios were calculated for all circular columns on the interior bents. Both the moment demand and capacity are determined below.

*Elastic Moment Demand.* The first step was to note the elastic moment demands for the top and bottom of each column in the transverse and longitudinal directions due to transverse, longitudinal, and vertical earthquake motions. They are listed in Tables 8.7, 8.8, and 8.9. The moments were then combined as per the rule discussed in Section 8.1.7.1.3.1. The resulting moments from the combination were algebraically combined with the moment due to the dead load. Finally, the total transverse moment demand and the total longitudinal moment demand are combined by squaring each term, summing them, and then taking the square root to get the final resulting moment demand. This final calculation yields the value that is ultimately used in C/D ratio calculations. These final moment demands are shown in Table 8.10.

*Moment Capacity.* To determine the capacities of these columns, the P-M interaction diagram for the given column cross-section was used. Given an axial compressive force due to the dead load (found from the bridge analysis), a moment capacity was found from the interaction diagram. From these moment capacities, column shear forces were found. From these shear forces, axial forces due to overturning were found. These axial forces due to overturning were combined with the axial dead loads to give new axial totals. From these new axial forces, new moment capacities were found from the interaction diagrams. These moments were then used to find new column shear forces. These shear forces were compared to the ones found previously (using the axial forces which did not include the overturning effect). If these shear forces were within 10% of the originals, no further iterations would be required. Otherwise, the cycle would need to be repeated until the shear forces were within the 10% limit (AASHTO, 1996). Refer to Figure 8.21 for this procedure. In this case, the shears were within the 10% limit, so no iterations were required. However, the final capacities used for the C/D ratios reflect the use of the newest shear values to obtain updated axial forces. The change was very minimal, but the final moment capacities do include the change.

Finally, the maximum demand from the possible combinations was then used in conjunction with the determined capacity for the column to determine a C/D ratio for the columns. In most cases, the C/D ratios were well below one, indicating insufficient column strength for elastic seismic demand. However, when the columns experience inelastic deformation, the seismic demand reduces due to energy dissipation. To account for the above effect, the ductility indicator was used with these ratios (FHWA, 1995). Since the two interior bents each had multiple columns, ductility of 5 was applied to each ratio (AASHTO, 1996). In all cases, this multiplier increased the ratios to values above one. Table 8.11 summarizes the moment C/D ratios. As noted above, the capacities in this table are slightly different than those in Figure 8.21, as they reflect the change

due to the updated shear and axial forces. This note was made simply for the sake of explaining the origin of the capacity values. Within the section where column moment capacities were examined, FHWA (1995) also outlined guidelines for examining capacities for the footings of the columns as well. Assuming a fixed pile cap, the moment and axial compressive strength for each pile foundation are both determined approximately by the vertical pile capacity. Using simple geometry concepts and forming relationships between axial compressive loads, moments, rotations of the footing (denoted as  $\theta$ ), and displacements due to these rotations (denoted as  $\delta$ ), capacities of the footings were calculated.

The procedure involved first determining moments corresponding to various  $\theta$  values. A moment-rotation curve was then plotted for a constant value of axial load (such as zero). The footing capacity corresponding to the case of  $P = 0$  kips was calculated for this bridge. Assuming that  $P = 0$ , various values of  $\theta$  were examined. For each different  $\theta$ , pile displacements were determined, and using these displacements multiplied by the pile stiffness, axial loads were found. These axial loads were then used in a basic summation of moment equation. It was from this summation of moments equation that the moment value was taken for the moment-rotation plot. The plateau of this curve is taken as the moment capacity

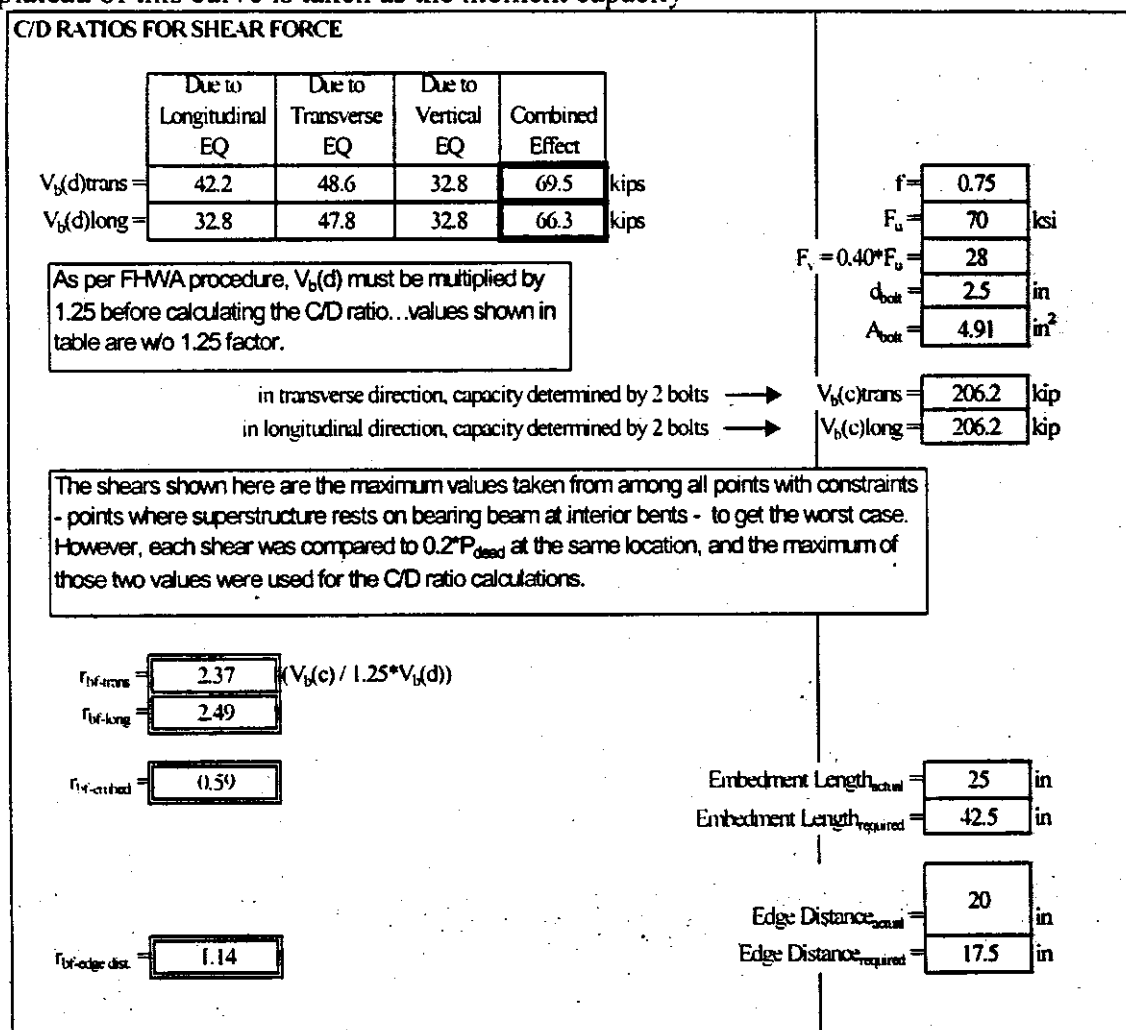


Figure 8.20 Shear Force Calculations

for the corresponding  $P$  value. It is well known that the moment capacity would increase with increasing  $P$  values so long as they are less than the balanced axial force. Because it was noted that the moment capacity for the case of  $P = 0$  is considerably higher than the capacities of the columns (several orders of magnitude greater), it was deemed unnecessary to proceed with the entire process of determining  $C/D$  ratios for these footings, as they would clearly be more than adequate. The moment versus rotation relation for the case of axial load equal to zero is plotted in Appendix H.

**Table 8.7 Elastic Moments Due to Transverse Acceleration**

(kip-inch units)			Transverse Moment, $M_T^{(T)}$	Longitudinal Moment, $M_L^{(T)}$
SAP fr. #	Location	Component	EQ	EQ
21	Bent 2, top	column 1	28416	8768
24	bottom	column 1	-53652	-12804
30	Bent 2, top	column 2	33884	12241
42	bottom	column 2	-56823	13912
52	Bent 2, top	column 3	27290	11790
64	bottom	column 3	-52163	-16809
16	Bent 3, top	column 4	27171	11744
96	bottom	column 4	-52043	-16778
103	Bent 3, top	column 5	33781	12191
216	bottom	column 5	-56689	-15938
300	Bent 3, top	column 6	28131	8663
529	bottom	column 6	-53427	-12698

**Table 8.8 Elastic Moments Due to Longitudinal Acceleration**

(kip-inch units)			Transverse Moment, $M_T^{(L)}$	Longitudinal Moment, $M_L^{(L)}$
SAP fr. #	Location	Component	EQ	EQ
21	Bent 2, top	column 1	-699	-263
24	bottom	column 1	1618	2227
30	Bent 2, top	column 2	790	303
42	bottom	column 2	1792	2136
52	Bent 2, top	column 3	-806	-306
64	bottom	column 3	1697	2074
16	Bent 3, top	column 4	-795	316
96	bottom	column 4	1717	2094
103	Bent 3, top	column 5	-922	296
216	bottom	column 5	1817	2136
300	Bent 3, top	column 6	-680	-245
529	bottom	column 6	1644	2207

**Table 8.9: Elastic Moments Due to Vertical Acceleration**

(kip-inch units)			Transverse Moment, $M_T^{(V)}$	Longitudinal Moment, $M_L^{(V)}$
SAP fr. #	Location	Component	EQ	EQ
21	Bent 2, top	column 1	-252	115
24	bottom	column 1	-975	-373
30	Bent 2, top	column 2	604	166
42	bottom	column 2	-1305	-463
52	Bent 2, top	column 3	940	346
64	bottom	column 3	-1532	-359
16	Bent 3, top	column 4	-865	-340
96	bottom	column 4	1438	468
103	Bent 3, top	column 5	-591	-172
216	bottom	column 5	1256	662
300	Bent 3, top	column 6	-297	115
529	bottom	column 6	900	615

**Table 8.10 Summary of All Moment Demands**

Elastic Moment Demands - TOTAL including combined 3 directions (kip-inch units)									
SAP fr. #	Location	Component	Transverse Moment			Longitudinal Moment			Elastic Moment Demand
			EQ (from transverse & longitudinal input)	EQ (from vertical input)	DL	EQ (from transverse & longitudinal input)	EQ (from vertical input)	DL	
21	Bent 2, top	column 1	28626	-252	-533	8847	115	-178	30525
24	bottom	column 1	54137	-975	543	13472	-373	-186	56370
30	Bent 2, top	column 2	34121	604	-89	12332	166	-17	36376
42	bottom	column 2	57361	-1305	258	14553	-463	-280	59513
52	Bent 2, top	column 3	27532	940	401	11882	346	114	30416
64	bottom	column 3	52672	-1532	-58	17431	-359	-348	55669
16	Bent 3, top	column 4	27410	-865	-377	11839	-340	-110	30261
96	bottom	column 4	52558	1438	25	17406	468	339	55517
103	Bent 3, top	column 5	34058	-591	116	12280	-172	17	36324
216	bottom	column 5	57234	1256	-293	16579	662	272	59961
300	Bent 3, top	column 6	28335	-297	561	8737	115	203	30249
529	bottom	column 6	53920	900	-576	13360	615	155	56158

1) Using P-M diagrams for columns from SAP2000 to create following table:

Bent	End	Axial Force		
		(due to DL)	1.3 Mu	Mu
2	top	262	38163	29356
2	bottom	335	56690	43608
3	top	260	38151	29347
3	bottom	332	56664	43588

2) Column Shear Forces (forces are per column, so total shear for one bent = 3 \* 266)

Bent 2:  $V_u = \frac{266}{3} (M_{top} + M_{bottom}) / L_{col}$   
 Bent 3:  $V_u = \frac{266}{3} (M_{top} + M_{bottom}) / L_{col}$

$L_{col-bent 2} = 29.7$  ft  
 $L_{col-bent 3} = 29.7$  ft

3) Axial Forces due to Overturning

Bent 2:  $P = \frac{730}{3} (3 * V_u * L_{col}) / D$   
 Bent 3:  $P = \frac{729}{3} (3 * V_u * L_{col}) / D$

$D = 32.5$  ft  
 (distance between columns)

4) Revision of Moment Capacity for Iterations

- Take new axial forces (P, from 3))
- Using P's, get new  $M_{top}$ ,  $M_{bottom}$
- Using new  $M_{top}$ ,  $M_{bottom}$ , get new column shear forces
- Compare new shear forces to original ones -- are they within 10%?
- If not, get new P's and try again, otherwise, use new shears to get new P's and move on

Bent	End	Axial Force	1.3 Mu	Mu
2	top	-468	31324	24095
2	top	992	43306	33312
2	bottom	-395	42405	32619
2	bottom	1065	63324	48711
3	top	-469	31303	24079
3	top	989	43284	33295
3	bottom	-397	42353	32579
3	bottom	1061	63283	48679

Revised Shear Capacity:

Bent 2:  $V_u = (M_{top} + M_{bottom})_{min} / L_{col} + (M_{top} + M_{bottom})_{max} / L_{col}$   
 $V_u = 759.1$

Bent 3:  $V_u = (M_{top} + M_{bottom})_{min} / L_{col} + (M_{top} + M_{bottom})_{max} / L_{col}$   
 $V_u = 758.5$

For each bent (2 & 3): This revised capacity accounts for 2 columns. Since the bent has 3 columns, multiply value by 1.5 to get shear for entire bent.

Compare to  $266 * 3$  (for one bent from above w/ 3 columns):  $798$   
 Check: YES - OK (within 10% - move on)

Figure 8.21 Calculations of Axial Loads and Column Shears

**Table 8.11 Summary of Moment C/D Ratios for Columns**

Bent	End	Axial Load	Column		$r_{ec}$ -initial	$r_{ec}$ -final
			Demand	Capacity		
2	top	minimum	36376	25225	0.69	3.47
2	top	maximum	36376	13462	0.37	1.85
2	bottom	minimum	59513	46083	0.77	3.87
2	bottom	maximum	59513	30952	0.52	2.60
3	top	minimum	36324	25225	0.69	3.47
3	top	maximum	36324	13462	0.37	1.85
3	bottom	minimum	59961	46083	0.77	3.84
3	bottom	maximum	59961	30952	0.52	2.58

Final C/D ratios are equal to initial ratios multiplied by 5, which is the ductility indicator.

NOTE: Capacities are *not* multiplied by 1.3

### 8.1.7.1.3.5 C/D Ratios for Hooked Anchorage in Columns

For both the top and bottom of the columns, the adequacy of the anchorage of longitudinal reinforcement must be checked. The capacity was determined simply by finding the length of hooked anchorage at both the top and bottom of the columns. The demand was determined from an equation outlined in the FHWA Seismic Retrofit Manual (1995).

In both the tops and the bottoms of the columns, the length of anchorage required was less than the actual length, as taken from the plans. The value for the C/D ratio was found from Figure 78 from the FHWA Manual, and this table was set up in terms of the anchorage geometry and location of the anchorage. In this case, the C/D ratio value of 1.0 was not the ratio of  $l_a(c)$  to  $l_a(d)$ . The aforementioned figure from the FHWA Manual assigned values for C/D ratios depending on the location of the anchorage (top/bent cap or bottom/footing), as well as the relationship of the capacity length to the demand length. Based on these parameters, the value assigned for these C/D ratios is 1.0. The calculations are shown in Figure 8.22.

### 8.1.7.1.3.6 C/D Ratios for Splices in Longitudinal Reinforcement

In this section, a C/D ratio was determined for the adequacy of the splicing of the longitudinal reinforcement. The formula used to determine the demand was again taken from the FHWA Retrofit Manual. The capacity was also found based on the definition from the Manual. Because the C/D ratio depends on the column moment C/D ratio,  $r_{ec}$ , an adjustment needed to be made. An attempt was made to determine the actual stress in the steel due to the external moment, and then divide the yield stress of the reinforcement (60 ksi) by this actual stress to form a ratio of the stresses. This ratio would likely be greater than one, therefore increasing the C/D ratio for the splices in the longitudinal reinforcement. The method used a reinforced concrete relationship to determine steel stresses at service loads. This method did increase the C/D ratio as expected. For all cases, both for 2% and 10% ground motions, the adjusted C/D ratios were raised above one, indicating that there will likely be minimal concerns with these splices. All calculations are shown in Figure 8.23.

C/D RATIOS FOR HOOKED ANCHORAGE IN COLUMNS, $r_{ca-bottom}$									
$l_a(c) = $ <table border="1"><tr><td>36</td><td>in</td></tr></table> $l_a(d) = $ <table border="1"><tr><td>19.477</td><td>in</td></tr></table> $r_{ca-bottom} = $ <table border="1"><tr><td>1.0</td></tr></table>	36	in	19.477	in	1.0	$1200 * k_{m1} * d_b * (f_y / (60000(f_c^{0.5})) \text{ or } 15 * d_b)$ (choose larger)			
36	in								
19.477	in								
1.0									
<table border="1"> <tr><td><math>k_{m1} = </math></td><td>0.7</td></tr> <tr><td><math>d_b = </math></td><td>1.27 in</td></tr> <tr><td><math>f_y = </math></td><td>60000 psi</td></tr> <tr><td><math>f_c = </math></td><td>3000 psi</td></tr> </table>		$k_{m1} = $	0.7	$d_b = $	1.27 in	$f_y = $	60000 psi	$f_c = $	3000 psi
$k_{m1} = $	0.7								
$d_b = $	1.27 in								
$f_y = $	60000 psi								
$f_c = $	3000 psi								
C/D RATIOS FOR HOOKED ANCHORAGE IN COLUMNS, $r_{ca-top}$									
$l_a(c) = $ <table border="1"><tr><td>36</td><td>in</td></tr></table> $l_a(d) = $ <table border="1"><tr><td>19.477</td><td>in</td></tr></table> $r_{ca-top} = $ <table border="1"><tr><td>1.0</td></tr></table>	36	in	19.477	in	1.0	$1200 * k_{m1} * d_b * (f_y / (60000(f_c^{0.5})) \text{ or } 15 * d_b)$ (choose larger)			
36	in								
19.477	in								
1.0									
<table border="1"> <tr><td><math>k_{m1} = </math></td><td>0.7</td></tr> <tr><td><math>d_b = </math></td><td>1.27 in</td></tr> <tr><td><math>f_y = </math></td><td>60000 psi</td></tr> <tr><td><math>f_c = </math></td><td>3000 psi</td></tr> </table>		$k_{m1} = $	0.7	$d_b = $	1.27 in	$f_y = $	60000 psi	$f_c = $	3000 psi
$k_{m1} = $	0.7								
$d_b = $	1.27 in								
$f_y = $	60000 psi								
$f_c = $	3000 psi								

Fi

Figure 8.22: Calculations for Hooked Anchorage in Columns

### 8.1.7.1.3.7 C/D Ratio for Transverse Confinement

The calculations in this section were similar to those in the previous section. Again, an FHWA-defined relationship was used to determine the adequacy of the transverse confinement. The relationship defined for the transverse confinement did include a multiplier. This multiplier was dependent on adequacy of transverse confinement. Also, this C/D ratio was again dependent on the column moment C/D ratio,  $r_{ec}$  (without including the ductility indicator), several factors, including geometry of the confinement as well as properties of the column reinforcement, the concrete, and the column cross-section.

The C/D ratios for all cases were above one. This indicates that there should be minimal problems with transverse confinement. All aforementioned calculations are shown in Figure 8.24.

### 8.1.7.1.3.8 C/D Ratio for Column Shear

In this section, a determination was made for column shear forces. On the spreadsheet, several parameters were calculated, as per the methodology outlined in the FHWA Manual. The maximum elastic shear force in the column was determined from the bridge analysis ( $V_e(d)$ ). The maximum column shear force,  $V_u(d)$  was found earlier when determining the ultimate moment capacities in Section 8.1.7.1.3.4. The other two parameters,  $V_i(c)$  and  $V_f(c)$ , are the initial and final shear capacities of the column, respectively. The initial shear capacity was determined using equation 11-4 from ACI 318-99. This equation was to be used to find the shear

### C/D RATIOS FOR SPLICES IN LONGITUDINAL REINFORCEMENT, $r_{cs}$

$$A_{tr}(d) = \frac{0.04536}{0.2} = ((s \cdot f_y) / (l_c \cdot f_{yt})) \cdot A_{b, \text{splice}}$$

$$r_{cs} = \frac{0.74}{0.2} = (A_{tr}(c) / A_{tr}(d)) \cdot r_{ec} \leq 2r_{ec}$$

NOTE:  $r_{ec}$  is from the moment section - using minimum  $r_{ec}$  value to obtain "worst case"; however, the initial value was used without the ductility indicator.

NOTE: because  $r_{cs}$  depends on the moment C/D ratio, which was increased by the ductility indicator, it must be determined whether  $r_{cs}$  can also be increased. Using the ACI equation for determining steel stress at service loads, we can form a ratio of the maximum stress in the steel to the actual stress in the steel under the given moment (output from SAP2000).

$$f_s = M / A_s \cdot j \cdot d$$

M =	23955	(from SAP2000 output -- moment from column corresponding to the $r_{cs}$ used above)
A <sub>s</sub> =	33.02	in <sup>2</sup>
j =	0.944	
d =	46.5	in
f <sub>s</sub> =	16.53	

(j = 1-k/3 ; k = (2pn+(pn)<sup>2</sup>)/2-pn ; p = A<sub>s</sub>/A<sub>concrete</sub> ; n = E<sub>s</sub>/E<sub>c</sub>  
where E<sub>s</sub> = 29000 ksi, E<sub>c</sub> = 3120 ksi)

$$r_{cs-adj} = 2.69$$

s =	3	in
f <sub>y</sub> =	60000	psi
l <sub>c</sub> =	84	in
f <sub>yt</sub> =	60000	psi
A <sub>b, splice</sub> =	1.27	in <sup>2</sup>

Figure 8.23 Calculations for Splices in Longitudinal Reinforcement

### C/D RATIOS FOR TRANSVERSE CONFINEMENT, $r_{cc}$

$$r_{cc} = 3.33 = \mu r_{ec}$$

NOTE:  $r_{ec}$  is from the moment section - using minimum  $r_{ec}$  value to obtain "worst case"; however, the initial value was used without the ductility indicator.

Assume transverse steel is effectively anchored, so  $k_3 = 1$

(r(d) according to AASHTO Specifications, Division I-A, Section 7.6)

μ =	6	
k <sub>1</sub> =	1	
k <sub>2</sub> =	1	
k <sub>3</sub> =	1	
ρ(c) =	0.0050	
ρ(d) =	0.00554	
P <sub>c</sub> =	355	kip
f <sub>c</sub> =	3	ksi
A <sub>s</sub> =	1809.6	in <sup>2</sup>
s =	3	in
d <sub>b</sub> =	1.27	in
b <sub>min</sub> =	48	in

Figure 8.24 Calculations for Transverse Confinement

capacity of members subjected to axial compression. The final shear capacity of the column was defined in the FHWA Manual. If the axial force, which was taken as approximately 425 k (the approximate largest axial load experienced by any column), divided by the column cross-sectional area was greater than 0.1 of  $f'_c$ , then  $2\sqrt{f'_c}$  was to be used (FHWA, 1995). If the axial stress was less than 0.1 $f'_c$ , then a value of zero was to be assumed for  $V_f(c)$ . In this case,  $V_f(c)$  was zero. In addition, by assuming a value of zero for the final capacity, the results are slightly more conservative. The procedure and formulas for these parameters are noted below. From these parameters, a "Case" needed to be chosen, based on the flow chart from Figure 81 in the FHWA Manual (1995). This flow chart outlined the process for determining the column shear C/D ratio. The original moment C/D ratios without the ductility indicator are used in these calculations.

In all cases of 2% motions, "Case B" was chosen, based on definitions from the FHWA Manual. This case was needed because at least one of the moment C/D ratios was less than one for each earthquake. This case was applicable when  $r_{ec}$  (column moment C/D ratio) was less than one and  $V_f(c) > V_u(d) > V_f(c)$ . When "Case B" was used, the relationship for the column shear C/D ratio was the column moment C/D ratio multiplied by an FHWA-defined multiplier. This multiplier, as shown in the spreadsheet, was based on column geometry ( $L_c$  = length of column and  $b_c$  = width of column) as well as the various shear parameters defined at the start of the section.

For the 10% motions, "Case B" did not apply because the initial C/D ratios for the columns under these earthquakes were above one. Therefore, the C/D ratios for these earthquakes were determined simply as a ratio of the initial capacity of the column to the maximum shear force in the column. All calculations are shown in Figure 8.25.

#### 8.1.7.1.3.9 C/D Ratio for Diaphragm and Cross-Frame Members

This section examines the damage caused to the diaphragm and cross-frame members for the bridge. Both the diaphragms and the cross-frames can be analyzed using the same method because they are both composed of the same sections (each consisted of two L 3x3x5/16 crossed over each other with L 4x4x5/16 as the top and bottom horizontal members). Because of very low moments on these members, the members were analyzed based on their axial load capacity and demand.

There are two calculations shown for the same capacity/demand ratio. The first uses the full length of the member spanning diagonally from top to bottom of the diaphragm/cross-frame. However, since there is a welded connection in the center where the diagonal members meet, the second calculation uses half of the total length of the member. This was done because of the possibility of failure within this connection, thus removing the intermediate brace. It should be noted that the members were modeled as two halves put together to make a full-length diagonal member for the diaphragms and cross-frames. This was done with the hopes of more closely modeling the actual bridge conditions.

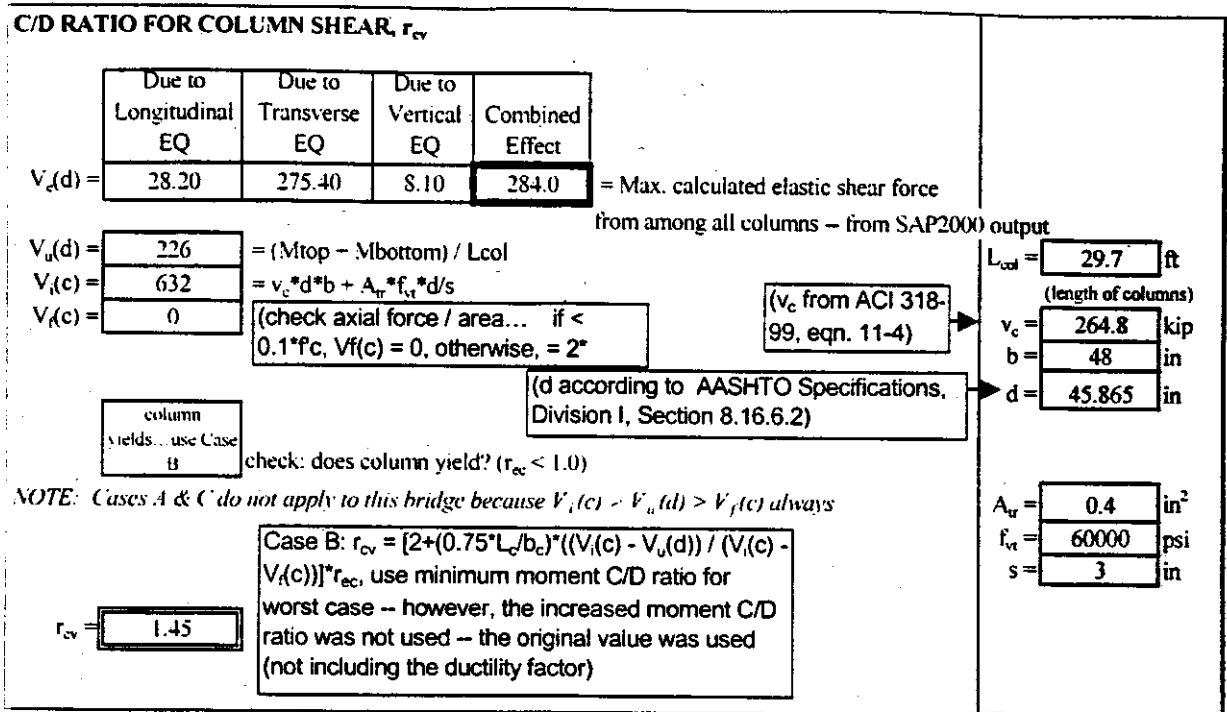
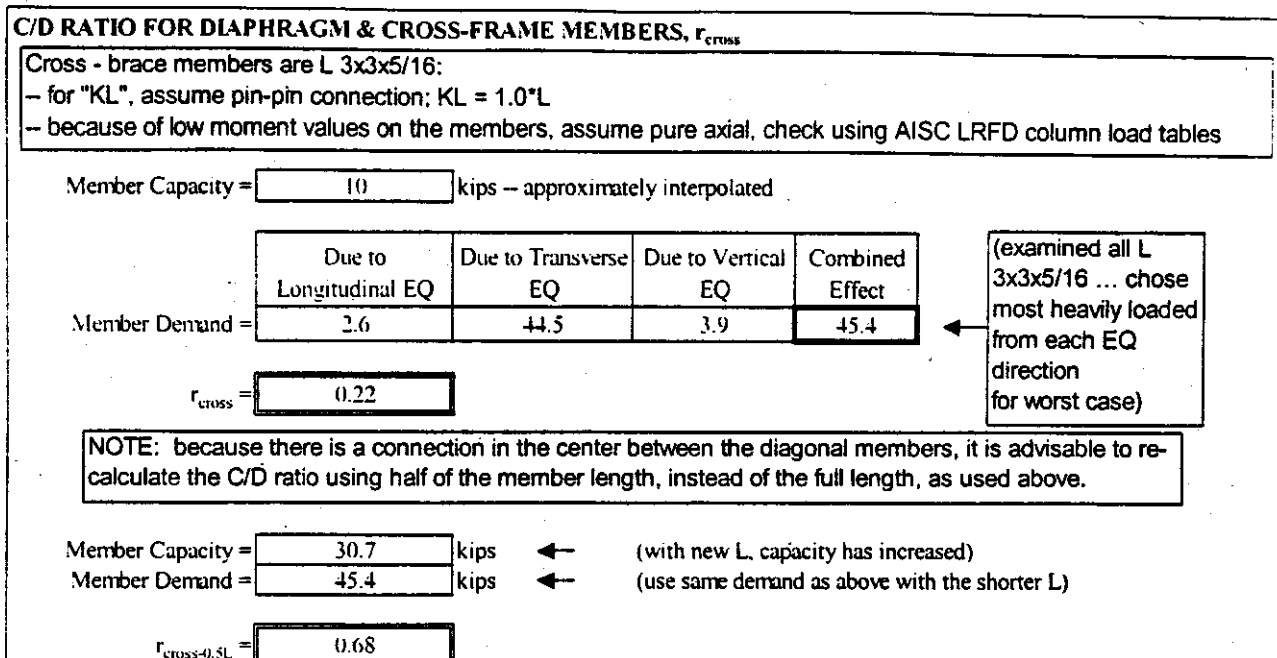


Figure 8.25 Calculations for Column Shear

The axial capacities for these members were estimated using load tables from the AISC Manual (1998). The total load demand on these members was determined using the combination rule described in Section 8.1.7.1.3.1. The calculations are shown in Figure 8.26.

#### 8.1.7.1.3.10 C/D Ratio for Abutment Displacements

The final section of the spreadsheet outlines the check for abutment adequacy. This test involves comparing the actual abutment displacements to maximum displacement values given by FHWA. These maximum values from FHWA are based on previous experiences due to past earthquakes and engineering judgment. The values are given as three inches of allowable displacement in the transverse direction and six inches of allowable displacement in the longitudinal direction.



**Figure 8.26** Calculations for Diaphragm and Cross-Frame Members

Similar to the determination of elastic moment demands for the columns, the abutment displacements due to all three directions of earthquake motions were also combined using the rule specified in Section 8.1.7.1.3.1. Figure 8.27 lists the maximum transverse and longitudinal abutment displacements due to the transverse, longitudinal, and vertical earthquake ground motions. The displacements were then combined as per the combination rule.

In all cases, no problems were encountered due to abutment displacements. The C/D ratios were always well over one, indicating that the abutments should remain relatively damage-free (at least due to displacement) in the event of an earthquake. Refer to Figure 8.27 for abutment displacements calculations.

#### 8.1.7.1.4 Summary of Problem Areas

Based on the step-by-step procedure illustrated in Section 8.1.7.1.3, the bridge was evaluated under twelve ground motions that were selected in Section 8.1.3. A sample summary table of all C/D ratios for one earthquake is shown in Table 8.12. A summary of all C/D ratios for all earthquakes for this bridge is shown in Table 8.13. It can be observed from Table 8.13 that the bridge experienced minimal problems. As expected, the bridge generally performed more poorly under the influence of the 2% likelihood earthquakes, which were considerably stronger than the 10%

C/D RATIOS FOR ABUTMENTS, $r_{ad}$				
	Due to Longitudinal EQ	Due to Transverse EQ	Due to Vertical EQ	Combined Effect
maximum transverse displacements:	0.002057	0.0700	0.0009462	0.070623
maximum longitudinal displacements:	0.0523	0.1259	0.018	0.142730

$r_{ad-trans}$	42.48	(= 3" capacity in transverse direction; maximum transverse displacement from above)
$r_{ad-long}$	42.04	(= 6" capacity in longitudinal direction; maximum longitudinal displacement from above)

**Figure 8.27** Calculations for Abutment Displacements

likelihood earthquakes. In some instances, C/D ratios for various components of the structure were increased by multipliers and thus indicated no problems because their values were raised above one. However, it would be advisable to pay careful attention to areas such as columns, for extensive inelastic deformations could occur at these locations.

Of main concern are the diagonal members in the cross-frames and diaphragms of the bridge. The C/D ratios for these members were raised above one in some cases by using the half-length of the member due to the presence of a weld connection between two diagonal members crossing over each other. However, for four of the 2% earthquakes, the ratios still fell below one, indicating that the members may need to be retrofitted. In the other two 2% earthquakes, the C/D ratio was raised to exactly one, indicating that the capacity is just barely enough.

The strength of the weld at the intermediate brace of the diagonals was calculated to be approximately 33.4 kips. According to the bridge analysis, several of the 2% PE motions would likely cause this weld to fail, since all the axial demands for those earthquakes are greater than 33.4 kips (range from 33 to 45 kips). However, the 10% PE motions do not appear to cause this problem, as the axial loads for those motions range from 9 to 18 kips.

#### 8.1.7.1.5 Time History Analysis vs. Response Spectrum Analysis

In order to verify that the response spectrum analysis is as reliable as the time history analysis, several cases of the response spectrum analysis were run on SAP2000 to compare to the time history results used for this evaluation.

Tables 8.14, 8.15, and 8.16 show the average of forces or displacements at several key locations (bottom of column 2, bottom of column 5 and for the maximum abutment displacement) on the structure for four 2% motions and also for four 10% motions. The averages for the response spectrum analysis were compared to the averages for the time history analysis to give an indication as to how closely these results coincide.

**Table 8.12 Summary of all C/D Ratios for New St. Francis Bridge Structure – For One 2% PE Earthquake**

<b>SUMMARY TABLE OF ALL C/D RATIOS FOR BRIDGE STRUCTURE</b>			
<i>Bridge A3709, PR020101 -- all three acceleration directions</i>			
<b>Element Description</b>	<b>C/D Ratio Name</b>	<b>C/D Ratio Value</b>	<b>NOTES</b>
bearing	$\Gamma_{bd}$	---	NOT APPLICABLE TO THIS BRIDGE
shear force - transverse	$\Gamma_{bf-trans}$	2.37	satisfactory
shear force - longitudinal	$\Gamma_{bf-long}$	2.49	satisfactory
bolt/anchor rod embedment length	$\Gamma_{bf-embed}$	0.59	Unsatisfactory...demand exceeds capacity
bolt/anchor rod edge distance	$\Gamma_{bf-edge dist.}$	1.14	satisfactory
column top, bent 2, $P_{min}$	$\Gamma_{ec-final}$	3.39	satisfactory
column top, bent 2, $P_{max}$	$\Gamma_{ec-final}$	4.55	satisfactory
column bottom, bent 2, $P_{min}$	$\Gamma_{ec-final}$	2.80	satisfactory
column bottom, bent 2, $P_{max}$	$\Gamma_{ec-final}$	4.07	satisfactory
column top, bent 3, $P_{min}$	$\Gamma_{ec-final}$	3.40	satisfactory
column top, bent 3, $P_{max}$	$\Gamma_{ec-final}$	4.56	satisfactory
column bottom, bent 3, $P_{min}$	$\Gamma_{ec-final}$	2.78	satisfactory
column bottom, bent 3, $P_{max}$	$\Gamma_{ec-final}$	4.04	satisfactory
hooked anchorage @ column bottom	$\Gamma_{ca-bottom}$	1.00	satisfactory
hooked anchorage @ column top	$\Gamma_{ca-top}$	1.00	satisfactory
splices in longitudinal reinforcement	$\Gamma_{cs}$	1.11	satisfactory
splices in longitudinal reinforcement, adjusted for stresses in steel	$\Gamma_{cs-adj}$	4.03	satisfactory
transverse confinement	$\Gamma_{cc}$	3.33	satisfactory
column shear	$\Gamma_{cv}$	2.06	satisfactory
diaphragm / cross-frame members	$\Gamma_{cross}$	0.22	Unsatisfactory...demand exceeds capacity
diaphragm / cross-frame members, using 1/2 of total member length	$\Gamma_{cross-0.5L}$	0.68	Unsatisfactory...demand exceeds capacity
abutments - transverse displacement	$\Gamma_{ad-trans}$	42.48	satisfactory
abutments - longitudinal displacement	$\Gamma_{ad-long}$	42.04	satisfactory

**Table 8.13 Summary of C/D Ratios For All Earthquakes at New St. Francis River Bridge**

C/D Ratio Name	020101	020103	020105	020201	020203	020205	100103	100104	100105	100201	100202	100205
$r_{bd}$	—	—	—	—	—	—	—	—	—	—	—	—
$r_{bf-trans}$	2.37	3.07	2.79	3.07	3.07	2.70	3.07	3.07	3.07	3.07	3.07	3.07
$r_{bf-long}$	2.49	3.05	2.97	3.07	3.07	2.69	3.07	3.07	3.07	3.07	3.07	3.07
$r_{bf-embed}$	<b>0.59</b>											
$r_{bf-edge\ dist.}$	1.14	1.14	1.14	1.14	1.14	1.14	1.14	1.14	1.14	1.14	1.14	1.14
$r_{ec-final}$	3.39	4.88	4.54	5.18	5.09	3.81	16.59	18.42	15.86	13.51	9.44	11.43
$r_{ec-final}$	4.55	6.55	6.10	6.94	6.83	5.11	22.25	24.71	21.28	18.12	12.66	15.34
$r_{ec-final}$	2.80	3.95	3.73	4.25	4.15	3.11	13.39	15.30	13.15	10.92	7.74	9.57
$r_{ec-final}$	4.07	5.74	5.42	6.17	6.02	4.52	19.45	22.23	19.10	15.86	11.24	13.90
$r_{ec-final}$	3.40	4.91	4.56	5.20	5.07	3.81	16.63	18.49	15.88	13.53	9.47	11.47
$r_{ec-final}$	4.56	6.58	6.12	6.97	6.80	5.12	22.32	24.80	21.30	18.15	12.71	15.39
$r_{ec-final}$	2.78	3.95	3.74	4.26	4.13	3.11	13.40	15.32	13.14	10.93	7.75	9.58
$r_{ec-final}$	4.04	5.75	5.43	6.19	6.00	4.52	19.48	22.27	19.10	15.88	11.26	13.92
$r_{ca-bottom}$	1.00	1.00	1.00	1.00	1.00	1.00	1.00	1.00	1.00	1.00	1.00	1.00
$r_{ca-top}$	1.00	1.00	1.00	1.00	1.00	1.00	1.00	1.00	1.00	1.00	1.00	1.00
$r_{cs}$	1.11	1.58	1.49	1.70	1.65	1.24	5.36	6.12	5.26	4.37	3.10	3.83
$r_{cs-adj}$	4.03	8.11	7.29	9.45	8.96	5.04	94.92	126.79	92.91	62.94	31.60	48.98
$r_{cc}$	3.33	4.74	4.48	5.10	4.96	3.73	16.07	18.37	15.77	13.11	9.29	11.48
$r_{cv}$	2.06	2.94	2.77	3.16	3.07	2.31	10.74	12.67	10.80	8.66	6.21	7.94
$r_{cross}$	<b>0.22</b>	<b>0.31</b>	<b>0.30</b>	<b>0.32</b>	<b>0.33</b>	<b>0.25</b>	1.04	1.06	<b>0.93</b>	<b>0.85</b>	<b>0.57</b>	<b>0.68</b>
$r_{cross-0.5L}$	<b>0.68</b>	<b>0.98</b>	<b>0.91</b>	1.00	1.00	<b>0.76</b>	3.19	3.24	2.85	2.61	1.74	2.08
$r_{ad-trans}$	42	59	59	67	63	48	211	262	220	171	121	162
$r_{ad-long}$	42	59	55	62	64	49	201	219	197	181	121	143

**Table 8.14 Comparison of Moments for Time History and Response Spectrum Analysis for Column 2 (New St. Francis River Bridge)**

<i>Due to 2% motions</i>					<i>Due to 10% motions</i>				
	transverse		longitudinal			transverse		longitudinal	
	time history	response spectra	time history	response spectra		time history	response spectra	time history	response spectra
Due to Transverse EQ					Due to Transverse EQ				
Column 2, bottom	56823	58252	13912	16363	Column 2, bottom	9966	14924	2795	4192
	41965	40841	11775	11470		11702	13059	3285	3668
	36840	38104	10358	10703		14162	14511	3986	4075
	37835	36107	10660	10143		16160	14081	4532	3954
average	43366	43326	11676	12170	average	12998	14144	3650	3972
Due to Longitudinal EQ					Due to Longitudinal EQ				
Column 2, bottom	1792	1958	2136	2319	Column 2, bottom	521	665	701	909
	1942	1833	2249	2503		500	517	593	682
	1484	1514	2089	1950		550	563	694	714
	1356	1328	1828	1668		828	619	848	838
average	1644	1658	2076	2110	average	600	591	709	786
Due to Vertical EQ					Due to Vertical EQ				
Column 2, bottom	1305	1222	463	462	Column 2, bottom	244	232	124	135
	1081	1040	398	408		267	260	121	141
	1133	1069	310	369		369	324	152	153
	923	1025	355	458		301	338	150	184
average	1111	1089	382	424	average	295	289	137	153

**Table 8.15 Comparison of Moments for Time History and Response Spectrum Analysis for Column 5 (New St. Francis River Bridge)**

<i>Due to 2% motions</i>					<i>Due to 10% motions</i>				
Due to Transverse EQ	transverse		longitudinal		Due to Transverse EQ	transverse		longitudinal	
	time history	response spectra	time history	response spectra		time history	response spectra	time history	response spectra
<b>Column 5, bottom</b>	56689	58104	15938	16292	<b>Column 5, bottom</b>	9907	14880	2776	4171
average	41820	40742	11722	11427	average	11663	13037	3272	3654
	36708	38010	10308	10658		14112	14475	3967	4058
	37924	36104	10665	10123		16085	14057	4507	3942
	43285	43240	12158	12125		12942	14112	3631	3956
Due to Longitudinal EQ	transverse		longitudinal		Due to Longitudinal EQ	transverse		longitudinal	
	time history	response spectra	time history	response spectra		time history	response spectra	time history	response spectra
<b>Column 5, bottom</b>	1817	1965	2136	2308	<b>Column 5, bottom</b>	536	667	697	904
average	1959	1841	2248	2490	average	507	518	591	678
	1478	1521	2086	1940		548	565	693	710
	1354	1336	1829	1660		837	623	848	834
	1652	1666	2075	2100		607	593	707	782
Due to Vertical EQ	transverse		longitudinal		Due to Vertical EQ	transverse		longitudinal	
	time history	response spectra	time history	response spectra		time history	response spectra	time history	response spectra
<b>Column 5, bottom</b>	1256	1165	662	531	<b>Column 5, bottom</b>	225	220	145	145
average	1011	983	509	480	average	253	245	143	154
	1092	1011	419	446		343	306	156	173
	874	967	464	520		284	312	166	202
	1058	1032	514	494		276	271	153	169

**Table 8.16 Comparison of Displacements for Time History and Response Spectrum Analysis for Maximum Abutment Displacement (New St. Francis River Bridge)**

<i>Due to 2% motions</i>					<i>Due to 10% motions</i>				
	transverse		longitudinal			transverse		longitudinal	
	time history	response spectra	time history	response spectra		time history	response spectra	time history	response spectra
Due to Transverse EQ					Due to Transverse EQ				
<b>Max. Abut. Disp.</b>	0.07	0.069	0.1259	0.1294	<b>Max. Abut. Disp.</b>	0.0113	0.0177	0.0227	0.0334
average	0.0506	0.0484	0.093	0.0907	0.0135	0.0155	0.0264	0.029	
	0.0442	0.0452	0.0824	0.0848	0.0174	0.0172	0.0281	0.0324	
	0.047	0.0429	0.0808	0.0792	0.0183	0.0167	0.0368	0.0312	
	0.053	0.05138	0.0955	0.09603	<b>average</b>	0.01513	0.01678	0.0285	0.0315
Due to Longitudinal EQ					Due to Longitudinal EQ				
<b>Max. Abut. Disp.</b>	0.0021	0.00167	0.0523	0.0485	<b>Max. Abut. Disp.</b>	0.00044	0.00046	0.0154	0.0193
average	0.0016	0.0013	0.05	0.0525	0.00036	0.00038	0.013	0.0144	
	0.0012	0.00117	0.0439	0.0408	0.00048	0.00044	0.0164	0.0151	
	0.0012	0.00106	0.039	0.035	0.00053	0.00043	0.0161	0.0178	
	0.0015	0.0013	0.0463	0.0442	<b>average</b>	0.00045	0.00043	0.01523	0.01665
Due to Vertical EQ					Due to Vertical EQ				
<b>Max. Abut. Disp.</b>	0.0009	0.00126	0.018	0.0171	<b>Max. Abut. Disp.</b>	0.00029	0.00029	0.0023	0.00255
average	0.0013	0.00098	0.0137	0.0143	0.00032	0.00026	0.00299	0.00305	
	0.0011	0.0009	0.0158	0.0152	0.0004	0.00038	0.00335	0.00422	
	0.0009	0.00111	0.0138	0.0138	0.00038	0.00036	0.00401	0.00409	
	0.0011	0.00106	0.0153	0.0151	<b>average</b>	0.00035	0.00032	0.00316	0.00348

It can be observed from Tables 8.16-8.18 that the results from the response spectrum analysis agree well with those of the linear time history analysis for the bridge. Therefore the response spectrum analysis can be used to replace the time history analysis for highway bridges with integral abutments that can be described with a linear model.

### 8.1.7.1.6 Comparison of AASHTO Response Spectrum vs. Site-Specific Response Spectrum

A response spectrum was generated based on the 1996 AASHTO Specifications. This response spectrum was used on both of the new bridges, both at the St. Francis River site and at the White Ditch site. The response spectrum was created using the following parameters: Soil Type III, which yielded an S value of 1.5, and an A value of 0.18, which represents the maximum ground motion in the area. The plot of the response spectrum that was used for the analyses is shown in Figure 8.28.

In Figure 8.28, two site specific response spectra were graphically compared to the AASHTO response spectrum. It should be noted that in the region of the structure's natural period (less than  $T = 0.5$  seconds) all the response spectrum data are relatively close to one another.

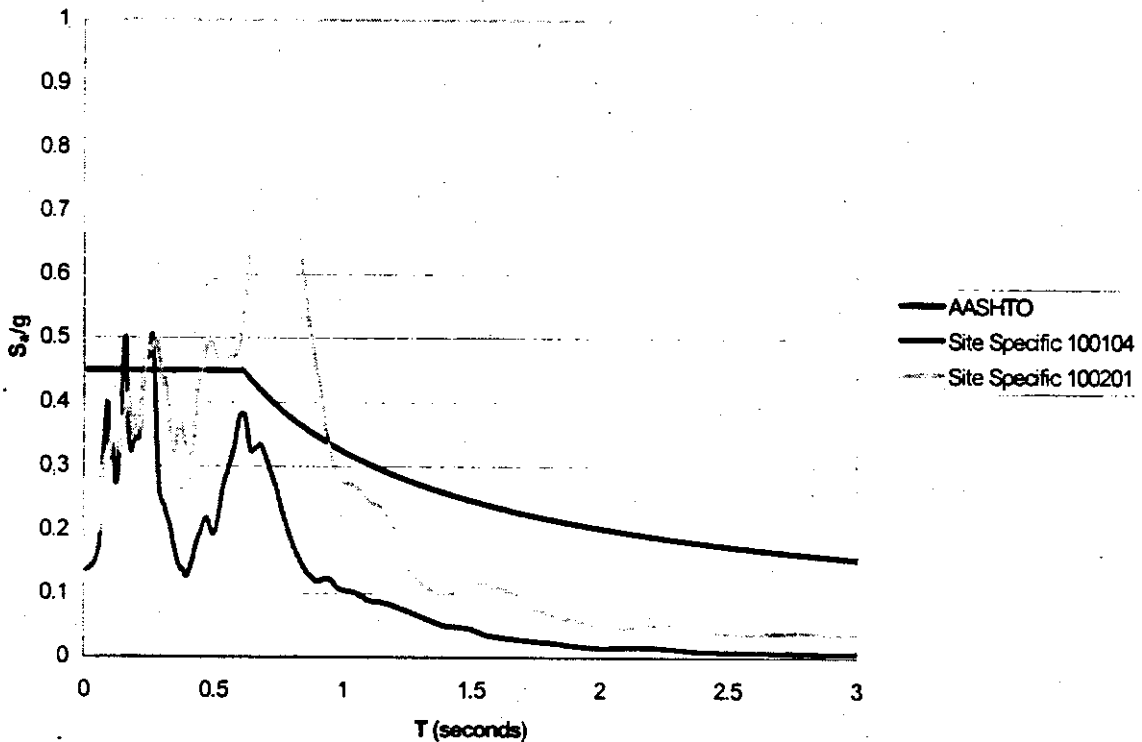


Figure 8.28 Comparison of AASHTO Response Spectrum & Site Specific Response Spectrum

**Table 8.17** Comparison of AASHTO Response Spectrum vs. Site Specific Response Spectrum (New St. Francis River Bridge)

Due to Transverse EQ	transverse		longitudinal	
	response spectra	AASHTO	response spectra	AASHTO
Column 2, bottom	14924		4192	
	13059		3668	
	14511		4075	
	14081		3954	
average	14144	14574	3972	4093

Due to Transverse EQ	transverse		longitudinal	
	response spectra	AASHTO	response spectra	AASHTO
Column 5, bottom	14880		4171	
	13037		3654	
	14475		4058	
	14057		3942	
average	14112	14525	3956	4073

Due to Longitudinal EQ	transverse		longitudinal	
	response spectra	AASHTO	response spectra	AASHTO
Column 2, bottom	665		909	
	517		682	
	563		714	
	619		838	
average	591	780	786	1050

Due to Longitudinal EQ	transverse		longitudinal	
	response spectra	AASHTO	response spectra	AASHTO
Column 5, bottom	667		904	
	518		678	
	565		710	
	623		834	
average	593	786	782	1046

The results from the AASHTO response spectrum analysis were compared to several of the 10% earthquake response spectrum analyses that were run on the New St. Francis River Bridge. It was expected that these results would be reasonably close to one another. These results are summarized in Table 8.17.

### 8.1.7.2 Old St. Francis River Bridge

#### 8.1.7.2.1 Bridge Description

The bridge under consideration is denoted as Bridge A-3708, located next to the new St. Francis River Bridge that was analyzed and evaluated in Section 8.1.7.1. It was designed in 1977 without seismic considerations. This 294 foot 1 inch bridge consists of three spans supported by steel plate girders, as shown in Figure 8.29. The dimensions of these plate girders varied slightly within a span depending on the location of the tension flange. The interior diaphragms and the cross-frames each consists of two L 3x2½x5/16 crossed over each other. The top and bottom horizontal members on the diaphragms and cross-frames were L 4x4x5/16. All interior diaphragms and cross-frames were placed parallel to the abutments of the bridge. The bridge, however, was skewed at a 20° angle, so the ends of the girders were offset from one another at the ends of the

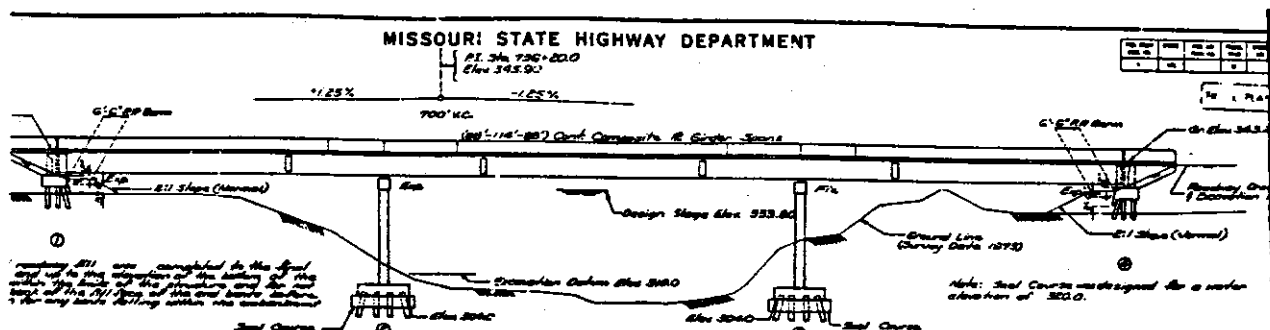


Figure 8.29 Bridge General Elevation (Old St. Francis River Bridge)

bridge. Therefore, these diaphragms and cross-frames were not perpendicular to the girders because of the angle of the structure.

The bridge superstructure is supported by two intermediate bents through one fixed bearing and one expansion bearing, along with seat-type abutments at its ends. Each bent consisted of a reinforced concrete cap beam and three reinforced concrete columns. Deep pile foundations support both bents and abutments. There are 12 piles for each column footing and 16 piles for each abutment footing. Two expansion joints were constructed at the ends of the bridge.

### 8.1.7.2.2 Bridge Model and Analysis

The bridge was modeled with the finite element method in the SAP2000 structural analysis program to analyze this bridge for susceptibility to earthquake damage.

All of the components of the structure were included in the bridge model. These components include the girders, diaphragms, cross-frames, interior bents and columns, and the bridge deck. The deck was represented by 52 shell elements with a thickness of 8.5 inches. All girders, cross-frames, and diaphragms were modeled as 633 frame members. Each frame section was then assigned member properties, such as material type and cross-section dimensions. The model also included 346 nodes.

To model ground soil conditions, springs and dashpots were used at the base of each column (six columns total, three on each interior bent). To account for passive soil pressure, "gap" elements with zero gap width were placed at the ends of the bridge on each abutment. A bilinear model was considered in the computer analysis. The soil body behind each abutment is considered to be mobilized when the displacement at the top of the abutment exceeds 0.5% of the abutment height (FHWA, 1995). The stiffness constants of the soil, which were input as part of the "gap" element information, were taken from Appendix F.

Rigid elements were used to model the abutments in SAP2000. However, unlike the New St. Francis River Bridge, the abutment rigid elements were modeled separated from the rest of the structure to represent the expansion joints between the abutment and the bridge structure. The expansion joints were modeled with several "gap" elements. Together with other "gap" elements on the abutments and the damper at the pile foundation, the bridge structure becomes a geometri-

cally nonlinear system. Therefore, a non-linear time-history analysis was used for the bridge model.

For each separate analysis using one directional earthquake excitation, 30 Ritz-vectors were considered associated with that earthquake direction. In Table 8.18, a sampling of five of the significant vibration modes are listed with its period in seconds and a brief description of the motion represented within the given mode. The mode shapes are shown in Figures 8.30-8.34.

The bridge was analyzed under a total of twelve earthquake ground motions described in Section 8.1.3. Six of the twelve motions correspond to a 10% PE level while the others to a 2% PE level. At each PE level of earthquakes, three were considered as near-field and the other three as far-field. The internal loads such as shear and moments and the abutment displacements were obtained at various critical locations. They will be presented together with the vulnerability evaluation of structural members in the next section. It is noted that one bridge analysis was conducted for each directional earthquake excitation due to the special directional combination rule specified in AASHTO Specifications (1996) and the nonlinear effect of the expansion joints and pile foundations on the bridge responses. Consequently, a total of 36 runs were completed.

### 8.1.7.2.3 Bridge Evaluation

The same procedure that was used for the New St. Francis River Bridge in Section 8.1.7.1.3 was followed for Old St. Francis River Bridge, denoted bridge A-3709. Again, C/D ratios were the main factor in determining whether a structural component would likely experience problems during

**Table 8.18** Natural Periods and their Corresponding Vibration Modes (Old St. Francis River Bridge)

Mode Number	Period (seconds)	Motion Description
1	1.3173	Longitudinal
2	0.4773	Transverse
3	0.3673	Transverse
4	0.2065	Vertical
5	0.1501	Longitudinal

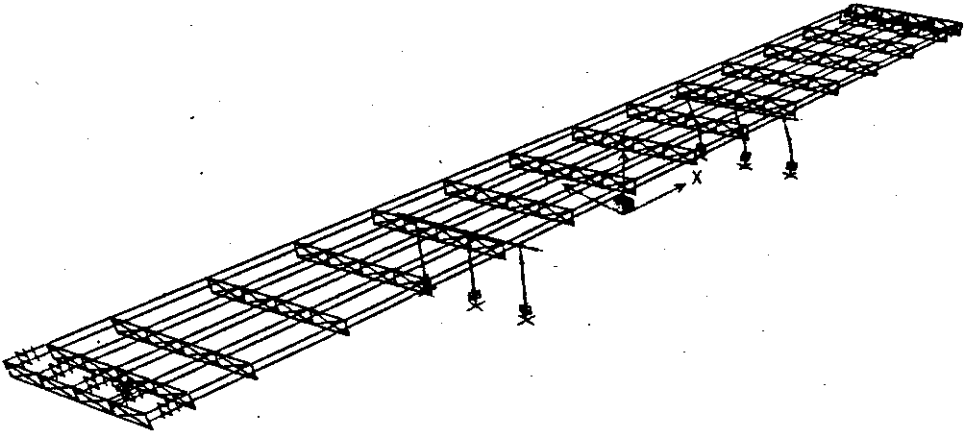


**Figure 8.30** Mode 1, Period 1.3173 Seconds (Old St. Francis River Bridge)

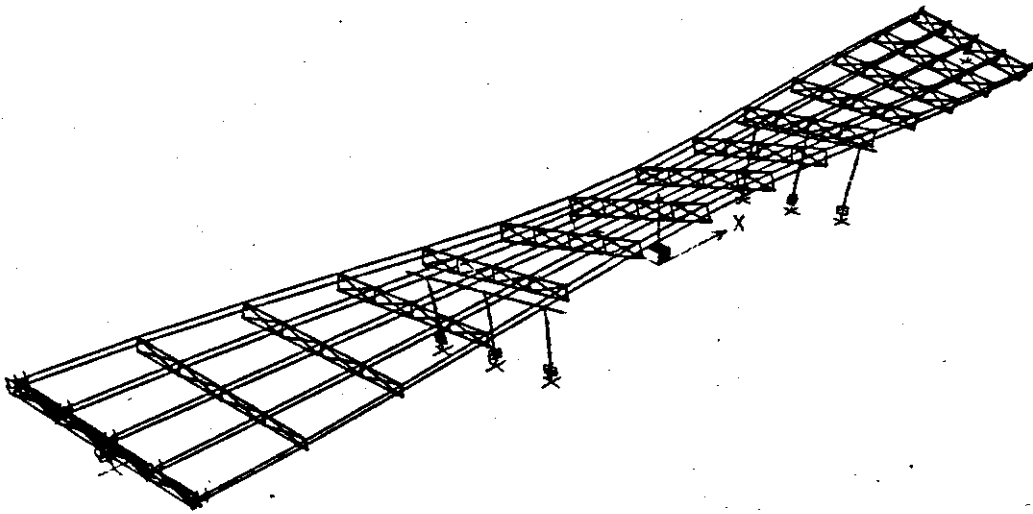


**Figure 8.31** Mode 2, Period 0.4773 Seconds (Old St. Francis River Bridge)

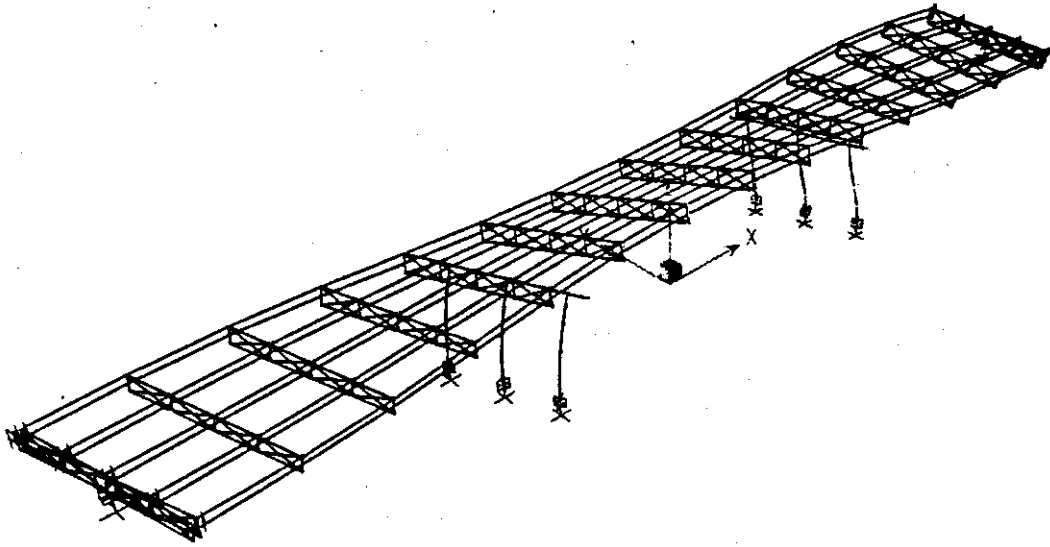


Figure 8.32 Mode 3, Period 0.3673 Seconds (Old St. Francis River Bridge)

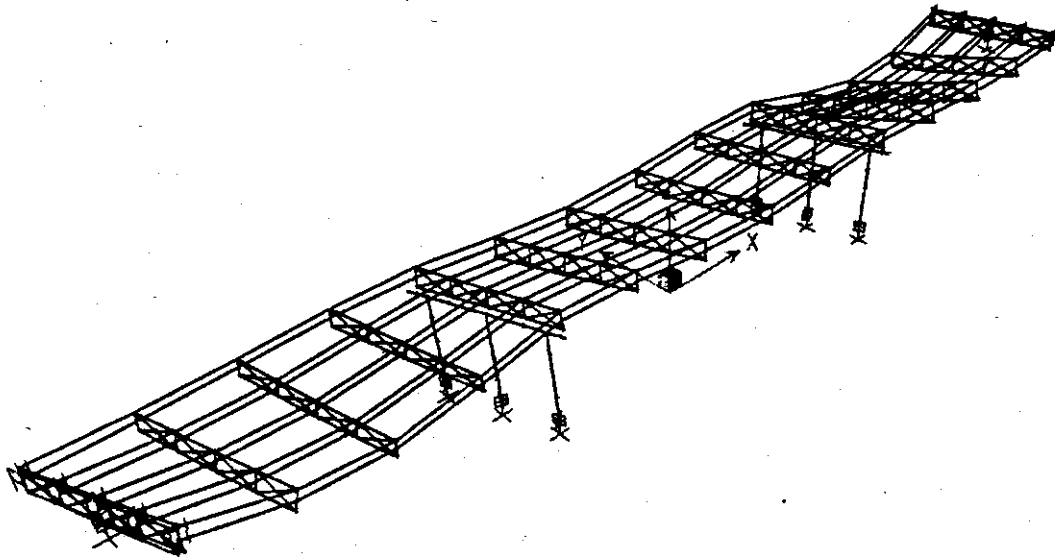
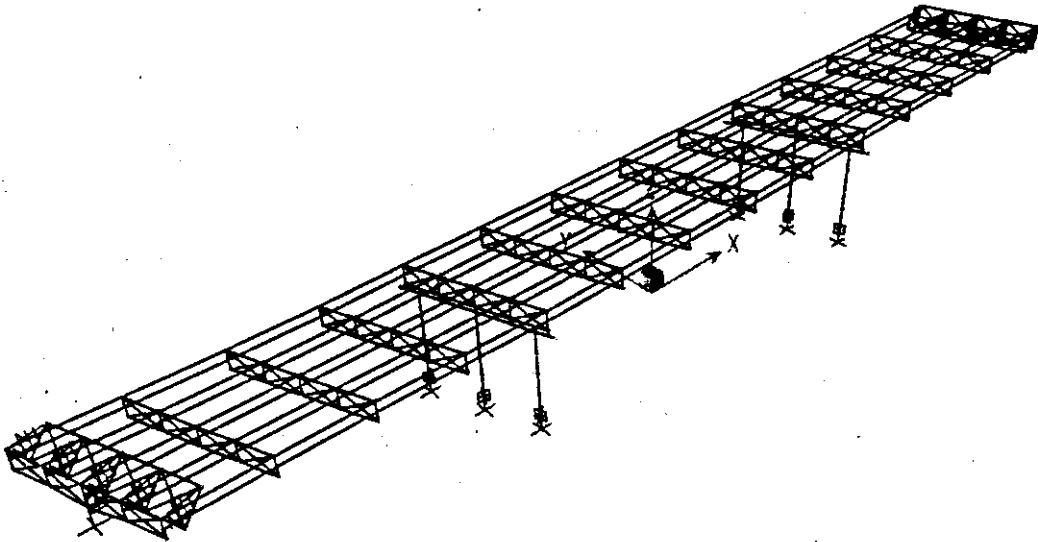


Figure 8.33 Mode 4, Period 0.2065 Seconds (Old St. Francis River Bridge)



**Figure 8.34 Mode 5, Period 0.1501 Seconds (Old St. Francis River Bridge)**

an earthquake. Any C/D ratio equal to or greater than one would indicate that the component would probably not experience major problems during earthquake motions.

#### **8.1.7.2.3.1 Load Combination Rule**

The same load combination rule that was used for the New St. Francis River Bridge evaluation was employed for this structure as well. This combination rule was used in several instances throughout these calculations for various types of demands on the structure (shear, moment, and axial forces, as well as transverse and longitudinal displacements).

#### **8.1.7.2.3.2 Minimum Support Length and C/D Ratio for Bearing**

Because this bridge uses seat-type abutments, bearing and support length are essential components that must be examined. For this structure, the support length is a small amount short of what is required. The capacity, or actual support length for this bridge, was estimated at 23 inches. However, based on the definition of required support by FHWA, approximately 24 inches of length was needed. This indicates that the capacity is slightly less than the demand, so the bearing and support length for this bridge need to be examined more closely, as it could lead to the dropping of exterior spans during an earthquake.

### **8.1.7.2.3.3 C/D Ratios for Shear Force at Bearings**

The first C/D ratios calculated in this section define the behavior of the bolts located at the bearing pads on the cap beams at the interior bents. In both the transverse and the longitudinal directions, there are two bolts for capacity. From the output of SAP2000 the shear demand at each of these points was determined and the maximum demand among these points was used to compute the C/D ratio for the "worst case". Before these shear values were used in determining the C/D ratios, the values were compared to 20% of the axial dead load at that location (FHWA, 1995). The greater of these two values were used in the subsequent calculations.

The force demands from each of the transverse, longitudinal, and vertical earthquake motions were combined to determine their total effect. The shear demands at these locations exceeded the capacities of these bolts for all of the 2% and 10% earthquakes. This indicates possible shear failures in the areas around the connecting bolts at the bearing pads.

The second set of C/D ratios in this section involves the embedment length and edge distance requirements for the bolts discussed in the previous paragraph. First, the required embedment length was found from Table 8-26 of the LRFD AISC Manual (1998). This length, for the 1.25-inch diameter rods that were used on this bridge, is 21.25 inches. From the plans, it is noted that the rods only extend 12 inches into the concrete. With the check, this results in a C/D ratio less than one, which would indicate a possible failure due to axial forces acting on the bolts. Finally, the edge distance was checked using another C/D ratio. From the same AISC table that provided the embedment lengths, allowable edge distances were also provided. For the rods used here, the required distance is 8.75 inches. The actual edge distance was estimated from the plans to be approximately 22 inches. This indicates that there should be no problems with the edge distance provided for the bolts.

### **8.1.7.2.3.4 C/D Ratios for Columns/Piers**

In this section, the C/D ratios were calculated for all columns on the interior bents. The first step was to note the elastic moment demands for the top and bottom of each column in the transverse and longitudinal directions due to the combined effect of transverse, longitudinal, and vertical earthquake motions. The resulting moments were algebraically combined with the moments due to the dead load. This final calculation yields the value that is ultimately used in C/D ratio calculations.

The capacities of these columns were found in the same way as for the columns of the New St. Francis River Bridge. Again, the P-M interaction diagrams were used in conjunction with the iterative method for determining the axial load due to overturning, as well as the resulting shear force.

Finally, the maximum demand from the possible combinations was then used in conjunction with the determined capacity for the column to determine a C/D ratio for the columns. In most cases, the C/D ratios were well below one, indicating insufficient column strength for elastic seismic demand. However, a multiplier of 5 was applied to each ratio for the multiple-column bents. In all cases except for one of the 2% earthquakes, this multiplier increased the ratios to values

above one. This indicates that the columns will probably not cause problems, as long as the re-bars are properly detailed in the plastic hinge zone.

As was outlined in the section discussing the New St. Francis River Bridge, capacities of the footings were also examined. The method used was identical to what was used previously, with the only adjustment accounting for the different number of piles and the different pile configurations. The plot of moment versus rotation for the case of axial load equal to zero is shown in Appendix H. It was noted that the moment capacity for this case is considerably higher than the capacities of the columns (several orders of magnitude greater). Therefore, it is unlikely that the footings would yield before the bottoms of the columns.

#### **8.1.7.2.3.5 C/D Ratios for Reinforcement Anchorage in Columns**

For both the top and bottom of the columns, the adequacy of the anchorage of longitudinal reinforcement must be checked. The capacity was determined simply by finding the length of anchorage at both the top and bottom of the columns. The demand was determined from an equation outlined in the FHWA Seismic Retrofit Manual.

At the tops of the columns, the anchorage was straight, whereas at the bottoms of the columns, the anchorage was hooked. However, in both cases, the actual length of the anchorage, which was estimated from the bridge plans, appeared to be less than the required lengths. These required lengths were determined from equations defined in FHWA (1995). The value for the C/D ratio was found from Figure 78 from the FHWA Manual, and this table was set up in terms of the anchorage geometry and location of the anchorage (top/bottom of the column, etc.). Because the capacity length was less than the demanded length, the resulting C/D ratio was simply the actual length divided by the required length, and then multiplied by the C/D ratio from the column. To determine the "worst-case" scenario, the minimum C/D ratio from among the columns was used without the ductility multiplier.

For this bridge, the initial C/D ratios for the columns were rather low, and this led to very low values for the C/D ratios for the reinforcement anchorage. These low ratios indicate that the anchorage of this longitudinal steel may be a component of concern.

#### **8.1.7.2.3.6 C/D Ratios for Splices in Longitudinal Reinforcement**

This section is not applicable to this structure, as the columns have no splices.

#### **8.1.7.2.3.7 C/D Ratio for Transverse Confinement**

In this section, a FHWA-defined relationship was used to determine the adequacy of transverse confinement. This C/D ratio was again dependent on the column moment C/D ratio,  $r_{ec}$ , without including the ductility indicator. The relationship defined for the transverse confinement included a multiplier as  $\mu$  (FHWA, 1995). This multiplier was dependent on several factors, including geometry of the confinement as well as properties of the column reinforcement, the concrete, and the column cross-section.

The C/D ratios for all cases were above one. This indicates that there should be minimal problems with the transverse confinement.

#### **8.1.7.2.3.8 C/D Ratio for Column Shear**

In this section, column shear forces were determined following the same procedure as applied to the New St. Francis River Bridge previously. The same parameters needed to be calculated, including the maximum elastic shear in the columns, the initial shear capacity of the column, the final shear capacity of the column, and the shear demand on the column. From these parameters, "Case B" was chosen in all cases of 2% and 10% motions based on definitions from the FHWA Manual. For this case, the relationship for the column shear C/D ratio was the column moment C/D ratio multiplied by an FHWA-defined multiplier. This multiplier was based on column geometry ( $L_c$  = length of column and  $b_c$  = width of column) as well as the various shear parameters defined in Section 8.1.7.1.3.8.

#### **8.1.7.2.3.9 C/D Ratio for Diaphragm and Cross-Frame Members**

This section examines the damage caused to the diaphragm and cross-frame members for the bridge. They are both composed of two L 3x2½x5/16 crossed over each other with L 4x4x5/16 as the top and bottom horizontal members. Because of very low moments on these members, the members were analyzed based on their axial load capacity and demand.

As done for the New St. Francis River Bridge, two calculations for the same C/D ratio were exercised. The first uses the full length of the member spanning diagonally from top to bottom of the diaphragm/cross-frame. The second calculation uses half of the total length of the member. This was done because of the possibility of failure within the connection where the diagonal members meet, thus removing the intermediate brace. It should be noted that the members were modeled as two halves put together to make a full-length diagonal member for the diaphragms and cross-frames. The axial capacity was found to be less than the demand in most cases, which indicates that these members may have problems under the influences of strong earthquake motions.

The strength of the weld at the intermediate brace of the diagonals was calculated to be approximately 15 kips. According to the analysis, all of the 2% PE motions would likely cause this weld to fail, since all the axial demands for those earthquakes are greater than the weld capacity (range from 47 to 69 kips). The 10% PE motions appeared to cause this problem in two of the six examined cases, as the axial loads for those motions range from 12 to 30 kips.

#### **8.1.7.2.3.10 C/D Ratio for Abutment Displacements**

The final section of the procedure outlines the check for abutment adequacy. This test involves comparing the actual abutment displacements to maximum displacement values given by FHWA. The values are given as three inches of allowable displacement in the transverse direction and six inches of allowable displacement in the longitudinal direction.

The abutment displacements due to all three directions of earthquake motions were determined to be less than the allowable displacements in all cases. This indicates that the abutments should remain relatively damage-free in the event of an earthquake.

#### 8.1.7.2.4 Summary of Problem Areas

The bridge experienced some serious problems that will be shown in more detail below. As expected, the bridge generally performed more poorly under the influence of the 2% likelihood earthquakes, which were considerably stronger than the 10% likelihood earthquakes.

Table 8.19 lists the C/D ratios of various components for all earthquakes. The following observations can be made from Table 8.19.

The first component of concern is the bearing length of this bridge. Because the capacity length is slightly less than the required length, this component could sustain damage in an earthquake. Next, the shear capacity at the bearing pads on the interior bents appears to be inadequate, as the demand outweighed the capacity in all cases. Also, the bolt embedment length and edge distance appear to be inadequate, indicating possible problems.

The next components of concern are the columns of this structure. Because the ductility indicator, which increases the column C/D ratios by five times, was used, all columns appeared to perform sufficiently, except at one point on two of the 2% ground motions. However, for all cases for both 2% and 10% ground motions, the longitudinal reinforcement anchorage was insufficient. This indicates that the ductile behavior of the columns may not be able to develop during a strong earthquake. Associated with the column ductility, the shear capacity of columns is also inadequate. For all of the 2% earthquakes, the column shear C/D ratio was less than one, which indicates some cause for concern.

The final components of concern are the diagonal members in the cross-frames and diaphragms of the bridge. As indicated by the C/D ratios, these members performed rather poorly.

The C/D ratios for these members were raised above one in some cases by using the half-length of the member. However, for all of the 2% earthquakes and two of the 10% earthquakes, the ratios still fell below one, indicating a problem that may warrant further investigation.

The strength of the weld at the intermediate brace of the diagonals was calculated to be approximately 15 kips. According to the analysis, all of the 2% PE motions would likely cause this weld to fail, since all the axial demands for those earthquakes are greater than the weld capacity (range from 47 to 69 kips). The 10% PE motions appeared to cause this problem in two of the six examined cases, as the axial loads for those motions range from 12 to 30 kips.

### 8.1.7.2.5 Time History Analysis vs. Response Spectrum Analysis

From the analysis of the New St. Francis River Bridge, it has been shown that a response spectrum analysis is reasonably accurate in the determination of elastic responses of structures. Due to the presence of the expansion joints in the Old St. Francis River Bridge, the bridge may behave in a nonlinear fashion due to the pounding effect. Therefore, it is necessary to compare the response spectrum analysis with the time history analysis again for this bridge to verify the accuracy of the spectrum analysis.

Tables 8.20, 8.21, and 8.21 show comparisons for moments and displacements at various locations on the structure (column 2, column 5 and the maximum abutment displacement). The values for the same location due to each of the 2% motions and 10% motions were averaged. The averages for time history results were then compared to those for the response spectra results. From these tables, the following observations can be made.

Bridge pounding in the longitudinal direction appears to be an issue when dealing with the 2% earthquake motions. This became apparent because of the "gap" elements that were used to model the expansion joints and the soil pressure on the back of the abutments in the non-linear time history analysis. In the response spectrum analysis, the structural model must be linear and the "gap" elements could not be used. Therefore, springs were used to model the soil stiffness behind the abutments, and the "gap" elements, which modeled the expansion joints between the abutment and the superstructure, were removed.

This caused noticeable differences on the moments and forces on the fixed interior bent (the other bent was an expansion bearing). Because this bent was fixed to the superstructure, it was allowed to move much more in the response spectra analysis, as the "gap" elements, which restrained the motion in the non-linear analysis, had been taken out. Therefore, it was noticed that the moments and forces on this bent were approximately two to three times larger than those noted from the time history analysis. This was only the case for longitudinal motion; the transverse and vertical direction earthquakes saw small variations. However, for the other bent, which was not fixed to the superstructure, the forces and moments were reasonably close to one another between the two analyses.

The above phenomenon was noticeable only on the stronger 2% earthquakes. The 10% earthquakes yielded different results. Pounding is apparently less of an issue with these motions, and therefore the moments and forces between the two analyses were closer to one another. There were some discrepancies, but these may have been attributed to differences in how damping is handled in the time history and response spectrum analyses.

**Table 8.19 Summary of C/D Ratios for All Earthquakes at Old St. Francis River Bridge**

C/D Ratio Name	020101	020103	020105	020201	020203	020204	100102	100104	100105	100201	100204	100205
$r_{bd}$	0.96	0.96	0.96	0.96	0.96	0.96	0.96	0.96	0.96	0.96	0.96	0.96
$r_{bf-trans}$	0.60	0.46	0.47	0.43	0.45	0.30	0.73	0.89	0.77	0.48	0.54	0.50
$r_{bf-long}$	0.62	0.52	0.57	0.58	0.71	0.71	0.89	0.89	0.89	0.74	0.89	0.78
$r_{bf-embed}$	0.56	0.56	0.56	0.56	0.56	0.56	0.56	0.56	0.56	0.56	0.56	0.56
$r_{bf-edge\ dist.}$	2.51	2.51	2.51	2.51	2.51	2.51	2.51	2.51	2.51	2.51	2.51	2.51
$r_{ec-final}$	1.91	2.54	1.70	2.40	2.35	2.51	8.95	12.46	9.56	5.40	5.84	5.92
$r_{ec-final}$	2.48	3.31	2.21	3.12	3.06	3.26	11.64	16.21	12.43	7.02	7.60	7.71
$r_{ec-final}$	1.34	1.33	1.16	1.53	1.43	1.63	6.48	8.19	7.27	3.34	4.09	3.24
$r_{ec-final}$	1.70	1.68	1.47	1.94	1.82	2.06	8.21	10.38	9.22	4.23	5.18	4.11
$r_{ec-final}$	1.77	1.54	1.67	1.66	2.17	2.19	5.01	7.28	5.65	2.93	3.25	2.96
$r_{ec-final}$	2.31	2.01	2.17	2.17	2.83	2.85	6.51	9.46	7.35	3.82	4.22	3.84
$r_{ec-final}$	1.24	0.90	1.05	1.05	1.12	0.95	2.13	3.18	2.46	1.28	1.40	1.31
$r_{ec-final}$	1.57	1.14	1.33	1.33	1.42	1.20	2.70	4.04	3.12	1.62	1.77	1.66
$r_{ca-bottom}$	0.16	0.11	0.13	0.13	0.14	0.12	0.27	0.40	0.31	0.16	0.18	0.17
$r_{ca-top}$	0.27	0.24	0.25	0.25	0.33	0.33	0.76	1.11	0.86	0.45	0.49	0.45
$r_{cs}$	--	--	--	--	--	--	--	--	--	--	--	--
$r_{cs-aq}$	--	--	--	--	--	--	--	--	--	--	--	--
$r_{cc}$	0.90	0.65	0.77	0.77	0.82	0.69	1.56	2.32	1.80	0.94	1.02	0.96
$r_{cv}$	0.95	0.69	0.81	0.81	0.86	0.73	1.64	2.45	1.90	0.99	1.08	1.01
$r_{cross}$	0.17	0.13	0.14	0.16	0.19	0.18	0.59	0.74	0.63	0.30	0.37	0.32
$r_{cross-0.5L}$	0.45	0.34	0.39	0.42	0.52	0.48	1.60	2.01	1.71	0.80	1.00	0.86
$r_{ad-trans}$	11.5	8.9	9.8	11.0	11.9	11.1	30.5	42.7	34.6	14.3	17.1	14.1
$r_{ad-long}$	14.9	6.7	7.9	9.4	10.9	7.4	40.8	62.9	45.6	10.1	13.3	10.0

To further check the response spectrum and time history a result, a third case was run, for the longitudinal direction only. This third case used the same model as from the response spectrum case (which had no "gap" elements on the abutments), but it was analyzed using a linear time history analysis. This case was run for four earthquakes, two each of the 2% and 10% motions. For the most part, the results lined up reasonably well with the response spectrum results. The only discrepancies were similar to the ones mentioned above due to the different ways of treating the damping matrix of the structure.

#### **8.1.7.2.6 Structure Response of Abutments**

The Old St. Francis River Bridge abutment (13.0 m x 2.1 m) is supported on 8 vertical piles and 8 battered piles. All piles are cylindrical concrete with 0.406 m (16 inch) diameter and 10.67 m (35 ft) length. The plan and cross section of the bridge abutment are shown in Figure 8.35.

The stiffness and damping factors are calculated using a pile length of 10.67 m (35 ft), a pile radius of 0.203 m (8 inch), and an elastic modulus of the pile material of  $2.15 \times 10^7$  kN/m ( $1.47 \times 10^6$  kips/ft) (Section F.6). Stiffness and damping factors of a single batter piles are 0.8 times that of a vertical pile. (Prakash and Subramanayam, 1964)

The vertical load acting on the top of bridge abutment is obtained from an analysis of the bridge superstructure. Accordingly, a vertical load (Q) of 100 kN (22481 lb) per m of abutment was used in this analysis. The self-weight of the bridge abutment was calculated by multiplying its area by the unit weight of the bridge abutment material ( $\gamma = 23.58$  kN/m<sup>3</sup>) (150.19 pcf). This calculation is done in the program itself. The lateral earth pressure behind the bridge abutment is calculated using a unit weight of soil of 19.54 kN/m<sup>3</sup> (122 pcf), internal friction angle of 33° and friction angle between soil and abutment of 33°. All of loads were modified by a time dependent seismic coefficient.

##### **8.1.7.2.6.1 Calculated Time Dependent Displacements of Abutment**

Table 8.23 shows for different magnitudes of earthquakes (M), the largest sliding, rocking and total displacement at the top of the bridge abutment for an earthquake with a PE of 10% in 50 years and one with a PE of 2 % in 50 years, respectively.

Figures 8.36a and b show the time histories of sliding, rocking and total permanent displacement of the Old St. Francis River Bridge abutment for a PE 10% in 50 years for earthquake magnitudes of M6.2 and M7.2 respectively. Figures 8.37a and b show the time histories of sliding, rocking and total permanent displacement of the Old St. Francis River Bridge abutment for a PE 2% in 50 years and magnitudes of M6.4 and M8.0 respectively.

Figure 8.36a shows a plot of magnitude and significant number of cycles. Table 8.22 also shows displacement in one significant cycle.

**Table 8.20 Comparison of Moments for Time History and Response Spectrum Analysis for Column 2 (Old St. Francis River Bridge)**

<i>Due to 2% motions</i>					<i>Due to 10% motions</i>				
Due to Transverse EQ	transverse		longitudinal		Due to Transverse EQ	transverse		longitudinal	
	time history	response spectra	time history	response spectra		time history	response spectra	time history	response spectra
<b>Column 2, bottom</b>	17677	16607	16125	18257	<b>Column 2, bottom</b>	2927	3158	2303	3448
average	19718	18457	19877	19745	average	3544	3332	2371	3449
	16591	16544	13460	15270	average	7148	7225	3441	6399
	13982	15119	17486	16400	average	5827	7142	4743	7574
	16992	16682	16737	17418	average	4862	5214	3215	5218
Due to Longitudinal EQ	transverse		longitudinal		Due to Longitudinal EQ	transverse		longitudinal	
	time history	response spectra	time history	response spectra		time history	response spectra	time history	response spectra
<b>Column 2, bottom</b>	6155	7495	14430	13499	<b>Column 2, bottom</b>	1794	1150	1564	2629
average	6630	6385	15559	14420	average	2234	1148	1648	2490
	5183	6486	10537	9923	average	3599	1917	4908	4035
	6367	6925	12146	12032	average	3879	2509	6069	5466
	6084	6823	13168	12469	average	2877	1681	3547	3655
Due to Vertical EQ	transverse		longitudinal		Due to Vertical EQ	transverse		longitudinal	
	time history	response spectra	time history	response spectra		time history	response spectra	time history	response spectra
<b>Column 2, bottom</b>	866	879	527	596	<b>Column 2, bottom</b>	135	146	146	149
average	539	565	339	408	average	116	148	141	152
	695	611	376	426	average	166	211	211	193
	636	623	506	508	average	164	208	191	215
	684	670	437	485	average	145	178	172	177

**Table 8.21 Comparison of Moments for Time History and Response Spectrum Analysis for Column 5 (Old St. Francis River Bridge)**

<i>Due to 2% motions</i>					<i>Due to 10% motions</i>				
	transverse		longitudinal			transverse		longitudinal	
	time history	response spectra	time history	response spectra		time history	response spectra	time history	response spectra
Due to Transverse EQ					Due to Transverse EQ				
Column 5, bottom	18491	18216	3457	5687	Column 5, bottom	3532	3395	1698	865
average	20032	20271	4515	5021	4168	3667	2097	921	
	19006	18621	3816	5466	7735	8136	4182	1870	
	14708	16619	4097	5286	6815	7879	4772	1991	
	18059	18432	3971	5365	5563	5769	3187	1412	
Due to Longitudinal EQ					Due to Longitudinal EQ				
Column 5, bottom	2834	8448	22867	75473	Column 5, bottom	610	1120	10821	9580
average	3810	6334	27989	54678	730	1170	14160	10161	
	3423	7719	29099	69563	4153	2015	27024	17573	
	3432	7909	28826	70868	4116	2563	26333	22335	
	3375	7603	27195	67646	2402	1717	19585	14912	
Due to Vertical EQ					Due to Vertical EQ				
Column 5, bottom	755	816	298	279	Column 5, bottom	157	135	181	66
average	489	529	167	171	124	141	230	73	
	631	577	221	201	217	229	305	138	
	668	578	272	222	182	207	261	114	
	636	625	240	218	170	178	244	98	

**Table 8.22 Comparison of Displacements for Time History and Response Spectrum Analysis for Maximum Abutment Displacement(Old St. Francis River Bridge)**

<i>Due to 2% motions</i>					<i>Due to 10% motions</i>				
	transverse		longitudinal			transverse		longitudinal	
	time history	response spectra	time history	response spectra		time history	response spectra	time history	response spectra
<b>Due to Transverse EQ</b>					<b>Due to Transverse EQ</b>				
<b>Max. Abut. Disp.</b>	0.2193	0.1805	0.1393	0.0858	<b>Max. Abut. Disp.</b>	0.0577	0.0536	0.0211	0.0328
	0.1982	0.2239	0.0582	0.1246		0.0595	0.0485	0.0207	0.0365
	0.1915	0.2121	0.0428	0.0837		0.0956	0.1005	0.051	0.0337
	0.1647	0.1614	0.0358	0.0841		0.0795	0.0778	0.0453	0.0391
<b>average</b>	0.1934	0.19448	0.069	0.09455	<b>average</b>	0.0731	0.0701	0.0345	0.03553
<b>Due to Longitudinal EQ</b>					<b>Due to Longitudinal EQ</b>				
<b>Max. Abut. Disp.</b>	0.0514	0.1037	0.3877	0.1741	<b>Max. Abut. Disp.</b>	0.0413	0.0309	0.0882	0.0849
	0.2477	0.1117	0.7396	0.26		0.0688	0.0332	0.1253	0.0883
	0.2147	0.0983	0.6232	0.172		0.1807	0.0296	0.5778	0.0715
	0.2023	0.1011	0.5379	0.1737		0.1894	0.0381	0.5865	0.087
<b>average</b>	0.179	0.1037	0.5721	0.19495	<b>average</b>	0.1201	0.03295	0.3445	0.08293
<b>Due to Vertical EQ</b>					<b>Due to Vertical EQ</b>				
<b>Max. Abut. Disp.</b>	0.008	0.00761	0.006	0.0121	<b>Max. Abut. Disp.</b>	0.0012	0.00149	0.0018	0.0007
	0.0057	0.0085	0.003	0.00519		0.0014	0.00135	0.0023	0.00074
	0.0068	0.00841	0.0035	0.00528		0.002	0.00177	0.0025	0.00125
	0.0068	0.00848	0.0042	0.00536		0.0017	0.00192	0.0024	0.00089
<b>average</b>	0.0068	0.00825	0.0042	0.00698	<b>average</b>	0.0016	0.00163	0.0023	0.0009



Several engineering properties of site soil units were measured in the field. These properties are recorded on the boring logs in Appendix A.

### 8.2.2 Selected Base Rock Motion

Herrmann, (2000) recommends 10 rock base motions for PE 10% in 50 years and another 10 for PE 2 % in 50 years. All of the 40 rock motions have been used for one-dimensional wave propagation analysis using the *SHAKE91* program. Based on wave propagation analysis, peak ground accelerations for each rock motion is obtained. Total of 12 ground motions were selected based on these peak ground acceleration values.

Table 8.24a lists 5-ground motion for PE 10% in 50 years with corresponding maximum peak ground accelerations for M6.4 with epicentral distance of 40 km. Five additional ground motions with M7.0 and epicentral distances of 65 km are given as well. Table 8.24b shows listing for PE 2 % in 50 years with different magnitudes and epicentral-distance. In these tables column 1-4 are basic data from Herrmann (2000).

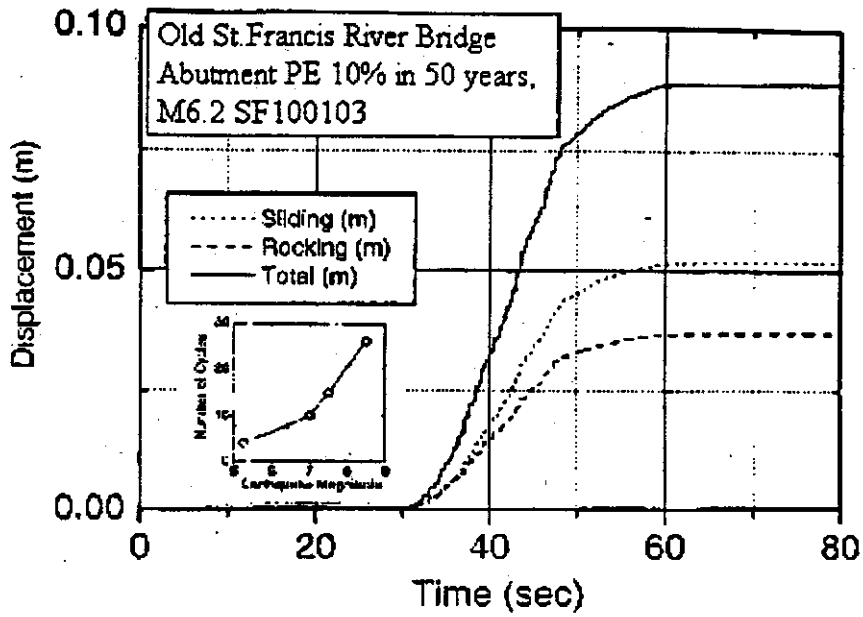
As for the St. Francis River site, 12- synthetic ground motions at the rock base (six for each PE) are selected as representative of the "worst case scenarios". They are given in Table 8.25. The associated acceleration-time histories are shown in Figure 8.39a-d.

### 8.2.3 Seismic Response of Soil

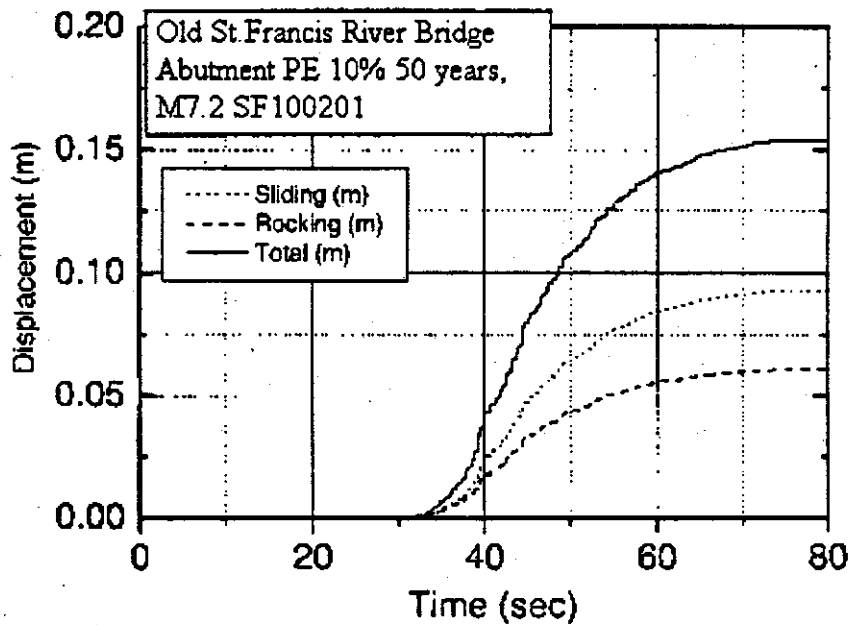
The *SHAKE* and *SHAKEDIT* programs were used to propagate the design earthquake base rock motions to the ground surface. This resulted in peak ground motions and time histories of acceleration at the soil surface, the base of bridge abutments and the piers Figure 8.40 shows the

**Table 8.23 Displacement at the Top of the Old St. Francis Bridge Abutment**

Displacement at top of abutment	PE 10% in 50 years		PE 2% in 50 years	
	M6.2	M7.2	M6.4	M8.0
Sliding (m)	0.052	0.093	0.096	0.31
Rocking (m)	0.037	0.061	0.069	0.21
Total (m)	0.089	0.154	0.165	0.52
Significant cycles	8	11	9	20
Displacement in 1-cycle	0.011	0.014	0.018	0.026

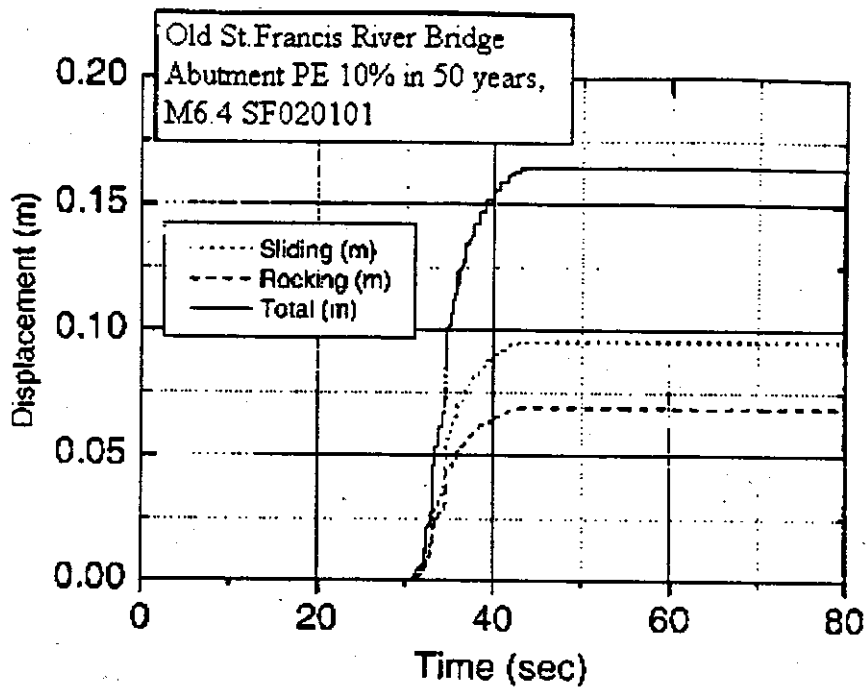


a. Magnitude 6.2

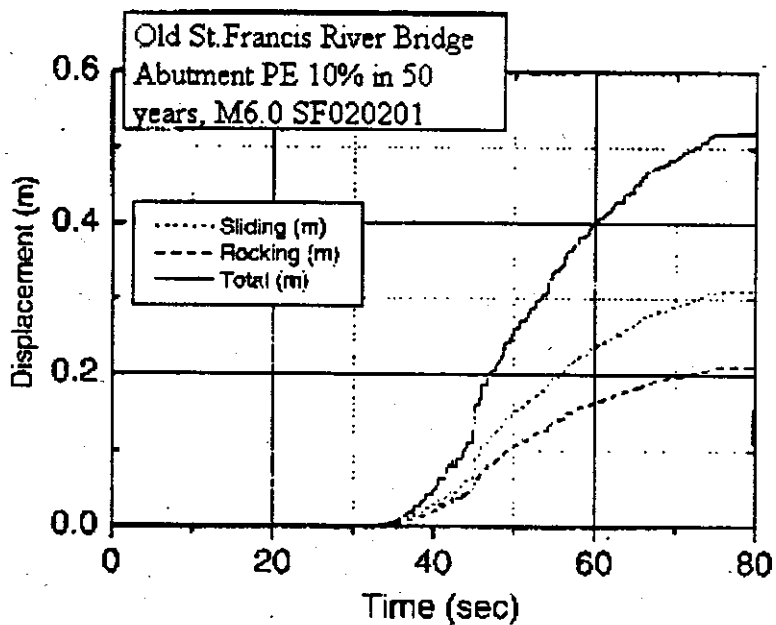


b. Magnitude 7.2

Figure 8.36 Time Histories of Sliding, Rocking and Total Permanent Displacement of the Old St. Francis River Bridge Abutment, PE 10% in 50 Years, Magnitudes 6.2 and 7.2



a. Magnitude 6.4



b. Magnitude 8.0

Figure 8.37 Time Histories of Sliding, Rocking and Total Permanent Displacement of the Old St. Francis River Bridge Abutment, PE 2% in 50 Years, Magnitudes 6.4 and 8.

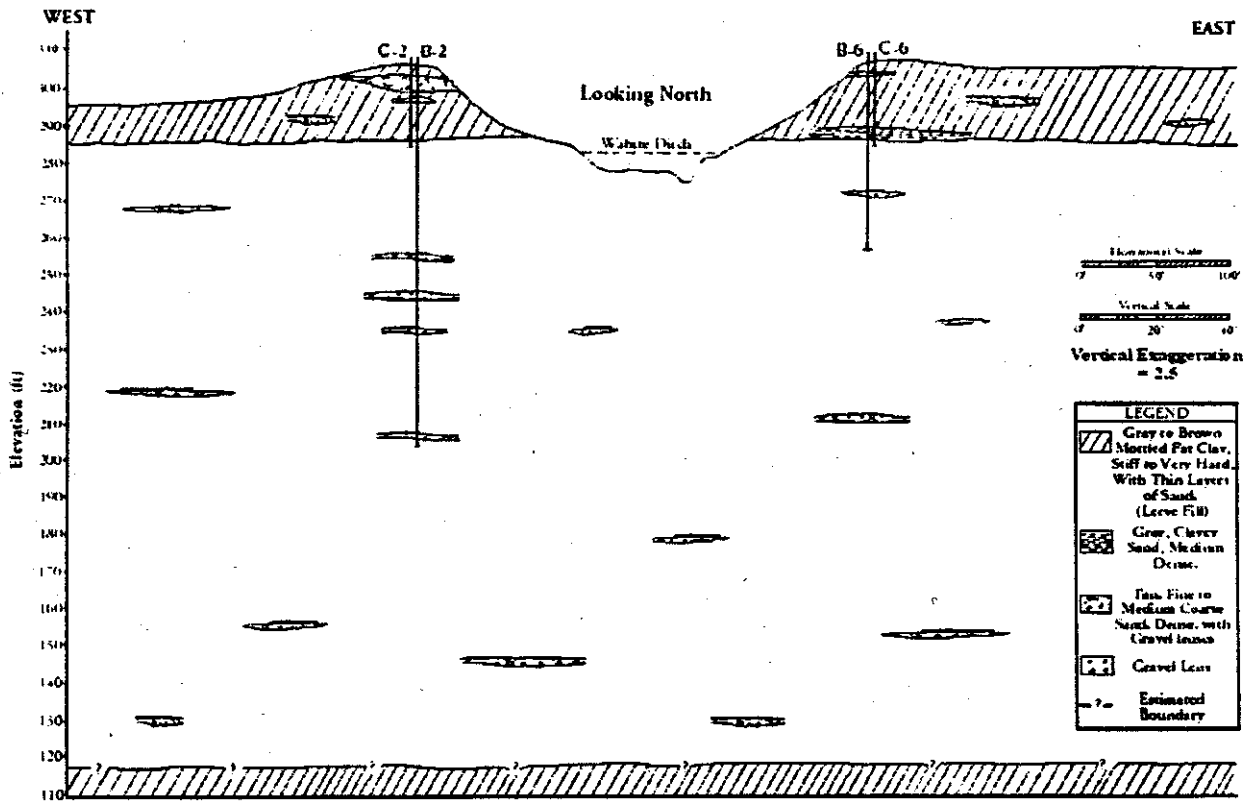


Figure 8.38 Cross-Section of Wahite Ditch Site Geology

location of the Wahite Ditch Site. A brief description of the soil profile including observed SPT ( $N_{obs}$ ) and corrected ( $N_1$ )<sub>60</sub> values are shown in Figure 8.41. The subsurface soil consists of 20 feet of high plasticity clay overlying about 170 ft of medium sand containing numerous thin gravel lenses.

### 8.2.3.1 Horizontal Seismic Response of Soil

The soil profile as developed from bore hole B1 (Figure 8.41), has been used in the seismic response analysis, because B1 is located close to the bridge abutment.

The initial shear modulus ( $G_0$ ) was computed using the seismic cone measurements of shear wave velocity. The seismic cone could be used only to a depth of 42 feet (13 m).  $G_0$  was calculated for depths below 42 ft (13 m) based on the measured  $N_{spt}$  values. This calculation is performed in the *SHAKEDIT* program itself. The non-linear soil properties, such as modulus degradation with shear strain and material damping with shear strain, have been employed for each soil type.

**Table 8.24.** Detail of Synthetic Ground Motion at the Rock Base of Wahite Ditch Site with Corresponding Maximum Peak Horizontal Ground Acceleration

**a. PE 10% In 50 Years**

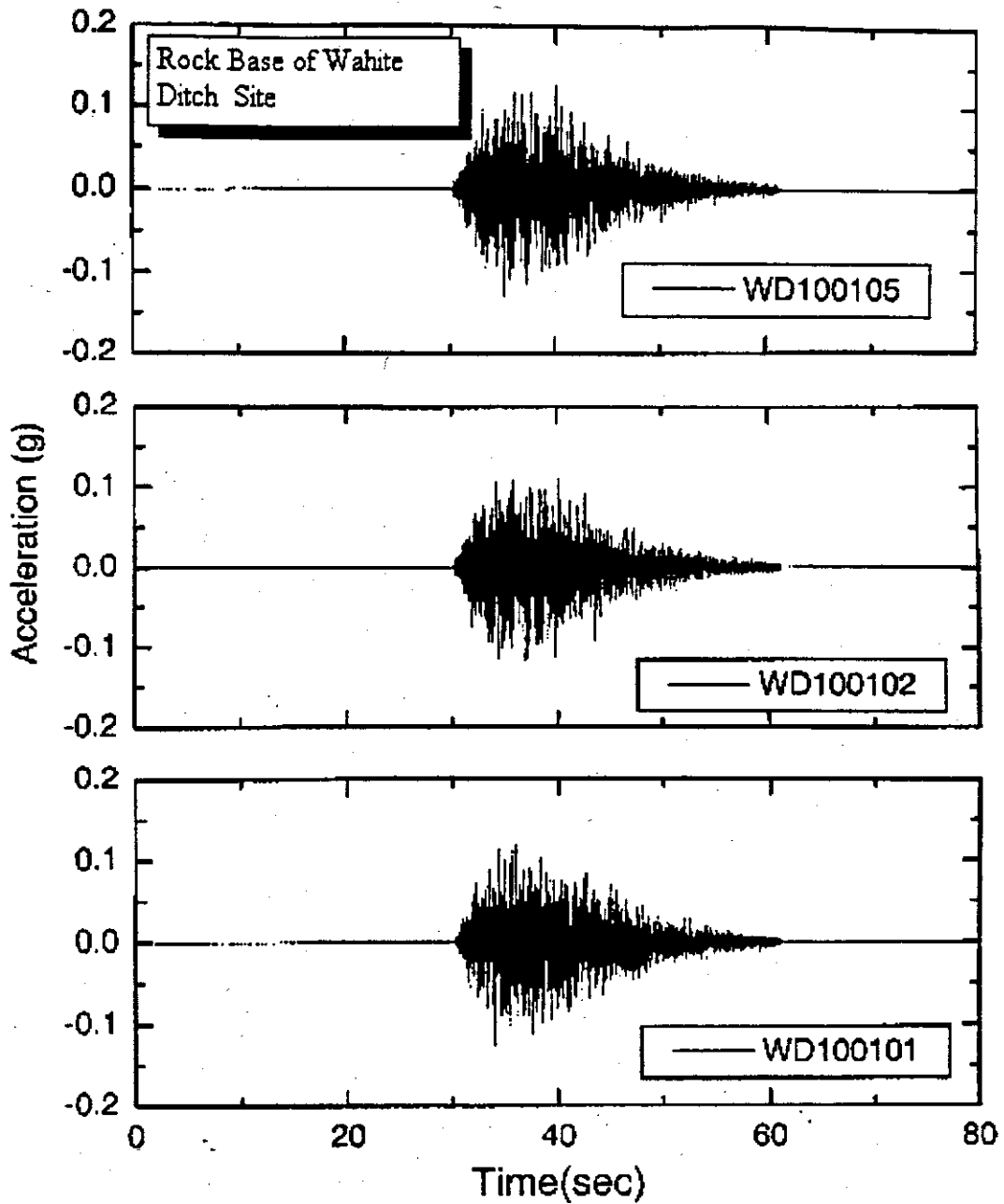
Name (1)	Mw (2)	R (km) (3)	Max acc. at rock-base(g) (4)	Max acc. at soil-surface(g) (5)
WD100101*	6.4	40	0.126	0.153
WD100102*	6.4	40	0.119	0.152
WD100103	6.4	40	0.136	0.127
WD100104	6.4	40	0.121	0.144
WD100105*	6.4	40	0.13	0.151
WD100201*	7.0	65	0.124	0.185
WD100202*	7.0	65	0.142	0.171
WD100203	7.0	65	0.173	0.171
WD100204	7.0	65	0.144	0.147
WD100205*	7.0	65	0.166	0.180
Mw = Magnitude R = Epicentral distance * Used in further analysis				

**b. PE 2% In 50 Years**

Name (1)	Mw (2)	R (km) (3)	Max acc. at rock-base(g) (4)	Max acc. at soil-surface(g) (5)
WD020101*	7.8	16	1.549	0.437
WD020102*	7.8	16	1.769	0.478
WD020103*	7.8	16	2.129	0.512
WD020104	7.8	16	1.996	0.415
WD020105	7.8	16	1.822	0.423
WD020201	8.0	20	1.442	0.440
WD020202	8.0	20	1.589	0.440
WD020203*	8.0	20	1.855	0.525
WD020204*	8.0	20	1.720	0.406
WD020205*	8.0	20	1.559	0.447
Mw = Magnitude R = Epicentral distance * Used in further analysis				

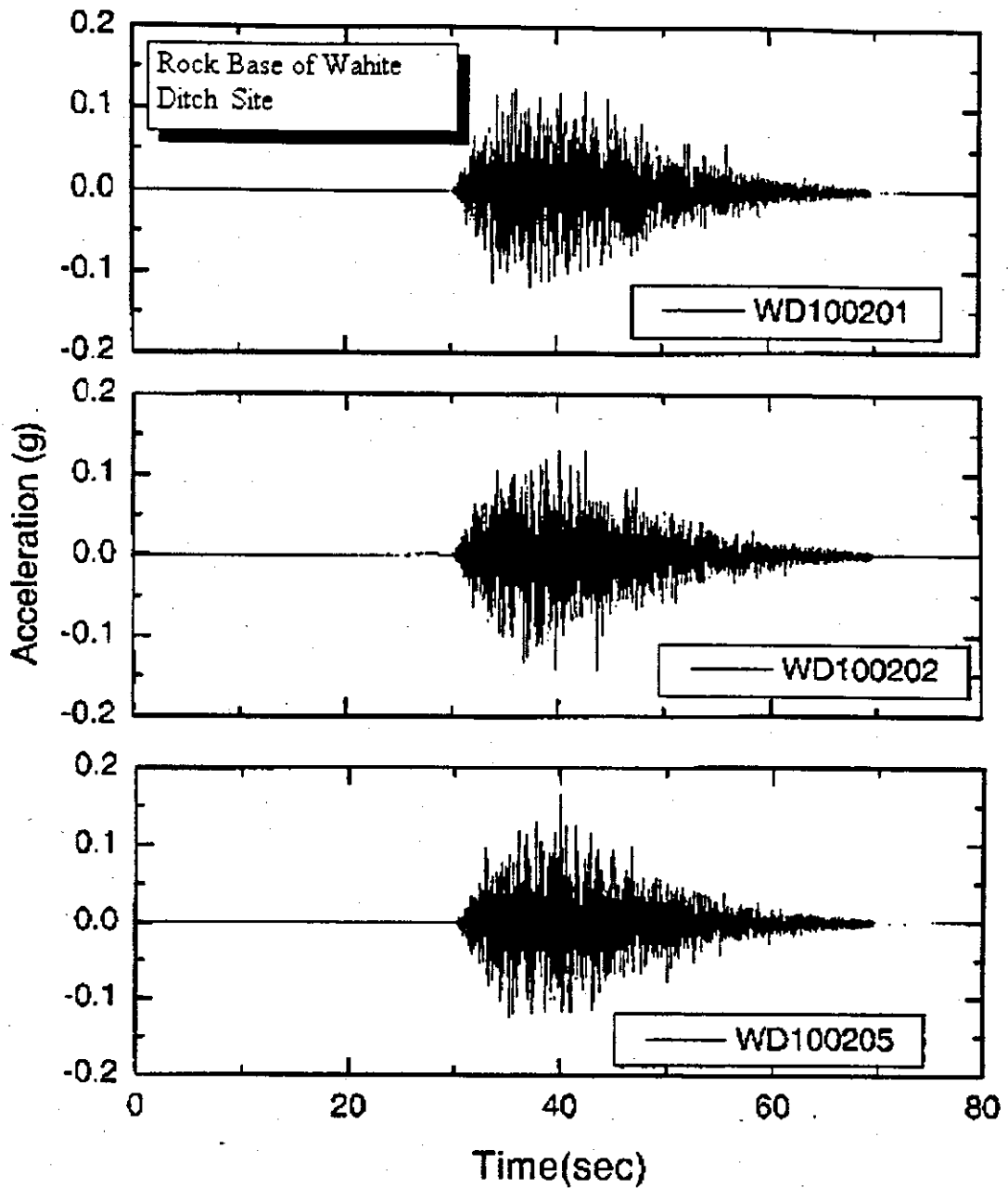
The calculated peak ground accelerations at each soil level, based on wave propagation analysis, were plotted against depth. Figures 8.42a and b show the peak acceleration for PE 10% in 50 years for M6.4 and M7.0 respectively. Figures 8.43a and b show the peak acceleration for PE 2% in 50 years for M7.8 and M8.0 respectively.

For PE 10 % in 50 years and M6.4 and M7.0 respectively, the peak accelerations at the soil surface are higher than those at the base-rock. However, for PE 2 % in 50 years, the peak accelerations at the soil surface are smaller than those at the base rock.



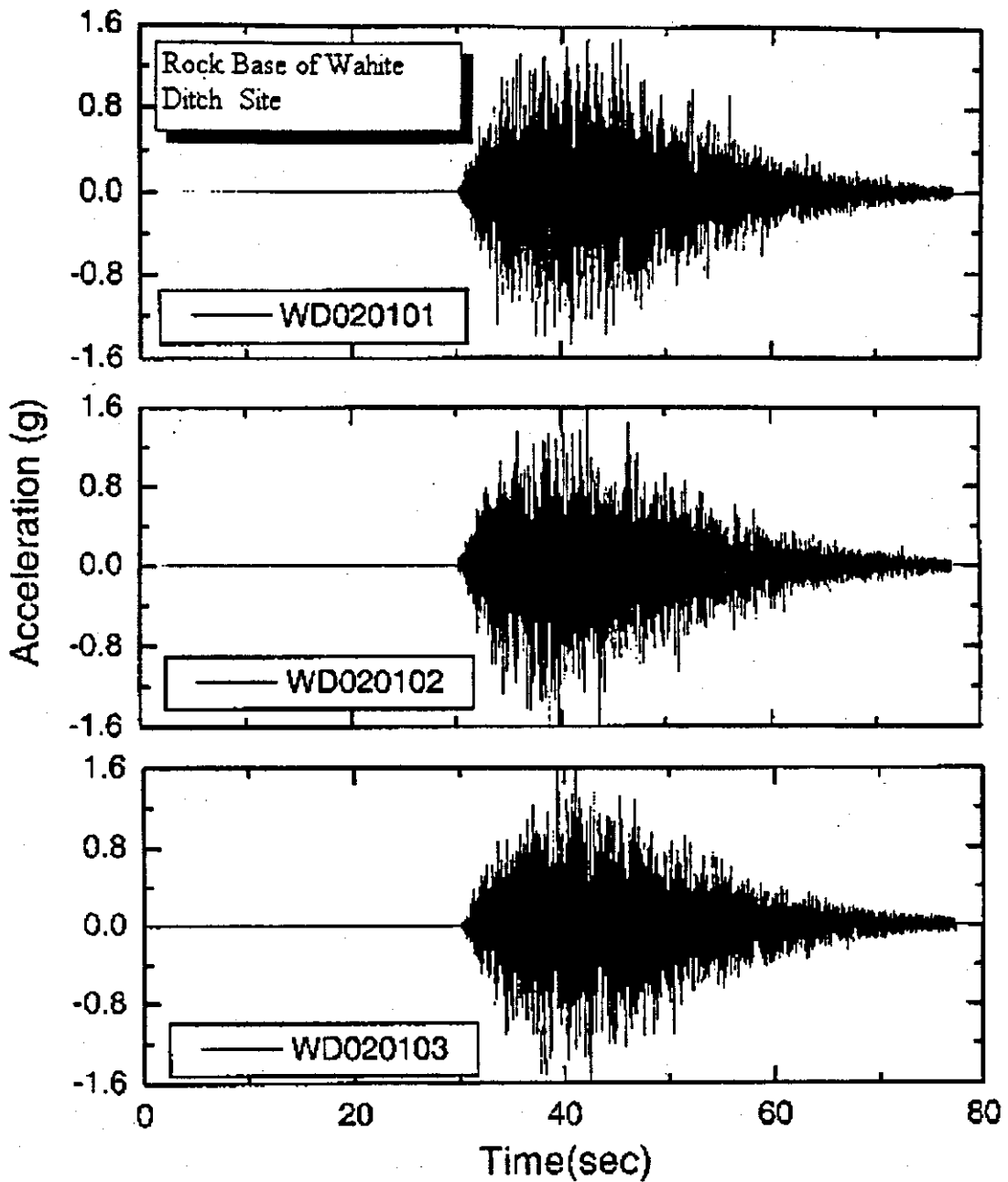
a. PE 2 % in 50 years, Magnitude = 6.4

Figure 8.39a Acceleration Time Histories for the Wahite Ditch Site, PE 2% in 50 Years, Magnitude = 6.4



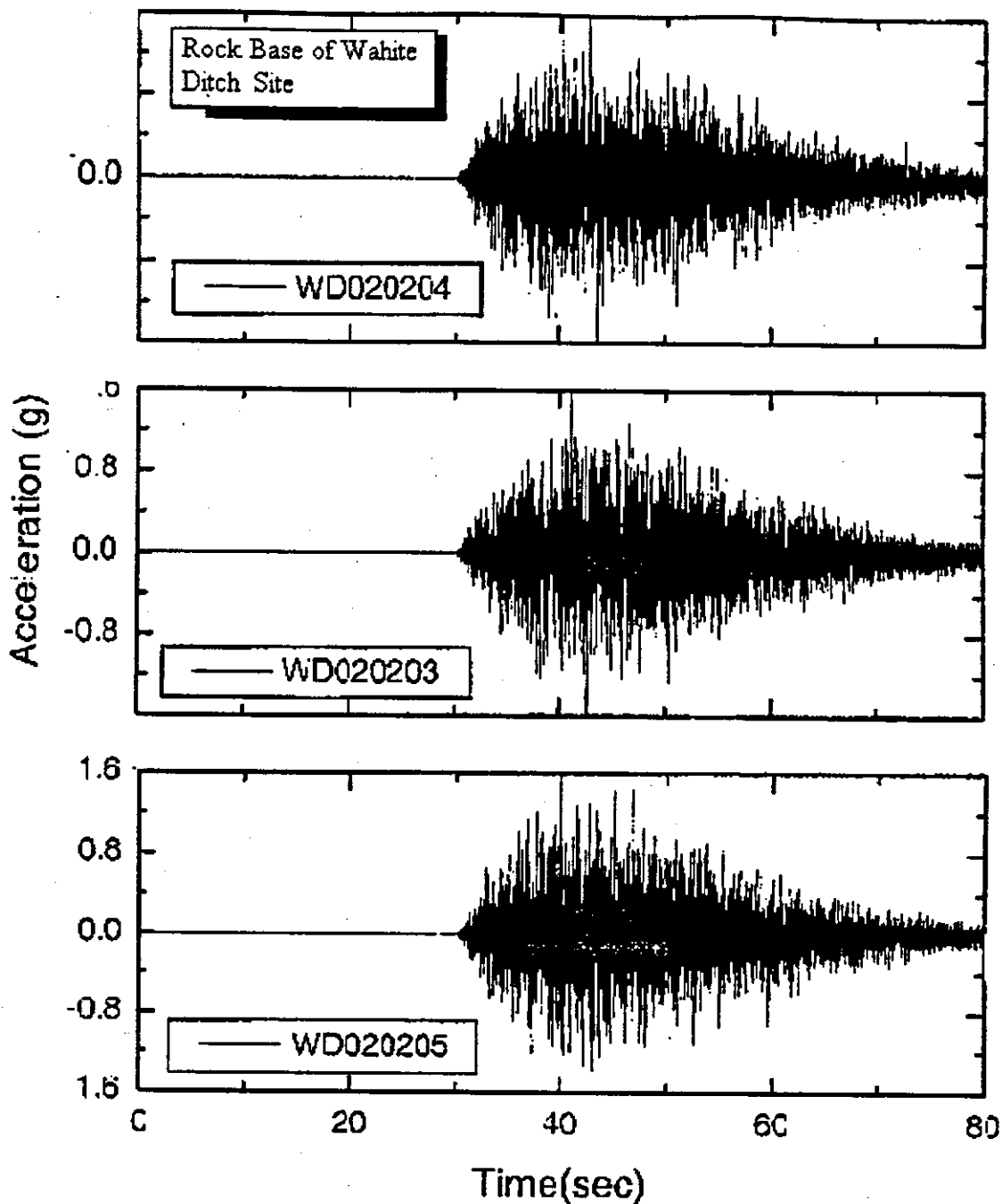
b. PE 10 % in 50 years, Magnitude = 7.0

Figure 8.39b Acceleration Time Histories for the Wahite Ditch Site, PE 10% in 50 Years, Magnitude = 7.0



c. PE 2 % in 50 years, Magnitude = 7.8

Figure 39c Acceleration Time Histories for the Wahite Ditch Site, PE 2% in 50 Years, Magnitude = 7.8



d. PE 2 % in 50 years, Magnitude = 8.0

Figure 8.39d Acceleration Time Histories for the Wahite Ditch Site, PE 2% in 50 Years, Magnitude = 8.0

Table 8.25a shows the peak horizontal acceleration for the design earthquake at the soil surface, bridge abutment and pier respectively for PE 10% in 50 years, Table 8.25b shows similar information for PE 2% in 50 years.

### 8.2.3.2 Resulting Ground Motion Time Histories

Figures 8.44a and b contain six-plots of surface ground acceleration at EL. 307.2 for PE 10% in 50 years and earthquake magnitude M6.4 and M7.0. Similarly Figures 8.44c and d contain plots for PE 2% in 50 years and M7.8 and M8.0 respectively.

Figures 8.45a, b, c and d contain plots of design acceleration time history at the abutment for (a) PE 10% in 50 years M6.4, (b) PE 10% in 50 years M7.0, (c) PE 2% in 50 years M7.8 and (d) PE 2% in 50 years M8.0.

Similarly, Figure 8.46a, b, c and d contain plots for the pier.

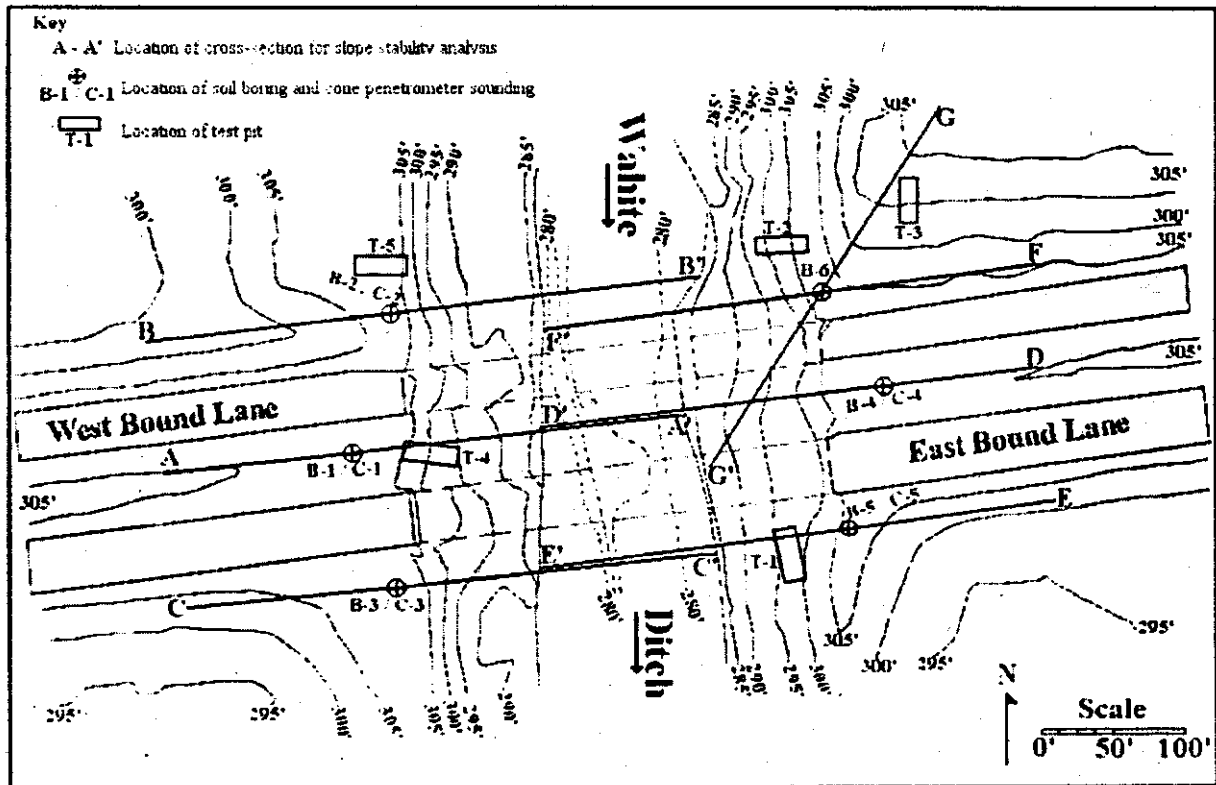


Figure 8.40 Wahite Ditch Site Topography, Cross-Section and Boring Locations

**Table 8.25** Detail of Peak Ground Motion Used at the Wahite Ditch Site Rock Base, Ground Surface, Bridge Abutment and Pier

**a. PE 10% in 50 years**

File Name	Max. acc. at rock-base EL. 106.0 (g)	Max acc. at soil-surface EL 307.2 (g)	Max acc. at bridge abutment EL 301.2 (g)	Max acc. at bridge pier EL 269.9 (g)
WD100101*	0.126	0.153	0.153	0.139
WD100102*	0.119	0.152	0.151	0.127
WD100105*	0.13	0.151	0.151	0.120
WD100201*	0.124	0.185	0.185	0.169
WD100202*	0.142	0.171	0.170	0.146
WD100205*	0.166	0.18	0.180	0.157

**b PE 2% in 50 years**

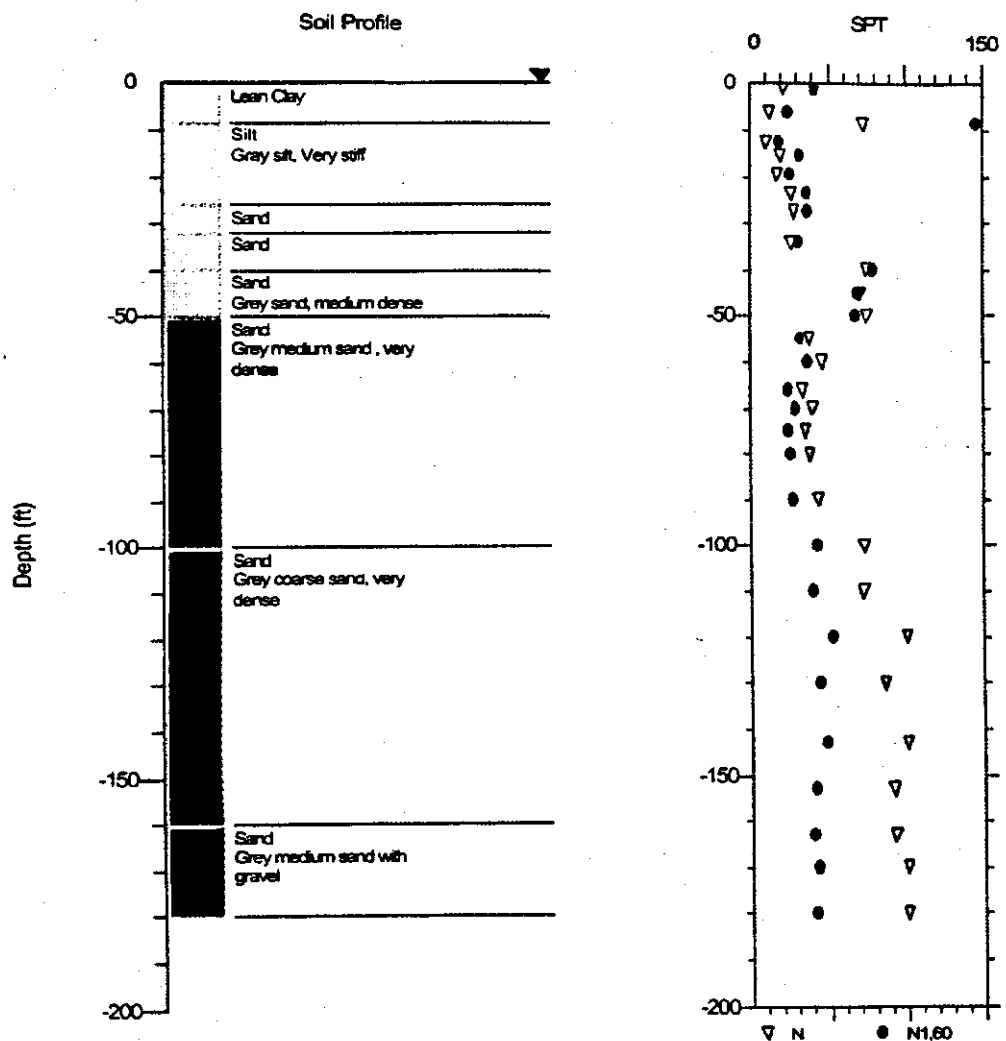
File Name	Max. acc. At rock-base EL. 106.0(g)	Max acc. at soil-surface EL 307.2 (g)	Max acc. at bridge abutment EL 301.2 (g)	Max acc. at bridge pier EL 269.9 (g)
WD020101*	1.549	0.437	0.440	0.430
WD020102*	1.769	0.478	0.482	0.512
WD020103*	2.129	0.512	0.514	0.522
WD020202*	1.589	0.44	0.446	0.466
WD020203*	1.855	0.525	0.527	0.538
WD020205*	1.559	0.447	0.449	0.444

**8.2.3.3 Vertical Seismic Response of Soil**

Herrmann (2000) stated that vertical rock motion is of the same order of magnitude as the horizontal rock motion. *SHAKE91* was used to transmit the horizontal rock motion from the rock base to the ground surface. No such solution is available for transmission of vertical motion. Therefore the following procedure was adopted for vertical ground motion determination:

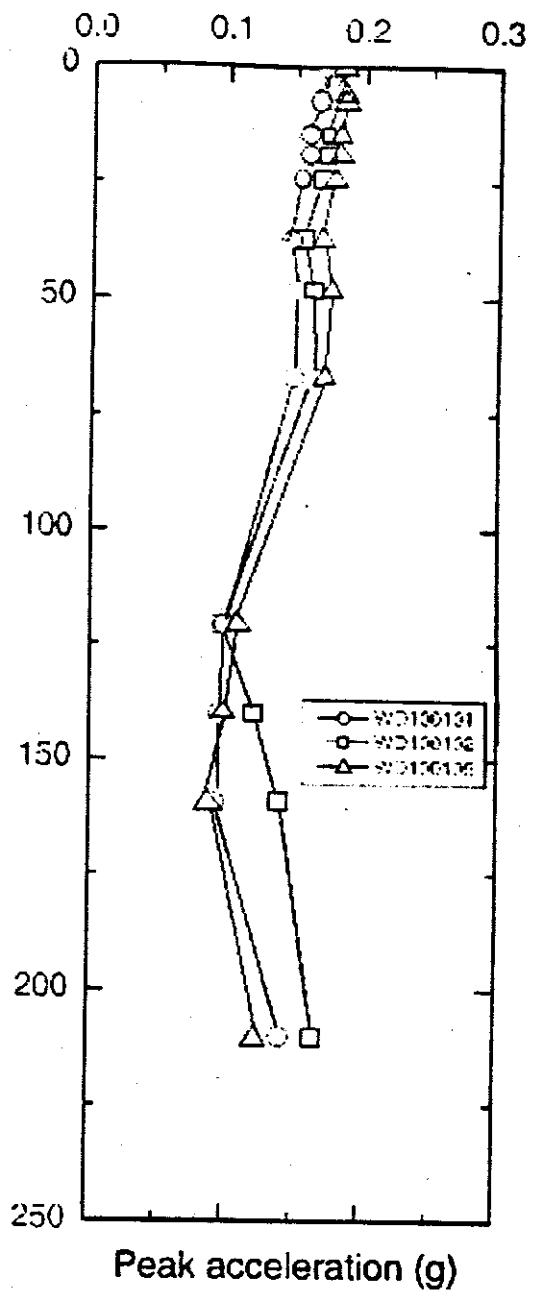
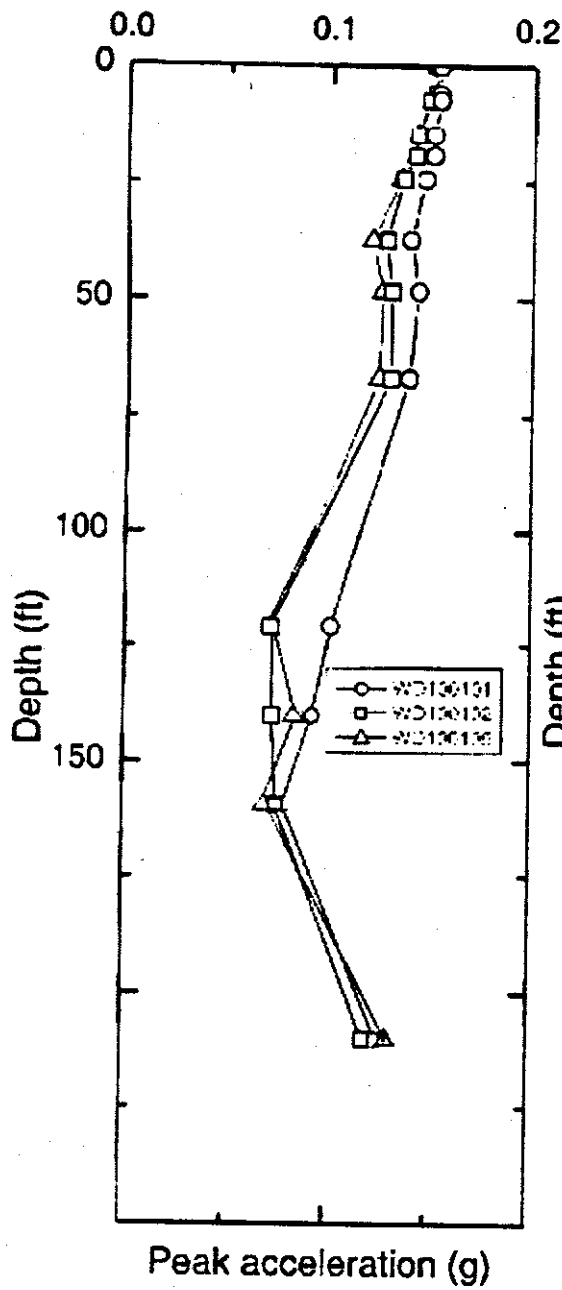
1. Use *SHAKE91* to transfer the P-wave.
2. Adjust peak vertical ground motion as 2/3 of peak horizontal ground motion.
3. Adjust the time history to reflect adjustment in (2) above.

The calculated vertical time histories of acceleration at soil surface, base of bridge abutment and at bridge pier were also modified as above.



Notes:  
 CSR analysis using SHAKE results.  
 CSR File: D:\I-O SF Vel08\SF100103\SF100103.grf  
 CSR using SPT Data and Seed et. al. Method in 1997 NCEER Workshop.  
 Earthquake File for SHAKE Analysis: D:\SF\SF100103.ACC  
 Earthquake Magnitude for CSR Analysis: 6.2  
 Magnitude Scaling Factor (MSF): 1.62  
 Depth to Water Table for CSR Analysis (ft): 0  
 Depth to Water Table for Cn Calculation (ft): 0  
 Depth to Base Layer for CSR Analysis (ft): 219.6  
 MSF Option: I.M. Idriss (1997)  
 Cn Option: Liao & Whitman (1986)  
 Ksigma Option: L.F. Harder & R. Boulanger (1997)  
 SPT Energy Ratio: USA/Safety/Rope: 0

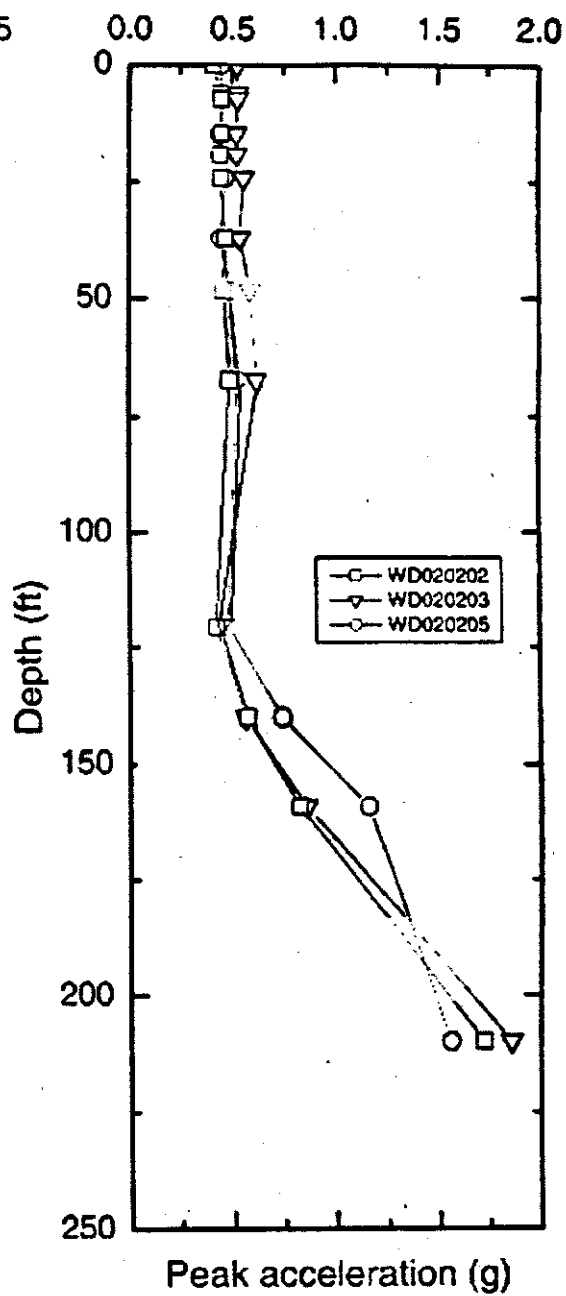
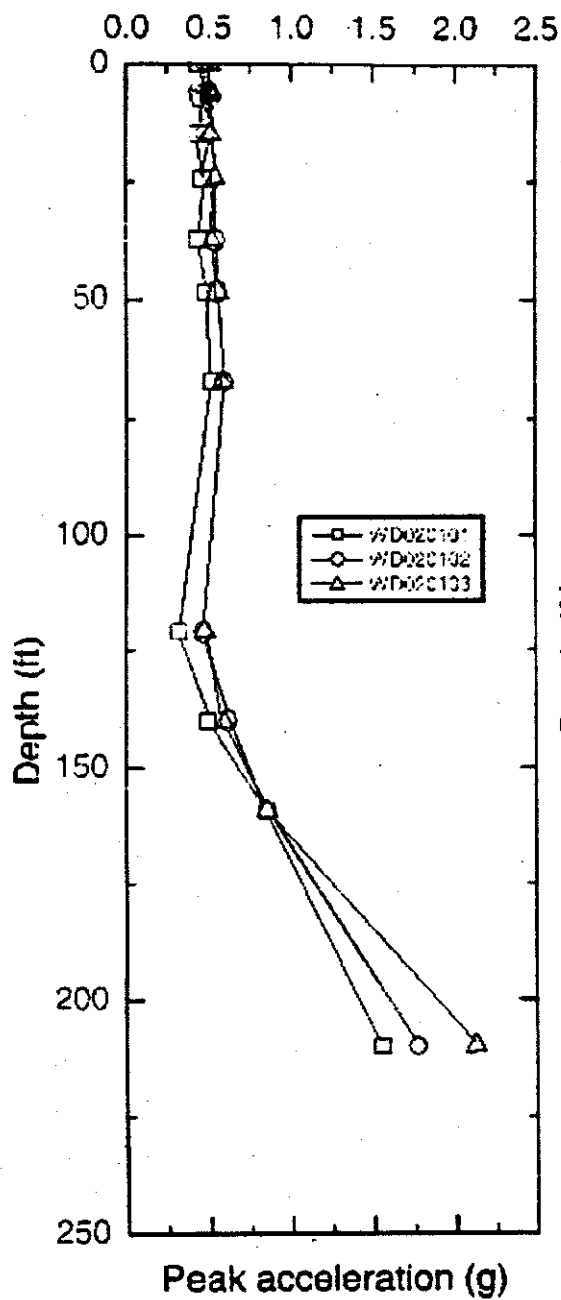
Figure 8.41 Soil Profile Wahite Ditch Site Boring B-1



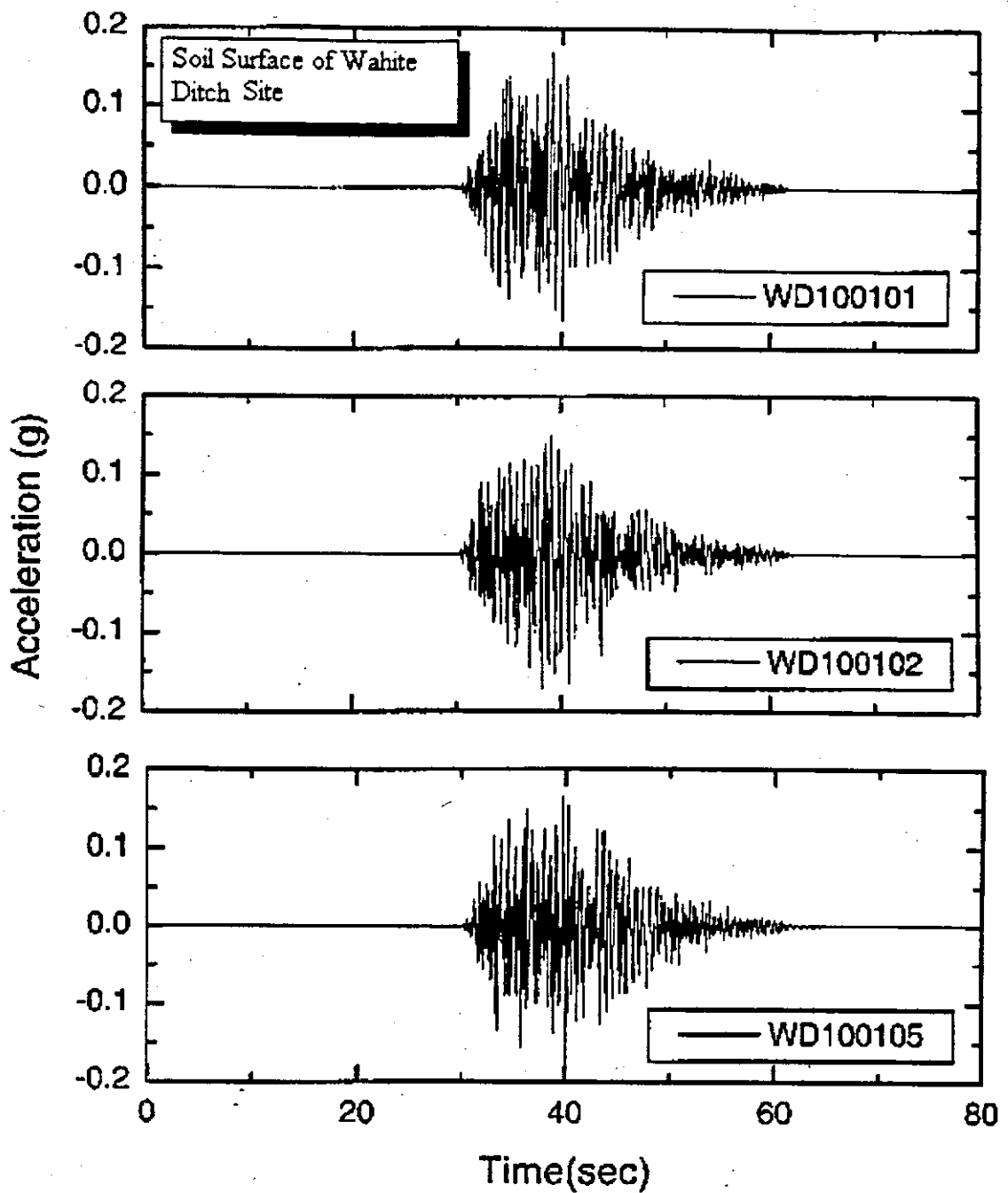
a) PE 10 % in 50 years, M6.4

b) PE 10 % in 50 years, M7.0

Figure 8.42 Peak Ground Acceleration vs. Depth for PE 10% in 50 Years Magnitudes 6.4 and 7.0 Wahite Ditch Site

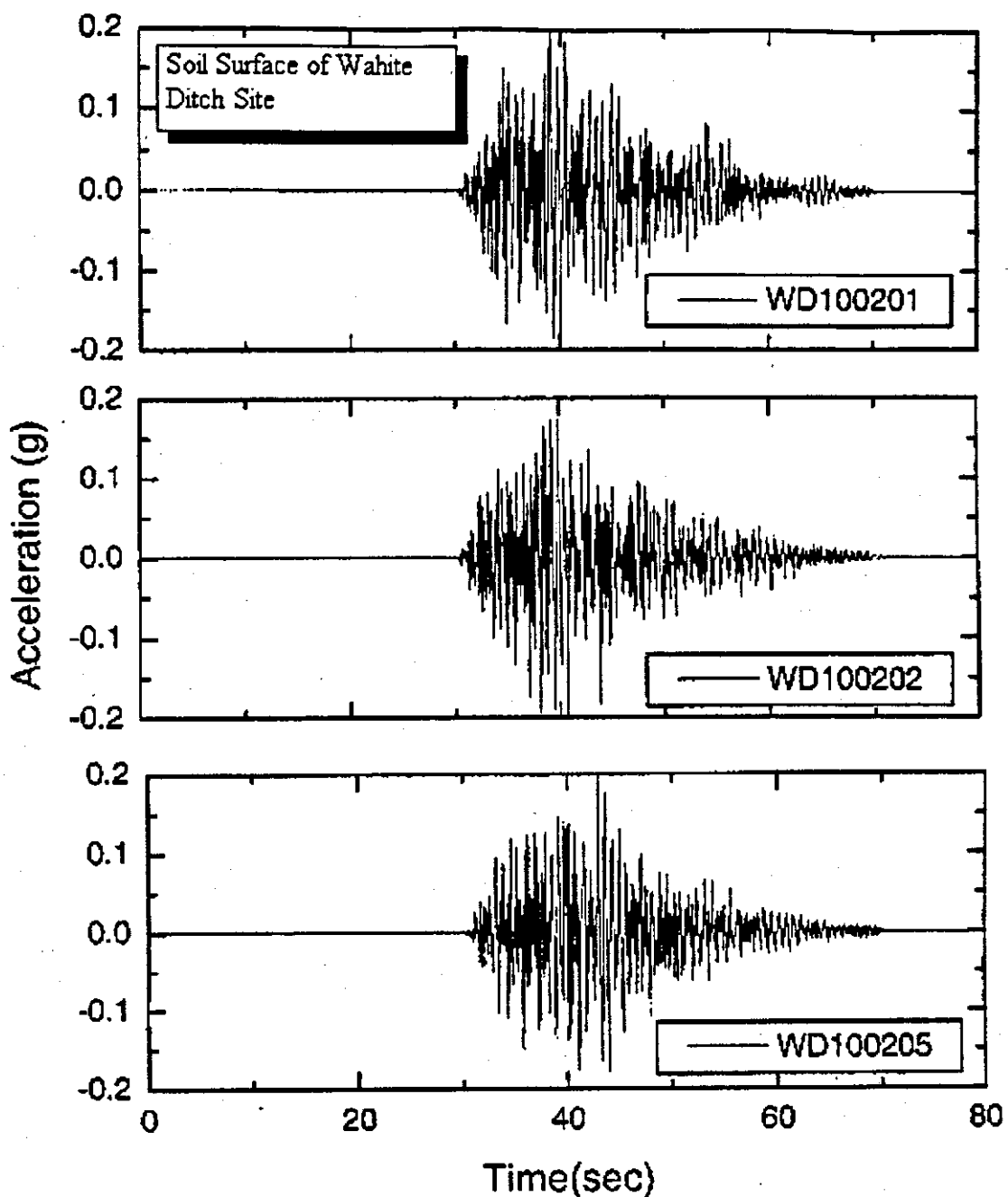


a) PE 2% in 50 years, M7.8      b) PE 2% in 50 years, M8.0  
 Figure 8.43 Peak Ground Acceleration vs. Depth for PE 2% in 50 Years Magnitudes 7.8 and 8.0  
 Wahite Ditch Site



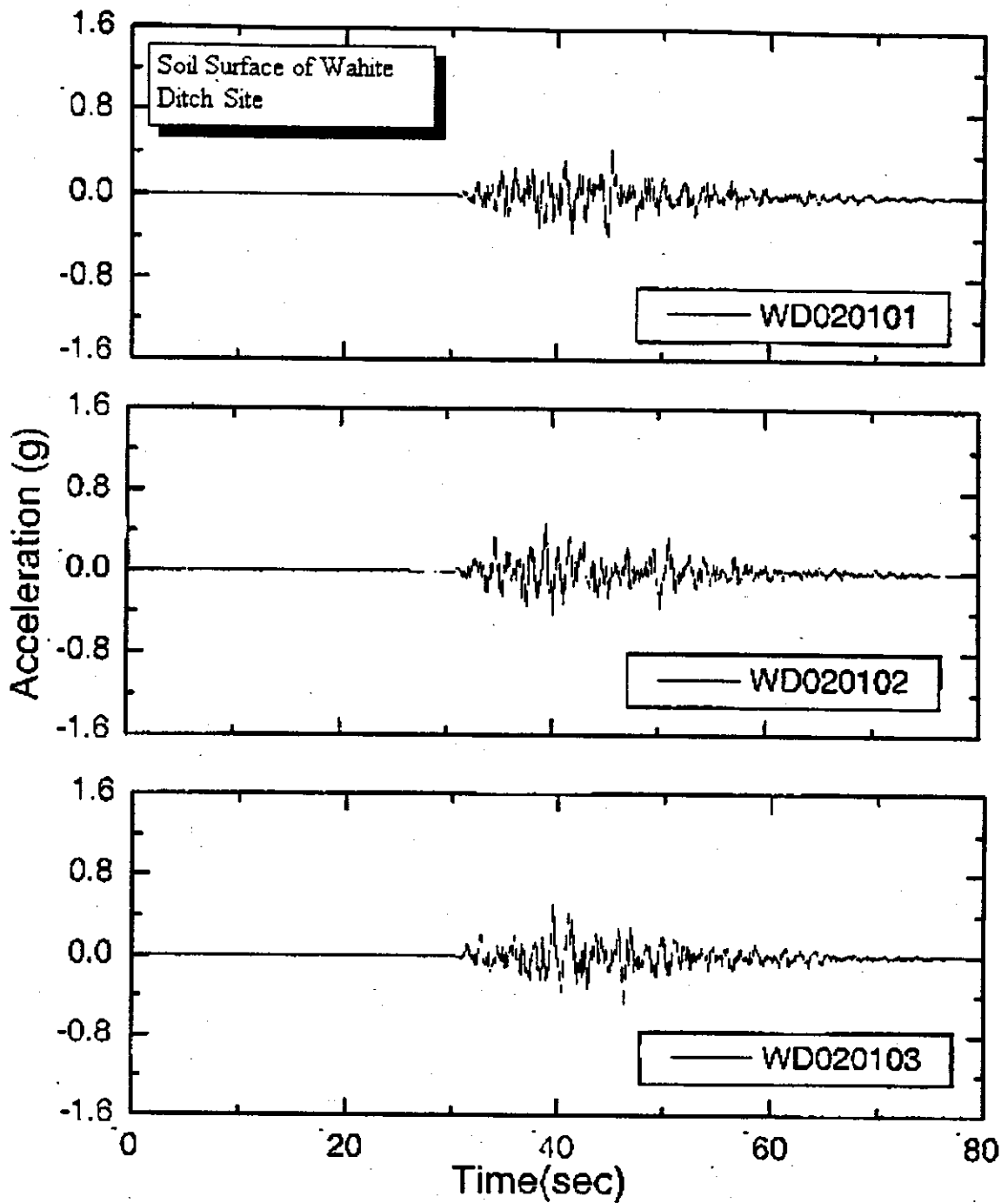
a. PE 10 % in 50 years, Magnitude = 6.4

Figure 8.44a Ground Acceleration at the surface of the Wahite Ditch Site, PE 10% in 50 years, Magnitude = 6.4



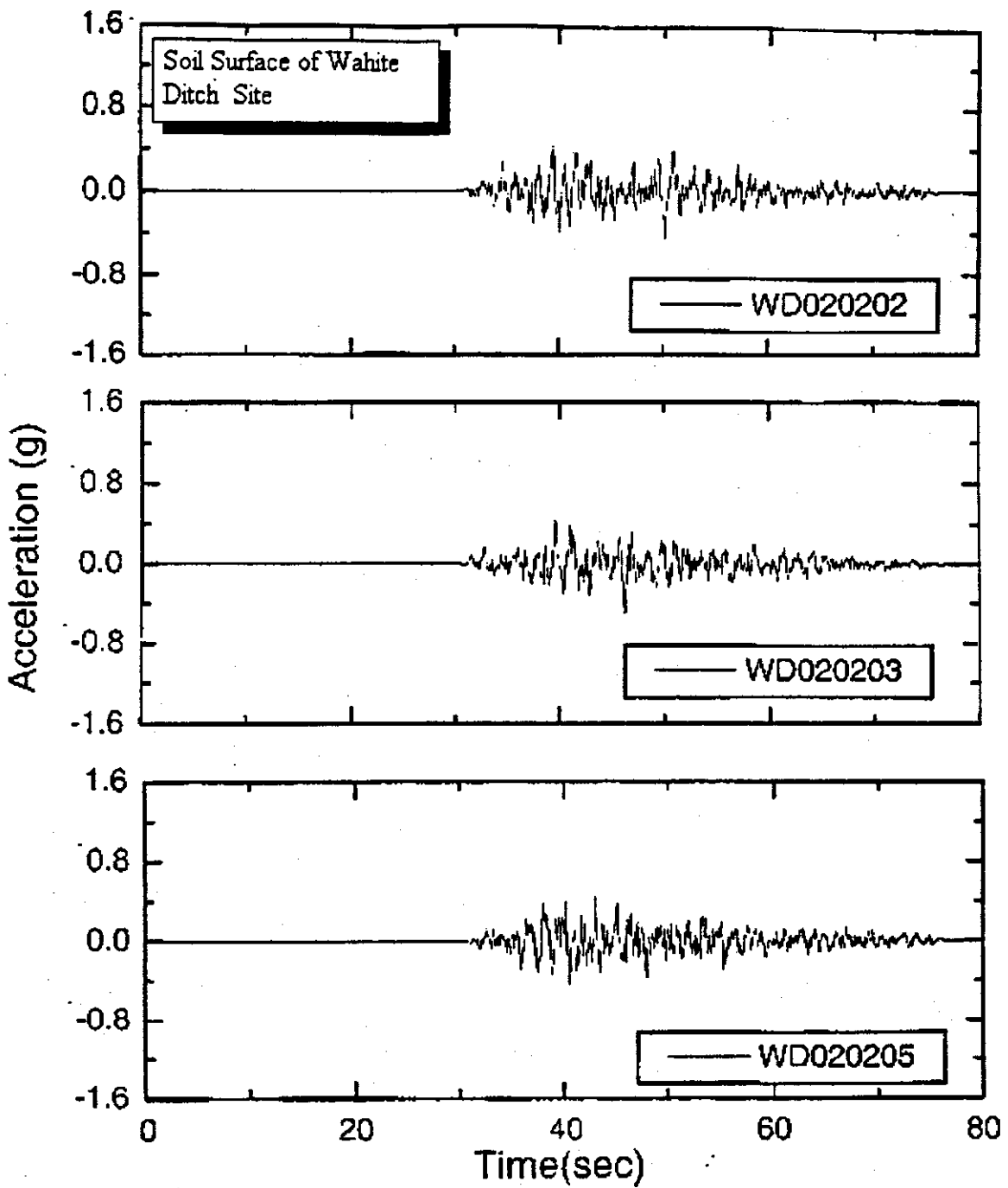
b. PE 10 % in 50 years, Magnitude = 7.0

Figure 8.44b Ground Acceleration at the surface of the Wahite Ditch Site, PE 10% in 50 years, Magnitude = 7.0



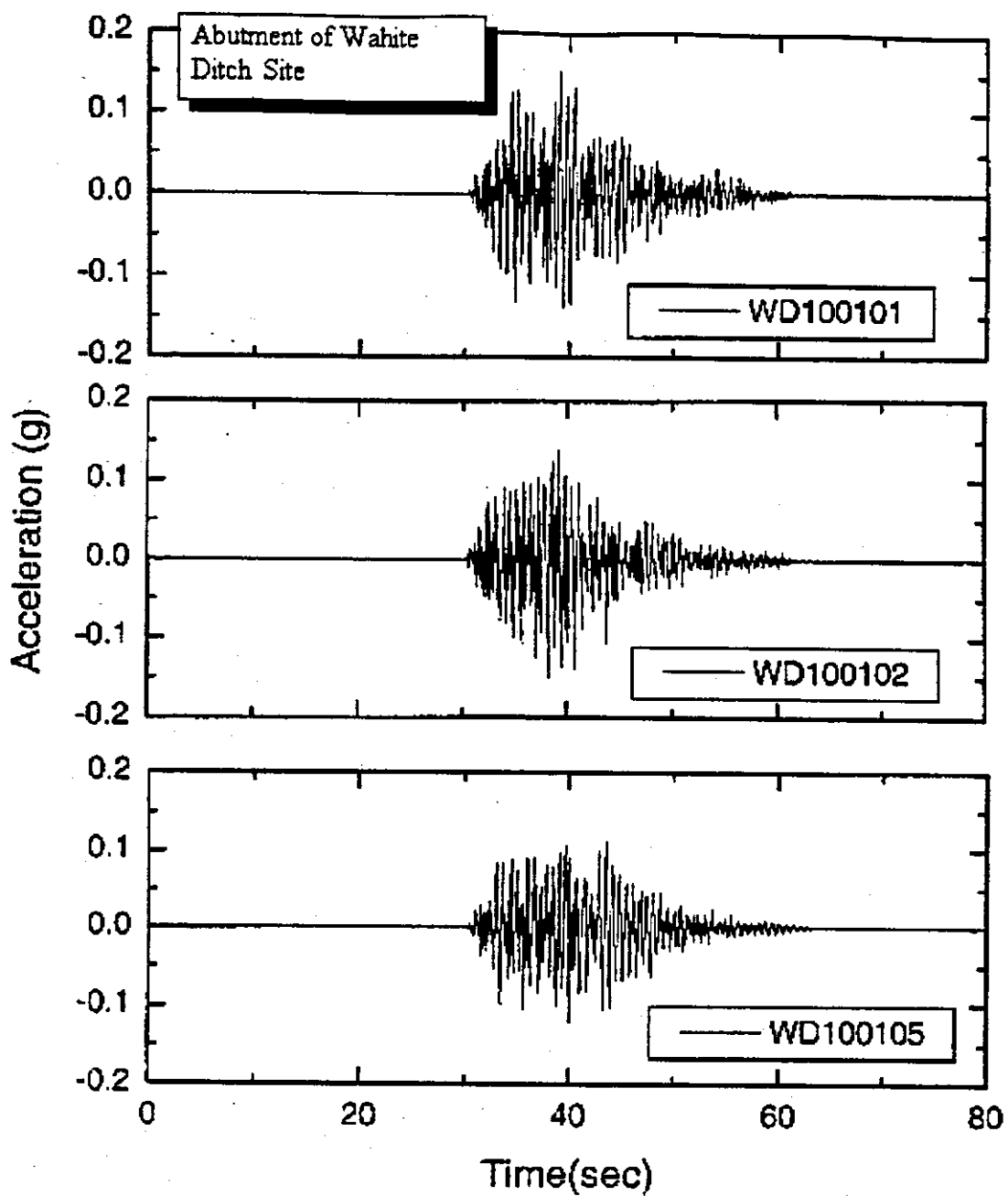
c. PE 2 % in 50 years, Magnitude = 7.8

Figure 8.44c Ground Acceleration at the surface of the Wahite Ditch Site, PE 2% in 50 years, Magnitude = 7.8



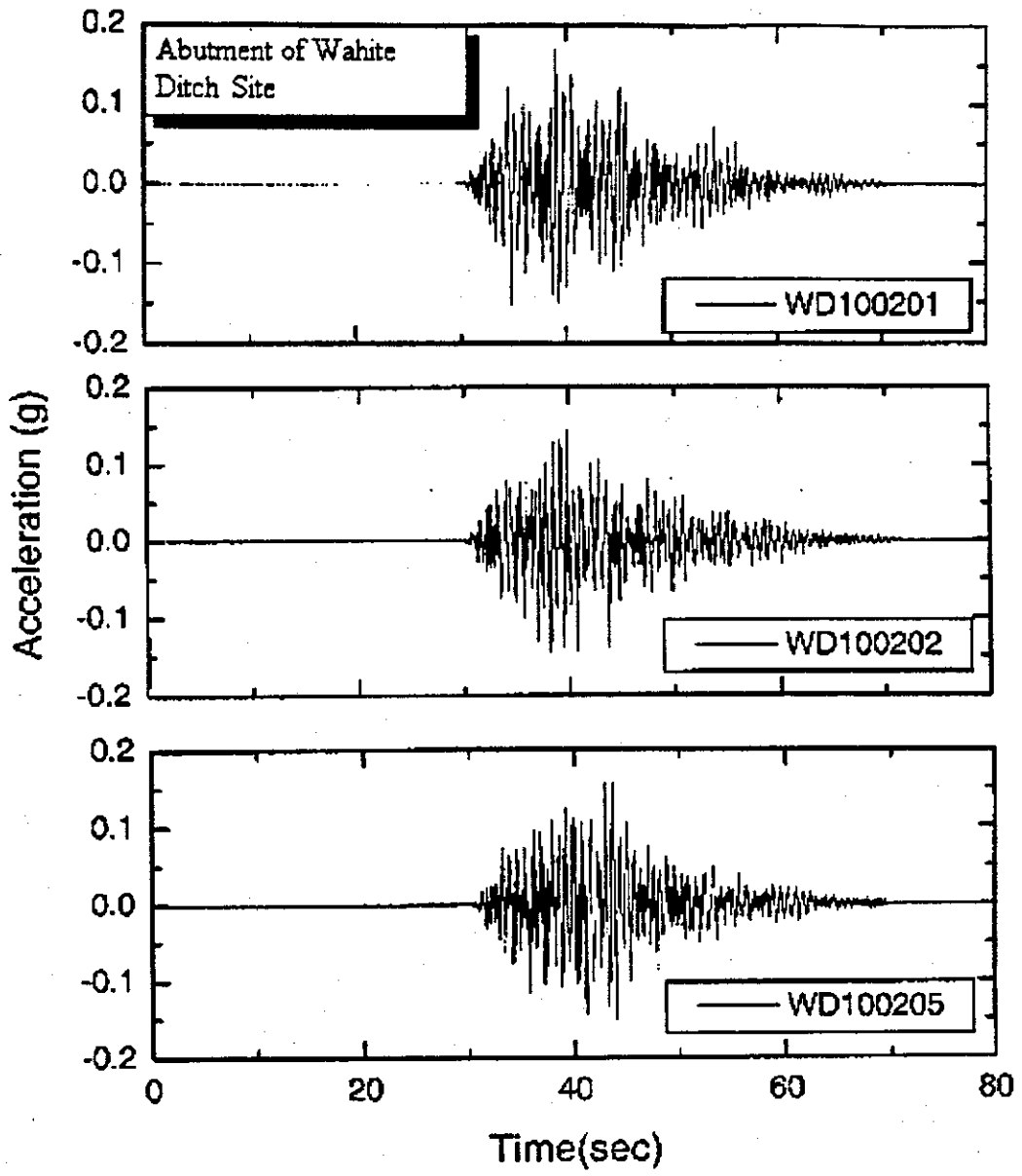
d. PE 2 % in 50 years, Magnitude = 8.0

Figure 8.44d Ground Acceleration at the surface of the Wahite Ditch Site, PE 2% in 50 years, Magnitude = 8.0



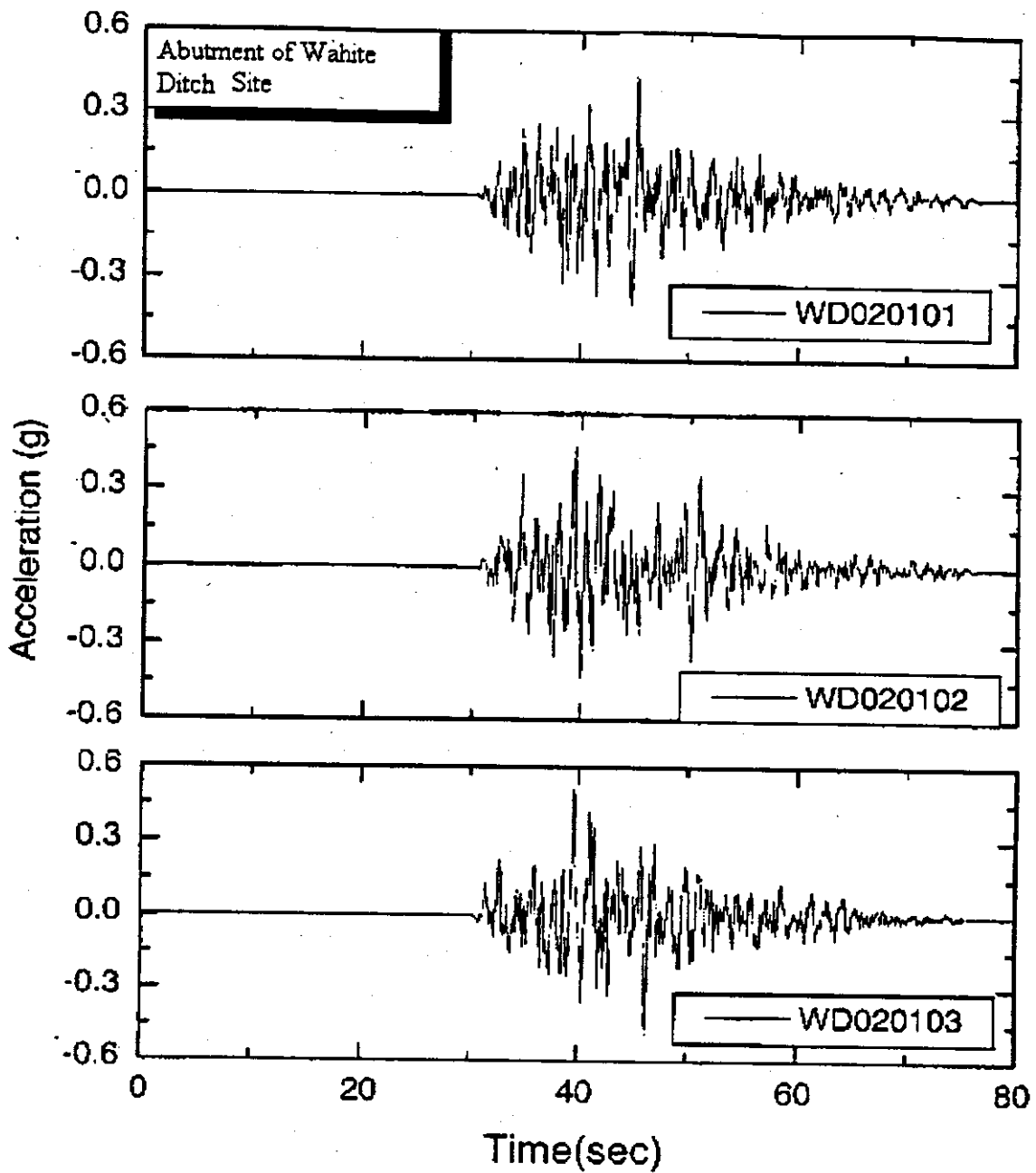
a. PE 10 % in 50 years, Magnitude = 6.4

Figure 8.45a Ground Acceleration at the Abutment of the Wahite Ditch Site, PE 10% in 50 years, Magnitude = 6.4



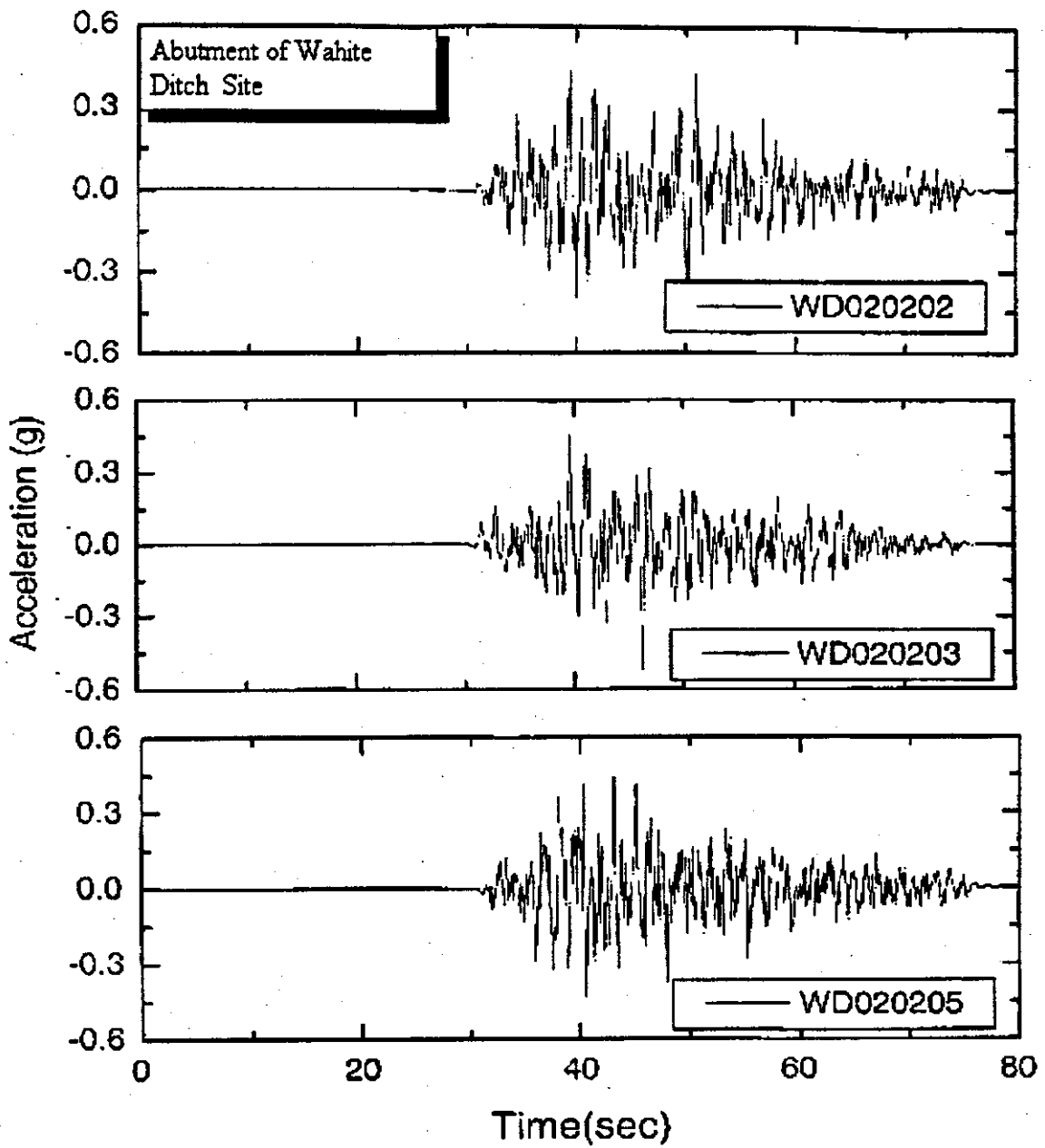
b. PE 10 % in 50 years, Magnitude = 7.0

Figure 8.45b Ground Acceleration at the Abutment of the Wahite Ditch Site, PE 10% in 50 years, Magnitude = 7.0



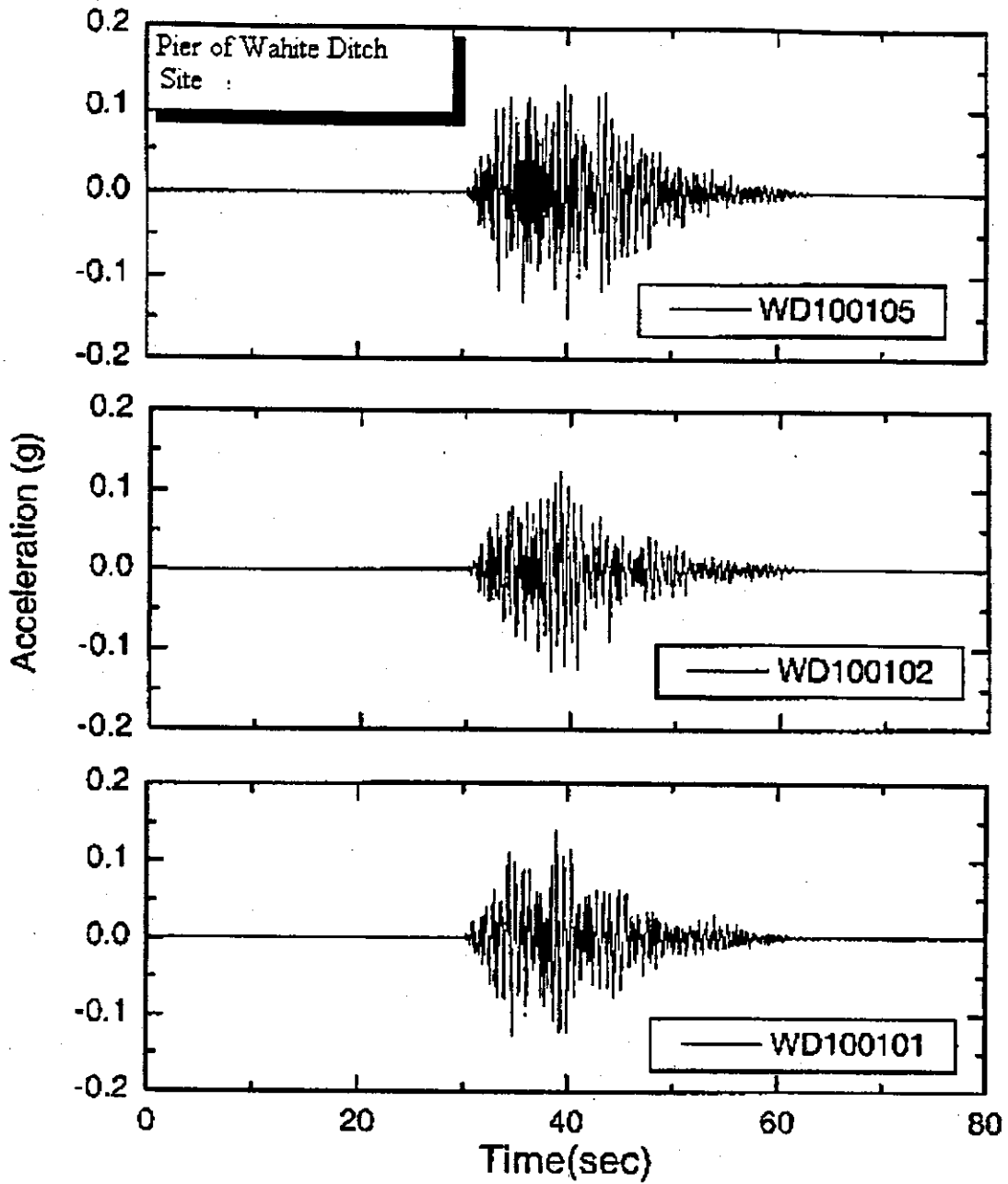
c. PE 2 % in 50 years, Magnitude = 7.8

Figure 8.45c Ground Acceleration at the Abutment of the Wahite Ditch Site, PE 2% in 50 years, Magnitude = 7.8



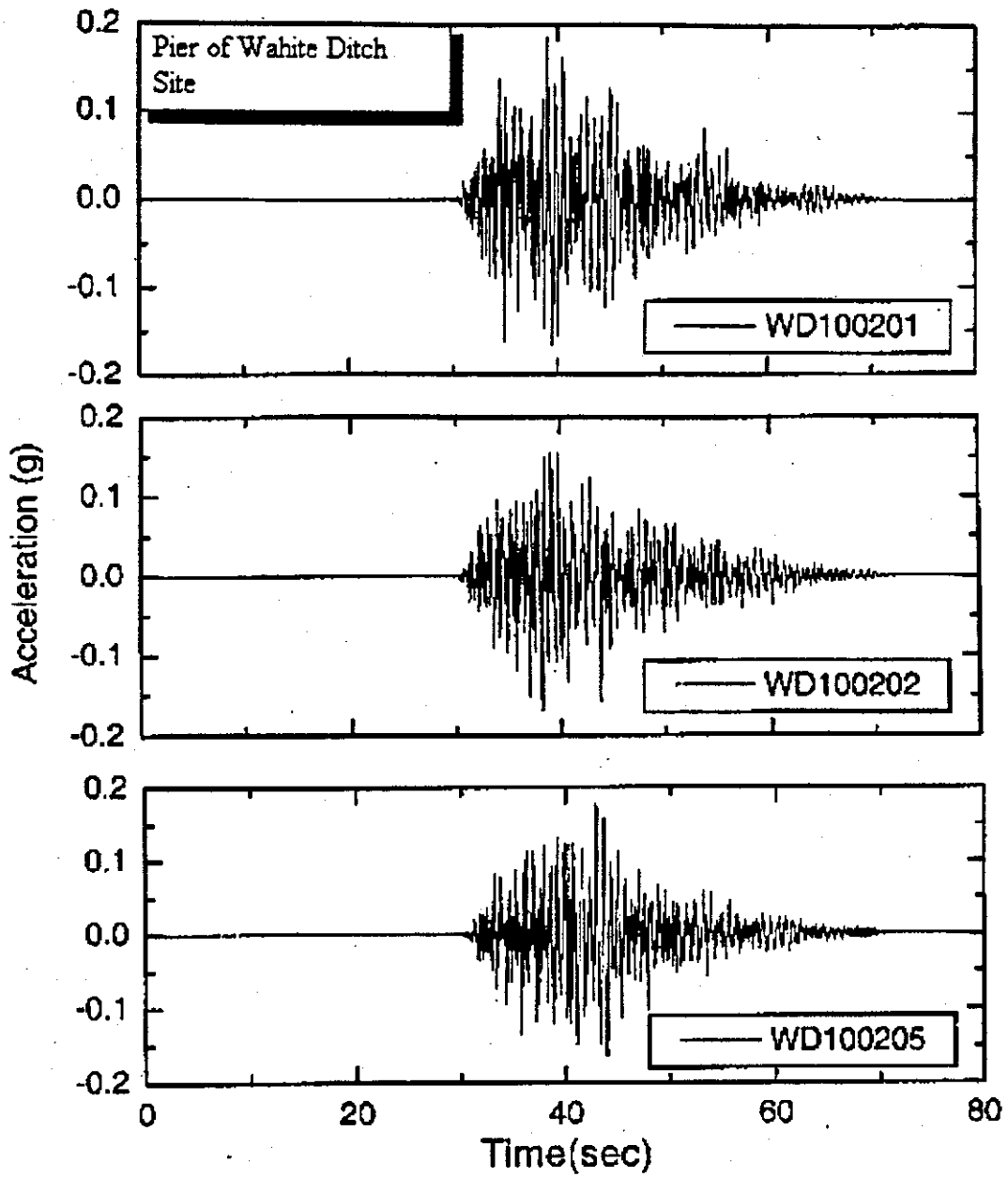
d. PE 2 % in 50 years, Magnitude = 8.0

Figure 8.45d Ground Acceleration at the Abutment of the Wahite Ditch Site, PE 2% in 50 years, Magnitude = 8.0



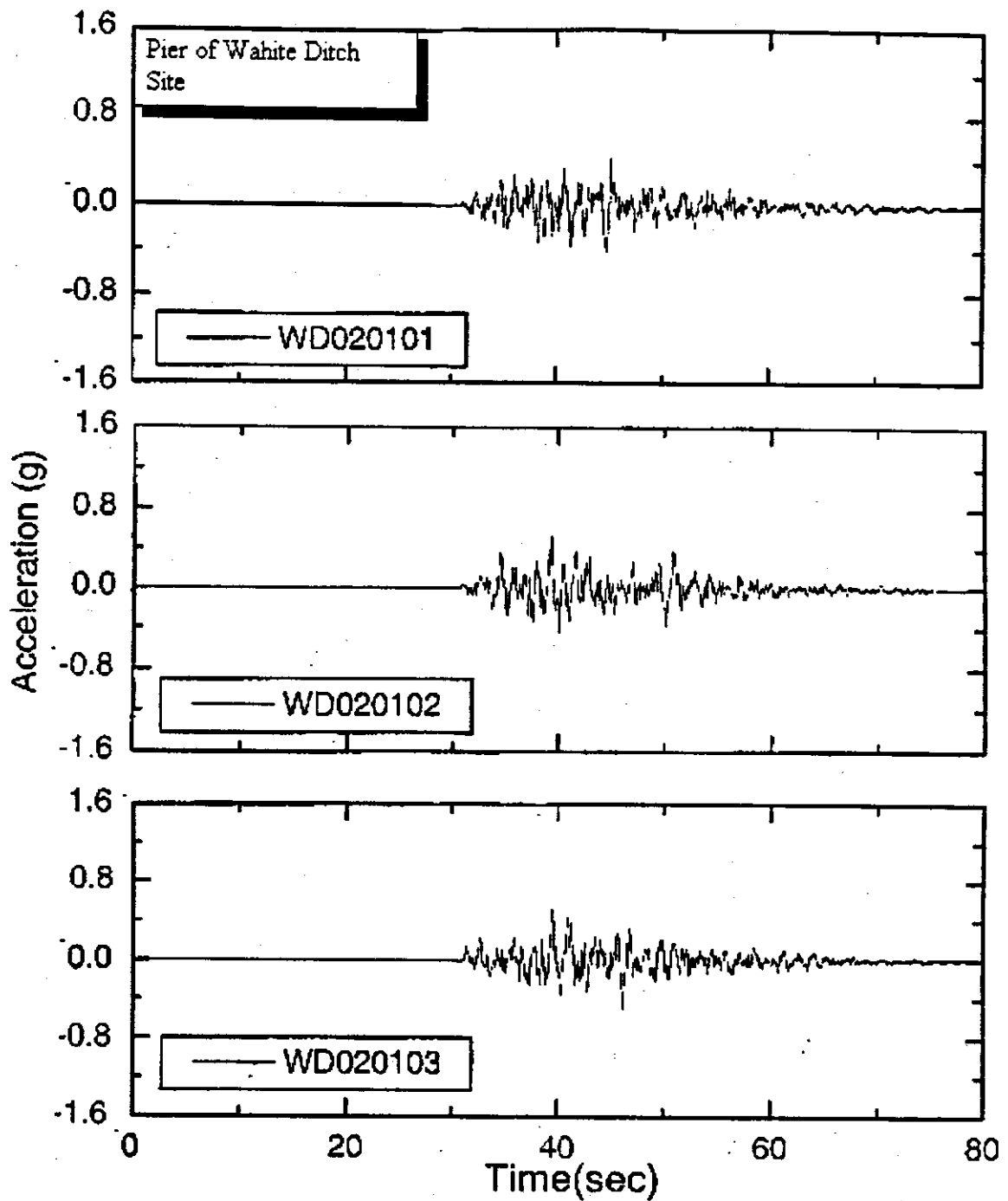
a. PE 10 % in 50 years, Magnitude = 6.4

Figure 8.46a Ground Acceleration at the Pier of the Wahite Ditch Site, PE 10% in 50 years, Magnitude = 6.4



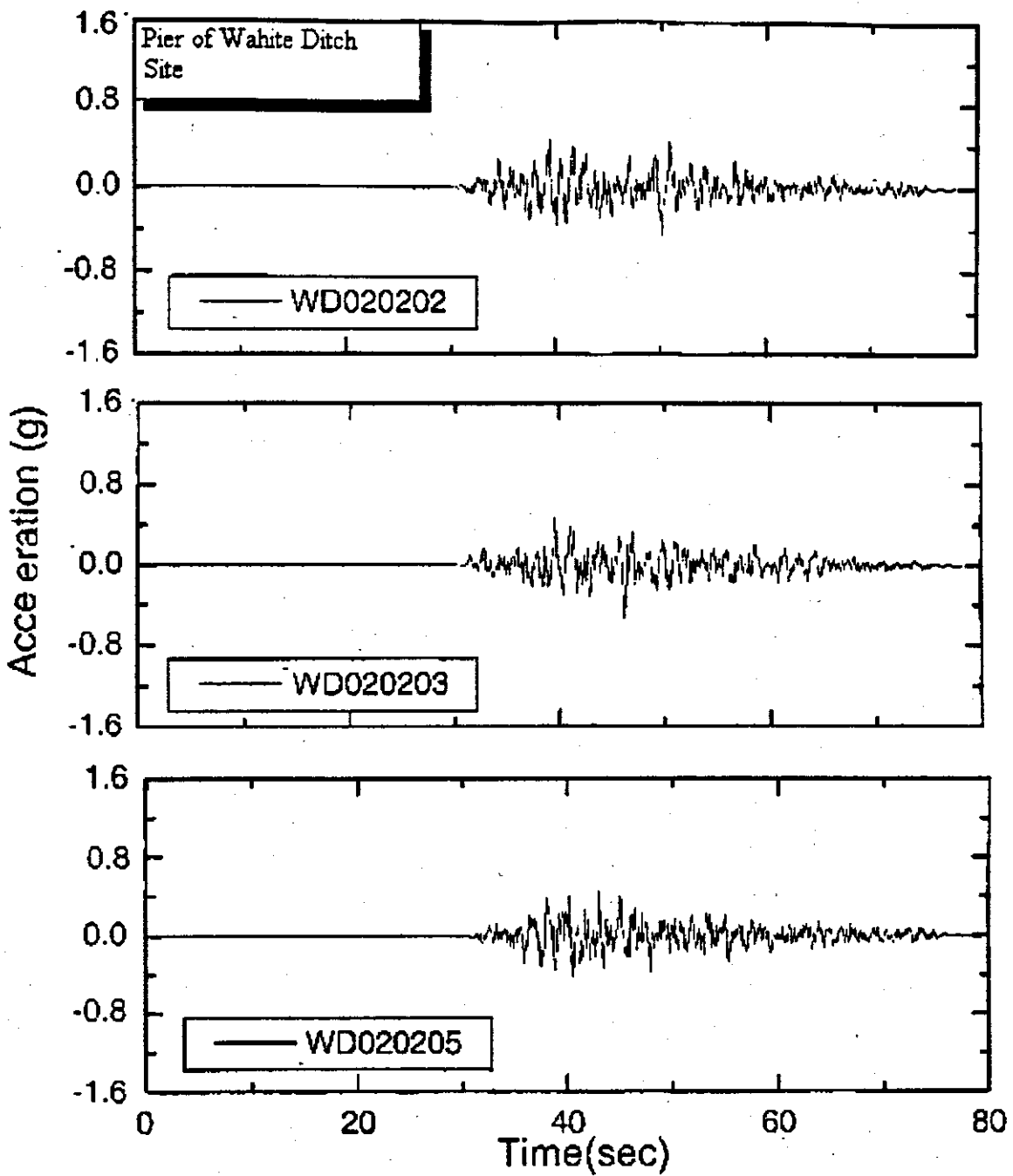
b. PE 10 % in 50 years, Magnitude = 7.0

Figure 8.46b Ground Acceleration at the Pier of the Wahite Ditch Site, PE 10% in 50 years, Magnitude = 7.0



c. PE 2 % in 50 years. Magnitude = 7.8

Figure 8.46c Ground Acceleration at the Pier of the Wahite Ditch Site, PE 2% in 50 years, Magnitude = 7.8



d. PE 2 % in 50 years, Magnitude = 8.0

Figure 8.46d Ground Acceleration at the Pier of the Wahite Ditch Site, PE 2% in 50 years, Magnitude = 8.0

The time histories of the modified vertical acceleration at soil surface, base of bridge abutment and pier of each site are presented in Appendix F. It appears by examination of the horizontal and vertical time histories of any one event that:

- $(k_h)_{\max}$  and  $(k_v)_{\max}$  do not occur at the same instant of time.
- The frequency content of these two ground motions are quite different.

#### **8.2.4 Liquefaction Potential Analysis**

The liquefaction potential of Wahite Ditch site is evaluated by the Seed and Idriss (1971) simplified method as modified by Youd and Idriss (1997). The procedure to obtain liquefaction potential is explained in Section 5.

##### **8.2.4.1 Cyclic Stress Ratio (CSR) and Cyclic Resistant Ratio (CRR) and Factor of Safety (FOS)**

Figure 8.47 shows soil profile and N-values with depth, which have been used for liquefaction analysis. A plot of CSR, CRR and factor of safety FOS, CRR/CSR with depth for PE 10% in 50 years and Magnitude 6.4 is plotted. For details see Appendix G.

It appears that the soil does not liquefy for an earthquake with a M6.4 PE 10% in 50 years. However, for a PE 10 % in 50 years and M7.0, the soil liquefies between depths of 120 to 130 ft.

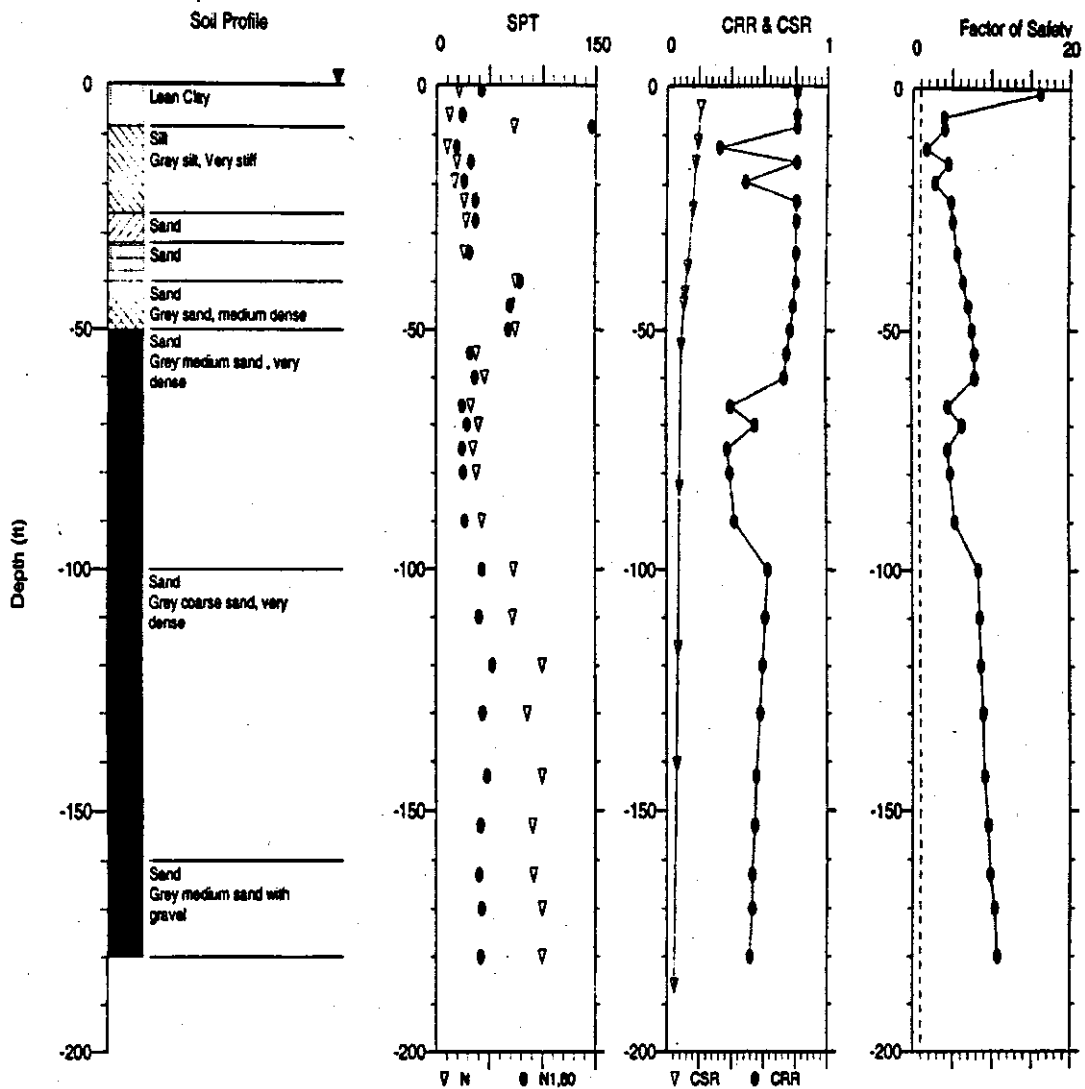
In this manner, the soil profile was analyzed for 4-ground motion for each magnitude that gives the greatest depths of liquefaction. A listing of FOS and the depth at which soil liquefy is given in Table 8.26.

#### **8.2.5 Slope Stability of Abutment Fills**

Slope stability analyses were performed for the Wahite Ditch site. Cross-section locations are shown on Figure 8.40. Soil properties used for the analysis are given in Table 8.27. An example analysis output for Cross-Section C-C' is shown on Figure 8.48. A summary of all analyses is included in Table 8.28.

The anticipated behavior is similar to that described for the St. Francis River Site. The site slopes are expected to be stable under static conditions (F.S. range from 3.48 to 7.76) and 10% PE loads (F.S. range from 2.05 to 7.40) for both low and high ground-water conditions. Under 2% PE loads, factors of safety are greater than one for all analyzed sections for low ground-water conditions. Under high water conditions factors of safety are greater than one but less than 1.10 for sections A-A', C-C', E-E', and F-F', indicating marginal stability.

This site is expected to be stable under small earthquake conditions. The site is less sensitive to ambient ground-water levels (which are affected by water levels in the river) than at the St. Francis River Site. Stability analysis under large earthquake conditions indicates marginal stability at the Wahite Ditch Site when ground-water levels are high.



Notes:  
 CSR analysis using SHAKE results.  
 CSR File: D:\I-0 SP Pe104\SP100101\SP100101.grf  
 CSR using SPT Data and Seed et. al. Method in 1997 NCEEK Workshop.  
 Earthquake File for SHAKE Analysis: D:\SP\SP100101.ACC  
 Earthquake Magnitude for CSR Analysis: 6.2  
 Magnitude Scaling Factor (MSF): 1.42  
 Depth to Water Table for CSR Analysis (ft): 0  
 Depth to Water Table for Ca Calculation (ft): 0  
 Depth to Base Layer for CSR Analysis (ft): 219.6  
 MSF Option: I.M. Idriss (1997)  
 Ca Option: Liao & Whitman (1986)  
 Ksiga Option: L.F. Harder & M. Boulanger (1997)  
 SPT Energy Ratio: USA/Safety/Bope: 0

Figure 8.47 Soil Profile, CSR, CRR and Factor of Safety Against Liquefaction at the Wa-white Ditch Bridge Site for PE 10% in 50 Years and Magnitude = 6.4

**Table 8.26 The Different Zones of Soil Liquefaction for Different Factors of Safety, Wahite Ditch Site**

Factor of Safety	Depth of soil Liquefy(ft)			
	PE10% in 50 years		PE 2% in 50 years	
	M6.4	M7.0	M7.8	M8.0
1.0	No	120 to 130	20 to 201	20 to 201
1.1	No	120 to 130	20 to 201	20 to 201
1.2	No	120 to 130	20 to 201	20 to 201
1.3	No	120 to 130	20 to 201	20 to 201
1.4	No	120 to 130	20 to 201	20 to 201

**Table 8.27 Soil Properties Used For Slope Stability Analysis, Wahite Ditch Site**

Soil Characteristics*				
	$\gamma_{moist}$ (pcf)	$\gamma_{saturated}$ (pcf)	c (psf)	$\phi$ (deg.)
Levee Fill	121.3	133.5	858	30
SP	134.9	141.9	0.0	40
Sand Lens	134.9	141.9	0.0	40
Gravel Lens	140.0	145.0	0.0	45

\* Soil characteristics obtained from slope stability procedures, Section (5.5.1)

## 8.2.6 Flood Hazard Analysis Results

Water levels appear to be too low during normal conditions to pose a significant risk of exiting the channel, even in the event of levee failure. Furthermore, the roadway is elevated above the surrounding land. One section of roadway located 0.1 to 0.5 miles west of the ditch is at low elevation and could potentially flood.

The remaining section of the roadway east of the Wahite Ditch appears to be elevated and is not anticipated to experience flooding due to levee failure.

## 8.2.7. Structure Response of Wahite Ditch Bridges and Abutments

### 8.2.7.1 New Wahite Ditch Bridge

#### 8.2.7.1.1 Bridge Description

The bridge under consideration in this section is denoted as Bridge A-5648, located in Stoddard County on US 60 where it crosses the Wahite drainage ditch. The bridge was designed in 1992 with seismic considerations. This 279 foot 9 inch bridge consists of three spans of prestressed concrete girders. The interior diaphragms each consist of a horizontally placed C15x33.9 channel section. The general elevation of the bridge is shown in Figure 8.49.

**Table 8.28 Slope Stability Results, Wahite Ditch Site**

<b>Factor of Safety for Most Sensitive Potential Failure Plane</b>							
<b>Cross-Section</b>	<b>A - A'</b>	<b>B - B'</b>	<b>C - C'</b>	<b>D - D'</b>	<b>E - E'</b>	<b>F - F'</b>	<b>G - G'</b>
<b>Static</b>							
Low GW	3.97	4.11	3.85	4.05	3.92	3.94	7.76
High GW	3.83	4.02	3.74	3.98	3.51	3.48	5.30
<b>Pseudo-Static Set 1*</b>							
<b>10% PE in 50 years</b>							
Low GW (0.123)	2.41	2.53	2.32	2.40	2.40	2.41	4.23
High GW (0.123)	2.14	2.39	2.06	2.20	2.07	2.10	2.79
<b>2% PE in 50 years</b>							
Low GW (0.350)	1.32	1.38	1.27	1.29	1.29	1.28	2.14
High GW (0.350)	1.10	1.25	1.06	1.11	1.10	1.10	1.39
<b>Pseudo-Static Set 2</b>							
<b>10% PE (HGA, VGA)</b>							
Low GW (0.123,+0.006)	2.40	2.52	2.31	2.38	2.38	2.39	4.22
Low GW (0.123,-0.006)	2.43	2.54	2.34	2.41	2.41	2.42	4.25
High GW (0.123,+0.006)	2.12	2.38	2.05	2.18	2.06	2.08	2.77
High GW (0.123,-0.006)	2.15	2.40	2.08	2.21	2.09	2.12	2.80
<b>2% PE (HGA, VGA)</b>							
Low GW (0.350,+0.007)	1.30	1.37	1.25	1.28	1.27	1.27	2.12
Low GW (0.350,-0.007)	1.33	1.39	1.28	1.30	1.30	1.30	2.15
High GW (0.350,+0.007)	1.09	1.24	1.05	1.10	1.09	1.09	1.38
High GW (0.350,-0.007)	1.12	1.26	1.07	1.12	1.11	1.11	1.41
<b>Pseudo-Static Set 3</b>							
<b>10% PE (HGA, VGA)</b>							
Low GW (0.008,+0.082)	3.69	3.90	3.57	3.74	3.70	3.68	7.40
Low GW (0.008,-0.082)	3.83	3.91	3.71	3.91	3.86	3.80	7.15
High GW (0.008,+0.082)	3.51	3.94	3.43	3.66	3.25	3.25	4.82
High GW (0.008,-0.082)	3.66	3.78	3.57	3.81	3.39	3.37	5.06
<b>2% PE (HGA, VGA)</b>							
Low GW (0.060,+0.233)	2.58	2.80	2.49	2.57	2.56	2.57	5.22
Low GW (0.060,-0.233)	3.26	3.27	3.15	3.30	3.26	3.24	5.54
High GW (0.060,+0.233)	2.27	2.86	2.20	2.35	2.18	2.22	3.00
High GW (0.060,-0.233)	3.03	3.13	2.94	3.13	2.88	2.91	4.10

\* Peak ground acceleration values calculated with the computer program *SHAKE*, Section 5.4

HGA - Horizontal Ground Acceleration

VGA - Vertical Ground Acceleration

PE - Probability of Exceedance in 50 years

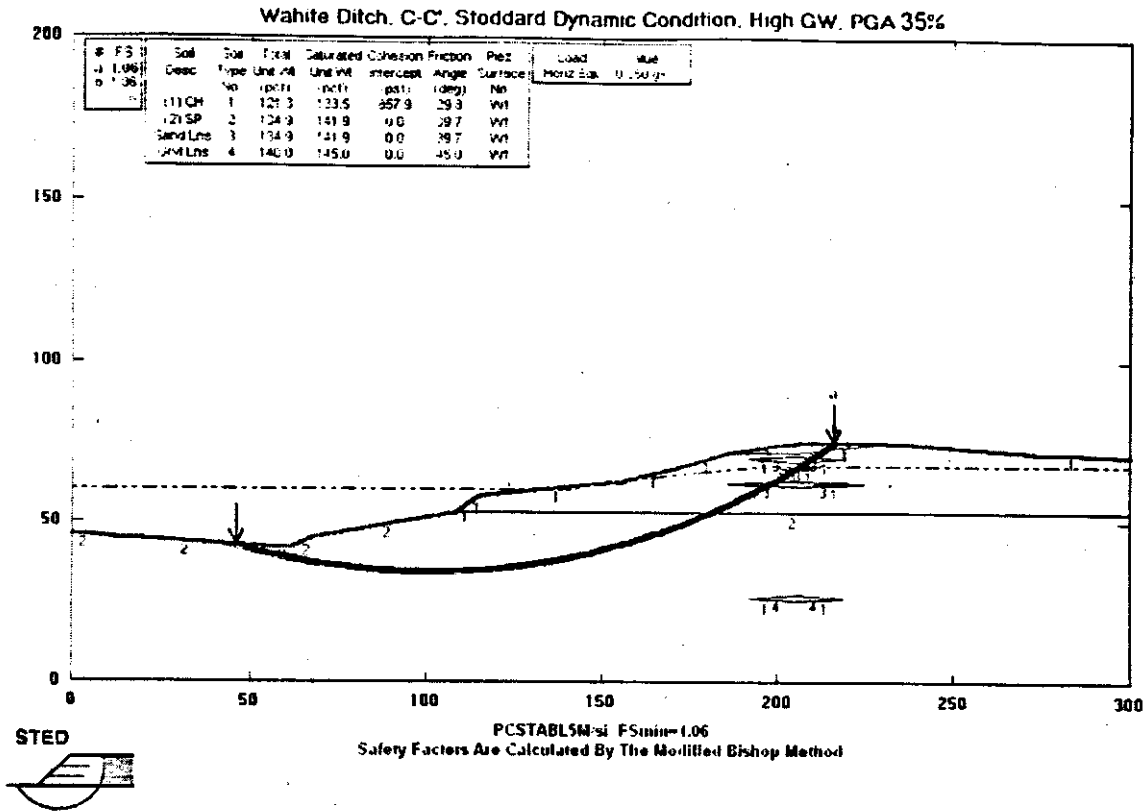


**Figure 8.48 Example Slope Stability Results for the Wahite Ditch Site**

The bridge superstructure is supported by two intermediate bents through fixed bearings and two integral abutments at its ends. Each bent consists of a reinforced concrete cap beam and two reinforced concrete columns. Deep pile foundations support both bents and abutments. There are 20 piles for each column footing and 14 piles for each abutment footing.

### 8.2.7.1.2 Bridge Model and Analysis

All of the components of the structure were included in the bridge model. These components include the girders, diaphragms, cross-frames, interior bents and columns, and the bridge deck. The deck was represented by 24 shell elements with a thickness of 8.5 inches. All girders, cross-frames, and diaphragms were modeled as 167 frame members. Each frame section was then assigned member properties, such as material type and cross-section dimensions. The model also included 120 nodes.

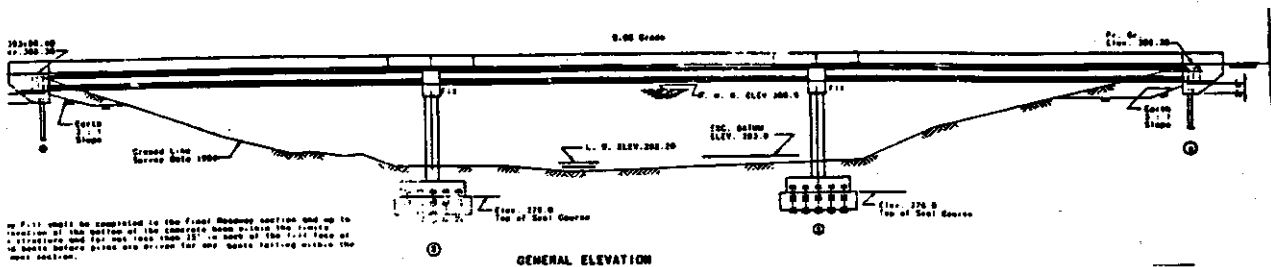


**Figure 8.49** Bridge General Elevation (New Wahite Ditch Bridge)

To further assist in modeling ground soil conditions in *SAP2000*, springs were used at the base of each column (six columns total, three on each interior bent). Springs were also placed at the ends of the bridge on each abutment footing. The stiffness constants of the springs were taken from Appendix F.

Rigid elements were used to model the integral abutments in *SAP2000*. Because of their presence, the bridge is relatively stiff and is expected to experience small displacements during earthquakes. Therefore, a response spectrum analysis was used for the bridge model. For each analysis with one directional earthquake excitation, 30 Ritz-vectors were considered associated with the earthquake direction. In Table 8.29, a sampling of five of the significant vibration modes are listed with its period in seconds and a brief description of the motion represented within the given mode. Their corresponding mode shapes are illustrated in Figures 8.50-8.54.

The bridge was analyzed under a total of twelve response spectra described in Section 8.1.3. Six of the spectra correspond to a 10% PE level while the others to a 2% PE level. At each PE level of earthquakes, three were considered as near-field and the other three as far-field. The internal loads such as shear and moments and the abutment displacements were obtained at various critical locations.

**Table 8.29** Natural Periods and their Corresponding Vibration Modes (New Wahite Ditch Bridge)

Mode Number	Period (seconds)	Motion Description
1	0.2686	Vertical
2	0.2558	Transverse twisting
3	0.0915	Longitudinal
4	0.0854	Vertical with twisting
5	0.0729	Transverse

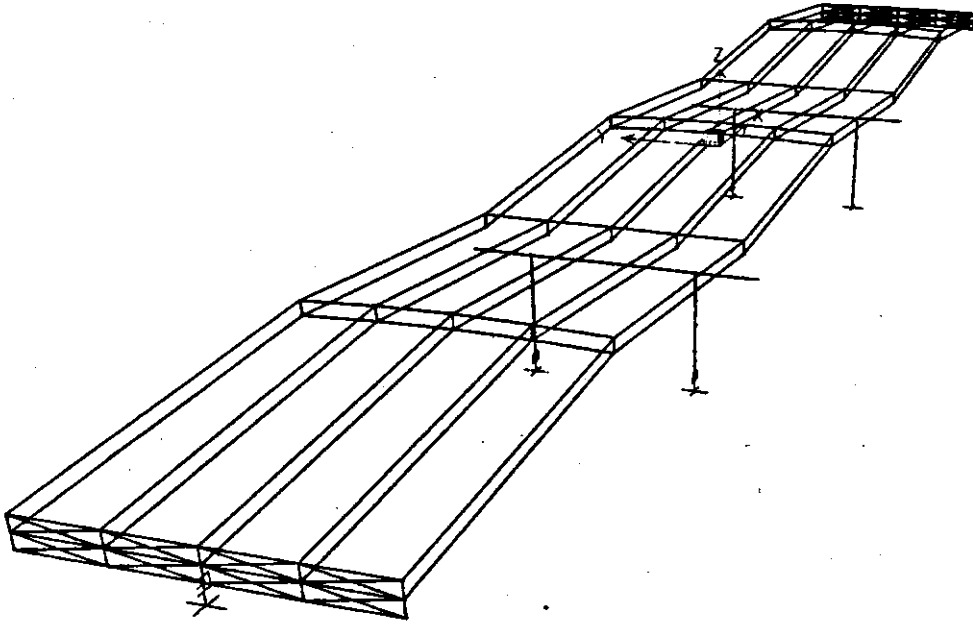


Figure 8.50 Mode 1, Period 0.2686 Seconds (New Wahite Ditch Bridge)

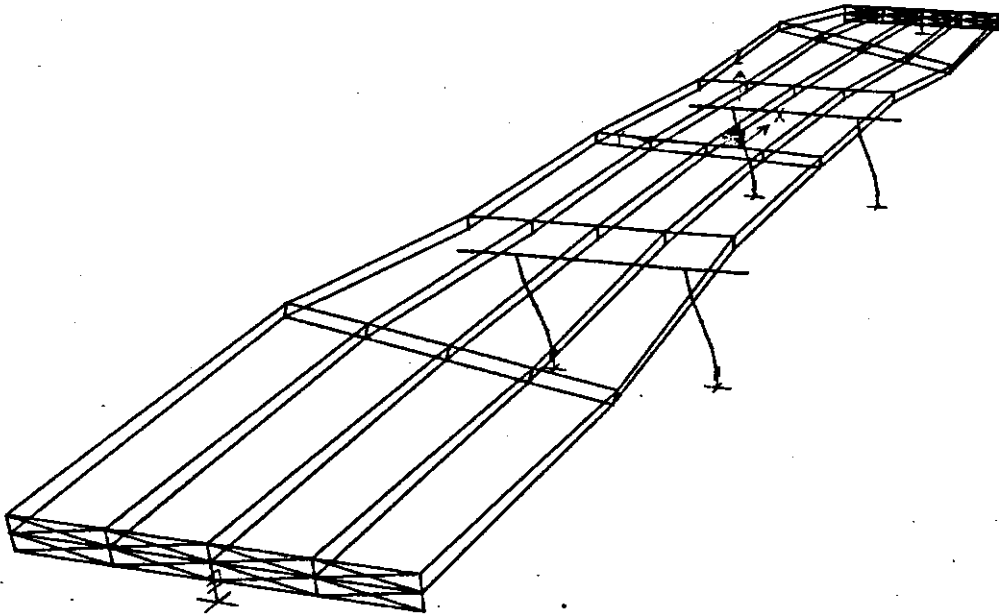
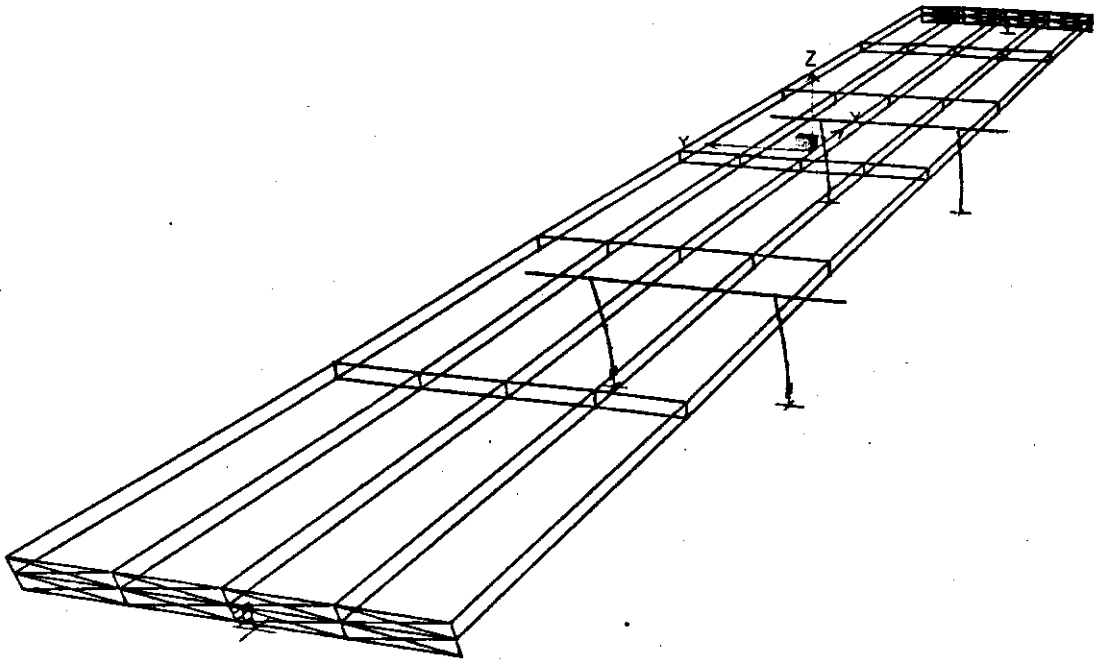
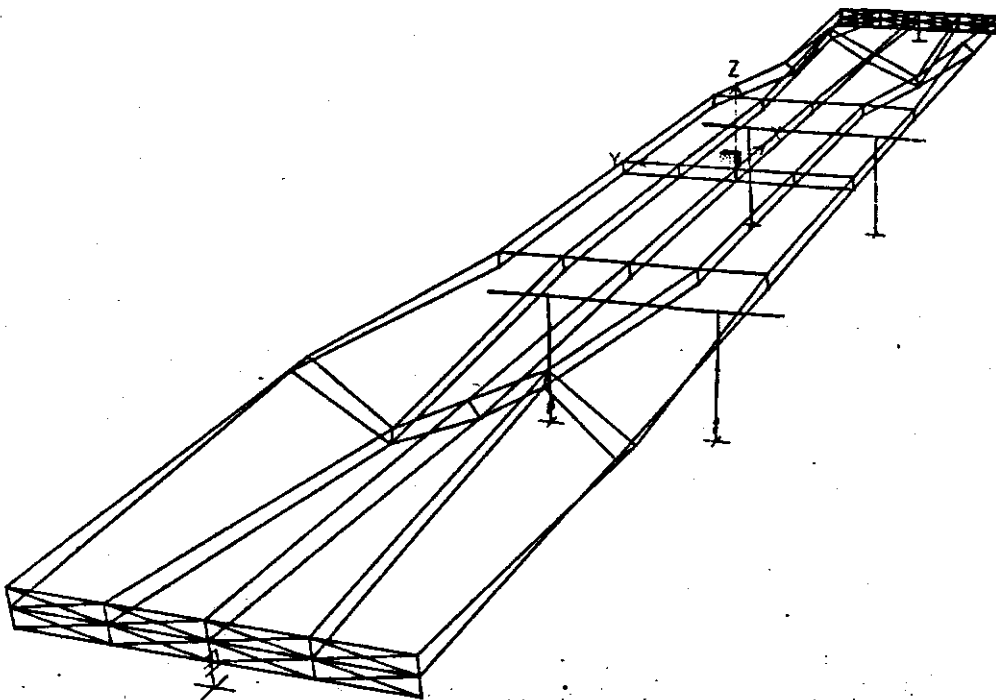


Figure 8.51 Mode 2, Period 0.2558 Seconds (New Wahite Ditch Bridge)



**Figure 8.52** Mode 3, Period 0.0915 Seconds (New Wahite Ditch Bridge)



**Figure 8.53** Mode 4, Period 0.0854 Seconds (New Wahite Ditch Bridge)

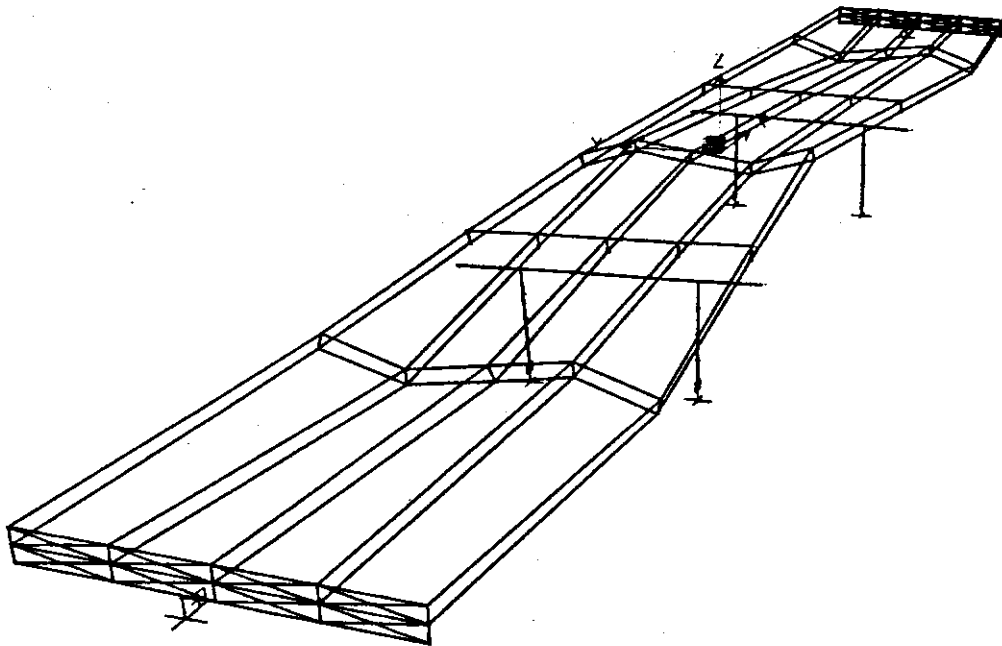


**Figure 8.54** Mode 5, Period 0.0729 Seconds (New Wahite Ditch Bridge)

### **8.2.7.1.3 Description of Bridge Evaluation**

The evaluation procedure is the same as used for the bridges at the St. Francis River Site. Whether or not the C/D ratios were greater than one indicated if their associated components would experience problems in an earthquake.

#### **8.2.7.1.3.1 Load Combination Rule**

The same load combination rule was used for the evaluations at the Wahite Ditch Bridge site as at the St. Francis River Site. This rule was used throughout these calculations for various types of demands on the structure (shear, moment, and axial forces, as well as transverse and longitudinal displacements).

#### **8.2.7.1.3.2 Minimum Support Length and C/D Ratio for Bearing**

This bridge has integral abutments without expansion joints. It is not susceptible to the dropping of exterior spans during earthquake excitations.

#### **8.2.7.1.3.3 C/D Ratios for Shear Force at Bearings**

The first C/D ratios calculated in this section define the behavior of the shear keys located at the bearing pads on the cap beams at the interior bents. There are four shear keys on each of the two interior bents, with 10 reinforcing bars in each key. From the bridge analysis the shear demand at each of these points was determined and the maximum demand among these points was used

to compute the C/D ratio for the "worst case". Before these shear values were used in determining the C/D ratios, the values were compared to 20% of the axial dead load at that location (FHWA, 1995). The greater of these two values were used in the subsequent calculations.

In all cases except for two of the 2% earthquakes, the shear capacities of the keys were adequate. For these two earthquakes, the capacity was only approximately 85% of the demand. However, in several other cases, the C/D ratio for the shear was very close to one, indicating that the capacity just barely exceeds the demand. In these cases, it is advisable to pay careful attention to the shear keys, as they could pose problems under the stronger earthquakes.

#### **8.2.7.1.3.4 C/D Ratios for Columns/Piers**

In this section, the C/D ratios were calculated for all columns on the interior bents. The elastic moment demands for the top and bottom of each column in the transverse and longitudinal directions due to transverse, longitudinal, and vertical earthquake motions were determined from the response spectrum analysis.

The maximum demand from the possible combinations was then used in conjunction with the determined capacity for the column to determine a C/D ratio for the columns. In most cases, the initial C/D ratios were below one, indicating insufficient column strength for elastic seismic demand. However, when the columns experience inelastic deformation, the seismic demand reduces due to energy dissipation. To account for the above effect, the ductility indicator was used with these ratios. Since the two interior bents each had multiple columns, a multiplier of 5 was applied to each ratio (AASHTO, 1996). In all cases, this multiplier increased the ratios to values above one.

As for the bridges at the St. Francis River Site, the footings of these columns were determined to have moment capacity considerably higher than the capacities of the columns even when the axial force is zero. Therefore, the footings are expected to perform satisfactorily. The plot for the moment versus rotation is presented in Appendix H for the case of axial load equal to zero.

#### **8.2.7.1.3.5 C/D Ratios for Reinforcement Anchorage in Columns**

For both the top and bottom of the columns, the adequacy of the anchorage of longitudinal reinforcement must be checked. The tops of the columns used straight anchorage, whereas the bottoms of the columns had hooked anchorage. Because in both cases (top and bottom) the capacity was greater than the demand, the C/D ratio was one for both cases, indicating that the anchorage should be adequate. As explained in Section 8.1.7.1.3.5, the values of the C/D ratios here are not actual ratios of the capacity length and the demand length. Rather, they are values dictated by the FHWA Manual based on the location of the anchorage and the relationship of the capacity length and the demand length.

#### **8.2.7.1.3.6 C/D Ratios for Splices in Longitudinal Reinforcement**

This section is not applicable to this structure, as the columns have no splices.

#### **8.2.7.1.3.7 C/D Ratio for Transverse Confinement**

The C/D ratios for all cases were above one. This indicates that there should be minimal problems with the transverse confinement on the columns of this bridge.

#### **8.2.7.1.3.8 C/D Ratio for Column Shear**

In all cases of 2% motions and for four of the 10% motions, "Case B" was chosen, based on definitions from the FHWA Manual (1995). This case was needed because at least one of the moment C/D ratios was less than one for each earthquake (before applying the ductility indicator) and  $V_i(c) > V_u(d) > V_i(c)$ . When "Case B" was used, the relationship for the column shear C/D ratio was the column moment C/D ratio multiplied by an FHWA-defined multiplier. This multiplier was based on column geometry ( $L_c$  = length of column and  $b_c$  = width of column) as well as the various shear parameters defined in Section 8.1.7.1.3.8.

For the remaining two 10% earthquakes, "Case B" did not apply because the initial C/D ratios for the columns under these earthquakes were above one. Therefore, the C/D ratios for these earthquakes were determined simply as a ratio of the initial capacity of the column to the maximum shear force in the column.

#### **8.2.7.1.3.9 C/D Ratio for Diaphragm Members**

The axial capacity of the diaphragm members (C15x33.9) was calculated based on critical buckling stress (Table 3-36 in AISC LRFD, 1998). This table gave values of the stress based on the effective length to radius of gyration ratio ( $KL/r$ ). In this case, K was taken to be one to simulate a pin-pin connection at the ends of the member.

In all cases, the axial capacity of these members appeared to be sufficient, as all C/D ratios were above one. This indicates that there should be minimal problems with these members.

#### **8.2.7.1.3.10 C/D Ratio for Abutment Displacements**

In all cases, the longitudinal and transverse displacements of the abutments under the combined effect of three earthquake effects were found to be less than their respective allowable values specified in the FHWA Manual (1995). This indicates that the abutments should remain damage-free in the event of an earthquake.

#### **8.2.7.1.4 Summary of Problem Areas**

A summary of all C/D ratios for all earthquakes for this bridge is shown in Table 8.30. Based on the above study, the bridge generally experienced minor problems.

The only components that warrant attention are the shear keys located on the bent cap beams of the structure. In several cases, the resulting C/D ratio was less than one, indicating the possibility of failure for these shear keys.

#### **8.2.7.1.5 Comparison of AASHTO Response Spectrum vs. Site-Specific Response Spectrum**

The same response spectrum shown for the New St. Francis Bridge was used for the New Wahite Bridge as well. The New Wahite Bridge Site is not far from the New St. Francis Bridge Site. Therefore, the maximum ground accelerations for these sites are nearly the same. For this reason, an A value of 0.18 was again used for this response spectrum.

The results from the AASHTO response spectrum analysis were compared to several of the site specific 10% earthquake response spectrum analyses that were run on the New Wahite Bridge. It was expected that these results would be reasonably close to one another. These results are summarized in Table 8.31.

**Table 8.30 Summary of all Earthquakes for New Wahite Ditch Bridge**

C/D Ratio Name	020101	020102	020103	020202	020203	020205	100101	100102	100105	100201	100202	100205
$\Gamma_{bd}$	---	---	---	---	---	---	---	---	---	---	---	---
$\Gamma_{bt-trans}$	1.23	1.07	0.83	1.17	0.84	1.00	1.84	2.38	2.51	1.81	1.78	2.00
$\Gamma_{bt-long}$	5.58	5.51	4.28	5.36	4.38	4.90	6.92	7.89	8.13	6.86	6.83	7.33
$\Gamma_{cc-final}$	2.95	2.55	1.95	2.80	1.98	2.40	4.47	5.98	6.39	4.38	4.32	4.91
$\Gamma_{cc-final}$	3.58	3.09	2.37	3.39	2.40	2.91	5.42	7.24	7.75	5.31	5.24	5.94
$\Gamma_{cc-final}$	2.75	2.38	1.83	2.60	1.85	2.24	4.16	5.55	5.93	4.07	4.02	4.56
$\Gamma_{cc-final}$	3.30	2.85	2.19	3.12	2.22	2.69	4.99	6.66	7.12	4.89	4.83	5.48
$\Gamma_{cc-final}$	2.95	2.55	1.95	2.80	1.98	2.40	4.47	5.98	6.39	4.38	4.32	4.91
$\Gamma_{cc-final}$	3.58	3.09	2.37	3.39	2.40	2.91	5.42	7.24	7.75	5.31	5.24	5.94
$\Gamma_{cc-final}$	2.75	2.38	1.83	2.60	1.85	2.24	4.16	5.55	5.93	4.07	4.02	4.56
$\Gamma_{cc-final}$	3.30	2.85	2.19	3.12	2.22	2.69	4.99	6.66	7.12	4.89	4.83	5.48
$\Gamma_{ca-bottom}$	1.00	1.00	1.00	1.00	1.00	1.00	1.00	1.00	1.00	1.00	1.00	1.00
$\Gamma_{ca-top}$	1.00	1.00	1.00	1.00	1.00	1.00	1.00	1.00	1.00	1.00	1.00	1.00
$\Gamma_{cs}$	---	---	---	---	---	---	---	---	---	---	---	---
$\Gamma_{cs-adj}$	---	---	---	---	---	---	---	---	---	---	---	---
$\Gamma_{cc}$	3.30	2.85	2.19	3.12	2.22	2.69	4.99	6.66	7.12	4.89	4.83	5.48
$\Gamma_{cc}$	2.33	2.01	1.54	2.20	1.56	1.89	3.52	6.37	6.80	3.45	3.40	3.86
$\Gamma_{upem}$	5.92	5.13	3.79	5.87	3.97	5.08	11.10	12.49	12.72	10.31	10.77	10.76
$\Gamma_{ad-trans}$	127.64	111.51	94.63	122.43	94.03	108.29	202.68	218.95	215.80	199.98	181.80	211.24
$\Gamma_{ad-long}$	89.52	77.69	61.50	84.98	62.07	74.38	136.34	174.20	180.07	133.18	131.17	142.25

**Table 8.31: Comparison of AASHTO Response Spectrum vs. Site Specific Response Spectrum (New Wahite)**

Due to Transverse EQ	transverse		longitudinal	
	response spectra	AASHTO	response spectra	AASHTO
Column 2, top	9490		560	
	7093		419	
	9685		571	
	8645		507	
average	8728		8781	

Due to Transverse EQ	transverse		longitudinal	
	response spectra	AASHTO	response spectra	AASHTO
Column 2, bottom	10336		734	
	7724		550	
	10546		749	
	9391		665	
average	9499		8085	

Due to Longitudinal EQ	transverse		longitudinal	
	response spectra	AASHTO	response spectra	AASHTO
Column 2, top	24		1	
	25		1	
	25		1	
	30		1	
average	26		36	

Due to Longitudinal EQ	transverse		longitudinal	
	response spectra	AASHTO	response spectra	AASHTO
Column 2, bottom	12		644	
	13		648	
	13		680	
	15		831	
average	13		19	

### 8.2.7.2 Old Wahite Ditch Bridge

#### 8.2.7.2.1 Bridge Description

The bridge under consideration in this section is denoted as Bridge L-927, located in Stoddard County on US 60 where it crosses the Wahite drainage ditch. The bridge was built in 1952 without seismic considerations in design. This 279 foot 9 inch bridge consists of five spans supported by steel girders. The interior diaphragms each consist of two diagonal L3x2½x5/16 members crossed over one another. The general elevation of the bridge is shown in Figure 8.55.

The bridge superstructure is supported by four intermediate bents through expansion and fixed bearings and two seat-type abutments at its ends. Each bent consists of a reinforced concrete cap beam and two reinforced concrete columns (tapered). There is a reinforced concrete diaphragm placed between each pair of columns on each bent for additional restraint in the transverse direction. Deep pile foundations support both bents and abutments. There are 6 piles for each column footing on bents 2 and 5, 8 piles for each column footing on bents 3 and 4, and 6 piles for each abutment footing.

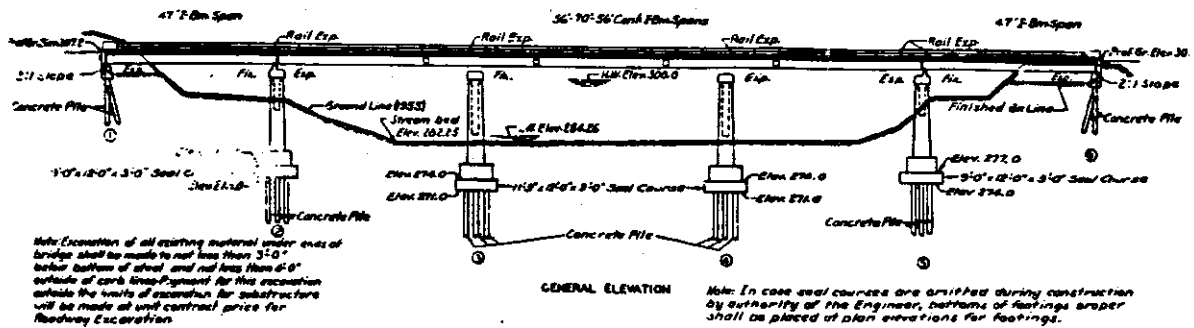


Figure 8.55: Bridge General Elevation (Old Wahite Ditch Bridge).

### 8.2.7.2.2 Bridge Model and Analysis

All of the components of the structure were included in the bridge model. These components include the girders, diaphragms, cross-frames, interior bents and columns, and the bridge deck. The deck was represented by 61 shell elements with a thickness of 6.5 inches. All girders, cross-frames, and diaphragms were modeled as 550 frame members. Each frame section was then assigned member properties, such as material type and cross-section dimensions. The model also included 356 nodes.

To take soil effect into account, springs and dashpots were used at the base of each column (eight columns total, two on each interior bent). Springs were also placed at the ends of the bridge on each abutment footing. The stiffness constants of the springs were taken from Appendix F.

Rigid elements were used to model the seat-type abutments in *SAP2000*. Because this bridge was to be analyzed using a response-spectrum analysis, no “gap” elements could be used (as they had been on the Old St. Francis Bridge). However, for comparison, several cases were run for this bridge using a non-linear time history analysis. This time history analysis did include the necessary “gap” elements to model the expansion joints.

In this way, the two models could then be compared to note how close the results were to one another. For each analysis with one directional earthquake excitation, 30 Ritz-vectors were considered associated with the earthquake direction. In Table 8.32, a sampling of five of the significant vibration modes are listed with its period in seconds and a brief description of the motion represented within the given mode. Their corresponding mode shapes are illustrated in Figures 8.56-8.60.

The bridge was analyzed under a total of twelve response spectra described in Section 8.1.3. Six of the spectra correspond to a 10% PE level while the others to a 2% PE level. At each PE level of earthquakes, three were considered as near-field and the other three as far-field. The internal loads—such as shear and moments and the abutment displacements were obtained at various critical locations.

**Table 8.32** Natural Periods and their Corresponding Vibration Modes (Old Wahite Ditch Bridge)

Mode Number	Period (seconds)	Motion Description
1	0.5641	Longitudinal
2	0.3518	Longitudinal
3	0.1809	Vertical
4	0.1229	Transverse
5	0.1025	Longitudinal

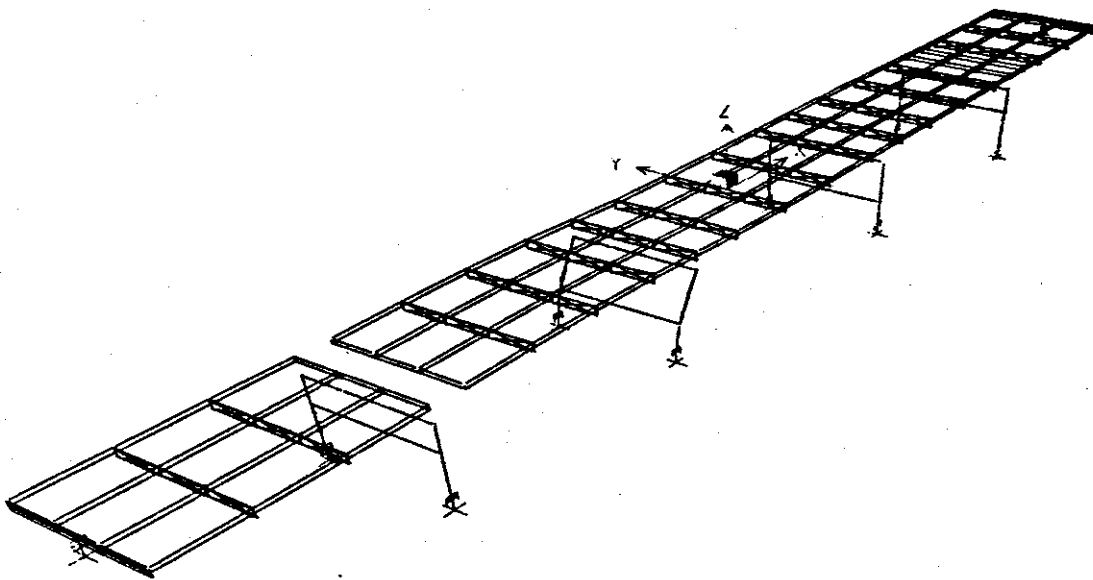


**Figure 8.56:** Mode 1, Period 0.5641 Seconds (Old Wahite Ditch Bridge)

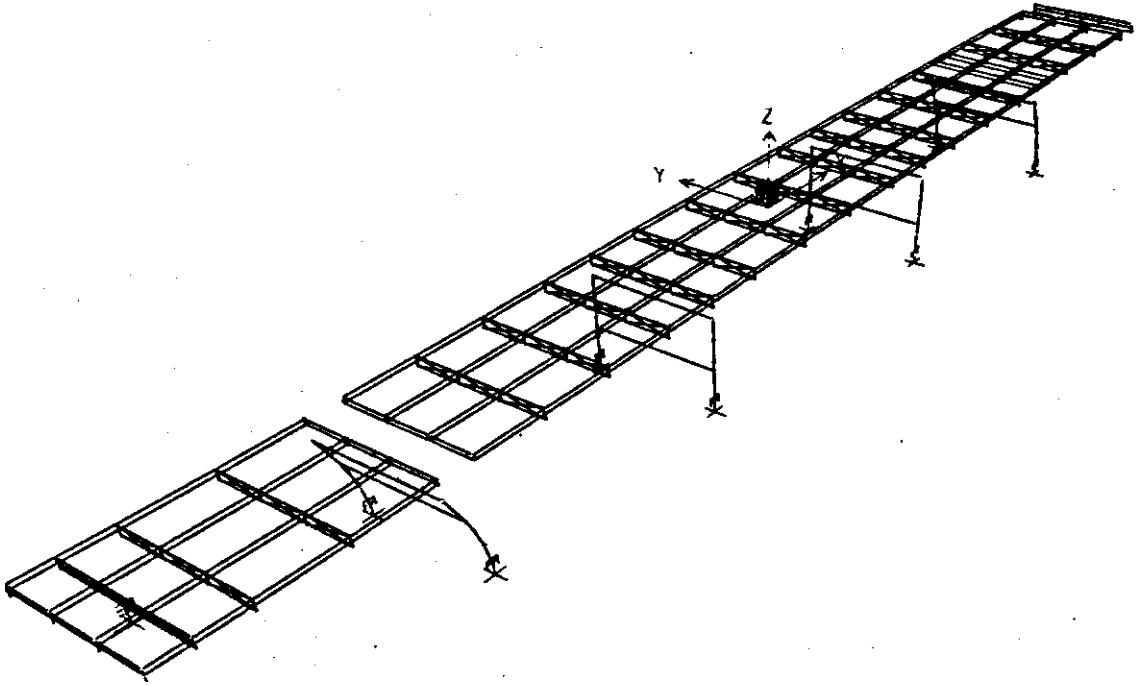


**Figure 8.57: Mode 2, Period 0.3518 Seconds (Old Wahite Ditch Bridge)**

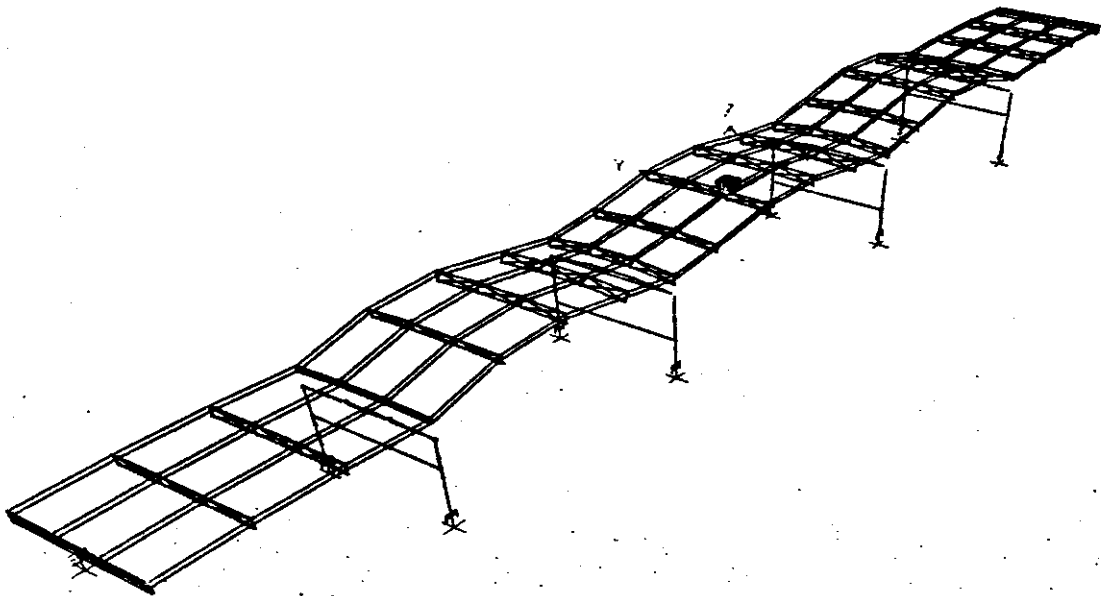


**Figure 8.58: Mode 3, Period 0.1809 Seconds (Old Wahite Ditch Bridge)**

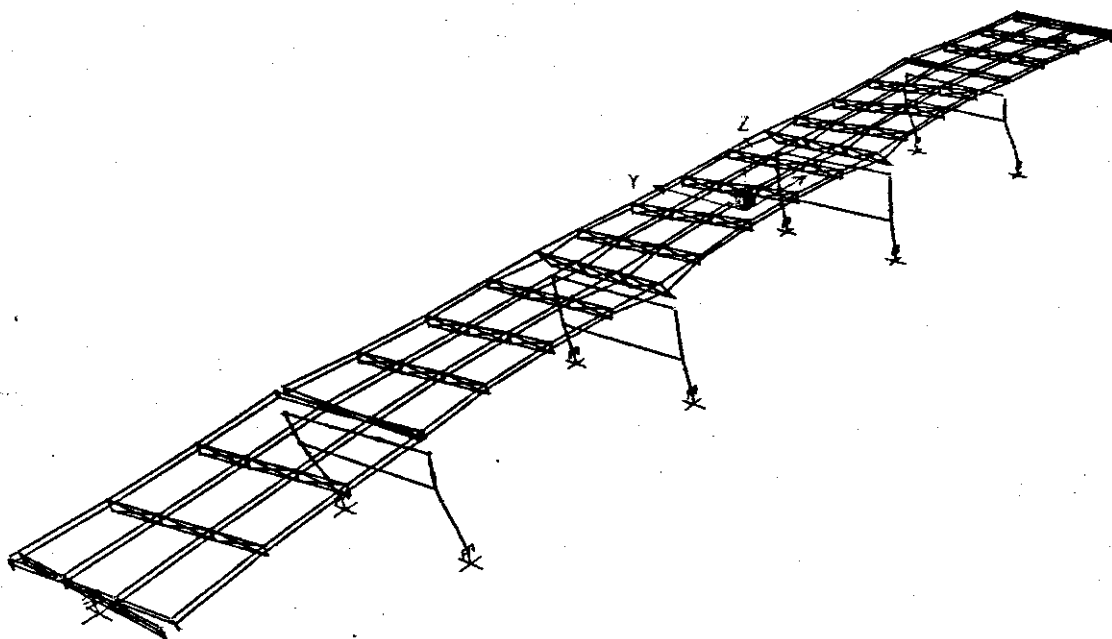


**Figure 8.59: Mode 4, Period 0.1229 Seconds (Old Wahite Ditch Bridge)**

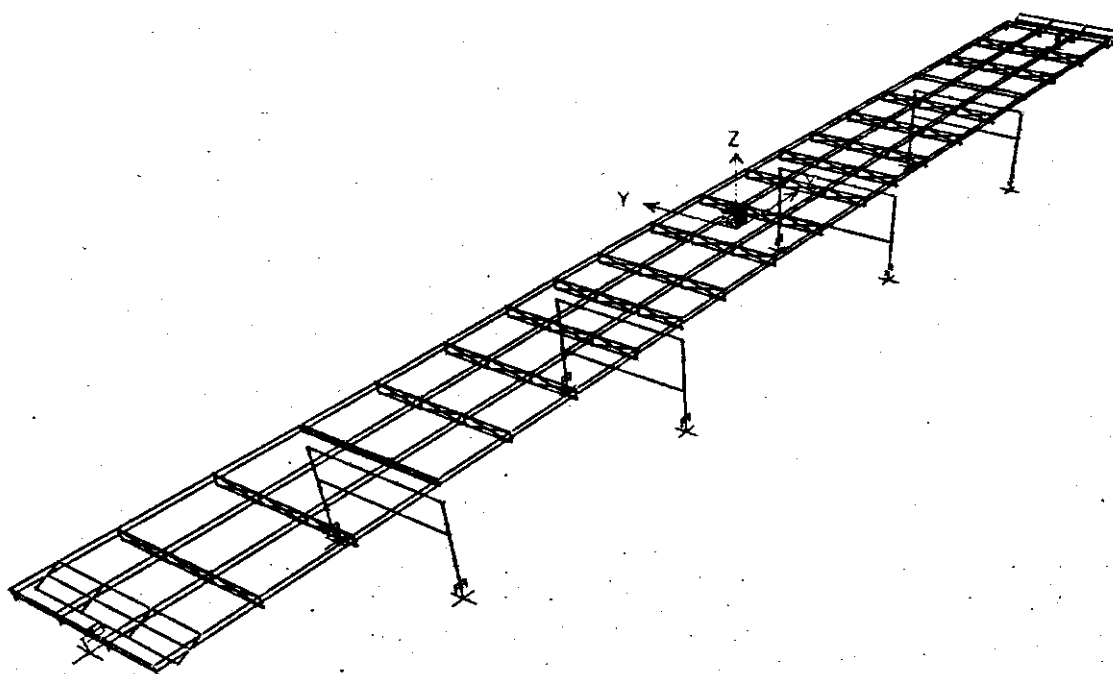


**Figure 8.60 Mode 5, Period 0.1025 Seconds (Old Wahite Ditch Bridge)**

### **8.2.7.2.3 Bridge Evaluation**

This section briefly presents the results and explains the reasoning behind the calculations in the evaluation of this bridge. The evaluation procedure is the same as used for the bridges at the St. Francis River Site. Whether or not the C/D ratios were greater than one indicated if their associated components would experience problems in an earthquake.

#### **8.2.7.2.3.1 Load Combination Rule**

The same load combination rule was used for the evaluations at the Wahite Ditch Site as at the St. Francis River Site. This rule was used throughout these calculations for various types of demands on the structure (shear, moment, and axial forces, as well as transverse and longitudinal displacements).

#### **8.2.7.2.3.2 Minimum Support Length and C/D Ratio for Bearing**

Because this bridge uses seat-type abutments, bearing and support length are essential components that must be examined. The capacity, or actual support length for this bridge, was estimated at 18 inches. However, based on the definition of required support by FHWA, approximately 20 inches of length was needed. This indicates that the bearing and support length for this bridge could lead to the dropping of spans during an earthquake.

#### **8.2.7.2.3.3 C/D Ratios for Shear Force at Bearings**

The shear forces from each of the transverse, longitudinal, and vertical earthquake motions were combined to determine their total effect. The force demands at the bearing pads on the cap beams at the interior bents exceeded the capacities of the two bolts available for all of the 2% and 10% earthquakes. This indicates possible shear failures in the areas around the connecting bolts at the bearing pads.

The C/D ratios for embedment length and edge distance requirements of the bolts are evaluated with the same procedures as used for the bridges at the St. Francis River site. The embedment length of the 1" diameter bolts appears to be inadequate, as the length taken from the bridge plans is 10 inches, and 17 inches are required for proper embedment. This indicates that there may be problems with the embedment caused by axial forces acting on these bolts.

The edge distance required for these bolts is 7 inches, and from the bridge plans, it appears that only approximately 6 inches are available. This would imply possible problems with the edge distances for these bolts.

#### **8.2.7.2.3.4 C/D Ratios for Columns/Piers**

In this section, the C/D ratios were calculated for all columns on the interior bents. The elastic moment demands for the top and bottom of each column in the transverse and longitudinal directions due to transverse, longitudinal, and vertical earthquake motions were determined from the response spectrum analysis.

The maximum demand from the possible combinations was then used in conjunction with the determined capacity for the column to determine a C/D ratio for the columns. In most cases, the initial C/D ratios were below one, indicating insufficient column strength for elastic seismic demand. However, when the columns experience inelastic deformation, the seismic demand reduces due to energy dissipation. To account for the above effect, the ductility indicator was used with these ratios. Since the four interior bents each had multiple columns, a multiplier of 5 was applied to each ratio (AASHTO, 1996). In most cases, this multiplier increased the ratios to values above one. However, on all of the 2% earthquakes, 2 of the columns had C/D ratios less than one even after the implementation of the ductility indicator. This was due to very high moments at the bottoms of the columns on the fixed bent.

As for the bridges at the St. Francis River site, the footings of these columns were determined to have moment capacity considerably higher than the capacities of the columns even when the axial force is zero. Therefore, the footings are expected to perform satisfactorily. The plot for the moment versus rotation is presented in Appendix H for the case of axial load equal to zero.

#### **8.2.7.2.3.5 C/D Ratios for Reinforcement Anchorage in Columns**

For both the top and bottom of the columns, the adequacy of the anchorage of longitudinal reinforcement must be checked. The tops and bottoms of the columns used straight anchorage. The anchorage at the tops of the columns caused somewhat of a problem, since the available length of anchorage was less than the required length of anchorage. All C/D ratios for top-of-column anchorage were less than one, indicating the possibility of failure within this region.

As for the bottom of the columns, further explanation is required. Because the capacity anchorage length was greater than the demand length, the FHWA Manual dictated that the C/D ratio was to be 1.5 multiplied by the C/D ratio of the footing. However, since the capacity of the footings was estimated to be much larger than that of the columns, it was deemed unnecessary to determine numerical values for the footing C/D ratios. Therefore, each C/D ratio for the bottoms of the columns was assigned a value of 1.0 to convey the fact that this anchorage should be adequate based on the capacities of the footings.

#### **8.2.7.2.3.6 C/D Ratios for Splices in Longitudinal Reinforcement**

This section is not applicable to this structure, as the columns have no splices.

#### **8.2.7.2.3.7 C/D Ratio for Transverse Confinement**

This section is not applicable, as the columns have no transverse reinforcement. This would indicate that the columns will perform inadequately. However, the C/D ratios for these columns were still computed for informational purposes.

#### **8.2.7.2.3.8 C/D Ratio for Column Shear**

In all cases of 2% motions and for 10% motions, "Case B" was chosen, based on definitions from the FHWA Manual (1995). This case was needed because at least one of the moment C/D ratios was less than one for each earthquake (before applying the ductility indicator) and  $V_i(c) > V_u(d) > V_i(c)$ . When "Case B" was used, the relationship for the column shear C/D ratio was the minimum column moment C/D ratio multiplied by an FHWA-defined multiplier, which is the same as was done for the previous bridges.

The shear forces seen by these columns were very large, especially at the bottoms of the columns. Because the maximum shear forces were always found at the column base, the dimensions of the column base were used in the calculations. These large shear forces and lack of transverse confinement of the columns led to very low C/D ratios for almost all cases. Only for one of the 10% earthquakes was the ratio above one. This indicates a problem with column shear capacity that must be retrofitted.

#### **8.2.7.2.3.9 C/D Ratio for Diaphragm Members**

The axial capacity of the diaphragm members (L3x2½x5/16) was obtained from AISC LRFD, 1998. This method is the same as was used for the bridges at the St. Francis River Site.

As done for the St. Francis River Bridges, two calculations for the same C/D ratio were exercised. The first uses the full length of the member spanning diagonally from top to bottom of the diaphragm/cross-frame. The second calculation uses half of the total length of the member. This was done because of the possibility of failure within the connection where the diagonal members meet, thus removing the intermediate brace. The axial capacity was found to be less than the demand in most cases, which indicates that these members may have problems under the influences of strong earthquake motions.

#### **8.2.7.2.3.10 C/D Ratio for Abutment Displacements**

In all cases, the longitudinal and transverse displacements of the abutments under the combined effect of three earthquake effects were found to be less than their respective allowable values specified in the FHWA Manual (1995). This indicates that the abutments should remain damage-free in the event of an earthquake.

#### **8.2.7.2.4 Summary of Problem Areas**

A summary of all C/D ratios for all earthquakes for this bridge is shown in Table 8.33. This bridge experienced problems with a variety of components.

First, the available support length is slightly less than the minimum requirement, indicating possible problem dropping of the exterior spans off their supports earthquake motion. Next, the shear capacity of bolts at the bearing pads on the interior bents appears to be inadequate, as the demand outweighed the capacity in all cases. Also, the bolt embedment length and edge distance appear to be inadequate, indicating possible problems with these components as well.

The next components of concern are the columns of the structure. Because the ductility indicator, which increases the column C/D ratios by five times, was used, all columns appeared to perform sufficiently, except for the bottoms of the columns on the fixed pier under five of the 2% ground motions. Associated with the column moment C/D ratios, the shear capacity of columns is also inadequate. For all of the 2% and five of the six 10% earthquakes, the column shear C/D ratio was less than one, which indicates some cause for concern. This is also in part due to the lack of transverse reinforcement in the columns.

The final components of concern are the diagonal members in the cross-frames and diaphragms of the bridge. As indicated by the C/D ratios, these members performed rather poorly. The C/D ratios for these members were raised above one in all cases by using the half-length of the member. However, there still exists the possibility of a problem that may warrant further investigation.

#### **8.2.7.2.5 Time History vs. Response Spectrum Analysis**

This bridge was analyzed using a response spectrum analysis, much like its new counterpart at the Wahite Ditch Site. However, this structure was more similar to the Old St. Francis River Bridge, which had been analyzed using a non-linear time history analysis. Therefore, several cases using a non-linear time history analysis needed to be run on this bridge to form a basis for comparison. The results from two analyses are compared in Table 8.34.

Four earthquake cases were run, choosing two each of 2% and 10% earthquakes, with one being near-field and one being far-field for each likelihood level. Only the longitudinal and transverse earthquake effects were analyzed, as they are the major contributors to the earthquake response of the structure. Also, the vertical responses seemed to change very little, as noted from the comparison of time history results to the response spectrum results for the St. Francis River bridges.

In all cases that were compared, the results of the two analyses were reasonably close. The differences between the values were typically low. These results indicate that the response spectrum analysis is an adequate alternative to the time history analysis for this bridge.

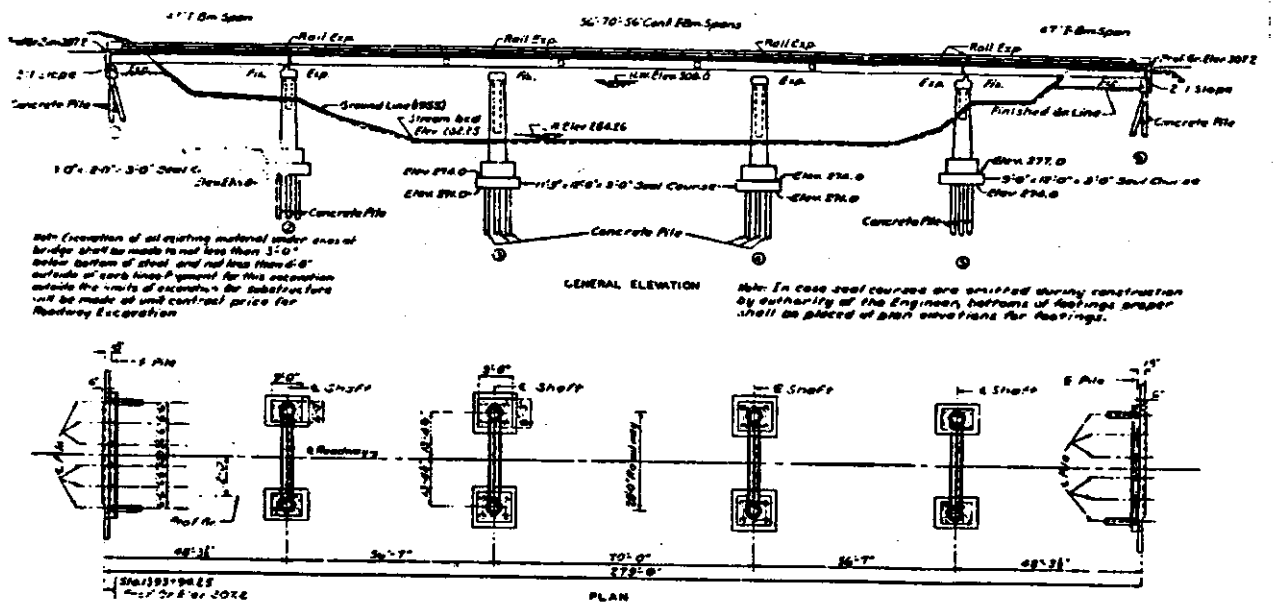


Figure 8.61 Bridge General Elevation (Old Wahite Ditch Bridge)

**Table 8.33 Summary of all Earthquakes for the Old Wahite Ditch Bridge**

<b>C/D Ratio Name</b>	<b>020101</b>	<b>020102</b>	<b>020103</b>	<b>020202</b>	<b>020203</b>	<b>020205</b>	<b>100101</b>	<b>100102</b>	<b>100105</b>	<b>100201</b>	<b>100202</b>	<b>100205</b>
$\Gamma_{\text{b}}$	0.90	0.90	0.90	0.90	0.90	0.90	0.90	0.90	0.90	0.90	0.90	0.90
$\Gamma_{\text{b-trans}}$	0.07	0.06	0.07	0.08	0.06	0.06	0.16	0.14	0.13	0.13	0.13	0.10
$\Gamma_{\text{b-long}}$	0.54	0.46	0.46	0.48	0.45	0.42	0.74	0.68	0.65	0.68	0.66	0.64
$\Gamma_{\text{b-embed}}$	0.59	0.59	0.59	0.59	0.59	0.59	0.59	0.59	0.59	0.59	0.59	0.59
$\Gamma_{\text{b-edge dist}}$	0.86	0.86	0.86	0.86	0.86	0.86	0.86	0.86	0.86	0.86	0.86	0.86
$\Gamma_{\text{cc-final}}$	5.30	4.80	4.94	4.99	4.88	4.77	6.51	6.31	6.23	6.26	6.21	6.10
$\Gamma_{\text{cc-final}}$	9.42	8.54	8.78	8.86	8.67	8.47	11.57	11.22	11.07	11.12	11.04	10.83
$\Gamma_{\text{cc-final}}$	0.80	0.75	0.65	0.74	0.66	0.61	2.97	2.76	2.98	2.43	2.52	2.29
$\Gamma_{\text{cc-final}}$	1.18	1.11	0.97	1.11	0.98	0.90	4.42	4.11	4.42	3.60	3.75	3.41
$\Gamma_{\text{cc-final}}$	6.44	5.78	6.14	6.01	6.13	6.08	8.15	8.04	8.11	7.94	7.97	7.81
$\Gamma_{\text{cc-final}}$	11.44	10.27	10.92	10.67	10.90	10.81	14.48	14.28	14.41	14.10	14.16	13.87
$\Gamma_{\text{cc-final}}$	0.34	0.30	0.31	0.37	0.29	0.27	0.80	0.65	0.63	0.62	0.62	0.49
$\Gamma_{\text{cc-final}}$	0.50	0.45	0.45	0.55	0.43	0.39	1.17	0.96	0.92	0.91	0.92	0.72
$\Gamma_{\text{cc-final}}$	6.51	5.85	6.22	6.05	6.22	6.19	8.16	8.05	8.12	7.96	7.99	7.84
$\Gamma_{\text{cc-final}}$	11.57	10.39	11.06	10.76	11.05	10.99	14.49	14.30	14.43	14.14	14.19	13.94
$\Gamma_{\text{cc-final}}$	3.16	2.48	2.51	2.67	2.59	2.09	5.24	4.83	4.36	4.65	4.24	3.88
$\Gamma_{\text{cc-final}}$	4.65	3.64	3.70	3.92	3.81	3.08	7.70	7.11	6.41	6.83	6.23	5.71
$\Gamma_{\text{cc-final}}$	5.33	4.83	4.96	5.00	4.90	4.79	6.54	6.34	6.27	6.29	6.24	6.14
$\Gamma_{\text{cc-final}}$	9.46	8.58	8.82	8.89	8.71	8.52	11.62	11.27	11.14	11.17	11.10	10.91
$\Gamma_{\text{cc-final}}$	0.80	0.75	0.65	0.74	0.66	0.61	2.98	2.77	2.98	2.43	2.52	2.29
$\Gamma_{\text{cc-final}}$	1.18	1.11	0.97	1.11	0.98	0.90	4.42	4.11	4.42	3.61	3.75	3.41
$\Gamma_{\text{ca-bottom}}$	1.00	1.00	1.00	1.00	1.00	1.00	1.00	1.00	1.00	1.00	1.00	1.00
$\Gamma_{\text{ca-top}}$	0.64	0.58	0.59	0.60	0.59	0.57	0.78	0.76	0.75	0.75	0.75	0.73
$\Gamma_{\text{cs}}$	---	---	---	---	---	---	---	---	---	---	---	---
$\Gamma_{\text{cs-adj}}$	---	---	---	---	---	---	---	---	---	---	---	---
$\Gamma_{\text{cc}}$	---	---	---	---	---	---	---	---	---	---	---	---
$\Gamma_{\text{cy}}$	0.28	0.25	0.25	0.31	0.24	0.22	0.65	0.54	0.51	0.51	0.51	0.40
$\Gamma_{\text{cross}}$	0.45	0.36	0.37	0.39	0.35	0.33	0.80	0.68	0.63	0.67	0.64	0.60
$\Gamma_{\text{cross-0.5L}}$	1.48	1.19	1.23	1.29	1.17	1.09	2.65	2.28	2.10	2.24	2.14	1.99
$\Gamma_{\text{ax-trans}}$	504	445	426	487	410	479	1286	1170	1179	1214	1060	1129
$\Gamma_{\text{ax-long}}$	91	78	81	81	76	80	143	126	128	122	119	123

**Table 8.34 Comparison of Column Moments for Old Wahite Ditch Bridge**

<i>Due to 2% motions</i>						<i>Due to 10% motions</i>					
Due to Transverse EQ	transverse		longitudinal			Due to Transverse EQ	transverse		longitudinal		
	time history	response spectra	time history	response spectra			time history	response spectra	time history	response spectra	
<b>Column 1, bottom</b>	11270	10721	908	1256		<b>Column 1, bottom</b>	4080	5175	372	578	
	10911	10152	917	1174			4611	6055	424	675	
average	11091	10437	913	1215		average	4346	5615	398	627	
Due to Longitudinal EQ	transverse		longitudinal			Due to Longitudinal EQ	transverse		longitudinal		
	time history	response spectra	time history	response spectra			time history	response spectra	time history	response spectra	
<b>Column 1, bottom</b>	28	27	45291	51199		<b>Column 1, bottom</b>	8	8	9130	10111	
	22	24	39931	44807			10	10	11287	12569	
average	25	26	42611	48003		average	9	9	10209	11340	
Due to Transverse EQ	transverse		longitudinal			Due to Transverse EQ	transverse		longitudinal		
	time history	response spectra	time history	response spectra			time history	response spectra	time history	response spectra	
<b>Column 3, bottom</b>	10943	10106	85	213		<b>Column 3, bottom</b>	3890	4855	50	90	
	10497	9572	70	190			4390	5676	54	106	
average	10720	9839	78	202		average	4140	5266	52	98	
Due to Longitudinal EQ	transverse		longitudinal			Due to Longitudinal EQ	transverse		longitudinal		
	time history	response spectra	time history	response spectra			time history	response spectra	time history	response spectra	
<b>Column 3, bottom</b>	17	20	125649	128584		<b>Column 3, bottom</b>	5	7	45961	49631	
	11	16	100706	105750			6	8	57793	64090	
average	14	18	113178	117167		average	6	8	51877	56861	

### 8.2.7.2.6 Structural Response of Abutments

The Old Wahite Ditch Bridge abutment (11.65 m x 0.91 m) is supported on vertical and battered piles. All of piles are cylindrical concrete with a 0.406 m (16 inch) diameter and 10.67 m (35 ft) length. The plan and cross-section of the bridge abutment are shown in Figure 8.61.

The stiffness and damping factors are calculated using a pile length of 10.67 m (35 ft), a pile radius of 0.203 m (8 inch), an elastic modulus of concrete of  $2.15 \times 10^7$  kN/m<sup>2</sup> ( $1.47 \times 10^6$  kips/ft)(Section F.6). Stiffness and damping factors of single batter piles are 0.8 times that of a vertical pile. (Prakash and Subramanayam, 1964)

The vertical load acting on the top of the bridge abutment is obtained from an analysis of the bridge structure. A vertical load of 51 kN (11365 lb) per meter of length was used in this analysis. The self-weight of the bridge abutment was calculated by multiplying its cross sectional area by the unit weight of the bridge abutment material (23.58 kN/m<sup>3</sup>) (150.19 pcf). This calculation is done in the program itself. The lateral earth pressure behind the bridge abutment was calculated using a soil unit weight of 19.54 kN/m<sup>3</sup> (122 pcf), angle of internal friction of 33° and friction angle between soil and abutment of 33°. All of the loads were modified by a time dependent seismic coefficient.

#### 8.2.7.2.6.1 Calculated Time Dependent Displacements of Abutment

Figure 8.63 a and b show the largest time histories of sliding, rocking and total permanent displacement of Old Wahite Ditch Bridge abutment for PE 10% in 50 years respectively. Fig. 8.64 a and b shows the time histories of sliding, rocking and total permanent displacement of Old Wahite Ditch Bridge abutment for PE 2% in 50 years respectively.

A plot of magnitude and significant number of cycles is given in Figure 8.63a. Table 8.35 shows displacement in one significant cycle. This is likely the displacement during a composite analysis.

**Table 8.35 Displacement at Top of Old Wahite Ditch Bridge Abutment**

Displacement at top of abutment	PE 10% in 50 years		PE 2% in 50 years	
	M6.4	M7.0	M7.8	M8.0
Sliding (m)	0.037	0.028	0.139	0.178
Rocking (m)	0.018	0.053	0.0513	0.064
Total (m)	0.056	0.080	0.190	0.242
Significant cycles	9	10	18	20
Disp. in 1-cycle	0.007	0.008	0.011	0.012

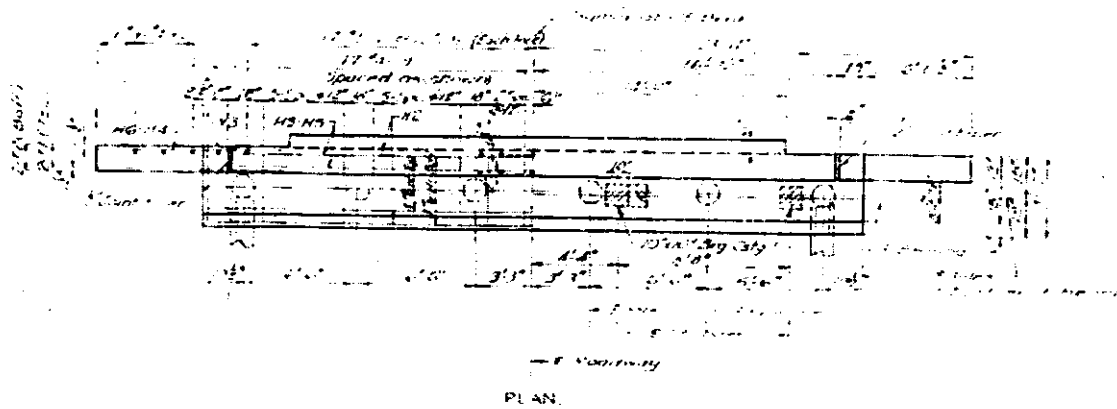


Figure 8.62a Plan of Old Wahite Ditch Bridge Abutment

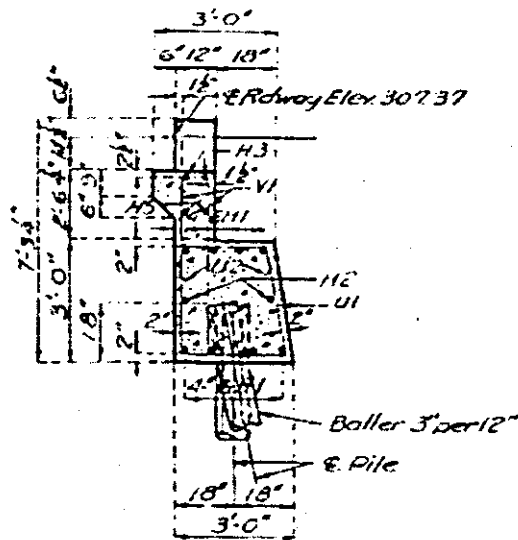
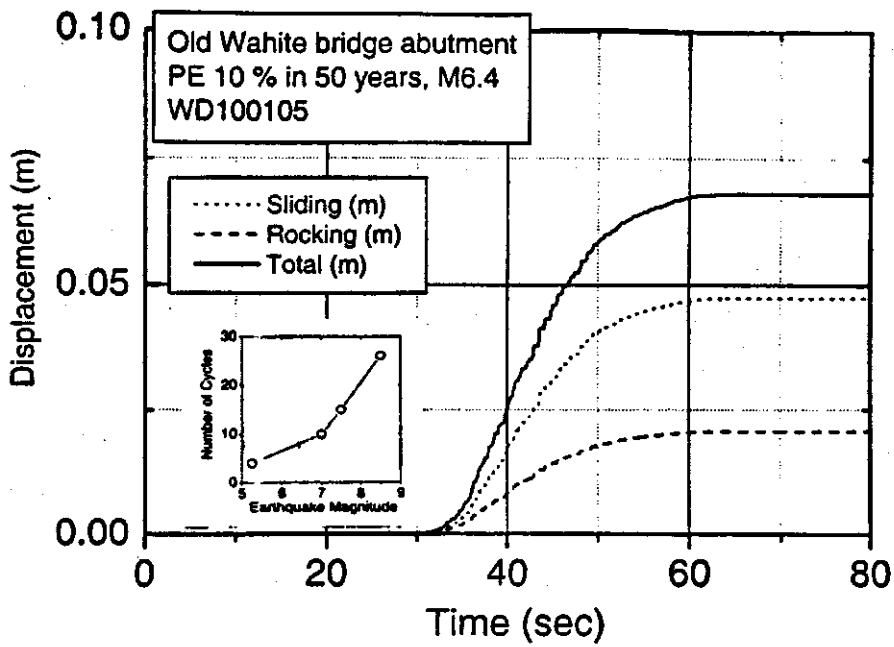
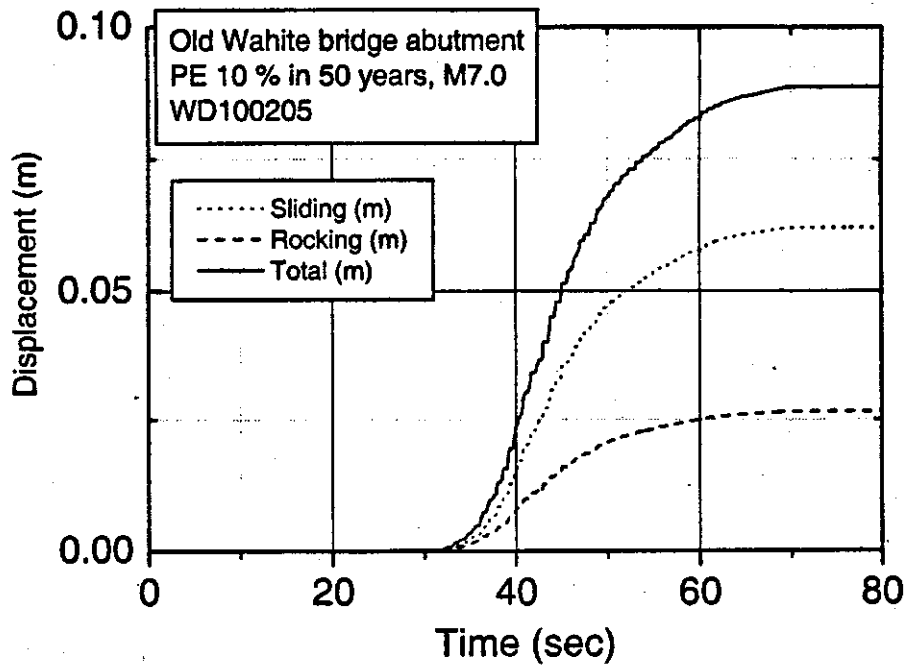


Figure 8.62b Cross Section of Old Wahite Ditch Bridge Abutment

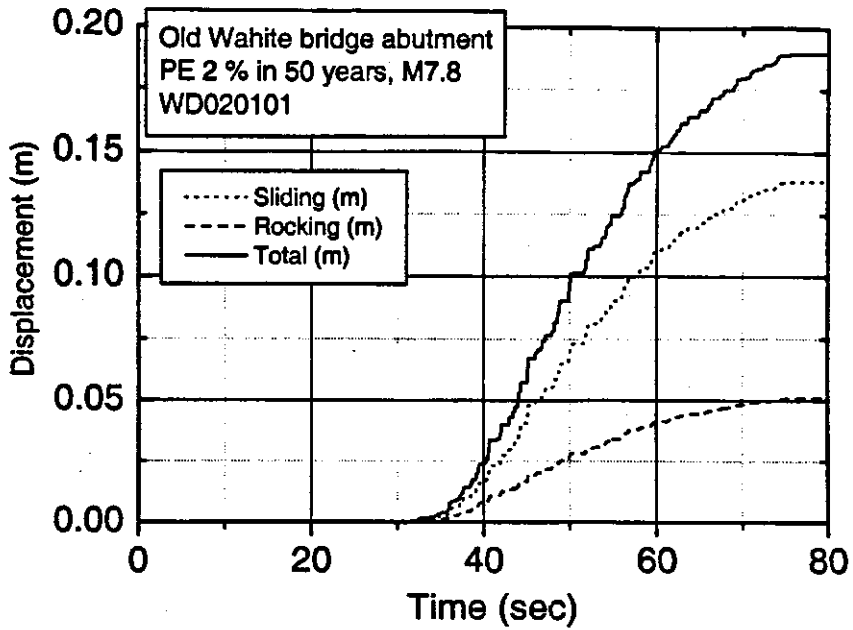


a. Magnitude 6.4

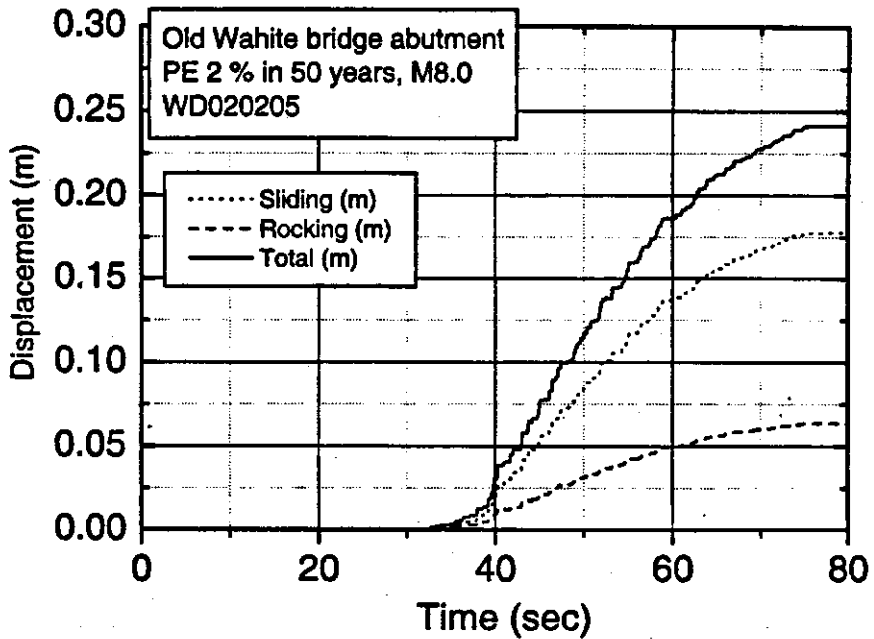


b. Magnitude 7.0

Figure 8.63 Time Histories of Sliding, Rocking and Total Permanent Displacement of the Old Wahite Ditch Bridge Abutment PE 10% in 50 Years, Magnitudes 6.4 and 7.0



a. Magnitude 7.8



b. Magnitude 8.0

Figure 8.64 Time Histories of Sliding, Rocking and Total Permanent Displacement of the Old Wahite Ditch Bridge Abutment PE 2% in 50 Years, Magnitudes 7.8 and 8.0

## **9.0 CONCLUSIONS**

### **9.1 Summary**

The primary objectives of this study were twofold. Objective 1 was to establish a current subsurface and earthquake design geographic information systems (GIS) database for the counties of Butler, Stoddard, New Madrid, Franklin and St. Louis. Objective 2 was to conduct detailed earthquake assessments at two sites along designated emergency vehicle priority access route US 60.

### **9.2 Geotechnical GIS Databases**

Databases have been established for earthquake design data for the US 60 corridor in Butler, Stoddard and New Madrid Counties and for the MO 100 corridor in Franklin and Saint Louis Counties. This includes appropriate data from Missouri Department of Transportation files. These databases will be integrated into the existing Missouri Department of Transportation GIS system for future access, and serve as the beginning of a larger regional or statewide database.

For future development and usage by Missouri Department of Transportation. Further details and access procedures may be found in "User Instructions for Data Entry and Editing-Database of Borehole and Other Geotechnical Data for Missouri Highway Structures".

### **9.3 Site Specific Earthquake Hazards Assessments**

Detailed earthquake site assessments were conducted for two critical US 60 roadway sites (White Ditch Site and St. Francis River Site). Site assessments included: subsurface exploration, and laboratory testing to identify subsurface materials and their engineering properties; evaluation of available seismic records and procedures to characterize the ground motions associated with various design earthquake events; and evaluation of the response of the subsurface materials and the existing bridge structures to the estimated ground motions.

The goals of the site assessments at these two locations were to:

1. Estimate peak magnitude and duration of ground surface motion (including amplification/damping) associated with various events at each site.
2. Evaluate the susceptibility of each site to quake-induced slope instability, liquefaction and flooding.
3. Estimate shaking effects on the various types of existing bridge structures at each site.
4. Compare ground motion and structural response parameters from site-specific earthquake analysis method with those from AASHTO response spectrum analysis method and provide preliminary guidance regarding selection of the analysis method at future sites.
5. Evaluate modified site assessment techniques and establish a basis for using these modified techniques at other sites along designated emergency access routes.

Site-specific seismic response evaluations of the four study bridges were completed. Liquefaction potential, slope stability, abutment stability, flooding potential, and structure stability analysis were performed at both sites for selected "worst case scenario bedrock ground motions" with PE of exceedance of 2% and 10% in 50 year, respectively. Ground motion analysis utilized synthetic ground motions for a New Madrid and other, source zones. Results are presented in Section 8.

### **9.3.1 St. Francis River Site**

The following conclusions may be drawn from this study:

#### **9.3.1.1 Liquefaction**

The soil does not liquefy under selected ground motion for PE 10 in 50 years. However, the soil at this site liquefied for PE 2% in 50 years to different depths depending on the magnitude and the factor of safety.

#### **9.3.1.2 Slope Stability**

The abutment slopes at the St. Francis River Bridge site are stable under all but the most extreme earthquake events.

#### **9.3.1.3 Flood Hazard**

Approximately 5.7 miles of US 60 roadway, from the St. Francis River eastward to approximately 0.4 miles west of Highway WW/TT (which leads to Dudley), and 3.4 miles of roadway from approximately 0.3 miles east of Highway WW/TT eastward to Highway ZZ would flood during and after an earthquake event that resulted in the failure of Lake Wappapelo Dam. Several additional stretches of roadway could flood as a result of levee failures.

#### **9.3.1.4 Structural Response of St. Francis River Bridges**

##### **9.3.1.4.1 New St. Francis River Bridge**

The three-span bridge with integral abutments was analyzed and evaluated in detail under the excitation of 12 ground motions. The overall performance of the bridge is satisfactory except for the following observations. It was found that the steel plates of the neoprene elastomeric pads are not anchored into the capbeam with the required embedment length. They may be pulled out during earthquakes. The diagonal members of the diaphragms or cross-frames are vulnerable to the 2% PE earthquakes. Comparison between the response spectrum analysis and the time history analysis verified the sufficient adequacy of analyzing the bridge with integral abutments using the simpler response spectrum procedure.

#### **9.3.1.4.2 Old St. Francis River Bridge**

Based on the extensive analysis and detailed evaluation of the bridge, the following conclusions can be drawn. The support length of bearings is slightly short based on the current requirement, which may result in the dropping of the spans adjacent to expansion joints. The shear capacity of anchor bolts and the embedment length of bearings are also inadequate for both 10% and 2% likelihood earthquakes. Another major concern is the stability of columns. Although the C/D ratios with a ductility indicator of 5 is greater than 1.0 for all columns, they are likely insufficient to sustain large deformations due to the poor detailing at joints. Associated with the poor detailing is a greater concern for shear capacity of the columns. Just like the New St. Francis River Bridge, it is likely that the diagonal members of the diaphragms and cross frames of this bridge would buckle during a strong earthquake event.

It is also observed from analyses that the response spectrum method can give internal shears and moments as well as displacements with satisfactory engineering accuracy for linear bridges with seat-type abutments. However, potential pounding at expansion joints during a strong earthquake event makes the spectrum method invalid.

#### **9.3.1.4.3 Old St. Francis River Bridge Abutment**

The maximum displacement at the top of this abutment varied from 0.43 inch to 1.02 inch for 10% PE and 2% PE for the different magnitudes of earthquakes. This displacement is tolerable without any damage to the abutments.

### **9.3.2 Wahite Ditch Site**

#### **9.3.2.1 Liquefaction**

The soils do not appear to liquefy for the 10% PE and M 6.4. However, the soils do liquefy marginally for a 10% PE earthquake with a magnitude of 7.0.

For a 2% PE and M 7.8 and 8.0 earthquake with factors of safety less than 1.0, the soils liquefy throughout.

#### **9.3.2.2 Slope Stability**

This site is expected to be stable under small earthquake conditions. The site is less sensitive to ambient ground-water levels (which are affected by water levels in the river) than at the St. Francis River site. Stability analysis under large earthquake conditions indicates marginal stability at the Wahite Ditch site when ground-water levels are high.

#### **9.3.2.3 Flood Hazard**

Water levels appear to be too low during normal conditions to pose a significant risk of exiting the channel, even in the event of levee failure. Furthermore, the roadway is elevated above the

surrounding land. One section of roadway located 0.1 to 0.5 miles west of the ditch is at low elevation and could potentially flood.

#### **9.3.2.4 Structure Stability of Wahite Ditch Bridges**

##### **9.3.2.4.1 New Wahite Ditch Bridge**

Extensive analyses and detailed evaluation of the bridge indicated that the bridge can sustain an earthquake at both 10% and 2% probability of exceedance. The only components that warrant attention are the shear keys on top of the capbeam. Their capacity is slightly inadequate for two out of the six earthquakes at high hazard levels.

##### **9.3.2.4.2 Old Wahite Ditch Bridge**

Based on the extensive analyses and evaluations of the bridge, some conclusions can be drawn as follows. The support length of the superstructures is insufficient so that it is likely that the bridge deck will drop off its support at expansion joints. Other load transferring components, such as bolts and their embedment lengths and edge distances, are also inadequate for earthquake loads. Even though a ductility indicator of 5 was used, the C/D ratios of the columns at Bent 3 are still less than one, indicating insufficient strength. Associated with the column bending, the shear capacity of the columns is significantly less than required due to the lack of transverse reinforcement. Like the diaphragms and cross frames built with angles at the St. Francis River Bridge site, the diagonal members are vulnerable to buckling.

##### **9.3.2.4.3 Old Wahite Ditch Bridge Abutment**

The maximum displacement at the top of this abutment for a 10% PE, M 6.4 and a 2% PE and M 8.0 earthquake varies from 0.28 inch to 0.47 inch. This displacement will not cause any damage to the abutments.

## **10.0 RECOMMENDATIONS**

### **10.1 Protocol**

Earthquake hazard assessment at both the St. Francis River and the Wahite Ditch Sites was essentially a six-component process consisting of the following inter-related analyses:

- 1) Determination of the appropriate earthquake induced strong ground motion.
- 2) Determination of liquefaction potential in response to strong ground motion.
- 3) Determination of slope stability in response to strong ground motion.
- 4) Evaluation of abutment stability in response to strong ground motion.
- 5) Evaluation of structure stability in response to strong ground motion.
- 6) Determination of potential for flooding in response to strong ground motion.

Based on this study, the following recommendations are made with respect to the development of an effective protocol for conducting these six analyzes.

### **10.1.1 Determination of Site-Specific Strong Rock Motion**

**Recommendation 1:** Acquire/develop capability to generate site-specific synthetic ground motion at bedrock based on earthquake magnitude, source signature (amplitude and phase spectrum), and source distance/depth.

**Recommendation 2:** Arbitrarily select two source zones, one proximal and one distal, based on recommendations from The Missouri Department of Natural Resources geologists. The Commerce Geophysical Lineament could serve as a reasonable proximal source zone for further studies along US 60. The New Madrid Fault zone could serve as a reasonable distal source zone.

**Recommendation 3:** Generate a representative suite of synthetic bedrock ground motions for both the proximal and distal sources. The representative suite of synthetic ground motions should cover a range of potentially damaging magnitudes (perhaps 4 to 8), and vary in duration and frequency.

**Recommendation 4:** Propagate the suite of bed rock synthetic ground motions to the surface, and assess damage as per analysis 2 through 5 (section 8.1).

**Recommendation 5:** Estimate probability of occurrence of each ground motion, based on input from USGS and other sources.

**Summary:** The procedure outlined above could be of more long-term utility to Missouri Department of Transportation than the “worst case New Madrid source zone scenario” process employed in this study. Earthquake probability estimates and prospective source zone locations are likely to change over time (in response to new data) – more so than the generated suite of synthetic ground motions. If this assumption is correct, Missouri Department of Transportation would merely be able to reassign new probabilities to each synthesized outcome – as opposed to having to generate new synthetic ground motions in response to changing probabilities.

### **10.1.2 Determination of Liquefaction Potential**

**Recommendation 1:** Liquefaction analysis should be conducted (using the entire suite of synthetic ground motions) at locations of all critical roadway structures and in roadway areas where there is a paucity of structures (to ensure valid statistical sampling). Areas along the roadways should be designated in accordance with their propensity for liquefaction (re: magnitude and source distance). Probabilities can be assigned thereafter, and reassigned as probability estimates change over time.

**Recommendation 2:** Seismic cone penetrometer data should be acquired to a depth of 50 feet (if possible) in immediate proximity to structures studied. Soil should be sampled from surface to bedrock, and SPT data should be acquired to enable the development of a vertical soil profile.

**Recommendation 3:** Bedrock ground motion should be propagated to surface. The propensity of each soil layer to liquefy under synthesized ground motion should be determined.

### **10.1.3 Determination of Slope Stability**

Recommendation 1: Slope stability analysis should be conducted (using the entire suite of synthetic ground motions) at all critical roadway bridge sites and in selected roadway areas where there may be some potential for lateral spreading. The sites studied should be designated in accordance with their propensity for slope failure (re: magnitude and source distance). Probabilities can be assigned thereafter, and reassigned as probability estimates change over time.

Recommendation 2: At each site, topographic data and shallow subsurface control (engineering properties of soil) should be acquired (trenching and boreholes).

Recommendation 3: Bedrock ground motion should be propagated to surface. The propensity of the slope to fail under synthesized ground motion should be determined.

### **10.1.4 Determination of Potential for Flooding in Response to Strong Ground Motion**

For future analysis of earthquake-induced flooding of roadway sections, we recommend the following procedure:

1. Preliminary identification of regions susceptible to flooding:
  - Collect report information on anticipated flood run out following catastrophic failure of nearby dams.
  - Collect 7.5-minute topographic maps and FEMA flood hazard maps along the alignment under evaluation.
  - Identify river, creek, and drainage ditch locations, approximate elevations of water levels, and approximate elevations of both natural and man-made levees flanking the waterways.
  - On the topographic maps, subdivide zones along the roadway by 5-foot contour intervals.
  - Mark areas where the land is below water levels in waterways as zones of potential flooding.
  - Field check each area to visually assess the elevation of the roadway compared to surrounding land.
2. Specific assessment of regions identified as susceptible:
  - Assemble more accurate data on range of water elevations in canals and streams through contact with local government offices for agriculture, flood control, and public works.
  - Measure ranges of water elevations in canals and streams using GPS devices.
  - Develop more accurate topographic analysis using DEM computer files analyzed with GIS software to compare water levels and roadway elevations.

- Confirm computer topographic analysis with GPS field measurements of roadway elevations.
- Use DEM computer files, soil survey information, and field reconnaissance data on soil type and strength to rank the susceptibility to slope failure of various stretches of waterway levees. Combine this analysis with roadway and water elevation analysis to identify critical areas where likelihood of levee failure is high and flooding potential in the event of levee failure is also high.

### **10.1.5 Evaluation of Flooding Potential**

Flood analysis (in accordance with methodologies outlined in this report) should be conducted for the entire designated roadway. Additionally, slope stability analysis (as outlined above) should be conducted at selected sites along river, drainage ditch and irrigation canals to determine likelihood of failure that could result in flow blockage and flooding.

### **10.1.6 Determination of Structural Stability**

#### **10.1.6.1 Evaluation of Abutment Stability**

Recommendation 1: Abutment stability analysis should be conducted (using the entire suite of synthetic ground motions) at all critical roadway structures. Sites studied should be designated in accordance with their propensity for abutment failure (re: magnitude and source distance). Probabilities can be assigned thereafter, and reassigned as probability estimates change over time.

Recommendation 2: Bedrock ground motion should be propagated to surface. The integrity of each abutment under synthesized ground motion should be determined.

#### **10.1.6.2 Evaluation of Stability of Integrated Bridge Abutments**

Recommendation 3: Structure stability analysis should be conducted (using entire suite of synthetic ground motions) for all critical roadway structures. Sites studied should be designated in accordance with their propensity to fail (re: magnitude and source distance). Probabilities can be assigned thereafter, and reassigned as probability estimates change over time.

Recommendation 4: Bedrock ground motion should be propagated to surface. The propensity of each designated structure to fail under synthesized ground motion should be determined.

#### **10.1.6.3 Evaluation of Stability of Structural Members**

Recommendation 5: For multiple span highway bridges with integral abutments, the response spectrum analysis is accurate enough for evaluation of structural members with a linear bridge model. For bridges supported by seat-type abutments at their ends, pounding at expansion joints makes it necessary to analyze a geometrically nonlinear system of the bridges.

Recommendation 6: For bridge seat-type abutments, the load transferring members such as bolts and their anchorage and edge distances must be evaluated together with the minimum support length requirements. For existing bridges, the shear and moment capacities of the columns must be evaluated with considerations of the detailing at the beam to column and the column to footing joints.

## **10.2 Further Work**

This study has provided a sound basis for developing a comprehensive evaluation of seismic response of highway structures in southeast Missouri. Based on these results and on discussions with Missouri Department of Transportation personnel the following recommendations are made for further work.

### **10.2.1 Proposed Study: Retrofit of Critical Structures along Designated Emergency Vehicle Priority Access Routes**

The results of this study have identified a number of critical locations where the bridge and embankment structures would fail under the severe earthquake loading forecasted for this area. Consequently, since these facilities must meet emergency access serviceability, it is proposed to develop seismic retrofit procedures for enhancing the ability of these structures to resist the severe earthquake forces. The procedures could include structural stiffening of the bridge members, enhanced resistance to embankment and foundation liquefaction and slope failure. This research should also include the development of a post-earthquake evaluation protocol such that the critical structures could be quickly and easily evaluated to determine their structural integrity following the earthquake event.

### **10.2.2 Proposed Study: Site Specific Earthquake Assessments along MO 100**

The Missouri Department of Transportation in conjunction with other state agencies has designated specific routes for vehicular access of emergency personnel, equipment and supplies in the event of a major earthquake event in southeast Missouri. These routes include portions of MO 100, US 50 and I-44. The routes traverse varied geologic settings and include or cross many critical roadway features such as bridges, slopes, box culverts, and retaining walls. The extent of damage and survivability of these critical roadway features in the event of a major earthquake event is not fully known and would impact the ability to use these designated routes to provide emergency vehicular access in a timely manner.

The goals of this proposed study are to use the results of this Phase I US 60 study to complete a regional overview and prioritization of seismic hazards and to conduct site specific studies along the next critical highway, which is judged to be MO 100. The specific objectives to complete these goals are given below. Detailed earthquake assessments will be conducted for two sites where critical roadway features exist. These site assessments will include subsurface exploration and laboratory testing to identify subsurface materials and their engineering properties; evaluation of available seismic records and procedures to characterize the ground motions associated with various design earthquake events and evaluation of the response of the subsurface materials

and the existing bridge structures to the estimated ground motions. Site assessment techniques will be selected based on their usefulness as determined from this study. In this way, comparisons in data quality, investigation time, and investigation costs may be made between the detailed US 60 study and the more streamlined MO 100 study.

It is proposed that members of the research team will survey MO 100 in St. Louis and Franklin Counties. Sites with critical roadway features will be visually evaluated and ranked based upon geologic factors, structural factors and perceived criticality/risk factors. The top two sites with differing geologic settings will then be selected for further study.

The goals of the site assessments at these locations would be to:

1. Estimate peak magnitude and duration of ground surface motion (including amplification/damping) associated with various events at each site.
2. Evaluate the susceptibility of each site to earthquake induced slope instability and liquefaction.
3. Estimate shaking effects on the various types of existing bridge structures at each site.
4. Compare ground motion and structural response parameters from site-specific earthquake analysis method with those from AASHTO response spectrum analysis method and provides preliminary guidance regarding selection of the analysis method at future sites.
5. Evaluate the modified site assessment techniques identified in the US 60 study and establish a basis for using these modified techniques at other sites along designated emergency access routes.

Finally, a qualitative assessment of slope stability along the entire length of MO 100 from near Linn to Manchester will be completed, as well as an assessment of evidence of previous earthquake activity (in the form of sand blows, prehistoric slope movement, etc.).

### **10.2.3 Proposed Study: Regional Liquefaction Hazard Analysis**

Liquefaction hazards will be identified and prioritized along the designated emergency vehicle routes US 60 and MO 100 using information in the GIS database prepared for Phase I and future work. Strip maps showing liquefaction potential along designated routes will be generated.

#### **10.2.4 Proposed Study: Geo-Referencing of Boring Locations**

The locations of geotechnical borings at the two bridges evaluated in Phase I and at the Phase II sites will be precisely identified in the GIS database using as-built drawings, survey information, and geo-referencing software. This will allow accurate cross-section generation from the database information without a field visit. Boring locations in the current GIS database are limited to station and offset coordinates, which are not precise enough for cross-section and mapping applications. Additionally, plans from approximately 104 bridges (4 plans per bridge) will be scanned and geo-referenced to permit accurate locating of proximal boreholes.

#### **10.2.5 Proposed Study: Regional Prioritization for Future Earthquake Hazards Assessments**

Part of the US 60 study included development of a GIS database of subsurface and earthquake data for both the US 60 and MO 100 corridors. This study will couple an assessment of this database with a regional review of geologic, hydrologic, and road structure information to prioritize future earthquake assessments along MO 100, US 50 and I-44. This type of assessment was completed for the Phase I study along US 60, and the methodology will be revised and conducted in more detail for the proposed Phase II study. The results this assessment are expected to provide the basis for gauging the sensitivity of various roadway and geologic conditions to earthquake damage and prioritizing locations for further study. In addition to bridges and roadway conditions, the assessment will also qualitatively evaluate slope stability hazards and flooding hazards related to levee, dam, or canal failure.

#### **10.2.6 Proposed Study: Laboratory Testing of Truss-Type Diaphragms or Cross Frames and Effective Retrofitting Techniques**

Three out of four bridges investigated in this project have diaphragms or cross frames consisting of angles. They are all subject to high potential for buckling during strong earthquakes. To ensure that the superstructure (deck, girder, diaphragms/cross frames) remains integrated to transfer load from it to the substructure, the diaphragms need to be further studied for the development of practical retrofitting techniques.

#### **10.2.7 Proposed Study: Integration of LOGMAIN Surficial Material Information**

Database elements will be identified to permit surficial materials information in LOGMAIN to be integrated into the Missouri Department of Transportation database.

#### **10.2.8 Proposed Study: Long Term Strategic Plan**

The site-specific and regional studies will be used to develop a long term strategic plan for earthquake hazards assessment in Southeast Missouri. The strategic plan will contain two elements: the first will be a prioritization of structures or sections of highway for further study of specific seismic hazards (shaking, slope movement, flooding, liquefaction, etc.), and the second will be a plan for solicitation of continued funding for continued funding of additional phases of the project. The primary agencies or programs targeted will be FEMA, USGS, NEHRP, and NSF.

## 11.0 BIBLIOGRAPHY

American Association of State Highway and Transportation Officials, Standard Specifications for Highway Bridges: Division I-A Seismic Design, 16 Edition, 1996,

Bowles, J. 1988. *Foundation Analysis and Design*. McGraw-Hill, New York.

Choudhry, M.S. 1999. "Seismic Analysis of Pile Supported Rigid-Bridge Abutments Using Material Geometric Non-linearity. Ph.D. Dissertation, University of Missouri Rolla.

Das, B.M. 1990. *Principles of Geotechnical Engineering*. 2nd Edition, PWS-Kent, Boston.

Federal Highway Administration (FHWA). Seismic Retrofitting Manual For Bridges, Buckle and Friedland, Eds., FHWA-RD-940942, May, 1995.

Grohskopf, J.G. 1955. *Subsurface Geology of the Mississippi Embayment of Southeast Missouri*: Missouri Geological Survey and Water Resources Vol. 37, Rolla, MO, 133 p.

Herrmann, R. (2000). "Report on credible synthetic ground motion " Personal communication. (see appendix D or website address <http://www.eas.slu.edu/People/RBHerrmann/MODOT.001014/>).

Holtz, R.D. and Kovacs, W. 1981. *An Introduction to Geotechnical Engineering*. Prentice-Hall, New Jersey.

Hunt, R.E. 1984. *Geotechnical Engineering Investigation Manual*. McGraw Hill, New York, pp. 190-191.

Idriss, I.M. and Sun, J.I. (1992), "Users Manual for SHAKE91. *A Computer Program for Conducting Equivalent Linear Seismic Response Analyses of Horizontally Layered Soil Deposit*". Center for Geotechnical Modeling, Department of Civil & Environmental Engineering, University of California, Davis, November.

Kagawa, T., and Kraft, L. M., Jr. (1980). *Lateral Load-Deflection Relationships for Piles Subjected to Dynamics Loadin.*, Soil Foundations, Japanese Society of Soil Mechanics and Foundation Engineering, Vol. 20, No. 4, pp 19-36.

Kramer, S. L. 1996. *Geotechnical Earthquake Engineering*. Prentice Hall, Inc., Upper Saddle River, NJ, p. 436.

Lambe, T. and Whitman, R., (1969), "Soil Mechanics", John Wiley and Sons, New York.

Liu, T.K. 1967., *A review of engineering soil classification system*. Highway Research Record, No. 156.

- Luna, R., and J.D. Frost. 1995. *Liquefaction Evaluation Using a Spatial Analysis System*, Report No. CEE/GIT-GEO-3, Georgia Institute of Technology, Atlanta, 202 p.
- McCarthy, D.F. 1998. *Essentials of Soil Mechanics and Foundations*, 5<sup>th</sup> Edition: Prentice Hall, Upper Saddle River, New Jersey, pp. 101, 148, 381.
- Meigh, A.C. 1987. *Cone Penetration Testing, Methods and Interpretation*. Butterworths, London, p. 24.
- Mitchell, J. K. 1993. *Fundamentals of Soil Behavior*, 2nd edition. John Wiley and Sons, New York.
- Mitchell, J.K. and W.S. Gardner. 1975. *In-Situ Measurement of Volume Change Characteristics*". *State of the Art Report*, Vol. II, 1975 Proc. of the American Society of Civil Engineers Specialty Conf. on In-Situ Measurement of Soil Properties, Raleigh, NC.
- Mononobe. N., Matsuo, H. (1929). *On the determination of Earth pressure during earthquakes*. World Engineering Congress Proceedings, Vol. IX, Tokyo 1929. Pp. 177-185.
- National Information Service for Earthquake Engineering (NISEE). University. of California, Berkeley. [Http://www.eerc.berkeley.edu/](http://www.eerc.berkeley.edu/)
- Novak, M. 1974. *Dynamics Stiffness and Damping of Piles*. Canadian Geotechnical Journal, Vol. 11, pp. 574-598.
- Novak, M., and B. El-Sharnouby. 1983. *Stiffness and Damping Constants of Single Piles*. Journal of the Geotechnical. Engineering. Division, American Society of Civil Engineers 109(GT-7) 961-974.
- Okabe, S. (1924). *General Theory on Earth pressure and Seismic Stability of Retaining Wall and Dam*, Journal of Japan Society of Civil Engineering, Vol. 10, 1277-1323.
- Poulos, H.G. 1968. *Analysis of the settlement of pile groups*. Geotechnique 18(4), 449-471.
- Poulos, H.G (1971), *Behavior of Laterally loaded piles. II Piles Groups*. Journal of the Soil Mechanics and Foundation. Engineering. Division, American Society of Civil Engineers. 97(SM-5), 733-751.
- Prakash, S. 1981., *Soil Dynamics*, McGraw-Hill, New York.
- Prakash, S. and H.D. Sharma. 1992. *Pile Foundations*. John Wiley and Sons, New York.
- Prakash, S and Subramanayam, G. (1964), *Load Carrying Capacity of Battered Piles* Rookee University Research Journal, Vol. VII, No. 1 and 2, September, pp 29-46.
- Rafnsson, E.A. (1991). *Displacement-Based Design of Rigid Retaining Walls Subjected to Dy-*

*namic Loads Considering Soil Non-linearity*. PhD Dissertation, University of Missouri Rolla.

Rumbaugh, Blaha M., et al. 1991. *Object-Oriented Modeling Design*, Prentice Hall, Inc., New Jersey, 500 pp.

Saucier, R.T. 1994. *Geomorphology and quaternary Geologic History of the Lower Mississippi Valley*: U.S. Army Corps of Engineers Waterways Experiment Station Portfolio, 28 plates.

Schnabel, B.; Lysmer, J. and Seed, H.B. (1972). *SHAKE. A Computer Program for Earthquake Response Analysis of Horizontally Layered Sites*. Report No. EERC 72-12, College of Engineering, University of California, Berkeley, December.

Seed, H.B. and I.M Idriss 1971. *Simplified Procedure for Evaluating Soil Liquefaction Potential*. Journal of the Soil Mechanics and Foundation Division, ASCE, Vol. 97, No. SM9, pp. 1249-1273.

Seed, H.B., K. Tokimatsu, L.F. Harder, and R.M. Chung. 1985. *Influence of SPT Procedures in Soil Liquefaction Resistance Evaluations*. Journal of the Geotechnical Engineering Division, ASCE, Vol. 112, No. GT11, pp. 1016-1032.

Segui, W.T., LRFD Steel Design, PWS Publishing Company, Boston, MA, 1996.

Sridharan, Asusri, and Narahimha Rao. 1972. *New Approach to Multistage Triaxial Test*. Technical Note, *Journal of Soil Mechanics and Foundation Engineering Division*, ASCE, Vol. SM11, November.

Turner, A.K., et. Al, (1996) " Landslides: Investigation and Mitigation", TRB Special Report 247, Robert L. Shuster, Washington D.C.

USGS, National Seismic Hazard Mapping Project, Golden, Colorado.  
[Http://geohazard.cr.usgs.gov/eq/](http://geohazard.cr.usgs.gov/eq/)

U.S. Army Corps of Engineers. 1985. *Below Wappapello Dam Emergency Notification Plan*: USACE Memphis District MDR 500-1-5.

Vucetic, M. and Dobry, R. (1991). *Effect of Soil Plasticity on Cyclic Response*. Journal of Geotechnical Engineering, Vol. 117, No. 1, ASCE. pp. 89-107.

Wen, Y.K. and C.L. Wu. 2000 *Generation of Ground Motions for Mid-America Cities*. MAE report currently under review.

Wesnousky, S.G. and L.M. Leffler. 1994. *A Search for Paleoliquefaction and Evidence Bearing on the Recurrence Behavior of the Great 1811-12 New Madrid Earthquakes*: USGS Professional Paper 1538-H, U.S. Government Printing office, Washington, 42 p.

Winterkorn, H and H. Fang. 1975. *Foundation Engineering Handbook*. Van Nostrad Reinhold,

New York.

Wu, Y. 1999. *Displacement-Based Analysis and Design of Rigid Retaining Walls During Earthquake*, PhD Dissertation, University of Missouri Rolla.

Youd, T.L. and I.M. Idriss. Editors. 1997. *Proceeding of the NCEER Workshop on Evaluation of Liquefaction Resistance of Soils*. National Center for Earthquake Engineering Research, Technical Report No. NCEER-97-0022, December 31, 1997.

## 12.0 LIST OF SYMBOLS

<u>Symbol</u>	<u>Definition</u>
A	Cross section of single pile
$A_{\text{bolt}}$	Cross-sectional area of one bolt
$A_{\text{b.splice}}$	Area of spliced bar
$A_g$	Gross area of column cross-section
$A_s$	Area of steel in cross-section
$A_{\text{tr}}$	Area of transverse steel reinforcement
$A_{\text{tr(e)}}$	Capacity for transverse confinement
$A_{\text{tr(d)}}$	Demand for transverse confinement
$a_{\text{(PGHA)}}$	Peak horizontal ground acceleration
$a_{\text{(PGVA)}}$	Peak vertical ground acceleration
$\text{acc}_x(t)$	Horizontal ground acceleration
$\text{acc}_y(t)$	Vertical ground acceleration
B	Footing (pile cap) width, bridge abutment width
b	Width of cross-section
c	Cohesion (psf)
CPT	Cone penetrometer test
CRR	Cyclic resistant ratio
CSR	Cyclic stress ratio
$c_x$	Damping of single pile for translation along x axis
$c_x^g$	Damping of piles group for translation along x axis
$c_{x\phi}$	Cross coupled damping of single pile for coupling sliding along x-axis
$c_{x\phi}^g$	Cross coupled damping of piles group for sliding along x-axis and
$c_y$	Damping of single pile for translation along y axis
$c_y^g$	Damping of piles group for translation along y axis
$c_{y\theta}$	Cross coupled damping of single pile for sliding along y-axis and
$c_{y\theta}^g$	Cross coupled damping of piles group for sliding along y-axis and
$c_z$	Damping of single pile for translation along z axis
$c_z^g$	Damping of piles group for translation along z axis
$c_\phi$	Damping of single pile for rocking about y axis
$c_\phi^g$	Damping of piles group for rocking about y axis
$c_\theta$	Damping of single pile for rocking about x axis
$c_\theta^g$	Damping of piles group for rocking about x axis
$c_{\psi}$	Damping of single pile for torsion about z axis
$c_{\psi}^g$	Damping of piles group for torsion about z axis
d	Effective width of cross-section
$d_b$	Diameter of reinforcing bar
$d_{\text{bolt}}$	Diameter of one bolt
D	Pile diameter
$D_r$	Relative density (unitless)
e	Void ratio (unitless)
$E_p, E_{\text{pile}}$	Modulus of elasticity of pile material
$F_u$	Ultimate stress for one bolt

$F_v$	Shear stress for one bolt
$f'_c$	Compressive strength of concrete
$f_s$	Stress in steel
$f_y$	Steel yield stress
$f_{yt}$	Transverse steel yield stress
$f_{w1}, f_{T1}, f_{x1}, f_{\phi1}, f_{x\phi1}$	Stiffness parameters
$f_{w2}, f_{T2}, f_{x2}, f_{\phi2}, f_{x\phi2}$	Damping parameter
$G_s$	Specific gravity of soil particles (unitless)
$g$	Acceleration due to gravity
$G_o$	Initial shear modulus of soil
$G_s$	Shear modulus of soil
$H$	Abutment height
$H_1$	Horizontal seismic force increment due to weight of abutment
$H_2$	Horizontal force increment as result of weight of girder and traffic load
$H_3$	Horizontal seismic force due to soil mass above wall
HGA	Horizontal ground acceleration (% of gravity)
$I_p$	Moment of inertia of single pile about x or y axis
$I_{pp}$	Polar moment of inertia of single pile
$j$	Parameter for concrete stress distribution
$k_1$	FHWA parameter for transverse confinement
$k_2$	FHWA parameter for transverse confinement
$k_3$	Effectiveness of transverse bar anchorage
$k_h, k_v$	Horizontal and vertical seismic coefficient, $k_h = acc_x(t)/g$ and $k_v = acc_y(t)/g$
$k_m$	FHWA parameter for longitudinal reinforcement
$k_x$	Stiffness of single pile for translation along x axis
$k_x^g$	Stiffness of group of piles in translation along x axis
$k_{x\phi}$	Cross coupled stiffness of single pile for coupling along x-axis and rocking about y axis
$k_{x\phi}^g$	Cross coupled stiffness of piles group for sliding along x-axis and rocking about y axis
$k_y$	Stiffness of single pile for translation along y axis
$k_y^g$	Stiffness of piles group for translation along y axis
$k_{y\theta}$	Cross coupled stiffness of single pile for sliding along y-axis and rocking about x axis
$k_{y\theta}^g$	Cross coupled stiffness of piles group for sliding along y-axis and rocking about x axis
$k_z$	Stiffness of single pile for translation along z axis
$k_z^g$	Stiffness of piles group for translation along z axis
$k_\phi$	Stiffness of single pile for rocking about y axis
$k_\phi^g$	Stiffness of piles group for rocking about y axis
$k_\theta$	Stiffness of single pile for rocking about x axis
$k_\theta^g$	Stiffness of piles group for rocking about x axis
$k_{\omega}$	Stiffness of single pile for torsional about z-axis
$k_{\omega}^g$	Stiffness of piles group for torsional about z-axis
$L$	Pile length

$I_{a(c)}$	Capacity of longitudinal anchorage
$I_{a(d)}$	Demand of longitudinal anchorage
$L_{cot}$	Length of column
$l_s$	Length of splice
$M$	Magnitude
$m$	Mass of bridge abutment
$Mm$	Mass moment of inertia of bridge abutment about the axis of rotation
$M_\phi$	Moment about y-axis.
$M_\theta$	Moment about x-axis
$N_1$	Field measured standard penetration value (number of blows per foot)
$N_{1,60}$	Corrected standard penetration value (number of blows per foot)
$N_{spt}$	Standard penetration value (number of blows per foot)
$P$	Axial compressive force
$P_a, \Delta P_{ae}$	Static and dynamic increment of earth pressure
$P_x, P_y$	Total horizontal force in x or y direction
$PHGA$	Peak horizontal ground acceleration (% of gravity)
$PVGA$	Peak vertical ground acceleration (% of gravity)
$Q$	Vertical force acting on the top of bridge abutment transmitted from girder
$\Gamma_{ad-long}$	C/D ratio for longitudinal abutment displacement
$\Gamma_{ad-trans}$	C/D ratio for transverse abutment displacement
$\Gamma_{bf-edge\ dist.}$	C/D ratio for edge distance of bolts
$\Gamma_{bf-embed}$	C/D ratio for bolt embedment length
$\Gamma_{bf-embed-adj}$	C/D ratio for bolt embedment length, adjusted for stresses
$\Gamma_{bf-long}$	C/D ratio for shear in longitudinal direction
$\Gamma_{bf-trans}$	C/D ratio for shear in transverse direction
$\Gamma_{ca-bottom}$	C/D ratio for reinforcement anchorage at column bottom
$\Gamma_{ca-top}$	C/D ratio for reinforcement anchorage at column top
$\Gamma_{cc}$	C/D ratio for transverse confinement
$\Gamma_{cross}$	C/D ratio for diaphragm and cross-frame members
$\Gamma_{cs}$	C/D ratio for splices
$\Gamma_{cs-adj}$	C/D ratio for splices, adjusted for steel stresses
$\Gamma_{cv}$	C/D ratio for column shear
$\Gamma_{ec}$	C/D ratio for column moment
$r_o$	Pile radius
$S$	Spacing (c/c distance of piles in all directions), saturation of soil (unitless)
$s$	Spacing of transverse reinforcement
$SPT$	Standard penetration test
$T$	Torsional moment
$V_1$	Vertical seismic force increment due to weight of abutment
$V_2$	Vertical force increment as result of weight of girder and traffic load
$V_3$	Vertical seismic force due to soil mass above wall
$V_{b(c)long}$	Shear capacity in longitudinal direction
$V_{b(d)long}$	Shear demand in longitudinal direction
$V_{b(c)trans}$	Shear capacity in transverse direction
$V_{b(d)trans}$	Shear demand in transverse direction

$V_{e(d)}$	Elastic shear demand in columns
$V_{i(c)}$	Initial shear capacity of column (concrete & steel)
$V_{f(c)}$	Final shear capacity of column
VGA	Vertical ground acceleration (% of gravity)
$V_p$	Shear wave velocity of pile material
$V_s$	Shear wave velocity of soil
$V_{u(d)}$	Maximum column shear from plastic hinging
$v_c$	Initial shear capacity of concrete in column
W	Weight of bridge abutment
W <sub>s</sub>	Weight of soil above of bridge abutment
X	Translation along x axis
x	Axis perpendicular to abutment and pier of bridge (direction of traffic), distance in x-direction
$x_r$	Distance between C.G. of footing (pile cap) and center to center of a pile
Y	Translation along y axis
y	Axis parallel to abutment and pier, distance in y-direction
Z	Translation along z-axis
z	Axis in vertical direction, distance in z-direction
$z_c$	Distance between center of gravity and base of footing (pile cap)
$\alpha_h$	Horizontal interaction factor
$\alpha_A$	Vertical interaction factor
$\alpha_{Lx}, \alpha_{Ly}$	Horizontal interaction factor in x and y direction
$\beta$	Departure angle
$\delta$	friction angle at interface of soil and wall
$\gamma_{water}$	Unit weight of water (pcf)
$\gamma_{dry}$	Dry unit weight of soil (pcf)
$\theta$	Footing rotation
$\mu$	FHWA multiplier for transverse confinement
$\phi$	Multiplier for shear capacity for bolts
$\phi$	Internal friction angle of soil, rotation about y axis
$\nu_p$	Poisson ratio of pile material
$\nu_s$	Poisson ratio of soil
$\rho(c)$	Volumetric ratio of existing transverse reinforcement
$\rho(d)$	Required volumetric ratio of transverse reinforcement
$\rho_p$	Mass density of pile material
$\rho_s$	Mass density of soil
$\sigma$	Total vertical stress
$\sigma_o'$	Effective initial vertical stress
$\psi$	Rotation about z axis
$\theta$	Rotation about x axis
$\tau$	Total shear stress

## A. FIELD DATA

### A.1 Symbols Used on Boring Information

COHESIVE SOILS (Modified after ASTM D2487-93 and D 2488-93)

Table 1: Fine Grained Soil Subclassification	Percent (by weight) of Total Sample
<b>Terms</b> <b>SILT, LEAN CLAY, FAT CLAY, ELASTIC SILT</b> Sandy, gravelly, abundant cobbles, abundant boulders, with sand, with gravel, with cobbles, with boulders, scattered sand, scattered gravel, scattered cobbles, scattered boulders, a trace sand, a trace gravel, a few cobbles, a few boulders	<b>PRIMARY CONSTITUENT</b> >30-50% >15-30%-Secondary coarse grained constituents 5-15% <1
*The relationship of clay and silt constituents is based on plasticity and normally determined by performing index tests. Refined classifications are based on Atterberg Limits tests and the Plasticity Chart.	

(Modified after Ref. Oregon DOT 1987, DM 7.1 1982 and FHWA 1997)

TERM	Number Of Blows Per 1 ft.	POCKET PENETROMETER (tsf)	FIELD TEST
Very Soft	0-1	0.25 or less	Squeezes between fingers when fist is closed, penetrated sever inches by fist.
Soft	2-4	0.25-0.50	Easily molded by fingers, easily penetrated several inches by thumb.
Medium Stiff	5-8	0.50-1.00	Molded by strong pressure of fingers, can be penetrated several inches by thumb with moderate effort.
Stiff	9-15	1.00-2.00	Dented by strong pressure of fingers, readily indented by thumb but can be penetrated only with great effort.
Very Stiff	16-30	2.00-4.00	Readily indented by thumbnail.
Hard	30-60	Over 4.00	Indented with difficulty by thumbnail.
Very Hard	61-		

MOISTURE CONDITION (Modified after ASTM D 2488-93)

DESCRIPTIVE TERM	GUIDE
Dry	No indication of water
Moist	Indication of water
Wet	Visible water

CRITERIA FOR DESCRIBING STRUCTURE (Modified after ASTM D 2488-93)

Description	Criteria
Stratified	Alternating layers of varying material or color with layers at least 1/6 inch (6mm) thick; note thickness
Laminated	Alternating layers of varying material or color with the layers less than 6 mm thick; note thickness
Fissured	Breaks along definite planes of fracture with little resistance to fracturing
Slickensided	Fracture planes appear polished or glossy, sometime striated.
Blocky	Cohesive soil that can be broken down into small angular lumps which resist further breakdown.
Lensed	Indication of small pockets of different soils, such as small lenses of sand scattered through a mass of clay, note thickness
Homogeneous	Same color and appearance throughout.
Layer	Inclusions greater than 3 inches thick (7.5 cm).
Seam	Inclusions 1/3 to 3 inches (3 to 75 mm) thick extending through the sample.
Parting	Inclusion less than 1/8 (3 mm) inch thick

NON-COHESIVE (GRANULAR) SOILS (Modified after ASTM D 2487-93 and D 2488-93)

Coarse Grained Soil Subclassification	Percent (by weight) of Total Sample
<b>Term</b> <b>GRAVEL, SAND, COBBLES, BOULDERS</b> Sandy, gravelly, abundant cobbles, abundant boulders With gravel, with sand, with cobbles, with boulders Scattered gravel, scattered sand, scattered cobbles, scattered boulders A trace gravel, a trace sand, a few cobbles, a few boulders	<b>PRIMARY CONSTITUENT</b> >30-50% >15-30% - Secondary coarse grained constituents 5-15% < 5%
Silty (MH. & ML) <sup>a</sup> , clayey (CL & CH) <sup>a</sup> (with silt, with clay) <sup>a</sup> (trace silt, trace clay) <sup>a</sup>	<15% 5-15% <5 %
<sup>a</sup> Index tests and/or plasticity tests are performed to determine whether the term "silt" or "clay" is used.	

**GRAIN SIZE IDENTIFICATION (Modified after Oregon DOT 1987 and FHWA 1997)**

NAME	SIZE LIMITS	FAMILIAR EXAMPLE
Boulder	12 in. (30 cm) or more	Larger than basketball
Cobbles	3 in (76 mm) – 12 in. (30 cm)	Grapefruit
Coarse Gravel	½ in. (19 mm) – 3 in (76 mm)	Orange or lemon
Fine Gravel	4.75 mm (No. 4 sieve) – ½ in. (19 mm)	Grape or Pea
Coarse Sand	2 mm (No. 10 sieve) 4.75 mm (No. 4 sieve)	Rocksalt
Medium Sand	0.42 mm (No. 40 sieve) – 2 mm (No. 10 sieve)	Sugar, Table Salt
Fine Sand	0.075 mm (No. 200 sieve) – 0.42 mm (No. 40 sieve)	Powdered Sugar
Fines	Less than 0075 mm (No. 200 sieve)	

\* Particles finer than fine sand cannot be discerned with the naked eye at a distance of 8 in. (20 cm).

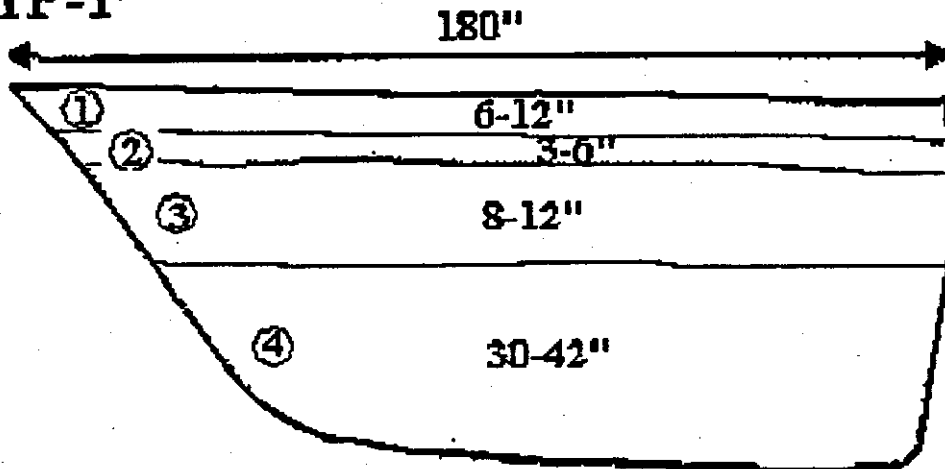
**(Modified after FHWA 1997)**

MOISTURE CONTITION		DENSITY	
DESCRIPTIVE TERM	GUIDE	TERM	N-VALUE (bp0)
Dry	No indication of water	Very Loose	00-04
Moist	Damp but no visible water	Loose	05-10
Wet	Visible free water, usually soil below water table	Medium Dense	11-24
		Dense	25-50
		Very Dense	Over 51

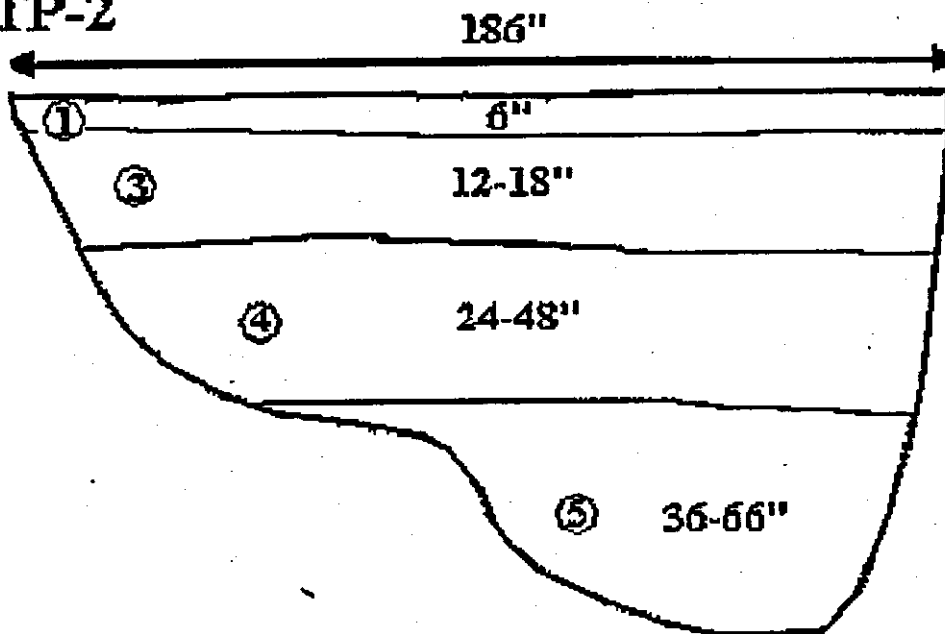
A.2 St. Francis River Bridge Site Test Pits

1. Brown, clayey Silt with roots, moist
2. Gray, Gravel Base course, dry
3. Light brown, silty Clay, very stiff, dry
4. Gray-brown, silty Clay, soft to slightly stiff, moist, rootlets present
5. Light to dark mottled silty Clay, soft to slightly stiff, moist

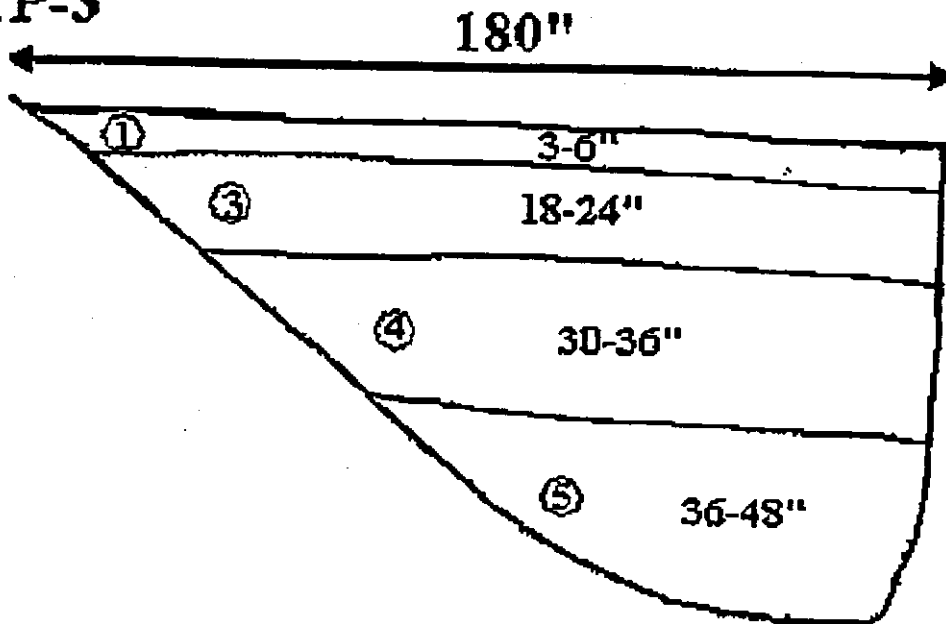
TP-1



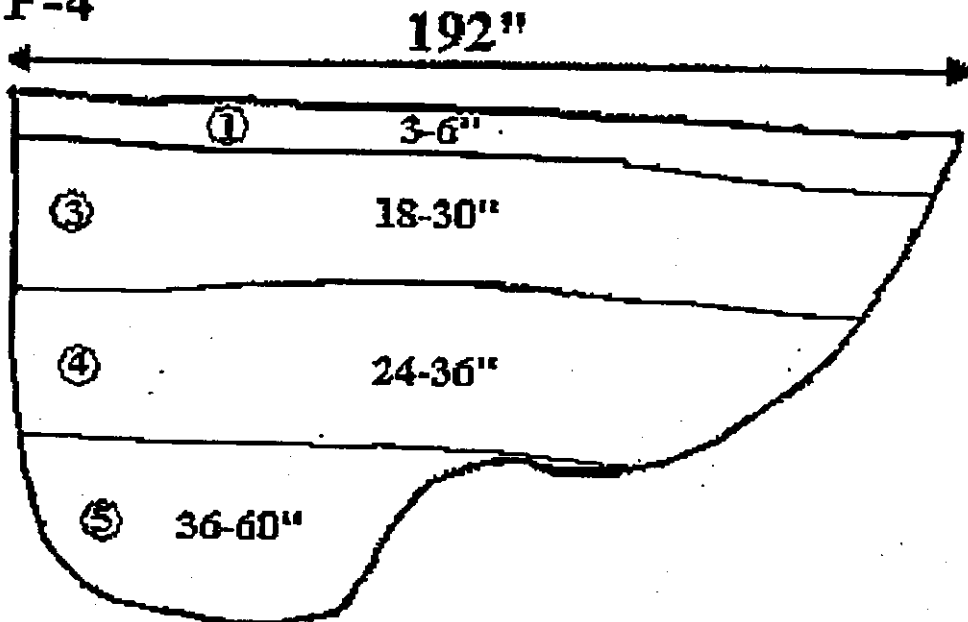
TP-2



TP-3

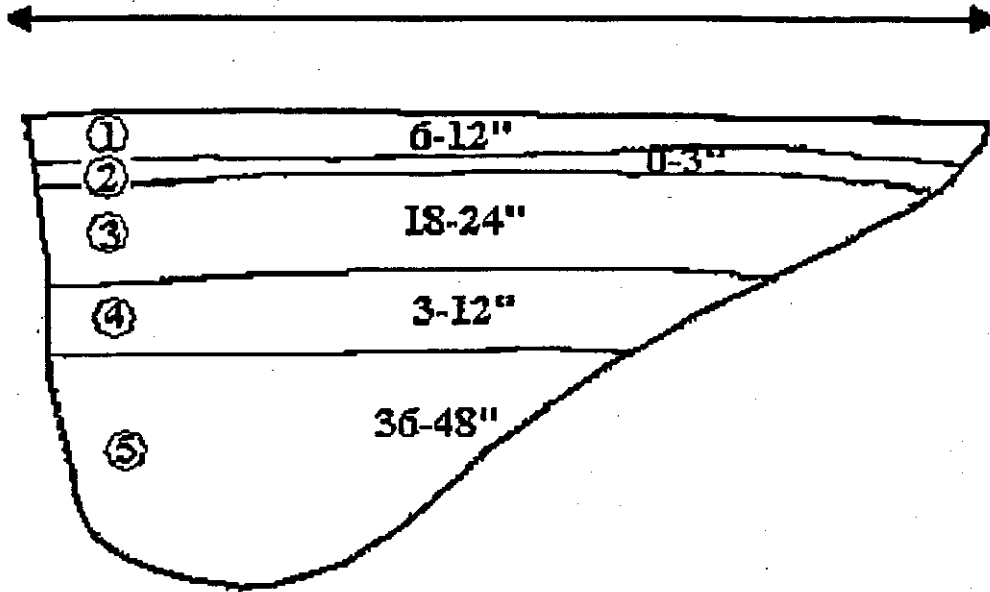


TP-4



TP-5

126"



St. francis river site

A.3 St. Francis River Bridge Site Boring Logs

St. Francis River													
BORING	SAMPLE	UMR	Depth	Description	PP (TSF)	Torvane (TSF)	N <sub>60</sub>	wc(%)	LL/PI	USC	q <sub>u</sub> (PSF)	CYCLIC TX	CU c(psi) †
B-1	473		0.0-1.0	Brn silty CLAY w/ gravel	4.3	0.60		11.3					
	474	*	0.0-1.0	Br. si lean CLAY					31/10				
	pen		1.0-2.5	Brn Silty lean CLAY	4.5		21						
	475		2.5-5.0	Brown silty lean CLAY	9.0	0.60		15.8	31/10	CL			300 32
	476		2.5-5.0	Brown silty lean CLAY	3.5	0.65					6446		
	pen		5.0-6.5	Br, silty lean CLAY	5.0	-	12	17.4					
	477		6.5-8.4	Br,gray mottled si CLAY	1.5	0.55							
	478	*	6.5-8.4	Br, gray mottled si CLAY		1.50		21.4					
	pen		8.4-9.9	Br/gr mottled si CLAY, intermix siltstone	9.0	-	73	19.5					
	479		10.0-12.5	Gray Clayey SILT	8.0	0.70		17.8					
	480		10.0-12.5	Gray Clayey SILT	4.5	0.35					6532		
	pen		12.5-14.0	Gray clayey SILT	1.2	-	10						
	481		14.0-15.5	Gray clayey SILT	3.0	0.40		19.1					
	482	*	14.0-15.5	Gray clayey SILT					29/12	CL		X	
	pen		15.5-17.0	Gray SILT to clayey SILT	2.5	-	19	20.6					
	483		17.0-19.5	Gray SILT to clayey SILT	2.8	0.65		22.5					
	484		17.0-19.5	Gray SILT to clayey SILT	2.8	0.65					2603		
	pen		19.5-21.0	Gray SILT, stiff to v. stiff	3.0	-	17	25.9					
	485		21.0-23.5	Gray SILT v. stiff	4.0	0.45		24.6					
	486	*	21.0-23.5	Gray SILT very stiff									
	pen		23.5-25.0	Gray SILT to 24.5, gray fine SAND	3.3	-	26	23.9					
	487		25.0-27.5	Brown Silty sand, too brittle to wrap									
	489		27.5-29.0	Brown fine grained Sand, dense, wet			28						
	490		35.0-36.5	Brown/gray fine grained Sand, dense, wet			26						
	491		40.0-41.5	Gray fine grained Sand, very dense, wet			75						
	492		45.0-46.5	Gray fine grained Sand, very dense, wet			71						

St. francis river site

St. Francis River													
BORING	SAMPLE	UMR	Depth	Description	PP (TSF)	Torvane (TSF)	N <sub>60</sub>	wc(%)	LL/PI	USC	q <sub>u</sub> (PSF)	CYCLIC TX	CU c(psi) †
	493		50.0-51.5	Gray fine-medium Sand, very dense, wet			75						
	494		55.0-56.5	Gray medium Sand, dense, wet			38						
	495		60.0-61.5	Gray medium Sand, very dense, wet			82						
	496		65.0-66.5	Gray medium Sand, dense			33						
	497		70.0-71.5	Gray medium Sand, dense			40						
	498		75.0-76.5	Gray medium Sand, dense			35						
	499		80.0-81.5	Drk gray fine-med silty sand, dense			38						
	500		90.0-91.5	Gray fine-med Sand, dense, fine gravel			43						
	501		100.0-101.5	Gray med Sand, fine gravel, v. dense			73						
	369		110.0-111.5	Gray med-coarse Sand w/ f. gravel v. dense			72						
	370		120.0-121.5	Gray Coarse Sand w/ m. sand and f. grav.			123						
	371		130.0-131.5	Brownish-gry coarse Sand w/ m. sa and fine grav			56						
			140.0-142.0	Coarse Sand and cobbles									
	372		143.0-144.5	Gray coarse Sand and coarse grav			142						
	373		153.0-157.5	Gray medium Sand, v. dense			91						
	374		163.0-164.5	Gray medium Sand, v. dense			92						
	375		170.0-171.5	Gray medium Sand, v. dense			139						
			180.0-180.2	Cobble									
			190.0-191.5	Cobbles and boulders									
B-2	pen		0.0-2.5	lt grey silty clay	1.8	0.65		17.0					
	346		2.5-4.0	reddish brn mottled CLAY	5.1		10						
	347		4.0-6.5	med. Gray lean CLAY v. stiff	3.8	0.46		20.0					
	348	*	4.0-6.5	Med. gray lean CLAY w/ silt, v. stiff									
	jar		6.5-7.5				6	16.4					
			10.5-12.0	no recovery			16						
	349		12.0-14.5		7.0	0.45		17.9					

St. francis river site

St. Francis River													
BORING	SAMPLE	JMR	Depth	Description	PP (TSF)	Torvane (TSF)	N <sub>60</sub>	wc(%)	LL/PI	USC	q <sub>u</sub> (PSF)	CYCLIC TX	CU c(psi) ↓
	350	*	12.0-14.5	Med. gray lean CLAY w/ silt, v. stiff									380 34
	351		14.7-16.0	lt to brn lean CLAY w/ silt v. stiff	2.0		12						
	bag		16.0-16.6										
	352		16.0-16.6		8.0	0.60							
	353		17.0-19.5	lt tan andy SILT	2.0	0.40							
	354		17.0-19.5	lt tan andy SILT				24.1			1328		
	358	*	21-23.5	Lt. Tan sa SILT stiff to v. stiff				25.5				X	
	359		24.5-25.0	Lt grey SILT			8						
	360		25.0-25.8	missing									
	361		25.8-27.5	lt brn silty SAND	0.5	0.23							
	362		25.8-27.5	lt brn silty SAND									
	363		27.5-28.5	lt brn med. Sand			15						
	364		29.0-31.5	lt. Gray medium Sand			15						
	365		35.0-36.5	lt. Gray medium Sand			18						
	366		40.0-41.5	lt. Gray medium Sand			59						
	367		45.0-46.5	lt. Gray medlum Sand			35						
	368		50.0-51.5	lt. Gray medium Sand			50						
B-3	AL		0.0-1.2	Brn sandy lean CLAY	4.5	0.95		10.9					
	jar		1.2-2.7	brn lean CLAY, v. stiff	4.5		19	15.7					
	42		3.0-5.5	ln Brn CLAY, v. stiff	1.3			23.2					
	43	*	3.0-5.5	ln Brn CLAY, v. stiff									280 35
	jar		5.5-7.0	ln Brn CLAY, v. stiff			6	23.2					
	44		7.0-9.5	ln Brn CLAY, v. stiff	2.8	0.90		23.5					
	45	*	7.0-9.5	Moist SILT									
	46		7.0-9.5	Moist SILT									
	jar		9.5-11.0	Moist SILT	2.5		7	21.9					

St. francis river site

St. Francis River													
BORING	SAMPLE	UMR	Depth	Description	PP (TSF)	Torvane (TSF)	N <sub>60</sub>	wc(%)	LL/PI	USC	q <sub>e</sub> (PSF)	CYCLIC TX	CU c(psi) ↓
	jar		10.5-14.0	Gray Clayey SILT	2.3		9	23.5					
	47		11.0-13.5	Gray Clayey SILT	2.8	0.90							
	48	*	11.0-13.5	Gray clayey SILT								X	
	jar		13.5-15.0	Gray clayey SILT			10						
	jar		14.5-15.0	tan fine SAND			19						
	49		15.0-16.1	gry bm fine SAND									
	50		16.1-17.6	Gray brown f. Sand, loose to med dense			16						
	51		18.0-19.5	Gray brown f. Sand, loose to med dense			9						
	52		19.5-21.0	Gray brown f. Sand, loose to med dense			9						
	53		21.0-22.5	gry-bm to tan f. Sand w/ lean clay			15						
	54		22.5-24.0	gry-bm to tan f. Sand w/ lean clay			24						
	55		24.0-25.5	Gray fine-med Sand			16						
	56		25.5-27.0	Gray fine-med Sand			28						
	57		27.5-28.5	Gray fine-med Sand			28						
	58		28.5-30.0	Gray fine-med Sand			23						
	59		30.0-31.5	Gray fine-med Sand			50						
	60		35.0-36.5	Gray fine-med Sand			56						
	61		40.0-41.5	Gray fine-med Sand			78						
	62		45.0-46.5	Gray fine-med Sand			26						
	63		50.0-51.5	Medium Sand			26						
	64		55.0-56.5	Gray fine-med Sand			41						
	65		60.0-61.5	Gray fine-med Sand			47						
	66		65.0-66.5	Gray fine-med Sand			46						
	67		70.0-71.5	Gray fine-med Sand			41						
	68		75.0-76.5	Gray fine-med Sand			49						
	69		80.0-81.5	Gray fine-med Sand			41						

St. francis river site

St. Francis River													
BORING	SAMPLE	JMR	Depth	Description	PP (TSF)	Torvane (TSF)	N <sub>60</sub>	wc(%)	LL/PI	USC	q <sub>u</sub> (PSF)	CYCLIC TX	CU c(psi) ↓
	70		90.0-91.5	Gray fine to med Sand w/ trace gravel			52						
	71		100.0-101.5	med to coarse Sand w. trace gravel			62						
B-4	80		0.0-2.5	brn lean CLAY w/ sa & grvl	4.5	0.86		12.4					
	81		4.0-6.5	med brown lean CLAY sft to me.	0.8	0.43		27.1					200 30
	82	*	4.0-6.5	Lean CLAY soft to med. stiff									
	jar		6.5-8.0					37.9					
	83		8.0-10.5	Lean CLAY soft to med. stiff									
	84	*	8.0-10.5	v. stiff lean CLAY				23.6	48/25	CL			
	Jar		10.5-12.0	Lean CLAY, v. stiff	2.8		12	23.5	36/15				
	85		10.5-12.0	Lean CLAY, v. stiff			15						
	jar		11.5-12.5	gry, brn lean CLAY, v. stiff and silty									
	86		12.5-14.5	lt brn lean Clay very silty and stiff	2.5	0.54	7	24.2					150 33
	87	*	12.0-14.5	Light brn lean silty CLAY v. stiff									
	88		14.5-16.0	Lt brn clayey SILT, stiff, moist			9?		23/4				
	450	*	16.0-18.5	Lt brn sandy silty CLAY			11	10.6	19/2				
	453	*	20.0-22.5	Br lean silty sandy CLAY				12.6				X	
	456	*	24.0-26.5	Brn gray sandy SILT, med. stiff				23.0					
	459	*	28.0-30.5	Brn gray fine grained				25.3					
	461		35.0-36.5	grey, fine SAND, med			16						
	462		40.0-41.5	Gry fine Sand, v. dense			29						
	463		45.0-46.5	Gr fine SAND v. dense			63						
	464		50.0-51.5	Gr fine SAND, m. dense			23						
	465		55.0-56.5	med SAND			75						
	466		60.0-61.5	med SAND, dense			26						
	467		65.0-66.5	med SAND, dense			55						
	468		70.0-71.5	med SAND, dense			47						

St. francis river site

St. Francis River													
BORING	SAMPLE	UMR	Depth	Description	PP (TSF)	Torvane (TSF)	N <sub>60</sub>	wc(%)	LL/PI	USC	q <sub>u</sub> (PSF)	CYCLIC TX	CU c(psi) †
	469		75.0-76.5	med SAND, dense			47						
	470		80.0-81.5	fine to med SAND, v. dense			85						
	471		90.0-91.5	fine to med SAND, v. dense			55						
	472		100.0-101.5	fine to med SAND, v. dense			45						
B-5	-		0.0-2.5	brn, lean CLAY									
	250		2.5-4.0	brn, lean CLAY			10						
	251		4.0-5.5	brn, lean CLAY									
	253		6.5-8.0	brn, lean CLAY									
	255		8.0-10.5	brn, clayey SILT, m. stiff			7						
	256		10.5-12.0	brn, clayey SILT, m. stiff			5						
	258	*	12.0-14.5	Brn clayey SILT, med. stiff to stiff									
	259		14.0-16.0	Brn clayey SILT, med. stiff to stiff			4						
	260		16.0-18.5	Brn clayey SILT, med. stiff to stiff									
	261		18.5-20.0	br silty fine SAND			4						
	262		20.0-21.5	br silty fine SAND			4						
	263		25.0-26.5	gray fine silty SAND			3						
	264		30.0-31.5	gray fine silty SAND			2						
	265		35.0-36.5	gray fine SAND, dense									
	266		40.0-41.5	gray fine SAND, dense									
	267		45.0-46.5	gray fine SAND, dense			30						
	268		50.0-51.5	gray fine SAND, dense			15						
B-6	10		0.0-2.3	Br, lean CLAY w/ f. Sand									
			2.3-4.8	Gravel									
	13	*	5.0-7.5	Brn clayey SILT, v. stiff									
	14		7.5-10.0	Brn clayey SILT, v. stiff									
	16	*	10.0-12.5	Brn clayey SILT, v. stiff									

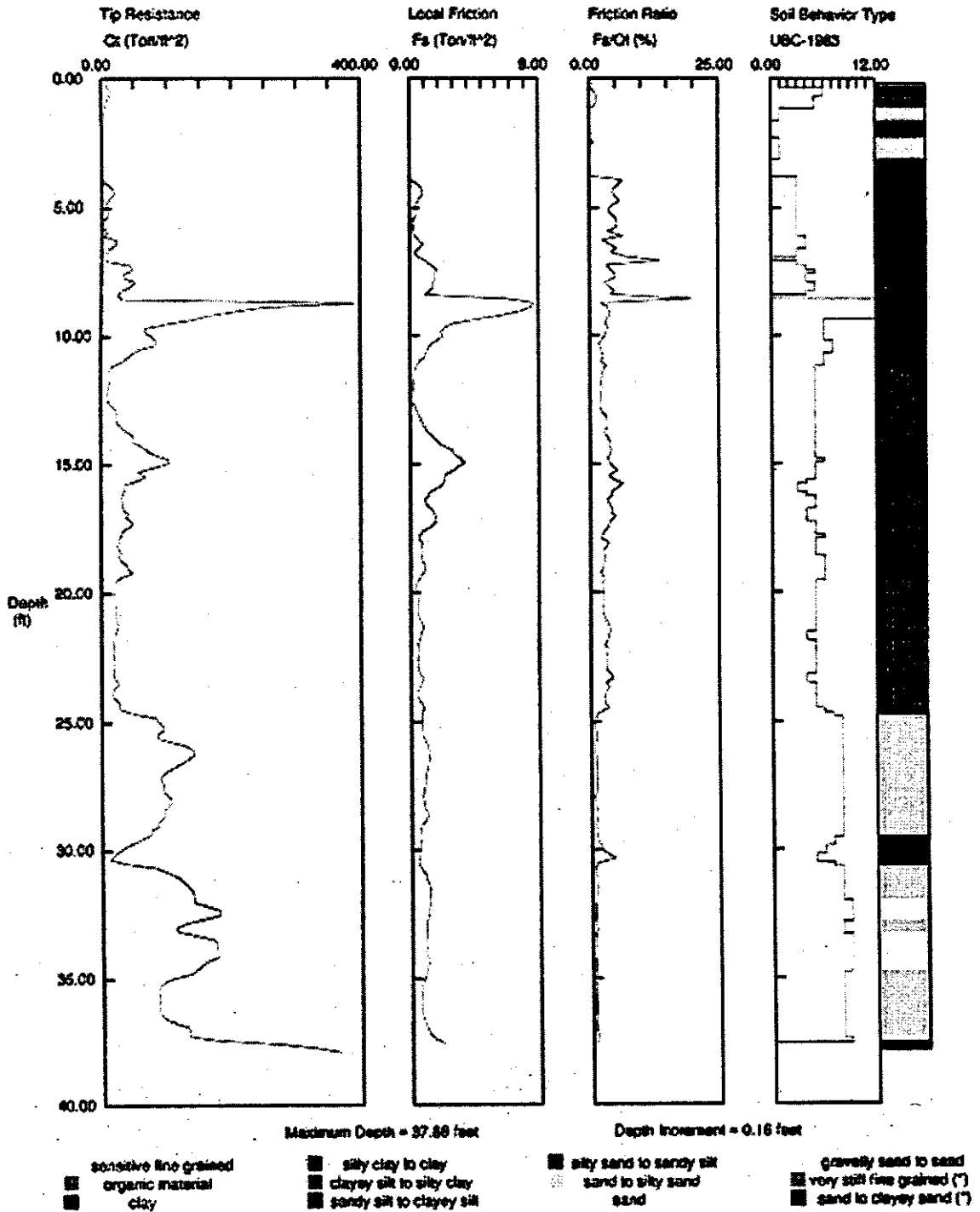
St. francis river site

St. Francis River													
BORING	SAMPLE	JMR	Depth	Description	PP (TSF)	Torvane (TSF)	N <sub>60</sub>	wc(%)	LL/PI	USC	q <sub>u</sub> (PSF)	CYCLIC TX	CU c(psi) $\phi$
	17		12.5-15.0	Bm clayey SILT, v. stiff									
	20	*	15.0-17.5	Bm clayey SILT, v. stiff									
	22		17.5-20.0	Bm silty fine SAND, trace clay									
	23		20.0-21.5	Bm silty fine SAND, trace clay			4						
	24		21.5-23.0	Bm silty fine SAND, trace clay			2						
	25		23.0-24.5	Bm silty fine SAND, trace clay			5						
	26		24.5-26.0	Bm silty fine SAND, trace clay			21						
	27		26.0-27.5	Bm silty fine SAND, trace clay			17						
	28		27.5-29.0	Gray brown fine to med SAND			22						
	29		29.0-30.5	Gray brown fine to med SAND			17						
	30		30.5-32.0	gray fine SAND			14						
	31		35.0-36.5	gray fine SAND			28						
	32		40.0-41.5	gray fine SAND			75						
	33		45.0-46.5	Gray brown fine SAND			75						
	34		50.0-51.5	Gray brown fine SAND			80						

# A.4 St. Francis River Bridge Site Cone Penetrometer Logs MODOT St. Francis River

Operator: KEVIN  
Sounding: #60b11  
Cone Used: 880tc

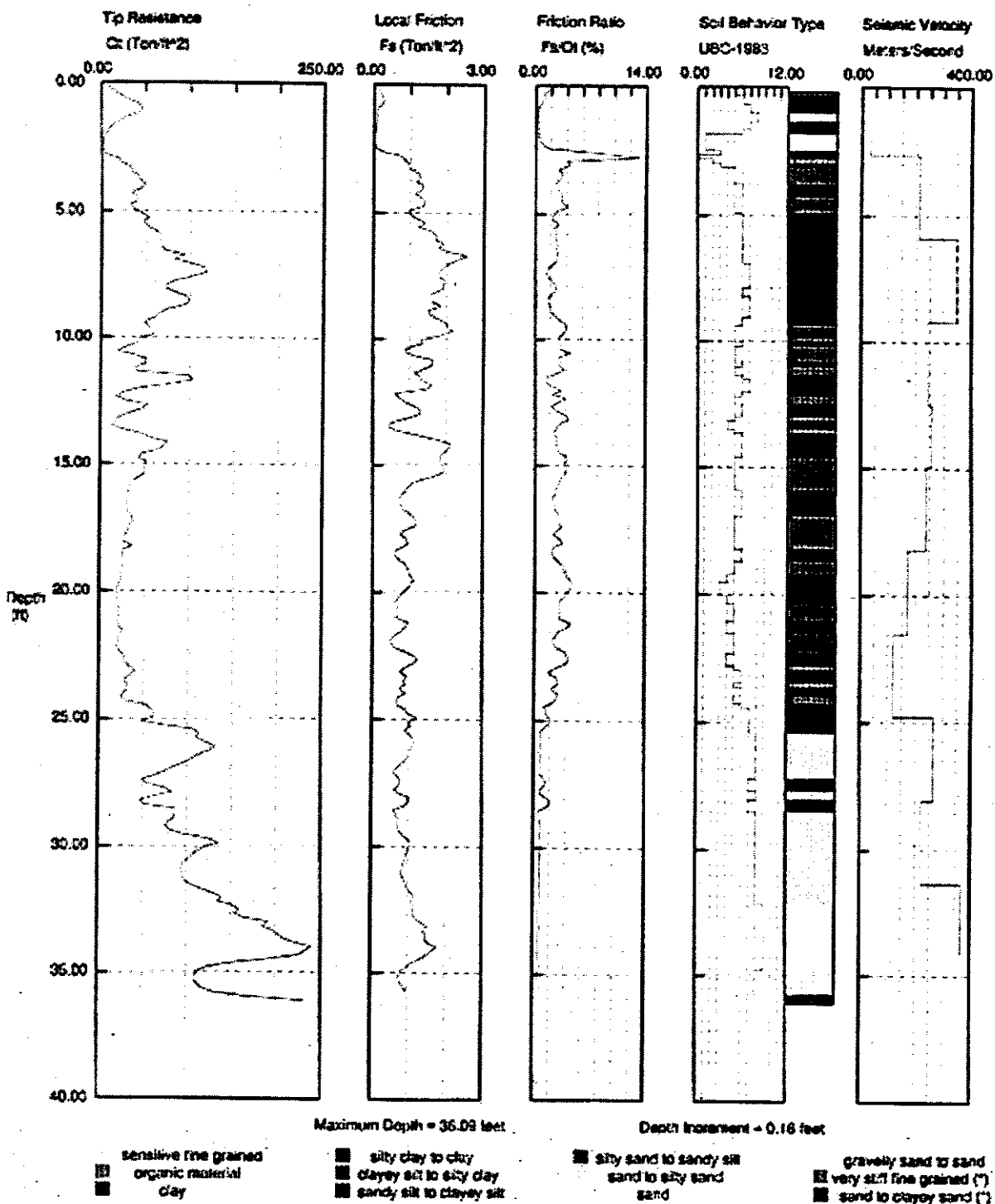
CPT Date: 06-14-99 14:50  
Location: Route 60  
Job No.: spr 98



# MODOT St. Francis River

Operator: KEVIN  
Sounding: r60021  
Cone Used: 880tc

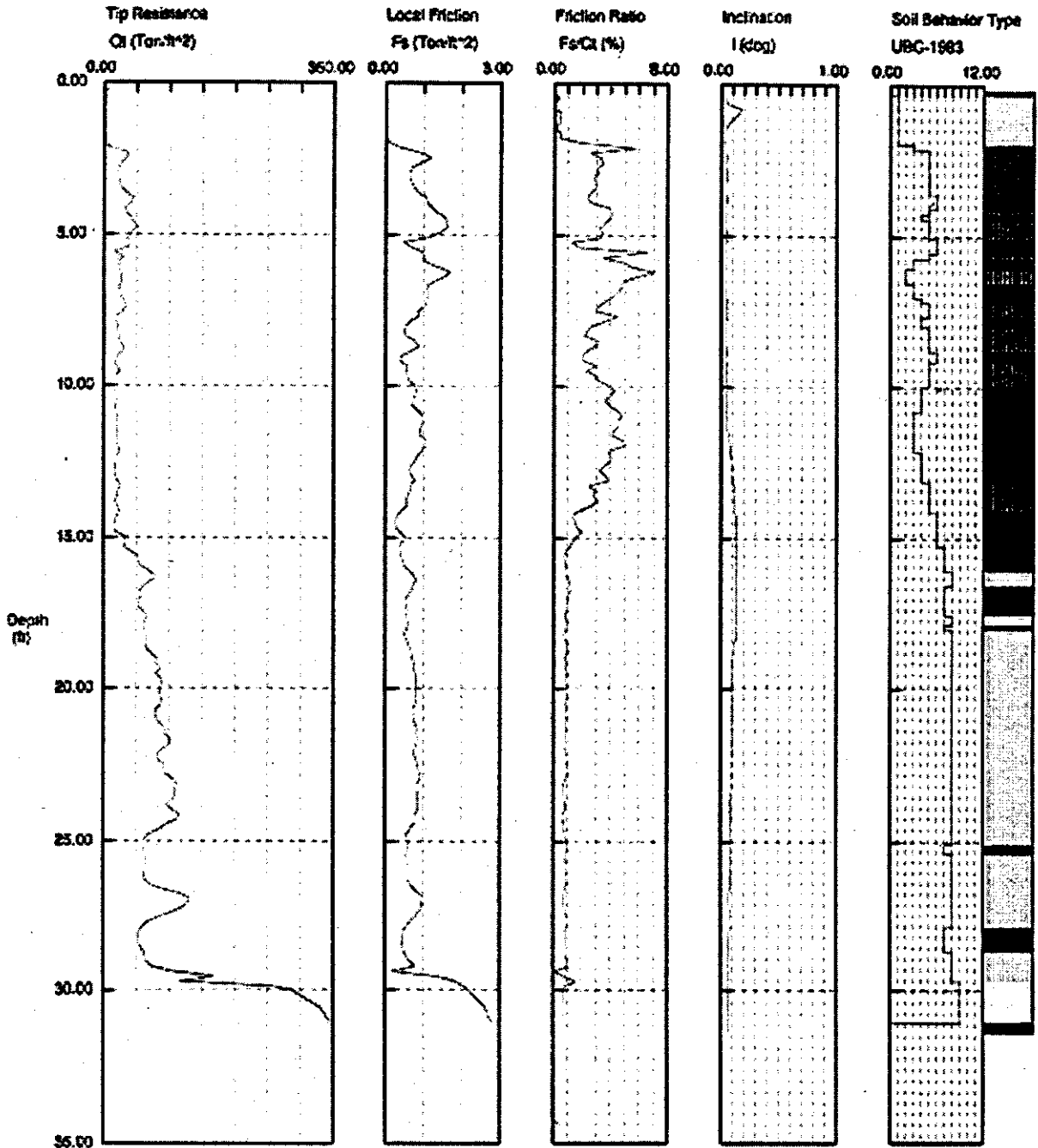
CPT Date: 05-08-99 09:19  
Location: route 60  
Job No.: spr 96



# MODOT St. Francis River

Operator: KEVIN  
 Sounding: r50601  
 Cores Used: 630c

CPT Date: 06-10-98 07:52  
 Location: route 80  
 Job No.: apr 98



Maximum Depth = 31.33 feet

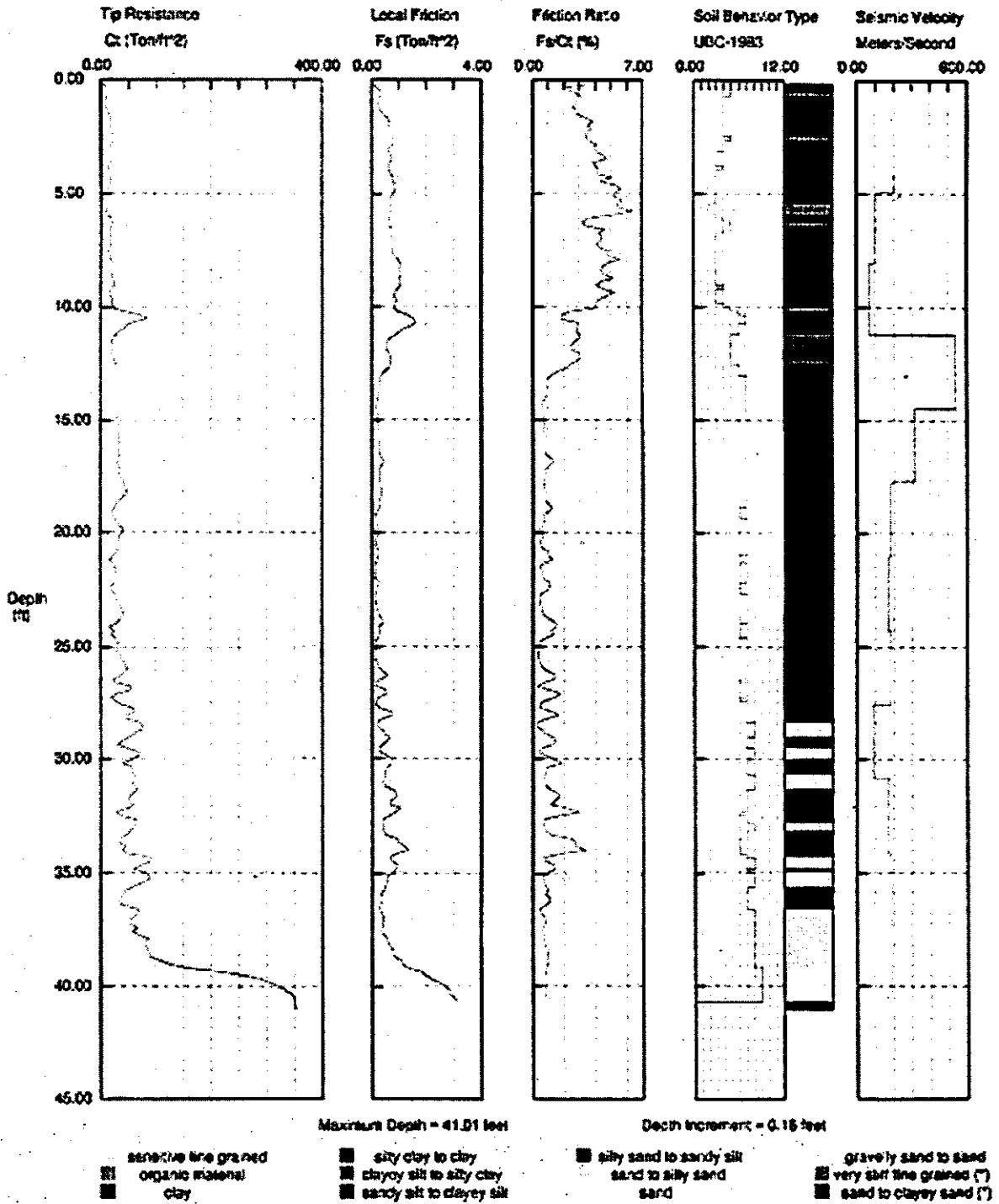
Depth Increment = 0.16 feet

- |  |  |  |   |
|--|--|--|---|
| <ul style="list-style-type: none"> <li>■ sensitive fine grained</li> <li>■ organic material</li> <li>■ clay</li> </ul> | <ul style="list-style-type: none"> <li>■ silty clay to clay</li> <li>■ clayey silt to silty clay</li> <li>■ sandy silt to clayey silt</li> </ul> | <ul style="list-style-type: none"> <li>■ silty sand to sandy silt</li> <li>■ sand to silty sand</li> <li>■ sand</li> </ul> | <ul style="list-style-type: none"> <li>■ gravelly sand to sand</li> <li>■ very stiff fine grained (?)</li> <li>■ sand to clayey sand (?)</li> </ul> |
|--|--|--|---|

# MODOT St. Francis River

Operator: KEVIN  
 Sounding: r60b41  
 Cone Used: 680k

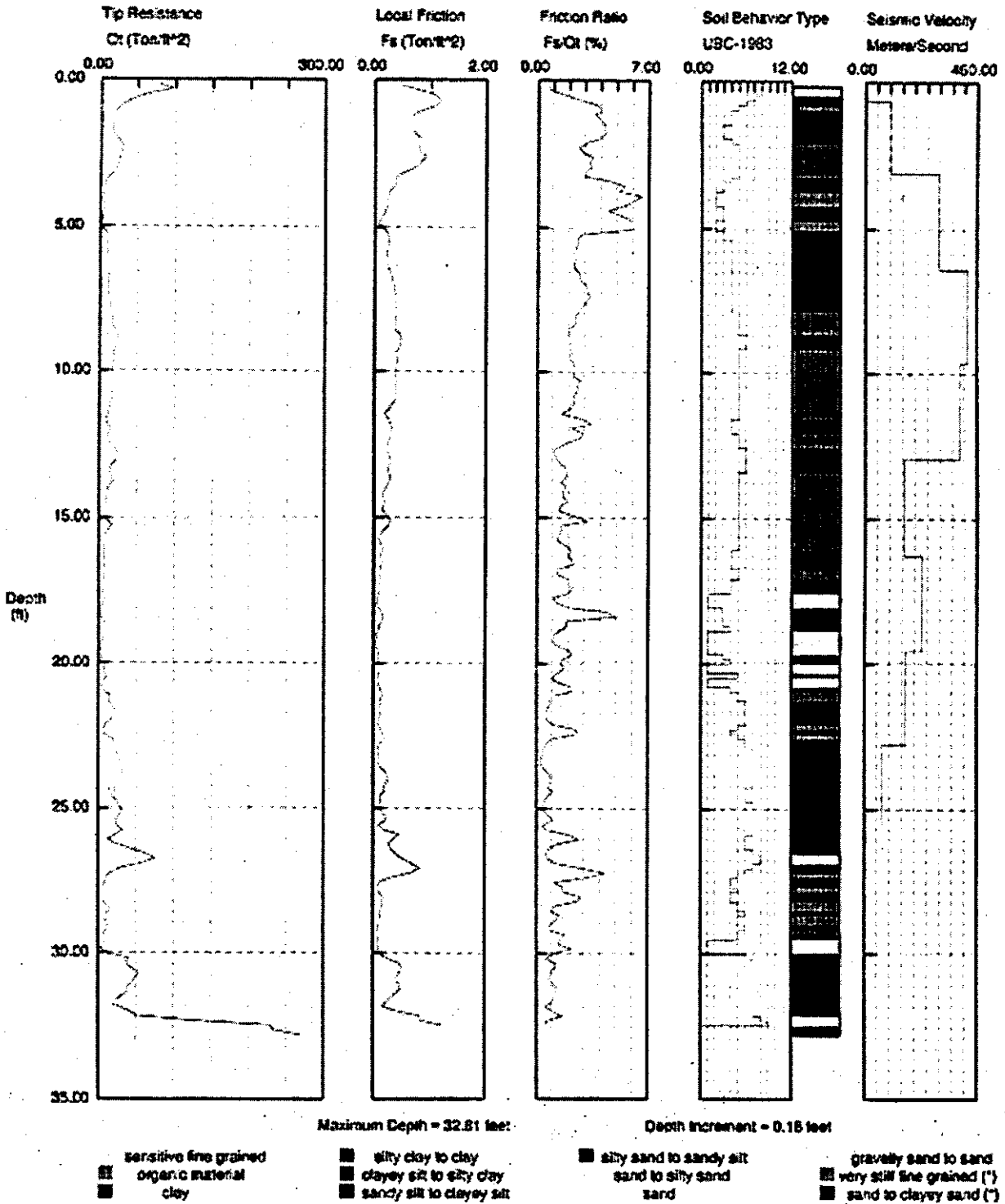
CPT Date: 06-09-99 08:43  
 Location: route 80  
 Job No.: spr 88



# MODOT St. Francis River

Operator: KEVIN  
 Sounding: #60652  
 Cone Used: 630tc

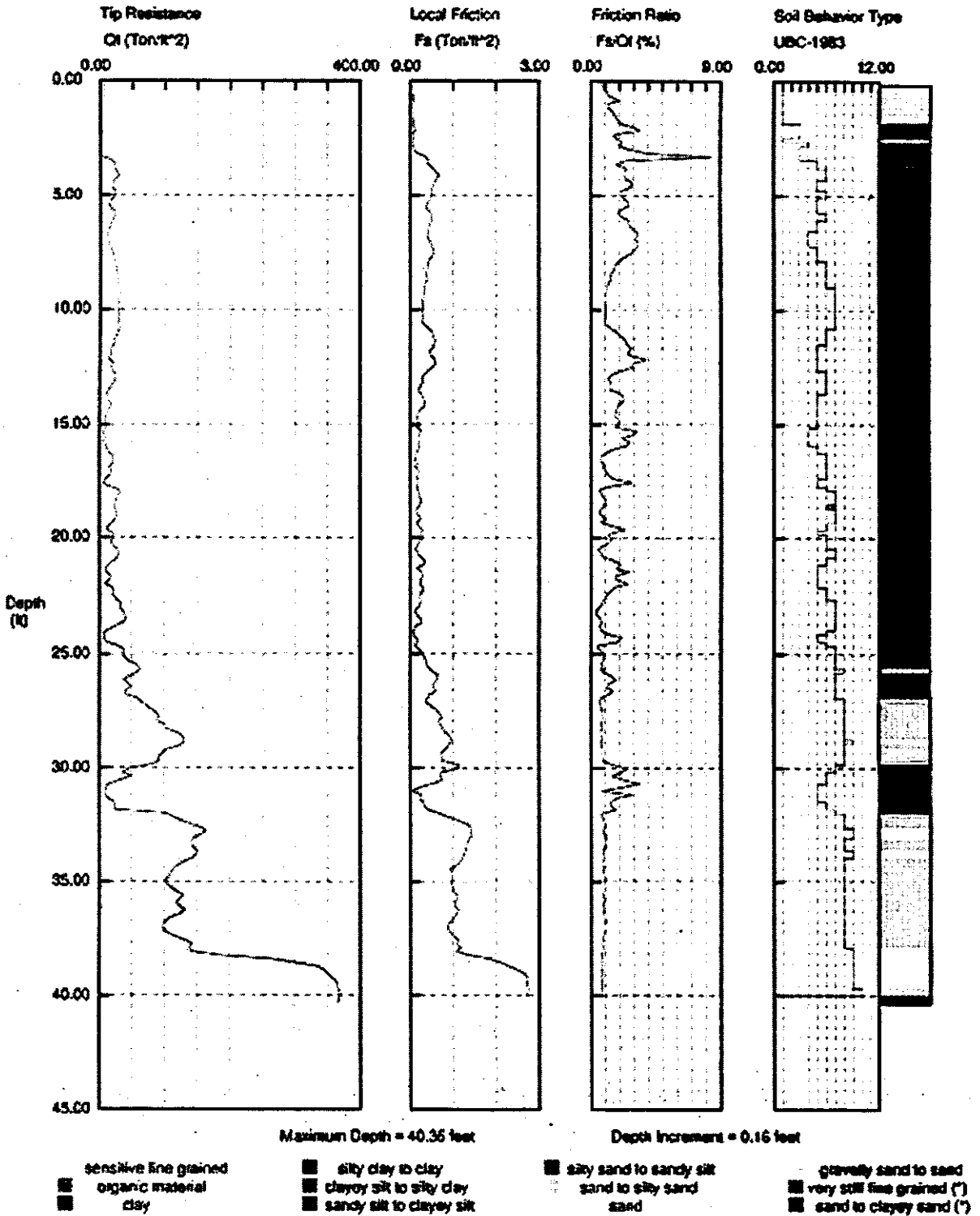
CPT Date: 06-08-99 15:18  
 Location: route 60  
 Job No.: spr 98



# MODOT St. Francis River

Operator: KEVIN  
 Sounding: r50b81  
 Cone Used: 680ic

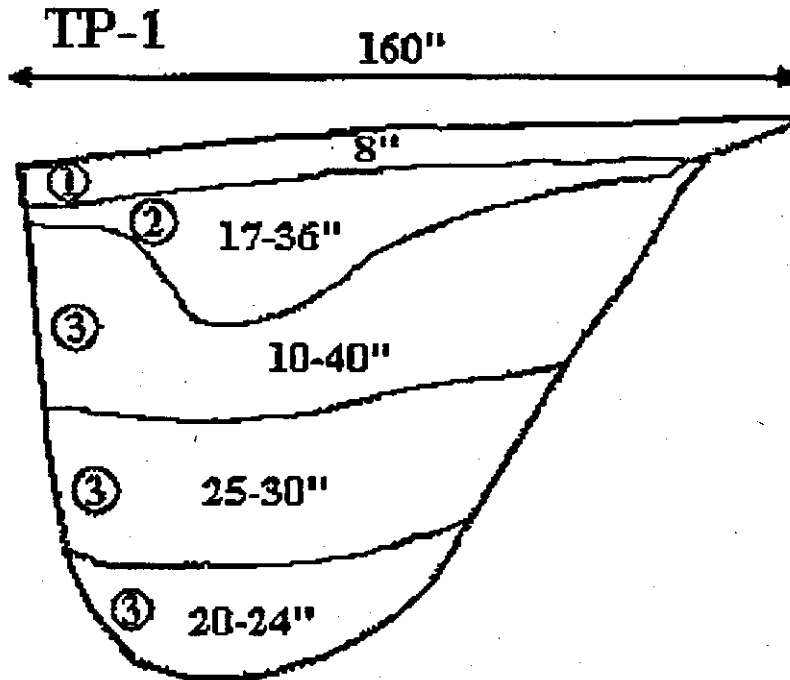
CPT Date: 08-09-99 12:27  
 Location: route 60  
 Job No.: spr 98

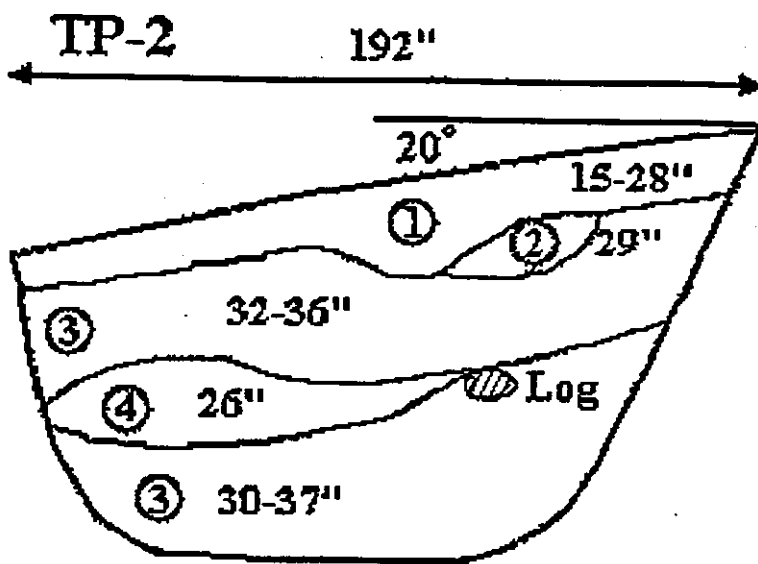


## A.5 Wahite Ditch Bridge Site Test Pits

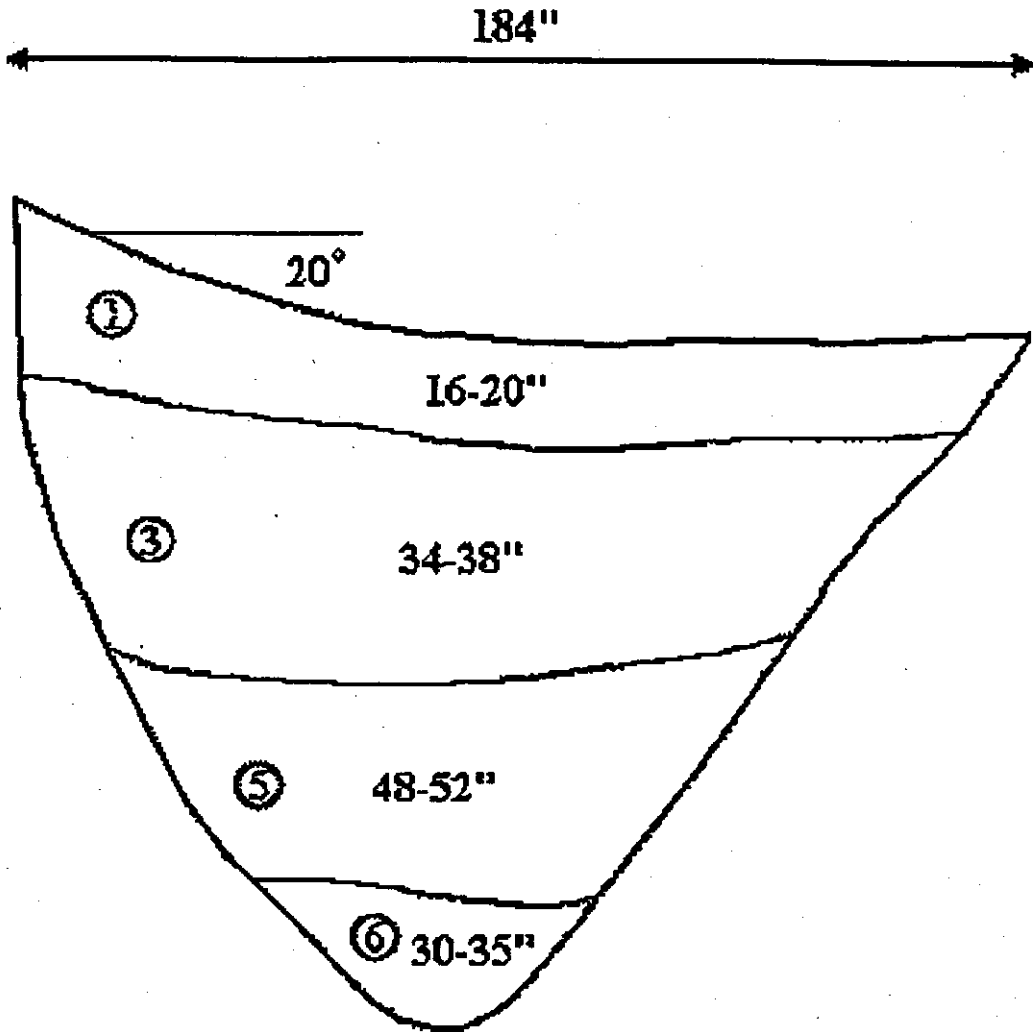
Not To Scale

1. Brown, sandy Gravel, with silt, dry, organics, angular to rounded
2. Brown-tan, medium coarse Sand, sub angular gravel, loose, dry, organics
3. Gray, mottled Clay, very plastic, moist, organics
4. Tan Sand, loose, very moist, rounded
5. Grey sandy Clay, soft, moist
6. Brown-red, clayey Sand, moist, gravel present

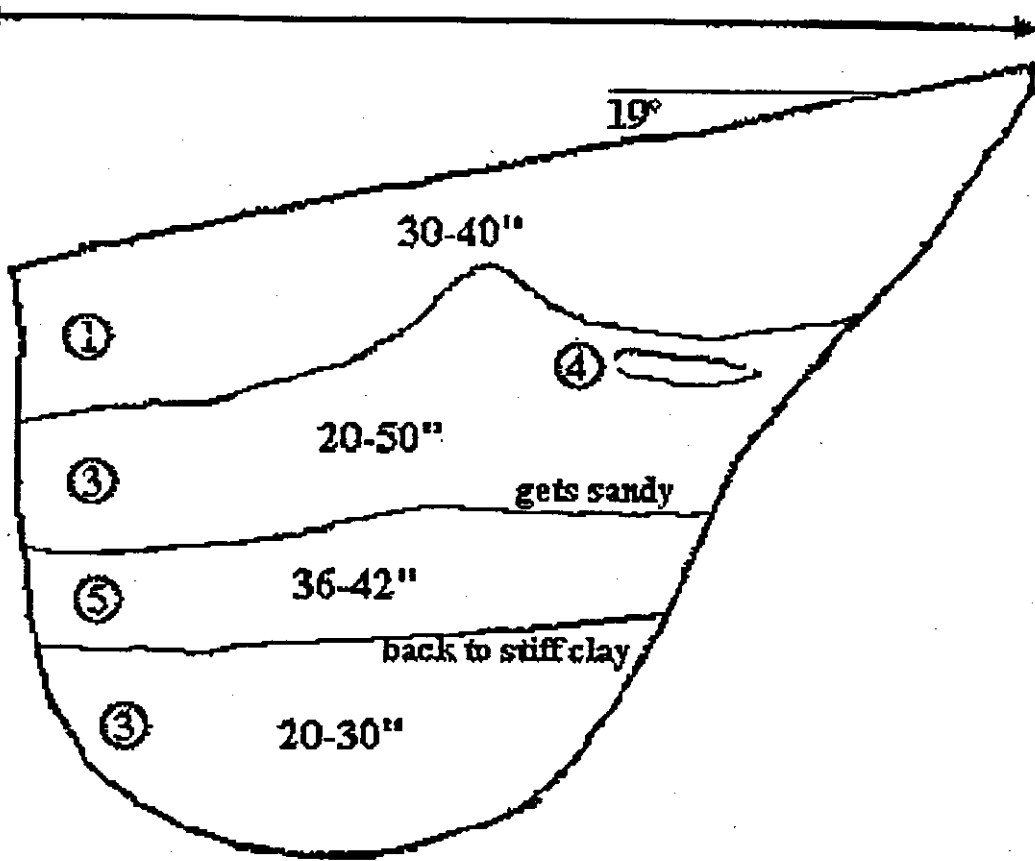




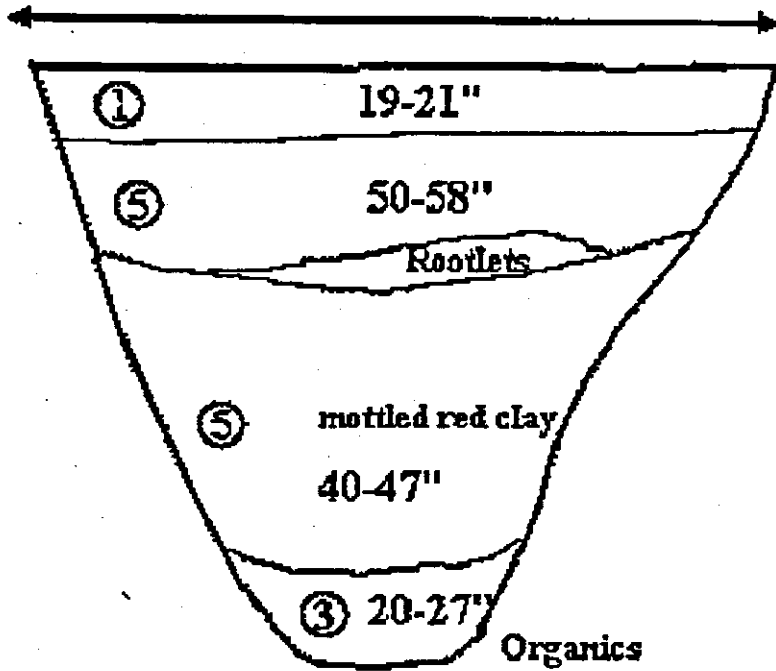
TP-3



TP-4



TP-5



Wahite Ditch Site

A.6 Wahite Ditch Bridge Site Boring Logs

Wahite Ditch													
BORING	SAMPLE	UMR	Depth	Description	PP (TSF)	Torvane (TSF)	N <sub>60</sub>	wc(%)	LL/PI	USC	q <sub>s</sub> (PSF)	CYCLICTX	CU
B-1	743	*	0.0-2.5	Br. gray fat clay with sand	9.0+	0.95		10.1%	51/29	CH			
	744		2.5-5.0	Br. gray fat clay with sand	1.50	0.55		15.4%					
	745		2.5-5.0	Br. gray fat clay with sand	-	-							
	746	*	5.0-7.3	Br. gray fat clay with sand	1.50	0.50		32.2%	33/17	CL			
	747		5.0-7.3	Br. gray fat clay with sand				29.1%			1783		
	748		7.5-10.0	Br. Fat clay with sand, stiff	1.50	0.75		35.6%					
	749		7.5-10.0	Br. Fat clay with sand, stiff									
	750	*	10.0-12.5	Br. Fat clay with sand, stiff	1.25	0.70		32.0%	73/46	CH			
	751		10.0-12.5	Br. Fat clay with sand, stiff				34.7%			1282		
	752		10.0-12.5	Br. Fat clay with sand, stiff									
	753		12.5-15.0	Br. Fat clay with sand, stiff	1.75	0.75		35.0%					
	754		12.5-15.0	Br. Fat clay with sand, stiff									
	755	*	15.0-17.5	Gr. Tan fat clay with sand, stiff	1.00	0.70		30.8%	81/50	CH			
	756		15.0-17.5	Gr. Tan fat clay with sand, stiff				30.6%			2101		
	757		15.0-17.5	Gr. Tan fat clay with sand, stiff									
	758		17.5-20.0	Gr. Tan fat clay with sand, stiff	1.50	0.70		35.1%					
	759		17.5-20.0	Gr. Tan fat clay with sand, stiff									
	760		20.0-21.5	Tan firm to med sand			58						
	761	*	21.5-23.0	Tan firm to med sand			51						
	762		23.0-24.5	Tan firm to med sand			72						
	763		24.5-26.0	Gr. & tan fine to med sand			63						
	764	*	26.0-27.5	Gr. & tan fine to med sand			49						
	765		27.5-29.0	Fine Sand			46						
	766		29.0-30.5	Gr. & tan fine to med sand			65						
	90	*	35.0-36.5	Scattered gravelly layers			66						
	91		40.0-41.5	Scattered gravelly layers			73						
	92		45.0-46.5	coarse sand			47						
	93	*	50.0-51.5	coarse sand			46						
	94		55.0-56.5	coarse sand			39						
	95	*	60.0-61.5	gravelly @ 62			38						
	96		65.0-66.5	Gr. & Tan medium sand			54						
	97	*	70.0-71.5	Gr. & Tan medium sand			51						

A24

White Ditch Site

White Ditch																							
BORING	SAMPLE	UMR	Depth	Description	PP (TSF)	Torvane (TSF)	N <sub>60</sub>	wc(%)	LL/PI	USC	q <sub>s</sub> (PSF)	CYCLICTX	CU										
	98		75.0-76.5	Gr. & Tan medium sand			54																
	99	*	80.0-81.5	Gr. & Tan medium sand			51																
	100		90.0-91.5	Gr. & Tan medium sand			51																
	101	*	100.0-101.5	Gr. & Tan medium sand			52																
	102		110.0-111.5	cobbles & Gravel @ 108			73																
	103	*	120.0-121.5	Tan fine to coarse sand with trace silt			24																
	104		130.0-131.5	Tan fine to coarse sand with trace silt			29																
	105		140.0-141.5	Tan fine to coarse sand with trace silt			61																
	106	*	150.0-151.5	cobbles & gravel @ 148.6			74																
	107		160.0-161.5	Tan fine to coarse sand with trace silt			56																
	108		170.0-171.5	Lt gr. and tan fine sand			82																
	109	*	180.0-181.5	Lt gr. and tan fine sand			96																
	110		190.0-191.5	Lt gr. and tan fine sand			82		38/22	CL													
	111	*	200.0-201.5	Gr. Lean clay with sand					42/19	CL													
	112		200.0-201.5	200-201.5 gr brown fat clay																			
B-2	680		2.5-5.0	Gray br fat clay	4.50	0.95																	
	681	*	5.0-7.5	Gray br fat clay	2.00	0.50			53/33	CH													
	682		7.5-10.0	Gray br fat clay	1.50	0.80																	
	683		7.5-10.0	Gray br fat clay																			
	684	*	10.0-12.5	Gray br fat clay	1.25	0.65			57/35	CH													
	685	*	12.5-15.0	Bluish grey fat clay with sand in lenses	1.25	0.70			75/46	CH													
	686		12.5-15.0	Bluish grey fat clay with sand in lenses																			
	687		15.2-17.5	Gray to tan fat clay with sand	1.50	0.65																	
	688		15.2-17.5	Gray to tan fat clay with sand				35.2%			1807												
	689	*	17.5-19.5	Gray to tan fat clay with sand	1.25	0.65			79/50	CH													
	690	*	20.0-20.7	Tan fine to med sand																			
	691		20.7-22.20	Tan fine to med sand			52																
	692		22.0-23.5	Tan fine to med sand			56																
	693		23.5-25.0	Tan fine to med sand			52																
	694		25.0-26.5	tan and light grey fine to med sand			39																
	695		26.5-28.0	tan and light grey fine to med sand			42																
	696		28.0-29.5	tan and light grey fine to med sand			49																

A25

Wahite Ditch Site

Wahite Ditch													
BORING	SAMPLE	UMR	Depth	Description	PP (TSF)	Torvane (TSF)	N <sub>60</sub>	wc(%)	LL/PI	USC	q <sub>c</sub> (PSF)	CYCLIC TX	CU
	697	*	29.5-31	tan and light grey fine to med sand			53						
	698		35.0-36.5	tan and light grey fine to med sand			57						
	699	*	40.0-41.5	tan and light grey fine to med sand									
	700		45.0-46.5	tan and light grey fine to med sand			52						
	701	*	50.0-51.5	tan and light grey fine to med sand			60						
	702		60.0-61.5	tan and light grey fine to med sand			82						
	703	*	65.0-66.5	tan and light grey fine to med sand			56						
	704		70.0-71.5	tan and light grey fine to med sand			108						
	705	*	75.0-76.5	tan and light grey fine to med sand			96						
	706		80.0-81.5	tan and light grey fine to med sand			75						
	707		90.0-91.5	tan and light grey fine to med sand			39						
	708	*	100.0-101.5	tan and light grey fine to med sand			73						
B-3	-		0.0-2.9	Tan sand with scattered gravel									
	591	*	2.90-4.0	Grey lt br. fat clay	2.75	0.95		23.4%					
	592	*	8.5-10.0	Grey fat clay stiff	1.50	0.70		37.3%					
	593		8.5-10.0	Grey fat clay stiff									
	594		10.0-12.3	Grey fat clay stiff				32.6%					
	595	*	14.1-15.0	Bluish grey fat clay, stiff	1.50	0.75		33.1%					
	596		14.1-15.0	Bluish grey fat clay, stiff									
	597	*	17.5-19.0	Bluish grey fat clay, stiff	1.50	0.70		32.3%	73/53	CH			
	598	*	22.5-242.0	tan medium sand			53						
	599		24.0-25.5	tan medium sand			61						
	600	*	25.5-27.0	tan medium sand			42						
	601		27.0-28.5	tan medium sand			45						
	602	*	28.5-30.0	tan medium sand			42						
	603		30.0-31.5	tan medium sand			53						
	604		35.0-36.5	tan medium sand			54						
	605	*	40.0-41.5	tan medium sand			51						
	606	*	45.0-46.5	tan medium sand			53						
	607		50.0-51.5	tan medium sand			36						
B-4	608	*	2.5-5.0	Drk Brown fat clay	10+	0.95		13.8%	39/22	CL			

A26

Wahite Ditch Site

Wahite Ditch														
BORING	SAMPLE	UMR	Depth	Description	PP (TSF)	Torvane (TSF)	N <sub>60</sub>	wc(%)	LL/PI	USC	q <sub>s</sub> (PSF)	CYCLICTX	CU	
	609		2.5-5.0	Drk Brown fat clay										
	610		5.0-5.7	Drk Brown fat clay	4.00	0.90		24.0%						
	611		5.0-5.7	Drk Brown fat clay	1.00	0.60								
	614	*	7.5-10.0	bluish gray fat clay	0.75	0.50		19.1%	33/17	CL				
	615		7.5-10.0	bluish gray fat clay										
	616		10.0-11.9	bluish gray fat clay	1.00	0.50		21.2%						
	617		10.0-11.9	bluish gray fat clay				22.9%			966			
	618	*	11.9-12.5	Drk gray fat clay	1.50	0.70		23.3%	45/21	CL				
	619	*	12.5-14.9	Bluish gray fat clay	1.25	0.55		21.7%	52/35	CH				
	620		12.5-14.9	Bluish gray fat clay										
	621	*	15.0-17.5	Gray fat clay	1.50	0.75		25.0%	59/37	CH				
	622		15.0-17.5	Gray fat clay										
	623		15.0-17.5	Gray fat clay										
	624	*	17.5-19.4	Gray fat clay	1.25			21.6%	46/27	CL				
	625		17.5-19.4	Gray fat clay										
	626	*	19.5-21.0	Tan fine to med sand			24							
	627		21.0-22.5	Tan fine to med sand			26							
	628		22.5-242.0	Tan fine to med sand			46							
	629		24.0-25.5	Tan fine to med sand			39							
	630	*	25.5-27.0	Tan fine to med sand			35							
	631		27.0-28.5	Tan fine to med sand			39							
	632		28.5-30.0	Tan fine to med sand			39							
	633		30.0-31.5	Tan fine to med sand			38							
	634	*	35.0-36.5	Tan fine to med sand			43							
	635		40.0-41.5	Tan fine to med sand			42							
	636		45.0-46.5	Tan fine to med sand			56							
	637	*	50.0-51.5	Tan fine to med sand			42							
<b>B-5</b>	709	*	2.5-5.0	Gray & brown to tan fat clay	8.00	0.95		20.6%	55/31	CH				
	710		2.5-5.0	Gray & brown to tan fat clay										
	711		5.0-7.5	Gray & brown to tan fat clay	2.00	0.90		26.1%						
	712		5.0-7.5	Gray & brown to tan fat clay				21.3%			1747			

A27

Wahite Ditch Site

Wahite Ditch													
BORING	SAMPLE	UMR	Depth	Description	PP (TSF)	Torvane (TSF)	N <sub>60</sub>	wc(%)	LL/PI	USC	q <sub>u</sub> (PSF)	CYCLIC TX	CU
	713	*	7.5-10.0	Gray & brown to tan fat clay	1.75	0.60		30.9%	63/38	CH			
	714		7.5-10.0	Gray & brown to tan fat clay									
	715		7.5-10.0	Gray & brown to tan fat clay									
	716		10.8-12.5	bluish gray fat clay	1.25	0.45		40.0%					
	717		10.8-12.5	bluish gray fat clay									
	718	*	12.5-13.4	bluish gray fat clay	1.50	0.70		30.6%	69/41	CH			
	719		12.5-13.4	bluish gray fat clay									
	720	*	15.0-17.5	Gray and tan fat clay	1.75	0.75		22.1%	60/39	CH			
	721		15.0-17.5	Gray and tan fat clay				27.1%			1157		
	722		15.0-17.5	Gray and tan fat clay									
	723		17.5-18.1	Gray and tan fat clay	1.50	0.70		22.5%					
	724	*	20.0-212.5	Tan fine to med sand			53						
	725		21.5-23.0	Tan fine to med sand			56						
	726		23.0-24.4	Tan fine to med sand			55						
	727	*	24.5-26.0	Tan and gray fine to med sand			48						
	728		26.0-27.5	Tan and gray fine to med sand			44						
	729		27.5-29.0	Tan and gray fine to med sand			48						
	730	*	29.0-30.5	Tan and gray fine to med sand			58						
	731		35.0-36.5	Tan and gray fine to med sand			62						
	732		40.0-41.5	Tan and gray fine to med sand			41						
	733	*	45.0-46.5	Tan and gray fine to med sand			46						
	734		50.0-51.5	Tan and gray fine to med sand			41						
	735	*	55.0-56.5	Tan and gray fine to med sand			68						
	736		60.0-61.5	Tan and gray fine to med sand			51						
	737		65.0-66.5	Tan and gray fine to med sand			54						
	738		70.0-71.5	Tan and gray fine to med sand			51						
	739	*	75.0-76.5	Tan and gray fine to med sand			80						
	740		80.0-81.5	Tan and gray fine to med sand			60						
	741	*	90.0-91.5	Tan and gray fine to med sand			43						
	742		100.0-101.5	Tan and gray fine to med sand			71						
B-6	638	*	2.5-5.0	Drk Brown Fat clay	7.00	0.95		17.8%	49/27	CL			

A28

White Ditch Site

White Ditch													
BORING	SAMPLE	UMR	Depth	Description	PP (TSF)	Torvane (TSF)	N <sub>60</sub>	wc(%)	LL/PI	USC	q <sub>s</sub> (PSF)	CYCLIC TX	CU
	639		2.5-5.0	Drk Brown Fat clay									
	640		5.0-7.5	Drk Brown Fat clay	2.50	0.85		24.5%					
	641	*	7.5-10.0	Drk Brown Fat clay	2.50	0.90		19.8%	35/19	CL			
	642		7.5-10.0	Drk Brown Fat clay									
	643	*	10.4-11.3	Gray Fat Clay	2.00	0.70		28.2%	64/40	CH			
	644	*	12.5-14.8	Bluish gray fat clay	1.50	0.75		22.2%	49/30	CL			
	645		12.5-14.8	Bluish gray fat clay									
	646	*	15.0-17.3	Gray and tan fat clay	2.00	0.80		21.5%	51/34	CH			
	647		15.0-17.3	Gray and tan fat clay				20.5%			2883		
	648		15.0-17.3	Gray and tan fat clay									
	649	*	17.5-20.0	Gray clayey sand	2.00	0.35		16.0%	34/17	CL			
	650		20.0-20.4	Gray clayey sand									
	651	*	20.0-21.5	Tan fine to med sand			27						
	652	*	21.5-23.0	Tan fine to med sand			34						
	653		23.0-24.5	Tan fine to med sand			38						
	654	*	24.5-26.0	Tan fine to med sand			42						
	655		26.0-27.5	Tan fine to med sand			39						
	656		27.5-29.0	Tan fine to med sand			48						
	657	*	29.0-30.5	Tan fine to med sand			39						
	658	*	35.0-36.5	Tan fine to med sand			58						
	659		40.0-41.5	Tan fine to med sand			58						
	660	*	45.0-46.5	Tan fine to med sand			58						
	661		50.0-51.5	Tan fine to med sand			30						

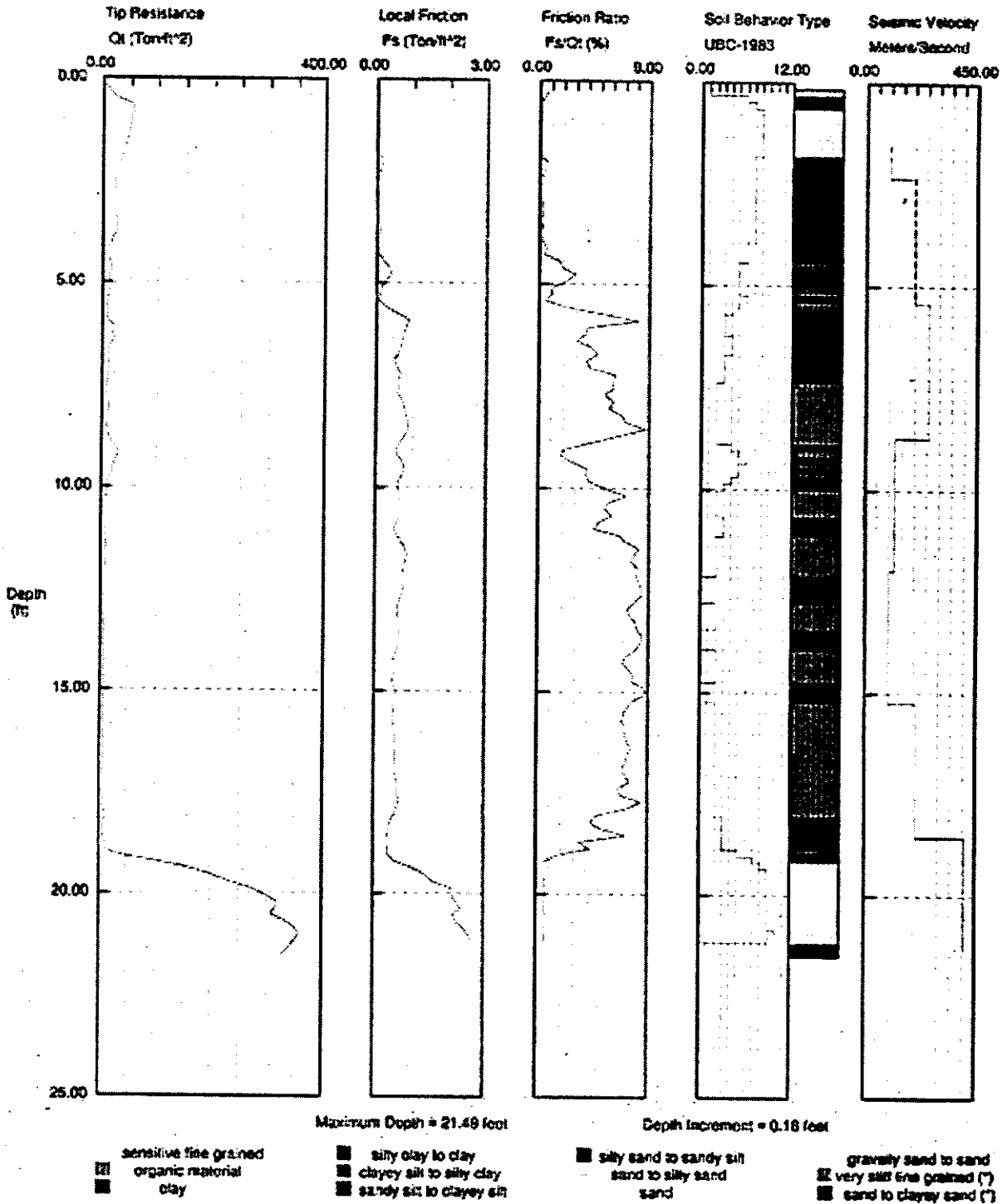
A29

# A.7 Wahite Ditch Bridge Site Cone Penetrometer Logs

## MODOT Wahite Ditch

Operator: SHERI  
 Sounding: r60c11  
 Cone Used: 66Cz

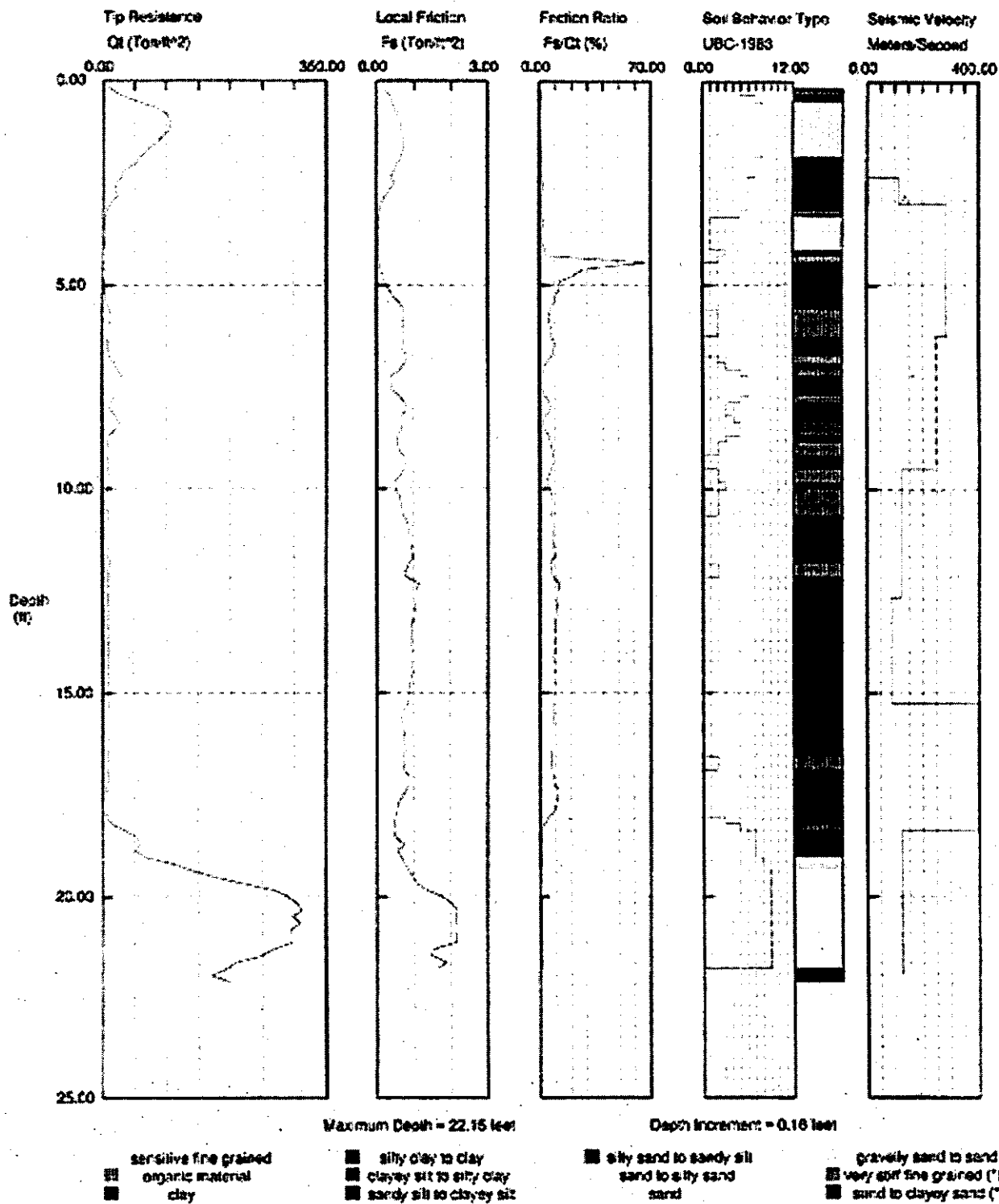
CPT Date: 08-31-99 14:14  
 Location: route 60  
 Job No.: spr 99



# MODOT Wahite Ditch

Operator: KEVIN  
 Sounding: r60c21  
 Cone Used: 600tc

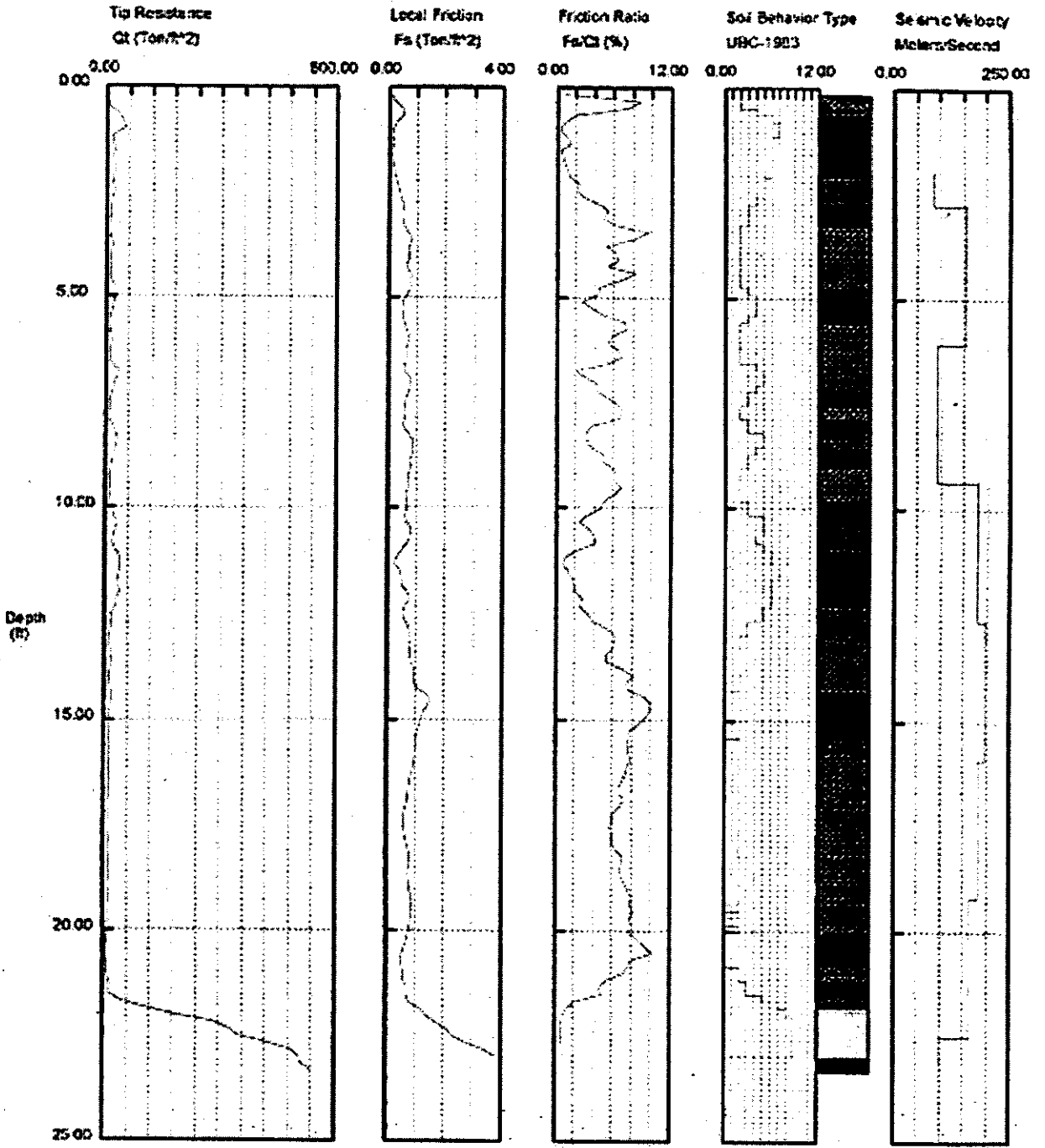
CPT Date: 09-31-99 10:35  
 Location: route 60  
 Job No.: sar 99



# MODOT C3 Wahite Ditch

Operator: paul  
 Seaming: 160c33  
 Cone Used: 850lc

CPT Date: 09-01-99 13:36  
 Location: route 80  
 Job No: apr93



Maximum Depth = 23.29 feet

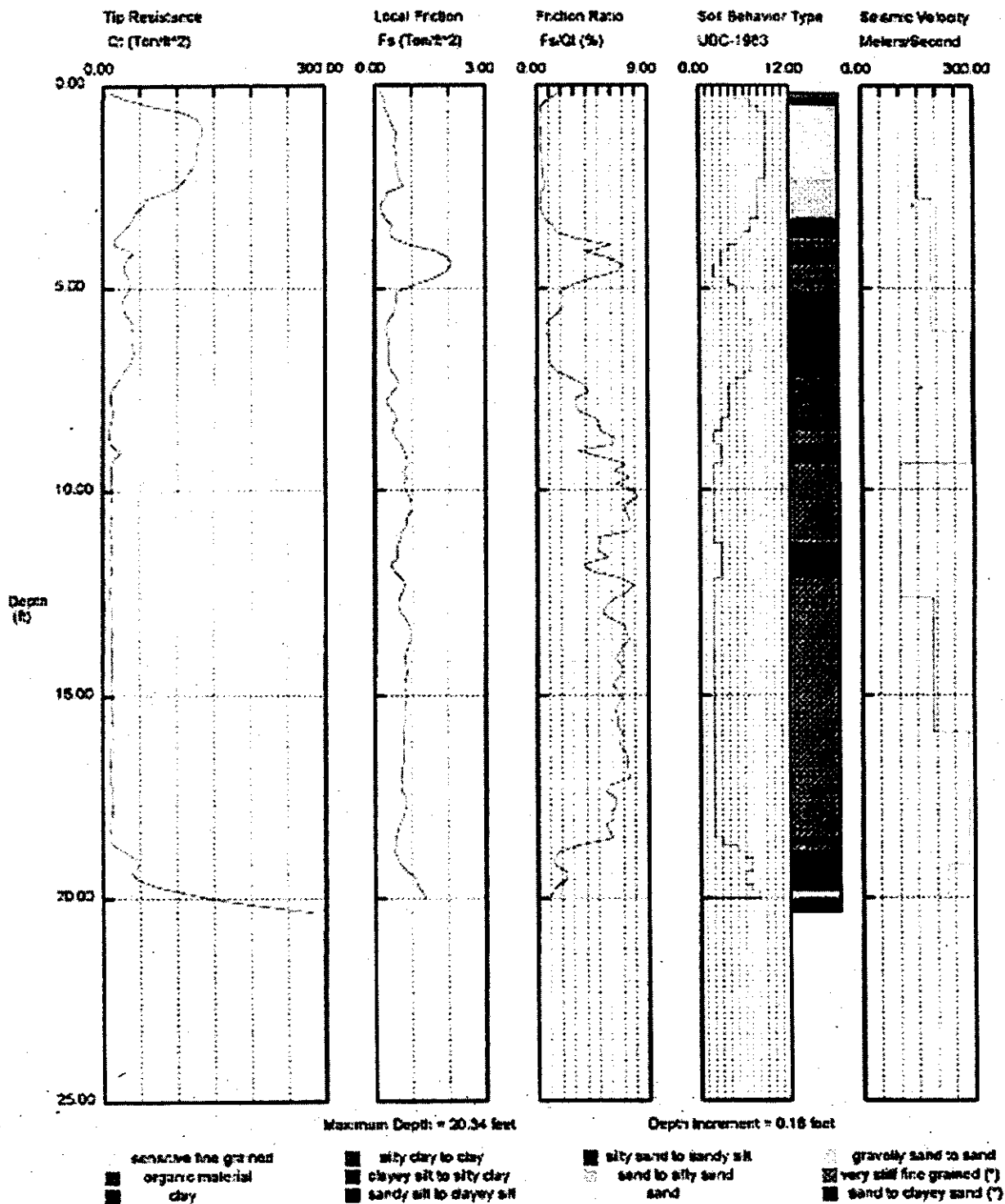
Depth Increment = 0.16 feet

- |  |  |  |   |
|--|--|--|---|
| <ul style="list-style-type: none"> <li>○ sensitive fine grained</li> <li>■ organic material</li> <li>■ clay</li> </ul> | <ul style="list-style-type: none"> <li>■ silty clay to clay</li> <li>■ clayey silt to silty clay</li> <li>■ sandy silt to clayey silt</li> </ul> | <ul style="list-style-type: none"> <li>■ silty sand to sandy silt</li> <li>○ sand to silty sand</li> <li>■ sand</li> </ul> | <ul style="list-style-type: none"> <li>○ gravelly sand to sand</li> <li>■ very stiff fine grained (*)</li> <li>■ sand to clayey sand (*)</li> </ul> |
|--|--|--|---|

# MODOT C4 Wahite Ditch

Operator: SHERI  
 Seunarg: r6C041  
 Cone Used: 5201c

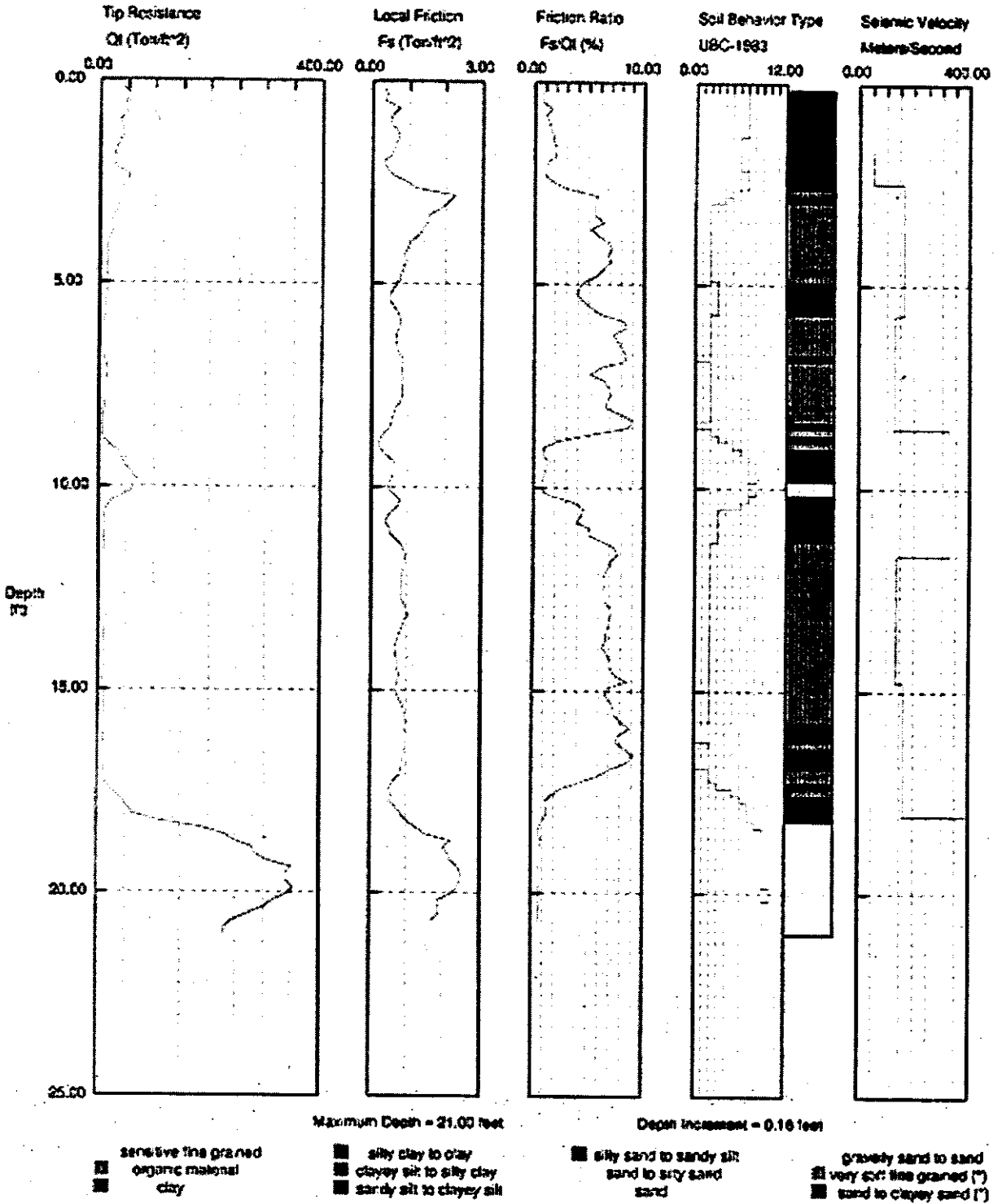
CPT Date: 09-02-99 08:52  
 Location: route 60  
 Job No.: spr 98



# MODOT Wahite Ditch

Operator: paul  
 Sounding: r60c61  
 Cone Used: 690ic

CPT Date: 09-01-99 15:27  
 Location: route 83  
 Job No.: spr 99



## B. LABORATORY DATA

### B.1 Cyclic Stress Test Results

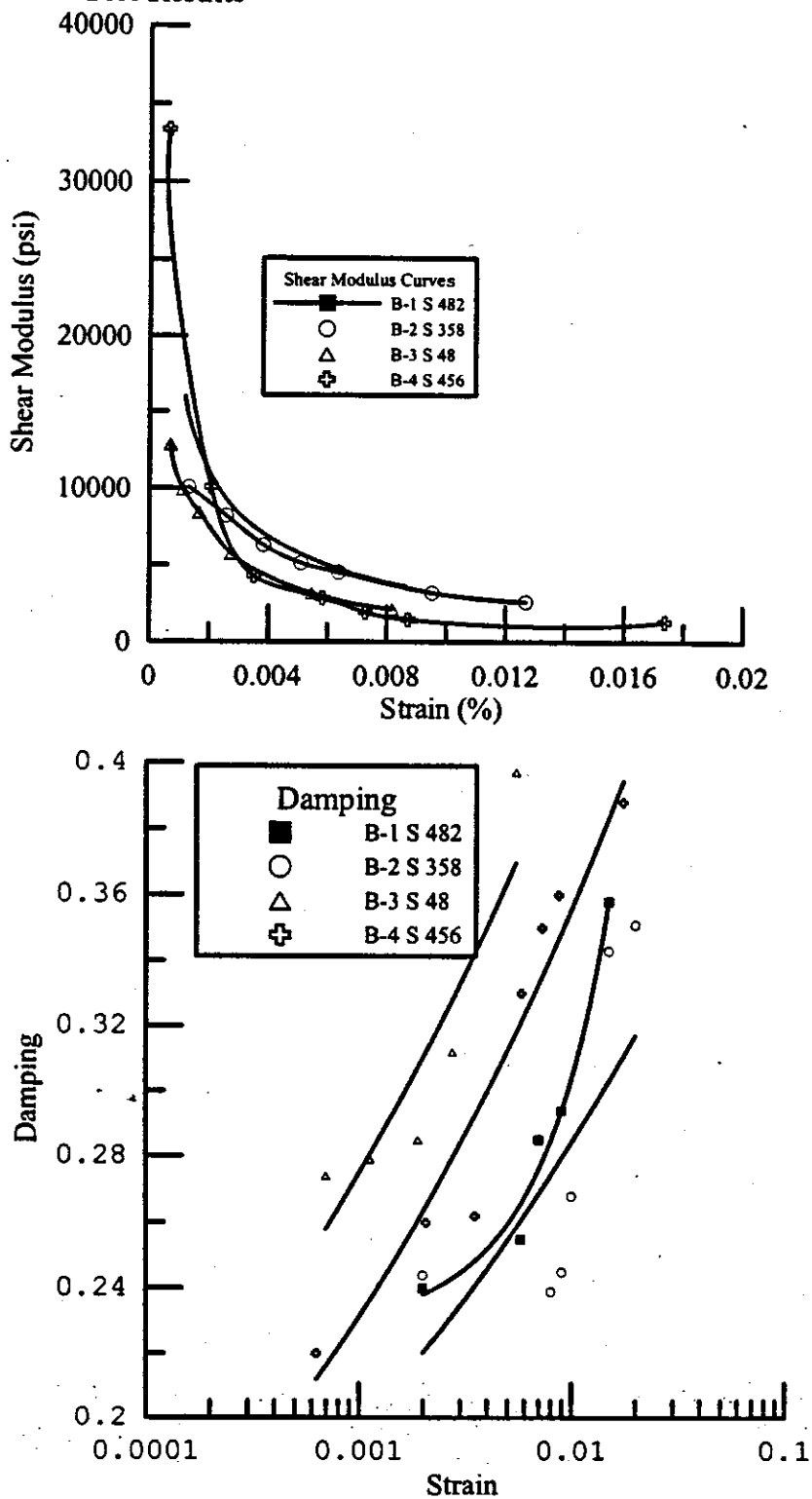
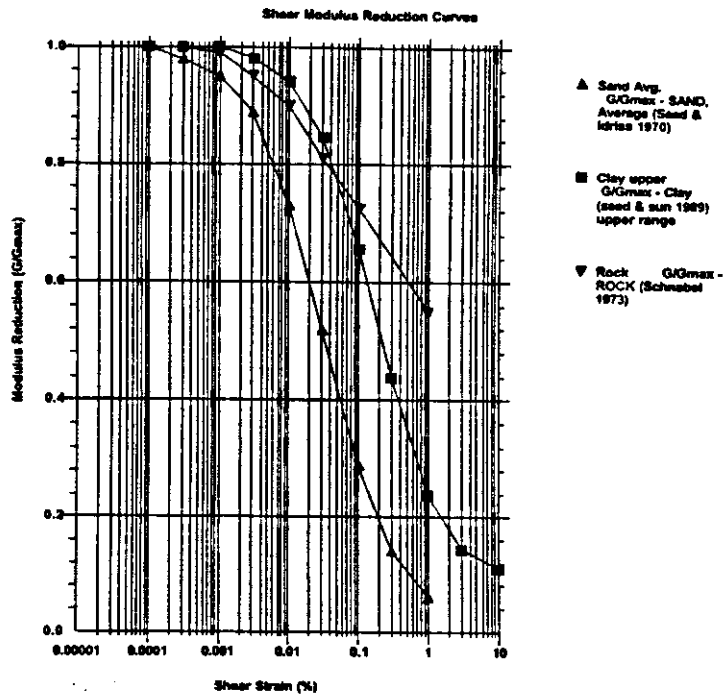
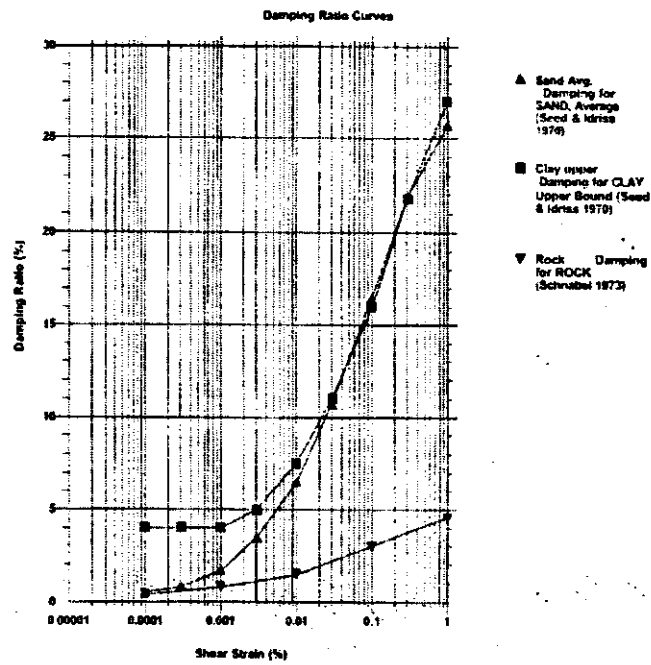


Figure B.1 Shear Modulus and Damping



**Figure B.2 Strain Dependent Modulus**



**Figure B.3 Strain Dependent Damping**

## B.2 St. Francis River Site Laboratory Results

St. Francis River														
BORING	SAMPLE	UMR	Depth	Description	PP (TSF)	Torvane (TSF)	N <sub>60</sub>	wc(%)	LL/PI	USC	q <sub>c</sub> (PSF)	Cyclic IX	CU (psi)	Φ
B-1	473		0.0-1.0	Brn silty CLAY w/ gravel	4.3	0.60		11.3						
	474	*	0.0-1.0	Br. si lean CLAY					31/10					
	pen		1.0-2.5	Brn Silty lean CLAY	4.5		21							
	475		2.5-5.0	Brown silty lean CLAY	9.0	0.60		15.8	31/10	CL			300	32
	476		2.5-5.0	Brown silty lean CLAY	3.5	0.65					6446			
	pen		5.0-6.5	Br. silty lean CLAY	5.0	-	12	17.4						
	477		6.5-8.4	Br,gray mottled si CLAY	1.5	0.55								
	478	*	6.5-8.4	Br, gray mottled si CLAY		1.50		21.4						
	pen		8.4-9.9	Br/gr mottled si CLAY, intermix siltstone	9.0	-	73	19.5						
	479		10.0-12.5	Gray Clayey SILT	8.0	0.70		17.8						
	480		10.0-12.5	Gray Clayey SILT	4.5	0.35					6532			
	pen		12.5-14.0	Gray clayey SILT	1.2	-	10							
	481		14.0-15.5	Gray clayey SILT	3.0	0.40		19.1						
	482	*	14.0-15.5	Gray clayey SILT					29/12	CL		X		
	pen		15.5-17.0	Gray SILT to clayey SILT	2.5	-	19	20.6						
	483		17.0-19.5	Gray SILT to clayey SILT	2.8	0.65		22.5						
	484		17.0-19.5	Gray SILT to clayey SILT	2.8	0.65					2603			
	pen		19.5-21.0	Gray SILT, stiff to v. stiff	3.0	-	17	25.9						
	485		21.0-23.5	Gray SILT v. stiff	4.0	0.45		24.6						
	486	*	21.0-23.5	Gray SILT very stiff										
	pen		23.5-25.0	Gray SILT to 24.5, gray fine SAND	3.3	-	26	23.9						
	487		25.0-27.5	Brown Silty sand, too brittle to wrap										
	489		27.5-29.0	Brown fine grained Sand, dense, wet			28							
	490		35.0-36.5	Brown/grey fine grained Sand, dense, wet			26							
	491		40.0-41.5	Gray fine grained Sand, very dense, wet			75							
	492		45.0-46.5	Gray fine grained Sand, very dense, wet			71							
	493		50.0-51.5	Gray fine-medium Sand, very dense, wet			75							
	494		55.0-56.5	Gray medium Sand, dense, wet			38							
	495		60.0-61.5	Gray medium Sand, very dense, wet			82							
	496		65.0-66.5	Gray medium Sand, dense			33							
	497		70.0-71.5	Gray medium Sand, dense			40							
	498		75.0-76.5	Gray medium Sand, dense			35							
	499		80.0-81.5	Drk gray fine-med silty sand, dense			38							

St. Francis River

Boring	Sample	UMR	Depth	Description	PP(TSF)	Torvane (TSF)	N <sub>60</sub>	wc(%)	LL/PI	USC	q <sub>u</sub> (psf) CYCLIC TX	CU(psi)	φ
	501		100.0-101.5	Gray med Sand, fine gravel, v. dense			73						
	369		110.0-111.5	Gray med-coarse Sand w/ f. gravel v. dense			72						
	370		120.0-121.5	Gray Coarse Sand w/ m. sand and f. grav.			123						
	371		130.0-131.5	Brownish-gry coarse Sand w/ m. sa and fine grav			56						
			140.0-142.0	Coarse Sand and cobbles									
	372		143.0-144.5	Gray coarse Sand and coarse grav			142						
	373		153.0-157.5	Gray medium Sand, v. dense			91						
	374		163.0-164.5	Gray medium Sand, v. dense			92						
	375		170.0-171.5	Gray medium Sand, v. dense			139						
			180.0-180.2	Cobble									
			190.0-191.5	Cobbles and boulders									
B-2	pen		0.0-2.5	lt grey silty clay	1.8	0.65		17.0					
	346		2.5-4.0	reddish brn mottled CLAY	5.1		10						
	347		4.0-6.5	med. Grey lean CLAY v. stiff	3.8	0.46		20.0					
	348	*	4.0-6.5	Med. gray lean CLAY w/ silt, v. stiff									
	jar		6.5-7.5				6	16.4					
			10.5-12.0	no recovery			16						
	349		12.0-14.5		7.0	0.45		17.9					
	350	*	12.0-14.5	Med. gray lean CLAY w/ silt, v. stiff								380	34
	351		14.7-16.0	lt to brn lean CLAY w/ silt v. stiff	2.0		12						
	bag		16.0-16.6										
	352		16.0-16.6		8.0	0.60							
	353		17.0-19.5	lt tan andy SILT	2.0	0.40							
	354		17.0-19.5	lt tan andy SILT				24.1			1328		
	358	*	21-23.5	Lt. Tan sa SILT stiff to v. stiff				25.5			X		
	359		24.5-25.0	Lt grey SILT			8						
	360		25.0-25.8	missing									
	361		25.8-27.5	lt brn silty SAND	0.5	0.23							
	362		25.8-27.5	lt brn silty SAND									
	363		27.5-28.5	lt brn med. Sand			15						

St. Francis River														
Boring	Sample	UMR	Depth	Description	PP(TSF)	Torvane (TSF)	N <sub>60</sub>	wc(%)	LL/PI	USC	qu(psf) CYCLICTX	Cu(psi)	φ	
	364		29.0-31.5	lt. Gray medium Sand			15							
	365		35.0-36.5	lt. Gray medium Sand			18							
	366		40.0-41.5	lt. Gray medium Sand			59							
	367		45.0-46.5	lt. Gray medium Sand			35							
	368		50.0-51.5	lt. Gray medium Sand			50							
B-3	AL		0.0-1.2	Bm sandy lean CLAY	4.5	0.95		10.9						
	jar		1.2-2.7	bm lean CLAY, v. stiff	4.5		19	15.7						
	42		3.0-5.5	In Bm CLAY, v. stiff	1.3			23.2						
	43	*	3.0-5.5	In Bm CLAY, v. stiff								280	35	
	jar		5.5-7.0	In Bm CLAY, v. stiff			6	23.2						
	44		7.0-9.5	In Bm CLAY, v. stiff	2.8	0.90		23.5						
	45	*	7.0-9.5	Moist SILT										
	46		7.0-9.5	Moist SILT										
	jar		9.5-11.0	Moist SILT	2.5		7	21.9						
	jar		10.5-14.0	Gray Clayey SILT	2.3		9	23.5						
	47		11.0-13.5	Gray Clayey SILT	2.8	0.90								
	48	*	11.0-13.5	Gray clayey SILT							X			
	jar		13.5-15.0	Gray clayey SILT			10							
	jar		14.5-15.0	tan fine SAND			19							
	49		15.0-16.1	gry bm fine SAND										
	50		16.1-17.6	Gray brown f. Sand, loose to med dense			16							
	51		18.0-19.5	Gray brown f. Sand, loose to med dense			9							
	52		19.5-21.0	Gray brown f. Sand, loose to med dense			9							
	53		21.0-22.5	gry-bm to tan f. Sand w/ lean clay			15							
	54		22.5-24.0	gry-bm to tan f. Sand w/ lean clay			24							
	55		24.0-25.5	Gray fine-med Sand			16							
	56		25.5-27.0	Gray fine-med Sand			28							
	57		275.0-28.5	Gray fine-med Sand			28							
	58		28.5-30.0	Gray fine-med Sand			23							
	59		30.0-31.5	Gray fine-med Sand			50							
	60		35.0-36.5	Gray fine-med Sand			56							
	61		40.0-41.5	Gray fine-med Sand			78							
	62		45.0-46.5	Gray fine-med Sand			26							
	63		50.0-51.5	Medium Sand			26							
	64		55.0-56.5	Gray fine-med Sand			41							

St. Francis River													
Boring	Sample	UMR	Depth	Description	PP(TSF)	Torvane (TSF)	N <sub>60</sub>	wc(%)	LL/PI	USC	qu(psf) CYCLIC TX	CU(psi)	Φ
	65		60.0-61.5	Gray fine-med Sand			47						
	66		65.0-66.5	Gray fine-med Sand			46						
	67		70.0-71.5	Gray fine-med Sand			41						
	68		75.0-76.5	Gray fine-med Sand			49						
	69		80.0-81.5	Gray fine-med Sand			41						
	70		90.0-91.5	Gray fine to med Sand w/ trace gravel			52						
	71		100.0-101.5	med to coarse Sand w. trace gravel			62						
B-4	80		0.0-2.5	br lean CLAY w/ sa & grvl	4.5	0.86		12.4					
	81		4.0-6.5	med brown lean CLAY sft to me.	0.8	0.43		27.1				200	30
	82	*	4.0-6.5	Lean CLAY soft to med. stiff									
	jar		6.5-8.0					37.9					
	83		8.0-10.5	Lean CLAY soft to med. stiff									
	84	*	8.0-10.5	v. stiff lean CLAY				23.6	48/25	CL			
	Jar		10.5-12.0	Lean CLAY, v. stiff	2.8		12	23.5	36/15				
	85		10.5-12.0	Lean CLAY, v. stiff			15						
	jar		11.5-12.5	gry, br lean CLAY, v. stiff and silty									
	86		12.5-14.5	lt br lean Clay very silty and stiff	2.5	0.54	7	24.2				150	33
	87	*	12.0-14.5	Light br lean silty CLAY v. stiff									
	88		14.5-16.0	Lt br clayey SILT, stiff, moist			9?		23/4				
	450	*	16.0-18.5	Lt br sandy silty CLAY			11	10.6	19/2				
	453	*	20.0-22.5	Br lean silty sandy CLAY				12.6			X		
	456	*	24.0-26.5	Br gray sandy SILT, med. stiff				23.0					
	459	*	28.0-30.5	Br gray fine grained				25.3					
	461		35.0-36.5	grey, fine SAND, med			16						
	462		40.0-41.5	Gry fine Sand, v. dense			29						
	463		45.0-46.5	Gr fine SAND v. dense			63						
	464		50.0-51.5	Gr fine SAND, m. dense			23						
	465		55.0-56.5	med SAND			75						
	466		60.0-61.5	med SAND, dense			26						
	467		65.0-66.5	med SAND, dense			55						
	468		70.0-71.5	med SAND, dense			47						
	469		75.0-76.5	med SAND, dense			47						
	470		80.0-81.5	fine to med SAND, v. dense			85						
	471		90.0-91.5	fine to med SAND, v. dense			55						
	472		100.0-101.5	fine to med SAND, v. dense			45						

St. Francis River													
Boring	Sample	UMR	Depth	Description	PP(TSF)	Torvac (TSF)	N <sub>60</sub>	wc(%)	LL/PI	USC	qu(psf) CYCLIC TX	CU(psi)	Φ
B-5	-		0.0-2.5	brn, lean CLAY									
	250		2.5-4.0	brn, lean CLAY			10						
	251		4.0-5.5	brn, lean CLAY									
	253		6.5-8.0	brn, lean CLAY									
	255		8.0-10.5	brn, clayey SILT, m. stiff			7						
	256		10.5-12.0	brn, clayey SILT, m. stiff			5						
	258	*	12.0-14.5	Brn clayey SILT, med. stiff to stiff									
	259		14.0-16.0	Brn clayey SILT, med. stiff to stiff			4						
	260		16.0-18.5	Brn clayey SILT, med. stiff to stiff									
	261		18.5-20.0	br silty fine SAND			4						
	262		20.0-21.5	br silty fine SAND			4						
	263		25.0-26.5	gray fine silty SAND			3						
	264		30.0-31.5	gray fine silty SAND			2						
	265		35.0-36.5	gray fine SAND, dense									
	266		40.0-41.5	gray fine SAND, dense									
	267		45.0-46.5	gray fine SAND, dense			30						
	268		50.0-51.5	gray fine SAND, dense			15						
B-6	10		0.0-2.3	Br, lean CLAY w/ f. Sand									
			2.3-4.8	Gravel									
	13	*	5.0-7.5	Brn clayey SILT, v. stiff									
	14		7.5-10.0	Brn clayey SILT, v. stiff									
	16	*	10.0-12.5	Brn clayey SILT, v. stiff									
	17		12.5-15.0	Brn clayey SILT, v. stiff									
	20	*	15.0-17.5	Brn clayey SILT, v. stiff									
	22		17.5-20.0	Brn silty fine SAND, trace clay									
	23		20.0-21.5	Brn silty fine SAND, trace clay			4						
	24		21.5-23.0	Brn silty fine SAND, trace clay			2						
	25		23.0-24.5	Brn silty fine SAND, trace clay			5						
	26		24.5-26.0	Brn silty fine SAND, trace clay			21						
	27		26.0-27.5	Brn silty fine SAND, trace clay			17						
	28		27.5-29.0	Gray brown fine to med SAND			22						
	29		29.0-30.5	Gray brown fine to med SAND			17						
	30		30.5-32.0	gray fine SAND			14						
	31		35.0-36.5	gray fine SAND			28						
	32		40.0-41.5	gray fine SAND			75						

St. Francis River													
Boring	Sample	UMR	Depth	Description	PP(TSF)	Torvane (TSF)	N <sub>60</sub>	wc(%)	LL/PI	USC	qu(psf) CYCLICTX	CU(psi)	Φ
	33		45.0-46.5	Gray brown fine SAND			75						
	34		50.0-51.5	Gray brown fine SAND			80						

### B.3 Wahite Ditch Bridge Site Laboratory Results

Wahite Ditch											CYCLICTX
BORING	SAMPLE	UMR	Depth	Description	PP (TSF)	Torvane (TSF)	N <sub>60</sub>	wc(%)	LL/PI	USC	
B-1	743	*	0.0-2.5	Br. gray fat clay with sand	9.0+	0.95		10.1%	51/29	CH	
	744		2.5-5.0	Br. gray fat clay with sand	1.50	0.55		15.4%			
	745		2.5-5.0	Br. gray fat clay with sand	-	-					
	746	*	5.0-7.3	Br. gray fat clay with sand	1.50	0.50		32.2%	33/17	CL	
	747		5.0-7.3	Br. gray fat clay with sand				29.1%			1783
	748		7.5-10.0	Br. Fat clay with sand, stiff	1.50	0.75		35.6%			
	749		7.5-10.0	Br. Fat clay with sand, stiff							
	750	*	10.0-12.5	Br. Fat clay with sand, stiff	1.25	0.70		32.0%	73/46	CH	
	751		10.0-12.5	Br. Fat clay with sand, stiff				34.7%			1282
	752		10.0-12.5	Br. Fat clay with sand, stiff							
	753		12.5-15.0	Br. Fat clay with sand, stiff	1.75	0.75		35.0%			
	754		12.5-15.0	Br. Fat clay with sand, stiff							
	755	*	15.0-17.5	Gr. Tan fat clay with sand, stiff	1.00	0.70		30.8%	81/50	CH	
	756		15.0-17.5	Gr. Tan fat clay with sand, stiff				30.6%			2101
	757		15.0-17.5	Gr. Tan fat clay with sand, stiff							
	758		17.5-20.0	Gr. Tan fat clay with sand, stiff	1.50	0.70		35.1%			
	759		17.5-20.0	Gr. Tan fat clay with sand, stiff							
	760		20.0-21.5	Tan firm to med sand				58			
	761	*	21.5-23.0	Tan firm to med sand				51			
	762		23.0-24.5	Tan firm to med sand				72			
	763		24.5-26.0	Gr. & tan fine to med sand				63			
	764	*	26.0-27.5	Gr. & tan fine to med sand				49			
	765		27.5-29.0	Fine Sand				46			
	766		29.0-30.5	Gr. & tan fine to med sand				65			
	90	*	35.0-36.5	Scattered gravelly layers				66			
	91		40.0-41.5	Scattered gravelly layers				73			
	92		45.0-46.5	Thin gravelly layers, medium with coarse sand				47			
	93	*	50.0-51.5	Thin gravelly layers, medium with coarse sand				46			
	94		55.0-56.5	Thin gravelly layers, medium with coarse sand				39			
	95	*	60.0-61.5	black with organics from 60.6-61.05, gravelly @ 62				38			
	96		65.0-66.5	Gr. & Tan medium sand				54			
	97	*	70.0-71.5	Gr. & Tan medium sand				51			
	98		75.0-76.5	Gr. & Tan medium sand				54			
	99	*	80.0-81.5	Gr. & Tan medium sand				51			
	100		90.0-91.5	Gr. & Tan medium sand				51			
	101	*	100.0-101.5	Gr. & Tan medium sand				52			
	102		110.0-111.5	cobbles & Gravel @ 108				73			
	103	*	120.0-121.5	Tan fine to coarse sand with trace silt				24			

Wahite Ditch												
BORING	SAMPLE	UMR	Depth	Description	PP (TSF)	Torvane (TSF)	N <sub>60</sub>	wc(%)	LL/PI	USC	q <sub>s</sub> (PSF)	CYCLIC FX
	104		130.0-131.5	Tan fine to coarse sand with trace silt			29					
	105		140.0-141.5	Tan fine to coarse sand with trace silt			61					
	106	*	150.0-151.5	cobbles & gravel @ 148.6			74					
	107		160.0-161.5	Tan fine to coarse sand with trace silt			56					
	108		170.0-171.5	Lt gr. and tan fine sand			82					
	109	*	180.0-181.5	Lt gr. and tan fine sand			96					
	110		190.0-191.5	Lt gr. and tan fine sand			82		38/22	CL		
	111	*	200.0-201.5	Gr. Lean clay with sand					42/19	CL		
	112		200.0-201.5	200-201.5 gr brown fat clay								
B-2	680		2.5-5.0	Gray br fat clay	4.50	0.95						
	681	*	5.0-7.5	Gray br fat clay	2.00	0.50			53/33	CH		
	682		7.5-10.0	Gray br fat clay	1.50	0.80						
	683		7.5-10.0	Gray br fat clay								
	684	*	10.0-12.5	Gray br fat clay	1.25	0.65			57/35	CH		
	685	*	12.5-15.0	Bluish grey fat clay with sand in lenses	1.25	0.70			75/46	CH		
	686		12.5-15.0	Bluish grey fat clay with sand in lenses								
	687		15.2-17.5	Gray to tan fat clay with sand	1.50	0.65						
	688		15.2-17.5	Gray to tan fat clay with sand				35.2%			1807	
	689	*	17.5-19.5	Gray to tan fat clay with sand	1.25	0.65			79/50	CH		
	690	*	20.0-20.7	Tan fine to med sand								
	691		20.7-22.20	Tan fine to med sand			52					
	692		22.0-23.5	Tan fine to med sand			56					
	693		23.5-25.0	Tan fine to med sand			52					
	694		25.0-26.5	tan and light grey fine to med sand			39					
	695		26.5-28.0	tan and light grey fine to med sand			42					
	696		28.0-29.5	tan and light grey fine to med sand			49					
	697	*	29.5-31	tan and light grey fine to med sand			53					
	698		35.0-36.5	tan and light grey fine to med sand			57					
	699	*	40.0-41.5	tan and light grey fine to med sand								
	700		45.0-46.5	tan and light grey fine to med sand			52					
	701	*	50.0-51.5	tan and light grey fine to med sand			60					
	702		60.0-61.5	tan and light grey fine to med sand			82					
	703	*	65.0-66.5	tan and light grey fine to med sand			56					
	704		70.0-71.5	tan and light grey fine to med sand			108					
	705	*	75.0-76.5	tan and light grey fine to med sand			96					
	706		80.0-81.5	tan and light grey fine to med sand			75					

White Ditch												
BORING	SAMPLE	UMR	Depth	Description	PP (TSF)	Torvane (TSF)	N <sub>60</sub>	wc(%)	LL/PI	USC	q <sub>s</sub> (PSF)	CYCLICTX
	707		90.0-91.5	tan and light grey fine to med sand			39					
	708	*	100.0-101.5	tan and light grey fine to med sand			73					
<b>B-3</b>	-		0.0-2.9	Tan sand with scattered gravel								
	591	*	2.90-4.0	Grey lt br. fat clay	2.75	0.95		23.4%				
	592	*	8.5-10.0	Grey fat clay stiff	1.50	0.70		37.3%				
	593		8.5-10.0	Grey fat clay stiff								
	594		10.0-12.3	Grey fat clay stiff				32.6%				
	595	*	14.1-15.0	Bluish grey fat clay, stiff	1.50	0.75		33.1%				
	596		14.1-15.0	Bluish grey fat clay, stiff								
	597	*	17.5-19.0	Bluish grey fat clay, stiff	1.50	0.70		32.3%	73/53	CH		
	598	*	22.5-242.0	tan mediium sand			53					
	599		24.0-25.5	tan mediium sand			61					
	600	*	25.5-27.0	tan mediium sand			42					
	601		27.0-28.5	tan mediium sand			45					
	602	*	28.5-30.0	tan mediium sand			42					
	603		30.0-31.5	tan mediium sand			53					
	604		35.0-36.5	tan mediium sand			54					
	605	*	40.0-41.5	tan mediium sand			51					
	606	*	45.0-46.5	tan mediium sand			53					
	607		50.0-51.5	tan mediium sand			36					
<b>B-4</b>	608	*	2.5-5.0	Drk Brown fat clay	10+	0.95		13.8%	39/22	CL		
	609		2.5-5.0	Drk Brown fat clay								
	610		5.0-5.7	Drk Brown fat clay	4.00	0.90		24.0%				
	611		5.0-5.7	Drk Brown fat clay	1.00	0.60						
	614	*	7.5-10.0	bluish gray fat clay	0.75	0.50		19.1%	33/17	CL		
	615		7.5-10.0	bluish gray fat clay								
	616		10.0-11.9	bluish gray fat clay	1.00	0.50		21.2%				
	617		10.0-11.9	bluish gray fat clay				22.9%			966	
	618	*	11.9-12.5	Drk gray fat clay	1.50	0.70		23.3%	45/21	CL		
	619	*	12.5-14.9	Bluish gray fat clay	1.25	0.55		21.7%	52/35	CH		
	620		12.5-14.9	Bluish gray fat clay								
	621	*	15.0-17.5	Gray fat clay	1.50	0.75		25.0%	59/37	CH		
	622		15.0-17.5	Gray fat clay								
	623		15.0-17.5	Gray fat clay								
	624	*	17.5-19.4	Gray fat clay	1.25-			21.6%	46/27	CL		
	625		17.5-19.4	Gray fat clay								
	626	*	19.5-21.0	Tan fine to med sand			24					
	627		21.0-22.5	Tan fine to med sand			26					
	628		22.5-242.0	Tan fine to med sand			46					
	629		24.0-25.5	Tan fine to med sand			39					
	630	*	25.5-27.0	Tan fine to med sand			35					
	631		27.0-28.5	Tan fine to med sand			39					
	632		28.5-30.0	Tan fine to med sand			39					

Wahite Ditch											CYCLIC TX	
BORING	SAMPLE	UMR	Depth	Description	PP (TSF)	Torvare (TSF)	N <sub>60</sub>	wc(%)	LL/PI	USC		q <sub>s</sub> (PSF)
	633		30.0-31.5	Tan fine to med sand			38					
	634	*	35.0-36.5	Tan fine to med sand			43					
	635		40.0-41.5	Tan fine to med sand			42					
	636		45.0-46.5	Tan fine to med sand			56					
	637	*	50.0-51.5	Tan fine to med sand			42					
<b>B-5</b>	709	*	2.5-5.0	Gray & brown to tan fat clay	8.00	0.95		20.6%	55/31	CH		
	710		2.5-5.0	Gray & brown to tan fat clay								
	711		5.0-7.5	Gray & brown to tan fat clay	2.00	0.90		26.1%				
	712		5.0-7.5	Gray & brown to tan fat clay				21.3%			1747	
	713	*	7.5-10.0	Gray & brown to tan fat clay	1.75	0.60		30.9%	63/38	CH		
	714		7.5-10.0	Gray & brown to tan fat clay								
	715		7.5-10.0	Gray & brown to tan fat clay								
	716		10.8-12.5	bluish gray fat clay	1.25	0.45		40.0%				
	717		10.8-12.5	bluish gray fat clay								
	718	*	12.5-13.4	bluish gray fat clay	1.50	0.70		30.6%	69/41	CH		
	719		12.5-13.4	bluish gray fat clay								
	720	*	15.0-17.5	Gray and tan fat clay	1.75	0.75		22.1%	60/39	CH		
	721		15.0-17.5	Gray and tan fat clay				27.1%			1157	
	722		15.0-17.5	Gray and tan fat clay								
	723		17.5-18.1	Gray and tan fat clay	1.50	0.70		22.5%				
	724	*	20.0-212.5	Tan fine to med sand			53					
	725		21.5-23.0	Tan fine to med sand			56					
	726		23.0-24.4	Tan fine to med sand			55					
	727	*	24.5-26.0	Tan and gray fine to med sand			48					
	728		26.0-27.5	Tan and gray fine to med sand			44					
	729		27.5-29.0	Tan and gray fine to med sand			48					
	730	*	29.0-30.5	Tan and gray fine to med sand			58					
	731		35.0-36.5	Tan and gray fine to med sand			62					
	732		40.0-41.5	Tan and gray fine to med sand			41					
	733	*	45.0-46.5	Tan and gray fine to med sand			46					
	734		50.0-51.5	Tan and gray fine to med sand			41					
	735	*	55.0-56.5	Tan and gray fine to med sand			68					
	736		60.0-61.5	Tan and gray fine to med sand			51					
	737		65.0-66.5	Tan and gray fine to med sand			54					
	738		70.0-71.5	Tan and gray fine to med sand			51					
	739	*	75.0-76.5	Tan and gray fine to med sand			80					
	740		80.0-81.5	Tan and gray fine to med sand			60					
	741	*	90.0-91.5	Tan and gray fine to med sand			43					
	742		100.0-101.5	Tan and gray fine to med sand			71					
<b>B-6</b>	638	*	2.5-5.0	Drk Brown Fat clay	7.00	0.95		17.8%	49/27	CL		
	639		2.5-5.0	Drk Brown Fat clay								
	640		5.0-7.5	Drk Brown Fat clay	2.50	0.85		24.5%				
	641	*	7.5-10.0	Drk Brown Fat clay	2.50	0.90		19.8%	35/19	CL		
	642		7.5-10.0	Drk Brown Fat clay								

White Ditch												
BORING	SAMPLE	UMR	Depth	Description	PP (TSF)	Torvane (TSF)	N <sub>60</sub>	wc(%)	LL/PI	USC	q <sub>s</sub> (PSF)	CYCLIC IX
	643	*	10.4-11.3	Gray Fat Clay	2.00	0.70		28.2%	64/40	CH		
	644	*	12.5-14.8	Bluish gray fat clay	1.50	0.75		22.2%	49/30	CL		
	645		12.5-14.8	Bluish gray fat clay								
	646	*	15.0-17.3	Gray and tan fat clay	2.00	0.80		21.5%	51/34	CH		
	647		15.0-17.3	Gray and tan fat clay				20.5%			2883	
	648		15.0-17.3	Gray and tan fat clay								
	649	*	17.5-20.0	Gray clayey sand	2.00	0.35		16.0%	34/17	CL		
	650		20.0-20.4	Gray clayey sand								
	651	*	20.0-21.5	Tan fine to med sand			27					
	652	*	21.5-23.0	Tan fine to med sand			34					
	653		23.0-24.5	Tan fine to med sand			38					
	654	*	24.5-26.0	Tan fine to med sand			42					
	655		26.0-27.5	Tan fine to med sand			39					
	656		27.5-29.0	Tan fine to med sand			41					
	657	*	29.0-30.5	Tan fine to med sand			39					
	658	*	35.0-36.5	Tan fine to med sand			55					
	659		40.0-41.5	Tan fine to med sand			58					
	660	*	45.0-46.5	Tan fine to med sand			58					
	661		50.0-51.5	Tan fine to med sand			34					

## C. SOFTWARE DESCRIPTION

Descriptions of the major analysis software are given below.

### C.1 *SHAKE91* and *SHAKEDIT*

#### C.1.1 *SHAKE91*

*SHAKE91* is a computer program for conducting equivalent linear seismic response analyses of horizontally layered soil deposits. Modified program is based on the original *SHAKE* program (Schnabel, Lysmer and Seed, 1972) and modifications by Idriss and Sun (1991).

#### C.1.2 *SHAKEDIT* Program

*SHAKEDIT* is a Windows based "pre-" and "post-"processor for *SHAKE91*. In a typical application, *SHAKEDIT* is used to create an input file for *SHAKE91*. User-friendly screens are provided to input the data for the different *SHAKE91* options, and then to create an input file. After executing *SHAKE91*, *SHAKEDIT* is used to process the output files, and to create a series of files containing acceleration and/or stress/strain time history data, response spectrum and amplification data, etc. The results can also be viewed graphically in *SHAKEDIT*, and the graphics created can be saved/printed for inclusion in documents. On-line help is provided for most editing and graphing operations. The information presented in this manual assumes that the reader is familiar with *SHAKE91* and the different options used in the program. However, all the results have been added to E-files.

### C.2 Modified *DDRW2* Program

The modified *DDRW2* program is used to calculate displacement of rigid retaining walls during real earthquake loading and considering nonlinear soil properties. The *DDRW2* program is a modification of *DDRW1* program in which only dry soil and sinusoidal ground motion were used. The former has been modified to include deck loads and their time dependent inertia forces as for bridge abutments for simply supported decks and assumed restrained by the deck with integral construction. Soil is considered non-linear. Therefore both material and radiation damping are included in the solution.

The following stiffness and damping factors were calculated by appropriate methods for 2-dimensional case.

$k_z, k_x, k_\phi, k_{y\theta}$  and  $c_z, c_x, c_\phi, c_{y\theta}$

Where;

- $k_z$  = stiffness of single pile for translation along z axis
- $k_x$  = stiffness of single pile for translation along x axis
- $k_\phi$  = stiffness of single pile for rocking about y axis
- $k_{y\theta}$  = cross couple stiffness of single pile for sliding along x-axis and rocking about y axis
- $c_z$  = damping of single pile for translation along z axis
- $c_x$  = damping of single pile for translation along x axis
- $c_\phi$  = damping of single pile for rocking about y axis
- $c_{y\theta}$  = cross couple stiffness of single pile for sliding along x-axis and rocking about y axis

These stiffness and damping parameter had been computed both as function of strain and linear-displacement.

The results give displacements (sliding, rocking and total displacement) of bridge abutment as a function time.

### **C.3 PCSTABL5**

The following program description is modified from the *STABL* homepage at <http://www.ecn.purdue.edu/STABL/>. Version 5 of the program was used for this study.

*PCSTABL* is a computer program written in FORTRAN for the general solution of slope stability problems by two-dimensional limiting equilibrium methods. The calculation of the factor of safety against instability of a slope is done using one of the following methods: Bishop Simplified Method (applicable to circular shaped failure surfaces), Janbu Simplified Method (applicable to failure surfaces of general shape), and Spencer's Method (applicable to any type of surface). The Janbu Simplified Method has an option to use a correction factor, developed by Janbu, which can be applied to the factor of safety to reduce the conservatism produced by the assumption of no interslice forces.

*PCSTABL* features unique random techniques for generation of potential failure surfaces for subsequent determination of the more critical surfaces and their corresponding factors of safety. One technique generates circular; another, surfaces of sliding block character; and a third, more general irregular surfaces of random shape. The user can also specify specific trial failure surface.

For this study, *PCSTABL5* was coupled with *STEDwin*, a pre- and post-processing program that simplifies data entry into the *PCSTABL5* program and improves the quality of graphical output diagrams.

### **C.4 SAP2000**

SAP2000 is a powerful structural analysis software tool. Many types of analyses may be completed in SAP2000, including static, dynamic, linear and nonlinear seismic, P-Delta, and vehicle live loads for bridges. A wide variety of frame and shell structural sections may be used

in modeling, including beam-columns, membranes, and plates. SAP2000 also offers multiple coordinate systems, a variety of joint constraints, many loading options, and capacity for very large structural models.

## **D. DETAILS OF SYNTHETIC GROUND MOTION**

### **D.1 Task**

The requirements are as follow:

Provide site-specific hard rock motions for two bridge sites in southeastern Missouri:

- St. Francis River Bridge (36.8°N, 90.2°W)
- Wahite Ditch Bridge (36.8°N, 89.7°W)

The rock motions are to be for annual probabilities of 2% probability of exceedance in 50 years, and 10% probability of exceedance in 50 years. The motions should consist of 5-horizontal and 5-vertical ground motions, considering both near-field and far-field earthquake events.

### **D.2. Overview of problem**

The location of the two sites is shown in Figure D.4.1 together with neighboring earthquake locations for the time period 1974-1995. The St. Francis site is about 37 - 150 km from possible earthquakes in the active part of the current seismicity zone, while the Wahite Ditch is about 15 - 150 km from active seismicity.

In the preparation of the 1996 NEHRP maps, the USGS considered other possible locations obtained by moving the 'Z' seismicity pattern westward slightly to the edge of the ancient right and eastward to the eastern boundary. They then assigned weights of 1/3 to each of the three patterns.

### **D.3. Defining earthquakes**

The USGS 1996 maps equally weighted two ground motion magnitude - distance relations: one based of the Toro and McGuire model for EPRI and the other a purely USGS model. The 1996 maps were generated for a nationwide NEHRP B-C soil condition boundary so that one could use the methodology in FEMA-273, for example, to adjust the mapped values to sites with other than the B-C soil condition in the upper 30 meters. The FEMA site adjustment factors are not applicable to these two bridges for two reasons: first, the surface soil conditions have shear-wave velocities closer to 150-200 m/sec (Paul Mayne and Glenn Rix, Georgia Tech, MAE Center research) and second, the soils are much deeper than 30 meters thick -- the depth to rock at the St. Francis and Wahite bridges site may be about 100 m and 200 m, respectively. Thus the ground motion values and the NEHRP site factors are not applicable to this study. The effect of the deep sediments on surface motions consists of two competing effects. The reduction of shear-wave going from the hard rock to the overlying soil introduces a site amplification that increases with frequency (basically amplitude increases as a wave propagates into a medium with lower impedance). This amplification is counteracted by a reduction in high frequency content due to intrinsic and scattering Q (damping) in the soil column. These effects are discussed in MAE

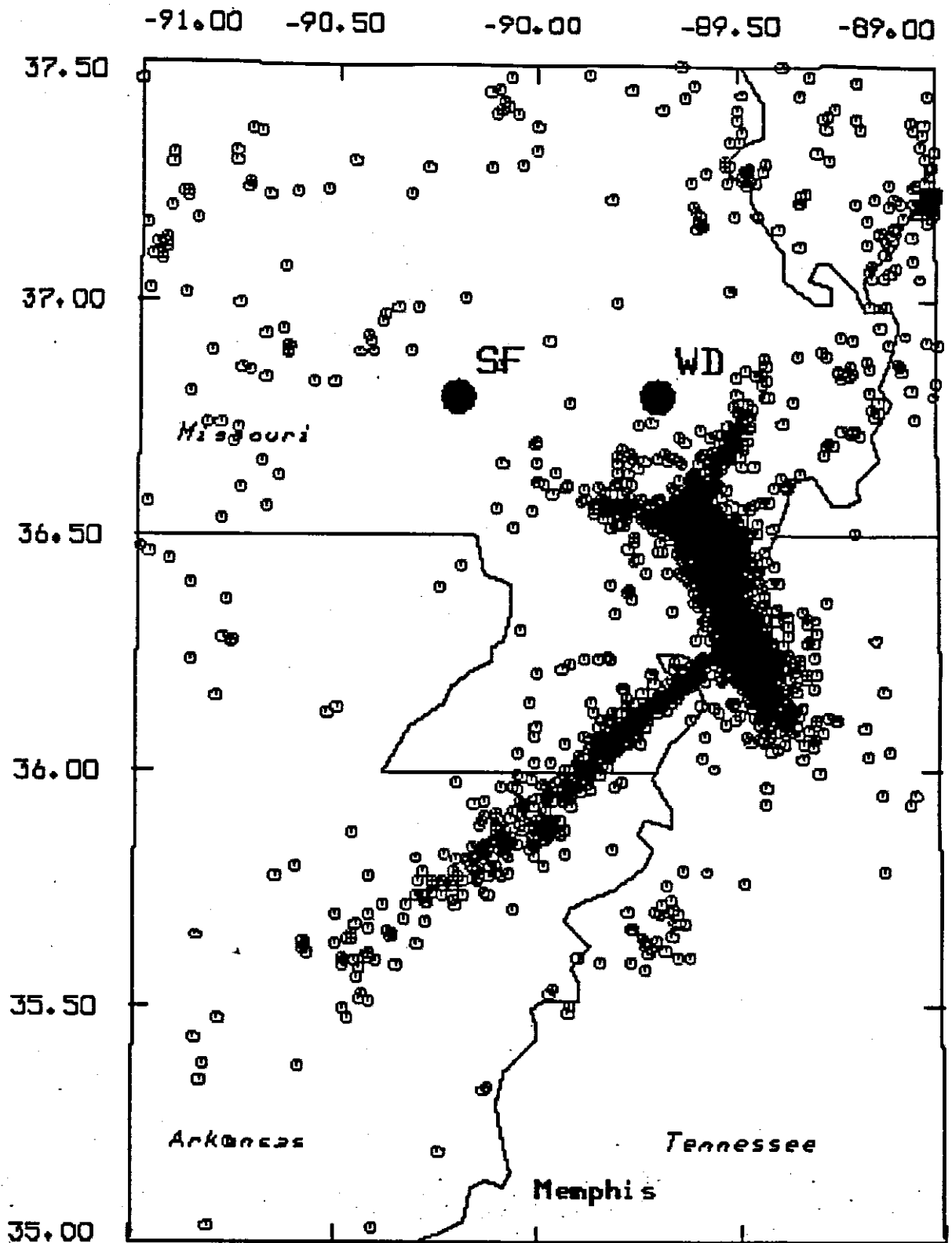


Fig. D.1 Seismicity in the 1974 - 1995 time period in the vicinity of the St. Francis River Site (SF) and the Wahite Ditch site (WD)

Center Ground Motion Models , Prototype CUS Hazard Maps , Prototype CUS Hazard Maps, Mmax effect , CUS Hazard Maps Project and FEMA Site Factors vs. Deep Soil . These studies used linear wave propagation theory to test the sensitivity of expected ground motions to the deep soil structure.

For site-specific studies, the effect of non-linear soil response must be considered though. The question is at what depth in a deep soil column, should one start using non-linear analysis. This is no easy response since fundamental experimental work must be done on the behavior of materials at the high confining pressures encountered at such depths. The Mid-America Earthquake Center is addressing this issue. It seems that linear motions can be propagated upward to about 100 - 200 meters depth, at which point non-linear analysis is required. Since the St. Francis and Wahite Bridge site soil sections are not excessively thick, standard non-linear or pseudo-non-linear analyses should be performed. However, the shear-wave velocity profile should be similar to that available from (MAEC GT-1 Deep Soil Model). In addition the non-linear analysis should have a low-strain damping floor of about 2.5% ( $Q=20$ ).

To provide suitable time series, we start with the USGS 1996 seismic hazard maps. By entering a latitude and longitude at the USGS - National Seismic Hazard Mapping Project , I obtained the following results:

**Table D.1 Time Series for Study Sites**

	<b>10 % PE in 50 Year (%g)</b>	<b>2 % PE in 50 Year (%g)</b>
<b>St. Francis River</b>		
PGA	15.83	64.32
0.2 sec SA	31.37	125.21
0.3 sec SA	24.01	105.10
1.0 sec SA	7.72	37.92
<b>Wahite Ditch</b>		
PGA	19.62	134.33
0.2 sec SA	38.17	275.53
0.3 sec SA	27.56	226.43
1.0 sec SA	18.68	89.11

The excess precision in the table is not meaningful, though. The next step is to find a suite of distances and magnitudes that provide these values. This is easy to do by a table lookup of the ground motion parameter as a function of magnitude and distance (the USGS ground motion model enters into the hazard analysis code by a table lookup) ; one need only search through this table for the best fit to these surface B-C mapped values. Performing this exercise, the following are acceptable combinations:

These magnitudes and distances will not be used to generate time series for each site and probability. To accomplish this, I use the band-limited Gaussian white noise technique of Boore (1922) (see CUS ground motion page for links to D. Boore's programs). Specifically I use the

program dorvt180 and td\_drvr together with auxiliary programs for display. I also use the CUS deep soil ground motion model with F96 (USGS96 source scaling) given on the CUS ground motion web page, with a soil thickness of 0 meters. Because the CUS model includes 1 km of Paleozoic layers, there is as light frequency dependent site amplification. The model uses recently determined, CUS specific, crustal wave propagation from the source to the site.

**Table D.2 Magnitude and Distance for Design Earthquakes**

**a. St. Francis River Site**

Probably Exceedance	Magnitude Mw	Distance, R (km)
10 % in 50 years	6.2	40
10 % in 50 years	7.2	100
2 % in 50 years	6.4	10
2 % in 50 years	8.0	40

**b. Wahite Ditch Site**

Probably Exceedance	Magnitude Mw	Distance, R (km)
10 % in 50 years	6.4	40
10 % in 50 years	7.0	65
2 % in 50 years	7.8	16
2 % in 50 years	8.0	20

For a given moment magnitude and distance, I first choose a random number seed and then perform 100 time domain simulations, saving the mean response spectra.

Next I perform one time domain simulation for each of five random number seeds. I examine the resultant time series by computing the corresponding response spectra to the mean of 100 simulations. If the comparison is good, then this time series is saved. The results for all the simulations are contained in the following table. The plot presents the time series acceleration, velocity and displacement time histories, the realized and target pseudo-acceleration, the Fourier acceleration spectra form the trace and an indicator of the magnitude, distance and random number seed. By clicking on the table the individual time series is presented.

**Table D.3 St. Francis River Site 10 % Probability of Exceedance in 50 Years**

M	DIST	SEED	Graph	Name
6.2	40	1234	Fig. D.2a	SF100101
6.2	40	2345	Fig. D.2b	SF100102
6.2	40	123	Fig. D.2c	SF100103
6.2	40	345	Fig. D.2d	SF100104
6.2	40	78	Fig. D.2e	SF100105
7.2	100	1234	Fig. D.3a	SF100201
7.2	100	2345	Fig. D.3b	SF100202
7.2	100	123	Fig. D.3c	SF100203
7.2	100	345	Fig. D.3d	SF100204
7.2	100	78	Fig. D.3e	SF100205

**Table D.4 St. Francis River Site 2 % Probability of Exceedance in 50 Years**

<b>M</b>	<b>DIST</b>	<b>SEED</b>	<b>Graph</b>	<b>Name</b>
6.4	10	1234	Fig. D.4a	SF020101
6.4	10	2345	Fig. D.4b	SF020102
6.4	10	123	Fig. D.4c	SF020103
6.4	10	345	Fig. D.4d	SF020104
6.4	10	78	Fig. D.4e	SF020105
8.0	40	1234	Fig. D.5a	SF020201
8.0	40	2345	Fig. D.5b	SF020202
8.0	40	123	Fig. D.5c	SF020203
8.0	40	345	Fig. D.5d	SF020204
8.0	40	78	Fig. D.5e	SF020205

**Table D.5 Wahite Ditch Site 10% Probability of Exceedance in 50 Years**

<b>M</b>	<b>DIST</b>	<b>SEED</b>	<b>Graph</b>	<b>Name</b>
6.4	40	1234	Fig. D.6a	WD100101
6.4	40	2345	Fig. D.6b	WD100102
6.4	40	123	Fig. D.6c	WD100103
6.4	40	345	Fig. D.6d	WD100104
6.4	40	78	Fig. D.6e	WD00105
7.0	65	1234	Fig. D.7a	WD100201
7.0	65	2345	Fig. D.7b	WD100202
7.0	65	123	Fig. D.7c	WD100203
7.0	65	345	Fig. D.7d	WD100204
7.0	65	78	Fig. D.7e	WD100205

**Table D.6 Wahite Ditch Site 2% Probability of Exceedance in 50 Years**

<b>M</b>	<b>DIST</b>	<b>SEED</b>	<b>Graph</b>	<b>Name</b>
7.8	16	1234	Fig. D.8a	WD020101
7.8	16	2345	Fig. D.8b	WD020102
7.8	16	123	Fig. D.8c	WD020103
7.8	16	345	Fig. D.8d	WD020104
7.8	16	78	Fig. D.8e	WD020105
8.0	20	1234	Fig. D.9a	WD020201
8.0	20	2345	Fig. D.9b	WD020202
8.0	20	123	Fig. D.9c	WD020203
8.0	20	345	Fig. D.9d	WD020204
8.0	20	78	Fig. D.9e	WD020205

Time series file format. An example of the first few lines of one time series file is

Acceleration acc.in

16384 0.0050

-0.89331E-08	-0.53218E-08	-0.78847E-08	-0.95266E-09	-0.45549E-08
0.18960E-08	0.13551E-10	0.41705E-08	0.30585E-08	0.75637E-08
0.43945E-08	0.89134E-08	0.61092E-08	0.10998E-07	0.10490E-07
0.14416E-07	0.12970E-07	0.16878E-07	0.16777E-07	0.20852E-07
0.19644E-07	0.23510E-07	0.20594E-07	0.24264E-07	0.22504E-07

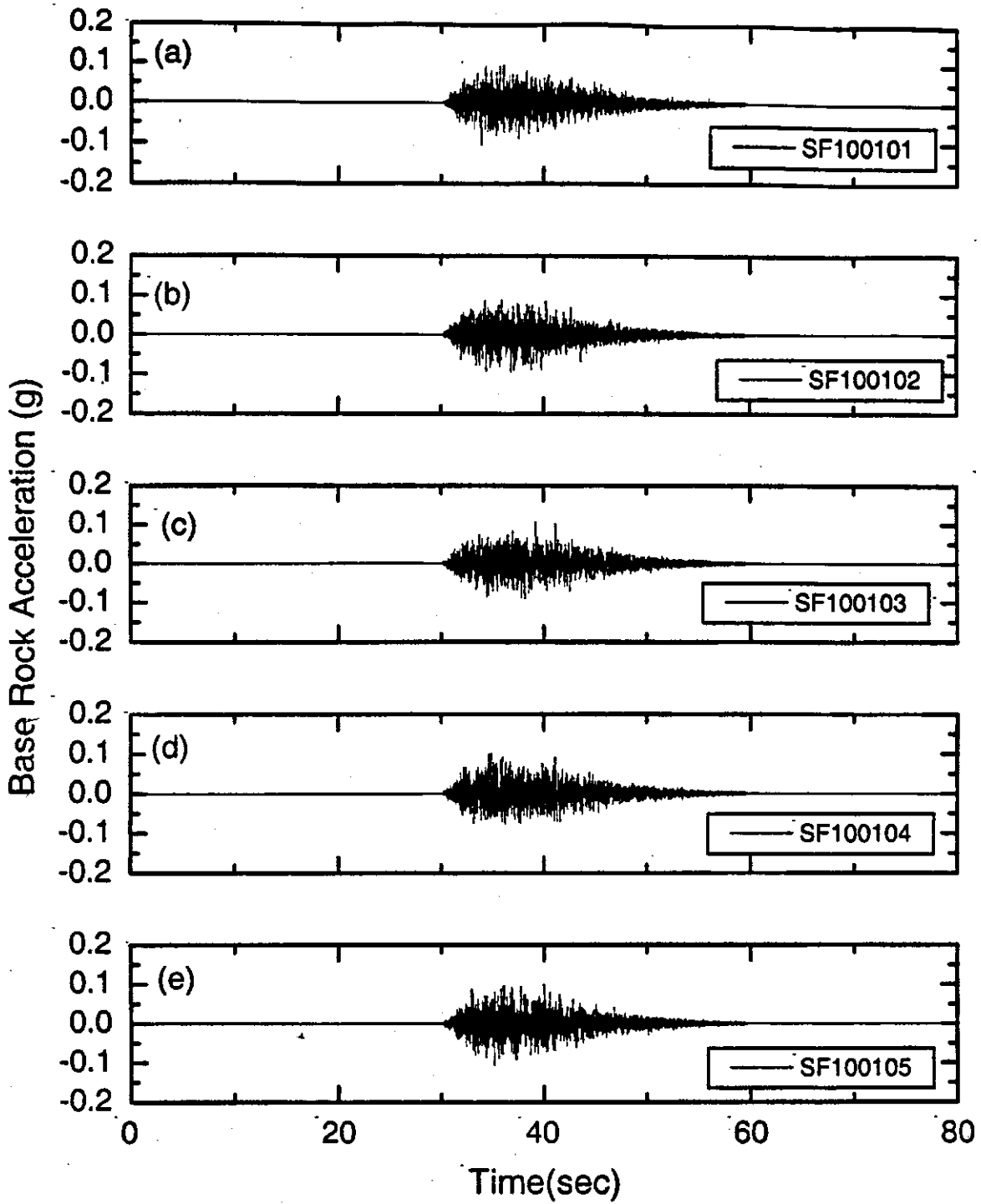
The first line is a comment line, which is the same for all simulations. The second line gives the number of data points (16384) and the sample interval (0.005 sec). The acceleration time series (units of g) follow on the succeeding lines. The reason for the long time series is that large earthquakes have long duration because of the total time of faulting.

#### **D.4 Discussion**

I have not presented vertical component time histories. I believe I know how to do this for the deep soil soils for which the surface vertical component motion in the shear-wave window is actually caused by the shear-wave in the hard rock converted into a P wave at the rock sediment interface. For motion on hard rock, though, the vertical motion is only slightly less than the horizontal. So use the horizontal motion for the vertical. The major site modifier is the deep soil condition.

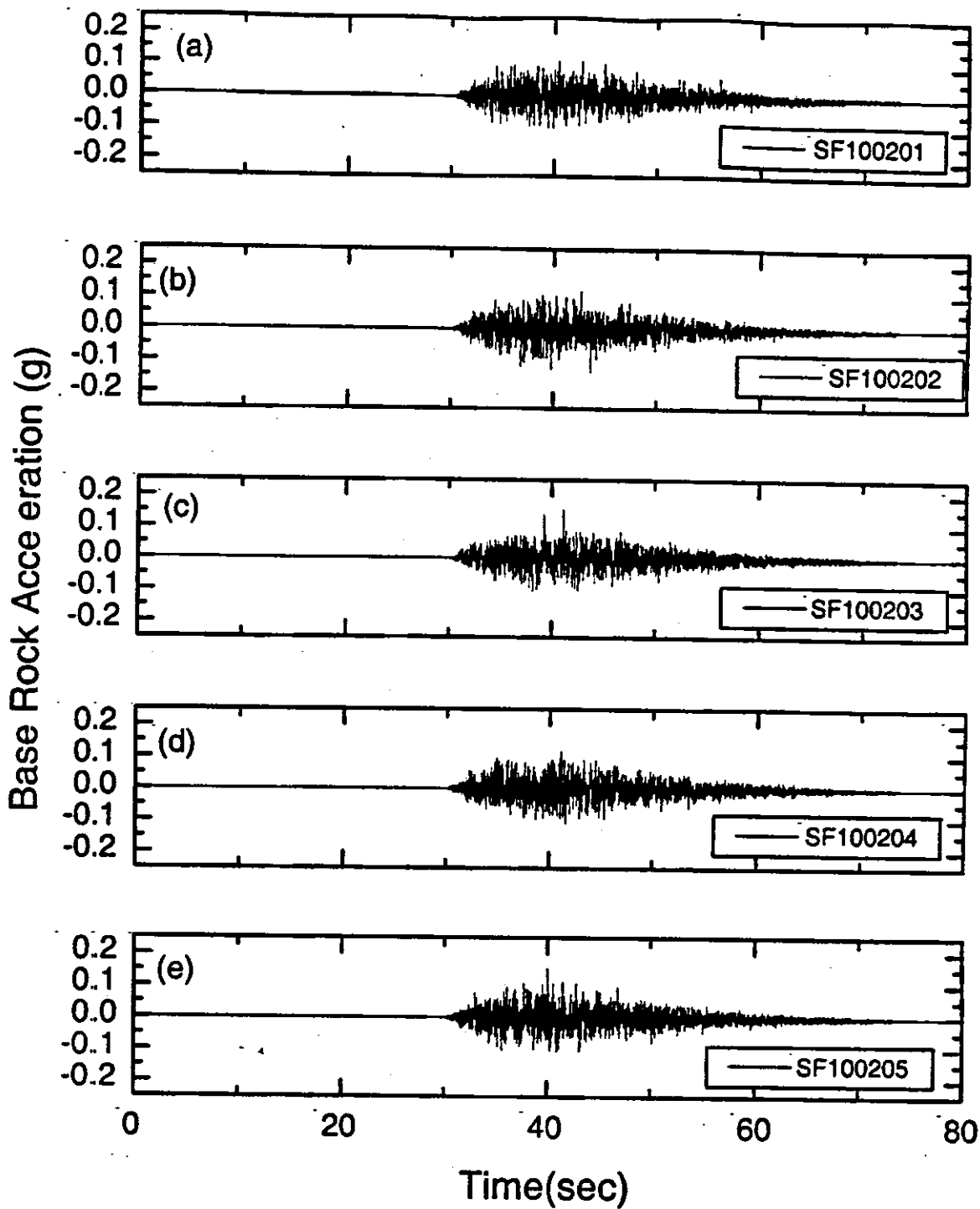
The simulations have not addressed any issues of coherency of ground motion, since the bridges are not very long in comparison to a seismic wavelength for the propagating wave (4000 meters/sec x period).

**Prof. Robert Herrmann**  
**Professor of St. Louis University**  
**St. Louis (MO)**



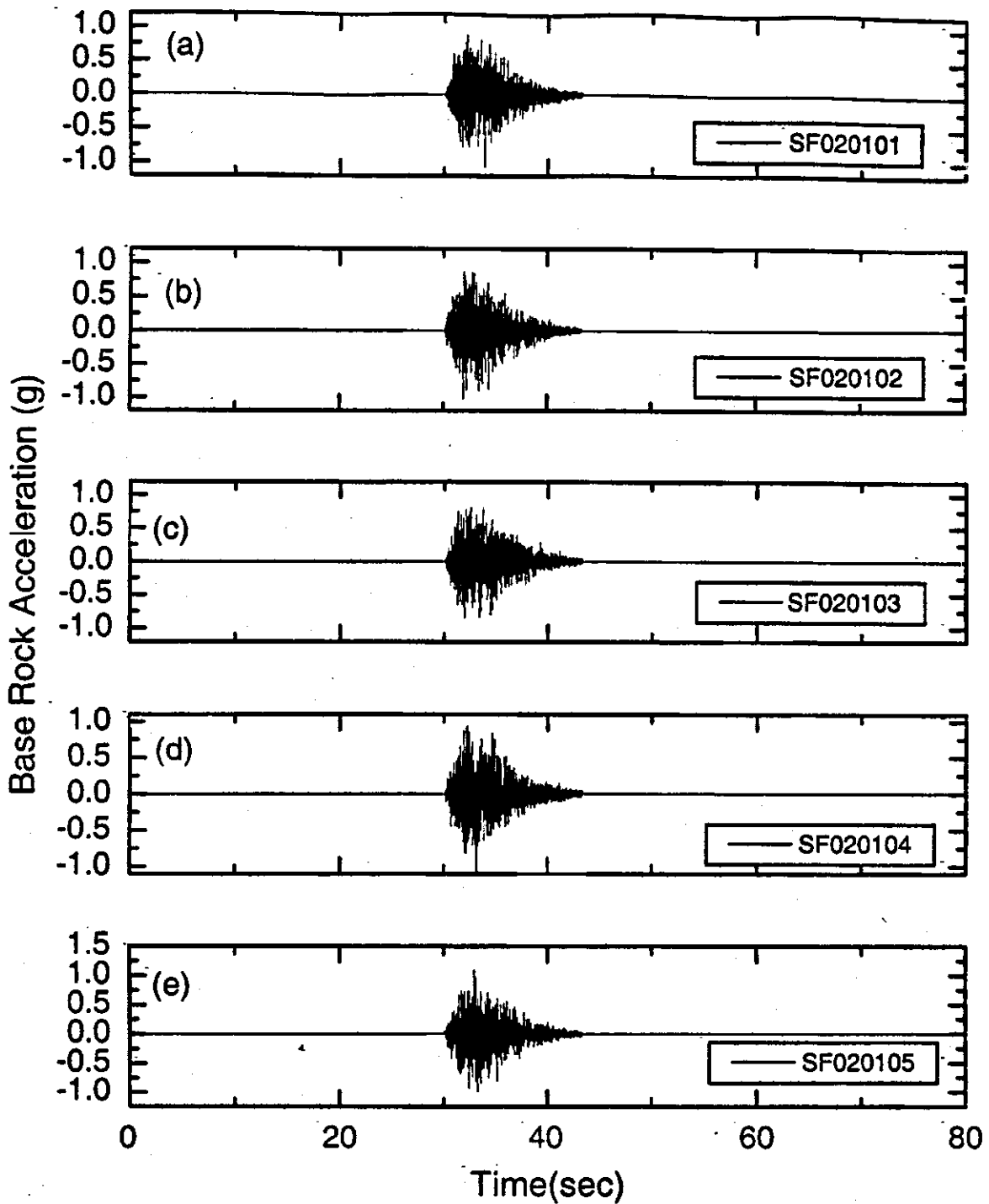
**PE 10 % in 50 years, Magnitude=6.2**

**Figure D.2 Acceleration Time Histories for St. Francis River Site, PE 10% in 50 Years  
M=6.2**



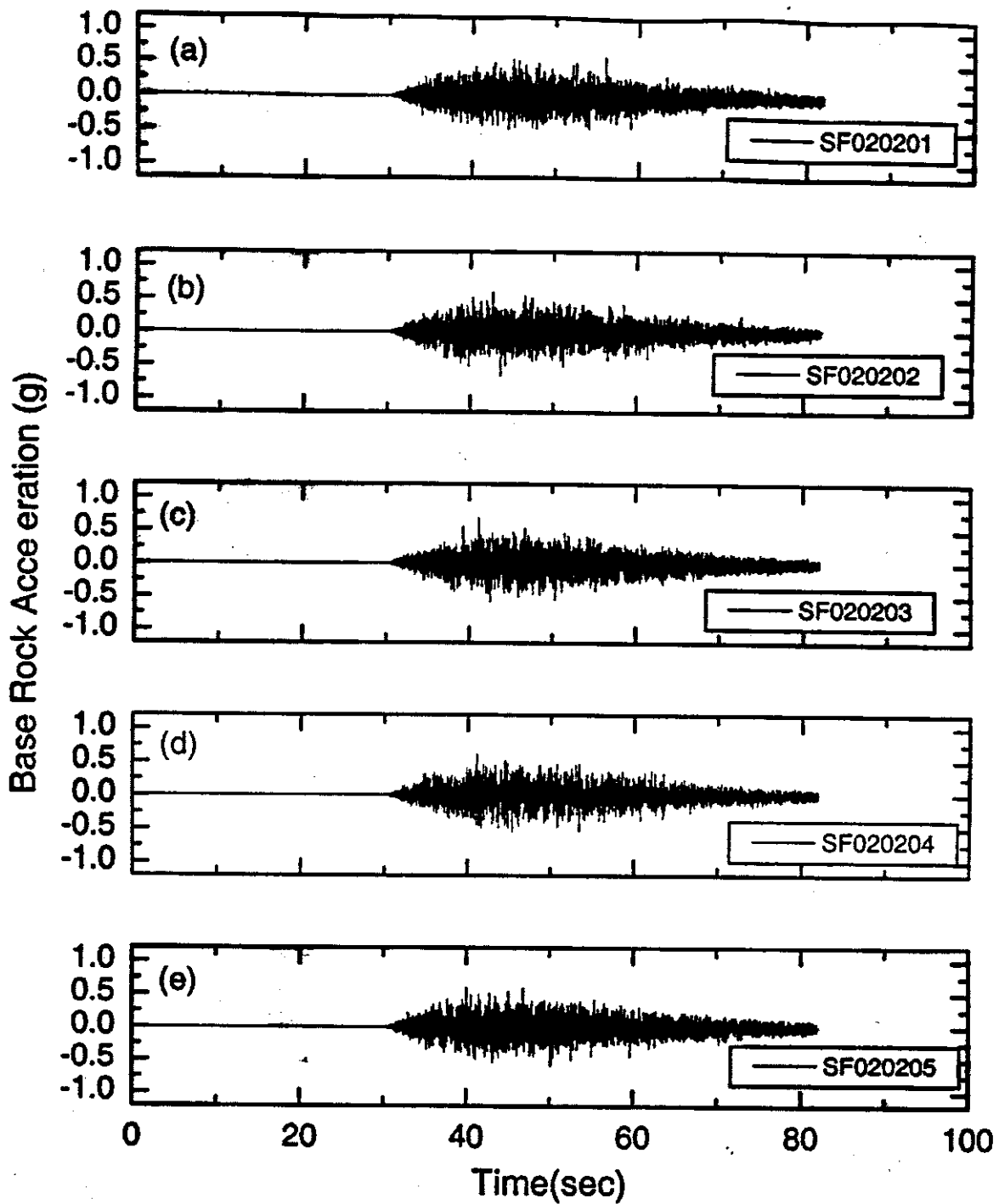
PE 10 % in 50 years, Magnitude=7.2

Figure D.3 Acceleration Time Histories for St. Francis River Site, PE 10% in 50 Years M=7.2



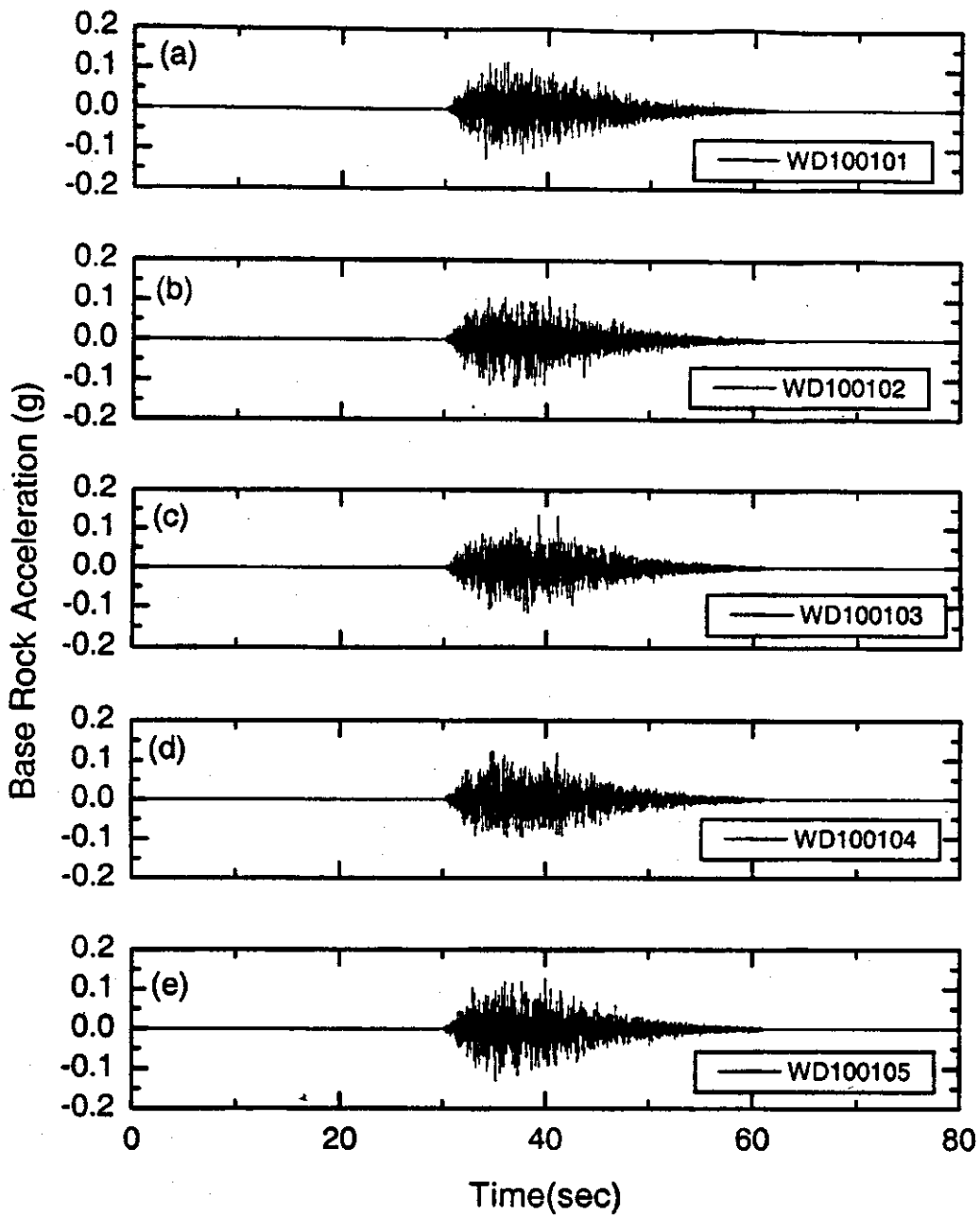
PE 2 % in 50 years, Magnitude=6.4

Figure D.4 Acceleration Time Histories for St. Francis River Site, PE 2% in 50 Years  
M=6.4



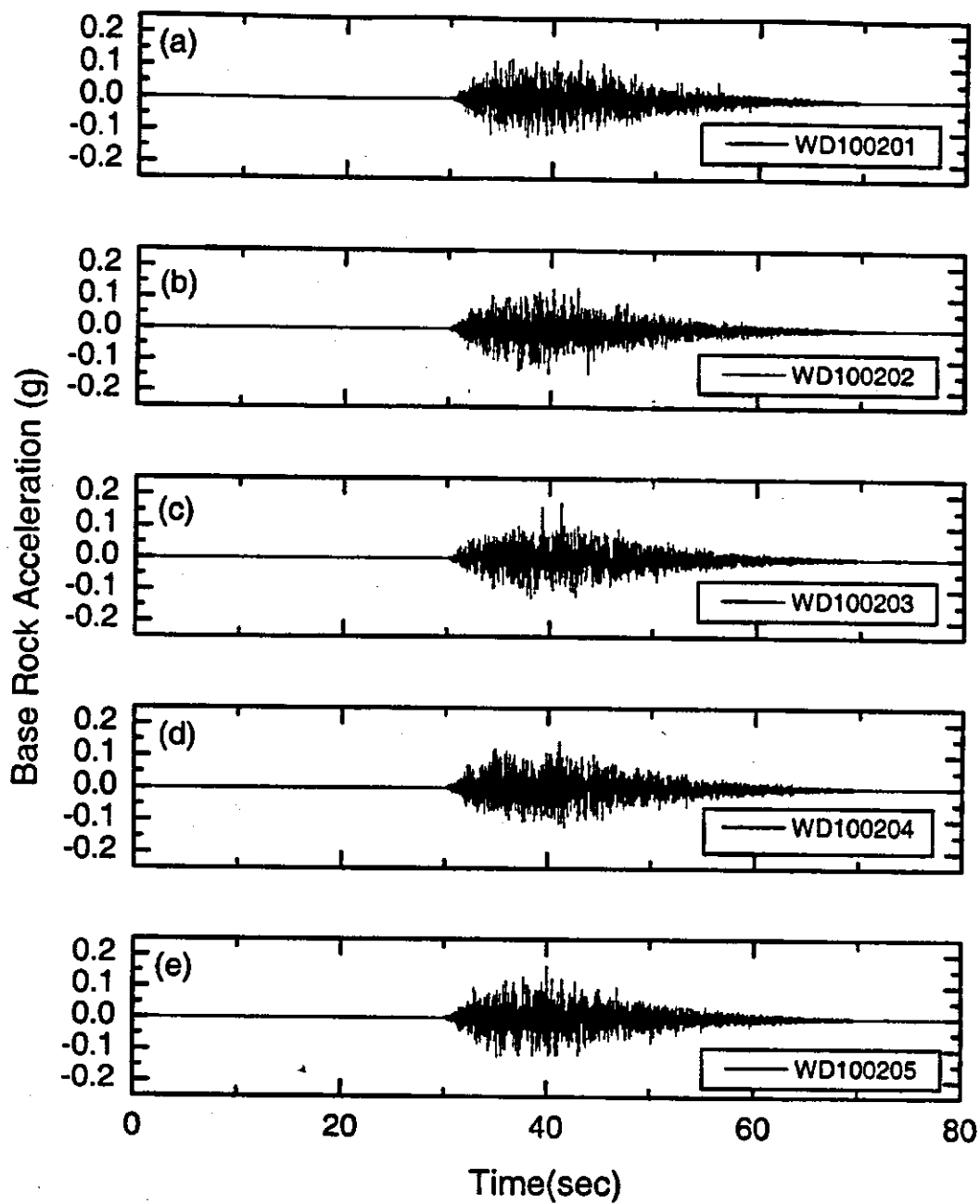
**PE 2 % in 50 years, Magnitude=8.0**

**Figure D.5 Acceleration Time Histories for St. Francis River Site, PE 2% in 50 Years M=8.0**



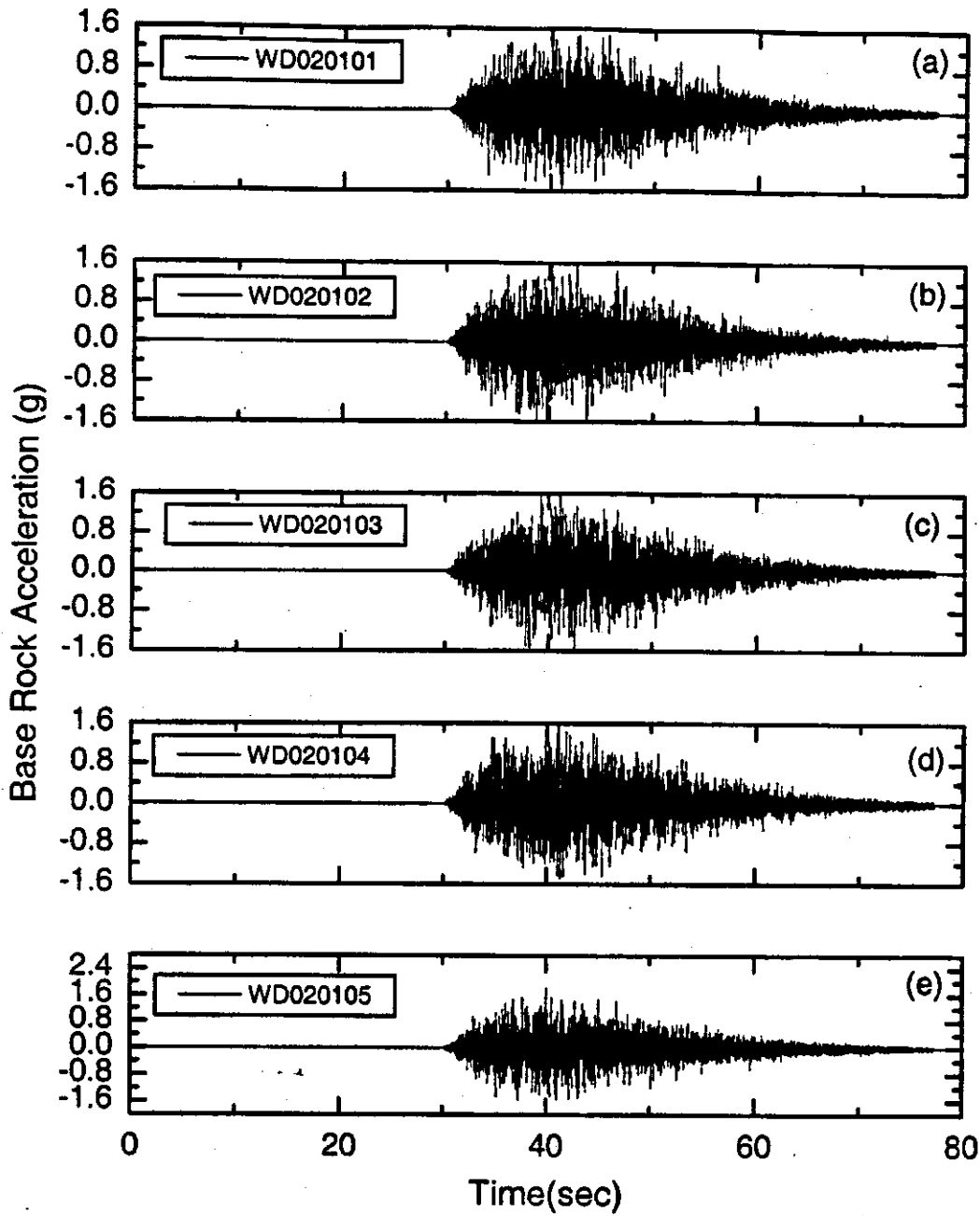
PE 10 % in 50 years, Magnitude=6.4

Figure D.6 Acceleration Time Histories for St. Francis River Site, PE 10% in 50 Years  
M=6.4



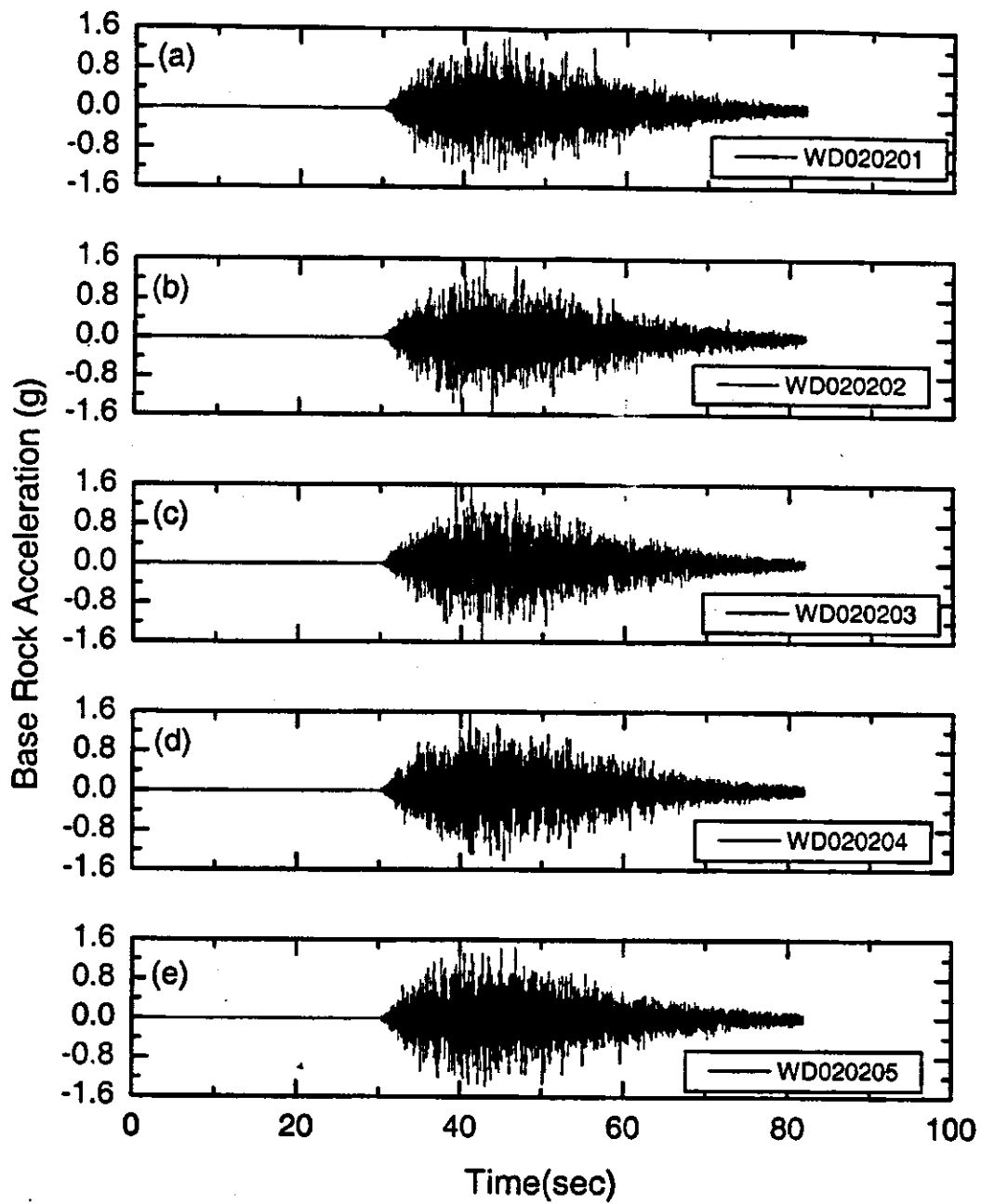
PE 10 % in 50 years, Magnitude=7.0

Figure D.7 Acceleration Time Histories for St. Francis River Site, PE 2% in 50 Years  
M=7.0



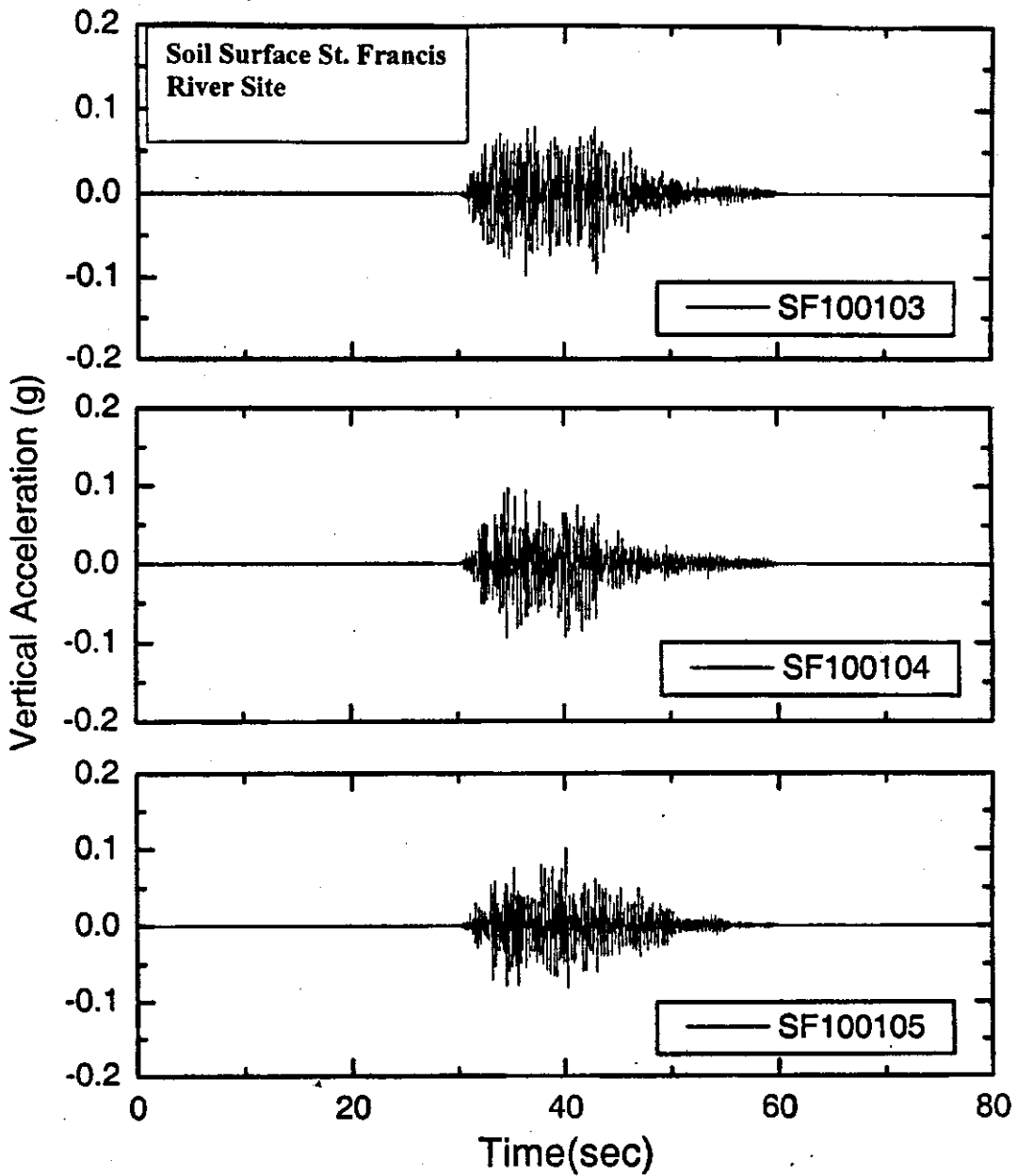
PE 2 % in 50 years, Magnitude=7.8

Figure D.8 Acceleration Time Histories for St. Francis River Site, PE 2% in 50 Years M=7.8



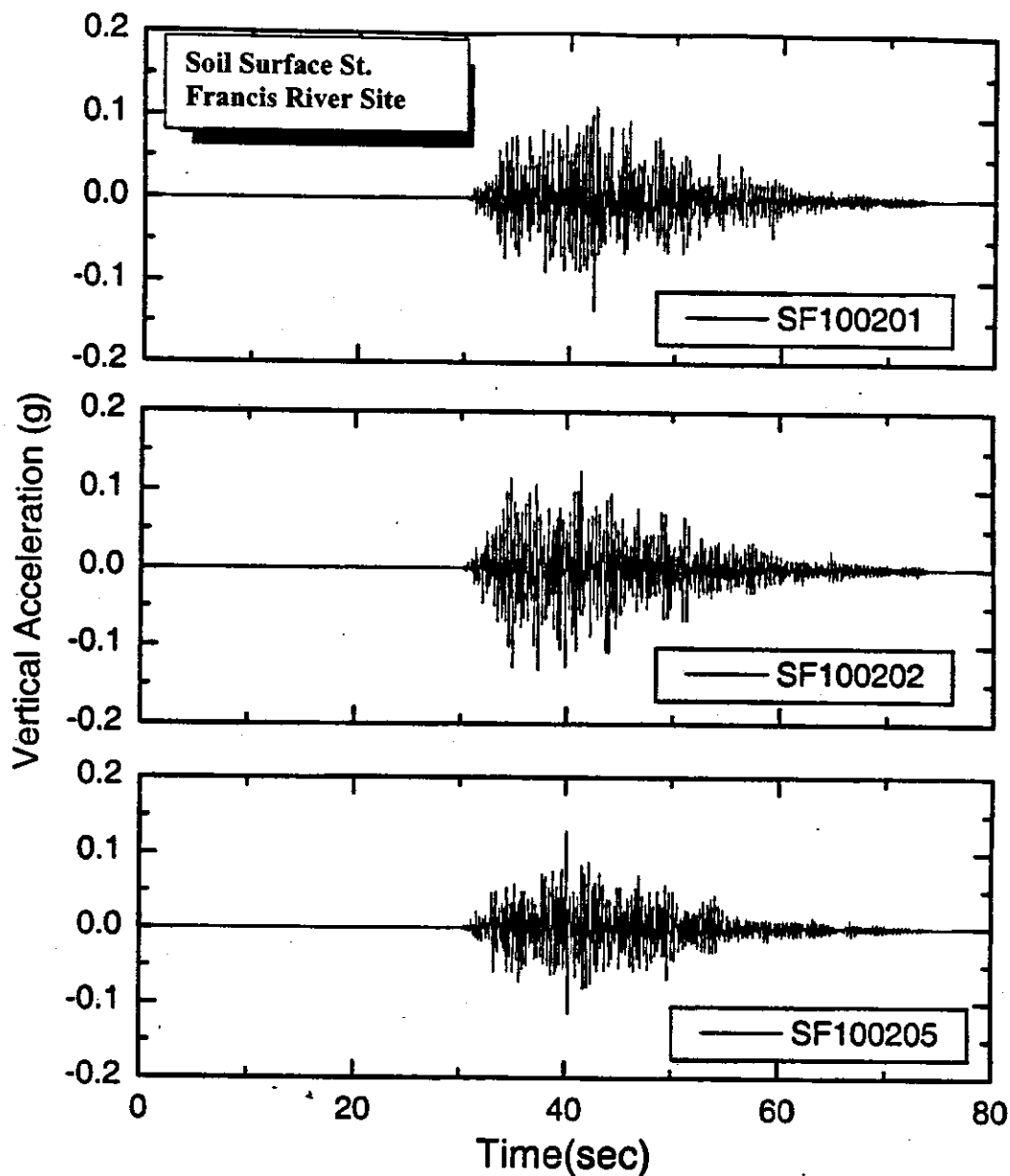
PE 2 % in 50 years, Magnitude=8.0

Figure D.9 Acceleration Time Histories for St. Francis River Site, PE 2% in 50 Years M=8.0



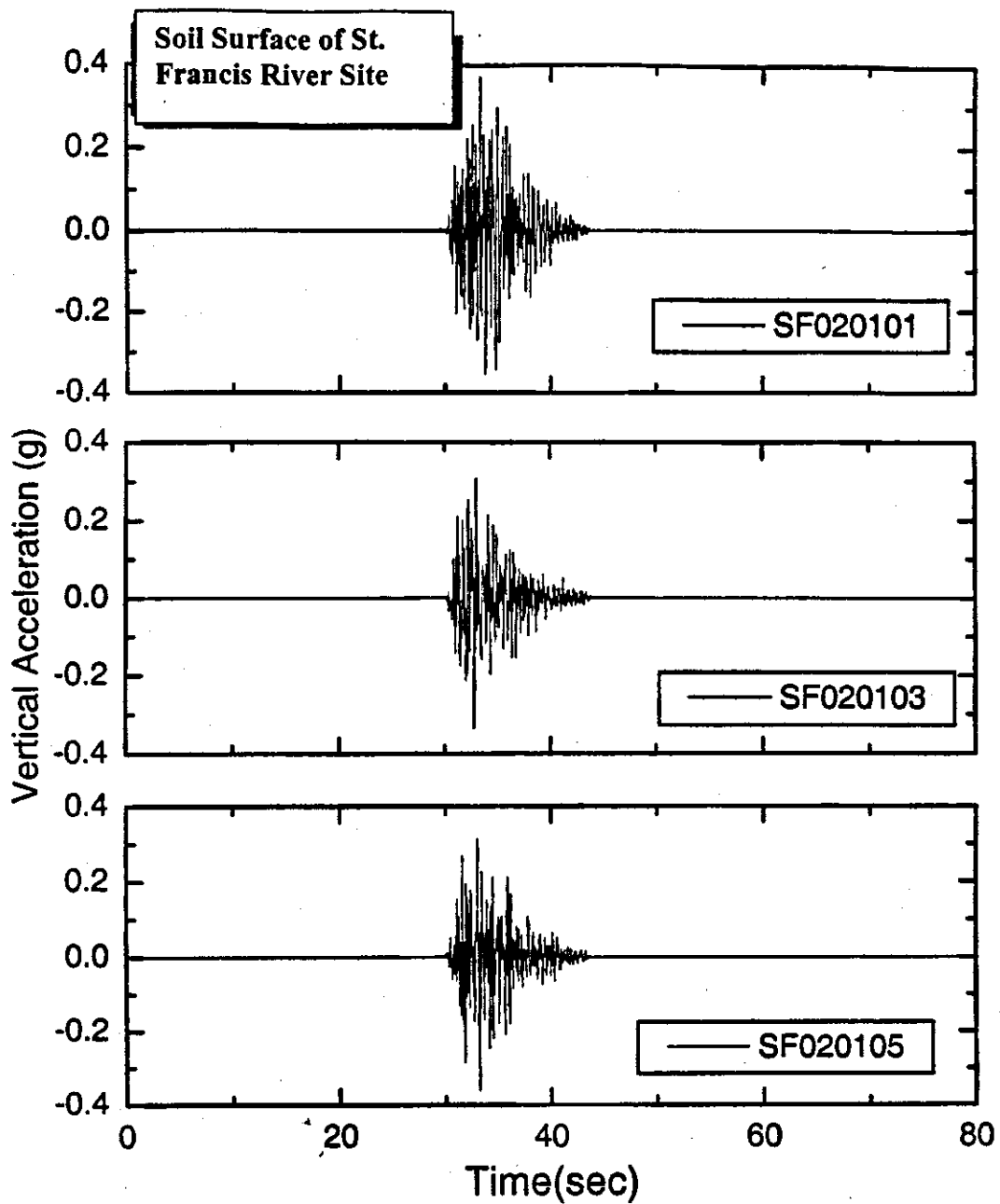
a. PE 10 % in 50 years, Magnitude = 6.2

Figure D.10a Time histories vertical acceleration at the soil surface of the St. Francis River Site, PE 10 % in 50 years, Magnitude=6.2



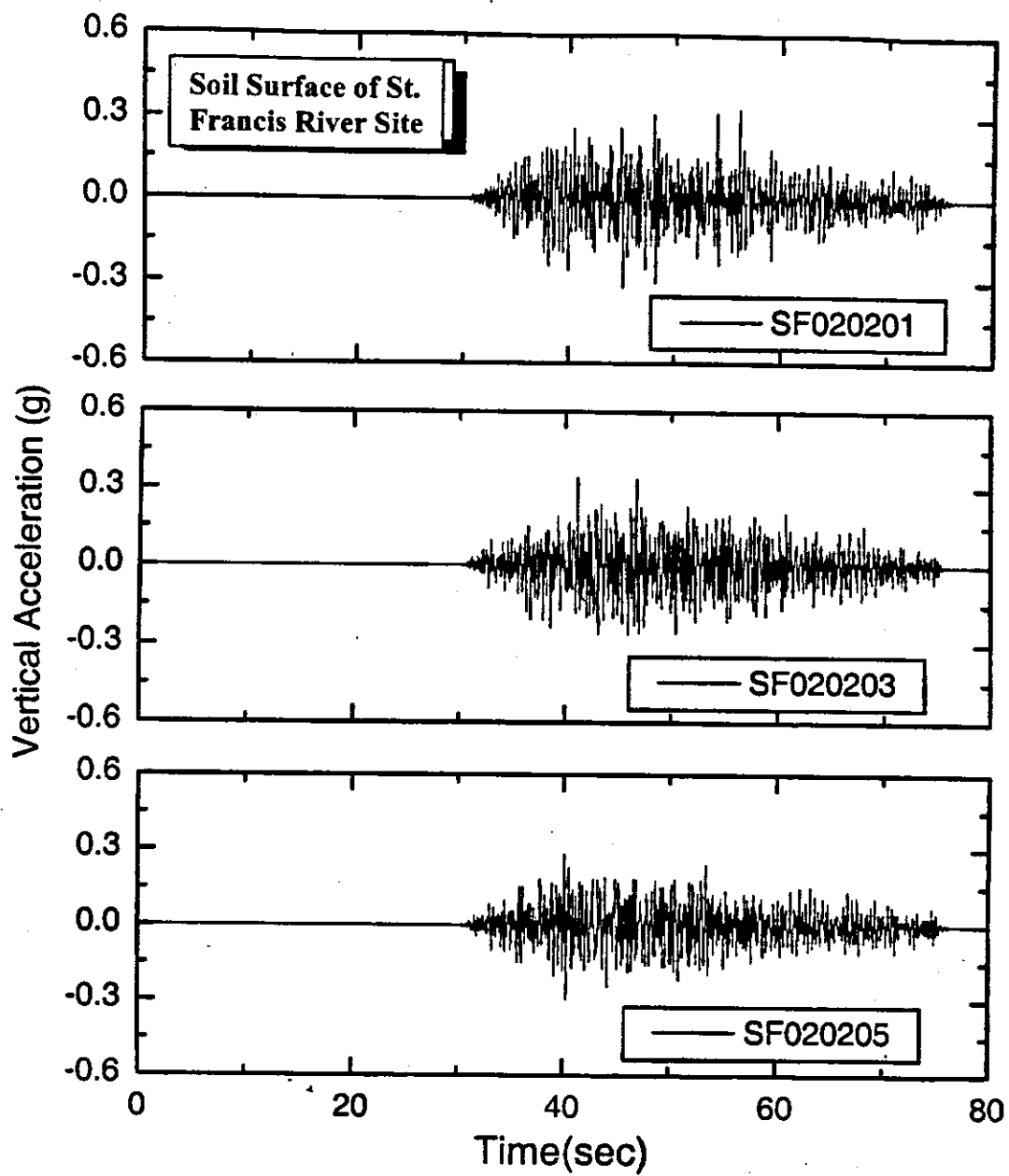
b. PE 10 % in 50 years, Magnitude = 7.2

Figure D.10b Time Histories Vertical Acceleration at the Soil Surface of the St. Francis River Site, PE 10 % in 50 years, Magnitude=7.2



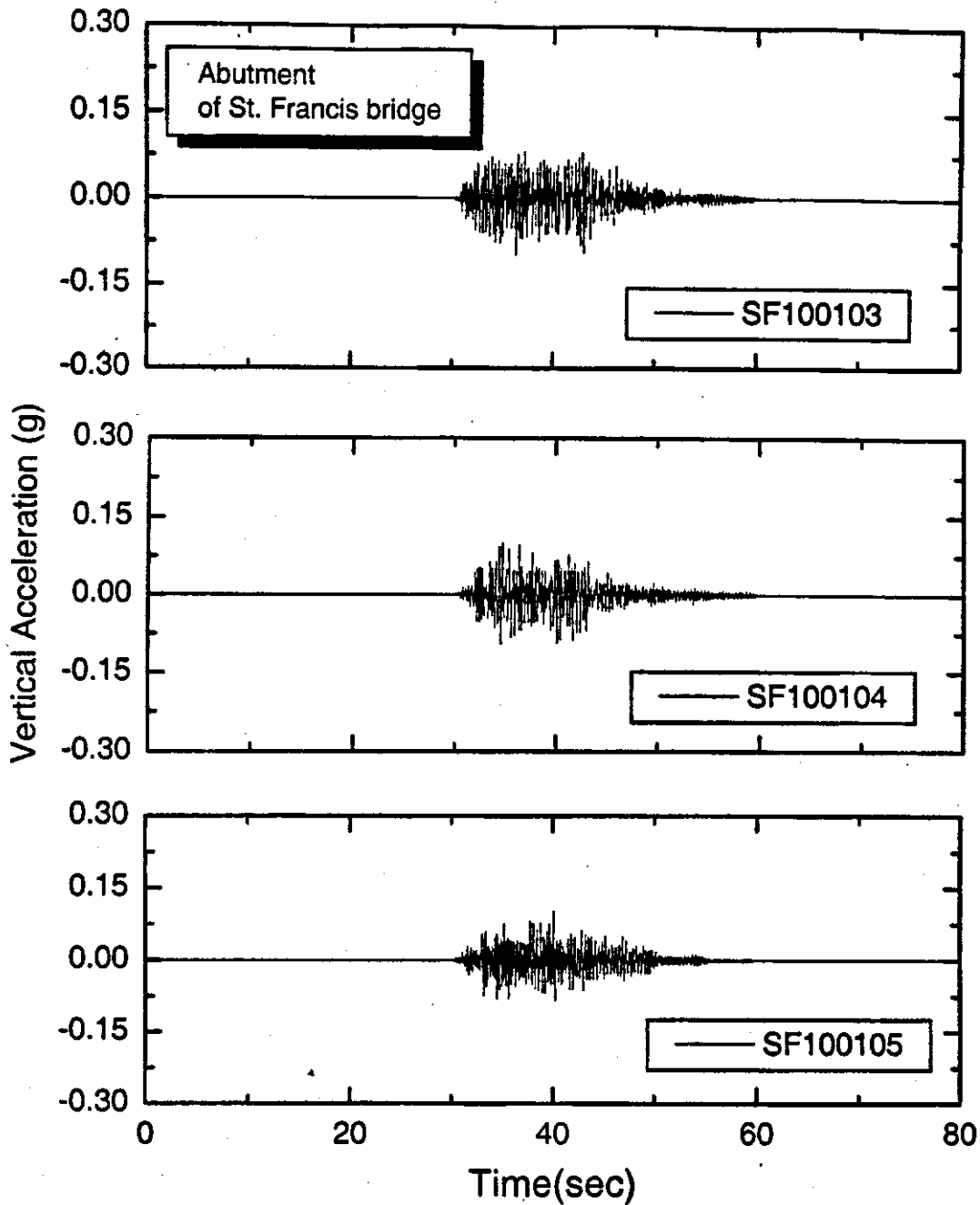
c. PE 2 % in 50 years, Magnitude = 6.4

Figure D.10c Time histories vertical acceleration at the soil surface of the St. Francis River Site, PE 10 % in 50 years, Magnitude=6.4



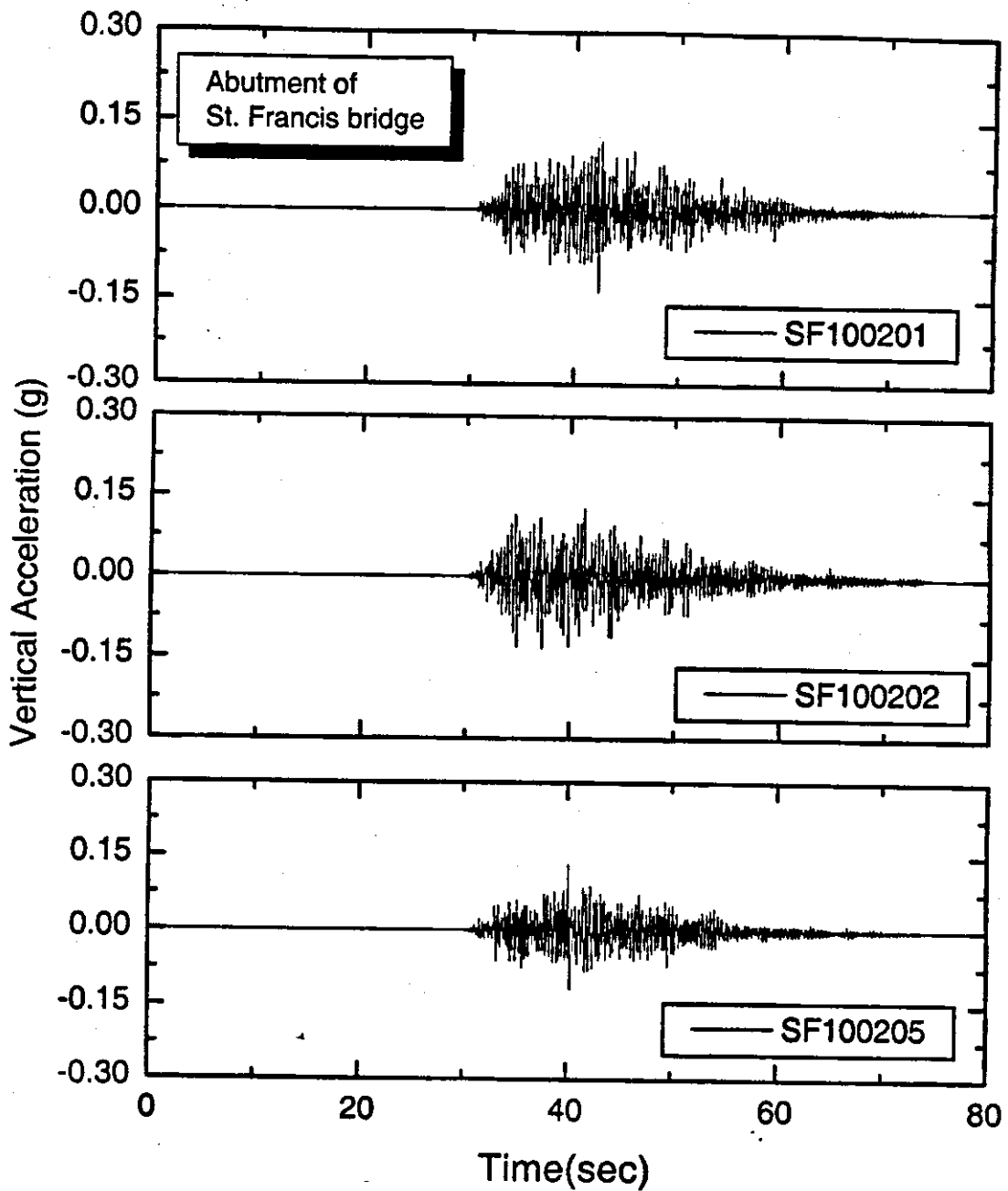
d. PE 2 % in 50 years, Magnitude = 8.0

Figure D.10d Time histories vertical acceleration at the soil surface of the St. Francis River Site, PE 10 % in 50 years, Magnitude=8.0



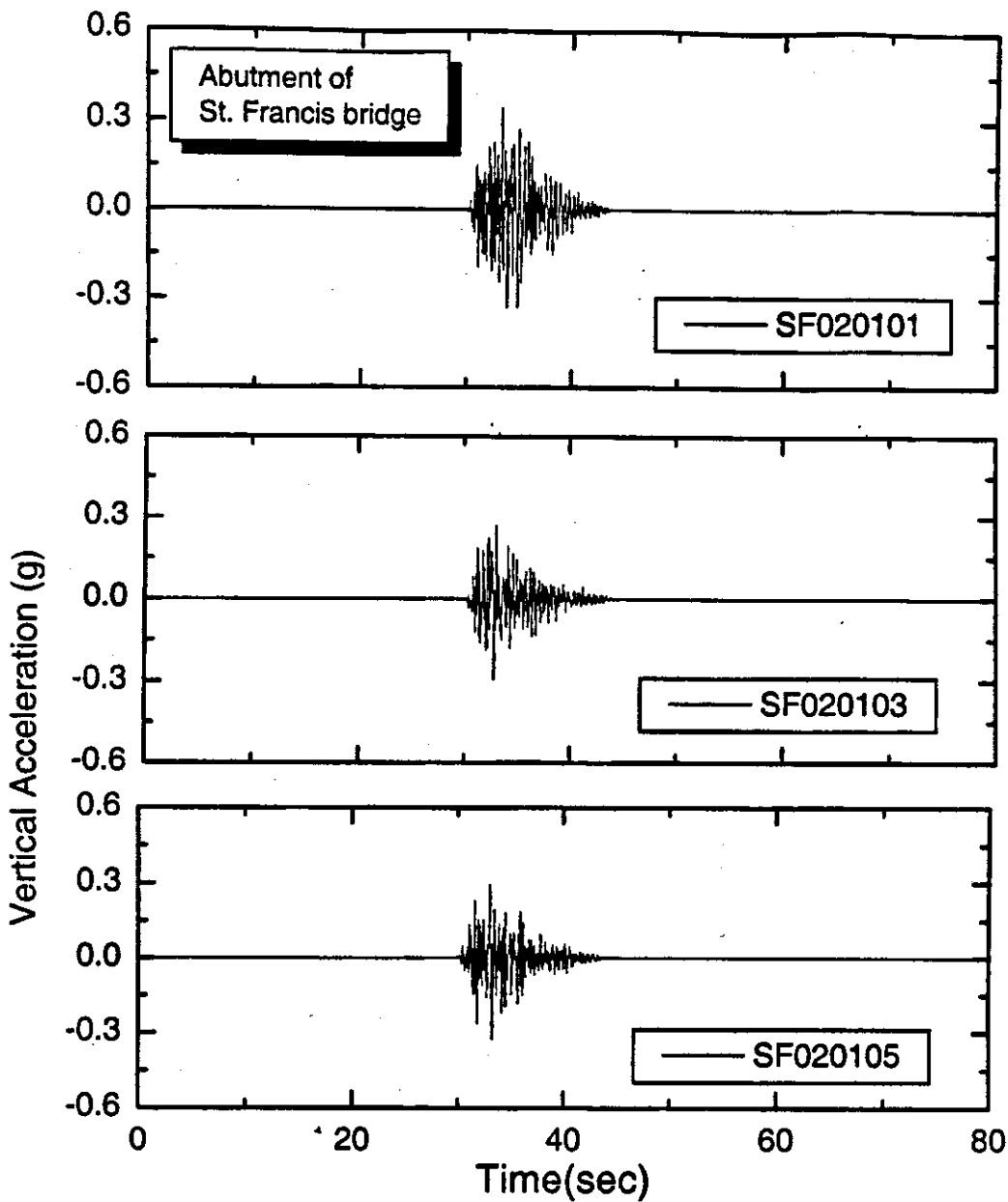
a. PE 10 % in 50 years, Magnitude = 6.2

Figure D.11a Time histories vertical acceleration at the bridge abutment of the St. Francis River Bridge; PE 10 % in 50 years, Magnitude=6.2



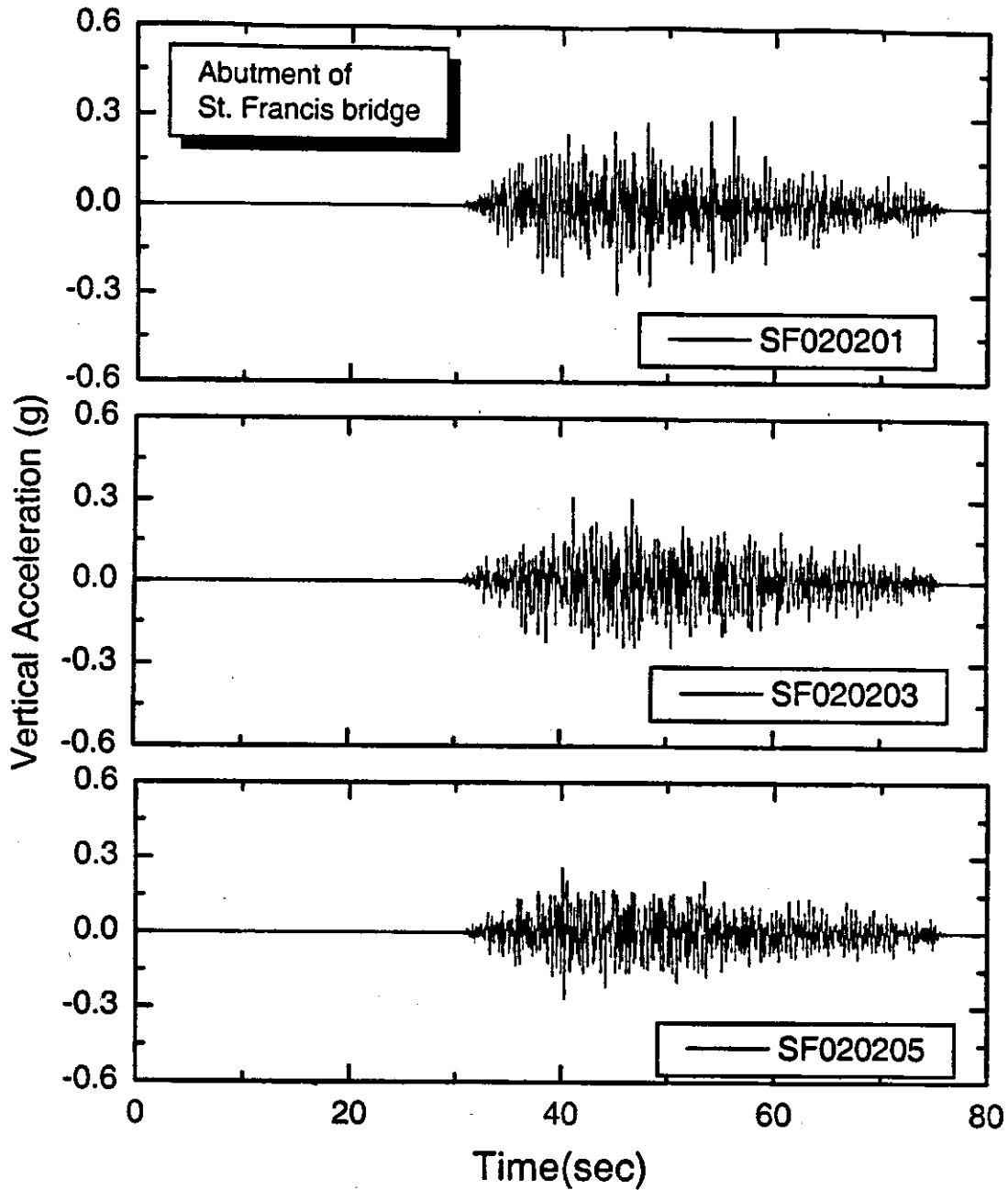
b. PE 10 % in 50 years, Magnitude = 7.2

Figure D.11b Time histories vertical acceleration at the bridge abutment of the St. Francis River Bridge, PE 10 % in 50 years, Magnitude=7.2



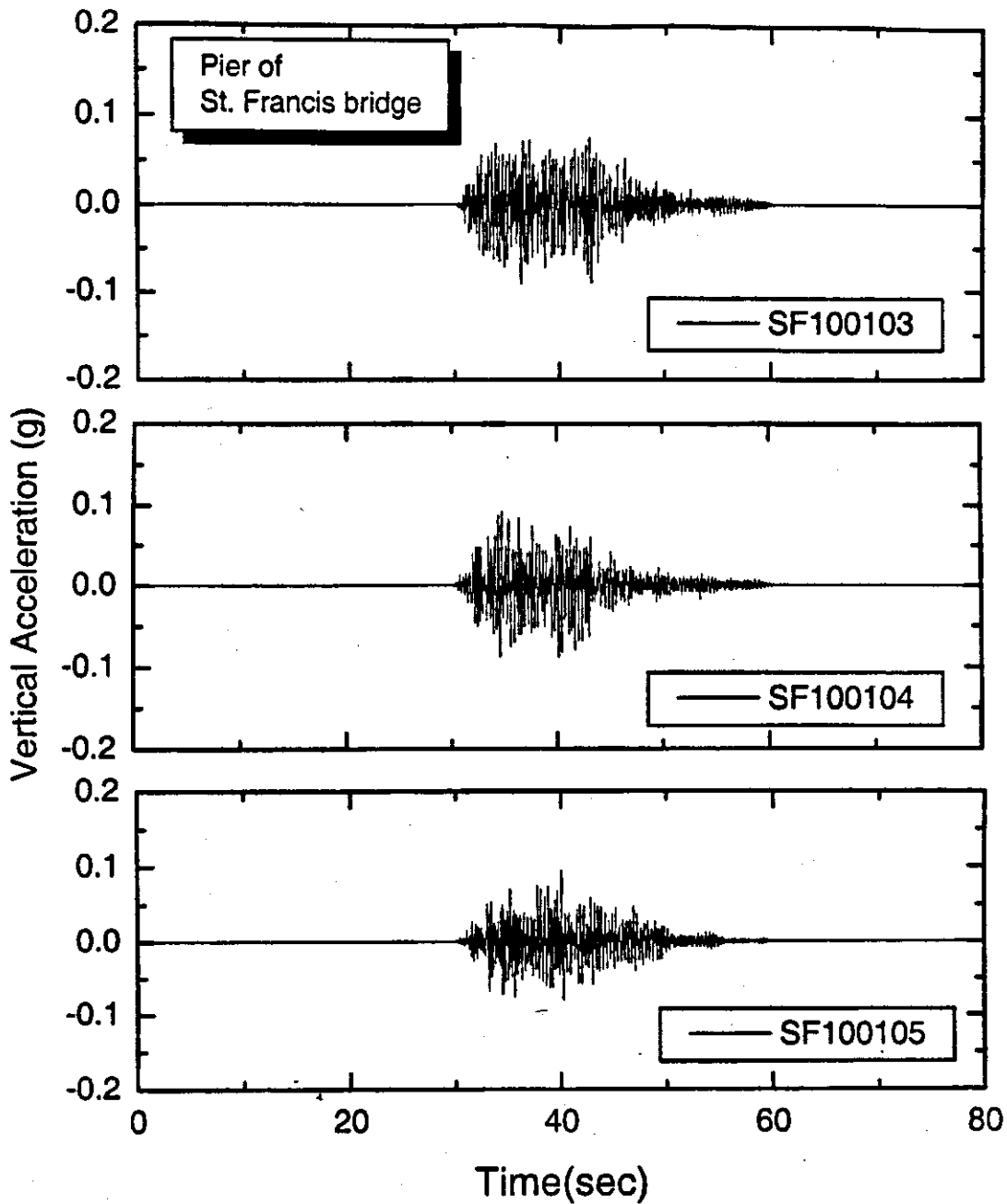
c. PE 2 % in 50 years, Magnitude = 6.4

**Figure D.11c** Time histories vertical acceleration at the bridge abutment of the St. Francis River Bridge, PE 10 % in 50 years, Magnitude=6.4



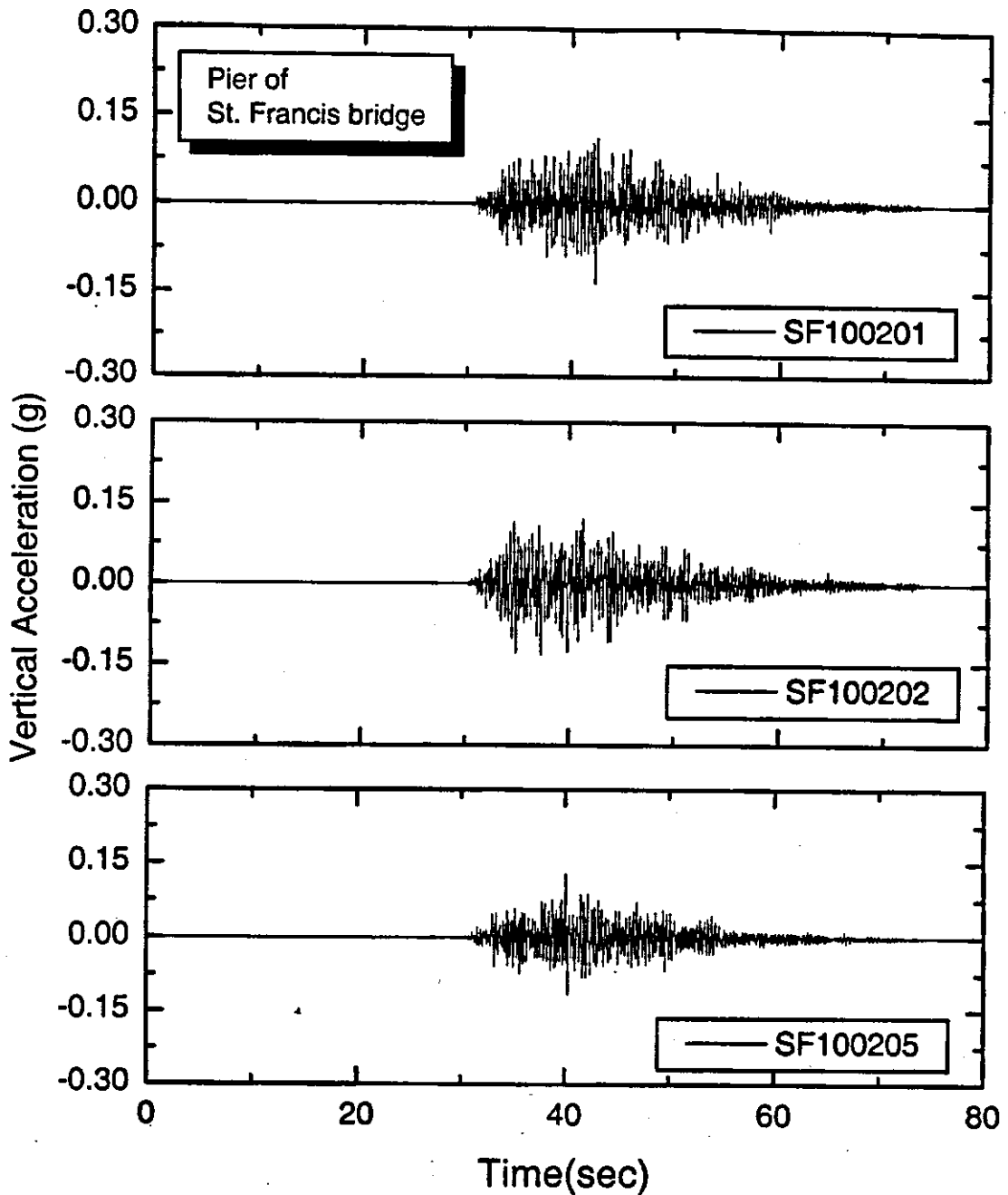
d. PE 2 % in 50 years, Magnitude = 8.0

Figure D.11d Time histories vertical acceleration at the bridge abutment of the St. Francis River Bridge, PE 10 % in 50 years, Magnitude=8.0



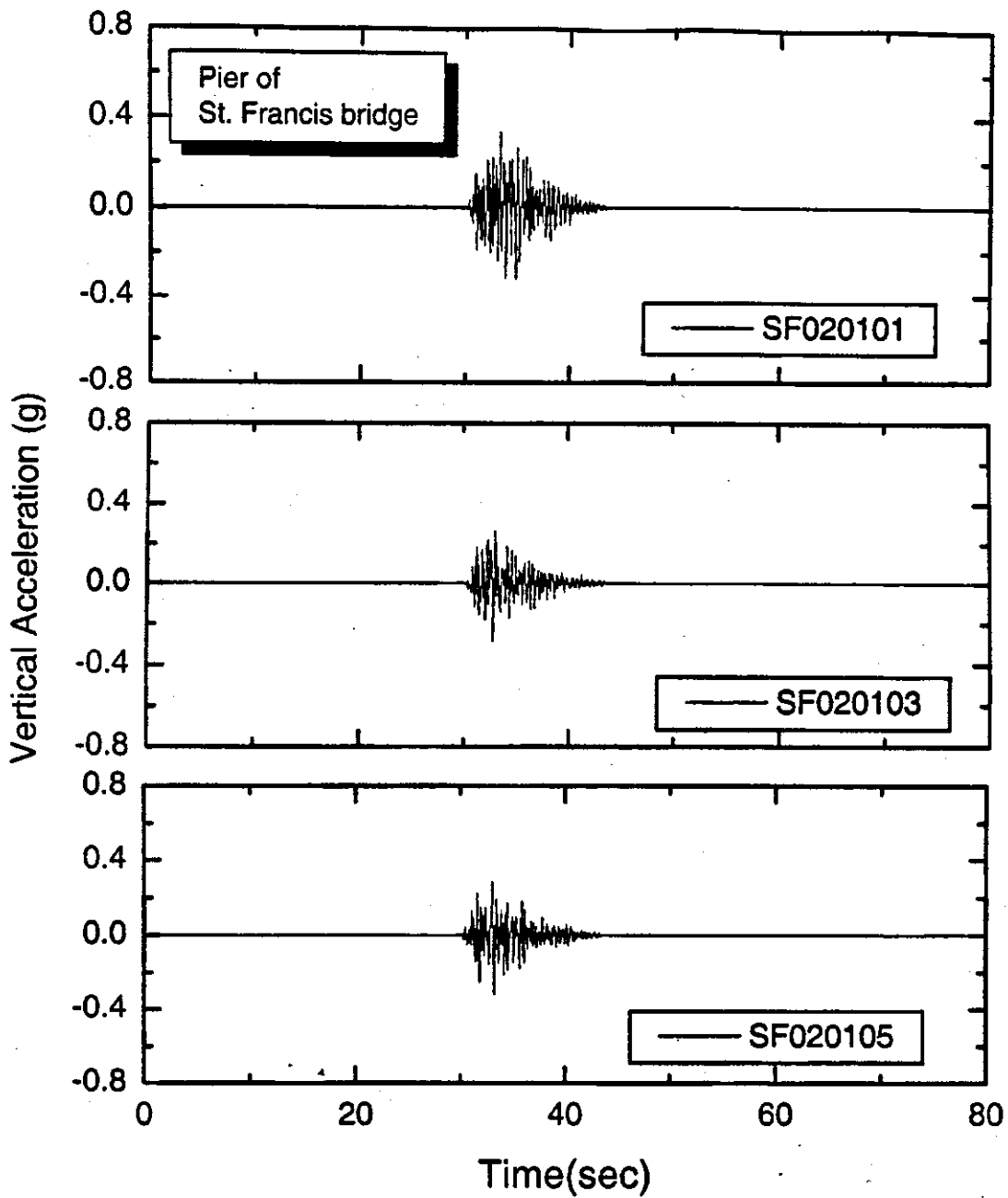
a. PE 10 % in 50 years, Magnitude = 6.2

Figure D.12a Time Histories Vertical Acceleration at the Bridge Pier, St. Francis River Bridge, PE 10 % in 50 years, Magnitude=6.2



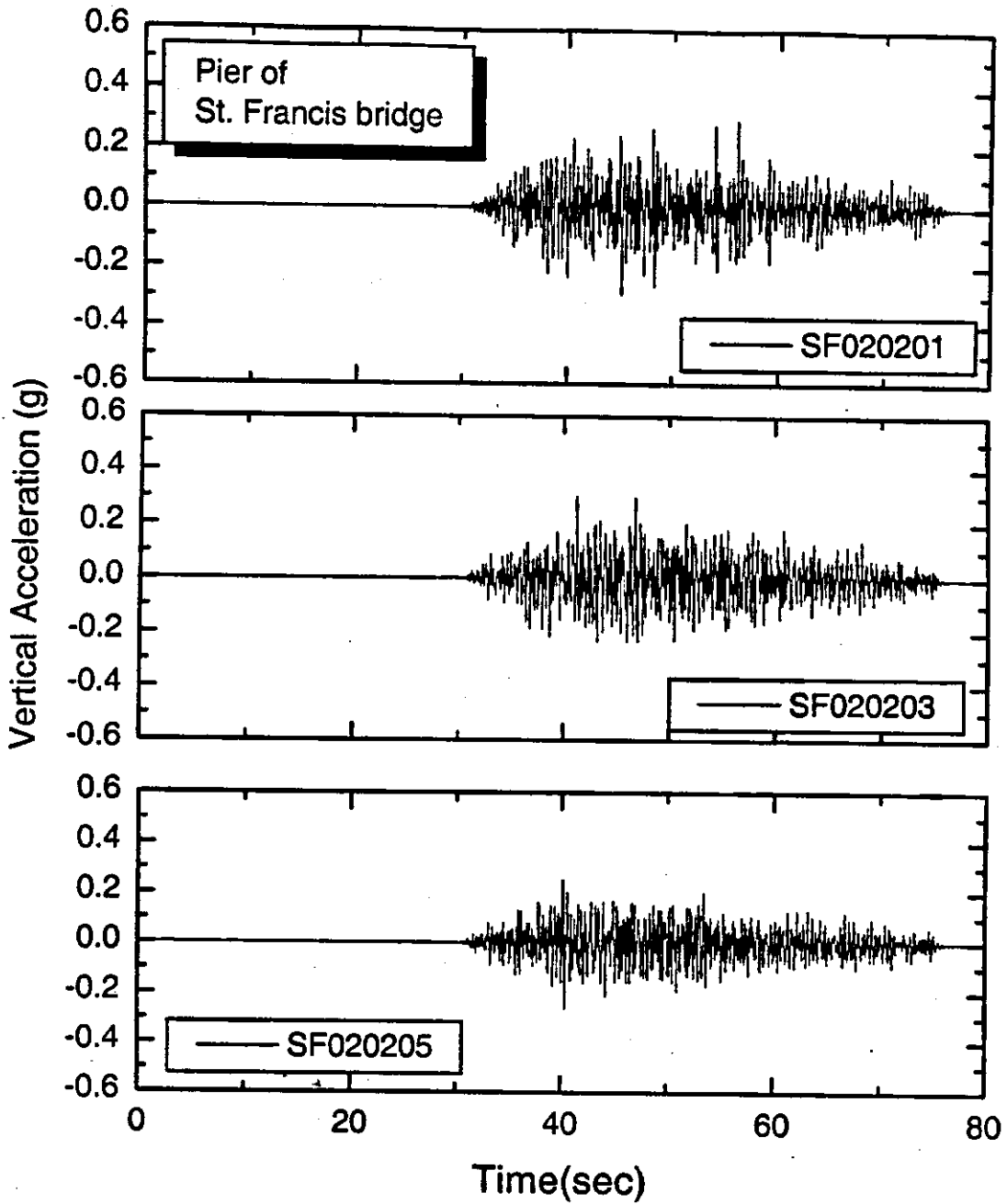
b. PE 10 % in 50 years, Magnitude = 7.2

Figure D.12b Time Histories Vertical Acceleration at the Bridge Pier, St. Francis River Bridge, PE 10 % in 50 years, Magnitude=7.2



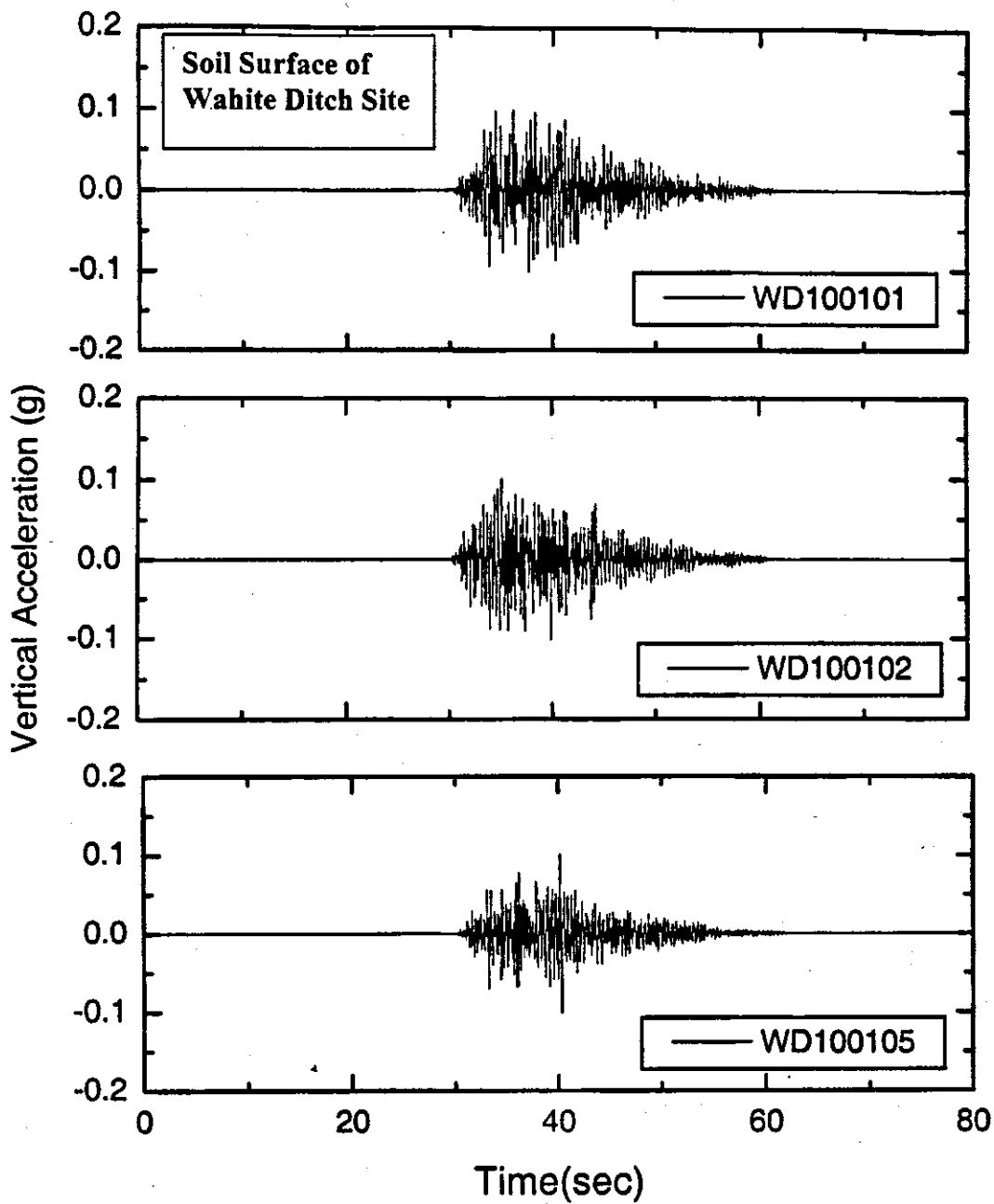
c. PE 2 % in 50 years, Magnitude = 6.4

Figure D.12c Time Histories Vertical Acceleration at the Bridge Pier, St. Francis River Bridge, PE 2 % in 50 years, Magnitude=6.4



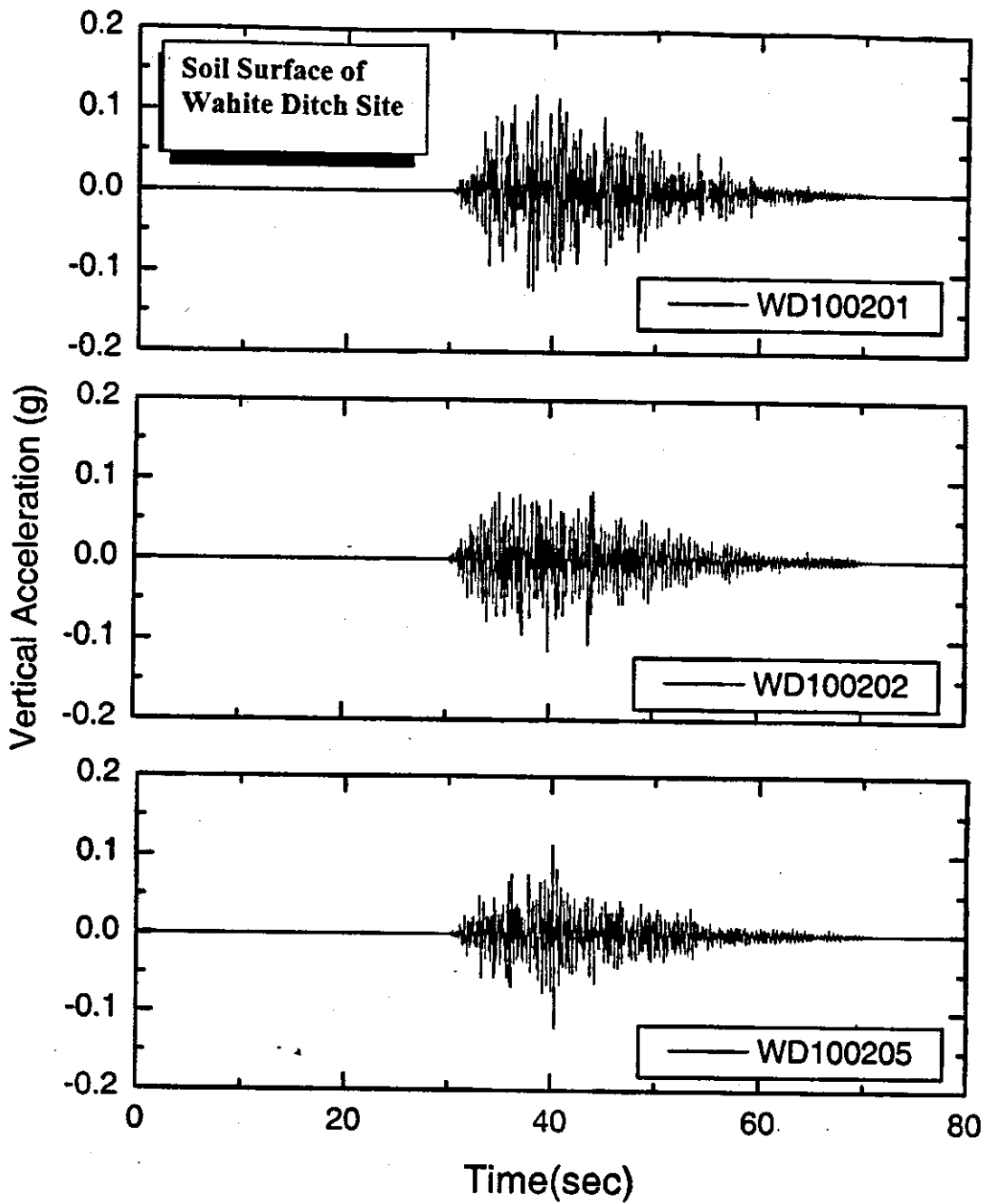
d. PE 2 % in 50 years, Magnitude = 8.0

Figure D.12d Time Histories Vertical Acceleration at the Bridge Pier, St. Francis River Bridge, PE 2 % in 50 years, Magnitude=8.0



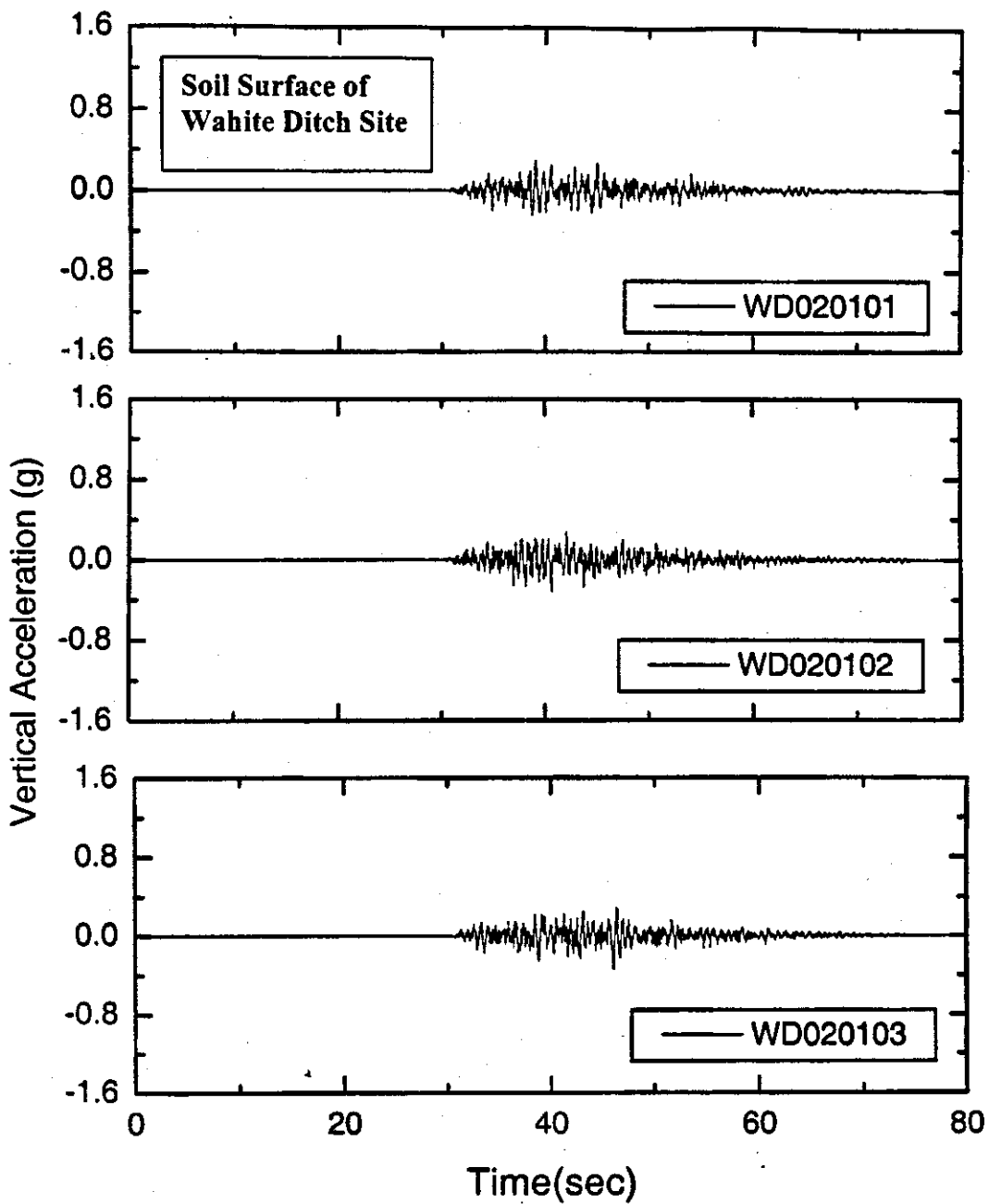
a. PE 10 % in 50 years, Magnitude = 6.4

Figure D.13a Time Histories Vertical Acceleration at the Soil Surface, Wahite Ditch Site, PE 10 % in 50 years, Magnitude=6.4



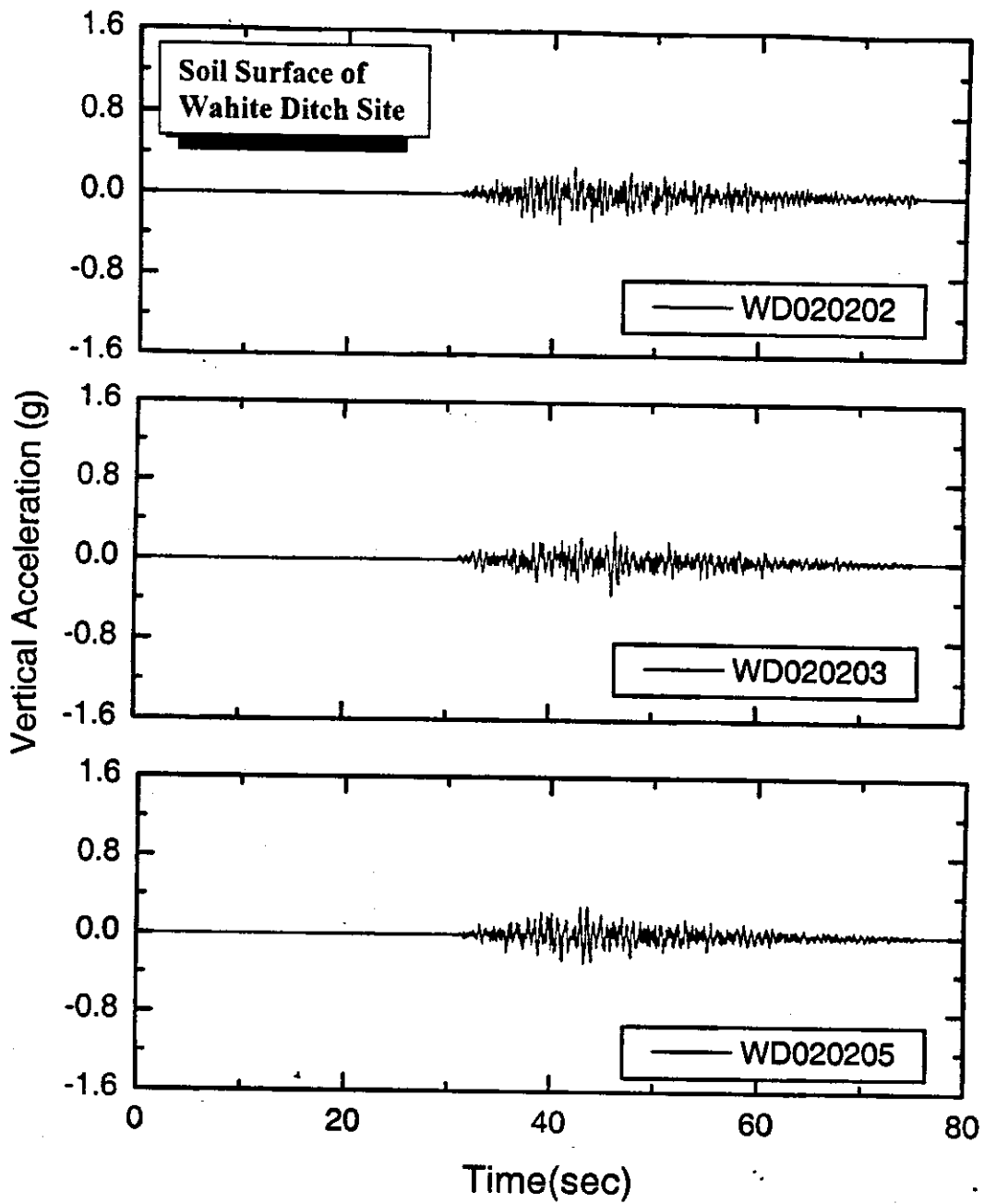
b. PE 10 % in 50 years, Magnitude = 7.0

Figure D.13b Time Histories Vertical Acceleration at the Soil Surface, Wahite Ditch Site, PE 10 % in 50 years, Magnitude=7.0



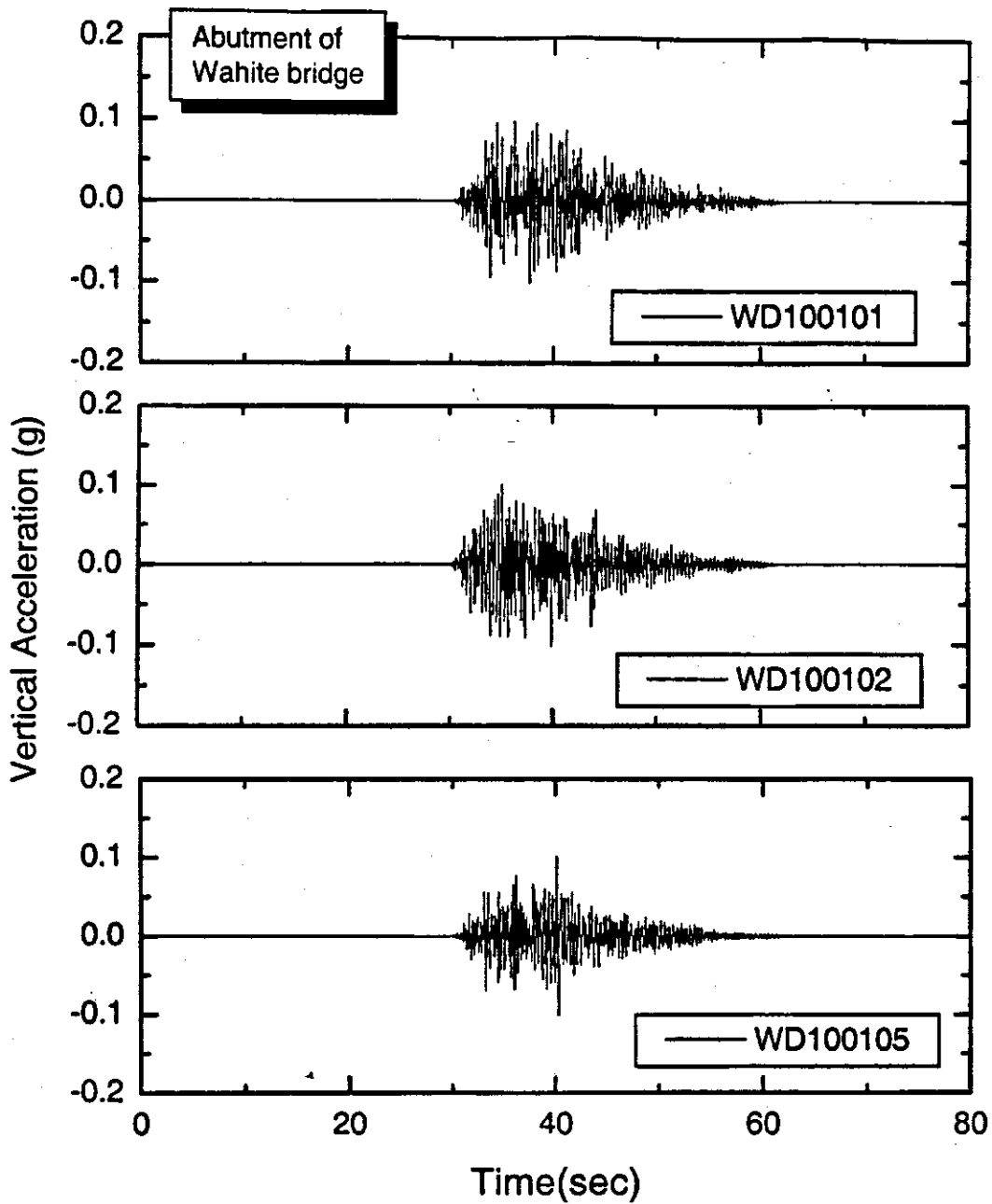
c. PE 2 % in 50 years, Magnitude = 7.8

Figure D.13c Time Histories Vertical Acceleration at the Soil Surface, Wahite Ditch Site, PE 2 % in 50 years, Magnitude=7.8



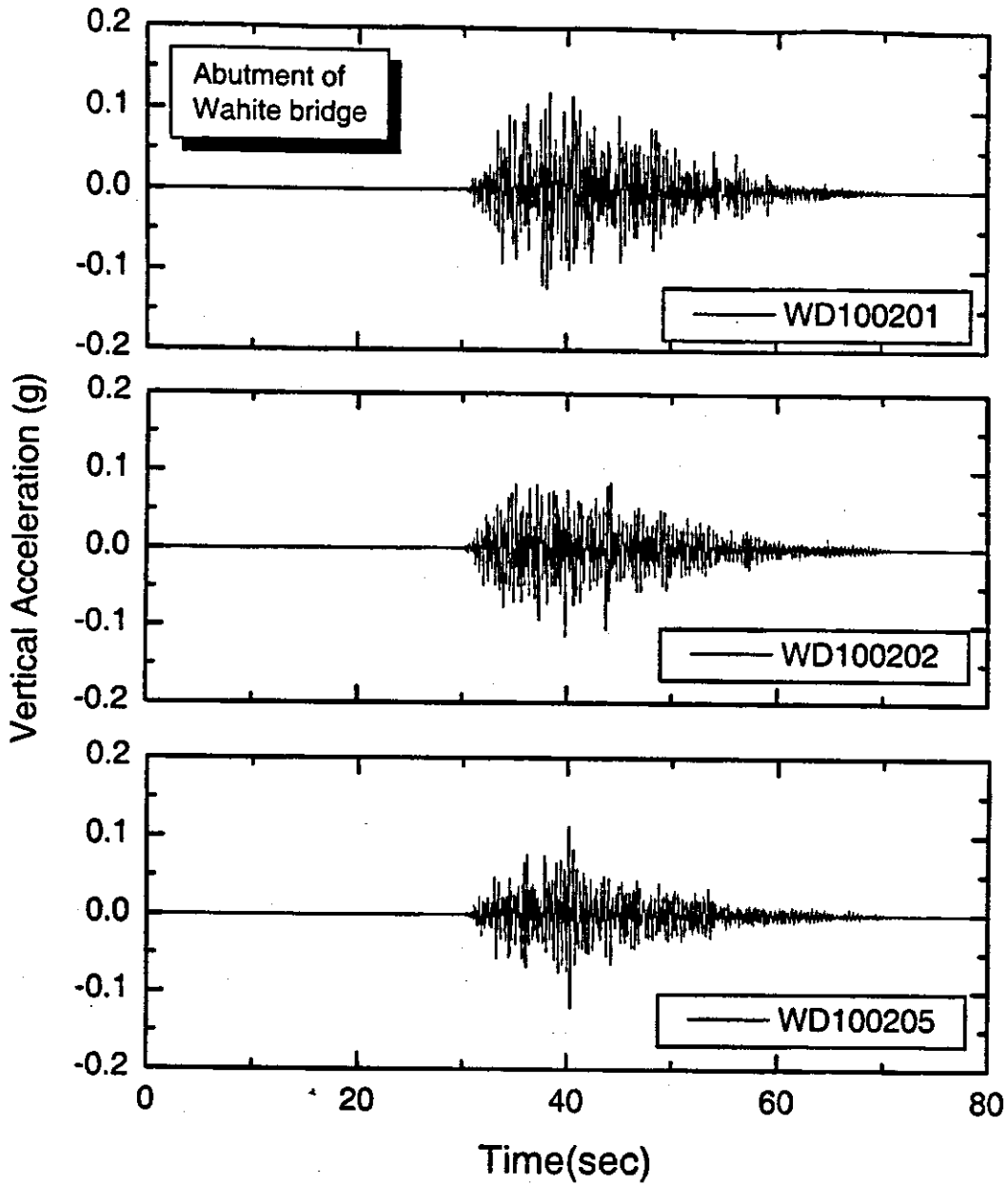
d. PE 2 % in 50 years, Magnitude = 8.0

Figure D.13d Time Histories Vertical Acceleration at the Soil Surface, Wahite Ditch Bridge Site, PE 2 % in 50 years, Magnitude=8.0



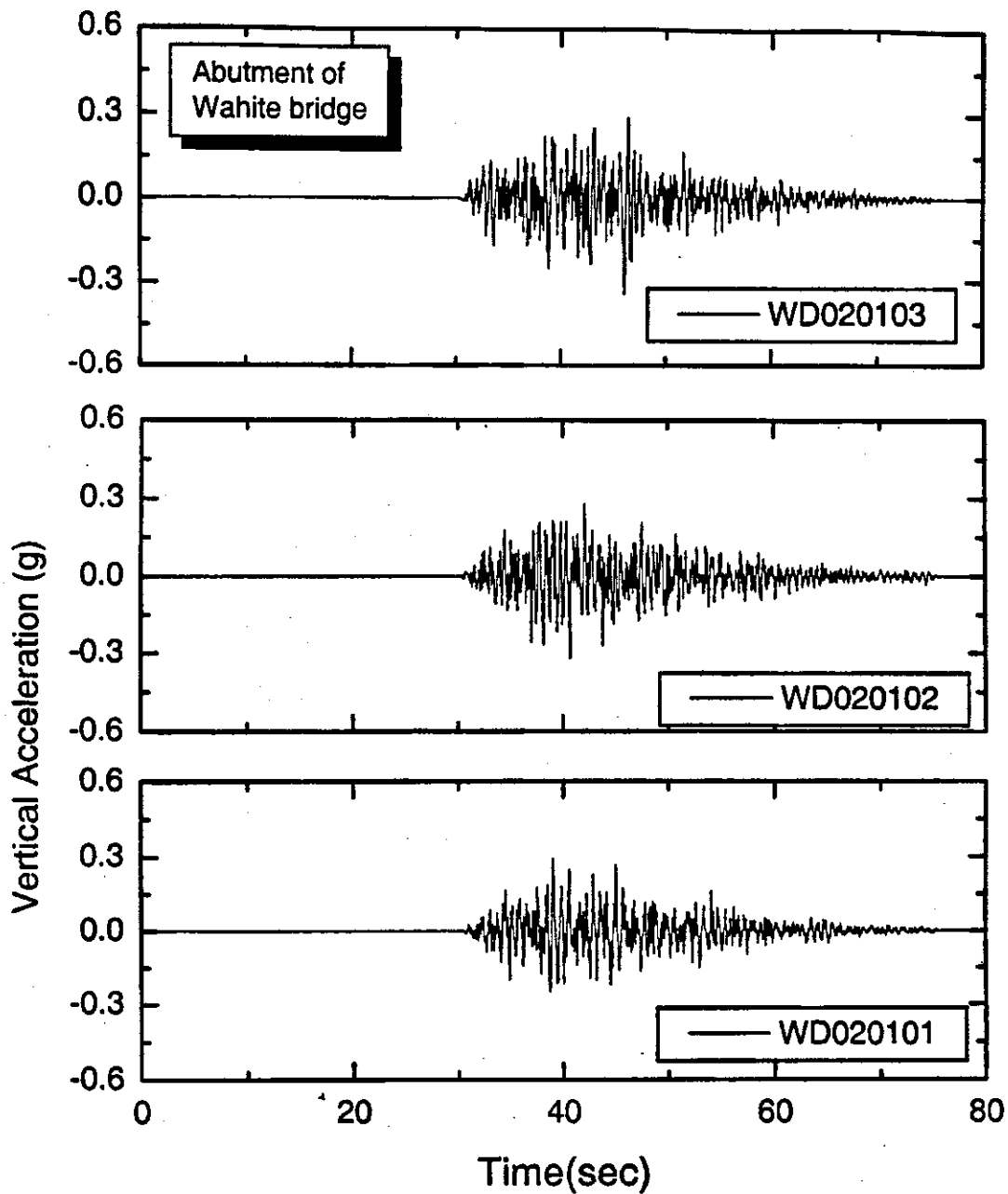
a. PE 10 % in 50 years, Magnitude = 6.4

**Figure D.14a** Time Histories Vertical Acceleration at the Bridge Abutment, Wahite Ditch Site, PE 10 % in 50 years, Magnitude=6.4



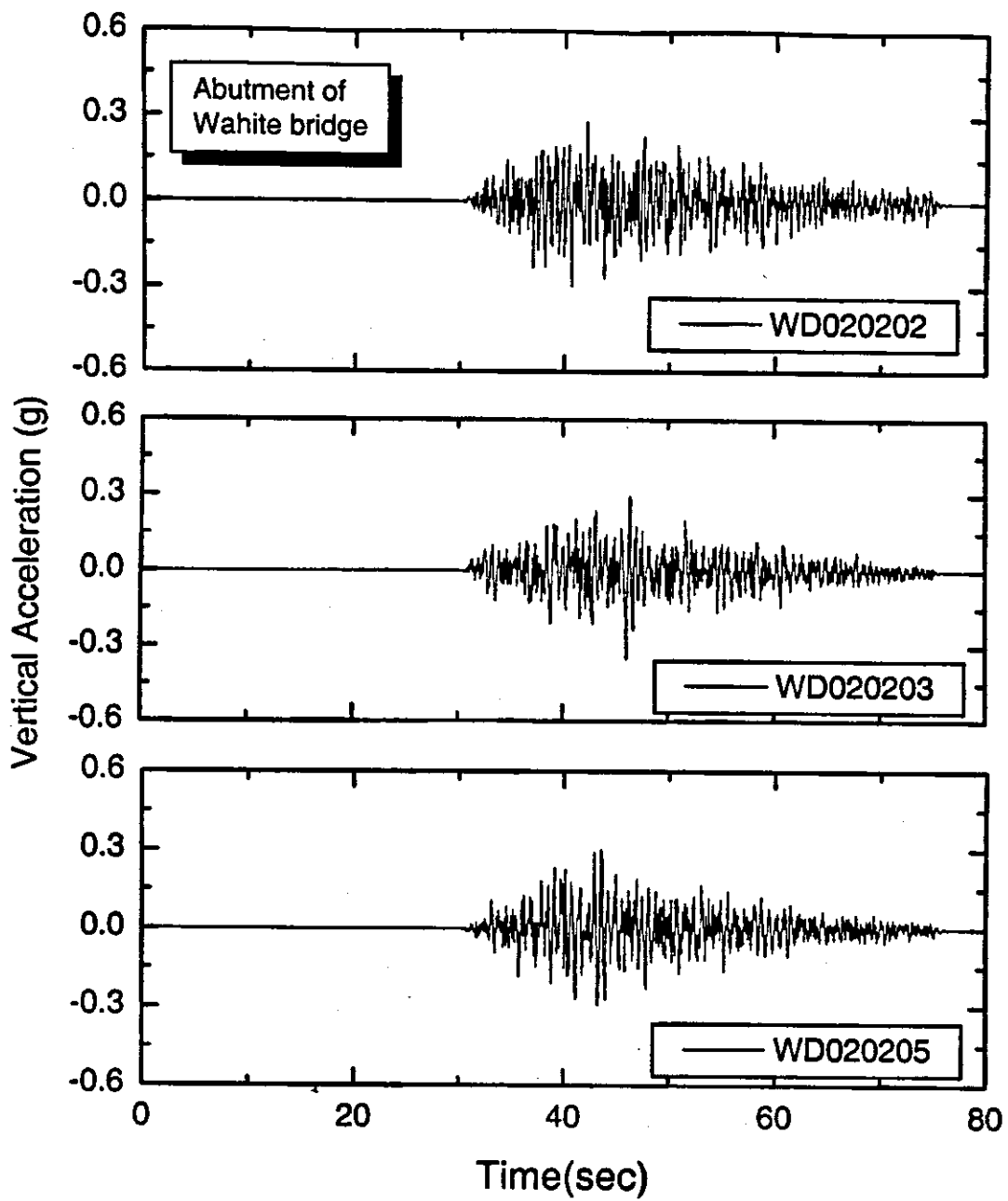
b. PE 10 % in 50 years, Magnitude = 7.0

Figure D.14b Time Histories Vertical Acceleration at the Bridge Abutment, Wahite Ditch Site, PE 10 % in 50 years, Magnitude=7.0



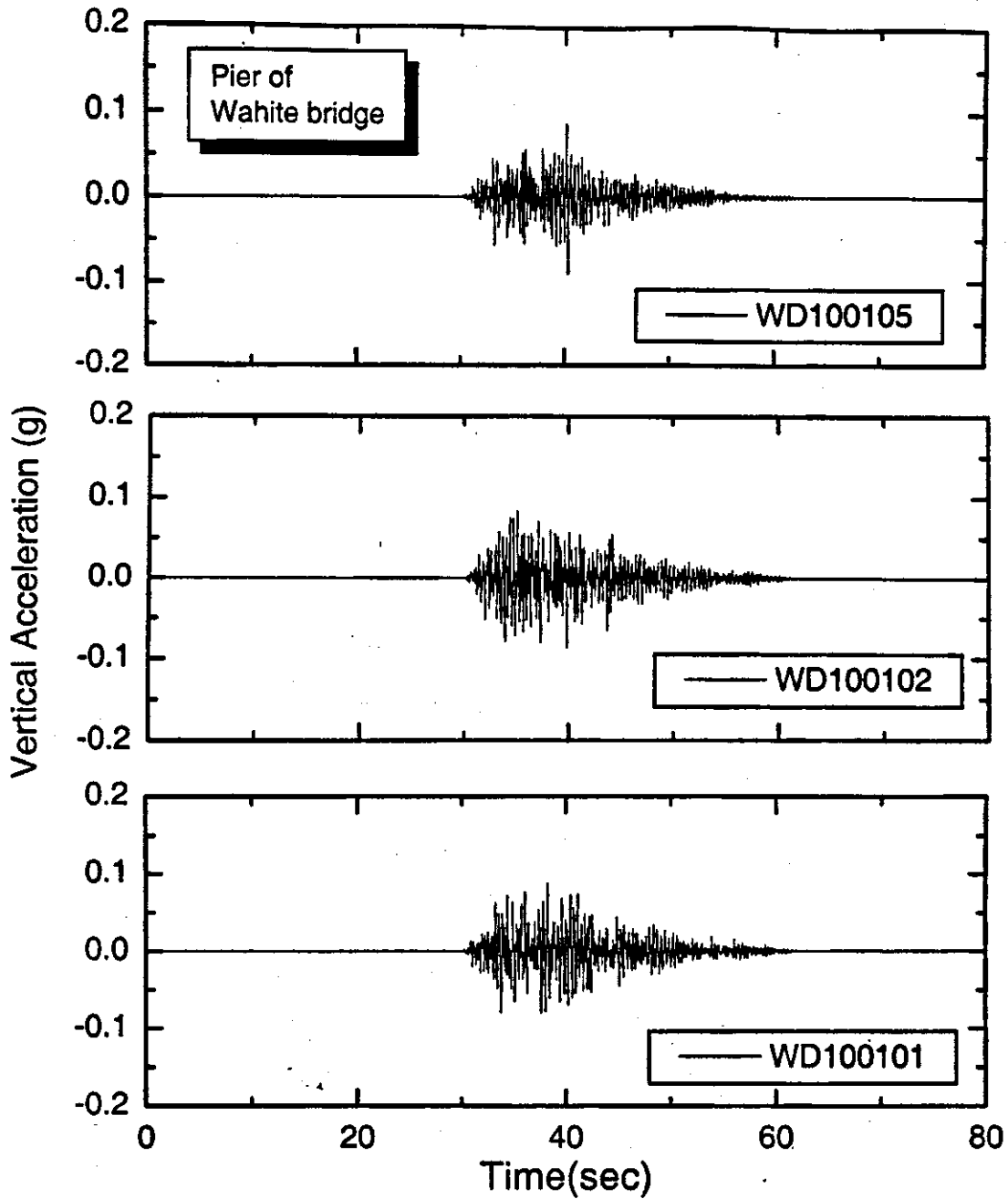
c. PE 2 % in 50 years, Magnitude = 7.8

Figure D.14c Time Histories Vertical Acceleration at the Bridge Abutment, Wahite Ditch Site, PE 2 % in 50 years, Magnitude=7.8



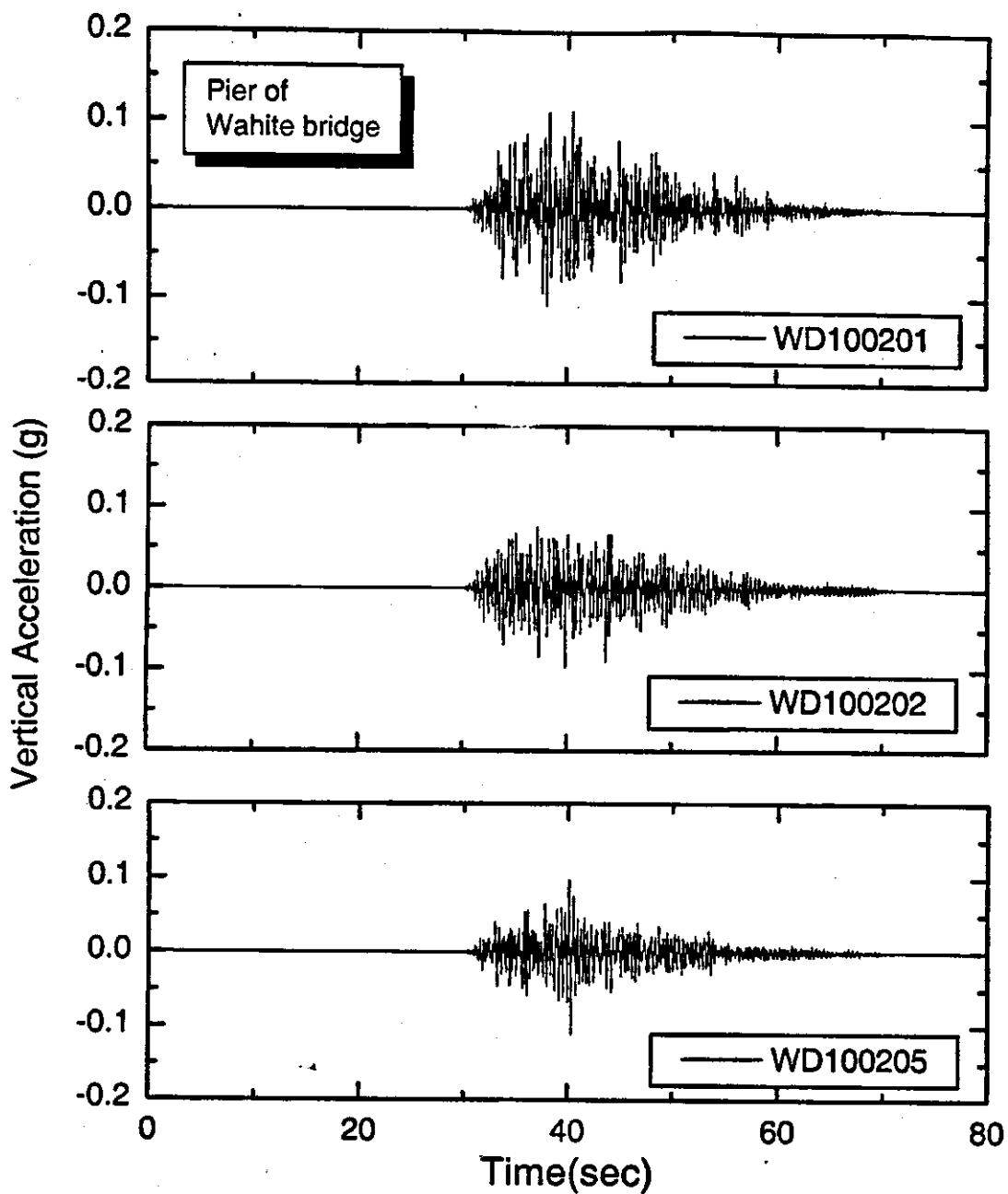
d. PE 2 % in 50 years, Magnitude = 8.0

Figure D.14d Time Histories Vertical Acceleration at the Bridge Abutment, Wahite Ditch Site, PE 2 % in 50 years, Magnitude=8.0



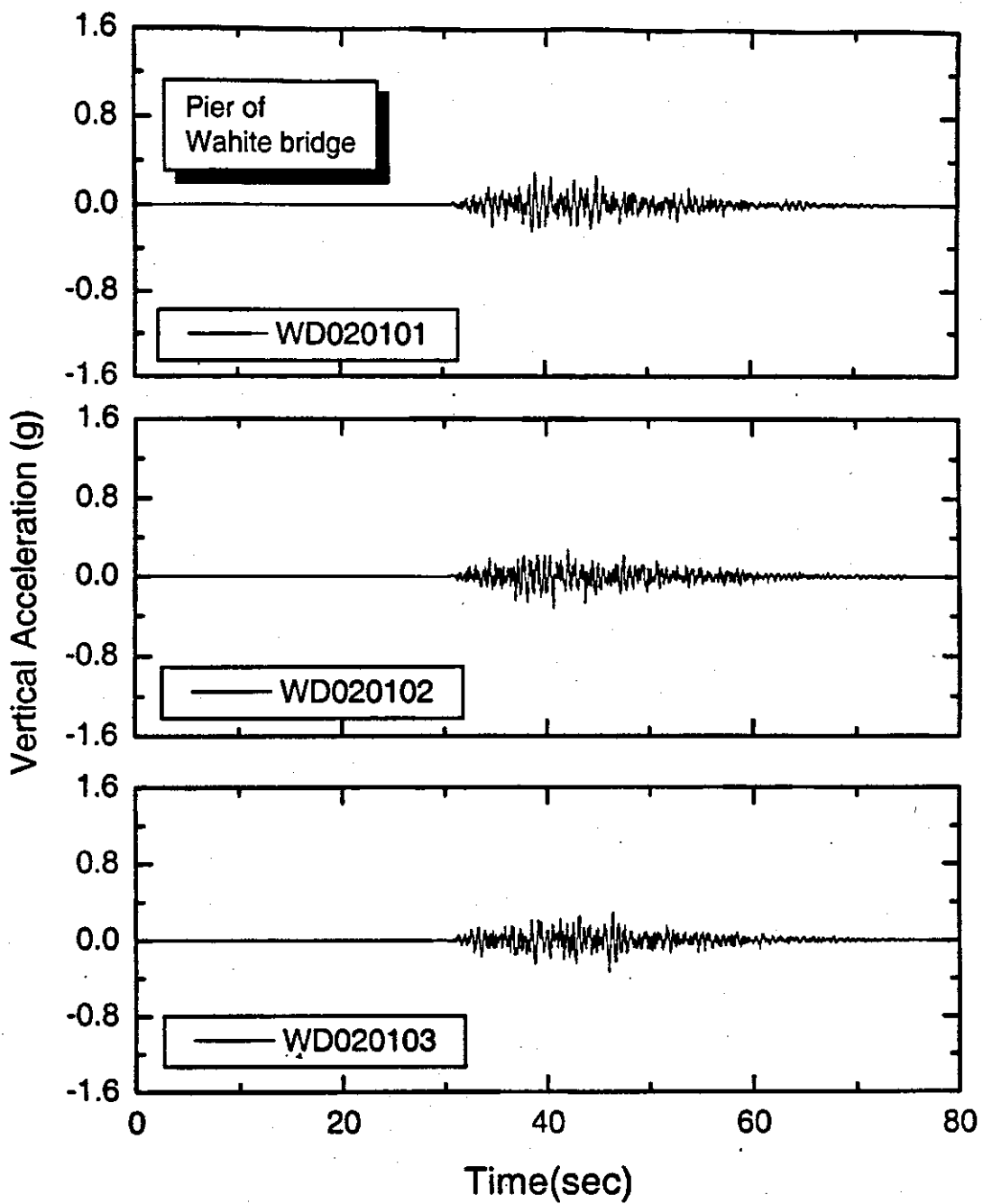
a. PE 10 % in 50 years, Magnitude = 6.4

Figure D.15a Time Histories Vertical Acceleration at the Bridge Pier, Wahite Ditch Bridge, PE 10 % in 50 years, Magnitude=6.4



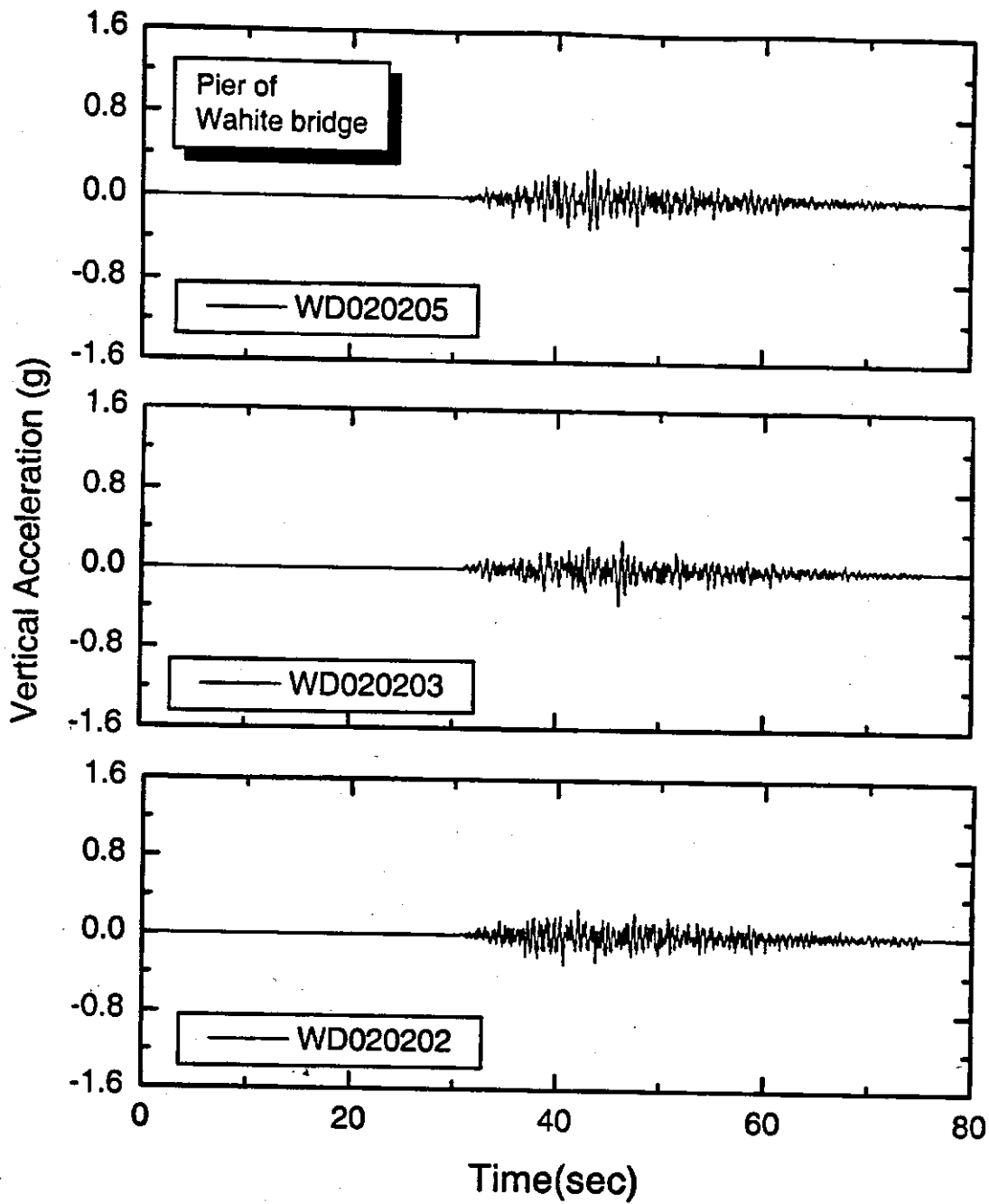
b. PE 10 % in 50 years, Magnitude = 7.0

Figure D.15b Time Histories Vertical Acceleration at the Bridge Pier, Wahite Ditch Bridge, PE 10 % in 50 years, Magnitude=7.0



c. PE 2 % in 50 years, Magnitude = 7.8

Figure D.15c Time Histories Vertical Acceleration at the Bridge Pier, Wahite Ditch Site, PE 2 % in 50 years, Magnitude=7.8



d. PE 2 % in 50 years, Magnitude = 8.0

Figure D.15d Time Histories Vertical Acceleration at the Bridge Pier, Wahite Ditch Site, PE 2 % in 50 years, Magnitude=8.0

## E. DATABASE FOR EARTHQUAKE ANALYSIS

5	sv	Effective vertical stress (middle layer)	N	10	2	9?	99?	kPa	10?	
6	less than 0.075	percent that passes 0.075 mm	N	5	2	0	100.00	%	20.00	
7	PI	Plasticity Index	N	3	0	0	200		50	Table 4.9 (Mitchell)
8	a th	Acceleration time histories	A						Elcentro	NISEE

## F. BRIDGE ABUTMENT AND PIER SUPPORTED ON A PILE GROUP

Novak's (1974) model has been used for the computation of stiffness and damping of single pile and a pile group, with appropriate interaction factors. Stiffness and damping in all the modes i.e. vertical, horizontal, rocking and torsion and cross coupling in both the x and y direction have been evaluated for the bridge abutments and the piers. (See Figure F.1 for sign convention).

The main assumptions in Novak's model are;

1. The pile is a circular and solid in cross section. For other than circular section, an equivalent radius  $r_o$  is determined in each mode of variation.
2. The pile material is linear elastic
3. The pile is perfectly connected to the soil (i.e., there is no separation between soil and pile during vibration).

### F.1 Stiffness and Damping Factors of Single Pile

#### F.1.1 Vertical Stiffness ( $k_z$ ) and Damping Factors ( $c_z$ )

$$k_z = \left[ \frac{E_p A}{r_o} \right] f_{w1} \quad (\text{F.1a})$$

$$c_z = \left[ \frac{E_p A}{V_s} \right] f_{w2} \quad (\text{F.1b})$$

Where;

- $E_p$  = modulus of elasticity of pile material  
 $A$  = cross section of single pile  
 $r_o$  = radius of a solid pile or equivalent pile radius  
 $V_s$  = shear wave velocity of soil along of the floating pile

$f_{w1}$  and  $f_{w2}$  are obtained from Figure F.2

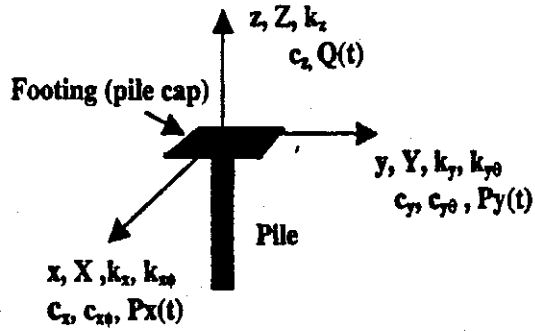
#### F.1.2 Torsional Stiffness ( $k_\psi$ ) and Damping Factors ( $c_\psi$ )

$$k_\psi = \left[ \frac{G_p I_{p_p}}{r_o} \right] f_{T,1} \quad (\text{F.2a})$$

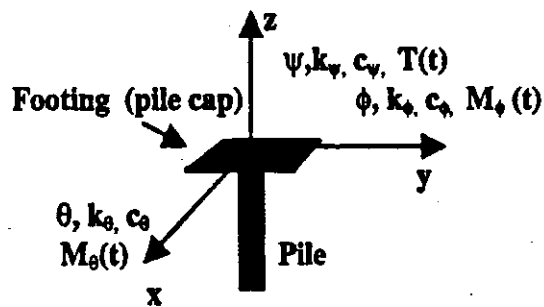
$$c_\psi = \left[ \frac{G_p I_{p_p}}{V_s} \right] f_{T,2} \quad (\text{F.2b})$$

Where;

- $G_p$  = shear modulus of elasticity of pile material  
 $I_{p_p}$  = Polar moment of inertia of single pile about z axis  
 $f_{T,1}$  and  $f_{T,2}$  are obtained from Figure F.3



a) Translational and coupled constants



b) Rotational constants

Figure F.1 Sign Convention

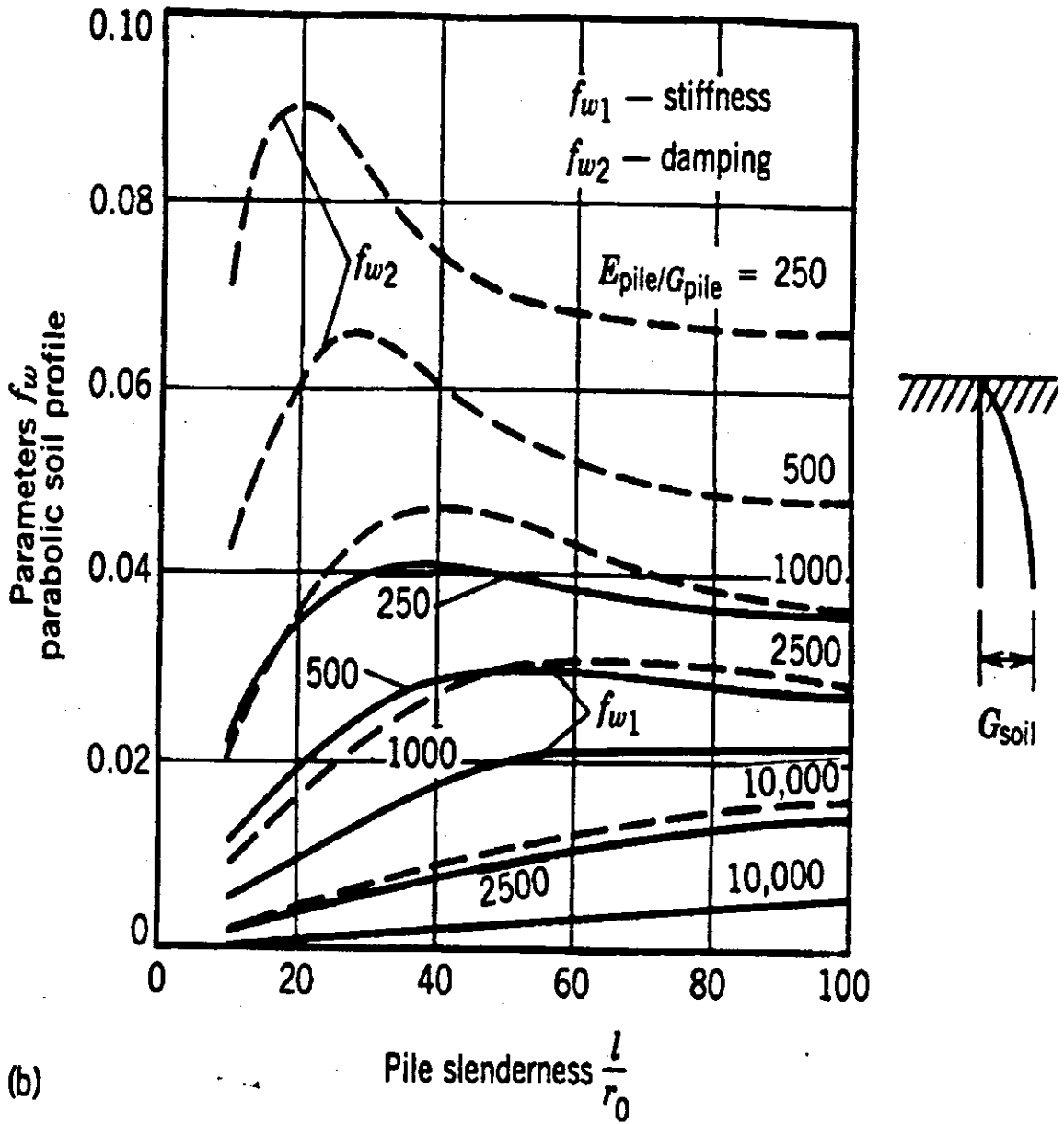


**Figure F.2** Stiffness and Damping Parameters for Vertical Response of Floating Piles (Novak and El-Shomouby, 1983)

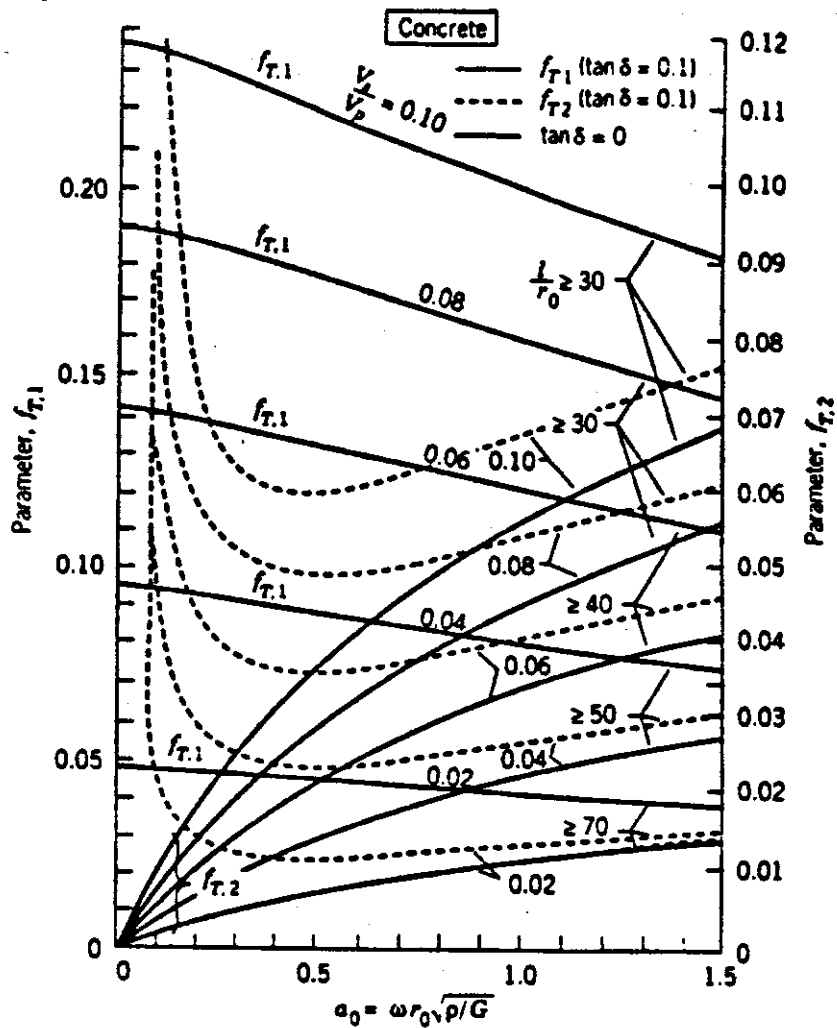


Figure. F.3 Torsional Stiffness and Damping Parameters for Reinforced Concrete (Novak and Howell, 1977)

### F.1.3 Sliding and Rocking Stiffness and Damping Factors

Because, the pile is assumed to be cylindrical with a radius  $r_0$ , its stiffness and damping factors in any horizontal direction are the same. However, in the pile group, the number of piles in the x and y directions may be different. Therefore the stiffness and damping factors of a pile group are dependent on the number of piles and their spacing in each direction.

### Sliding ( $k_x, c_x$ )

$$k_x = \left[ \frac{E_p I_p}{r_o^3} \right] f_{x1} \quad (\text{F.3a})$$

$$c_x = \left[ \frac{E_p I_p}{r_o^2 V_s} \right] f_{x2} \dots \quad (\text{F.3b})$$

### Rocking ( $k_\theta, c_\theta$ ) and ( $k_\phi, c_\phi$ )

$$k_\theta = k_\phi = \left[ \frac{E_p I_p}{r_o^2} \right] f_{\theta1} \quad (\text{F.4a})$$

$$c_\theta = c_\phi = \left[ \frac{E_p I_p}{r_o^2 V_s} \right] f_{\theta2} \quad (\text{F.4b})$$

### Cross-coupling ( $k_{x\phi}, c_{x\phi}$ ) and ( $k_{y\theta}, c_{y\theta}$ )

$$k_{x\phi} = k_{y\theta} = \left[ \frac{E_p I_p}{r_o^2} \right] f_{x\theta1} \quad (\text{F.5a})$$

$$c_{x\phi} = c_{y\theta} = \left[ \frac{E_p I_p}{r_o V_s} \right] f_{x\theta2} \quad (\text{F.5b})$$

Where;

$I_p$  = moment of inertia of single pile about x or y axis  
 $r_o$  = pile radius

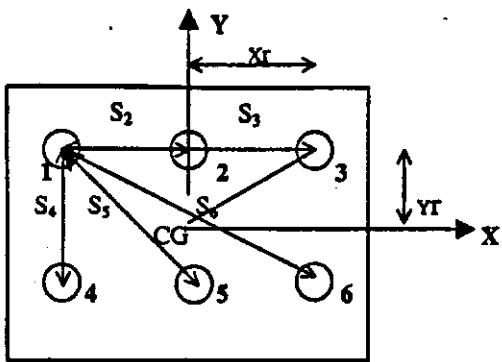
$f_{x1}, f_{x2}, f_{\phi1}, f_{\phi2}, f_{x\phi1}, f_{x\phi2}$  Novak's coefficient and have obtained from Table F.1 for parabolic soil profile, with appropriate interpolation and for  $\nu = 0.25$

## F.2 Group Interaction Factor

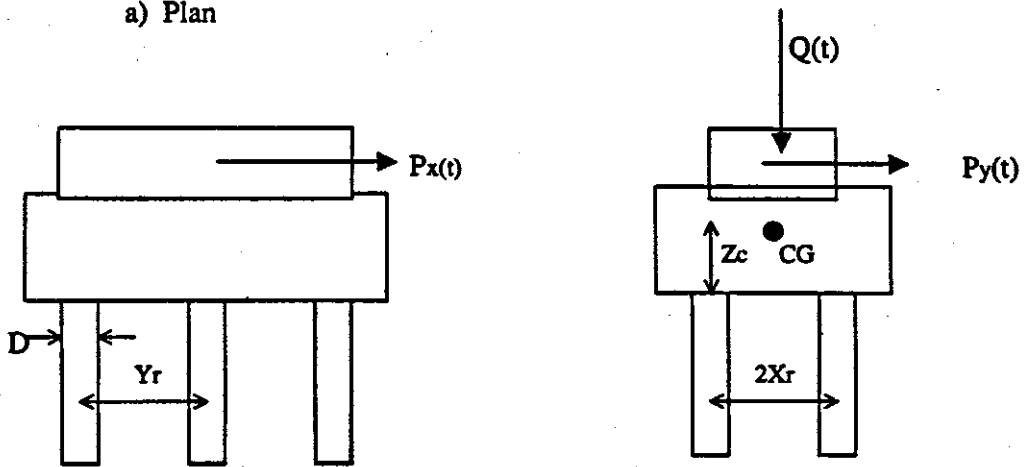
To consider group effect, (Paulos, 1968) assume a pile in the group as reference pile. In the illustration Figure F.4, pile No. 1 is assumed as a reference pile and distance 'S' is measured from the center of other pile to center of the reference pile.

For vertical direction use Figure F.5 to obtain  $\alpha_A$  for each pile for appropriate  $S/2r_o$  values  $\alpha_A$ 's are function of length of the pile (L) and radius ( $r_o$ ).

Use Figure F.6 (Paulos, 1971), to obtain  $\alpha_L$  for each pile in the horizontal x-direction, considering departure angle  $\beta$  (degree).  $\alpha_L$ 's are a function of L,  $r_o$  and flexibility  $K_R$  as defined in Figure F.6 and departure angle ( $\beta$ ). This procedure will also apply for horizontal direction.



a) Plan



b) Cross section

Figure F.4 Plan and Cross Section of Pile Group

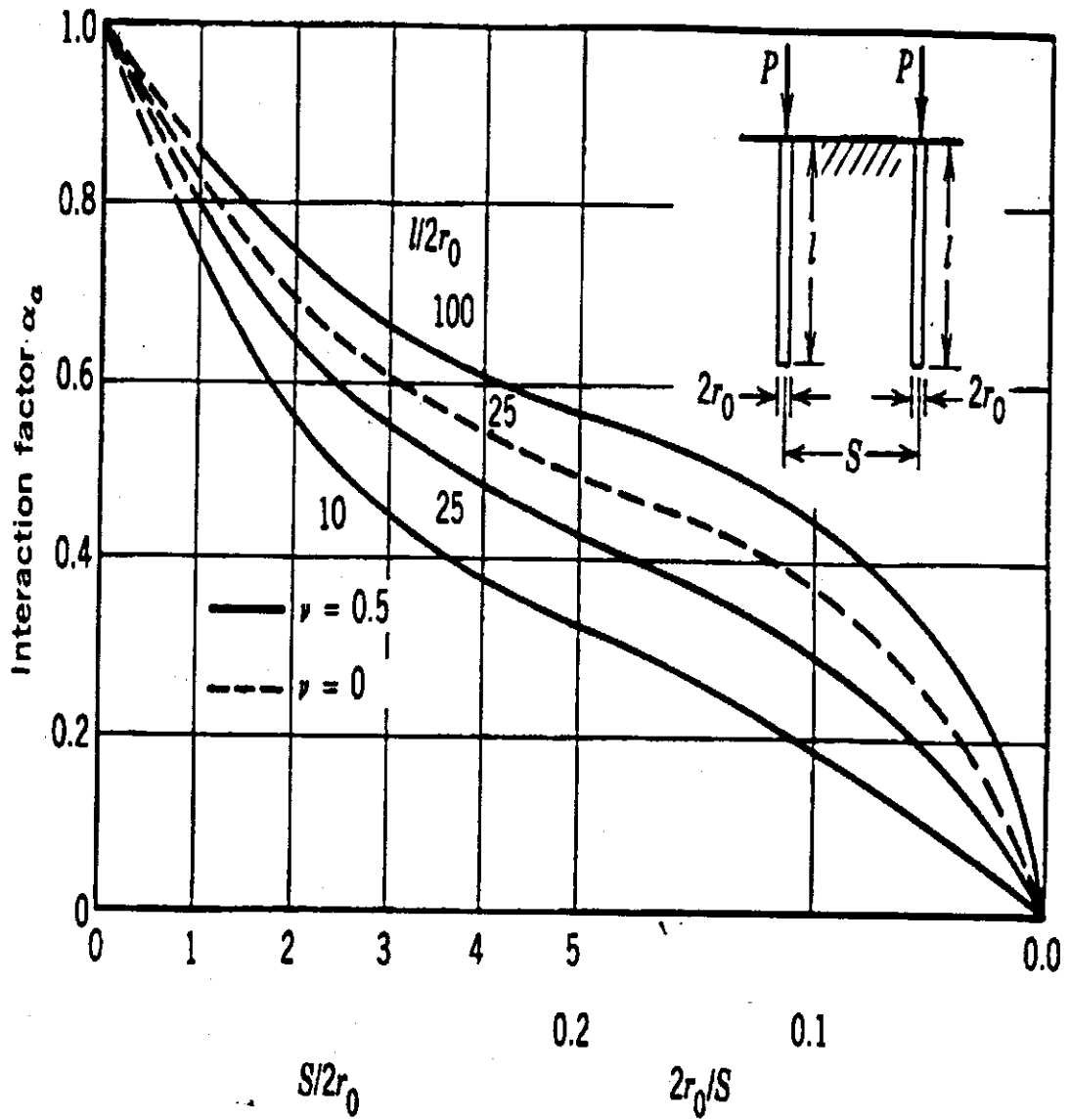


Figure F.5  $\alpha_A$  as a Function of Pile Length and Spacing (Poulos, 1968)

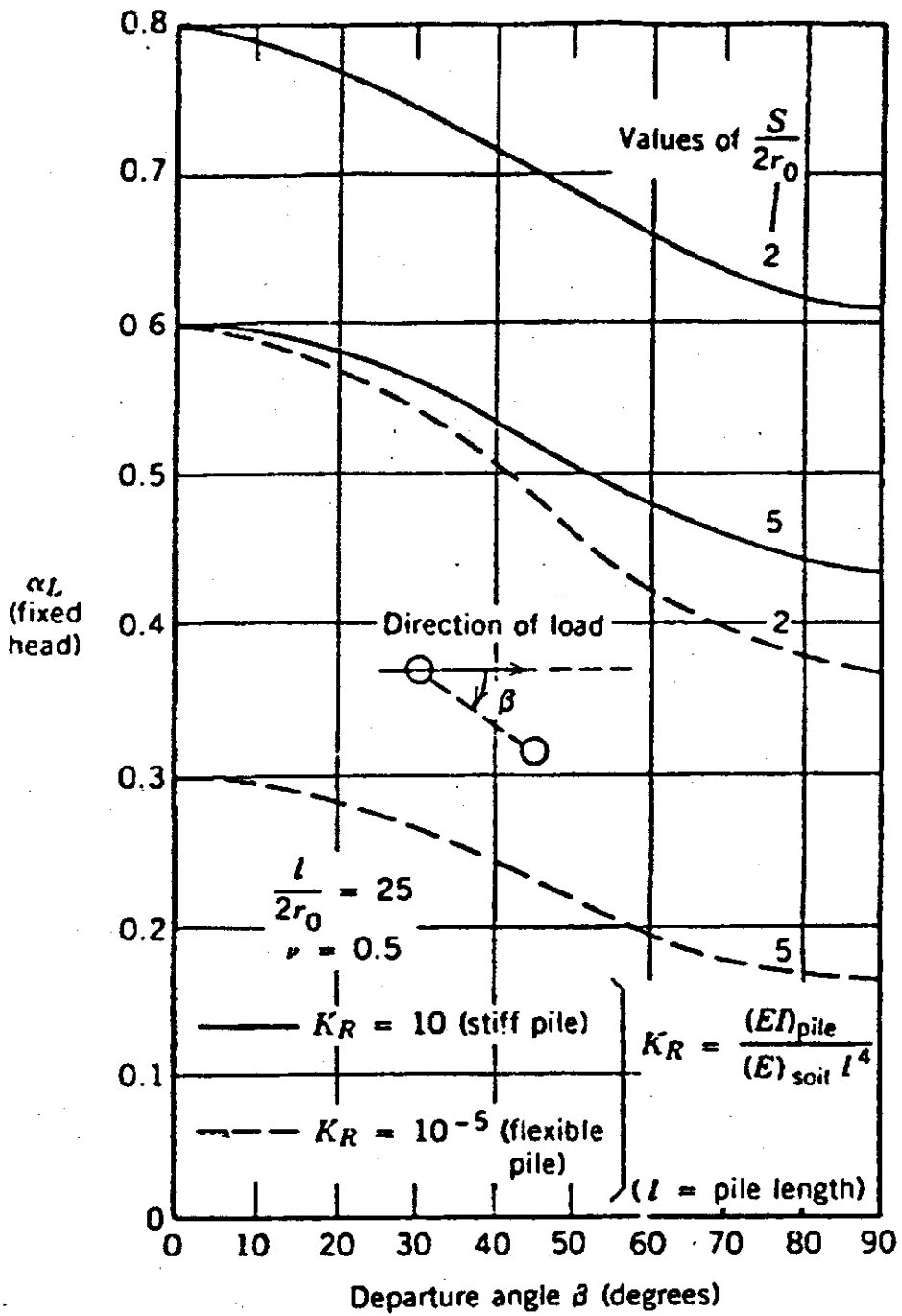


Figure F.6 Graphical Solution of  $\alpha_L$  (Poulos, 1972)

**Table F.1** Stiffness and Damping Parameters of Horizontal Response For Pile With  $L/R_o > 25$  For Homogeneous Soil Profile and  $L/R_o > 30$  For Parabolic Soil Profile

$\nu$ (1)	$E_{pile}/G_{soil}$ (2)	Stiffness Parameters				Damping Parameters				
		$f_{s1}$ (3)	$f_{s4}$ (4)	$f_{s1}^*$ (5)	$f_{s1}^{**}$ (6)	$f_{d2}$ (7)	$f_{d2}^*$ (8)	$f_{d2}$ (9)	$f_{d2}^{**}$ (10)	
(a) Homogeneous Soil Profile										
0.25	10,000	0.2135	-0.0217	0.0042	0.0021	0.1577	-0.0333	0.0107	0.0054	
	2,500	0.2998	-0.0429	0.0119	0.0061	0.2152	-0.0646	0.0297	0.0154	
	1,000	0.3741	-0.0668	0.0236	0.0123	0.2598	-0.0985	0.0579	0.0306	
	500	0.4411	-0.0929	0.0395	0.0210	0.2953	-0.1337	0.0953	0.0514	
0.40	10,000	0.5186	-0.1281	0.0659	0.0358	0.3299	-0.1786	0.1556	0.0864	
	2,500	0.2207	-0.0232	0.0047	0.0024	0.1634	-0.0358	0.0119	0.0060	
	1,000	0.3097	-0.0459	0.0132	0.0068	0.2224	-0.0692	0.0329	0.0171	
	500	0.3860	-0.0714	0.0261	0.0136	0.2677	-0.1052	0.0641	0.0339	
	10,000	0.4547	-0.0991	0.0436	0.0231	0.3034	-0.1425	0.1054	0.0570	
	2,500	0.5336	-0.1365	0.0726	0.0394	0.3377	-0.1896	0.1717	0.0957	
	(b) Parabolic Soil Profile									
	0.25	10,000	0.1800	-0.0144	0.0019	0.0008	0.1450	-0.0252	0.0060	0.0028
2,500		0.2452	-0.0267	0.0047	0.0020	0.2025	-0.0484	0.0159	0.0076	
1,000		0.3000	-0.0400	0.0086	0.0037	0.2499	-0.0737	0.0303	0.0147	
500		0.3469	-0.0543	0.0136	0.0059	0.2910	-0.1008	0.0491	0.0241	
0.40	10,000	0.4049	-0.0734	0.0215	0.0094	0.3361	-0.1370	0.0793	0.0398	
	2,500	0.1857	-0.0153	0.0020	0.0009	0.1508	-0.0271	0.0067	0.0031	
	1,000	0.2529	-0.0284	0.0051	0.0022	0.2101	-0.0519	0.0177	0.0084	
	500	0.3094	-0.0426	0.0094	0.0041	0.2589	-0.0790	0.0336	0.0163	
	10,000	0.3596	-0.0577	0.0149	0.0065	0.3009	-0.1079	0.0544	0.0269	
	2,500	0.4170	-0.0780	0.0236	0.0103	0.3468	-0.1461	0.0880	0.0443	

Source: Novak and El-Sharnouby (1983).  $f_{s1}^*$  and  $f_{s2}^*$  are parameters for pinned end.

The group interaction factor ( $\Sigma\alpha_L$ ) is the summation  $\alpha_L$  for all the piles. Note that the group interaction factor in horizontal x-direction and y-direction may be different depending on number and spacing of piles in each direction.

### F.3 Group Stiffness and Damping Factors

Figure F.4 shows schematically the plan and cross sections of an arbitrary pile group foundation. This figure will be used to explain and obtain the stiffness and damping factors group of pile for all direction. They are presented as follows:

#### F.3.1 Vertical group stiffness ( $k_z^g$ ) and damping factors ( $c_z^g$ )

$$k_z^g = \frac{\sum k_z}{\sum \alpha_A} \quad (F.6.a)$$

$$c_z^g = \frac{\sum c_z}{\sum \alpha_A} \quad (F.6.b)$$

#### F.3.2 Torsional group stiffness ( $k_\psi^g$ ) and damping factors ( $c_\psi^g$ )

$$k_\psi^g = \frac{1}{\sum \alpha_A} [k_\psi + k_x(x_r^2 + y_r^2)] \quad (F.7.a)$$

$$c_v^g = \frac{1}{\sum \alpha_A} [c_v + c_x(x_r^2 + y_r^2)] \quad (\text{F.7b})$$

### F.3.3 Sliding and Rocking and Cross Coupled Group Stiffness and Damping Factors

#### Sliding and Rocking and Cross Coupled Group Stiffness and Damping Factors

$$k_x^g = \frac{\sum k_x}{\sum \alpha_{Lx}} \quad (\text{F.8a})$$

$$c_x^g = \frac{\sum c_x}{\sum \alpha_{Lx}} \quad (\text{F.8b})$$

#### Translation Along Y Axis ( $k_y^g, c_y^g$ )

$$k_y^g = \frac{\sum k_y}{\sum \alpha_{Ly}} \quad (\text{F.9a})$$

$$c_y^g = \frac{\sum c_y}{\sum \alpha_{Ly}} \quad (\text{F.9b})$$

#### Rocking About Y Axis ( $k_\phi^g, c_\phi^g$ )

$$k_\phi^g = \frac{1}{\sum \alpha_{Lx}} [k_\phi + k_z x_r^2 + k_x z_c^2 - 2z_c k_{x\phi}] \quad (\text{F.10a})$$

$$c_\phi^g = \frac{1}{\sum \alpha_{Lx}} [c_\phi + c_z x_r^2 + c_x z_c^2 - 2z_c c_{x\phi}] \quad (\text{F.10b})$$

#### Rocking About X Axis ( $k_\theta^g, c_\theta^g$ )

$$k_\theta^g = \frac{1}{\sum \alpha_{Ly}} [k_\theta + k_z y_r^2 + k_y z_c^2 - 2z_c k_{y\theta}] \quad (\text{F.11a})$$

$$c_\theta^g = \frac{1}{\sum \alpha_{Ly}} [c_\theta + c_z y_r^2 + c_y z_c^2 - 2z_c c_{y\theta}] \quad (\text{F.11b})$$

#### Cross-Coupling Translation in X Axis and Rotation About Y Axis. ( $k_{x\phi}^g, c_{x\phi}^g$ )

$$k_{x\phi}^g = \frac{1}{\alpha_{Lx}} \sum (k_{x\phi} - k_x z_c) \quad (\text{F.12a})$$

$$c_{x\phi}^g = \frac{1}{\alpha_{Lx}} \sum (c_{x\phi} - c_x z_c) \quad (\text{F.12b})$$

### Cross-Coupling Translation in Y-Axis and Rotation About X Axis. ( $k_{y\theta}$ , $c_{y\theta}$ )

$$k_{y\theta}^g = \frac{1}{\alpha_{ly}} \sum (k_{y\theta} - k_y z_c) \quad (\text{F.13a})$$

$$c_{y\theta}^g = \frac{1}{\alpha_{ly}} \sum (c_{y\theta} - c_y z_c) \quad (\text{F.13b})$$

#### F.4 Strain-Displacement Relationships

The shear strain and displacement relationship is not well defined in practical problems occurring in the field. However, the relationship has been recommended by Prakash and Puri (1981) as:

$$\gamma = \text{amplitude of foundation vibration/average width of foundation} \quad (\text{F.14})$$

Because evaluation of shear strain in the field is, in many cases, not clear, reasonable expressions must be assumed and used as the basis for evaluating the shear strain in each particular case.

Kagawa and Kraft (1980) used a following relationship for horizontal displacement

$$\lambda_x = \frac{(1+\nu)X}{2.5D} \quad (\text{F.15})$$

Where,  
 $\nu$  = Poisson's ratio  
 $X$  = horizontal displacement in x-direction  
 $D$  = diameter of pile

Rafnsson (1992) stated that, the shear strain due to rocking can be reasonably determined as;

$$\gamma_\phi = \frac{\phi}{3} \quad (\text{F.16})$$

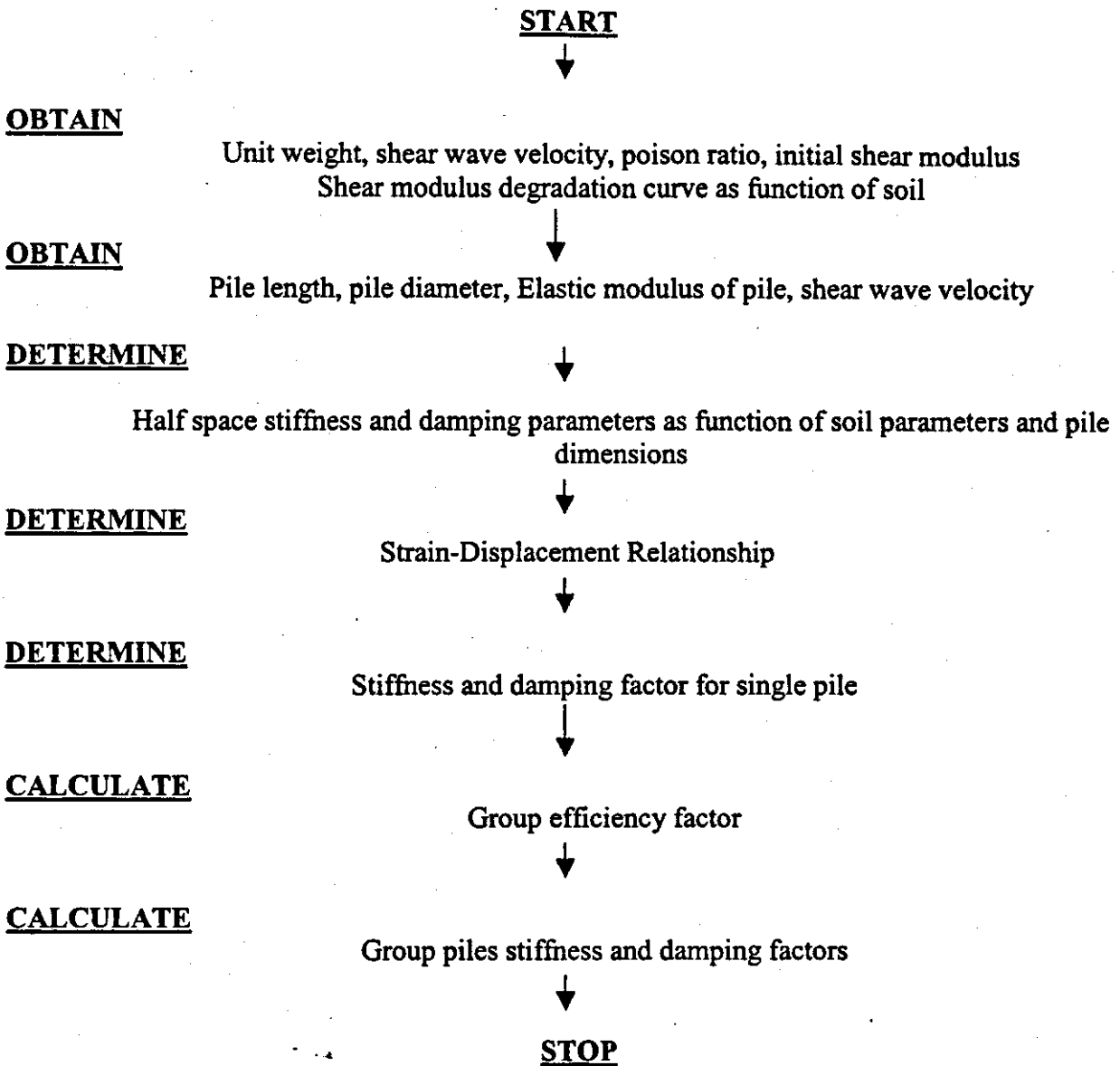
Where,  
 $\phi$  = rotation of foundation about y axis

The shear strain- displacement relationship for couple sliding and rocking can be determined as:

$$\gamma_x = \frac{(1+\nu)X}{2.5D} + \frac{\phi}{3} \quad (\text{F.17})$$

Note that, equations F.15, F.16 and F.17 have been adopted for other directions respectively.

## F.5 Solution Technique for Displacement Dependent $k$ 's and $c$ 's



The stiffness and damping factors are plotted against displacement for bridge abutment and pier of old St Francis, new St. Francis, new Wahite and old Wahite bridges. They are presented in Figure F.7a through F.25c.

## F.6 Equations of Motion

Under dynamic loading, the equilibrium of forces is derived based on the second Newton's law. This equilibrium in two-dimensional analysis will give three-equations of motion in the vertical and two horizontal directions.

### Vertical equation of motion

$$m.Z + c_z^g . Z + k_z^g Z = Q(t) \quad (F.18)$$

### Torsional equation of motion

$$m. \psi + c_\psi^g . \psi + k_\psi^g . \psi = T(t) \quad (F.19)$$

### Two-Dimensional Sliding and Rocking Equation of Motion

In the horizontal x direction

$$\begin{Bmatrix} m & 0 \\ 0 & Mm \end{Bmatrix} \begin{Bmatrix} X \\ \phi \end{Bmatrix} + \begin{Bmatrix} c_x^g & -c_{\phi x}^g \\ -c_{\phi x}^g & c_\phi^g \end{Bmatrix} \begin{Bmatrix} X \\ \phi \end{Bmatrix} + \begin{Bmatrix} k_x^g & -k_{\phi x}^g \\ -k_{\phi x}^g & k_\phi^g \end{Bmatrix} \begin{Bmatrix} X \\ \phi \end{Bmatrix} = \begin{Bmatrix} P_x(t) \\ M_\phi(t) \end{Bmatrix} \quad (F.20)$$

In the horizontal y direction

$$\begin{Bmatrix} m & 0 \\ 0 & Mm \end{Bmatrix} \begin{Bmatrix} Y \\ \theta \end{Bmatrix} + \begin{Bmatrix} c_y^g & -c_{\theta y}^g \\ -c_{\theta y}^g & c_\theta^g \end{Bmatrix} \begin{Bmatrix} Y \\ \theta \end{Bmatrix} + \begin{Bmatrix} k_y^g & -k_{\theta y}^g \\ -k_{\theta y}^g & k_\theta^g \end{Bmatrix} \begin{Bmatrix} Y \\ \theta \end{Bmatrix} = \begin{Bmatrix} P_y(t) \\ M_\theta(t) \end{Bmatrix} \quad (F.21)$$

where:

$m$  = mass of bridge abutment

$Mm$  = mass inertia of bridge abutment about the axis of rotation

$Q(t)$  = total vertical force

$P_x(t)$  = total horizontal force x-direction

$T(t)$  = total torsional force

$P_y(t)$  = total horizontal force y-direction

$M_\phi(t)$  = moment about y-axis

$M_\theta(t)$  = moment about x-axis

### Three-Dimensional Equation of Motion

$$[m]\{X\} + [C]\{X\} + [K]\{X\} = \{P(t)\} \quad (F.22)$$

where, matrix mass  $[m]$  is

$$\{m\} = \begin{Bmatrix} m & 0 & 0 & 0 & 0 & 0 \\ 0 & m & 0 & 0 & 0 & 0 \\ 0 & 0 & m & 0 & 0 & 0 \\ 0 & 0 & 0 & Mm & 0 & 0 \\ 0 & 0 & 0 & 0 & m & 0 \\ 0 & 0 & 0 & 0 & 0 & Mm \end{Bmatrix} \quad (F.22a)$$

Matrix damping  $[C]$  is

$$\{C\} = \begin{Bmatrix} C_z^g & 0 & 0 & 0 & 0 & 0 \\ 0 & C_v^g & 0 & 0 & 0 & 0 \\ 0 & 0 & C_x^g & -C_{\phi x}^g & 0 & 0 \\ 0 & 0 & -C_{\phi x}^g & C_\phi^g & 0 & 0 \\ 0 & 0 & 0 & 0 & C_y^g & -C_{\theta y}^g \\ 0 & 0 & 0 & 0 & -C_{\theta y}^g & C_\theta^g \end{Bmatrix} \quad \text{F.22b)}$$

Matrix stiffness [K] is

$$\{K\} = \begin{Bmatrix} k_z^g & 0 & 0 & 0 & 0 & 0 \\ 0 & k_v^g & 0 & 0 & 0 & 0 \\ 0 & 0 & k_x^g & -k_{\phi x}^g & 0 & 0 \\ 0 & 0 & -k_{\phi x}^g & k_\phi^g & 0 & 0 \\ 0 & 0 & 0 & 0 & k_y^g & -k_{\theta y}^g \\ 0 & 0 & 0 & 0 & -k_{\theta y}^g & k_\theta^g \end{Bmatrix} \quad \text{(F.22c)}$$

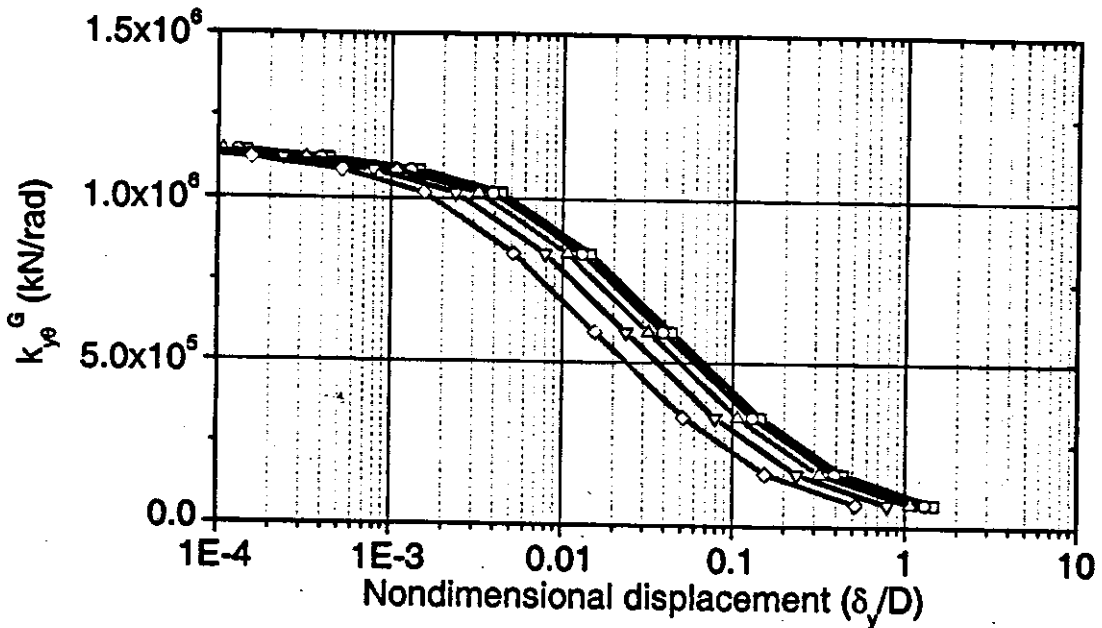
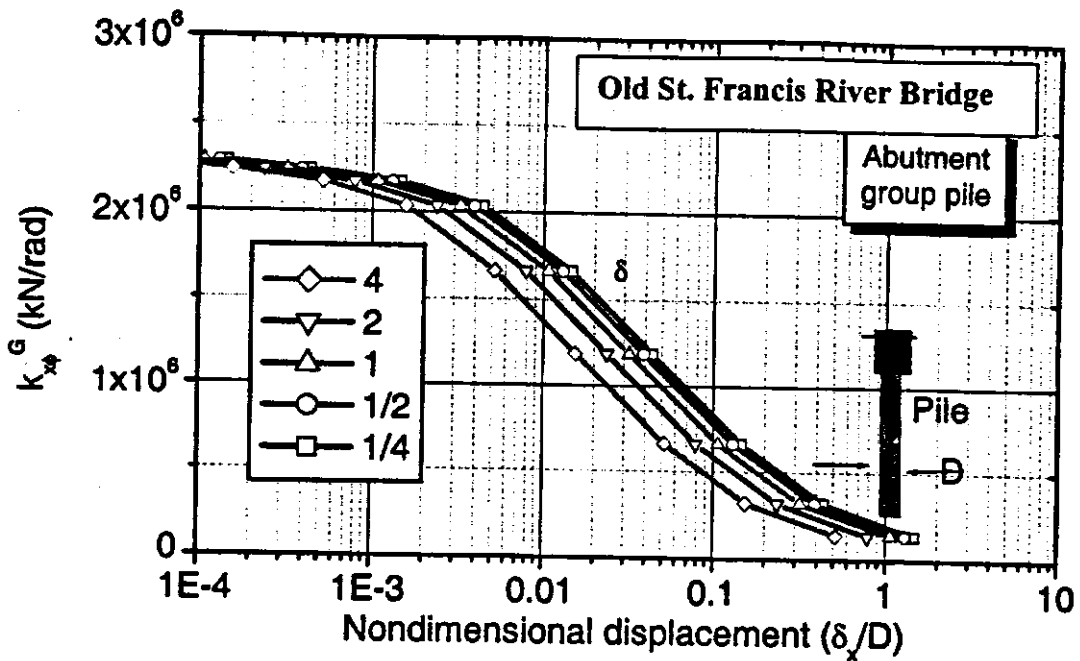
Vector load {P(t)} is;

$$\begin{Bmatrix} Q(t) \\ T(t) \\ P_x(t) \\ M_\phi(t) \\ P_y(t) \\ M_\theta(t) \end{Bmatrix}$$

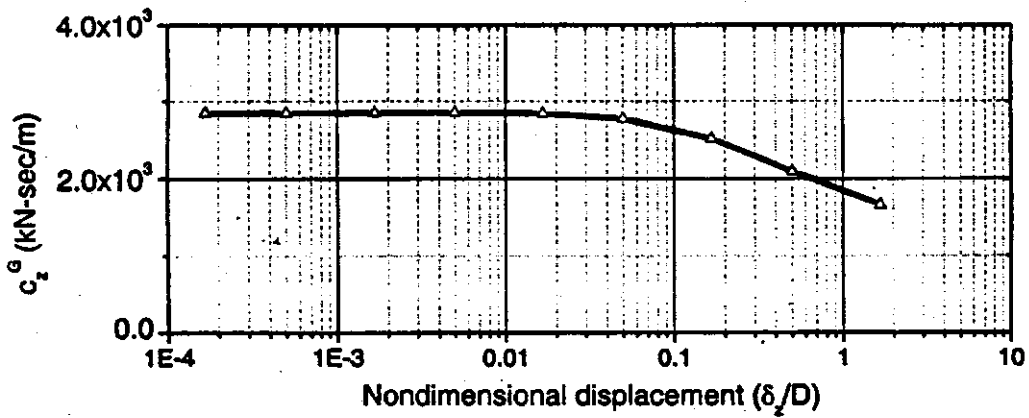
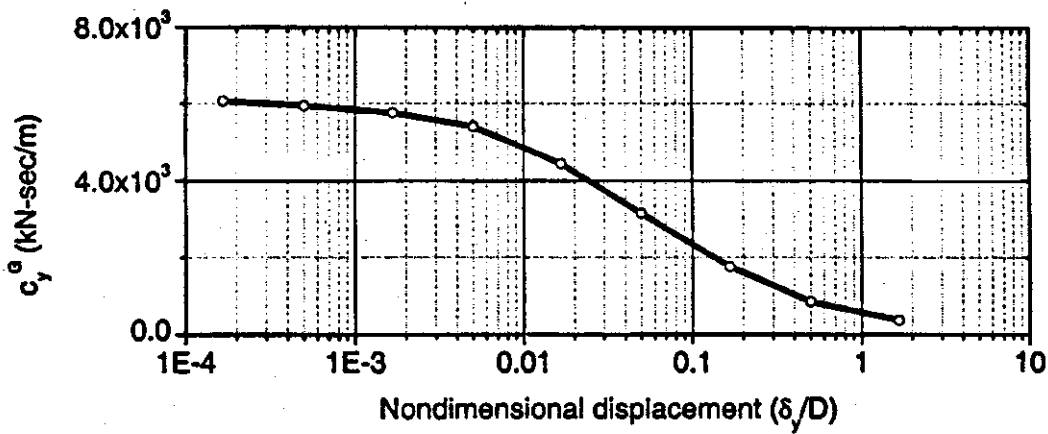
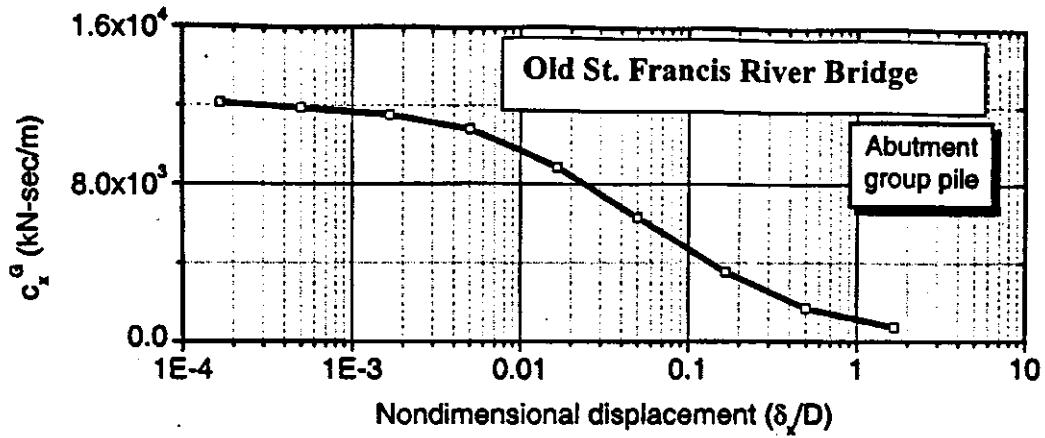
Vector displacement {X} is

$$\begin{Bmatrix} Z \\ \psi \\ X \\ \phi \\ Y \\ \theta \end{Bmatrix}$$

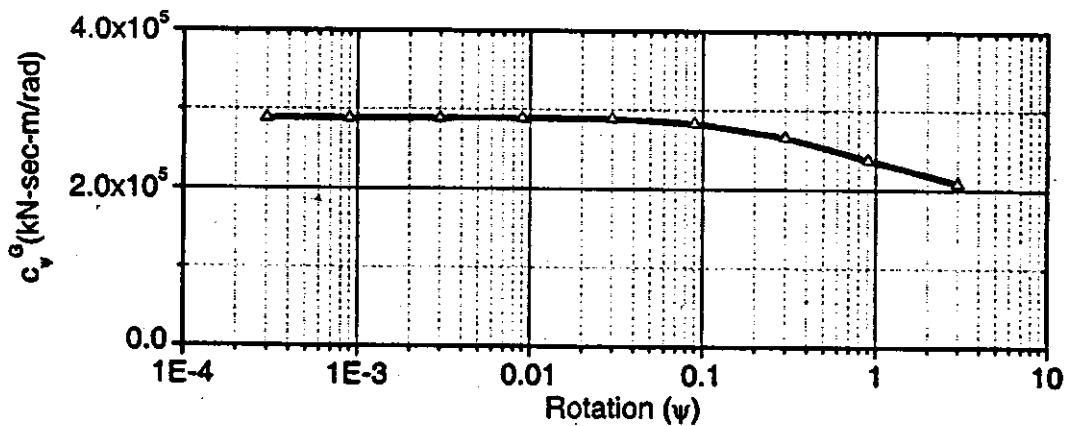
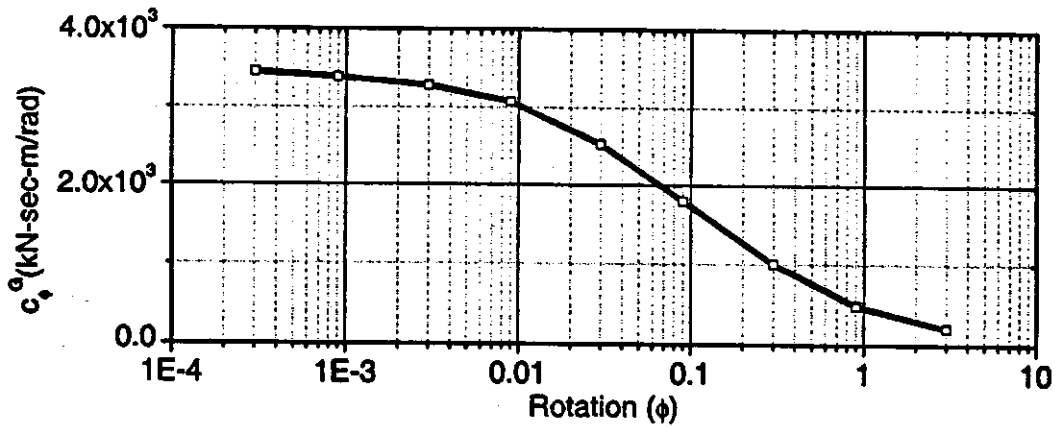
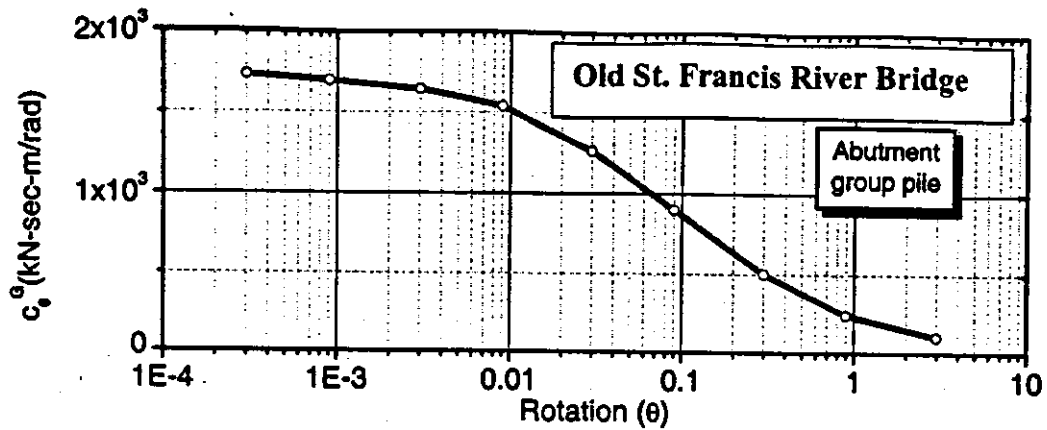
(F.22d)



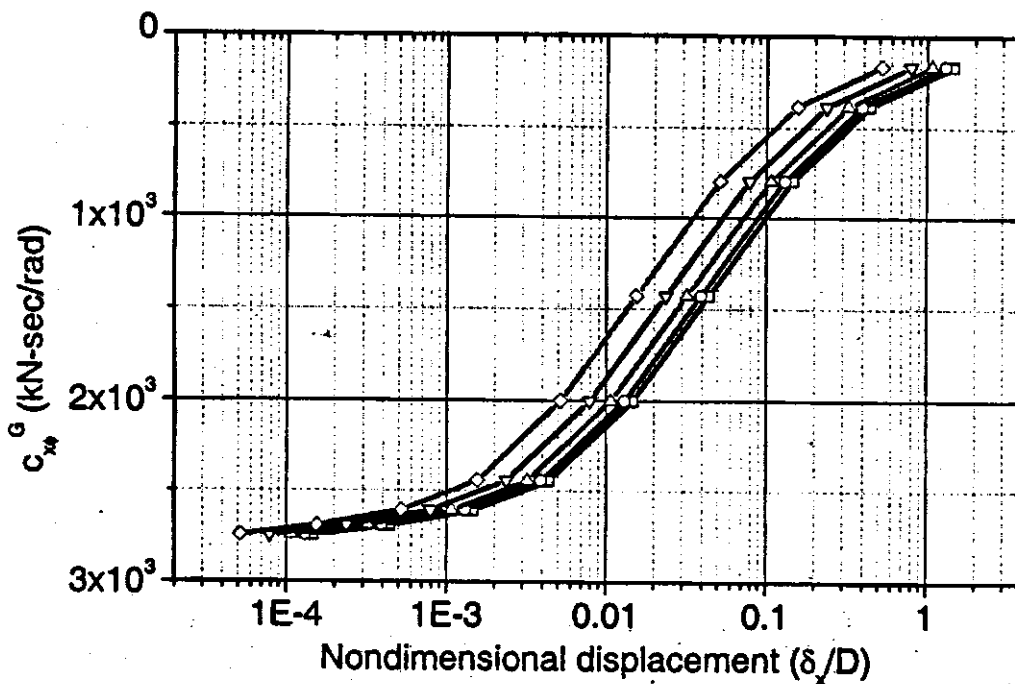
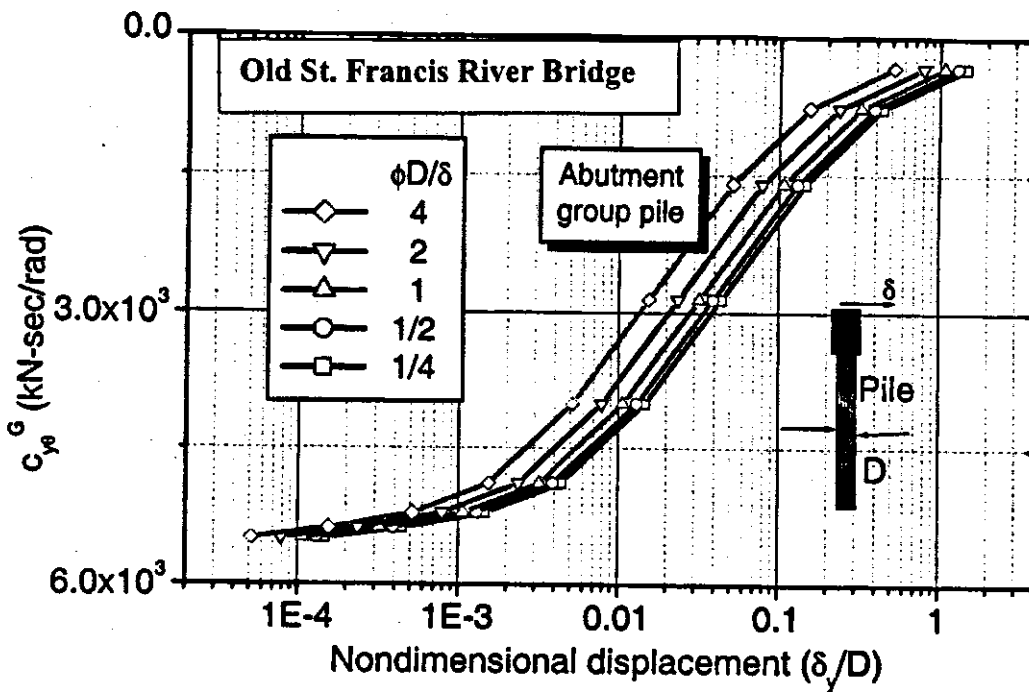
**F.7a Cross-Coupling Translation in X and Y-Axis vs. Nondimensional Displacement for the Abutment Group Pile, Old St. Francis River Bridge**



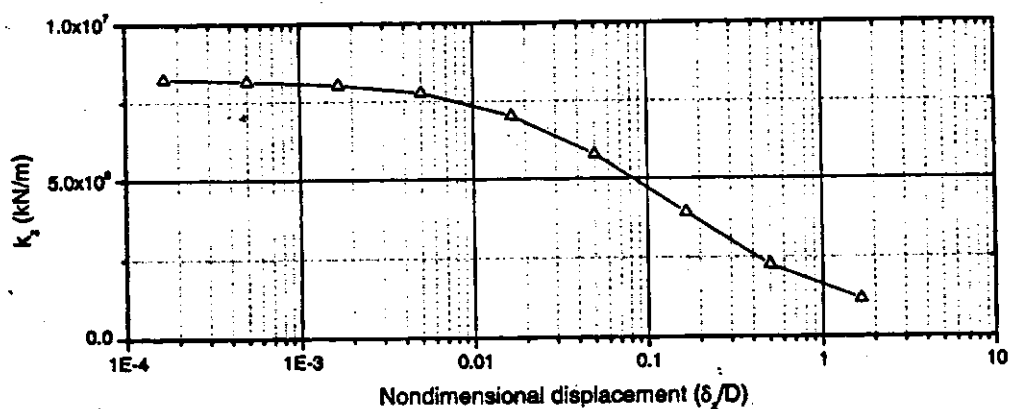
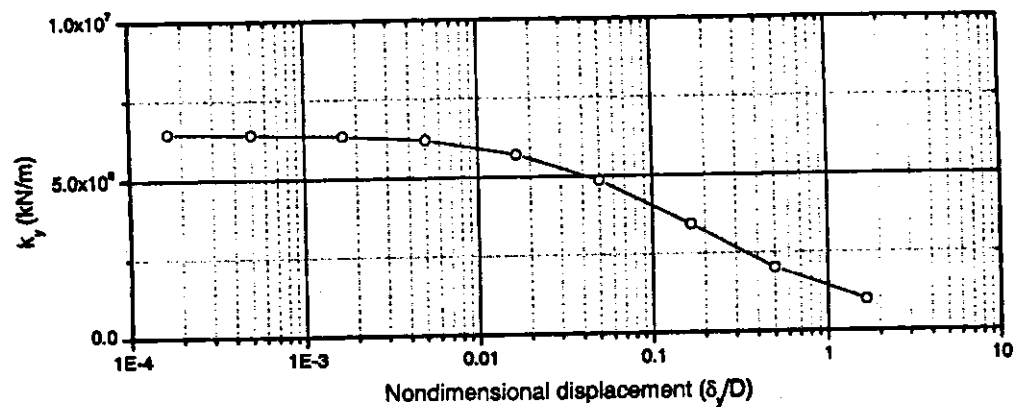
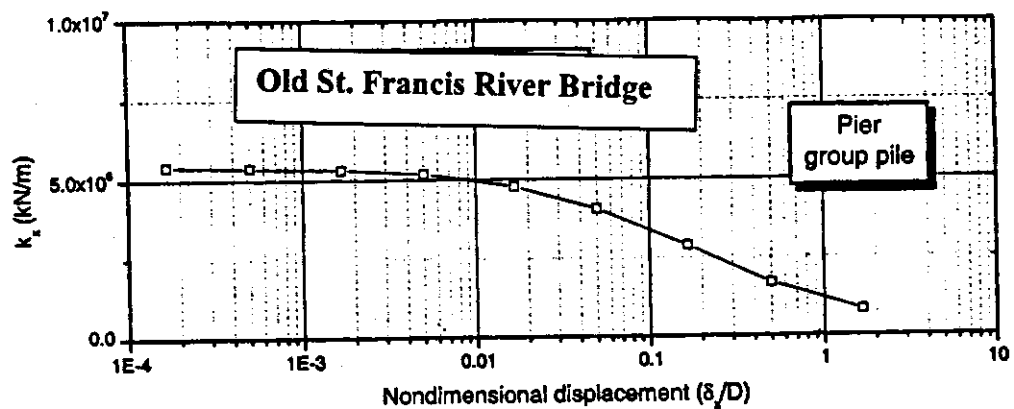
**F.7b Damping Due to Vertical and Sliding Along the X and Y Axis vs. Rotation for the Abutment Group Pile, Old St. Francis River Bridge**



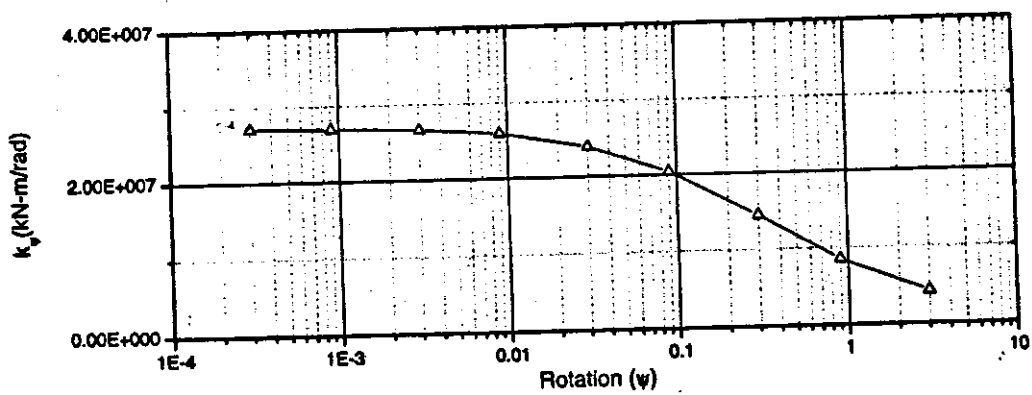
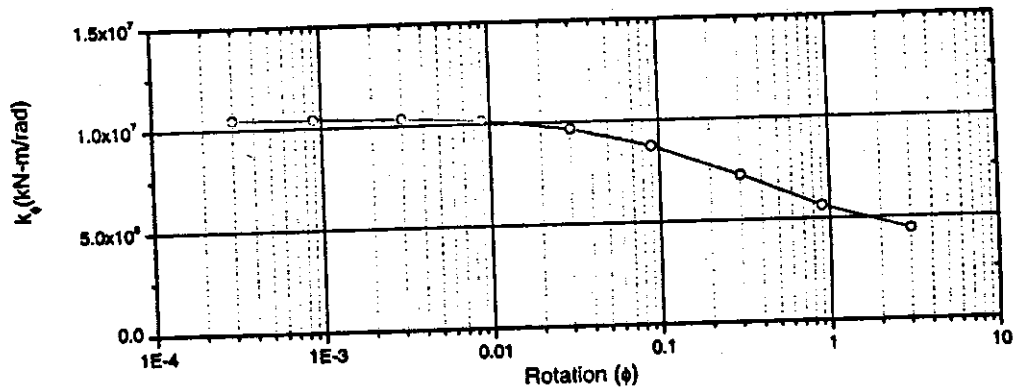
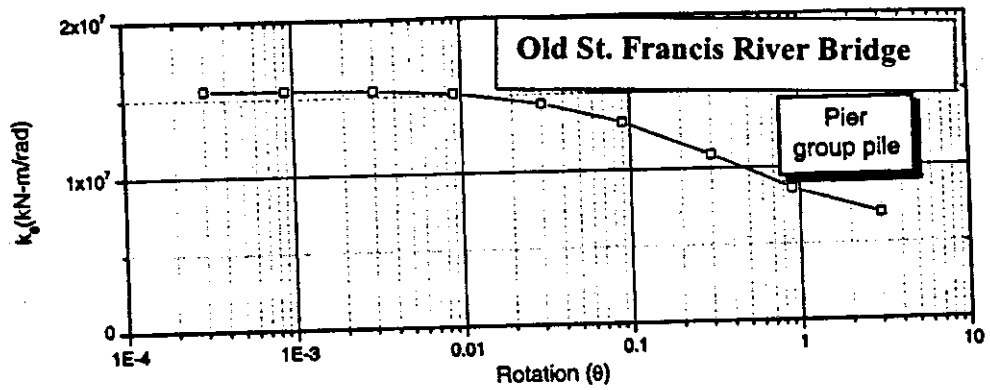
**F.7c. Damping Due to Torsion and Rocking About the X and Y Axis vs. Rotation for the Abutment Group Pile, Old St. Francis River Bridge**



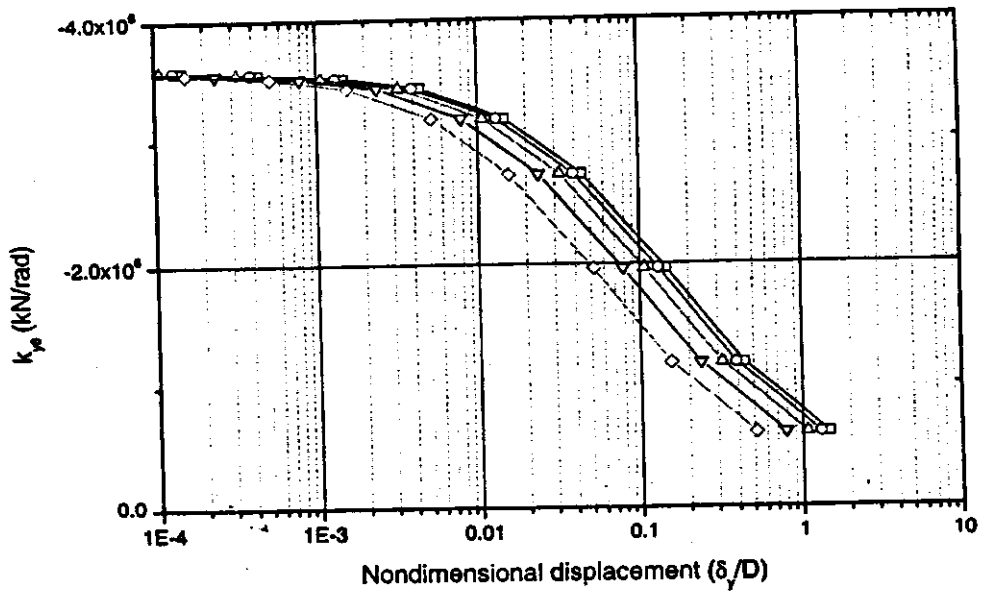
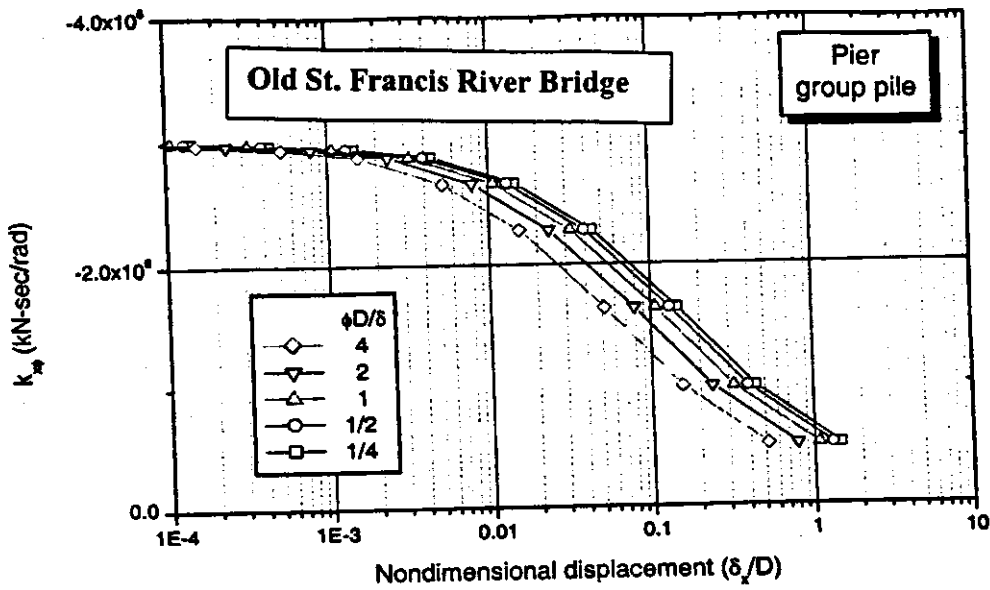
**F.7d Cross-Coupled Damping About the X and Y Axis vs. Nondimensional Displacement for the Abutment Group Pile, Old St. Francis River Bridge**



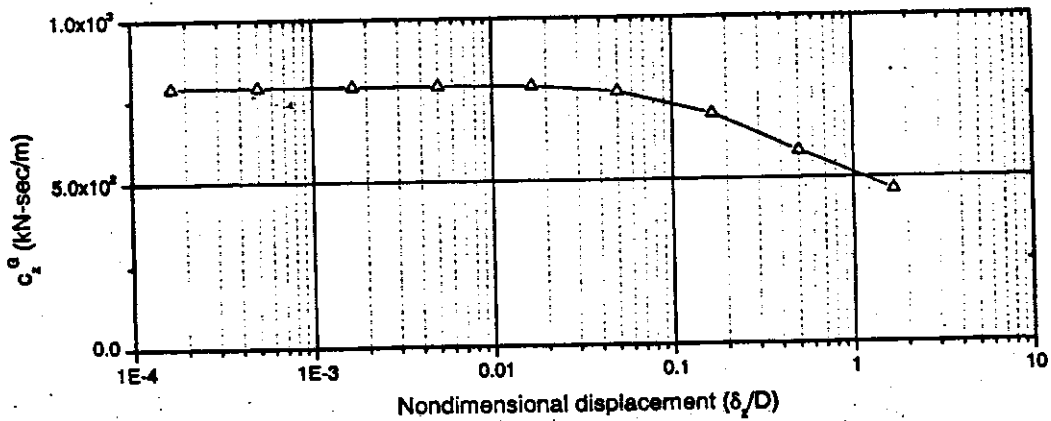
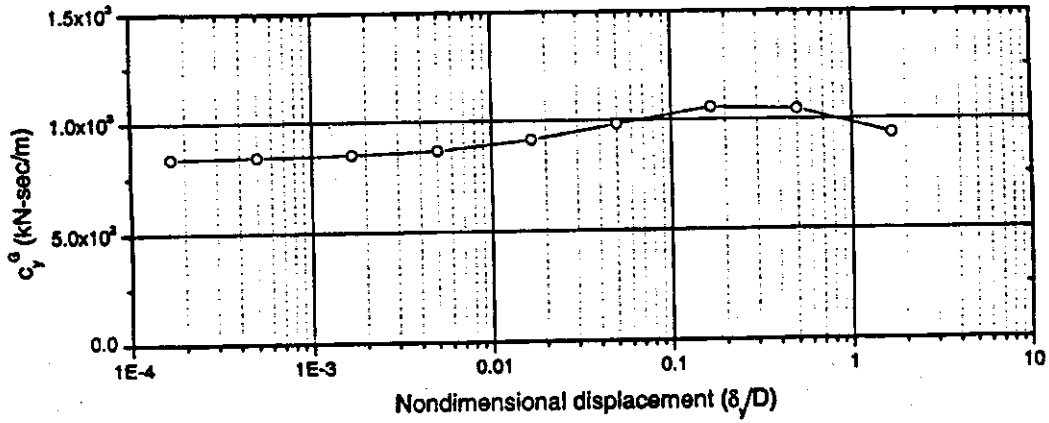
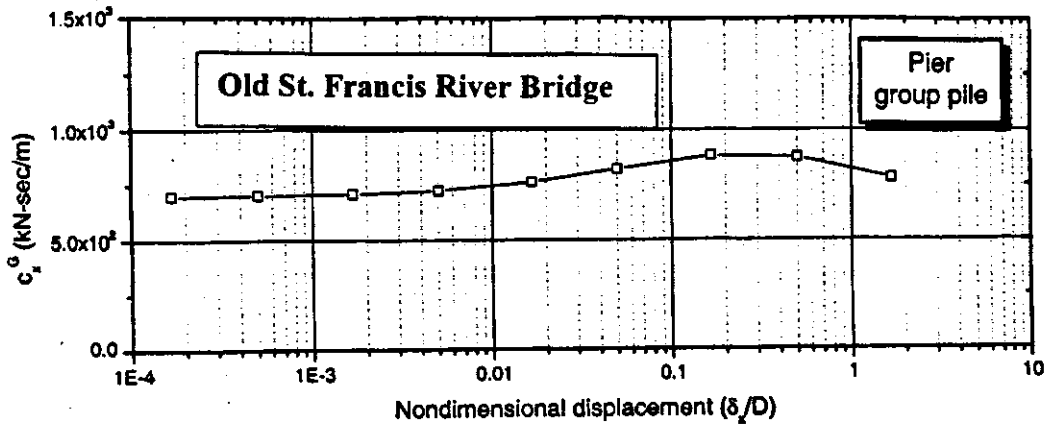
**F.7e Group Stiffness in Vertical and X and Y Translation vs. Nondimensional Displacement for the Pier Group Pile, Old St. Francis River Bridge**



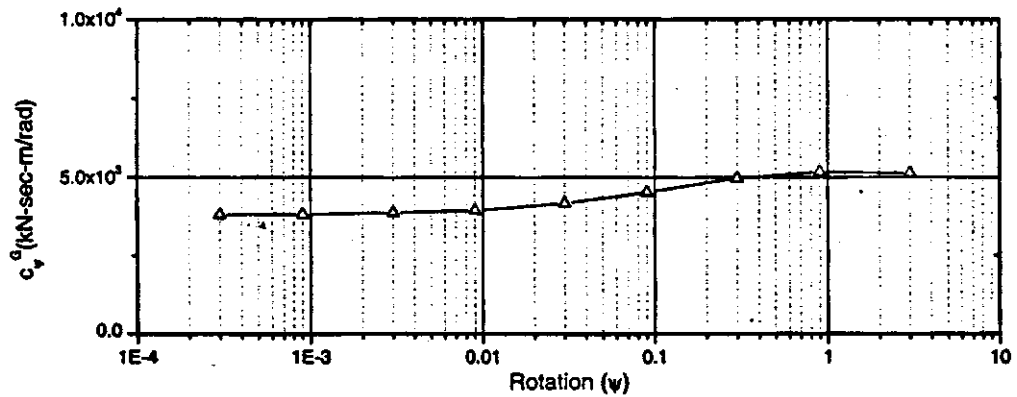
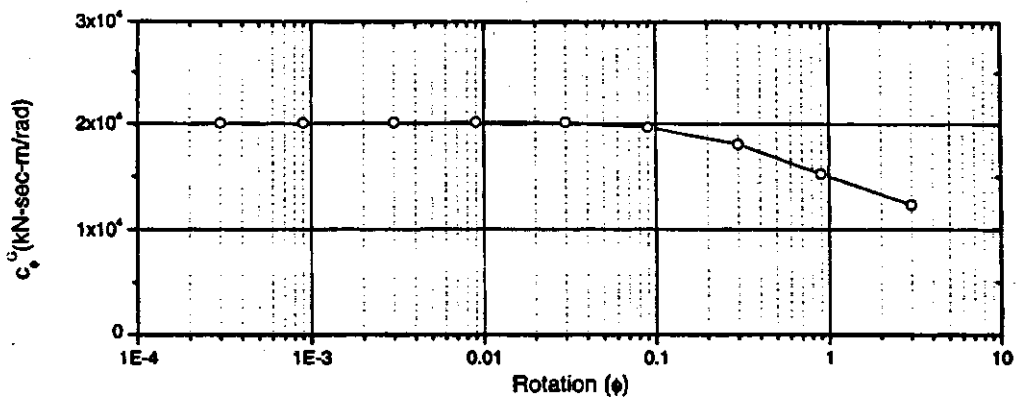
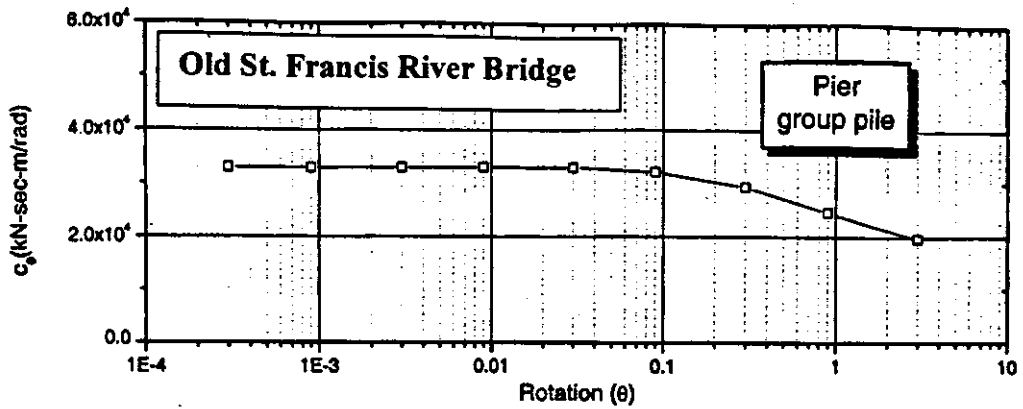
**F.7f Group Stiffness Due to Torsion and Rocking About the X and Y Axis vs. Rotation for the Pier Group Pile, Old St. Francis River Bridge**



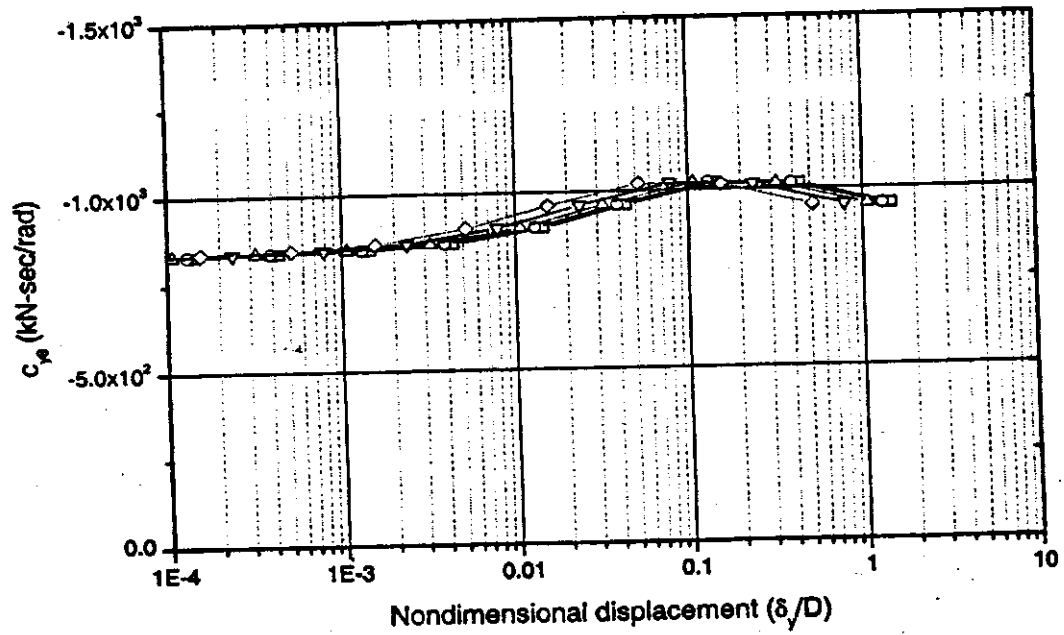
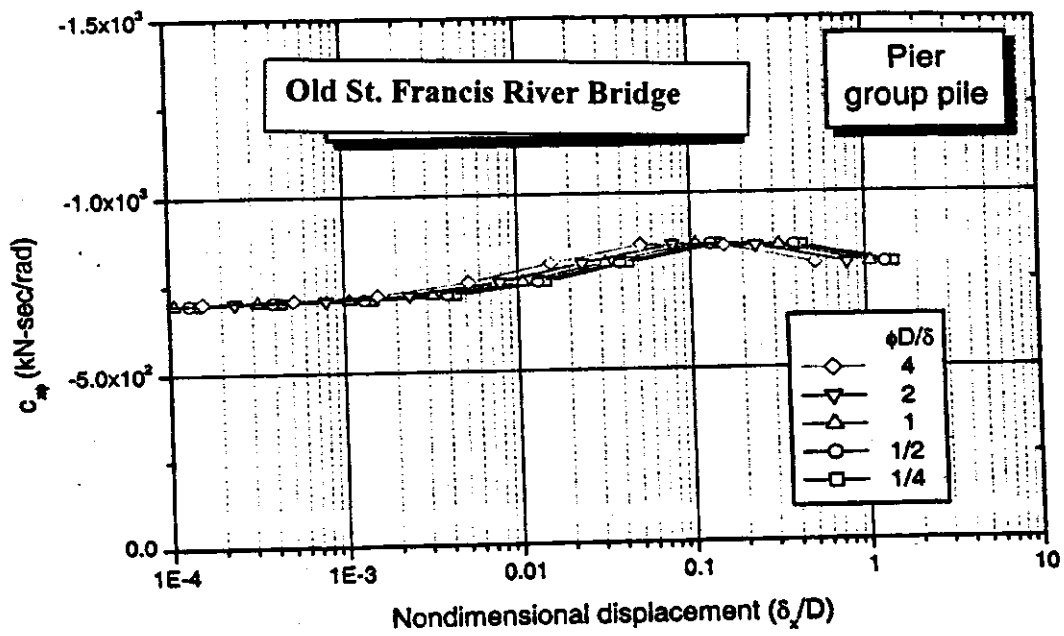
**F.7g Cross-Coupling Translation in X and Y-Axis vs. Nondimensional Displacement for the Pier Group Pile, Old St. Francis River Bridge**



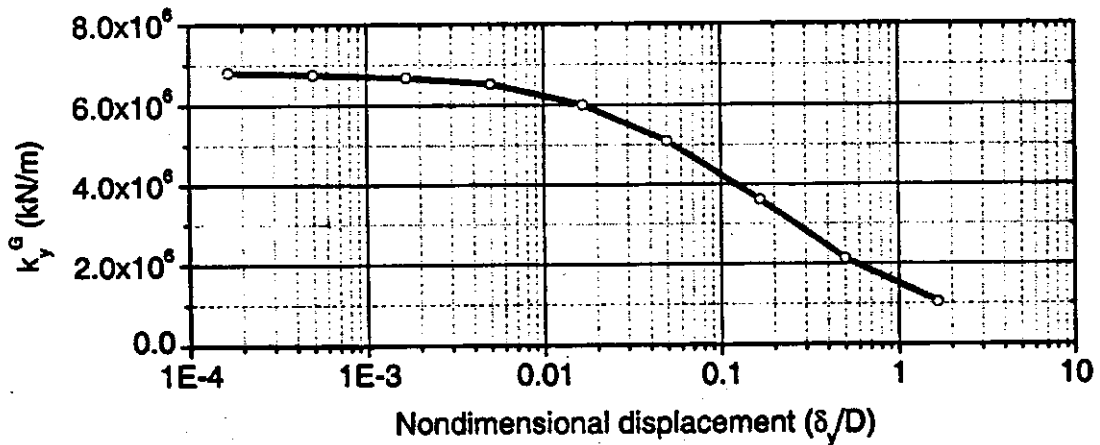
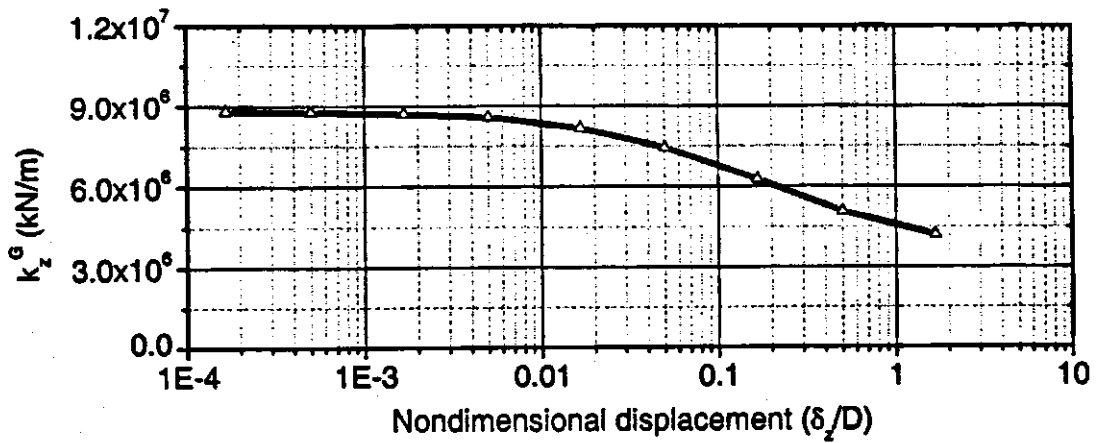
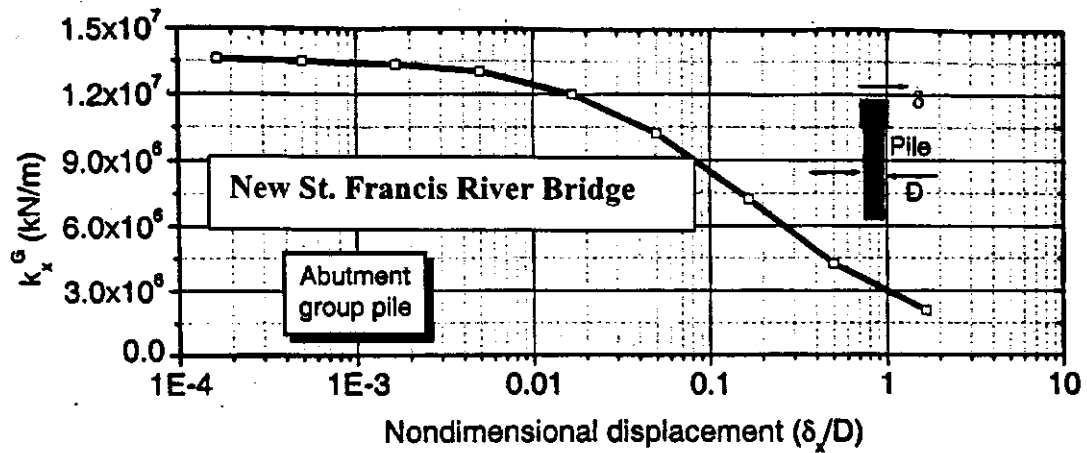
**F.7h Damping Due to Vertical and Sliding Along the X and Y Axis vs. Rotation for the Pier Group Pile, Old St. Francis River Bridge**



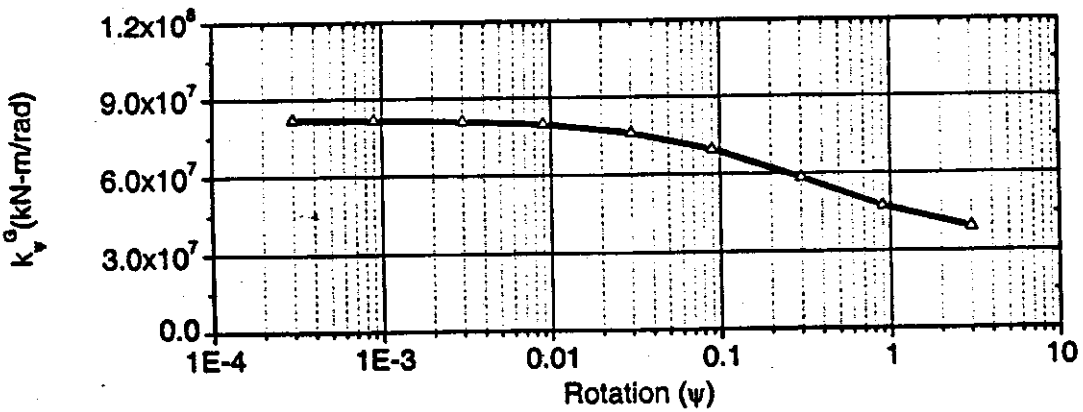
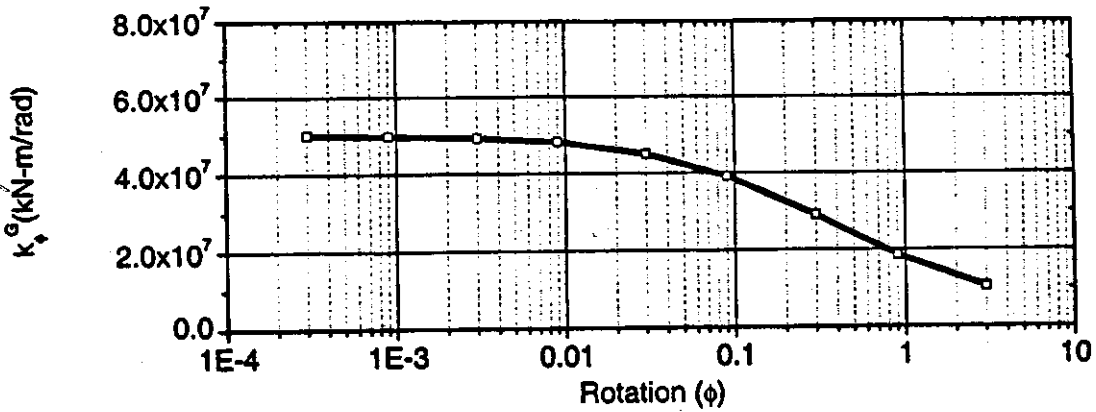
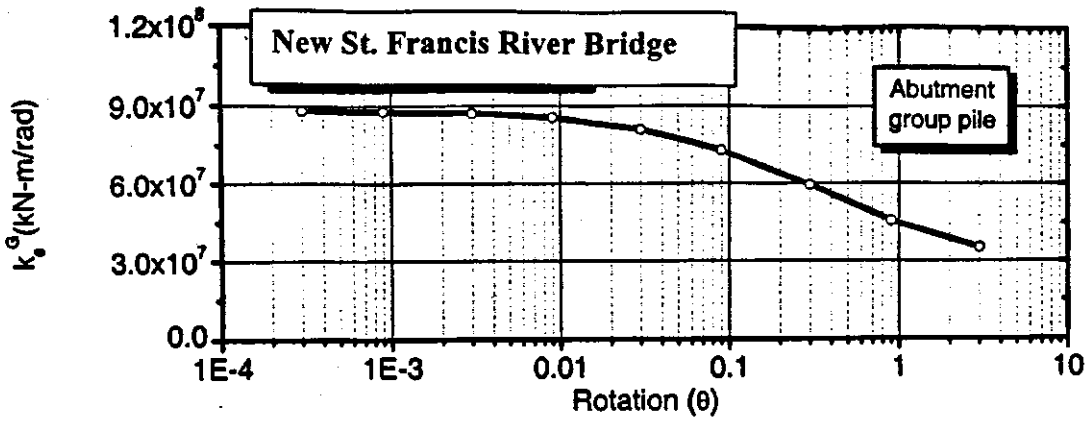
**F.7i Damping Due to Torsion and Rocking About the X and Y Axis vs. Rotation for the Pier Group Pile, Old St. Francis River Bridge**



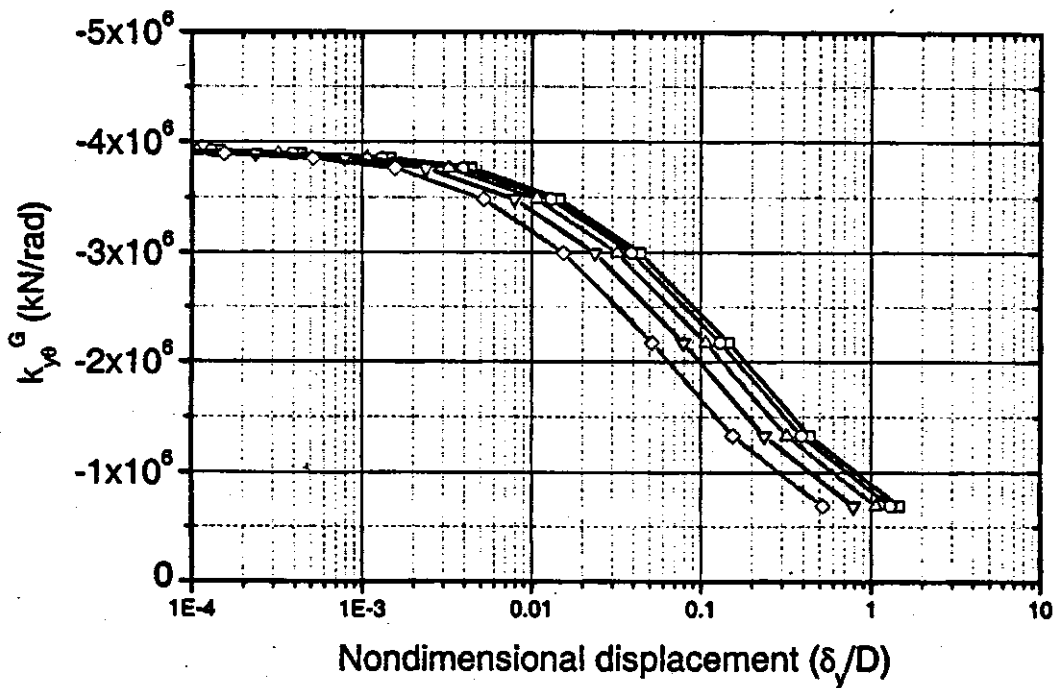
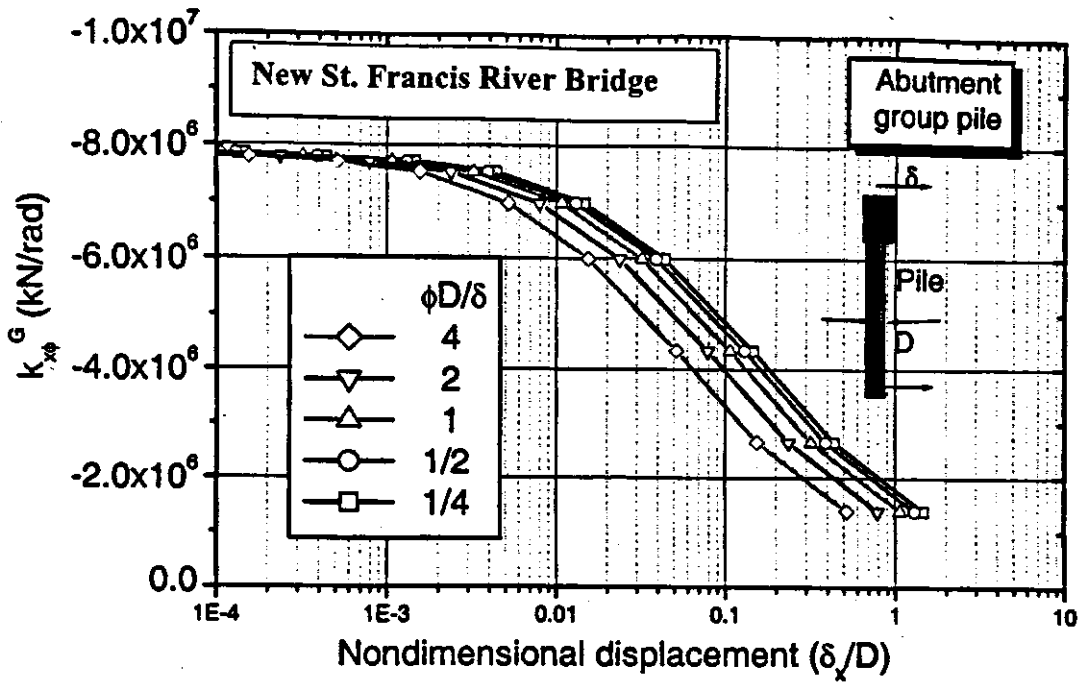
**F.7j Cross-Coupled Damping About the X and Y Axis vs. Nondimensional Displacement for the Pier Group Pile, Old St. Francis River Bridge**



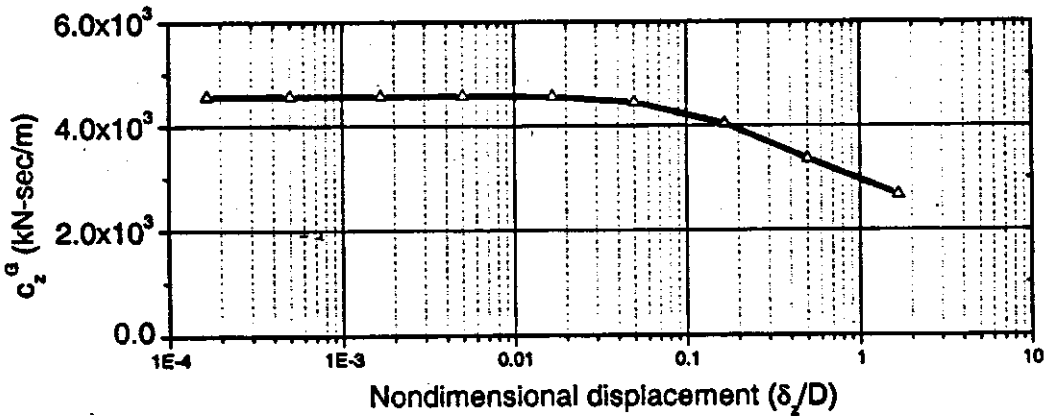
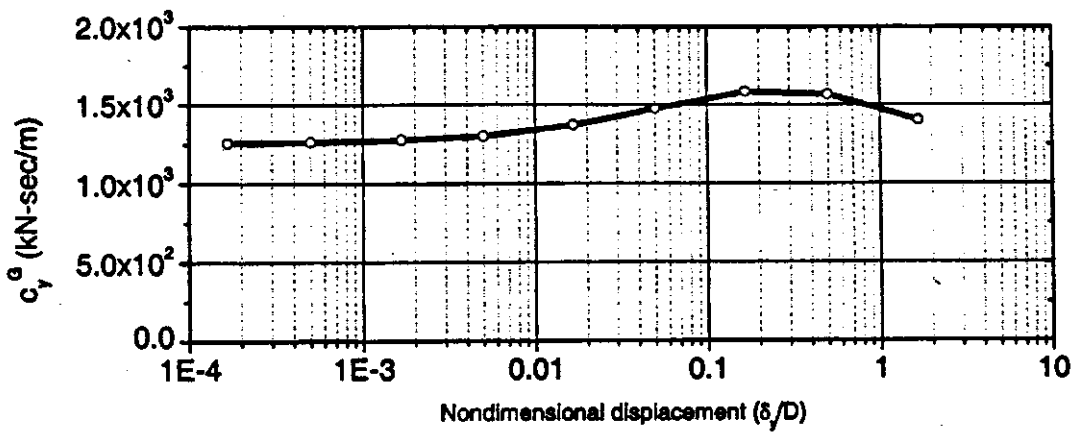
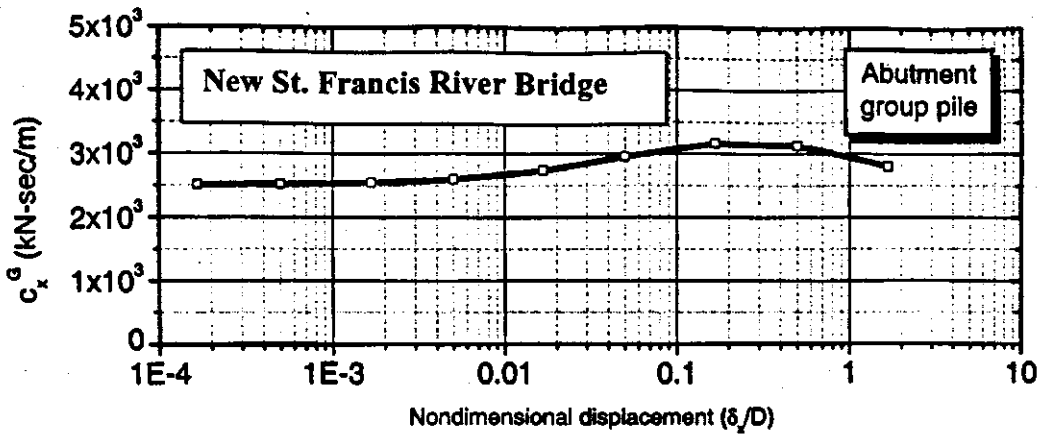
**F7.k Group Stiffness in Vertical and X and Y Translation vs. Nondimensional Displacement for the Abutment Group Pile, New St. Francis River Bridge**



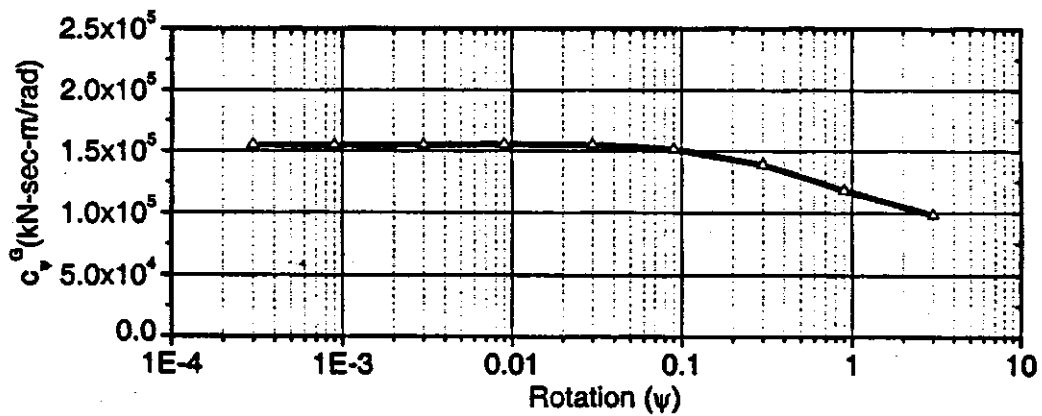
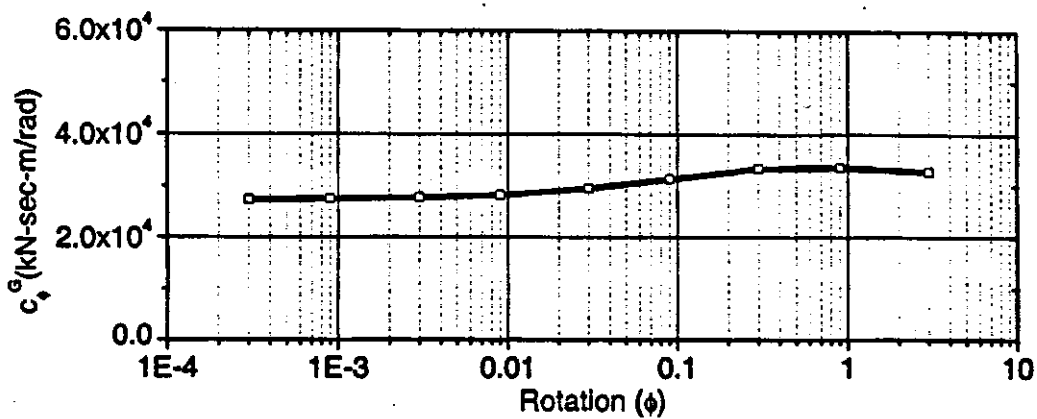
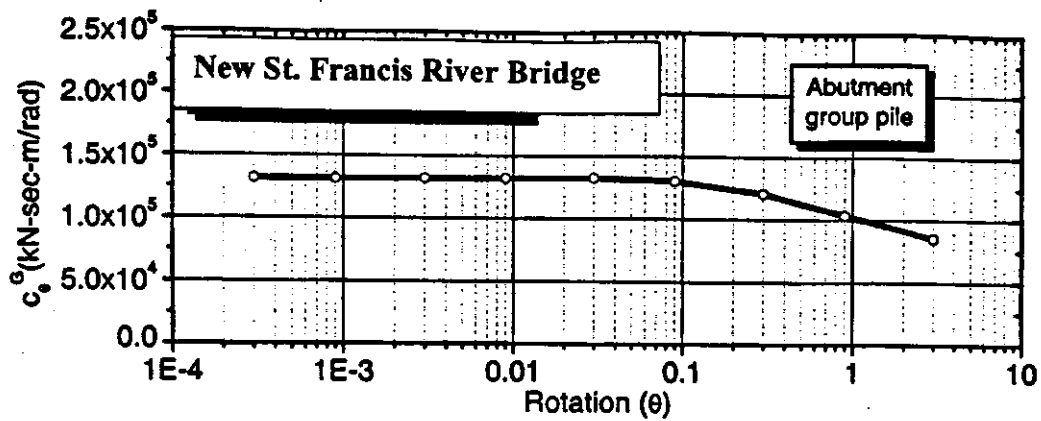
**F.7I Group Stiffness Due to Torsion and Rocking About the X and Y Axis vs. Rotation for the Abutment Group Pile, New St. Francis River Bridge**



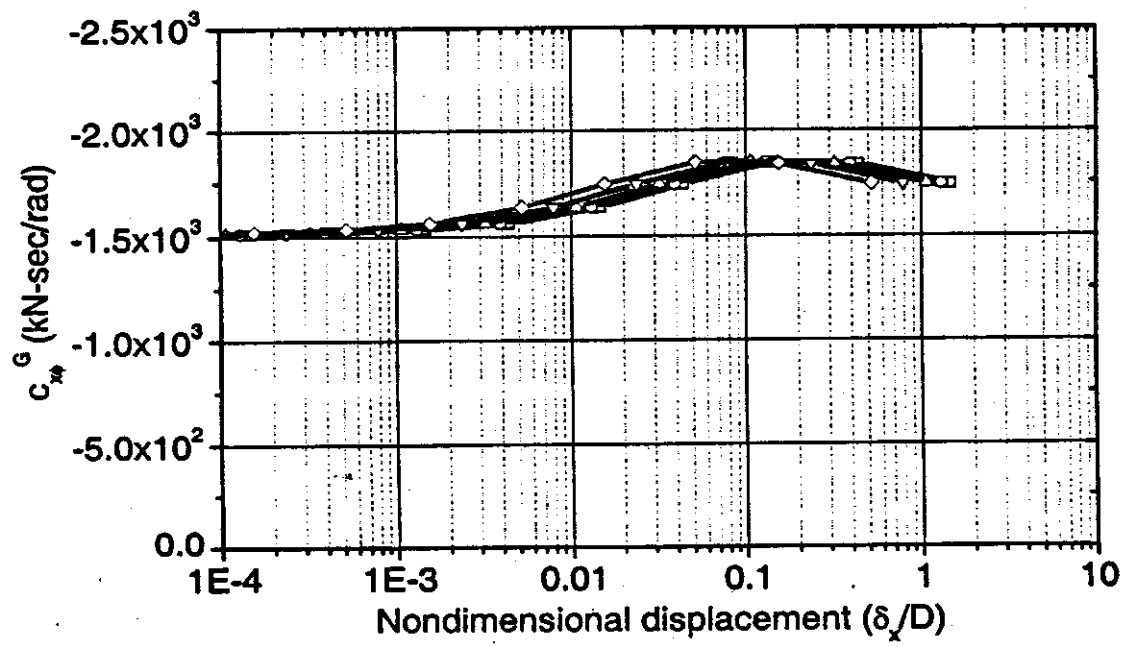
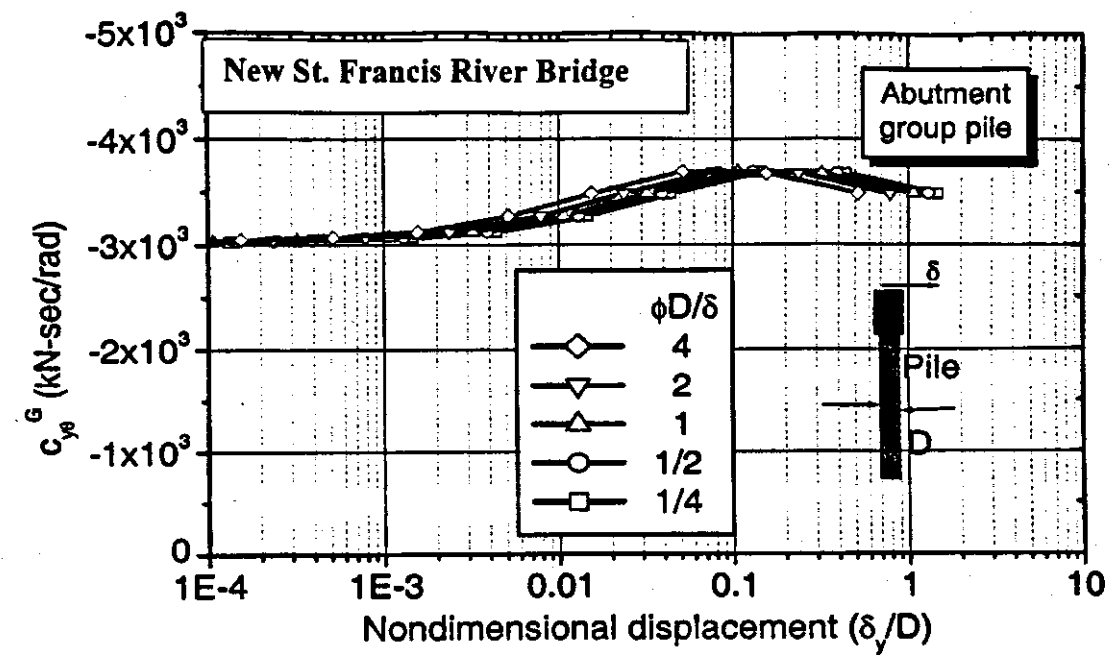
**F.7m Cross-Coupling Translation in X and Y-Axis vs. Nondimensional Displacement for the Abutment Group Pile, New St. Francis River Bridge**



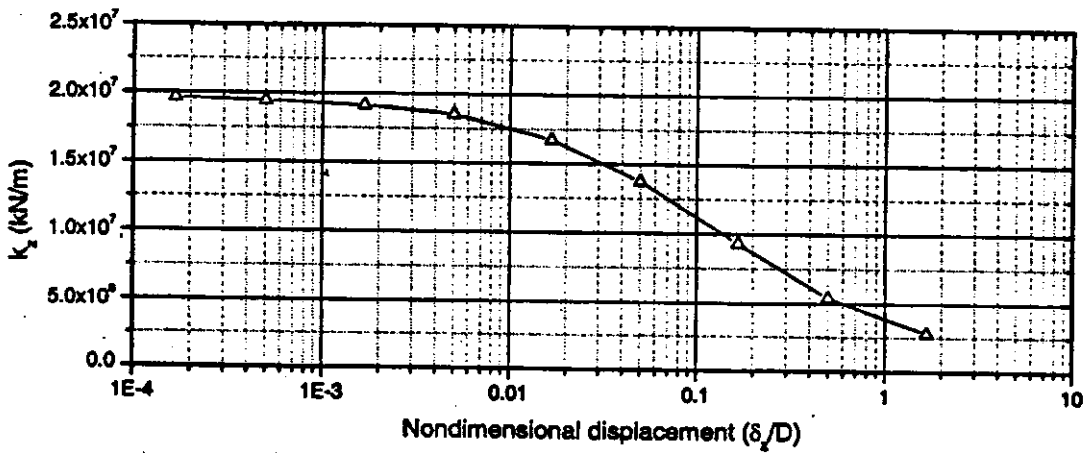
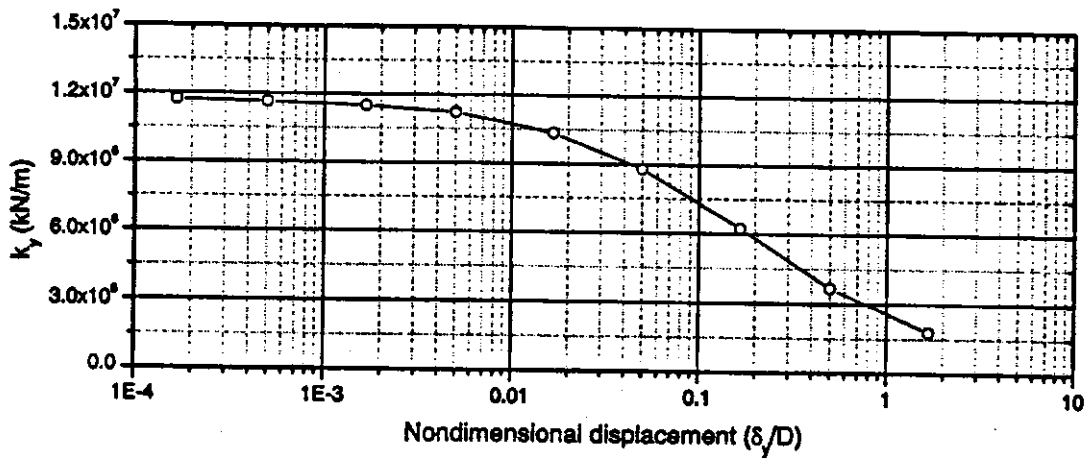
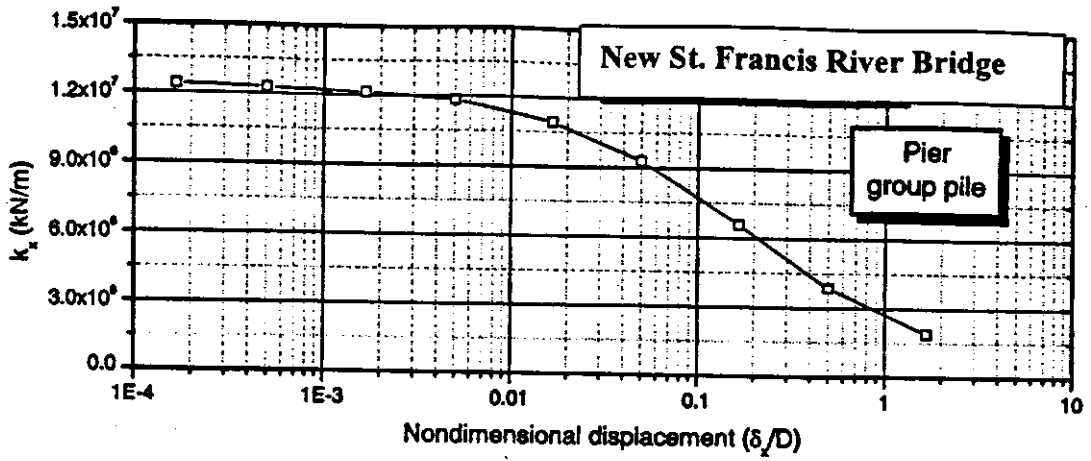
**F.7n Damping Due to Vertical and Sliding Along the X and Y Axis vs. Rotation for the Abutment Group Pile, New St. Francis River Bridge**



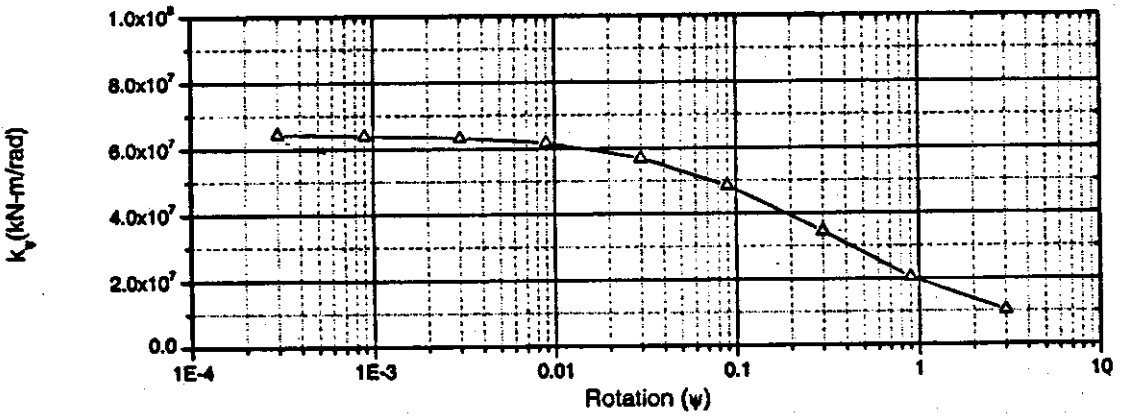
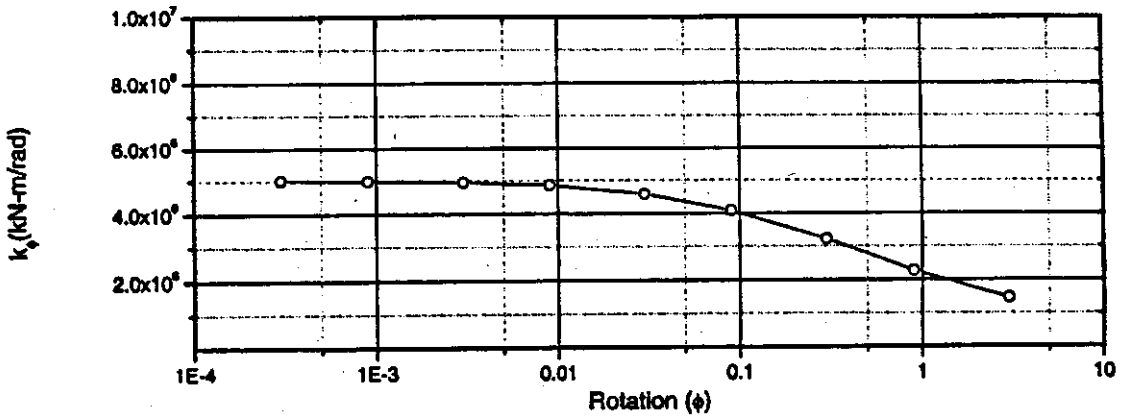
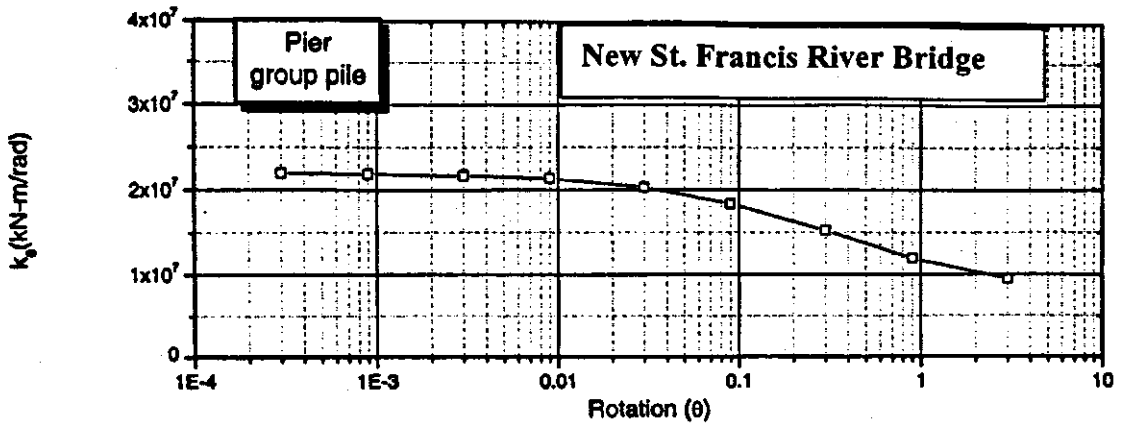
**F.7o Damping Due to Torsion and Rocking About the X and Y Axis vs. Rotation for the Abutment Group Pile, New St. Francis River Bridge**



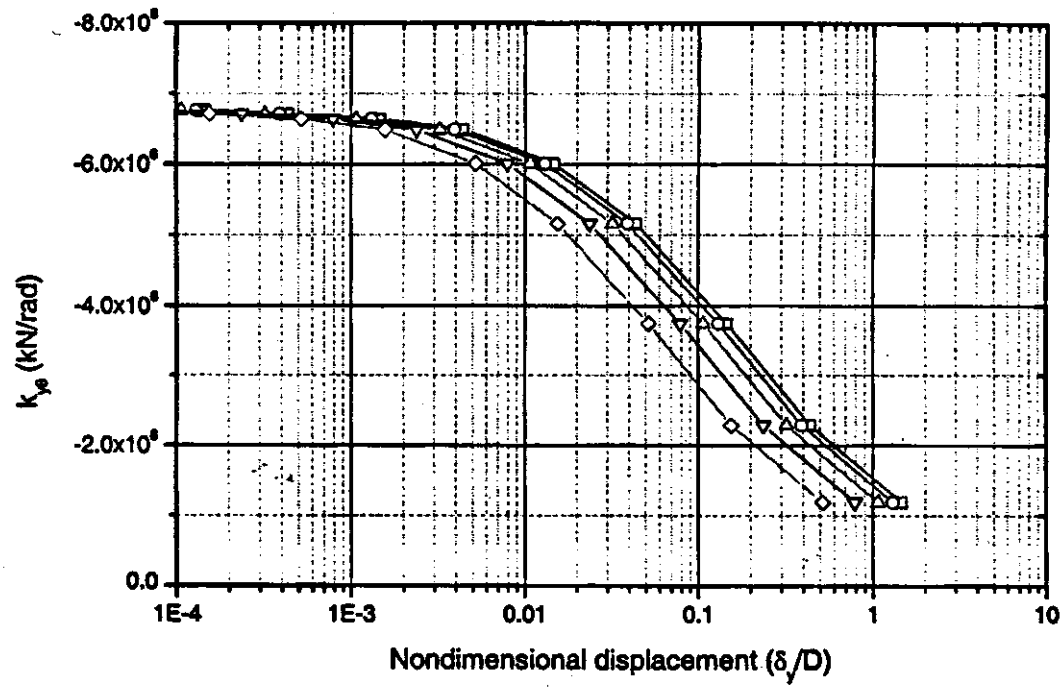
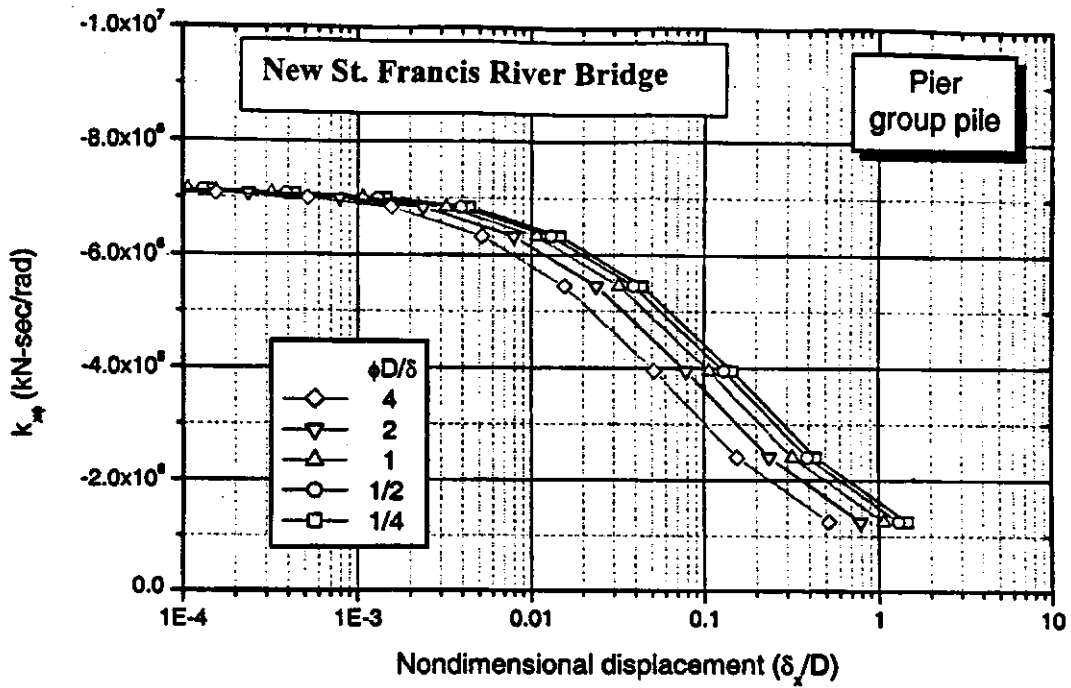
**F.7p Cross-Coupled Damping About the X and Y Axis vs. Nondimensional Displacement for the Abutment Group Pile, New St. Francis River Bridge**



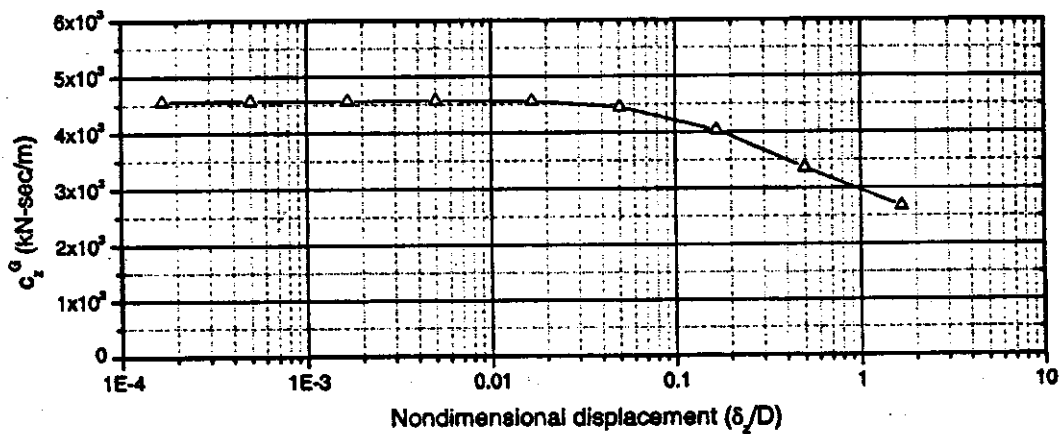
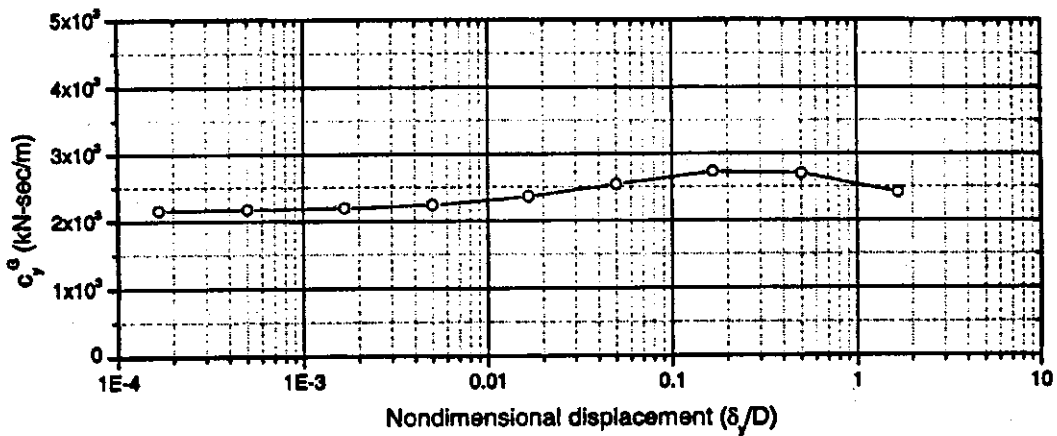
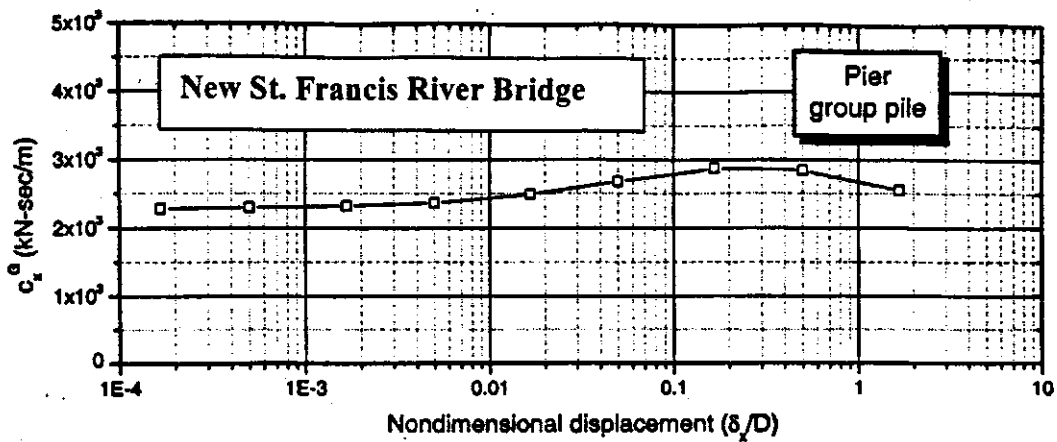
**F.7q Group Stiffness in Vertical and X and Y Translation vs. Nondimensional Displacement for the Pier Group Pile, New St. Francis River Bridge**



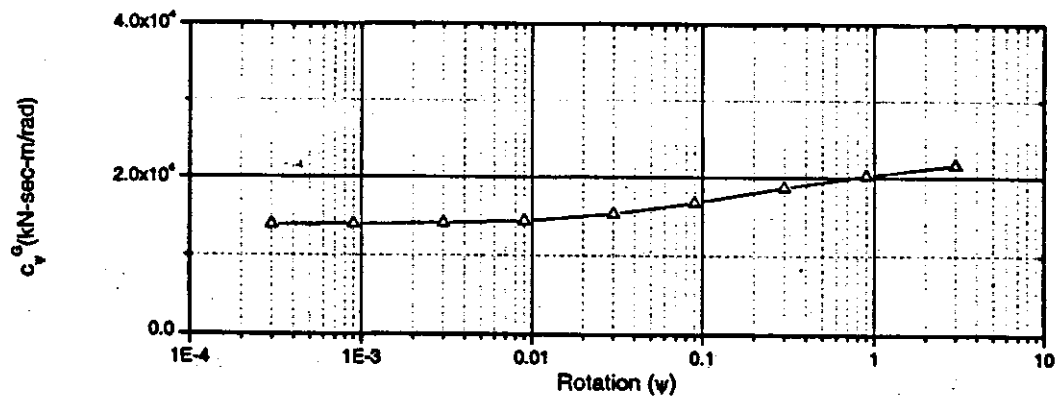
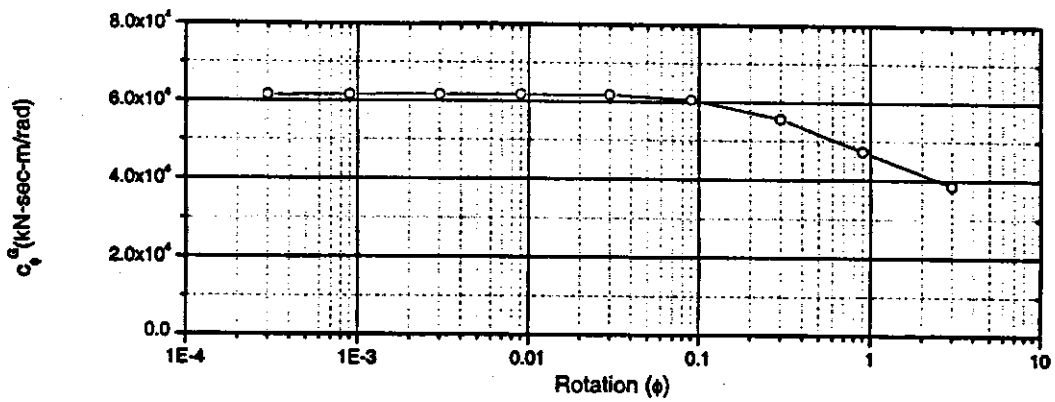
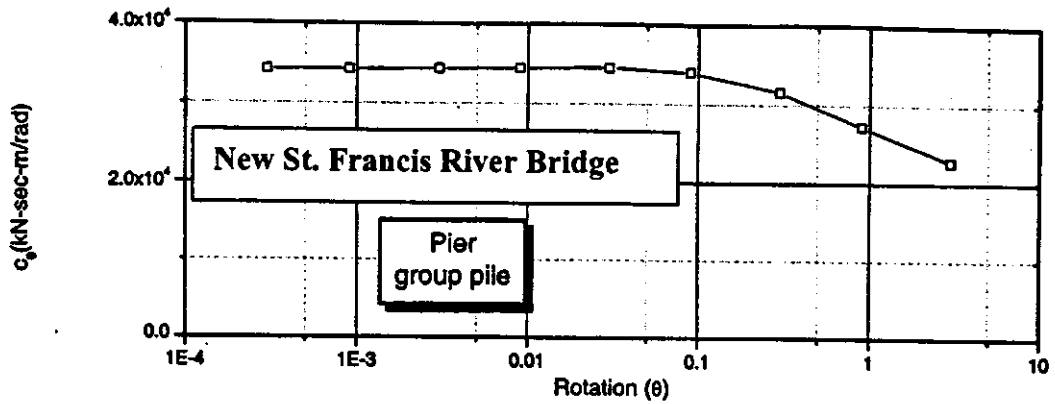
**F.7r Group Stiffness Due to Torsion and Rocking About the X and Y Axis vs. Rotation for the Pier Group Pile, New St. Francis River Bridge**



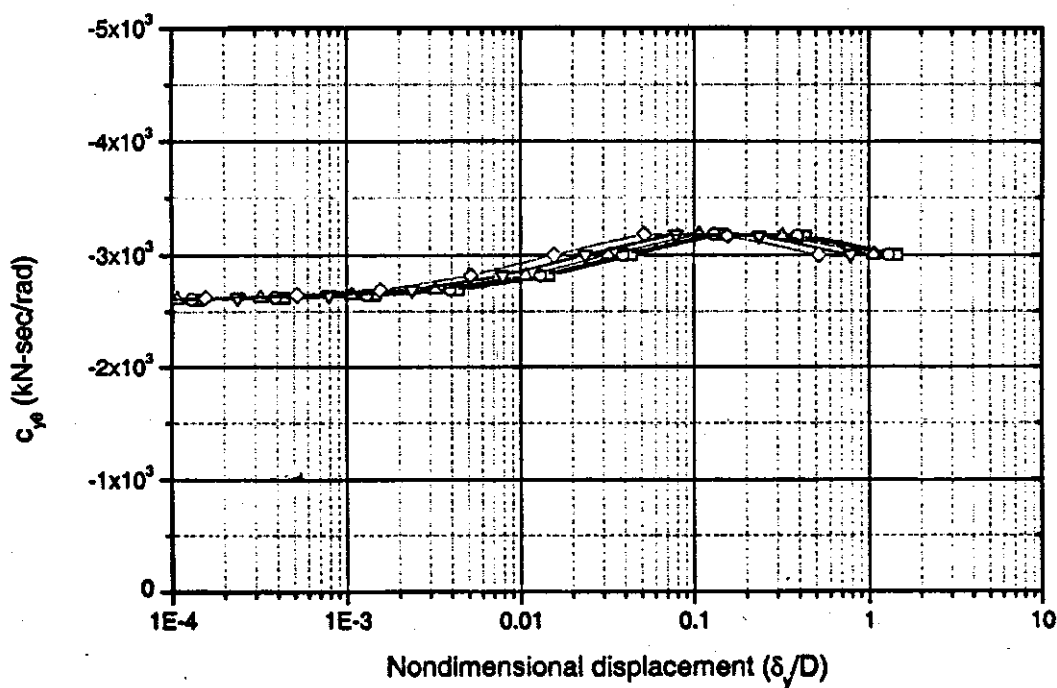
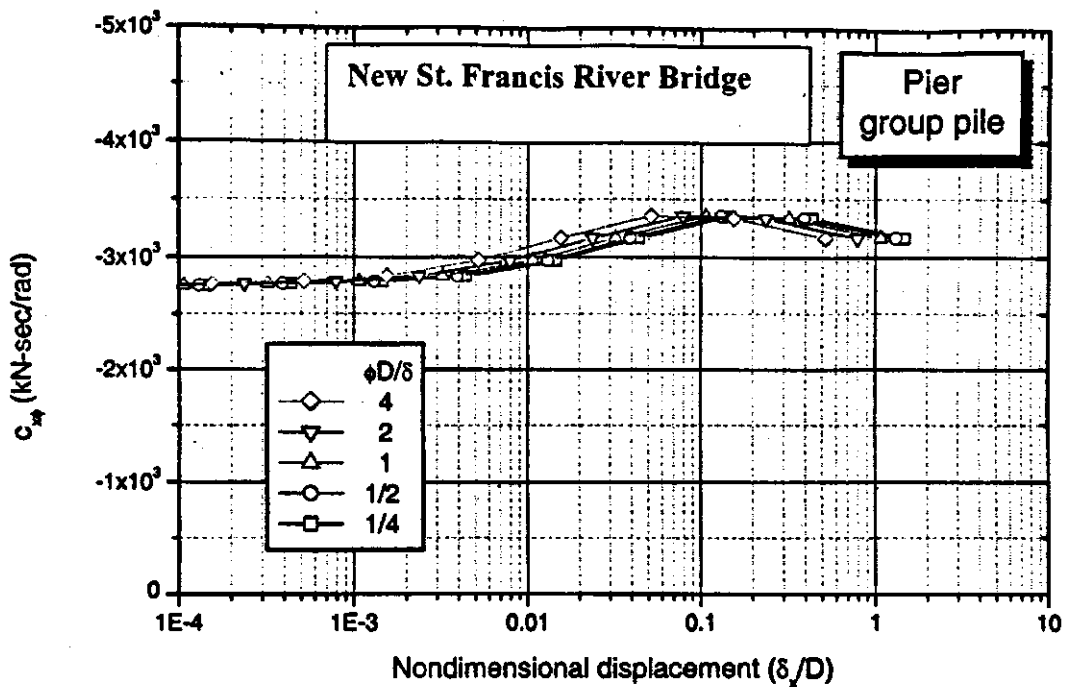
**F.7s Cross-Coupling Translation in X and Y-Axis vs. Nondimensional Displacement for the Pier Group Pile, New St. Francis River Bridge**



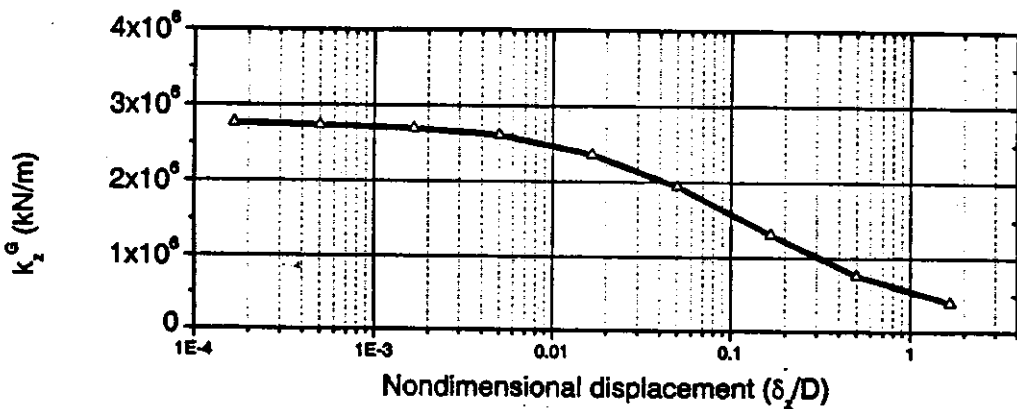
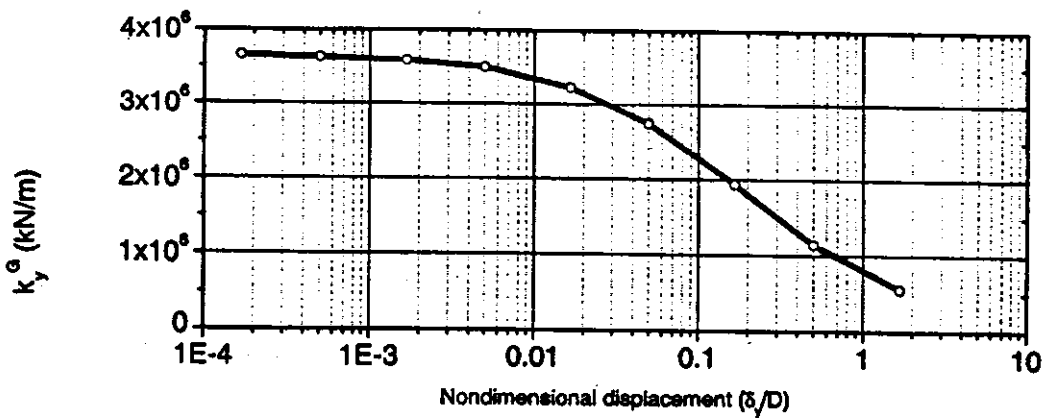
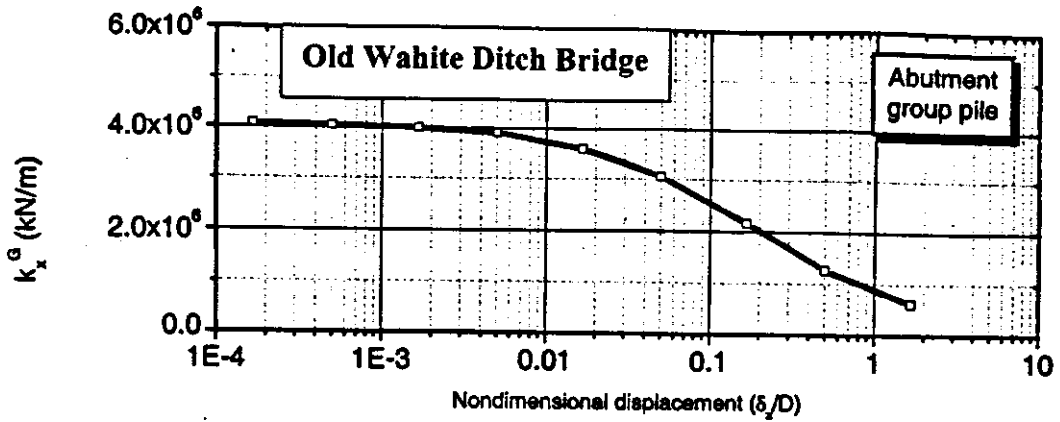
**F.7t Damping Due to Vertical and Sliding Along the X and Y Axis vs. Rotation for the Pier Group Pile, New St. Francis River Bridge**



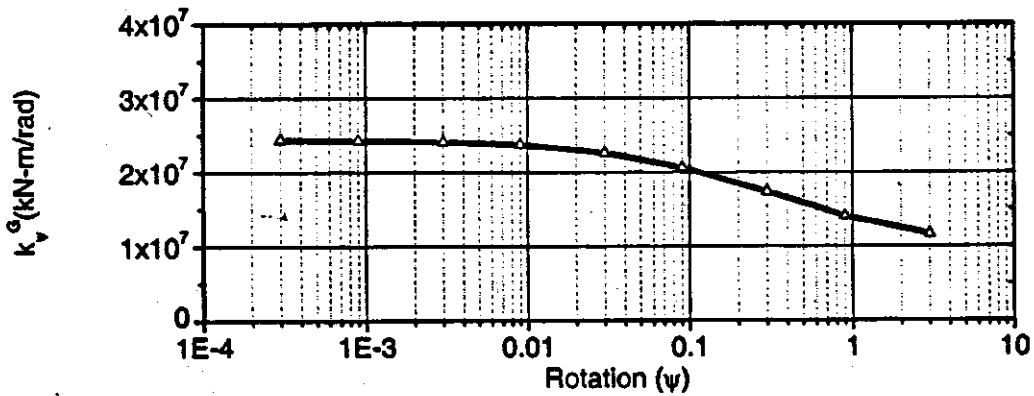
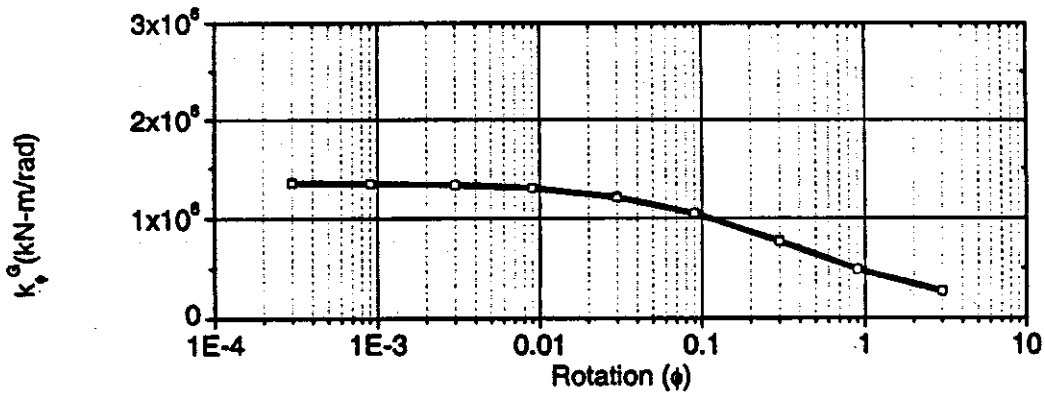
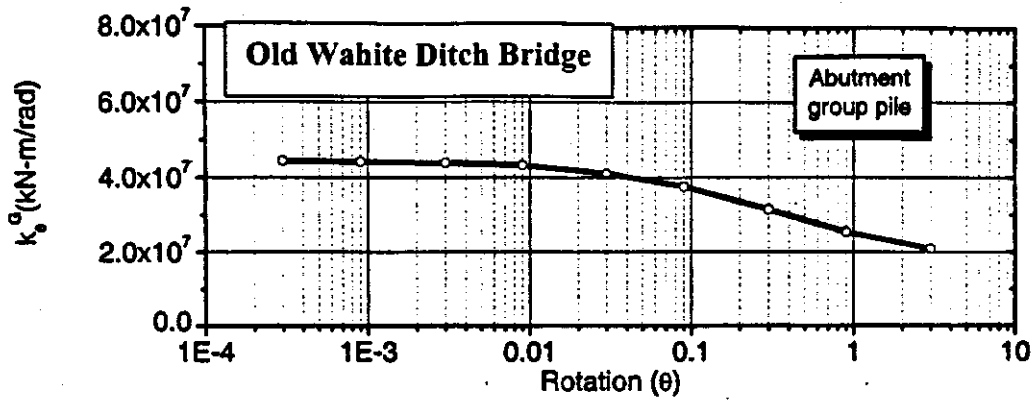
**F.7u Damping Due to Torsion and Rocking About the X and Y Axis vs. Rotation for the Pier Group Pile, New St. Francis River Bridge**



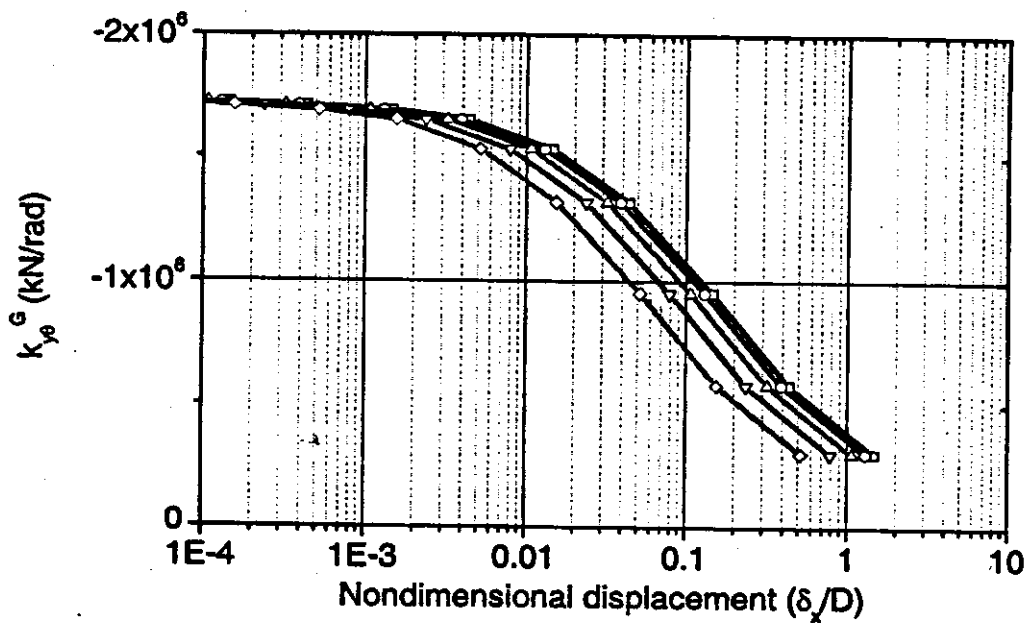
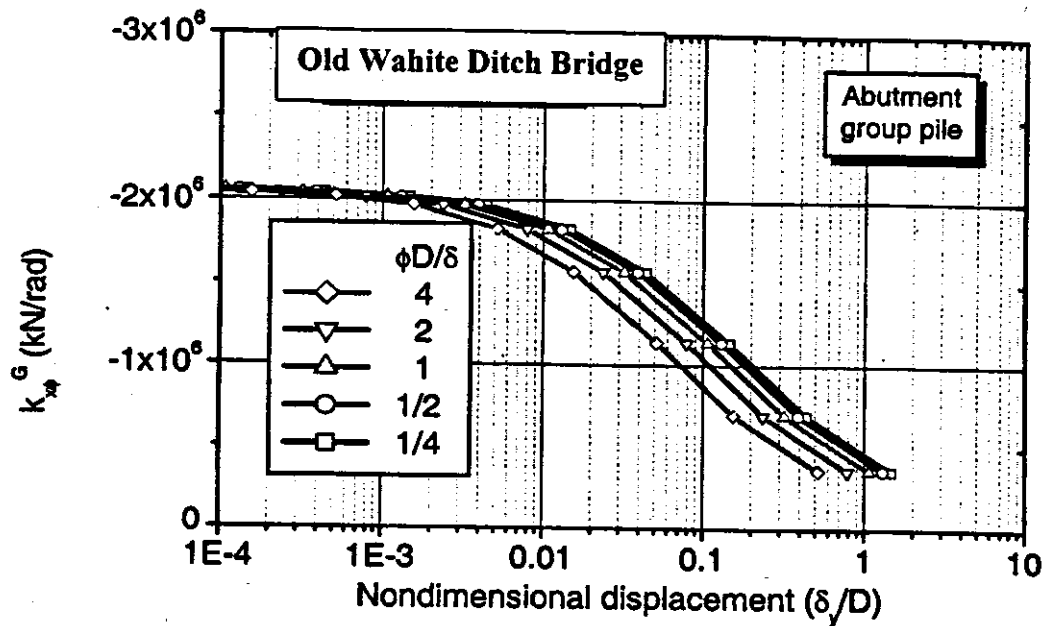
**F.7v Cross-Coupled Damping About the X and Y Axis vs. Nondimensional Displacement for the Pier Group Pile, New St. Francis River Bridge**



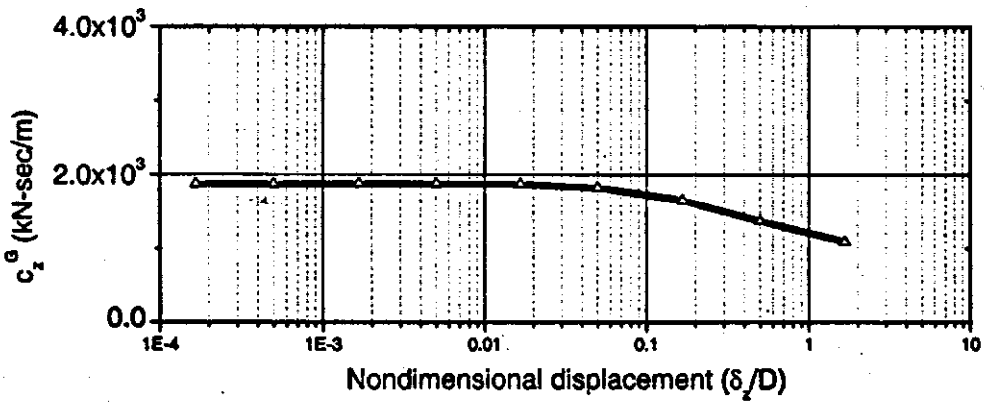
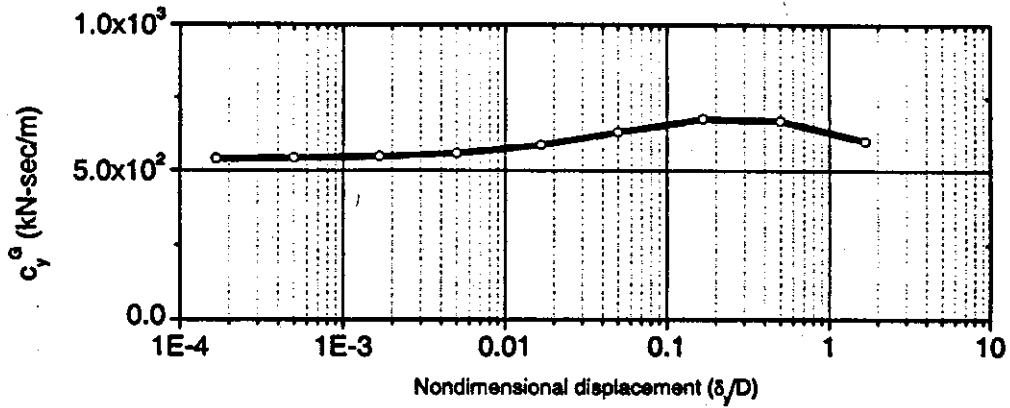
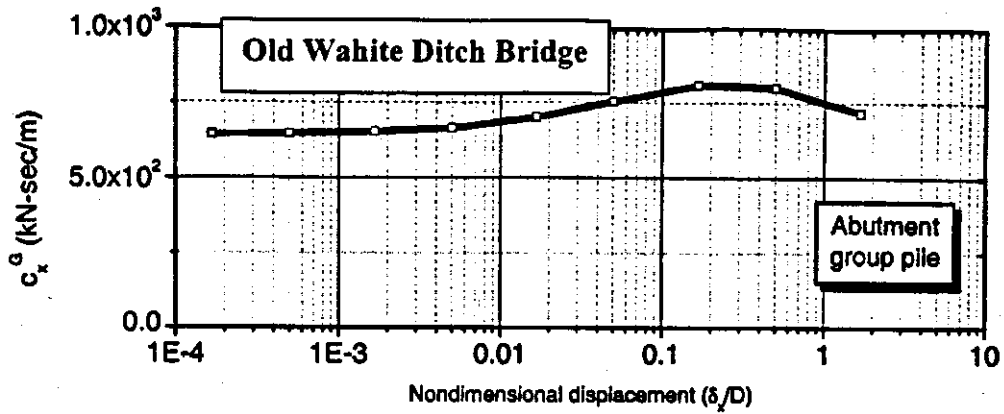
**F.7w Group Stiffness in Vertical and X and Y Translation vs. Nondimensional Displacement for the Abutment Group Pile, Old Wahite Ditch Bridge**



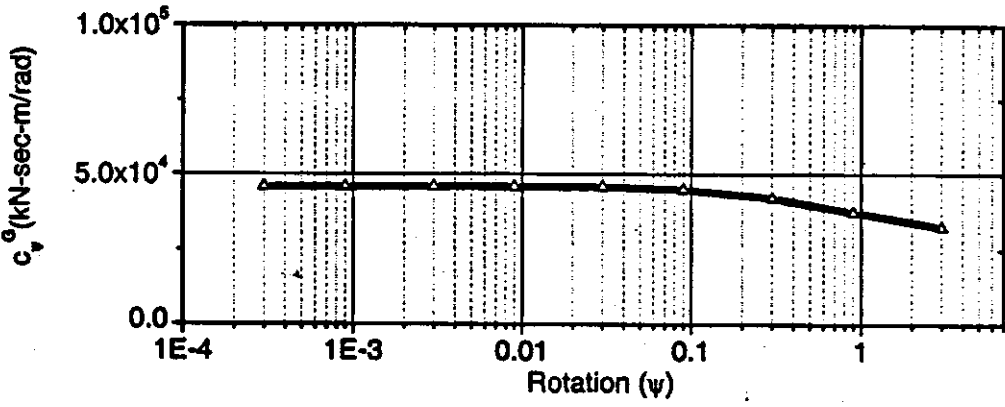
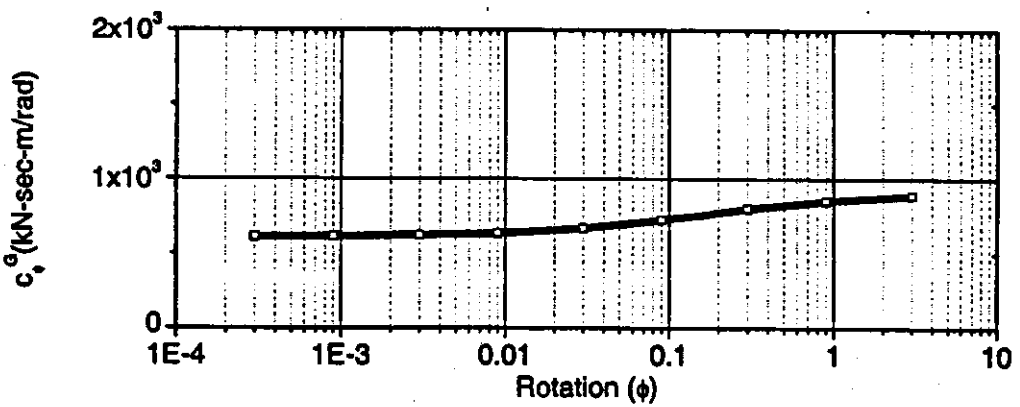
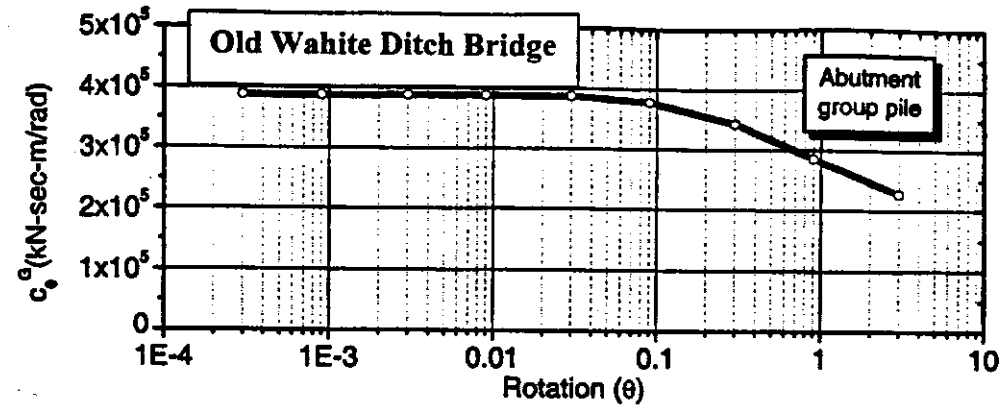
**F.7x Group Stiffness Due to Torsion and Rocking About the X and Y Axis vs. Rotation for the Abutment Group Pile, Old Wahite Ditch Bridge**



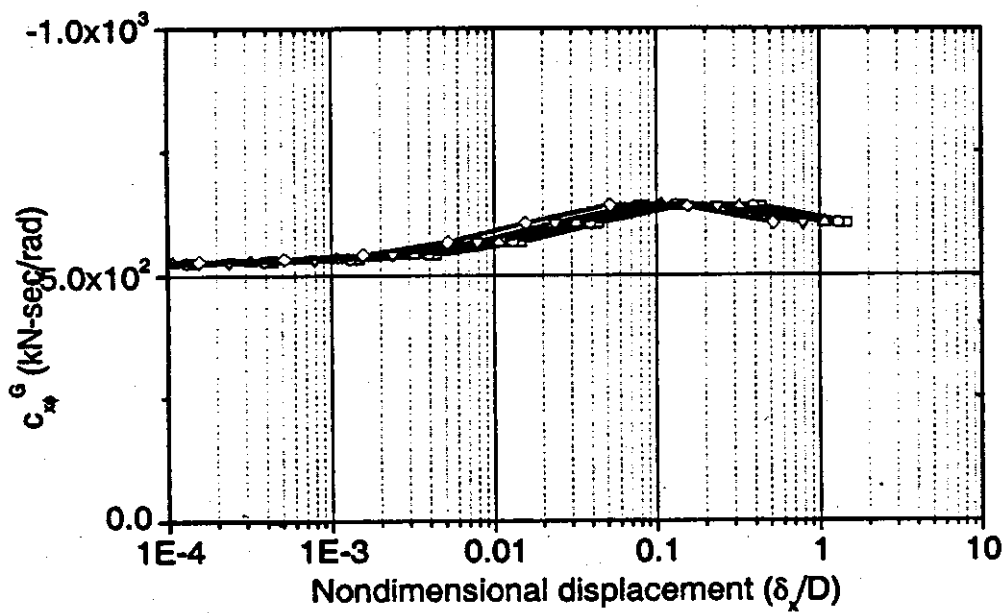
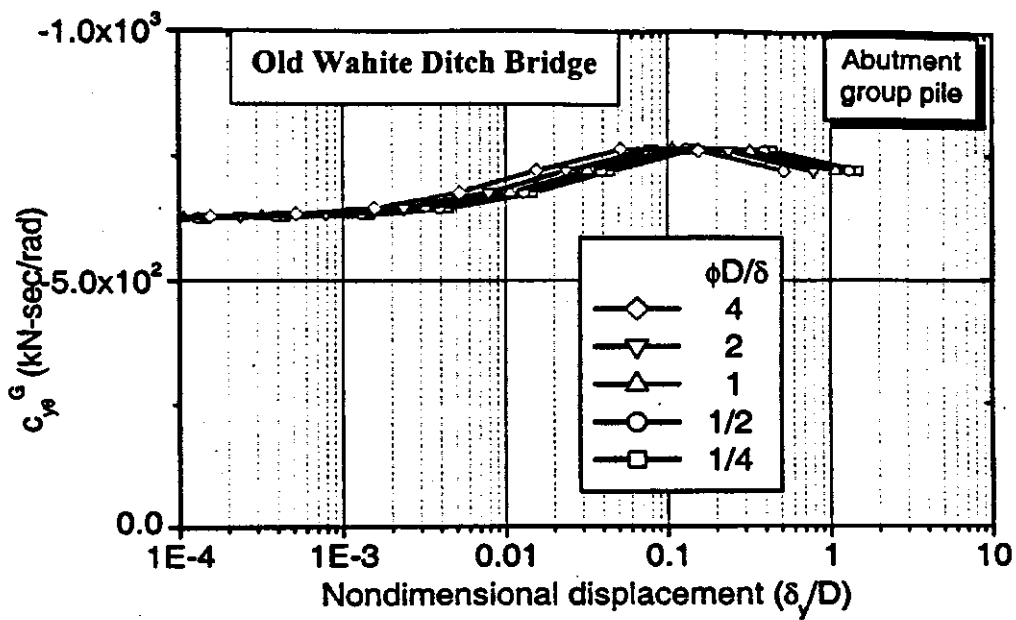
**F.7y Cross-Coupling Translation in X and Y-Axis vs. Nondimensional Displacement for the Abutment Group Pile, Old Wahite Ditch Bridge**



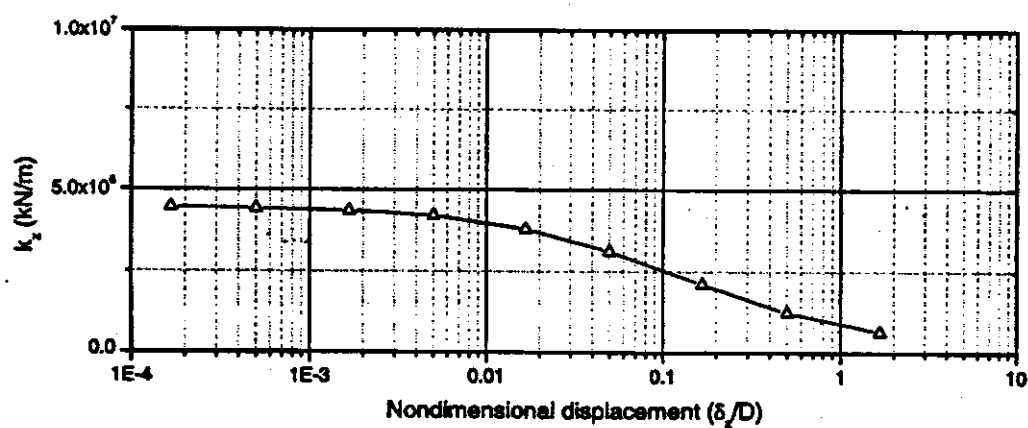
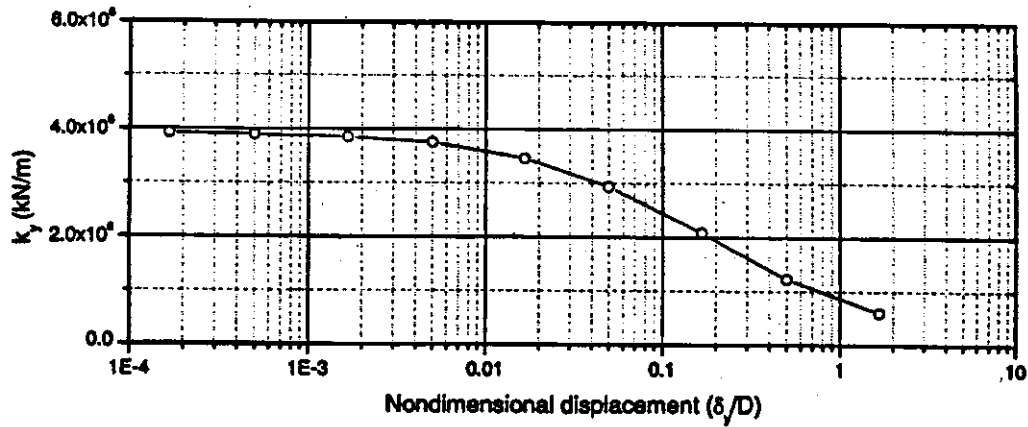
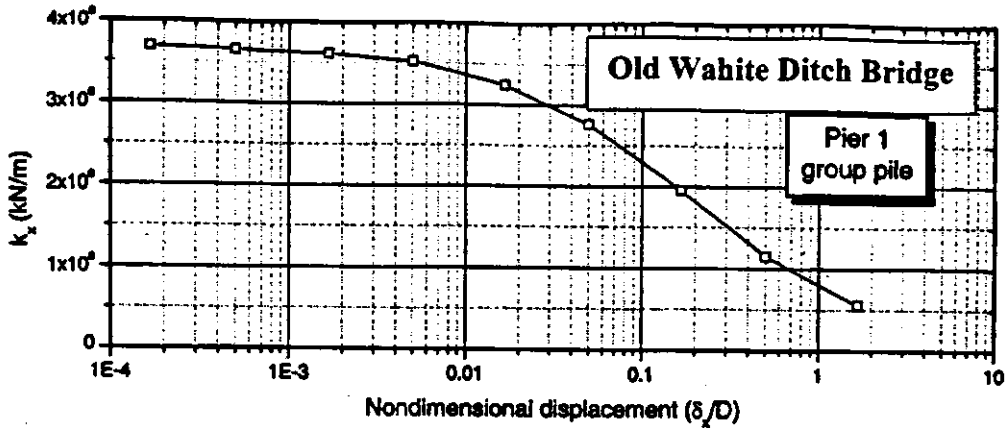
**F.7z Damping Due to Vertical and Sliding Along the X and Y Axis vs. Rotation for the Pier Group Pile, Old Wahite Ditch Bridge**



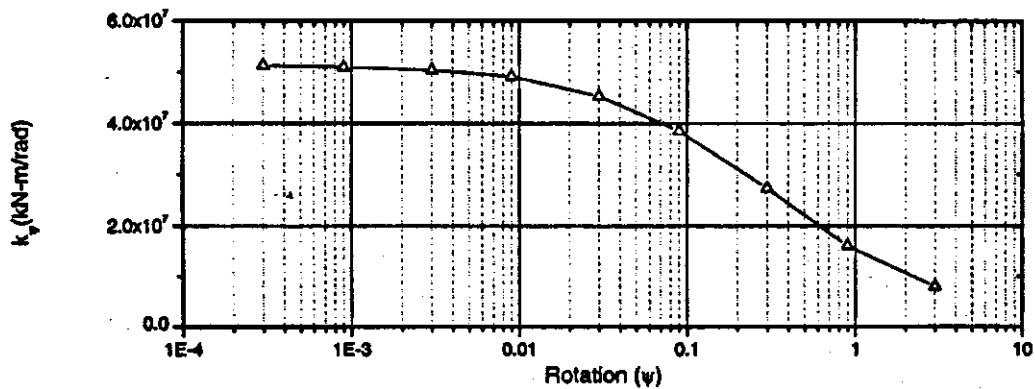
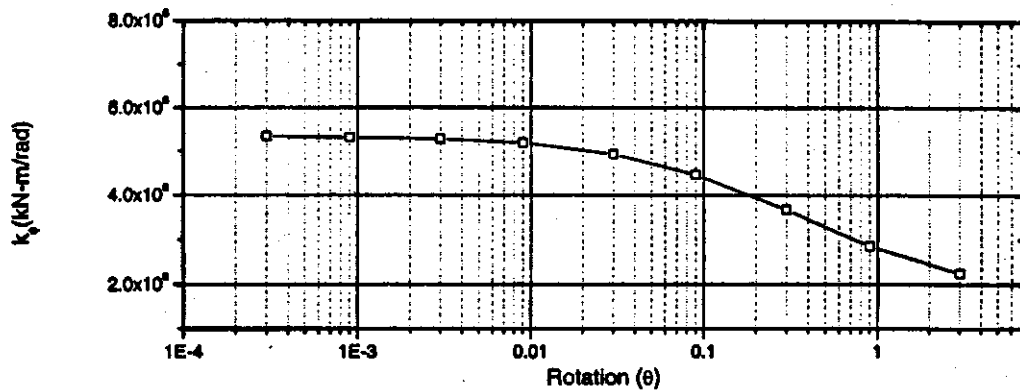
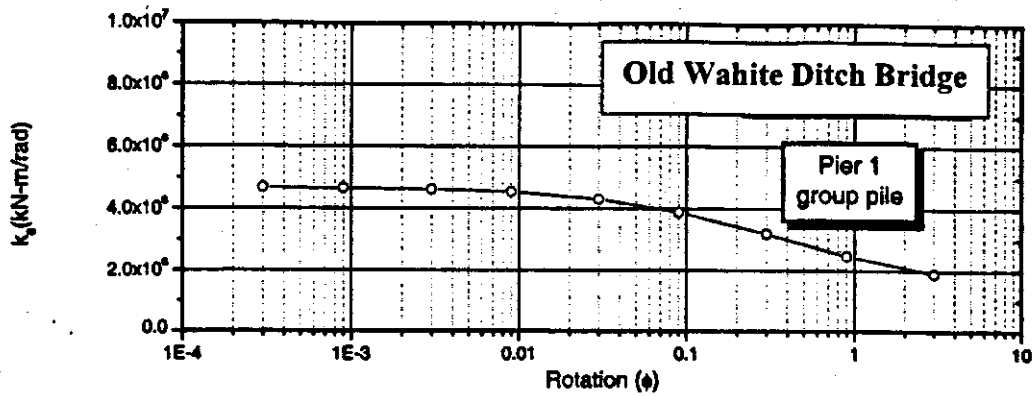
**F.7aa Damping Due to Torsion and Rocking About the X and Y Axis vs. Rotation for the Abutment Group Pile, Old Wahite Ditch Bridge**



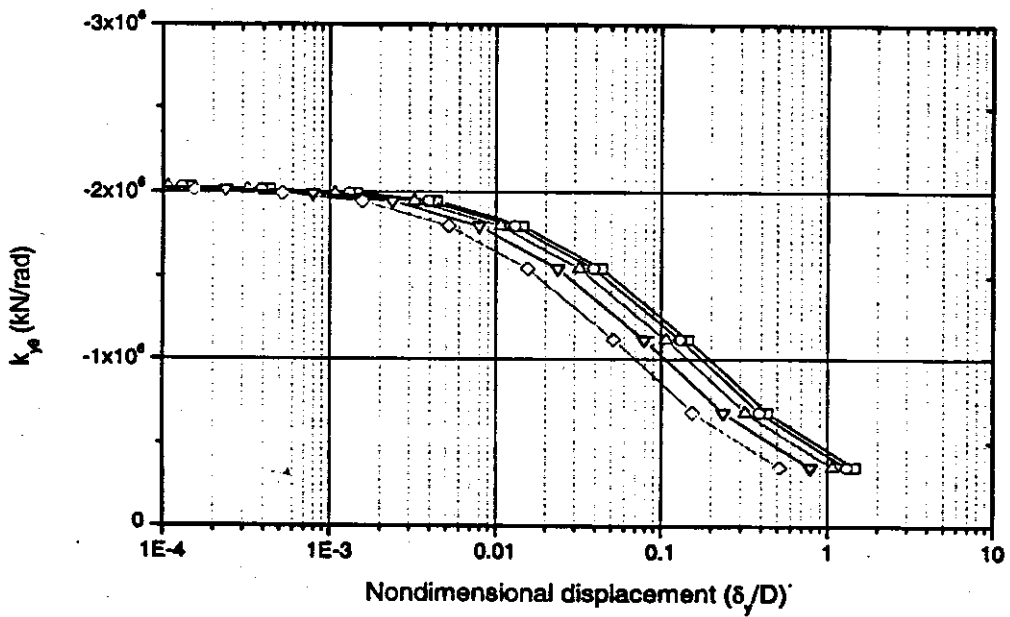
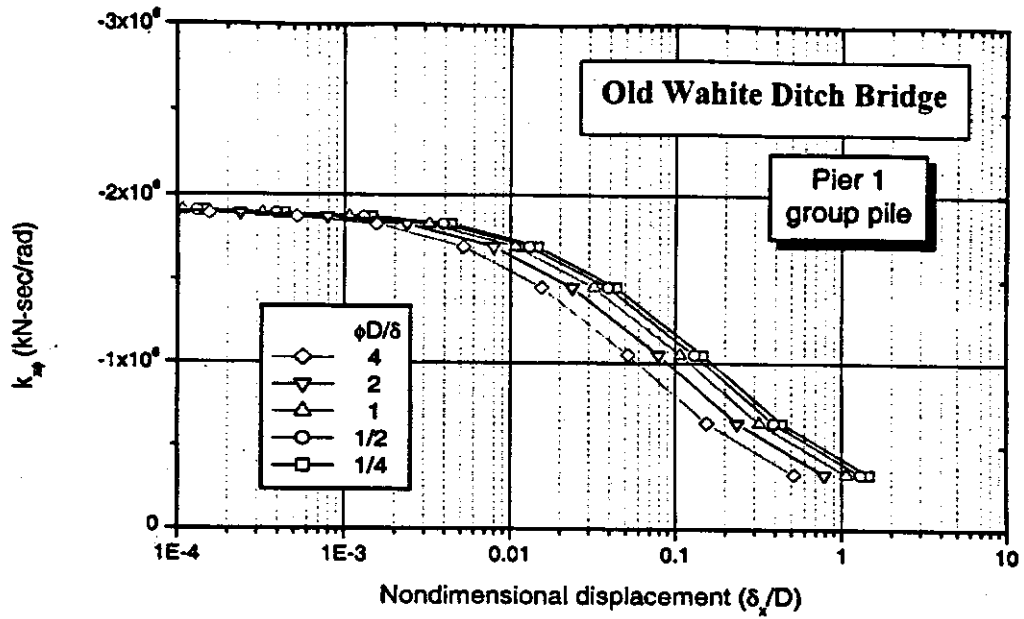
**F.7ab Cross-Coupled Damping About the X and Y Axis vs. Nondimensional Displacement for the Abutment Group Pile, Old Wahite Ditch Bridge**



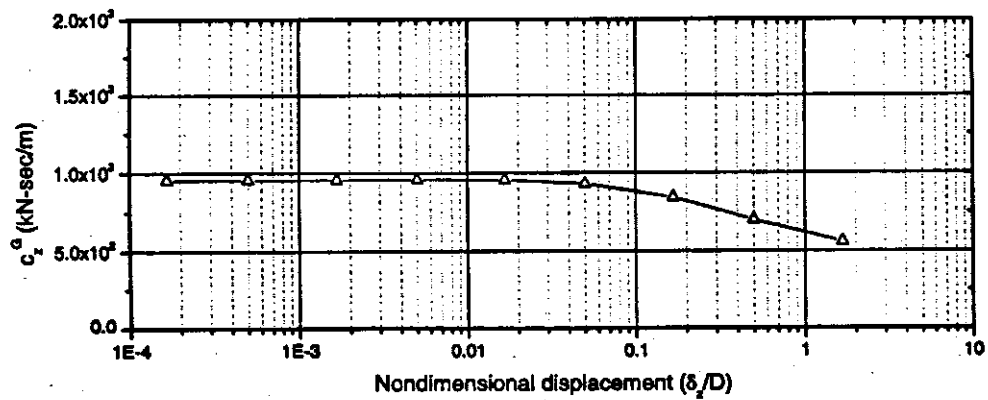
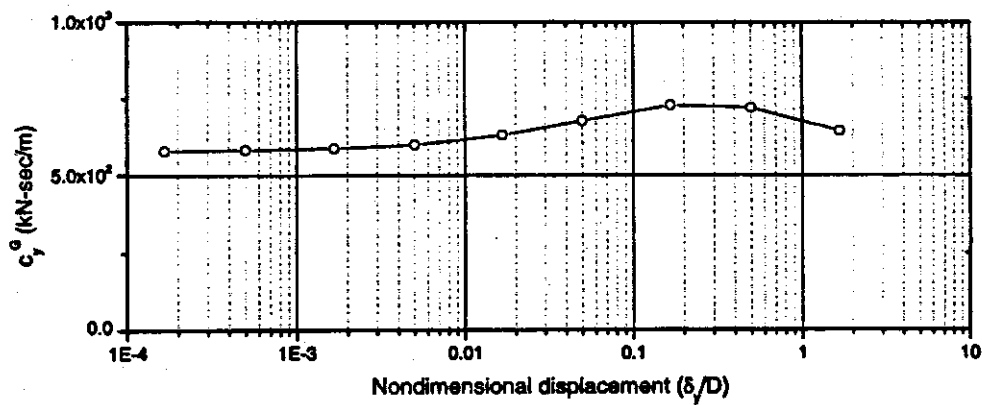
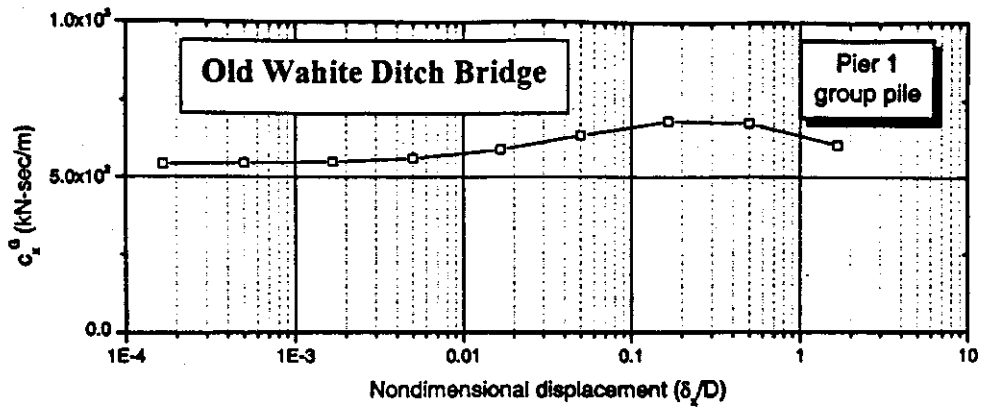
**F.7ac Group Stiffness in Vertical and X and Y Translation vs. Nondimensional Displacement for the Pier 1 Group Pile, Old Wahite Ditch Bridge**



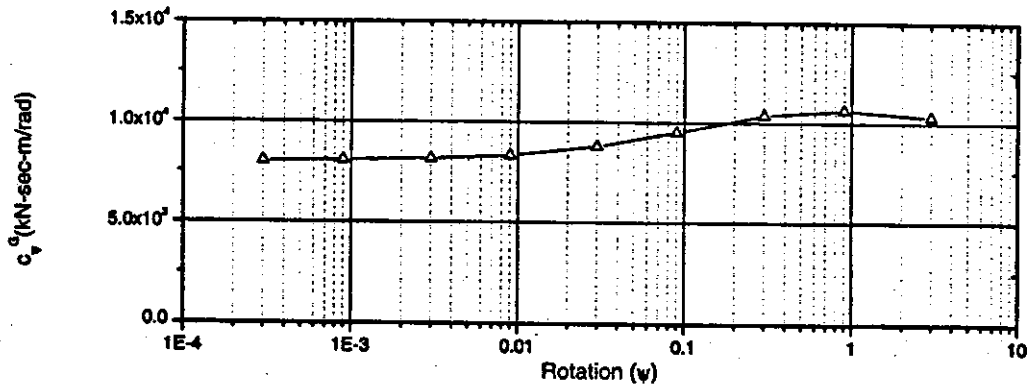
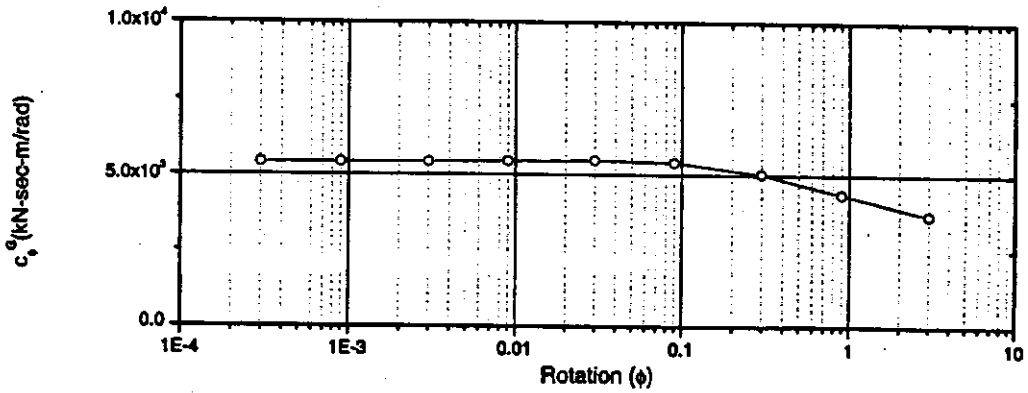
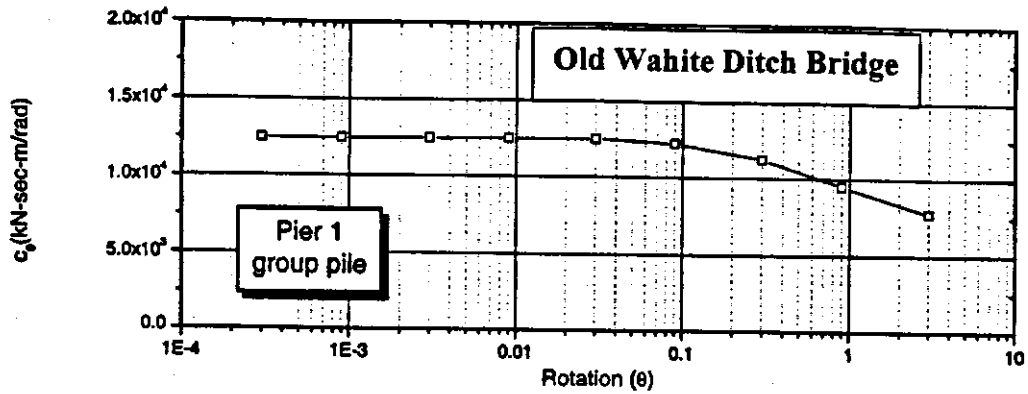
**F.7ad Group Stiffness Due to Torsion and Rocking About the X and Y Axis vs. Rotation for the Pier 1 Group Pile, Old Wahite Ditch Bridge**



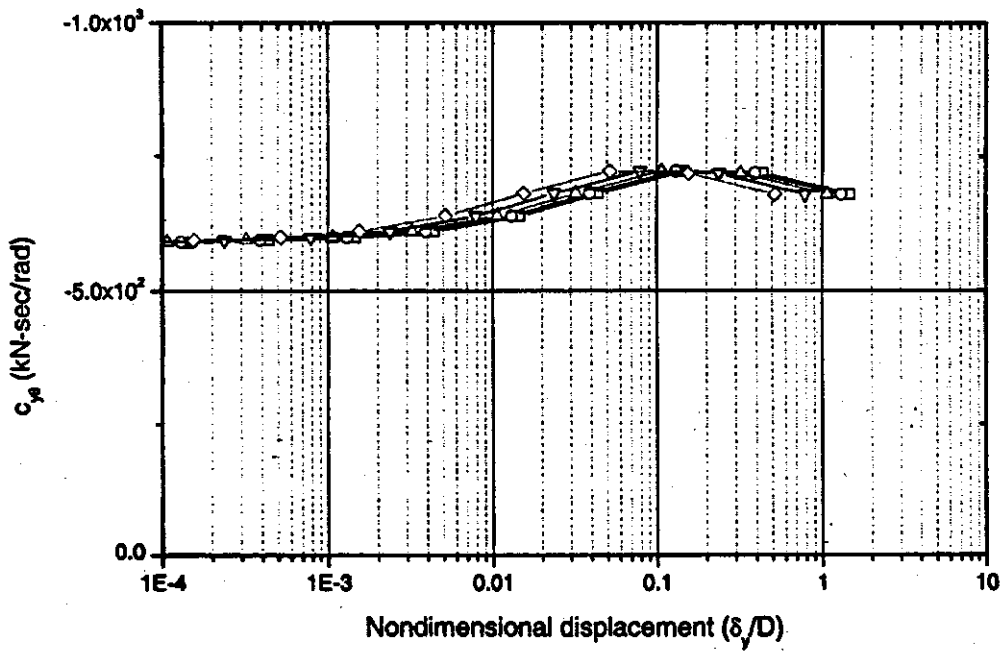
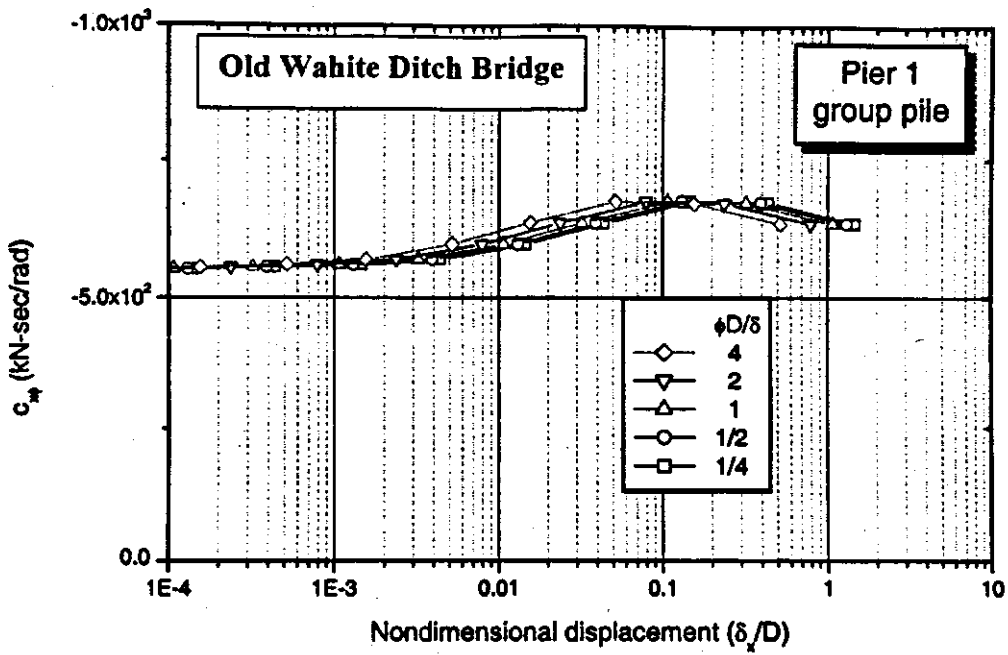
**F.7ae Cross-Coupling Translation in X and Y-Axis vs. Nondimensional Displacement for the Pier 1 Group Pile, Old Wahite Ditch Bridge**



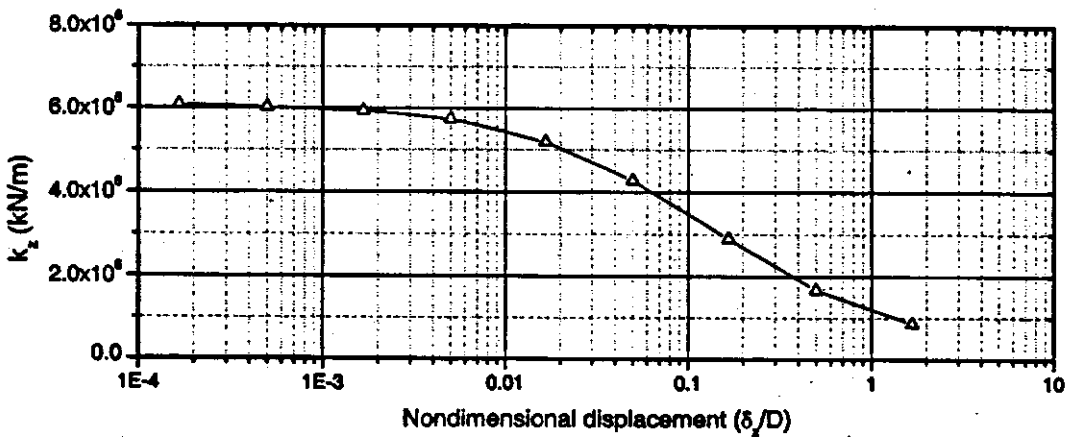
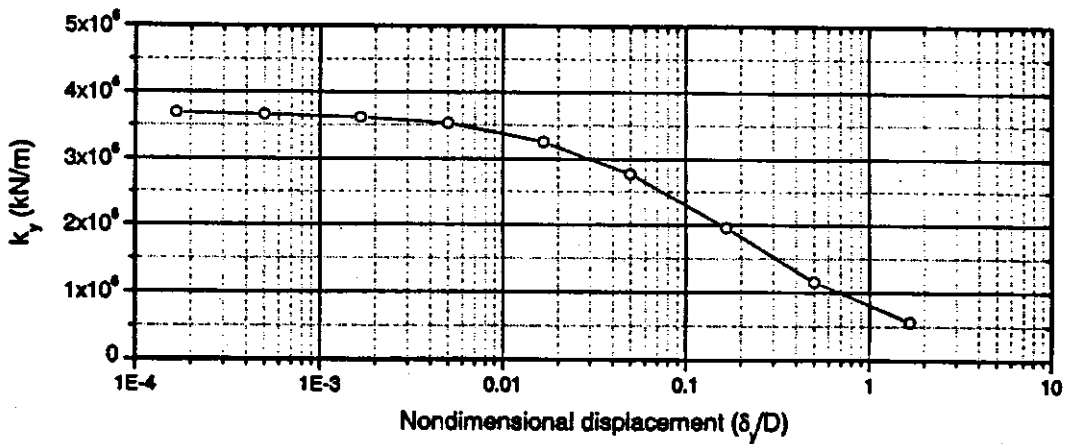
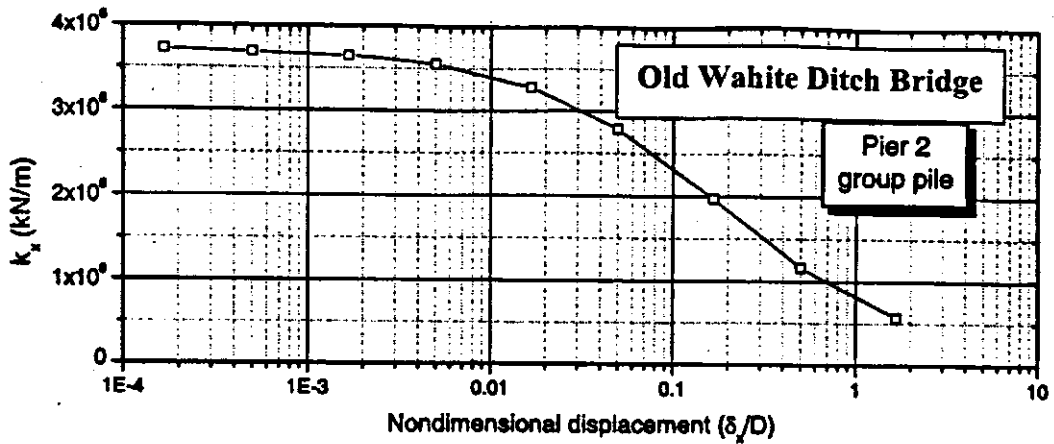
**F.7af Damping Due to Vertical and Sliding Along the X and Y Axis vs. Rotation for the Pier 1 Group Pile, Old Wahite Ditch Bridge**



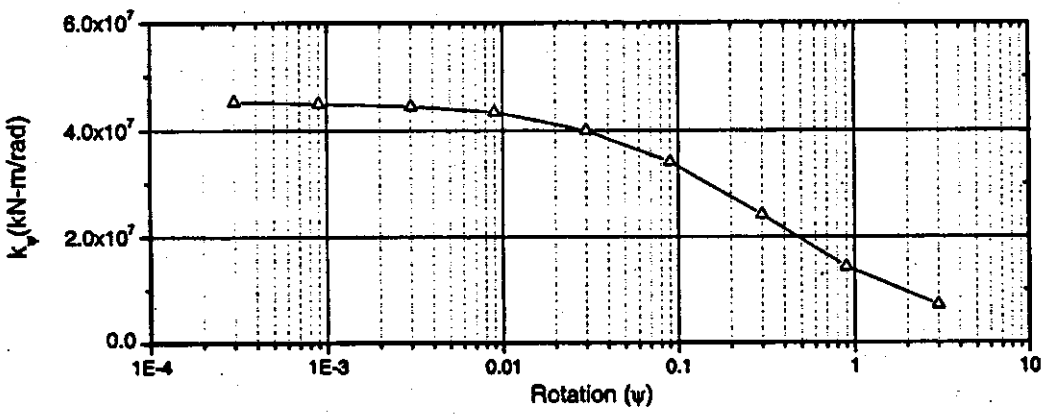
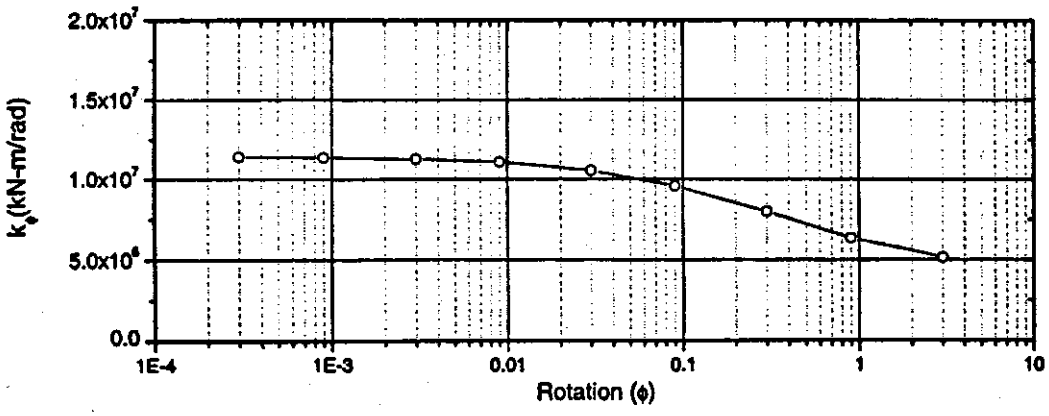
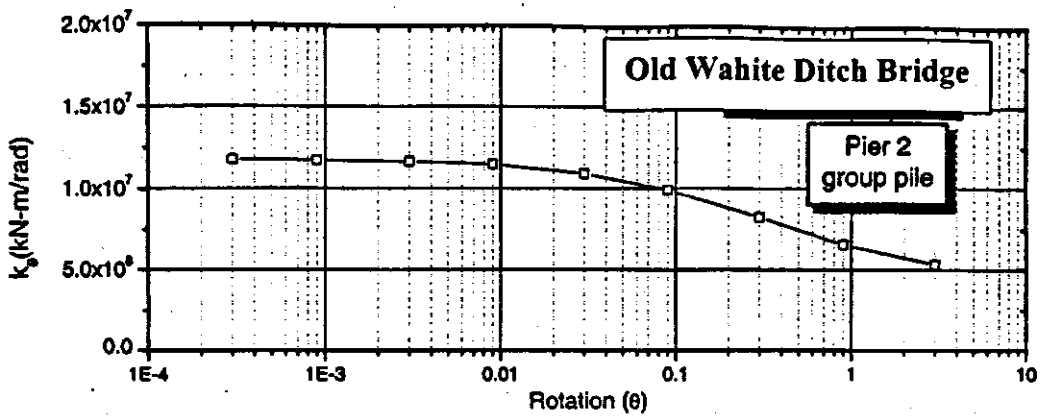
**F.7ag Damping Due to Torsion and Rocking About the X and Y Axis vs. Rotation for the Pier 1 Group Pile, Old Wahite Ditch Bridge**



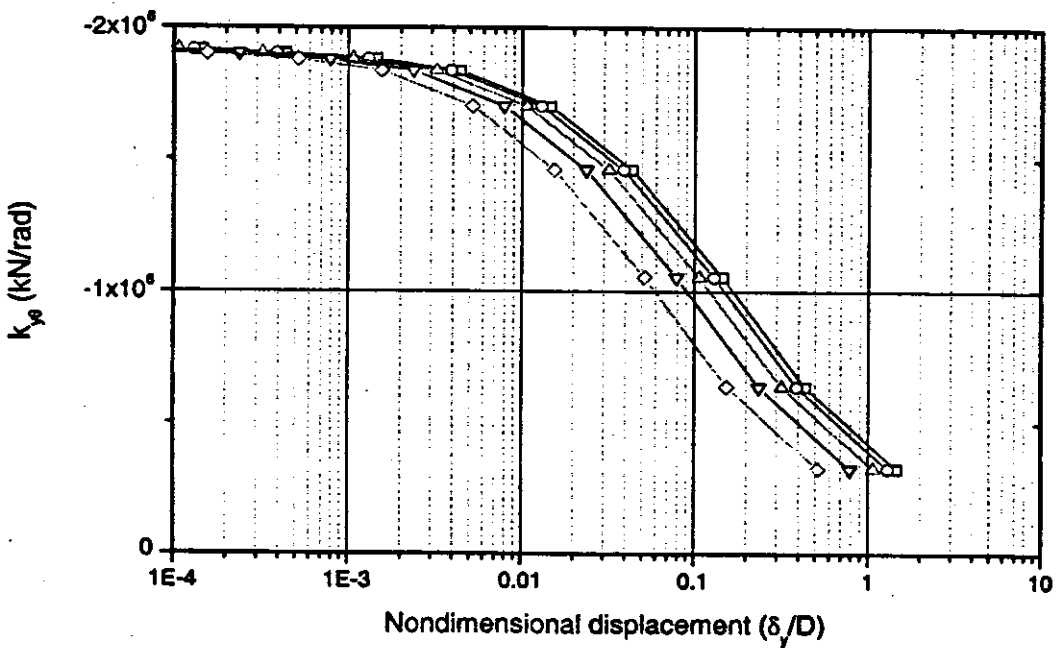
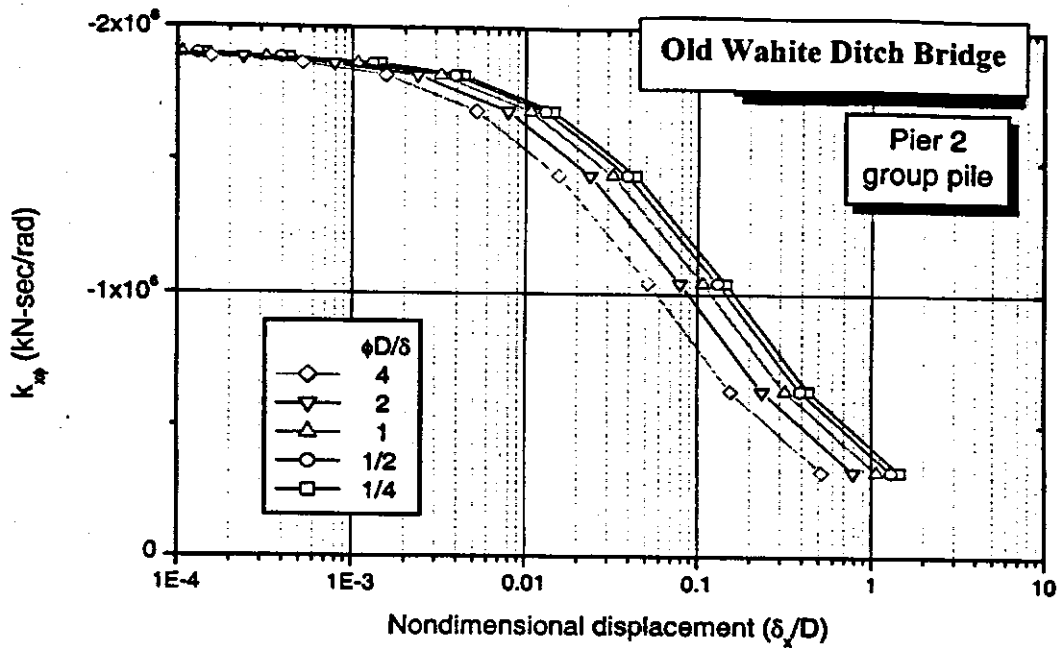
**F.7ah Cross-Coupled Damping About the X and Y Axis vs. Nondimensional Displacement for the Pier 1 Group Pile, Old Wahite Ditch Bridge**



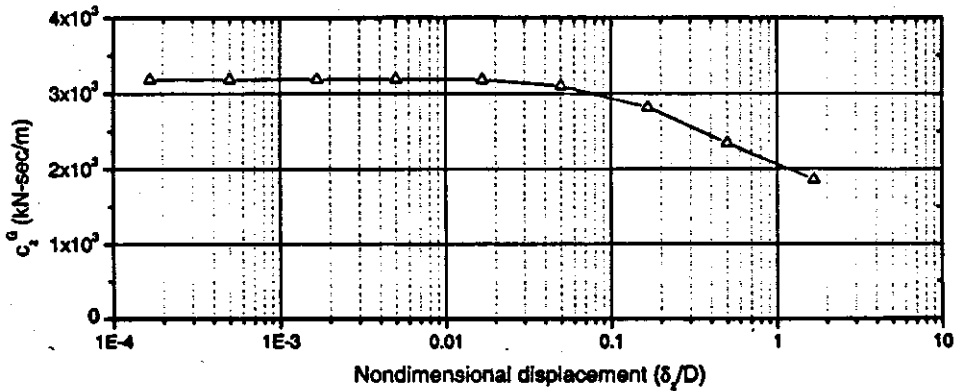
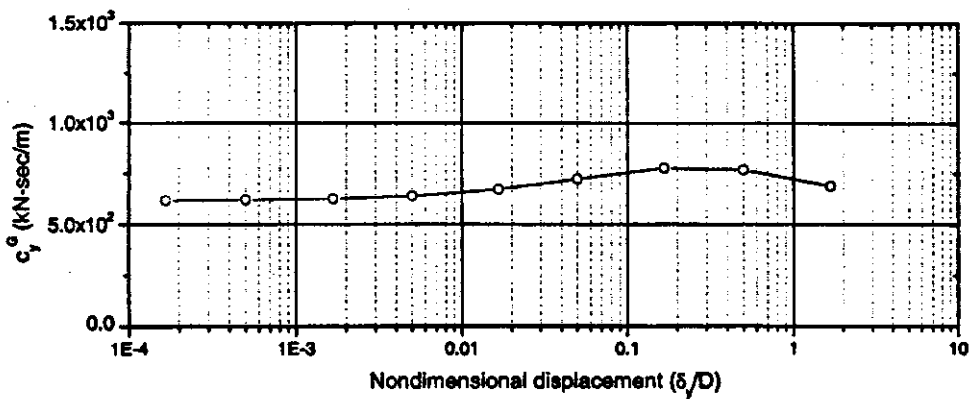
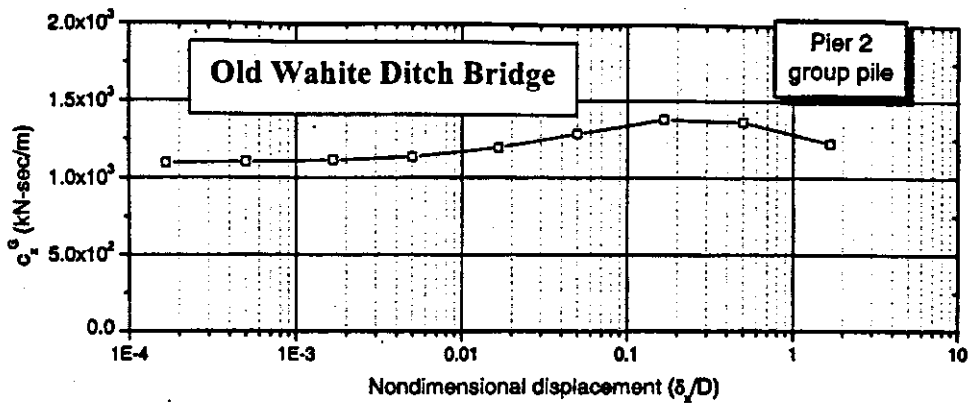
**F.7ai Group Stiffness in Vertical and X and Y Translation vs. Nondimensional Displacement for the Pier 2 Group Pile, Old Wahite Ditch Bridge**



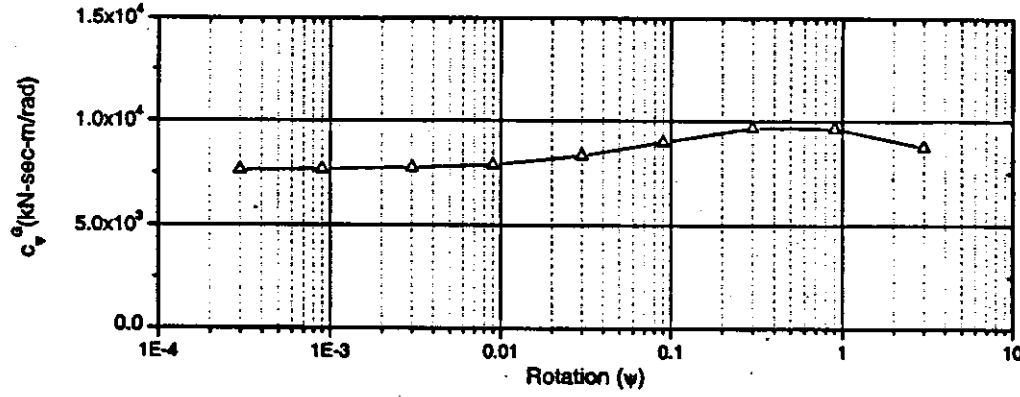
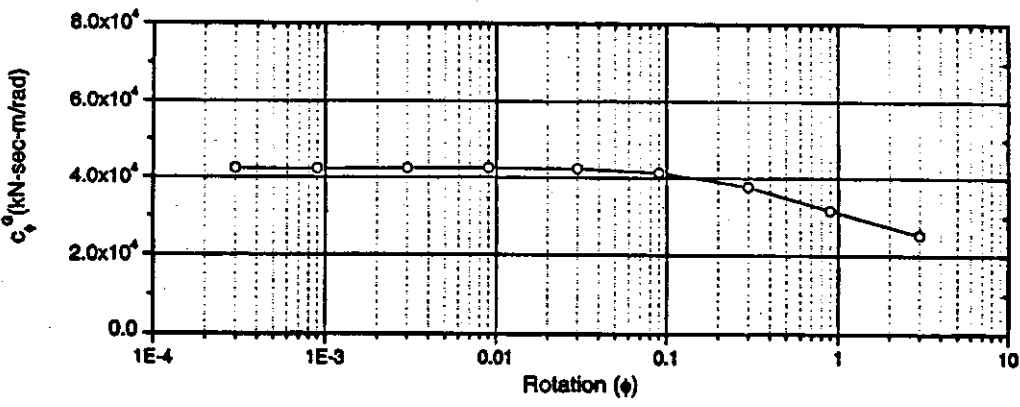
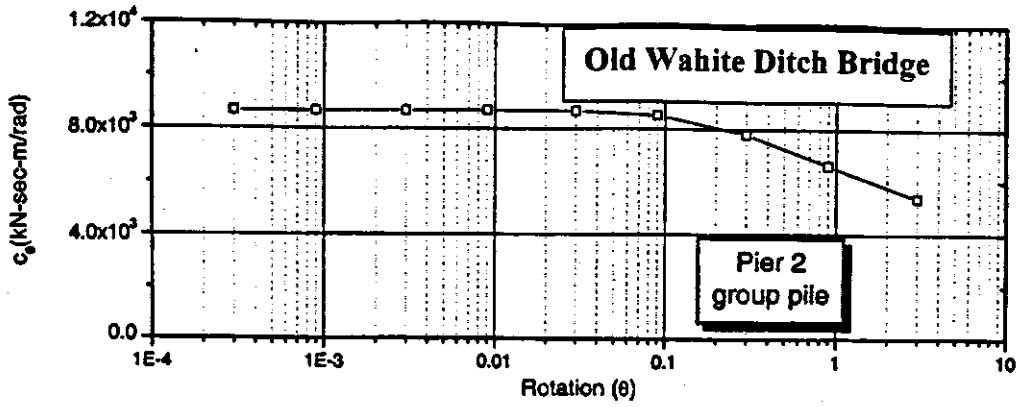
**F.7aj Group Stiffness Due to Torsion and Rocking About the X and Y Axis vs. Rotation for the Pier 2 Group Pile, Old Wahite Ditch Bridge**



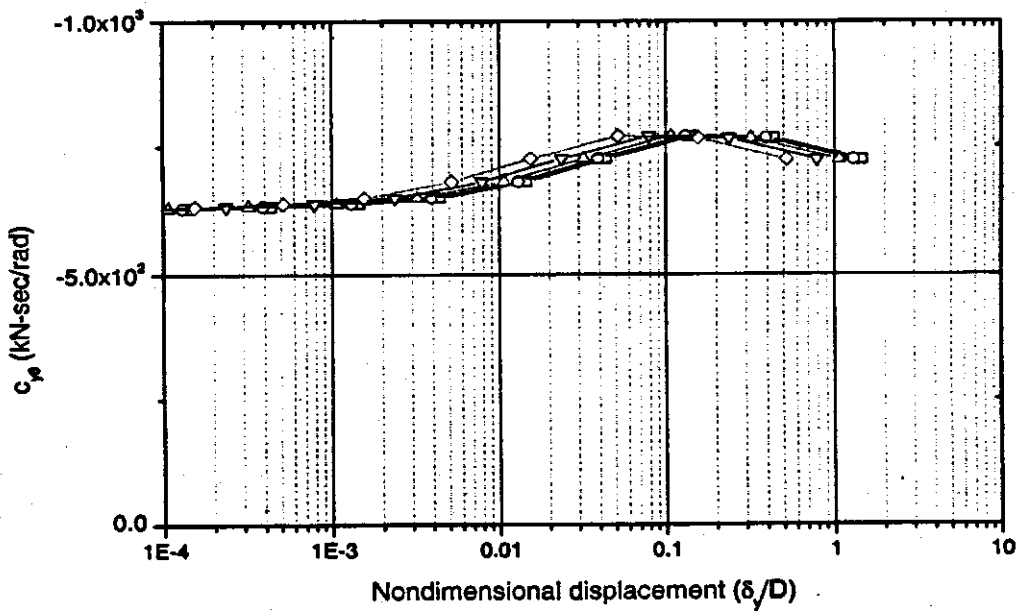
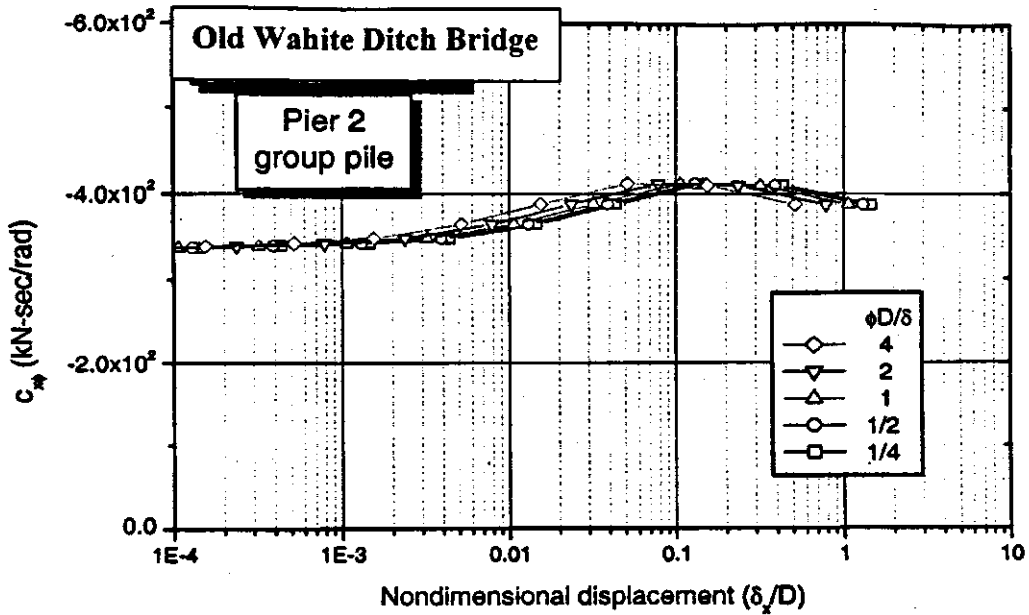
**F.7ak Cross-Coupling Translation in X and Y-Axis vs. Nondimensional Displacement for the Pier 2 Group Pile, Old Wahite Ditch Bridge**



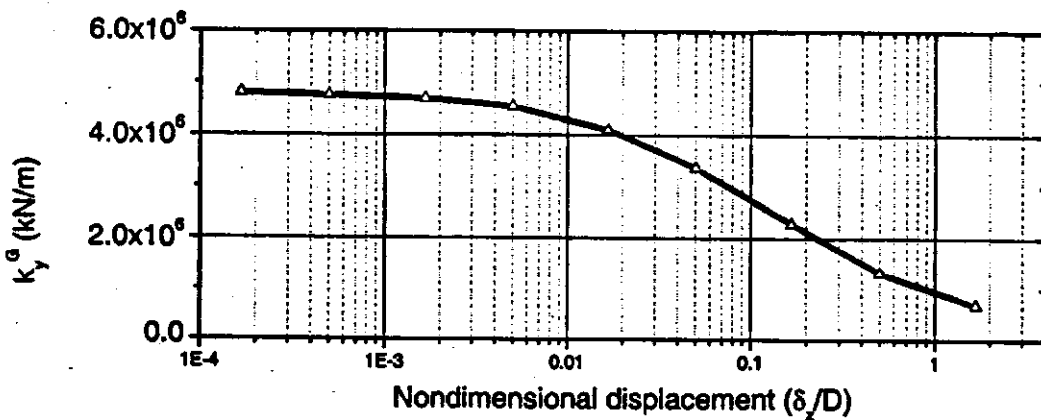
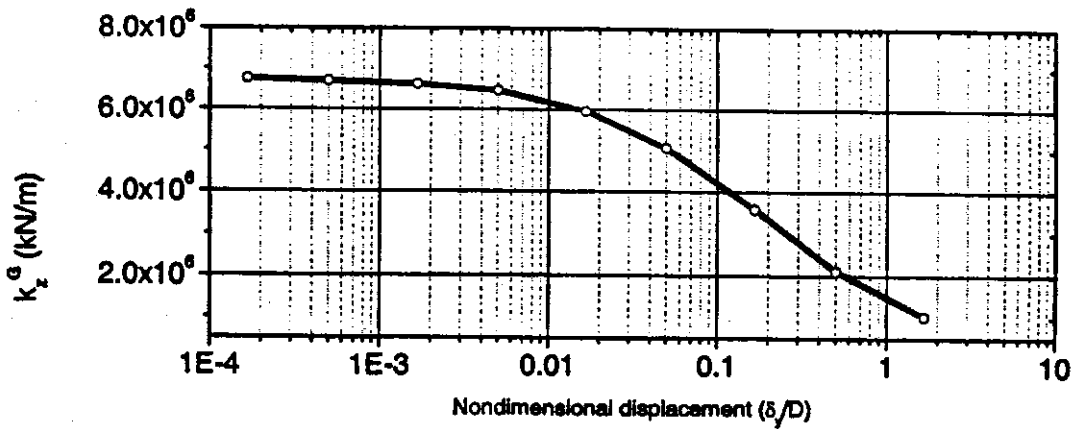
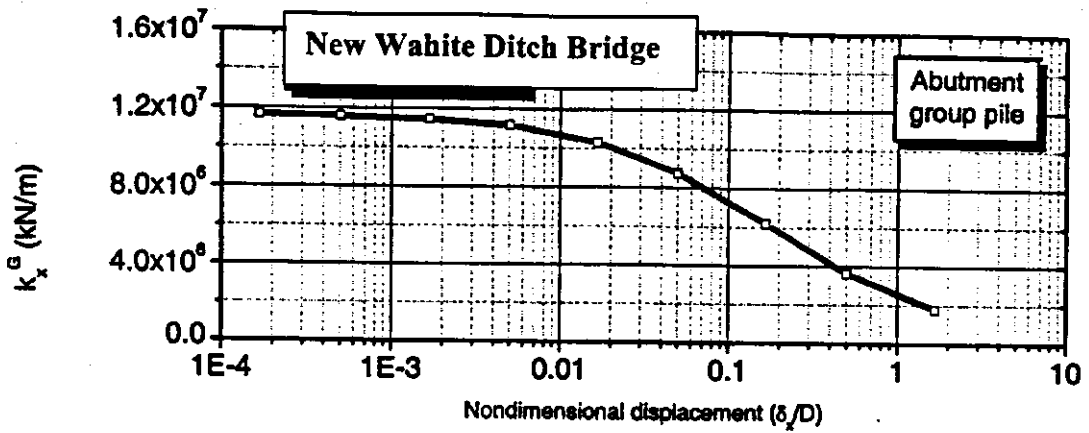
**F.7al Damping Due to Vertical and Sliding Along the X and Y Axis vs. Rotation for the Pier 2 Group Pile, Old Wahite Ditch Bridge**



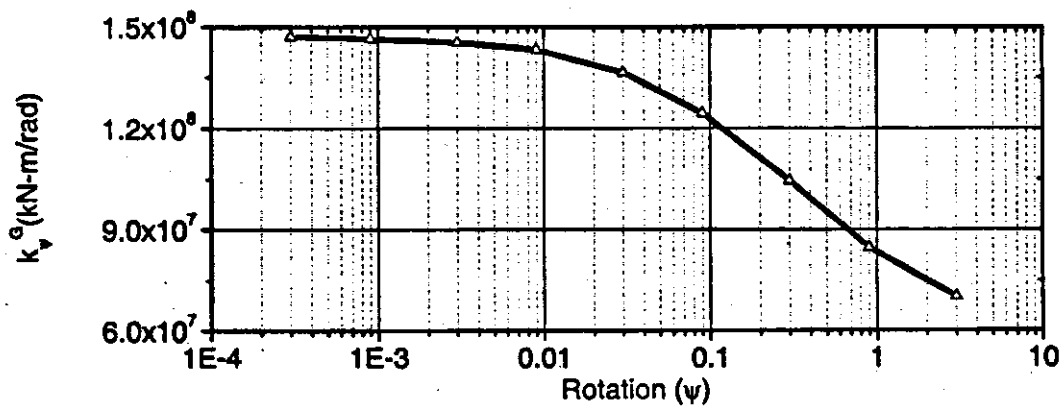
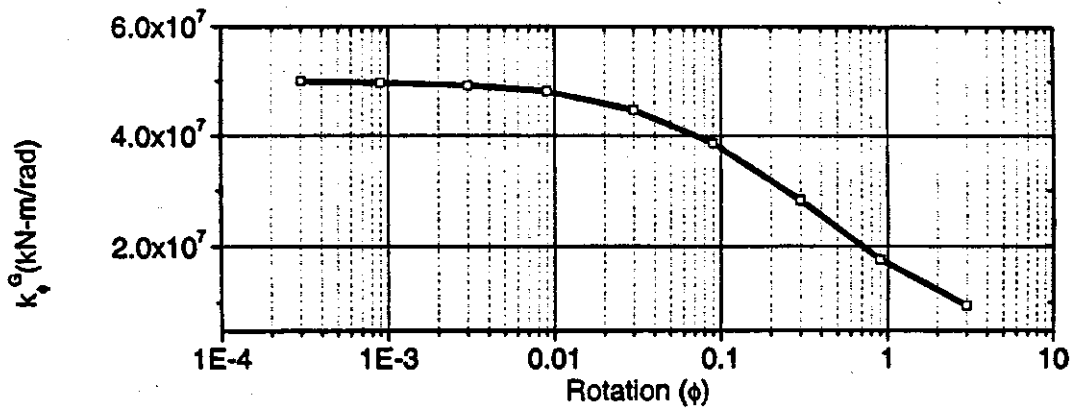
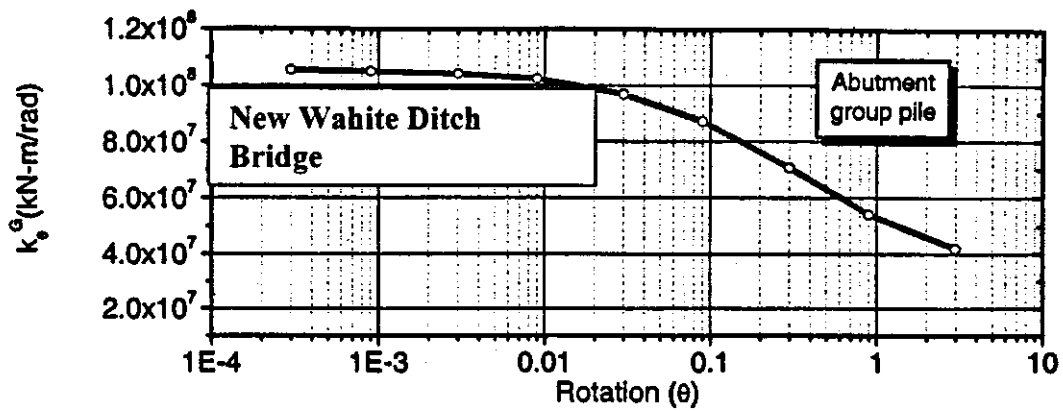
**F.7am Damping Due to Torsion and Rocking About the X and Y Axis vs. Rotation for the Pier 2 Group Pile, Old Wahite Ditch Bridge**



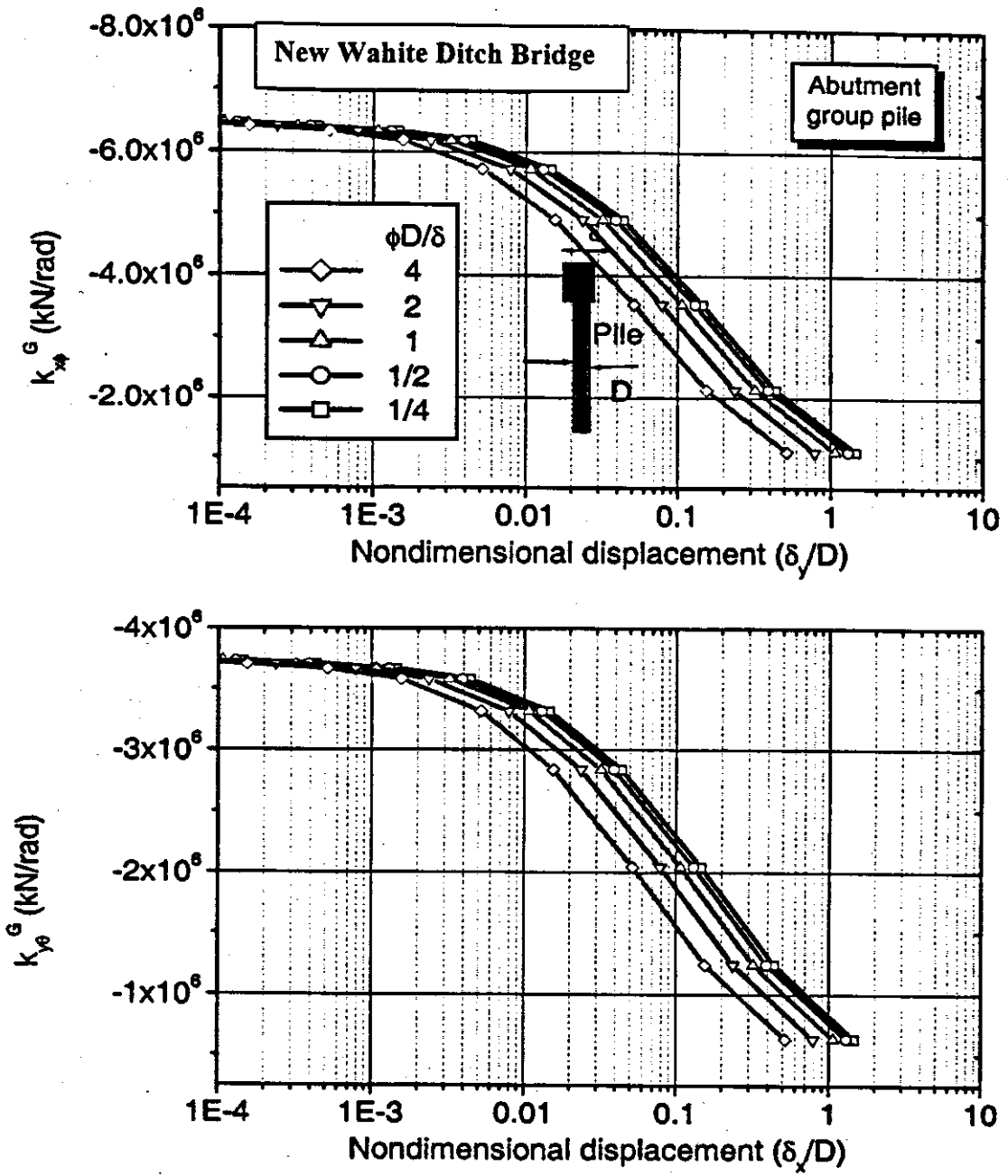
**F.7an Cross-Coupled Damping About the X and Y Axis vs. Nondimensional Displacement for the Pier 2 Group Pile, Old Wahite Ditch Bridge**



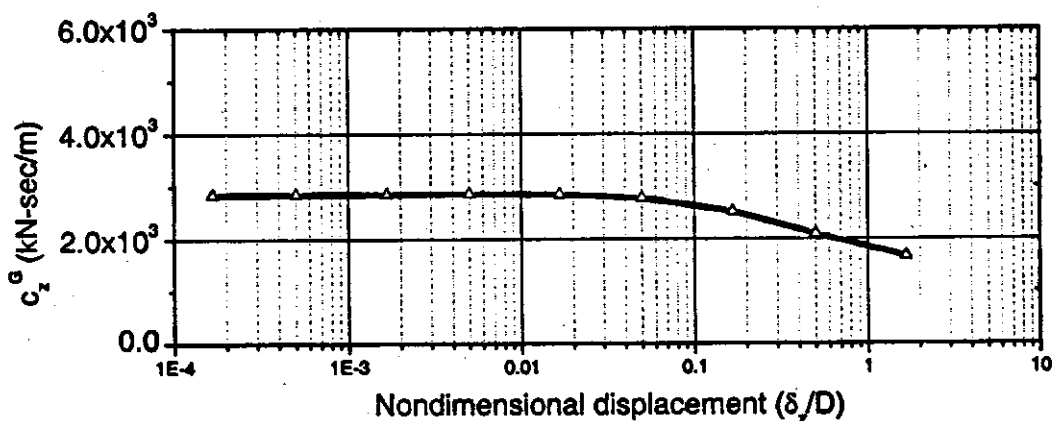
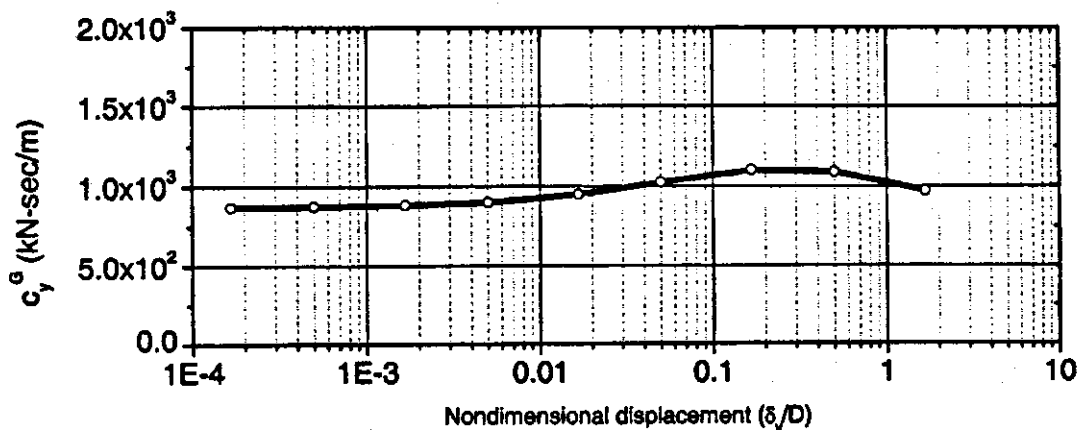
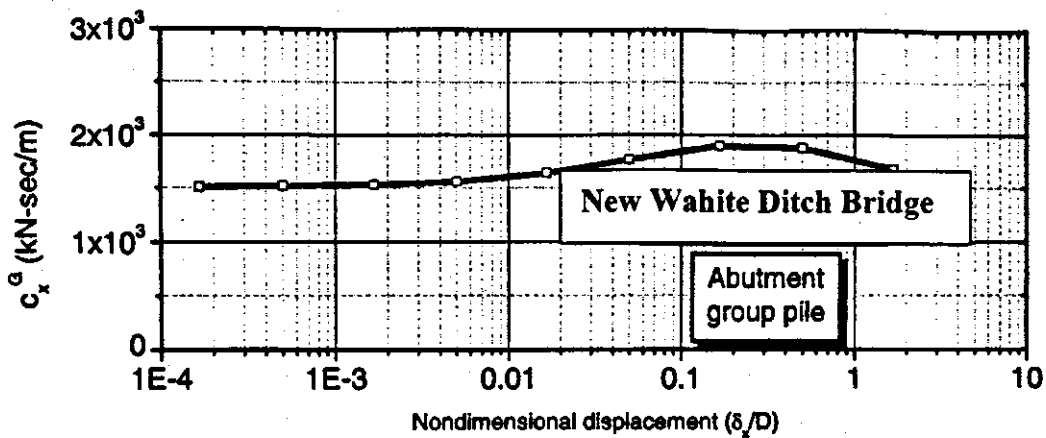
**F.7ao Group Stiffness in Vertical and X and Y Translation vs. Nondimensional Displacement for the Abutment Group Pile, New Wahite Ditch Bridge**



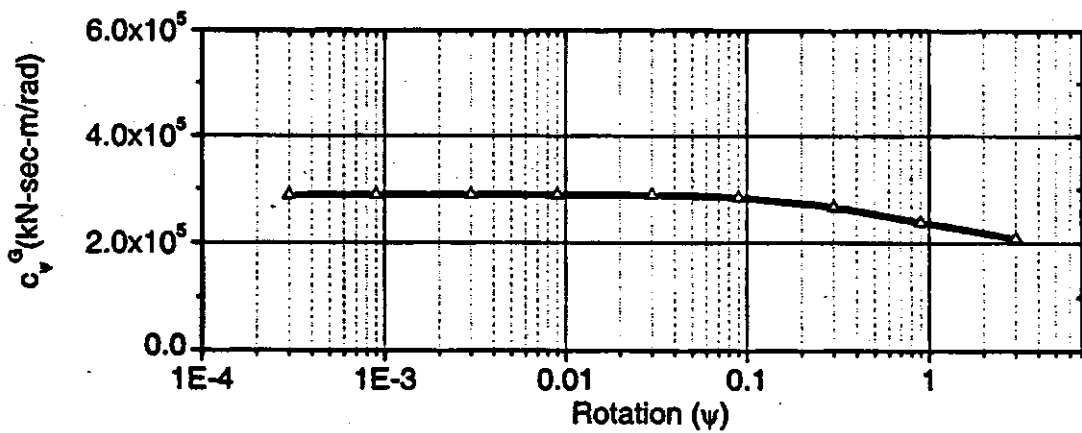
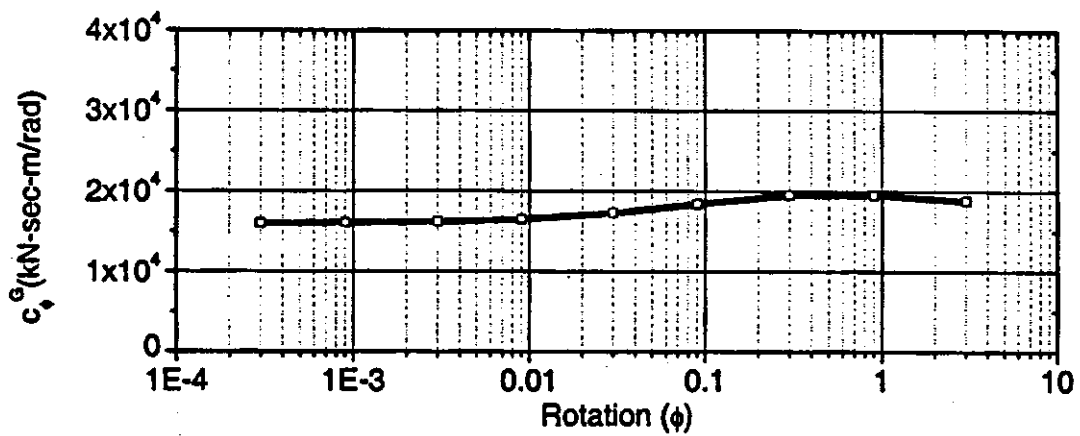
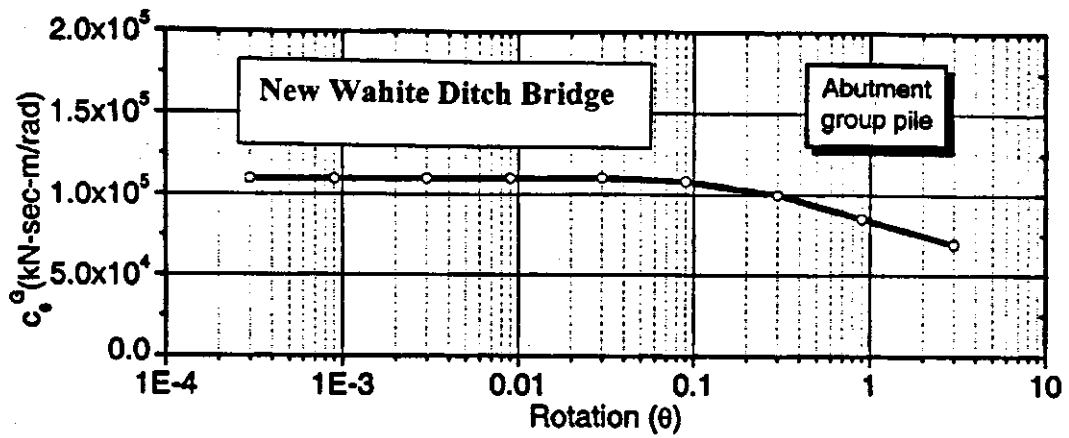
**F.7ap Group Stiffness Due to Torsion and Rocking About the X and Y Axis vs. Rotation for the Abutment Group Pile, New Wahite Ditch Bridge**



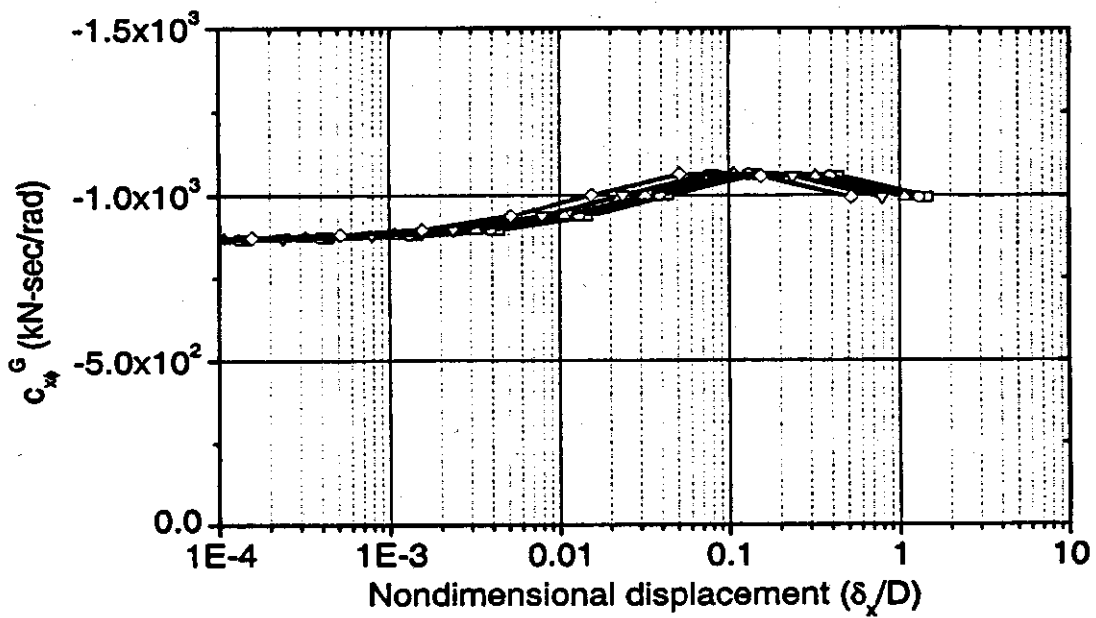
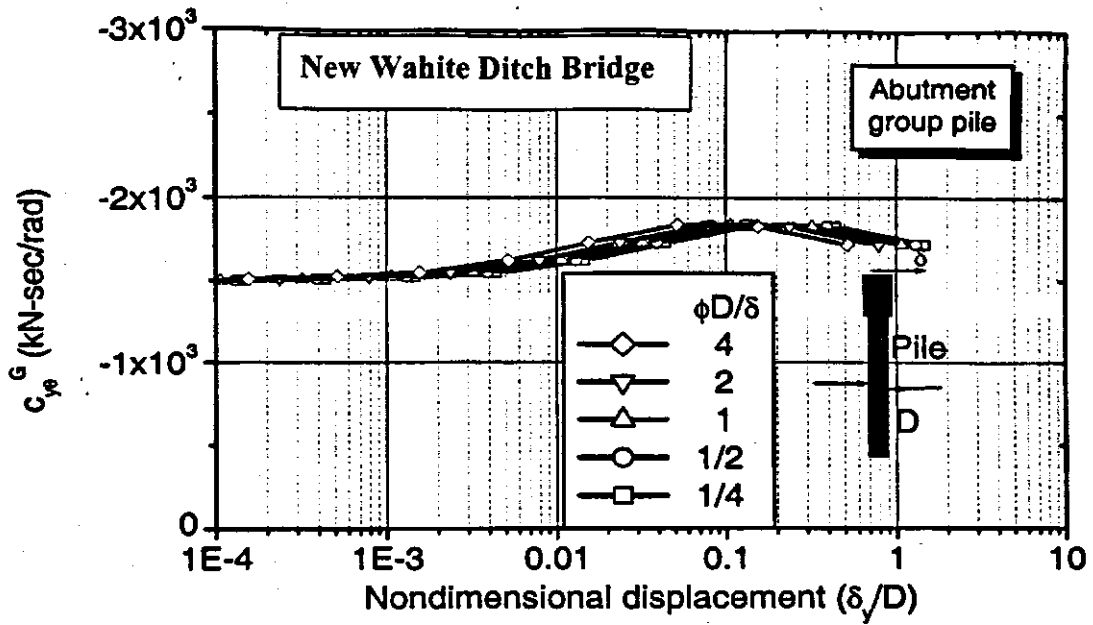
**F.7aq Cross-Coupling Translation in X and Y-Axis vs. Nondimensional Displacement for the Abutment Group Pile, New Wahite Ditch Bridge**



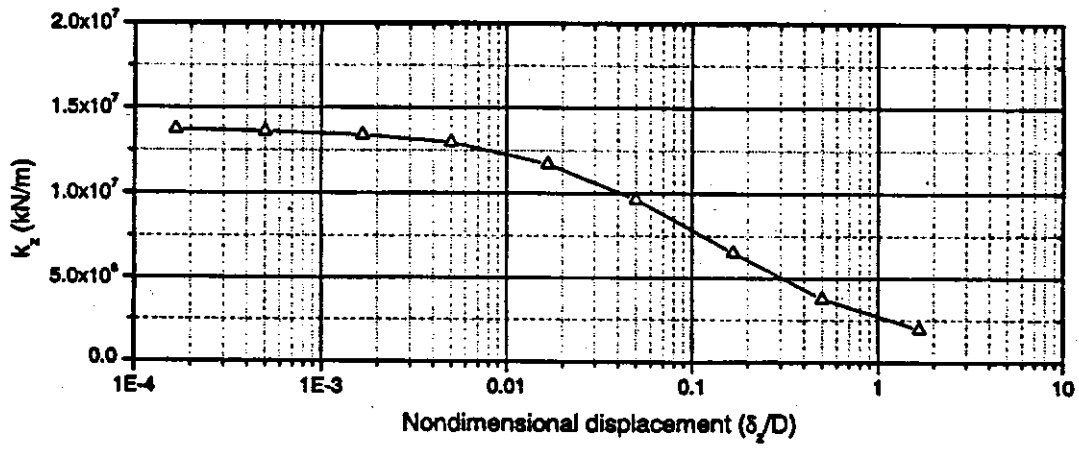
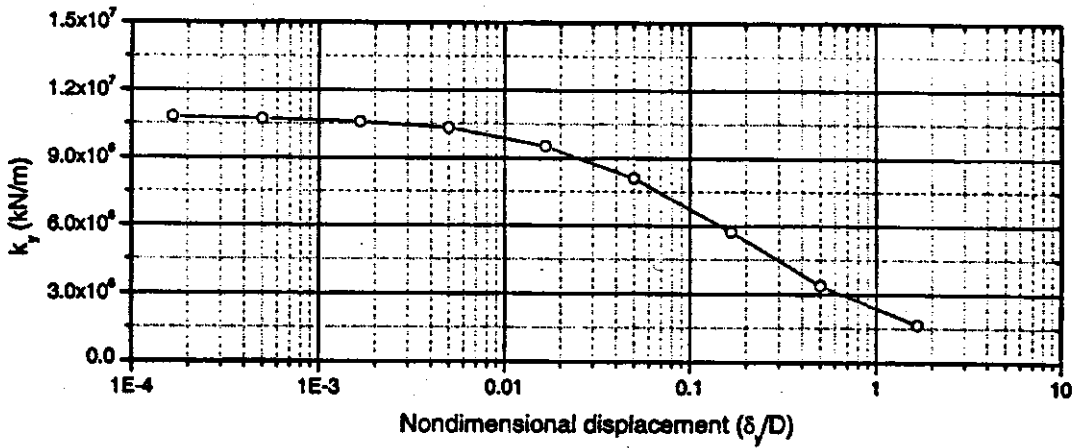
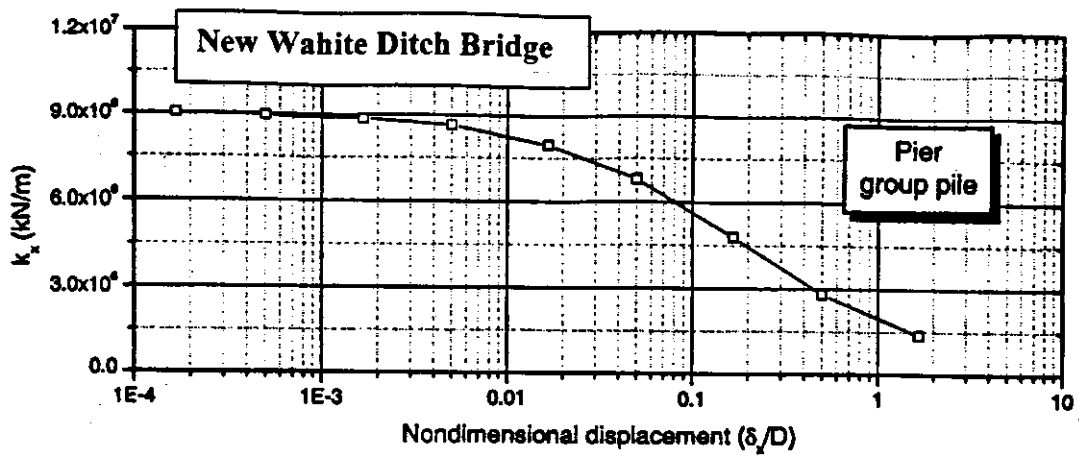
**F.7ar Damping Due to Vertical and Sliding Along the X and Y Axis vs. Rotation for the Abutment Group Pile, New Wahite Ditch Bridge**



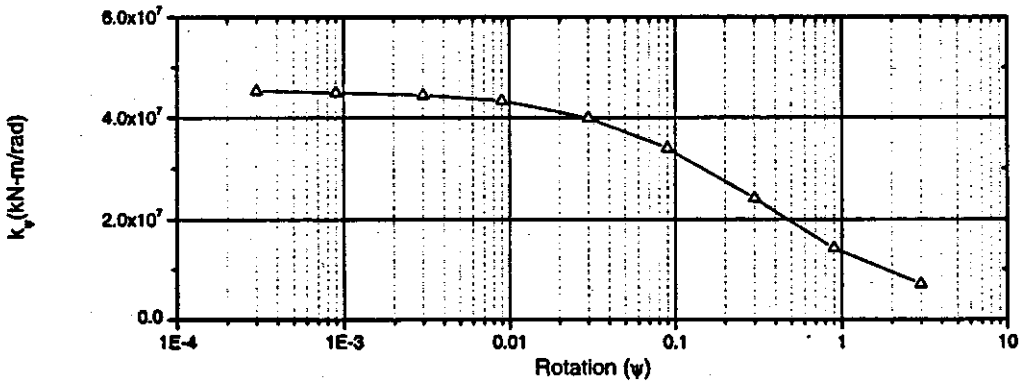
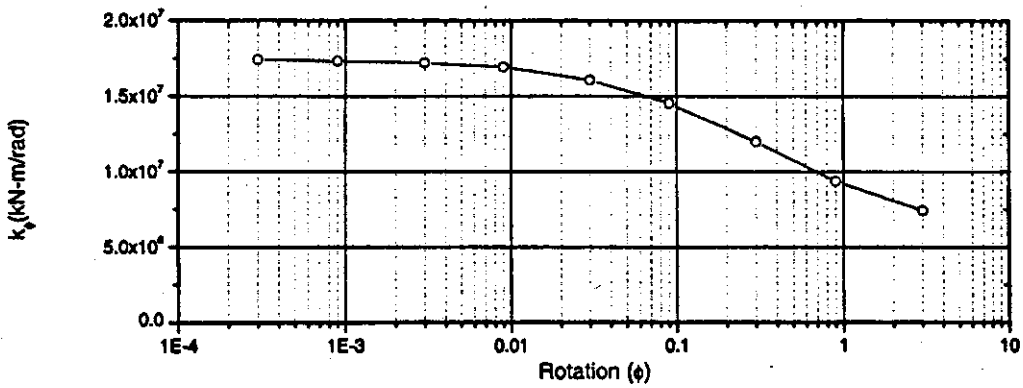
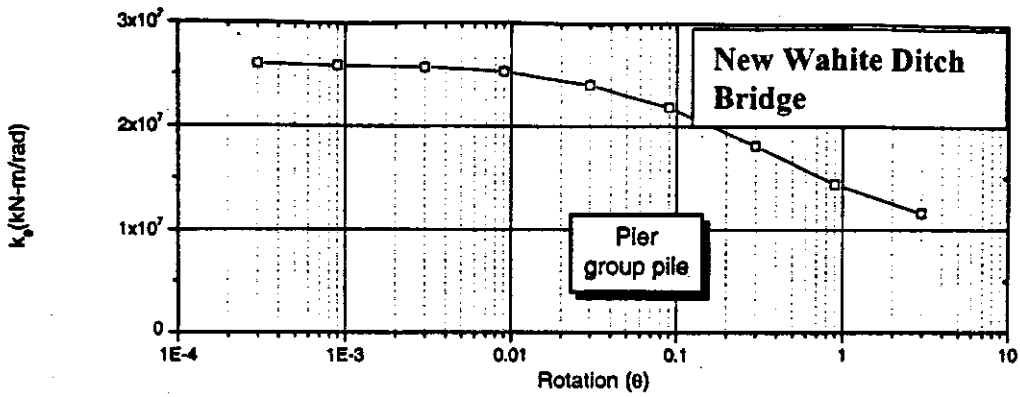
**F.7as Damping Due to Torsion and Rocking About the X and Y Axis vs. Rotation for the Abutment Group Pile, New Wahite Ditch Bridge**



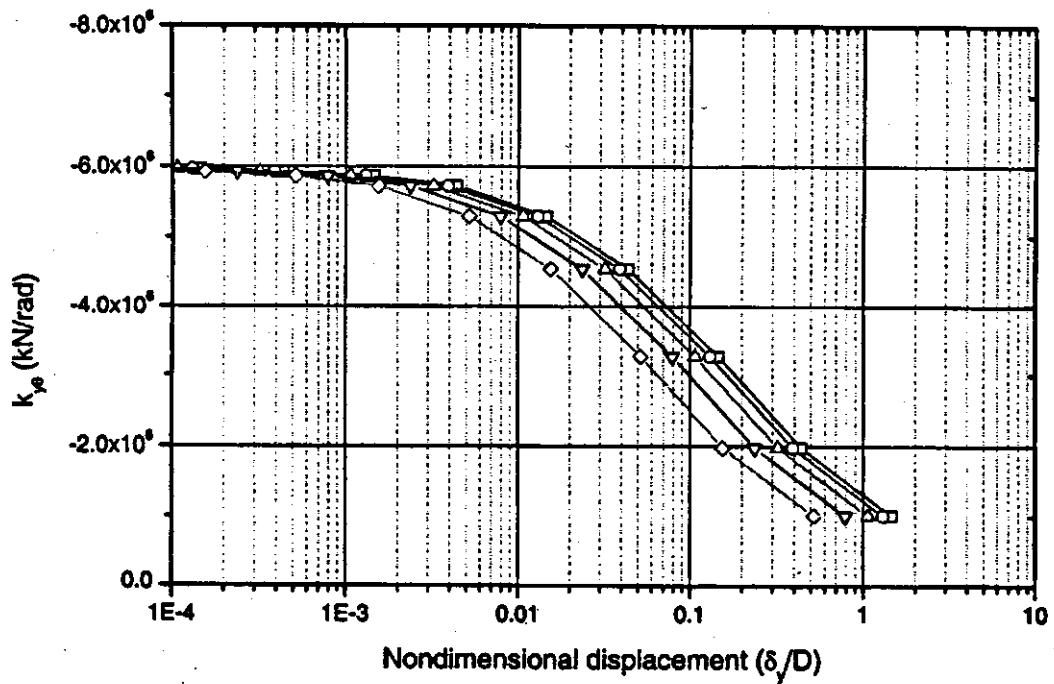
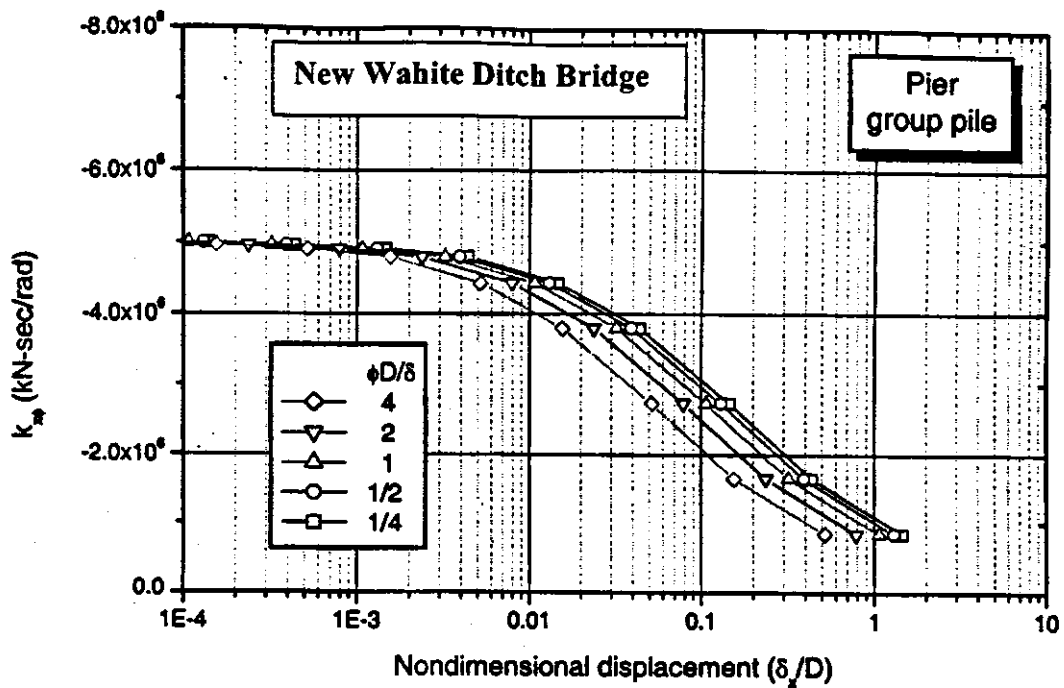
**F.7at Cross-Coupled Damping About the X and Y Axis vs. Nondimensional Displacement for the Abutment Group Pile, New Wahite Ditch Bridge**



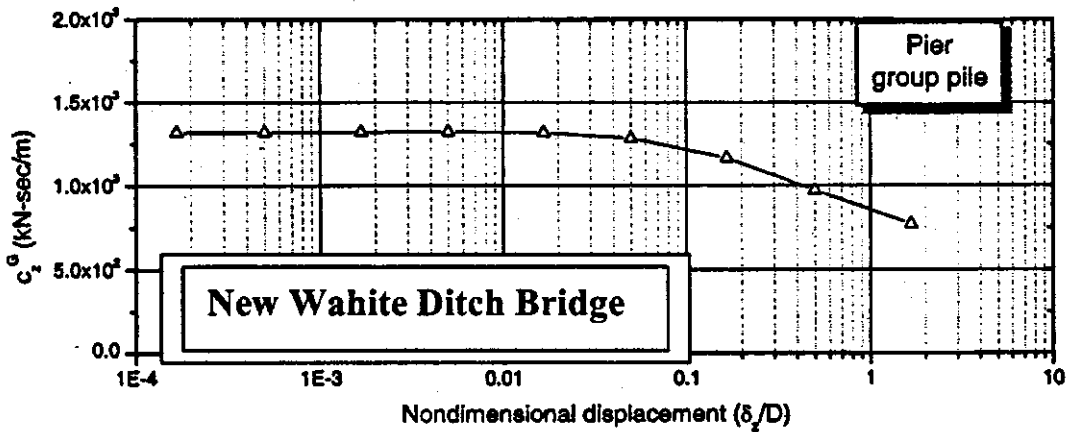
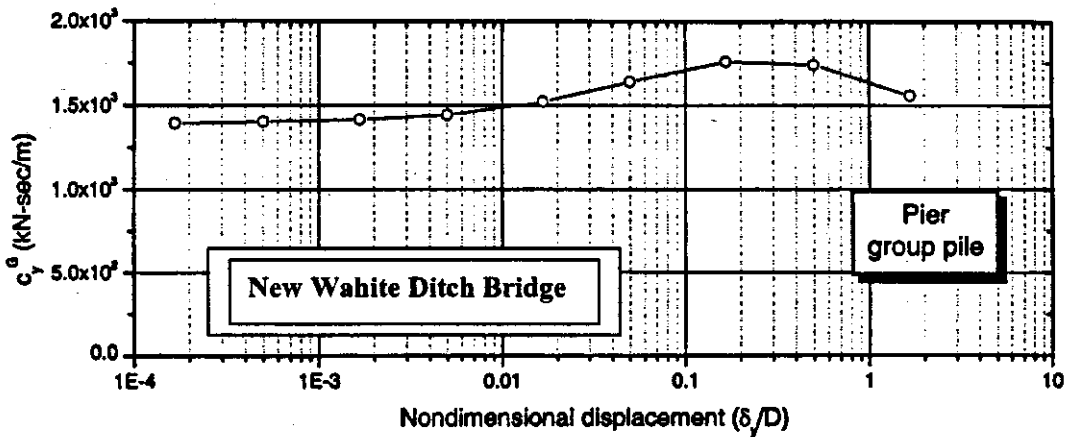
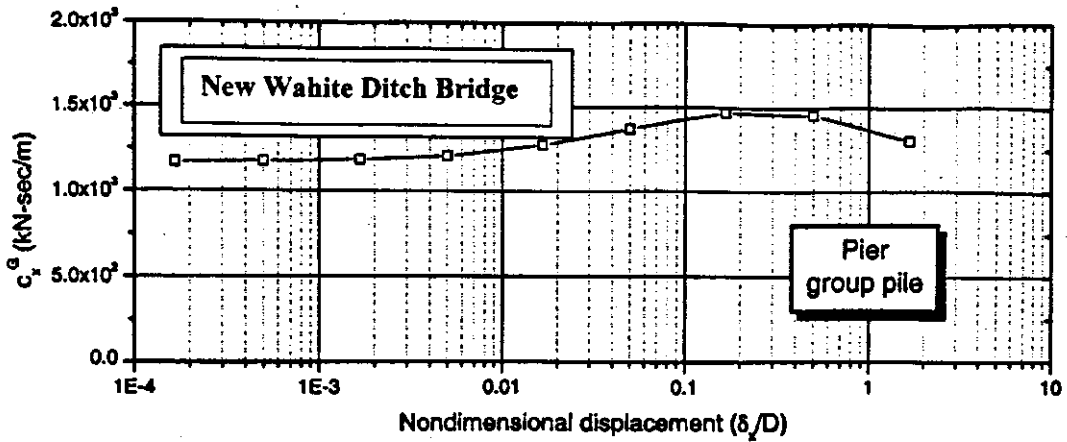
**F.7au Group Stiffness in Vertical and X and Y Translation vs. Nondimensional Displacement for the Pier Group Pile, New Wahite Ditch Bridge**



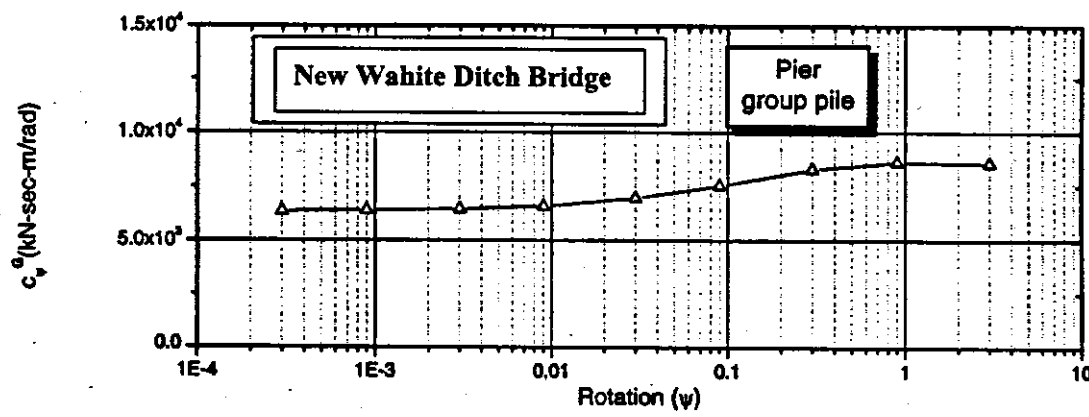
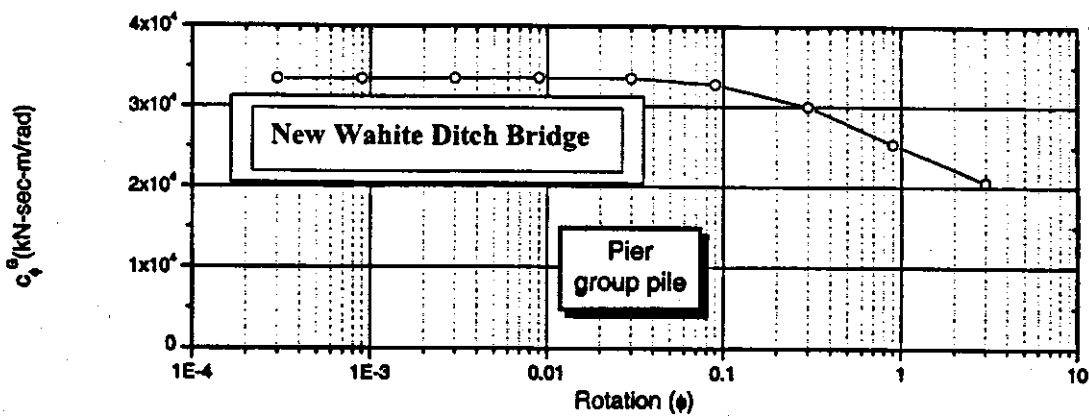
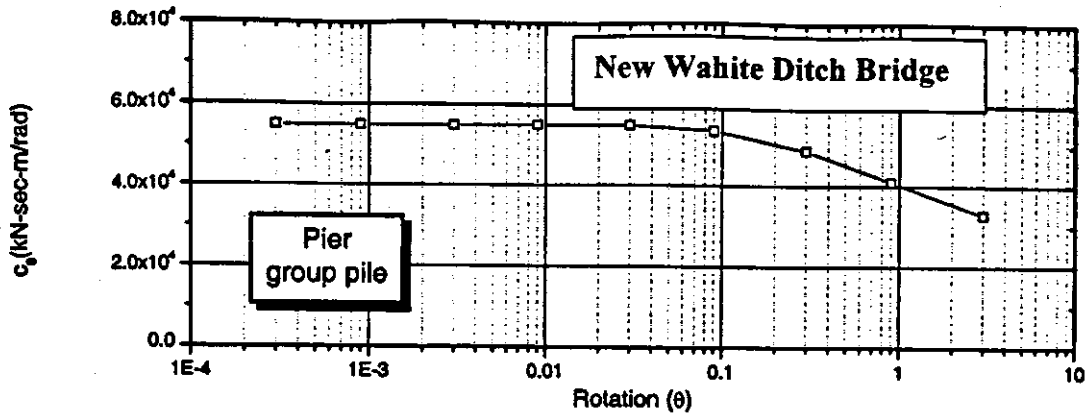
**F.7av Group Stiffness Due to Torsion and Rocking About the X and Y Axis vs. Rotation for the Pier Group Pile, New Wahite Ditch Bridge**



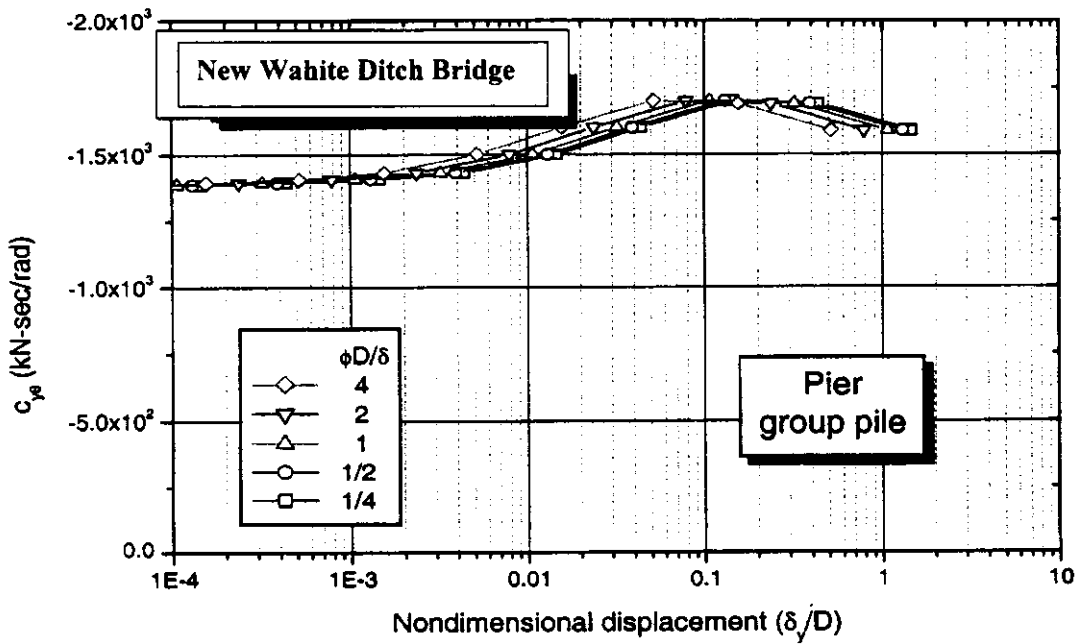
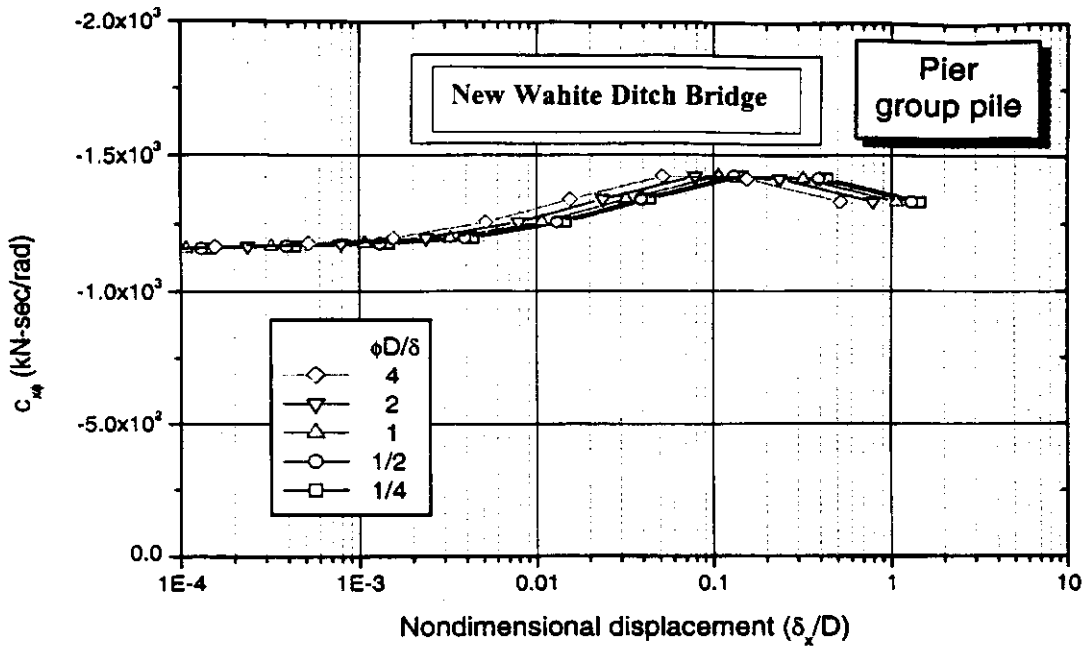
**F.7aw Cross-Coupling Translation in X and Y-Axis vs. Nondimensional Displacement for the Pier Group Pile, New Wahite Ditch Bridge**



**F.7ax Damping Due to Vertical and Sliding Along the X and Y Axis vs. Rotation for the Pier Group Pile, New Wahite Ditch Bridge**



**F.7ay Damping Due to Torsion and Rocking About the X and Y Axis vs. Rotation for the Pier Group Pile, New Wahite Ditch Bridge**



**F.7az Cross-Coupled Damping About the X and Y Axis vs. Nondimensional Displacement for the Pier Group Pile, New Wahite Ditch Bridge**

# G. LIQUEFACTION ANALYSIS

Table G.1 Liquefaction Analysis

St. Francis River Site  
Ground Motion SF100103

SPT No.	Depth (ft)	N field	Energy Factor	Rod Factor	Sampler Factor	Borehole Factor	Total Stress (psf)	Effective Stress (psf)	Cn	(N1)60	Fines Content (%)	N1,60cs	Alpha	Ksigma	Kalpha	CRR	CSR	Safety Factor
1	1	21	1	1	1	1		285.6	2	42	91	55.4		1		.81	.05	16.19
2	6	12	1	1	1	1	660	285.6	2	24	91	33.8		1		.81	.205	3.95
3	8.4	73	1	1	1	1	923.99	399.83	2	146	0	146		1		.81	.2	4.04
4	12.5	10	1	1	1	1	1375	595	1.88	18.8	0	18.8		1		.33	.189	1.74
5	15.5	19	1	1	1	1	1705	737.8	1.69	32.1	0	32.1		1		.81	.179	4.52
6	19.5	17	1	1	1	1	2118	901.19	1.53	26	0	26		1		.49	.172	2.84
7	23.5	26	1	1	1	1	2518	1051.6	1.41	36.8	0	36.8		1		.81	.165	4.9
8	27.5	28	1	1	1	1	2918	1202	1.32	36.9	0	36.9		1		.81	.157	5.15
9	34	26	1	1	1	1	3584.79	1483.19	1.2	31.2	0	31.2		1		.81	.141	5.74
10	40	75	1	1	1	1	4352.79	1856.79	1.06	79.4	0	79.4		1		.81	.124	6.53
11	45	71	1	1	1	1	4990.29	2182.29	.98	69.5	0	69.5		.98		.793	.11	7.2
12	50	75	1	1	1	1	5660.3	2540.29	.91	68.2	0	68.2		.96		.777	.101	7.69
13	55	38	1	1	1	1	6330.3	2898.29	.85	32.3	0	32.3		.93		.753	.094	8.01
14	60	46	1	1	1	1	7000.3	3256.29	.8	36.8	0	36.8		.91		.737	.092	8.01
15	66	33	1	1	1	1	7787.1	3668.7	.75	24.7	0	24.7		.89		.703	.089	4.52
16	70	40	1	1	1	1	8307.09	3839.09	.73	29.2	0	29.2		.87		.554	.067	6.36
17	75	35	1	1	1	1	8957.09	4277.09	.7	24.5	0	24.5		.85		.381	.064	4.53
18	80	38	1	1	1	1	9607.09	4615.09	.67	25.4	0	25.4		.84		.367	.062	4.94
19	90	43	1	1	1	1	10907.1	5291.09	.63	27	0	27		.81		.424	.078	5.43
20	100	73	1	1	1	1	12207.1	5967.09	.59	43	0	43		.78		.631	.075	8.41
21	110	72	1	1	1	1	13530.3	6666.3	.56	40.3	0	40.3		.76		.615	.072	8.54
22	120	100	1	1	1	1	14870.3	7382.3	.53	52.9	0	52.9		.74		.599	.069	8.68
23	130	86	1	1	1	1	16210.29	8098.29	.51	43.8	0	43.8		.72		.583	.065	8.96
24	143	100	1	1	1	1	17952.29	9029.09	.48	48	0	48		.69		.558	.061	9.14
25	153	91	1	1	1	1	19294.69	9747.49	.46	41.8	0	41.8		.68		.55	.057	9.64
26	163	92	1	1	1	1	20694.69	10523.49	.44	40.4	0	40.4		.66		.534	.054	9.88
27	170	100	1	1	1	1	21674.7	11066.69	.43	43	0	43		.66		.534	.051	10.47
28	180	100	1	1	1	1	23074.7	11842.69	.42	42	0	42		.64		.518	.048	10.79

Notes:  
 CSR analysis using SHAKE results.  
 CSR File: D:\4-O SF\10103\SF100103\S100103.rpt  
 CRR using SPT Data and Seed et al. Method in 1997 NCEER Workshop.  
 Earthquake File for SHAKE Analysis: D:\SF\SF100103.ACC  
 Earthquake Magnitude for CRR Analysis: 6.2  
 Magnitude Scaling Factor (MSF): 1.82  
 Depth to Water Table for CRR Analysis (ft): 0  
 Depth to Water Table for Cn Calculation (ft): 0  
 Depth to Base Layer for CSR Analysis (ft): 218.6  
 MSF Option: I.M. Idriss (1987)  
 Cn Option: Luo & Whitman (1986)  
 Ksigma Option: L.F. Harder & R. Boulanger (1997)  
 SPT Energy Ratio: USASafetyFactor: 0  
 \*Effective Stress column computed using Depth to Water Table for CRR Analysis

**Table G.2 Liquefaction Analysis**

St. Francis Site  
Ground Motion SF100104

SPT No.	Depth (ft)	N field	Energy Factor	Rod Factor	Sampler Factor	Borehole Factor	Total Stress (psf)	Effective Stress (psf)	Cn	(N1)60	Fines Content (%)	N1,60cs	Alpha	Ksigma	Kalpha	CRR	CSR	Safety Factor
1	1	21	1	1	1	1		285.6	2	42	91	55.4		1		.81	.05	16.19
2	6	12	1	1	1	1	660	285.6	2	24	91	33.8		1		.81	.208	3.89
3	8.4	73	1	1	1	1	923.99	399.83	2	146	0	146		1		.81	.201	4.02
4	12.5	10	1	1	1	1	1375	595	1.88	18.8	0	18.8		1		.33	.187	1.76
5	15.5	19	1	1	1	1	1705	737.8	1.69	32.1	0	32.1		1		.81	.173	4.68
6	19.5	17	1	1	1	1	2118	901.19	1.53	26	0	26		1		.49	.164	2.98
7	23.5	26	1	1	1	1	2518	1051.6	1.41	36.6	0	36.6		1		.81	.156	5.19
8	27.5	28	1	1	1	1	2918	1202	1.32	36.9	0	36.9		1		.81	.149	5.43
9	34	26	1	1	1	1	3584.79	1463.19	1.2	31.2	0	31.2		1		.81	.139	5.82
10	40	75	1	1	1	1	4352.79	1856.79	1.06	79.4	0	79.4		1		.81	.126	6.42
11	45	71	1	1	1	1	4990.29	2182.29	.98	69.5	0	69.5		.98		.793	.112	7.08
12	50	75	1	1	1	1	5660.3	2540.29	.91	68.2	0	68.2		.96		.777	.104	7.47
13	55	38	1	1	1	1	6330.3	2898.29	.85	32.3	0	32.3		.93		.753	.098	7.68
14	60	46	1	1	1	1	7000.3	3256.29	.8	36.8	0	36.8		.91		.737	.094	7.84
15	66	33	1	1	1	1	7787.1	3668.7	.75	24.7	0	24.7		.89		.403	.09	4.47
16	70	40	1	1	1	1	8307.09	3939.09	.73	29.2	0	29.2		.87		.554	.087	6.36
17	75	35	1	1	1	1	8957.09	4277.09	.7	24.5	0	24.5		.85		.381	.084	4.53
18	80	38	1	1	1	1	9607.09	4615.09	.67	25.4	0	25.4		.84		.397	.08	4.96
19	90	43	1	1	1	1	10907.1	5291.09	.63	27	0	27		.81		.424	.075	5.65
20	100	73	1	1	1	1	12207.1	5967.09	.59	43	0	43		.78		.631	.072	8.76
21	110	72	1	1	1	1	13530.3	6666.3	.56	40.3	0	40.3		.76		.615	.068	9.04
22	120	100	1	1	1	1	14870.3	7382.3	.53	52.9	0	52.9		.74		.599	.065	9.21
23	130	86	1	1	1	1	16210.29	8098.29	.51	43.8	0	43.8		.72		.583	.061	9.55
24	143	100	1	1	1	1	17952.29	9029.09	.48	48	0	48		.69		.558	.057	9.78
25	153	91	1	1	1	1	19294.69	9747.49	.46	41.8	0	41.8		.68		.55	.053	10.37
26	163	92	1	1	1	1	20694.69	10523.49	.44	40.4	0	40.4		.66		.534	.05	10.67
27	170	100	1	1	1	1	21674.7	11066.69	.43	43	0	43		.66		.534	.048	11.12
28	180	100	1	1	1	1	23074.7	11842.69	.42	42	0	42		.64		.518	.044	11.77

**Notes:**

CSR analysis using SHAKE results.  
 CSR File: D:\1-0\_SF\_Ps10104\SF100104\SI100104.gtl  
 CRR using SPT Data and Seed et. al. Method in 1997 NCEER Workshop.  
 Earthquake File for SHAKE Analysis: D:\SF\SF100104\ACC  
 Earthquake Magnitude for CRR Analysis: 6.2  
 Magnitude Scaling Factor (MSF): 1.63  
 Depth to Water Table for CRR Analysis (ft): 0  
 Depth to Water Table for Cn Calculation (ft): 0  
 Depth to Base Layer for CRR Analysis (ft): 218.6  
 MSF Option: LM, Idriss (1997)  
 Cn Option: Liao & Whitman (1988)  
 Ksigma Option: L.F. Harder & R. Boulanger (1997)  
 SPT Energy Ratio: USA Safety Program  
 \*Effective Stress column computed using Depth to Water Table for CRR Analysis

**Table G.3 Liquefaction Analysis**

St. Francis Site  
Ground Motion SF100105

SPT No.	Depth (ft)	N field	Energy Factor	Rod Factor	Sampler Factor	Borehole Factor	Total Stress (psf)	Effective Stress (psf)	Cn	(N1)60	Fines Content (%)	N1,60cs	Alpha	Ksigma	Kalpha	CRR	CSR	Safety Factor
1	1	21	1	1	1	1		285.6	2	42	91	55.4		1		.81	.063	15.28
2	6	12	1	1	1	1	660	285.6	2	24	91	33.8		1		.81	.218	3.71
3	8.4	73	1	1	1	1	323.99	389.83	2	146	0	146		1		.81	.211	3.83
4	12.5	10	1	1	1	1	1375	595	1.88	18.8	0	18.8		1		.33	.199	1.65
5	15.5	19	1	1	1	1	1705	737.8	1.69	32.1	0	32.1		1		.81	.187	4.33
6	19.5	17	1	1	1	1	2118	901.19	1.53	26	0	26		1		.49	.176	2.78
7	23.5	26	1	1	1	1	2518	1051.6	1.41	36.6	0	36.6		1		.81	.166	4.87
8	27.5	28	1	1	1	1	2918	1202	1.32	36.9	0	36.9		1		.81	.158	5.12
9	34	28	1	1	1	1	3584.79	1463.19	1.2	31.2	0	31.2		1		.81	.147	5.51
10	40	75	1	1	1	1	4352.79	1856.79	1.06	79.4	0	79.4		1		.81	.137	5.91
11	45	71	1	1	1	1	4990.29	2182.29	.98	69.5	0	69.5		.98		.793	.13	6.1
12	50	75	1	1	1	1	5660.3	2540.29	.91	68.2	0	68.2		.96		.777	.125	6.21
13	55	38	1	1	1	1	6330.3	2898.29	.85	32.3	0	32.3		.93		.753	.121	6.22
14	60	46	1	1	1	1	7000.3	3256.29	.8	36.8	0	36.8		.91		.737	.118	6.24
15	66	33	1	1	1	1	7787.1	3668.7	.75	24.7	0	24.7		.89		.403	.114	3.53
16	70	40	1	1	1	1	8307.09	3939.09	.73	29.2	0	29.2		.87		.554	.112	4.94
17	75	35	1	1	1	1	8957.09	4277.09	.7	24.5	0	24.5		.85		.381	.109	3.49
18	80	38	1	1	1	1	9607.09	4615.09	.67	25.4	0	25.4		.84		.397	.106	3.74
19	90	43	1	1	1	1	10907.1	5291.09	.63	27	0	27		.81		.424	.1	4.23
20	100	73	1	1	1	1	12207.1	5967.09	.59	43	0	43		.78		.631	.094	6.71
21	110	72	1	1	1	1	13530.3	6666.3	.56	40.3	0	40.3		.76		.615	.088	6.98
22	120	100	1	1	1	1	14870.3	7382.3	.53	52.9	0	52.9		.74		.599	.083	7.21
23	130	86	1	1	1	1	16210.29	8098.29	.51	43.8	0	43.8		.72		.583	.079	7.37
24	143	100	1	1	1	1	17952.29	9029.09	.48	48	0	48		.69		.558	.074	7.54
25	153	91	1	1	1	1	19294.69	9747.49	.46	41.8	0	41.8		.68		.55	.07	7.85
26	163	92	1	1	1	1	20694.69	10523.49	.44	40.4	0	40.4		.66		.534	.066	8.09
27	170	100	1	1	1	1	21674.7	11066.69	.43	43	0	43		.66		.534	.063	8.47
28	180	100	1	1	1	1	23074.7	11842.69	.42	42	0	42		.64		.518	.058	8.93

**Notes:**

CSR analysis using SHAKE results.  
 CSR File: C:\O-SF\F\K95\SH100105\SH100105.csf  
 CRR using SPT Data and Seed et. al. Method in 1997 NCEER Workshop.  
 Earthquake File for SHAKE Analysis: C:\SF\100105\ACC  
 Earthquake Magnitude for CRR Analysis: 6.2  
 Magnitude Scaling Factor (MSF): 1.62  
 Depth to Water Table for CRR Analysis (ft): 0  
 Depth to Water Table for Cn Calculation (ft): 0  
 Depth to Base Layer for CRR Analysis (ft): 218.6  
 MSF Option: LAL, Iliens (1987)  
 Cn Option: Liao & Whitman (1989)  
 Ksigma Option: L.F. Harder & R. Boulanger (1987)  
 SPT Energy Ratio: USA\SafetyFactor: 0  
 \*Effective Stress column computed using Depth to Water Table for CRR Analysis

**Table G.4 Liquefaction Analysis**

St. Francis Site  
Ground Motion SF100201

SPT No.	Depth (ft)	N field	Energy Factor	Rod Factor	Sampler Factor	Borehole Factor	Total Stress (psf)	Effective Stress (psf)	Cn	(N1)60	Fines Content (%)	N1,60cs	Alpha	Ksigma	Kalpha	CRR	CSR	Safety Factor
1	1	21	1	1	1	1		285.6	2	42	91	55.4		1		.555	.071	7.81
2	6	12	1	1	1	1	660	285.6	2	24	91	33.8		1		.555	.3	1.84
3	8.4	73	1	1	1	1	923.99	399.83	2	146	0	146		1		.555	.298	1.86
4	12.5	10	1	1	1	1	1375	595	1.88	18.8	0	18.8		1		.226	.293	.77
5	15.5	19	1	1	1	1	1705	737.8	1.69	32.1	0	32.1		1		.555	.288	1.92
6	19.5	17	1	1	1	1	2118	901.19	1.53	26	0	26		1		.336	.288	1.16
7	23.5	25	1	1	1	1	2518	1051.6	1.41	35.6	0	36.6		1		.555	.287	1.93
8	27.5	28	1	1	1	1	2918	1202	1.32	36.9	0	36.9		1		.555	.283	1.96
9	34	26	1	1	1	1	3584.79	1463.19	1.2	31.2	0	31.2		1		.555	.272	2.04
10	40	75	1	1	1	1	4352.79	1856.79	1.06	79.4	0	79.4		1		.555	.257	2.15
11	45	71	1	1	1	1	4950.29	2182.29	.98	69.5	0	69.5		.98		.543	.242	2.24
12	50	75	1	1	1	1	5660.3	2540.29	.91	68.2	0	68.2		.96		.532	.229	2.32
13	55	38	1	1	1	1	6330.3	2898.29	.85	32.3	0	32.3		.93		.516	.219	2.35
14	60	46	1	1	1	1	7000.3	3256.29	.8	36.8	0	36.8		.91		.505	.213	2.37
15	66	33	1	1	1	1	7787.1	3668.7	.75	24.7	0	24.7		.89		.276	.206	1.33
16	70	40	1	1	1	1	8307.09	3939.09	.73	29.2	0	29.2		.87		.38	.202	1.88
17	75	35	1	1	1	1	8957.09	4277.09	.7	24.5	0	24.5		.85		.261	.196	1.33
18	80	38	1	1	1	1	9507.09	4615.09	.67	25.4	0	25.4		.84		.272	.191	1.42
19	90	43	1	1	1	1	10907.1	5291.09	.63	27	0	27		.81		.29	.178	1.62
20	100	73	1	1	1	1	12207.1	5967.09	.59	43	0	43		.78		.432	.165	2.61
21	110	72	1	1	1	1	13530.3	6666.3	.56	40.3	0	40.3		.76		.421	.152	2.76
22	120	100	1	1	1	1	14870.3	7382.3	.53	52.9	0	52.9		.74		.41	.14	2.92
23	130	86	1	1	1	1	16210.29	8098.29	.51	43.8	0	43.8		.72		.399	.129	3.09
24	143	100	1	1	1	1	17952.29	9029.09	.48	48	0	48		.69		.382	.115	3.32
25	153	91	1	1	1	1	19294.69	9747.49	.46	41.8	0	41.8		.68		.377	.109	3.45
26	163	92	1	1	1	1	20694.69	10523.49	.44	40.4	0	40.4		.66		.366	.103	3.55
27	170	100	1	1	1	1	21674.7	11066.69	.43	43	0	43		.66		.366	.098	3.73
28	180	100	1	1	1	1	23074.7	11842.69	.42	42	0	42		.64		.355	.092	3.85

Notes:

CSR analysis using SHAKE results.  
 CSR File: D:\0 SF Pe10%\SF100201\SF100201.gr  
 CRR using SPT Data and Seed et al. Method in 1997 NCEER Workshop.  
 Earthquake File for SHAKE Analysis: D:\SF100201 ACC  
 Earthquake Magnitude for CRR Analysis: 7.2  
 Magnitude Scaling Factor (MSF): 1.11  
 Depth to Water Table for CRR Analysis (ft): 0  
 Depth to Water Table for Cn Calculations (ft): 0  
 Depth to Base Layer for CSR Analysis (ft): 219.6  
 MSF Option: I.M. Jones (1987)  
 Cn Option: Liao & Whitman (1988)  
 Ksigma Option: L.F. Harder & R. Boulanger (1997)  
 SPT Energy Ratio: USA-Safety/Ropic: 0  
 \*Effective Stress column calculated using Depth to Water Table for CRR Analysis

**Table G.5 Liquefaction Analysis**

St. Francis Site  
Ground Motion SF100202

SPT No.	Depth (ft)	N field	Energy Factor	Rod Factor	Sampler Factor	Borehole Factor	Total Stress (psf)	Effective Stress (psf)	Cn	(N1)60	Fines Content (%)	N1,60cs	Alpha	Ksigma	Kalpha	CRR	CSR	Safety Factor
1	1	21	1	1	1	1		285.6	2	42	91	55.4		1		.555	.071	7.81
2	6	12	1	1	1	1	660	285.6	2	24	91	33.8		1		.555	.296	1.87
3	8.4	73	1	1	1	1	923.99	399.83	2	146	0	146		1		.555	.293	1.89
4	12.5	10	1	1	1	1	1375	595	1.88	18.8	0	18.8		1		.226	.266	.79
5	15.5	19	1	1	1	1	1705	737.8	1.69	32.1	0	32.1		1		.555	.278	1.99
6	19.5	17	1	1	1	1	2118	901.19	1.53	26	0	26		1		.336	.272	1.23
7	23.5	28	1	1	1	1	2518	1051.6	1.41	36.6	0	36.6		1		.555	.266	2.08
8	27.5	28	1	1	1	1	2918	1202	1.32	36.9	0	36.9		1		.555	.259	2.14
9	34	26	1	1	1	1	3584.79	1463.19	1.2	31.2	0	31.2		1		.555	.248	2.23
10	40	75	1	1	1	1	4352.79	1856.79	1.06	79.4	0	79.4		1		.555	.234	2.37
11	45	71	1	1	1	1	4990.29	2182.29	.98	69.5	0	69.5		.98		.543	.22	2.46
12	50	75	1	1	1	1	5660.3	2540.29	.91	68.2	0	68.2		.96		.532	.21	2.53
13	55	38	1	1	1	1	6330.3	2898.29	.85	32.3	0	32.3		.93		.516	.202	2.55
14	60	46	1	1	1	1	7000.3	3256.29	.8	36.8	0	36.8		.91		.505	.195	2.58
15	66	33	1	1	1	1	7787.1	3668.7	.75	24.7	0	24.7		.89		.278	.187	1.47
16	70	40	1	1	1	1	8307.09	3939.09	.73	29.2	0	29.2		.87		.38	.181	2.09
17	75	35	1	1	1	1	8957.09	4277.09	.7	24.5	0	24.5		.85		.261	.175	1.49
18	80	38	1	1	1	1	9607.09	4615.09	.67	25.4	0	25.4		.84		.272	.168	1.61
19	90	43	1	1	1	1	10907.1	5291.09	.63	27	0	27		.81		.29	.155	1.87
20	100	73	1	1	1	1	12207.1	5967.09	.59	43	0	43		.78		.432	.142	3.04
21	110	72	1	1	1	1	13530.3	6668.3	.56	40.3	0	40.3		.76		.421	.129	3.26
22	120	100	1	1	1	1	14870.3	7382.3	.53	52.9	0	52.9		.74		.41	.119	3.44
23	130	86	1	1	1	1	16210.29	8098.29	.51	43.8	0	43.8		.72		.389	.113	3.53
24	143	100	1	1	1	1	17952.29	9029.09	.48	48	0	48		.69		.382	.107	3.57
25	153	91	1	1	1	1	19294.69	9747.49	.46	41.8	0	41.8		.68		.377	.102	3.69
26	163	92	1	1	1	1	20694.69	10523.49	.44	40.4	0	40.4		.66		.366	.098	3.73
27	170	100	1	1	1	1	21674.7	11066.69	.43	43	0	43		.66		.366	.094	3.89
28	180	100	1	1	1	1	23074.7	11842.69	.42	42	0	42		.64		.355	.09	3.94

**Notes:**

CSR analysis using SHAKE results.  
 CSR File: D:\V-O SF Proj\99SF100202\SF100202.gnl  
 CRR using SPT Data and Seed et. al. Method in 1987 NCEER Workshop.  
 Earthquake File for SHAKE Analysis: D:\SF\SF100202.ACC  
 Earthquake Magnitude for CRR Analysis: 7.2  
 Magnitude Scaling Factor (MSF): 1.11  
 Depth to Water Table for CRR Analysis (ft): 0  
 Depth to Water Table for Cn Calculation (ft): 0  
 Depth to Base Layer for CSR Analysis (ft): 218.8  
 MSF Option: LML Issues (1997)  
 Cn Option: Liao & Whitman (1988)  
 Ksigma Option: L.F. Harder & R. Boulanger (1987)  
 SPT Energy Ratio: USA Safety Paper: 0  
 \*Effective Stress column computed using Depth to Water Table for CRR Analysis

**Table G.6 Liquefaction Analysis**

St. Francis Site  
Ground Motion SF100205

SPT No.	Depth (ft)	N field	Energy Factor	Rod Factor	Sampler Factor	Borehole Factor	Total Stress (psf)	Effective Stress (psf)	Cn	(N1)60	Fines Content (%)	N1,60cs	Alpha	Ksigma	Kalpha	CRR	CSR	Safety Factor
1	1	21	1	1	1	1		285.6	2	42	91	55.4		1		.555	.066	8.4
2	6	12	1	1	1	1	660	285.6	2	24	91	33.8		1		.555	.278	1.99
3	8.4	73	1	1	1	1	923.99	399.83	2	146	0	146		1		.555	.275	2.01
4	12.5	10	1	1	1	1	1375	595	1.88	18.8	0	18.8		1		.226	.269	.84
5	15.5	19	1	1	1	1	1705	737.8	1.69	32.1	0	32.1		1		.555	.264	2.1
6	19.5	17	1	1	1	1	2118	901.19	1.53	26	0	26		1		.336	.263	1.27
7	23.5	26	1	1	1	1	2518	1051.6	1.41	36.6	0	36.6		1		.555	.263	2.11
8	27.5	28	1	1	1	1	2918	1202	1.32	36.9	0	36.9		1		.555	.26	2.13
9	34	28	1	1	1	1	3584.79	1463.19	1.2	31.2	0	31.2		1		.555	.253	2.19
10	40	75	1	1	1	1	4352.79	1856.79	1.06	79.4	0	79.4		1		.555	.241	2.3
11	45	71	1	1	1	1	4990.29	2182.29	.98	69.5	0	69.5		.98		.543	.23	2.36
12	50	75	1	1	1	1	5660.3	2540.29	.91	68.2	0	68.2		.96		.532	.22	2.41
13	55	38	1	1	1	1	6330.3	2898.29	.85	32.3	0	32.3		.93		.516	.212	2.43
14	60	48	1	1	1	1	7000.3	3256.29	.8	36.8	0	36.8		.91		.505	.208	2.42
15	66	33	1	1	1	1	7787.1	3668.7	.75	24.7	0	24.7		.89		.276	.202	1.36
16	70	40	1	1	1	1	8307.09	3939.09	.73	29.2	0	29.2		.87		.38	.198	1.91
17	75	35	1	1	1	1	8957.09	4277.09	.7	24.5	0	24.5		.85		.261	.193	1.35
18	80	38	1	1	1	1	9607.09	4615.09	.67	25.4	0	25.4		.84		.272	.189	1.43
19	90	43	1	1	1	1	10907.1	5291.09	.63	27	0	27		.81		.29	.177	1.63
20	100	73	1	1	1	1	12207.1	5967.09	.59	43	0	43		.78		.432	.165	2.61
21	110	72	1	1	1	1	13530.3	6666.3	.56	40.3	0	40.3		.76		.421	.152	2.76
22	120	100	1	1	1	1	14870.3	7382.3	.53	52.9	0	52.9		.74		.41	.141	2.9
23	130	86	1	1	1	1	16210.29	8098.29	.51	43.8	0	43.8		.72		.399	.131	3.04
24	143	100	1	1	1	1	17952.29	9029.09	.48	48	0	48		.69		.382	.118	3.23
25	153	91	1	1	1	1	19294.69	9747.49	.46	41.8	0	41.8		.68		.377	.11	3.42
26	163	92	1	1	1	1	20694.69	10523.49	.44	40.4	0	40.4		.66		.366	.102	3.58
27	170	100	1	1	1	1	21674.7	11066.69	.43	43	0	43		.66		.366	.097	3.77
28	180	100	1	1	1	1	23074.7	11842.69	.42	42	0	42		.64		.355	.089	3.98

Notes:

CSR analysis using SHAKE results.  
 CSR File: D:\40 SF P\167\SF100205\SF100205.grf  
 CRR using SPT Data and Seed et. al. Method in 1997 NCEER Workshop.  
 Earthquake File for SHAKE Analysis: C:\Y1\SF100205LACC  
 Earthquake Magnitude for CRR Analysis: 7.2  
 Magnitude Scaling Factor (MSF): 1.11  
 Depth to Water Table for CRR Analysis (ft): 0  
 Depth to Water Table for Cn Calculation (ft): 0  
 Depth to Base Layer for CSR Analysis (ft): 219.6  
 MSF Option: LM, Idriss (1997)  
 Cn Option: Liao & Whitman (1986)  
 Ksigma Option: L.F. Harder & R. Boulanger (1987)  
 SPT Energy Ratio: USA/SafetyFactor: 0  
 \*Effective Stress column computed using Depth to Water Table for CRR Analysis

**Table G.7 Liquefaction Analysis**

St. Francis Site  
Ground Motion SF020101

SPT No	Depth (ft)	N field	Energy Factor	Rod Factor	Sampler Factor	Borehole Factor	Total Stress (psf)	Effective Stress (psf)	Cn	(N1/60)	Fines Content (%)	N1,50cs	Alpha	Ksigma	Kalpha	CRR	CSR	Safety Factor
1	1	21	1	1	1	1		285.6	2	42	91	55.4		1		.75	.178	4.21
2	6	12	1	1	1	1	660	285.6	2	24	91	33.8		1		.75	.744	1
3	8.4	73	1	1	1	1	923.99	399.83	2	146	0	146		1		.75	.736	1.01
4	12.5	10	1	1	1	1	1375	595	1.88	18.8	0	18.8		1		.306	.719	.42
5	15.5	19	1	1	1	1	1705	737.8	1.69	32.1	0	32.1		1		.75	.701	1.06
6	19.5	17	1	1	1	1	2118	901.19	1.53	26	0	26		1		.454	.691	.65
7	23.5	26	1	1	1	1	2518	1051.6	1.41	36.6	0	36.6		1		.75	.681	1.1
8	27.5	28	1	1	1	1	2918	1202	1.32	36.9	0	36.9		1		.75	.666	1.12
9	34	26	1	1	1	1	3584.79	1463.19	1.2	31.2	0	31.2		1		.75	.638	1.17
10	40	75	1	1	1	1	4352.79	1856.79	1.06	79.4	0	79.4		1		.75	.599	1.25
11	45	71	1	1	1	1	4990.29	2182.29	.98	69.5	0	69.5		.98		.735	.559	1.31
12	50	75	1	1	1	1	5660.3	2540.29	.91	68.2	0	68.2		.96		.719	.523	1.37
13	55	38	1	1	1	1	6330.3	2898.29	.85	32.3	0	32.3		.93		.697	.49	1.42
14	60	46	1	1	1	1	7000.3	3256.29	.8	36.8	0	36.8		.91		.682	.462	1.47
15	66	33	1	1	1	1	7787.1	3668.7	.75	24.7	0	24.7		.89		.373	.429	.86
16	70	40	1	1	1	1	8307.09	3939.09	.73	29.2	0	29.2		.87		.513	.407	1.26
17	75	35	1	1	1	1	8957.09	4277.09	.7	24.5	0	24.5		.85		.353	.379	.93
18	80	38	1	1	1	1	9607.09	4615.09	.67	25.4	0	25.4		.84		.367	.351	1.04
19	90	43	1	1	1	1	10907.1	5291.09	.63	27	0	27		.81		.392	.322	1.21
20	100	73	1	1	1	1	12207.1	5967.09	.59	43	0	43		.78		.585	.304	1.92
21	110	72	1	1	1	1	13530.3	6666.3	.56	40.3	0	40.3		.76		.57	.286	1.99
22	120	100	1	1	1	1	14870.3	7382.3	.53	52.9	0	52.9		.74		.555	.272	2.04
23	130	86	1	1	1	1	16210.29	8096.29	.51	43.8	0	43.8		.72		.54	.265	2.03
24	143	100	1	1	1	1	17952.29	9029.09	.48	46	0	46		.69		.517	.254	2.03
25	153	91	1	1	1	1	19294.69	9747.49	.46	41.8	0	41.8		.68		.51	.24	2.12
26	163	92	1	1	1	1	20694.69	10523.49	.44	40.4	0	40.4		.66		.495	.226	2.19
27	170	100	1	1	1	1	21674.7	11066.69	.43	43	0	43		.66		.495	.216	2.29
28	180	100	1	1	1	1	23074.7	11842.69	.42	42	0	42		.64		.48	.202	2.37

Notes:

CSR analysis using SHAKE results.  
 CSR File: D:\0 SF Pe 2\USF020101\SI020101.grd  
 CRR using SPT Data and Seed et. al. Method in 1997 NCEER Workshop.  
 Earthquake File for SHAKE Analysis: D:\USF020101.ACC  
 Earthquake Magnitude for CRR Analysis: 6.4  
 Magnitude Scaling Factor (MSF): 1.5  
 Depth to Water Table for CRR Analysis (ft): 0  
 Depth to Water Table for Cn Calculations (ft): 0  
 Depth to Base Layer for CSR Analysis (ft): 218.6  
 MSF Option: I.M. Idriss (1987)  
 Cn Option: Liao & Whelan (1986)  
 Ksigma Option: L.F. Harder & R. Boussanger (1997)  
 SPT Energy Ratio: USA/SafetyFactor: 0  
 Effective Stress column computed using Depth to Water Table for CRR Analysis

**Table G.8 Liquefaction Analysis**

St. Francis Site  
Ground Motion SF020103

SPT No.	Depth (ft)	N field	Energy Factor	Rod Factor	Sampler Factor	Borehole Factor	Total Stress (psf)	Effective Stress (psf)	Cn	(N1)60	Fines Content (%)	N1,60cs	Alpha	Ksigma	Kalpha	CRR	CSR	Safety Factor
1	1	21	1	1	1	1		285.6	2	42	91	55.4		1		.75	.155	4.83
2	6	12	1	1	1	1	660	285.6	2	24	91	33.8		1		.75	.653	1.14
3	8.4	73	1	1	1	1	923.99	399.83	2	146	0	146		1		.75	.652	1.15
4	12.5	10	1	1	1	1	1375	595	1.88	18.8	0	18.8		1		.306	.647	.47
5	15.5	19	1	1	1	1	1705	737.8	1.69	32.1	0	32.1		1		.75	.641	1.17
6	19.5	17	1	1	1	1	2118	901.19	1.53	26	0	26		1		.454	.643	.7
7	23.5	26	1	1	1	1	2518	1051.6	1.41	36.6	0	36.6		1		.75	.645	1.16
8	27.5	28	1	1	1	1	2918	1202	1.32	36.9	0	36.9		1		.75	.641	1.17
9	34	26	1	1	1	1	3584.79	1463.19	1.2	31.2	0	31.2		1		.75	.626	1.19
10	40	75	1	1	1	1	4352.79	1856.79	1.06	79.4	0	79.4		1		.75	.597	1.25
11	45	71	1	1	1	1	4990.29	2182.29	.98	69.5	0	69.5		.98		.735	.561	1.31
12	50	75	1	1	1	1	5660.3	2540.29	.91	68.2	0	68.2		.96		.719	.526	1.36
13	55	38	1	1	1	1	6330.3	2898.29	.85	32.3	0	32.3		.93		.697	.496	1.4
14	60	46	1	1	1	1	7000.3	3256.29	.8	36.8	0	36.8		.91		.682	.475	1.43
15	66	33	1	1	1	1	7787.1	3668.7	.75	24.7	0	24.7		.89		.373	.448	.83
16	70	40	1	1	1	1	8307.09	3939.09	.73	29.2	0	29.2		.87		.513	.432	1.18
17	75	35	1	1	1	1	8957.09	4277.09	.7	24.5	0	24.5		.85		.353	.411	.85
18	80	38	1	1	1	1	9607.09	4615.09	.67	25.4	0	25.4		.84		.367	.39	.94
19	90	43	1	1	1	1	10907.1	5291.09	.63	27	0	27		.81		.392	.364	1.07
20	100	73	1	1	1	1	12207.1	5967.09	.59	43	0	43		.78		.585	.345	1.69
21	110	72	1	1	1	1	13530.3	6666.3	.56	40.3	0	40.3		.76		.57	.326	1.74
22	120	100	1	1	1	1	14870.3	7382.3	.53	52.9	0	52.9		.74		.555	.307	1.8
23	130	86	1	1	1	1	16210.29	8098.29	.51	43.8	0	43.8		.72		.54	.288	1.87
24	143	100	1	1	1	1	17952.29	9029.09	.48	48	0	48		.69		.517	.268	1.92
25	153	91	1	1	1	1	19294.69	9747.49	.46	41.8	0	41.8		.68		.51	.264	1.93
26	163	92	1	1	1	1	20694.69	10523.49	.44	40.4	0	40.4		.66		.495	.26	1.9
27	170	100	1	1	1	1	21674.7	11066.69	.43	43	0	43		.66		.495	.258	1.91
28	180	100	1	1	1	1	23074.7	11842.69	.42	42	0	42		.64		.48	.254	1.88

Notes:

CSR analysis using SHAKE results.  
 CSR File: D:\14-SF-Pa 2\GIS020103\S020103.gcf  
 CRR using SPT Data and Seed et. al. Method in 1987 NCEER Workshop.  
 Earthquake File for SHAKE Analysis: D:\SF020103.LACC  
 Earthquake Magnitude for CRR Analysis: 8.4  
 Magnitude Scaling Factor (MSF): 1.5  
 Depth to Water Table for CRR Analysis (ft): 0  
 Depth to Water Table for Cn Calculation (ft): 0  
 Depth to Base Layer for CSR Analysis (ft): 219.6  
 MSF Option: LM, Idriss (1987)  
 Cn Option: Ueo & Whitman (1988)  
 Ksigma Option: L.F. Harder & R. Boulanger (1987)  
 SPT Energy Ratio: USASafetyFactor: 0  
 \*Effective Stress column computed using Depth to Water Table for CRR Analysis

**Table G.9 Liquefaction Analysis**

St. Francis Site  
Ground Motion SF020105

SPT No.	Depth (ft)	N Field	Energy Factor	Rod Factor	Sampler Factor	Borehole Factor	Total Stress (psf)	Effective Stress (psf)	Cn	(N1)60	Fines Content (%)	N1,60cs	Alpha	Ksigma	Kalpha	CRR	CSR	Safety Factor
1	1	21	1	1	1	1		265.6	2	42	91	55.4		1		75	168	4.46
2	6	12	1	1	1	1	660	265.6	2	24	91	33.8		1		75	697	1.07
3	8.4	73	1	1	1	1	923.99	399.83	2	146	0	146		1		75	685	1.09
4	12.5	10	1	1	1	1	1375	595	1.88	18.8	0	18.8		1		306	661	.46
5	15.5	19	1	1	1	1	1705	737.8	1.69	32.1	0	32.1		1		75	639	1.17
6	19.5	17	1	1	1	1	2118	901.19	1.53	26	0	26		1		454	625	.72
7	23.5	26	1	1	1	1	2518	1051.6	1.41	36.6	0	36.6		1		75	612	1.22
8	27.5	28	1	1	1	1	2918	1202	1.32	36.9	0	36.9		1		75	596	1.25
9	34	26	1	1	1	1	3584.79	1463.19	1.2	31.2	0	31.2		1		75	564	1.32
10	40	75	1	1	1	1	4352.79	1856.79	1.06	79.4	0	79.4		1		75	525	1.42
11	45	71	1	1	1	1	4990.29	2182.29	.98	69.5	0	69.5		.98		735	491	1.49
12	50	75	1	1	1	1	5650.3	2540.29	.91	68.2	0	68.2		.96		719	463	1.55
13	55	38	1	1	1	1	6330.3	2698.29	.85	32.3	0	32.3		.93		697	439	1.58
14	60	46	1	1	1	1	7000.3	3256.29	.8	36.8	0	36.8		.91		682	42	1.62
15	66	33	1	1	1	1	7787.1	3668.7	.75	24.7	0	24.7		.89		373	397	.93
16	70	40	1	1	1	1	8307.09	3939.09	.73	29.2	0	29.2		.87		513	382	1.34
17	75	35	1	1	1	1	8957.09	4277.09	.7	24.5	0	24.5		.85		353	363	.97
18	80	38	1	1	1	1	9607.09	4615.09	.67	25.4	0	25.4		.84		367	344	1.06
19	90	43	1	1	1	1	10907.1	5291.09	.63	27	0	27		.81		392	319	1.22
20	100	73	1	1	1	1	12207.1	5967.09	.59	43	0	43		.78		585	298	1.96
21	110	72	1	1	1	1	13530.3	6668.3	.56	40.3	0	40.3		.76		57	278	2.05
22	120	100	1	1	1	1	14870.3	7382.3	.53	52.9	0	52.9		.74		555	257	2.15
23	130	86	1	1	1	1	16210.29	8098.29	.51	43.8	0	43.8		.72		54	236	2.28
24	143	100	1	1	1	1	17952.29	9029.09	.48	48	0	48		.69		517	214	2.41
25	153	91	1	1	1	1	19294.69	9747.49	.46	41.8	0	41.8		.68		51	212	2.4
26	163	92	1	1	1	1	20694.69	10523.49	.44	40.4	0	40.4		.66		495	21	2.35
27	170	100	1	1	1	1	21674.7	11066.69	.43	43	0	43		.66		495	209	2.36
28	180	100	1	1	1	1	23074.7	11842.69	.42	42	0	42		.64		48	207	2.31

Notes:

CSR analysis using SHAKE results.  
 CSR File: D:\3-0 SF Pa 2\%S020105\S020105.pr  
 CRR using SPT Data and Seed et. al. Method in 1997 NCEER Workshop.  
 Earthquake File for SHAKE Analysis: D:\SFS020105.ACC  
 Earthquake Magnitude for CRR Analysis: 6.4  
 Magnitude Scaling Factor (MSF): 1.5  
 Depth to Water Table for CRR Analysis (ft): 0  
 Depth to Water Table for Cn Calculation (ft): 0  
 Depth to Base Layer for CSR Analysis (ft): 219.6  
 MSF Option: I.M. Idias (1999)  
 Cn Option: Geo & Whitman (1989)  
 Ksigma Option: L.F. Harder & R. Boulanger (1997)  
 SPT Energy Ratio: USA/SafetyFactor 0  
 \*Effective Stress column computed using Depth to Water Table for CRR Analysis

**Table G.10 Liquefaction Analysis**

St. Francis Site  
Ground Motion SF020201

SPT No.	Depth (ft)	N field	Energy Factor	Rod Factor	Sampler Factor	Borehole Factor	Total Stress (psf)	Effective Stress (psf)	Cn	(N1)60	Fines Content (%)	N1,60cs	Alpha	Ksigma	Kalpha	CRR	CSR	Safety Factor
1	1	21	1	1	1	1		285.6	2	42	91	55.4		1		42	159	2.64
2	6	12	1	1	1	1	660	285.6	2	24	91	33.8		1		42	668	.62
3	8.4	73	1	1	1	1	923.99	399.83	2	146	0	146		1		42	667	.62
4	12.5	10	1	1	1	1	1375	595	1.88	18.8	0	18.8		1		171	665	.25
5	15.5	19	1	1	1	1	1705	737.8	1.59	32.1	0	32.1		1		42	663	.63
6	19.5	17	1	1	1	1	2118	901.19	1.53	26	0	26		1		254	669	.37
7	23.5	26	1	1	1	1	2518	1051.6	1.41	36.6	0	36.6		1		42	675	.62
8	27.5	28	1	1	1	1	2918	1202	1.32	36.9	0	36.9		1		42	673	.62
9	34	26	1	1	1	1	3584.79	1483.19	1.2	31.2	0	31.2		1		42	661	.63
10	40	75	1	1	1	1	4352.79	1856.79	1.06	79.4	0	79.4		1		42	633	.66
11	45	71	1	1	1	1	4990.29	2182.29	.98	69.5	0	69.5		.98		411	596	.66
12	50	75	1	1	1	1	5660.3	2540.29	.91	68.2	0	68.2		.96		403	558	.72
13	55	38	1	1	1	1	6330.3	2898.29	.85	32.3	0	32.3		.93		39	523	.74
14	60	46	1	1	1	1	7060.3	3256.29	.8	36.8	0	36.8		.91		382	496	.77
15	66	33	1	1	1	1	7787.1	3668.7	.75	24.7	0	24.7		.89		209	464	.45
16	70	40	1	1	1	1	8307.09	3939.09	.73	29.2	0	29.2		.87		287	442	.64
17	75	35	1	1	1	1	8957.09	4277.09	.7	24.5	0	24.5		.85		197	415	.47
18	80	38	1	1	1	1	9607.09	4615.09	.57	25.4	0	25.4		.84		206	388	.52
19	90	43	1	1	1	1	10907.1	5291.09	.63	27	0	27		.81		219	352	.62
20	100	73	1	1	1	1	12207.1	5967.09	.59	43	0	43		.78		327	322	1.01
21	110	72	1	1	1	1	13530.3	6666.3	.56	40.3	0	40.3		.76		319	292	1.09
22	120	100	1	1	1	1	14870.3	7382.3	.53	52.9	0	52.9		.74		31	267	1.16
23	130	86	1	1	1	1	16210.29	8098.29	.51	43.8	0	43.8		.72		302	25	1.2
24	143	100	1	1	1	1	17952.29	9029.09	.48	48	0	48		.69		289	229	1.26
25	153	91	1	1	1	1	19294.69	9747.49	.46	41.8	0	41.8		.68		285	218	1.3
26	163	92	1	1	1	1	20694.69	10523.49	.44	40.4	0	40.4		.66		277	207	1.33
27	170	100	1	1	1	1	21674.7	11066.69	.43	43	0	43		.66		277	199	1.39
28	180	100	1	1	1	1	23074.7	11842.69	.42	42	0	42		.64		268	189	1.41

Notes:

CSR analysis using SHAKE results.  
 CSR File: D:\0 SF Pa 2% SF020201\SF020201.cr  
 CRR using SPT Data and Seed et al. Method in 1997 NCEER Workshop.  
 Earthquake File for SHAKE Analysis: O:\SP\SF020201.ACC  
 Earthquake Magnitude for CRR Analysis: 8  
 Magnitude Scaling Factor (MSF): .84  
 Depth to Water Table for CRR Analysis (ft): 0  
 Depth to Water Table for Cn Calculation (ft): 0  
 Depth to Base Layer for CSR Analysis (ft): 219.6  
 MSF Option: L.M. Idriss (1987)  
 Cn Option: Leo & Whitman (1988)  
 Ksigma Option: L.F. Harder & R. Boulanger (1987)  
 SPT Energy Ratio: USA/SafetyFactor: 0  
 Effective Stress column computed using Depth to Water Table for CRR Analysis

**Table G.11 Liquefaction Analysis**

St. Francis Site  
Ground Motion SF020203

SPT No.	Depth (ft)	N field	Energy Factor	Rod Factor	Sampler Factor	Borehole Factor	Total Stress (psf)	Effective Stress (psf)	Cn	(N1)60	Fines Content (%)	N1,60cs	Alpha	Ksigma	Kalpha	CRR	CSR	Safety Factor
1	1	21	1	1	1	1		285.6	2	42	91	55.4		1		.42	.159	2.64
2	6	12	1	1	1	1	660	285.6	2	24	91	33.8		1		.42	.663	.63
3	8.4	73	1	1	1	1	923.99	399.83	2	146	0	146		1		.42	.655	.64
4	12.5	10	1	1	1	1	1375	595	1.88	18.8	0	18.8		1		.171	.639	.26
5	15.5	19	1	1	1	1	1705	737.8	1.69	32.1	0	32.1		1		.42	.624	.67
6	19.5	17	1	1	1	1	2118	901.19	1.53	26	0	26		1		.254	.62	.4
7	23.5	26	1	1	1	1	2518	1051.6	1.41	36.6	0	36.6		1		.42	.617	.68
8	27.5	28	1	1	1	1	2918	1202	1.32	36.9	0	36.9		1		.42	.606	.69
9	34	26	1	1	1	1	3584.79	1463.19	1.2	31.2	0	31.2		1		.42	.582	.72
10	40	75	1	1	1	1	4352.79	1856.79	1.06	79.4	0	79.4		1		.42	.551	.76
11	45	71	1	1	1	1	4990.29	2182.29	.98	69.5	0	69.5		.98		.411	.521	.78
12	50	75	1	1	1	1	5660.3	2540.29	.91	68.2	0	68.2		.96		.403	.496	.81
13	55	38	1	1	1	1	6330.3	2898.29	.85	32.3	0	32.3		.93		.39	.474	.82
14	60	46	1	1	1	1	7000.3	3256.29	.8	36.8	0	36.8		.91		.382	.459	.83
15	66	33	1	1	1	1	7787.1	3668.7	.75	24.7	0	24.7		.89		.209	.441	.47
16	70	40	1	1	1	1	8307.09	3939.09	.73	29.2	0	29.2		.87		.287	.429	.66
17	75	35	1	1	1	1	8957.09	4277.09	.7	24.5	0	24.5		.85		.197	.414	.47
18	80	38	1	1	1	1	9607.09	4615.09	.67	25.4	0	25.4		.84		.205	.399	.51
19	90	43	1	1	1	1	10907.1	5291.09	.63	27	0	27		.81		.219	.372	.58
20	100	73	1	1	1	1	12207.1	5967.09	.59	43	0	43		.78		.327	.346	.94
21	110	72	1	1	1	1	13530.3	6666.3	.56	40.3	0	40.3		.76		.319	.32	.99
22	120	100	1	1	1	1	14870.3	7382.3	.53	52.9	0	52.9		.74		.31	.298	1.04
23	130	86	1	1	1	1	16210.29	8098.29	.51	43.8	0	43.8		.72		.302	.282	1.07
24	143	100	1	1	1	1	17952.29	9029.09	.48	48	0	48		.69		.289	.263	1.09
25	153	91	1	1	1	1	19294.69	9747.49	.46	41.8	0	41.8		.68		.285	.252	1.13
26	163	92	1	1	1	1	20694.69	10523.49	.44	40.4	0	40.4		.66		.277	.241	1.14
27	170	100	1	1	1	1	21674.7	11066.69	.43	43	0	43		.66		.277	.233	1.18
28	180	100	1	1	1	1	23074.7	11842.69	.42	42	0	42		.64		.268	.223	1.2

Notes:  
 CSR analysis using SHAKE results.  
 CSR File: D:\40 SF Pa 2\6\SM020203\SF020203.gr  
 CRR using SPT Data and Seed et. al. Method in 1987 NCEER Workshop.  
 Earthquake File for SHAKE Analysis: D:\SF\SF020203.ACC  
 Earthquake Magnitude for CRR Analysis: 8  
 Magnitude Scaling Factor (MSF): .84  
 Depth to Water Table for CRR Analysis (ft): 0  
 Depth to Water Table for Cn Calculation (ft): 0  
 Depth to Base Layer for CRR Analysis (ft): 219.8  
 MSF Option: I.M. Jelliss (1987)  
 Cn Option: Liao & Whitman (1988)  
 Ksigma Option: L.F. Harder & P. Boulanger (1987)  
 SPT Energy Ratio: USA/SafetyFactor: 0  
 \*Effective Stress column computed using Depth to Water Table for CRR Analysis

**Table G.12 Liquefaction Analysis**

St. Francis Site  
Ground Motion SF020205

SPT No.	Depth (ft)	N field	Energy Factor	Rod Factor	Sampler Factor	Borehole Factor	Total Stress (psf)	Effective Stress (psf)	Cn	(N1)60	Fines Content (%)	N1,60cs	Alpha	Ksigma	Kalpha	CRR	CSR	Safety Factor
1	1	21	1	1	1	1		285.6	2	42	91	55.4		1		42	137	3.06
2	6	12	1	1	1	1	660	285.6	2	24	91	33.8		1		42	571	.73
3	8.4	73	1	1	1	1	923.99	399.83	2	146	0	146		1		42	565	.74
4	12.5	10	1	1	1	1	1375	595	1.88	18.8	0	18.8		1		171	553	.3
5	15.5	19	1	1	1	1	1705	737.8	1.69	32.1	0	32.1		1		42	543	.77
6	19.5	17	1	1	1	1	2118	901.19	1.53	26	0	26		1		254	546	.46
7	23.5	26	1	1	1	1	2518	1051.8	1.41	36.6	0	36.6		1		42	549	.76
8	27.5	28	1	1	1	1	2918	1202	1.32	36.9	0	36.9		1		42	547	.76
9	34	26	1	1	1	1	3584.79	1463.19	1.2	31.2	0	31.2		1		42	539	.77
10	40	75	1	1	1	1	4352.79	1856.79	1.06	79.4	0	79.4		1		42	517	.81
11	45	71	1	1	1	1	4990.29	2182.29	.96	69.5	0	69.5		.96		411	486	.84
12	50	75	1	1	1	1	5660.3	2540.29	.91	68.2	0	68.2		.96		403	458	.87
13	55	38	1	1	1	1	6330.3	2898.29	.85	32.3	0	32.3		.93		39	434	.89
14	60	46	1	1	1	1	7000.3	3256.29	.8	36.8	0	36.8		.91		382	418	.91
15	66	33	1	1	1	1	7787.1	3668.7	.75	24.7	0	24.7		.89		209	399	.52
16	70	40	1	1	1	1	8307.09	3939.09	.73	29.2	0	29.2		.87		287	386	.74
17	75	35	1	1	1	1	8957.09	4277.09	.7	24.5	0	24.5		.85		197	37	.53
18	80	38	1	1	1	1	9607.09	4615.09	.67	25.4	0	25.4		.84		205	353	.58
19	90	43	1	1	1	1	10907.1	5291.09	.63	27	0	27		.81		219	327	.66
20	100	73	1	1	1	1	12207.1	5967.09	.59	43	0	43		.78		327	302	1.08
21	110	72	1	1	1	1	13530.3	6666.3	.56	40.3	0	40.3		.76		319	277	1.15
22	120	100	1	1	1	1	14870.3	7382.3	.53	52.9	0	52.9		.74		31	259	1.19
23	130	86	1	1	1	1	16210.29	8098.29	.51	43.8	0	43.8		.72		302	251	1.2
24	143	100	1	1	1	1	17952.29	9029.09	.48	48	0	48		.69		289	24	1.2
25	153	91	1	1	1	1	19294.69	9747.49	.46	41.8	0	41.8		.68		285	23	1.23
26	163	92	1	1	1	1	20694.69	10523.49	.44	40.4	0	40.4		.66		277	219	1.26
27	170	100	1	1	1	1	21674.7	11066.69	.43	43	0	43		.66		277	212	1.3
28	180	100	1	1	1	1	23074.7	11842.69	.42	42	0	42		.64		268	201	1.33

**Notes:**

CSR analysis using SHAKE results.  
 CSR File: D:\4-SF-Pa 2\4\S020205\S020205.csf  
 CRR using SPT Data and Seed et. al. Method in 1987 NCEER Workshop.  
 Earthquake File for SHAKE Analysis: D:\SF\S020205.ACC  
 Earthquake Magnitude for CRR Analysis: 8  
 Magnitude Scaling Factor (MSF): .34  
 Depth to Water Table for CRR Analysis (ft): 0  
 Depth to Water Table for Cn Calculation (ft): 0  
 Depth to Base Layer for CSR Analysis (ft): 218.6  
 MSF Option: LM, Ilnan (1987)  
 Cn Option: Liao & Whitman (1988)  
 Ksigma Option: L.F. Harder & R. Boulanger (1987)  
 SPT Energy Ratio: USA Safety Procs: 0  
 \*Effective Stress column computed using Depth to Water Table for CRR Analysis

Table G.13 Liquefaction Analysis

Wahite Ditch Site  
Ground Motion WD100101

SPT No.	Depth (ft)	N field	Energy Factor	Rod Factor	Sampler Factor	Borehole Factor	Total Stress (psf)	Effective Stress (psf)	Cn	(N1)60	Fines Content (%)	N1,60cs	Alpha	Ksigma	Kalpha	CRR	CSR	Safety Factor
1	20	58	1	1	1	1		47.6	2	116	91	144.2		1		.75	.336	2.23
2	21.5	51	1	1	1	1	1932.59	590.99	1.89	96.3	91	120.5		1		.75	.331	2.26
3	23	72	1	1	1	1	2072.09	636.89	1.82	131	91	162.2		1		.75	.319	2.35
4	24.5	63	1	1	1	1	2219.79	690.99	1.74	109.6	91	136.5		1		.75	.305	2.45
5	26	49	1	1	1	1	2420.79	796.39	1.62	79.3	91	100.1		1		.75	.292	2.56
6	27.5	46	1	1	1	1	2621.79	905.79	1.52	69.9	91	88.8		1		.75	.279	2.68
7	29	65	1	1	1	1	2822.79	1013.19	1.44	93.6	91	117.3		1		.75	.266	2.81
8	35	66	1	1	1	1	3626.79	1442.79	1.21	79.8	26	93.9		1		.75	.231	3.24
9	40	73	1	1	1	1	4291.4	1795.39	1.08	78.8	20	88.6		1		.75	.207	3.62
10	45	47	1	1	1	1	4951.4	2143.39	.99	46.5	8	47.3	.98			.735	.19	3.86
11	50	46	1	1	1	1	5613	2493	.92	42.3	0	42.3	.96			.719	.181	3.97
12	55	39	1	1	1	1	6278	2946	.86	33.5	0	33.5	.94			.705	.171	4.12
13	60	38	1	1	1	1	6942.99	3198.99	.81	30.7	0	30.7	.91			.682	.164	4.15
14	60	46	1	1	1	1	6942.99	3198.99	.81	37.2	0	37.2	.91			.682	.164	4.15
15	65	54	1	1	1	1	7607.99	3551.99	.77	41.5	8	42.3	.89			.667	.161	4.14
16	70	51	1	1	1	1	8252.69	3884.69	.73	37.2	0	37.2	.87			.652	.158	4.12
17	75	54	1	1	1	1	8882.69	4202.69	.7	37.8	0	37.8	.86			.645	.154	4.18
18	80	51	1	1	1	1	9512.69	4520.69	.68	34.6	0	34.6	.84			.63	.151	4.17
19	90	51	1	1	1	1	10772.69	5156.69	.64	32.6	0	32.6	.81			.607	.144	4.21
20	100	82	1	1	1	1	12032.69	5792.69	.6	49.2	0	49.2	.79			.592	.135	4.36
21	110	73	1	1	1	1	13292.69	6428.69	.57	41.6	0	41.6	.77			.577	.125	4.61
22	120	24	1	1	1	1	14552.69	7064.69	.54	12.9	0	12.9	.74			.158	.115	1.35
23	130	29	1	1	1	1	15895.49	7773.49	.52	15	7	15.2	.72			.178	.105	1.69
24	140	61	1	1	1	1	17225.5	8499.5	.49	29.8	0	29.8	.71			.475	.098	4.84
25	150	71	1	1	1	1	18545.69	9185.69	.47	33.3	0	33.3	.69			.517	.09	5.74
26	160	56	1	1	1	1	19865.69	9881.69	.46	25.7	0	25.7	.68			.303	.084	3.6
27	170	82	1	1	1	1	21185.7	10577.69	.44	36	0	36	.66			.495	.08	6.18
28	180	96	1	1	1	1	22578.49	11346.49	.43	41.2	0	41.2	.65			.487	.075	6.49
29	190	82	1	1	1	1	23978.49	12122.49	.41	33.6	0	33.6	.64			.48	.071	6.76
30	201	81	1	1	1	1	25517.7	12975.29	.4	32.4	0	32.4	.63			.472	.067	7.04

Notes:

CSR analysis using SHAKE results.  
 CSR File: D:\4-8 WH PE10\WH100101\WH100101.prj  
 CRR using SPT Data and Seed et. al. Method in 1987 NCEER Workshop.  
 Earthquake File for SHAKE Analysis: D:\WH100101\ACC  
 Earthquake Magnitude for CRR Analysis: 6.4  
 Magnitude Scaling Factor (MSF): 1.5  
 Depth to Water Table for CRR Analysis (ft): 0  
 Depth to Water Table for Cn Calculation (ft): 0  
 Depth to Base Layer for CSR Analysis (ft): 205.9  
 MSF Option: L.M. Idriss (1987)  
 Cn Option: Liao & Whitman (1986)  
 Ksigma Option: L.F. Harder & R. Boulanger (1997)  
 SPT Energy Ratio: USA/SafetyHope: 1

**Table G.14 Liquefaction Analysis**

White Ditch Site  
Ground Motion WD100102

SPT No.	Depth (ft)	N field	Energy Factor	Rod Factor	Sampler Factor	Borehole Factor	Total Stress (psf)	Effective Stress (psf)	Cn	(N1)60	Fines Content (%)	N1,60cs	Alpha	Ksigma	Kalpha	CRR	CSR	Safety Factor
1	20	58	1	1	1	1		47.6	2	116	91	144.2		1		.75	.3	2.5
2	21.5	51	1	1	1	1	1932.59	590.99	1.89	96.3	91	120.5		1		.75	.292	2.56
3	23	72	1	1	1	1	2072.09	636.89	1.82	131	91	162.2		1		.75	.279	2.68
4	24.5	63	1	1	1	1	2219.79	690.99	1.74	109.6	91	136.5		1		.75	.266	2.81
5	26	49	1	1	1	1	2420.79	798.39	1.62	79.3	91	100.1		1		.75	.252	2.97
6	27.5	46	1	1	1	1	2621.79	905.79	1.52	69.9	91	88.8		1		.75	.238	3.15
7	29	65	1	1	1	1	2822.79	1013.19	1.44	93.6	91	117.3		1		.75	.224	3.34
8	35	66	1	1	1	1	3626.79	1442.79	1.21	79.8	26	93.9		1		.75	.192	3.9
9	40	73	1	1	1	1	4291.4	1795.39	1.08	78.8	20	86.6		1		.75	.174	4.31
10	45	47	1	1	1	1	4951.4	2143.39	.99	46.5	8	47.3	.98			.735	.159	4.62
11	50	46	1	1	1	1	5613	2493	.92	42.3	0	42.3	.96			.719	.151	4.76
12	55	39	1	1	1	1	6278	2846	.86	33.5	0	33.5	.94			.705	.143	4.93
13	60	38	1	1	1	1	6942.99	3198.99	.81	30.7	0	30.7	.91			.682	.137	4.97
14	60	46	1	1	1	1	6942.99	3198.99	.81	37.2	0	37.2	.91			.682	.137	4.97
15	65	54	1	1	1	1	7607.99	3551.99	.77	41.5	8	42.3	.89			.667	.133	5.01
16	70	51	1	1	1	1	8252.69	3884.69	.73	37.2	0	37.2	.87			.652	.13	5.01
17	75	54	1	1	1	1	8882.69	4202.69	.7	37.8	0	37.8	.86			.645	.126	5.11
18	80	51	1	1	1	1	9512.69	4520.69	.68	34.6	0	34.6	.84			.63	.123	5.12
19	90	51	1	1	1	1	10772.69	5156.69	.64	32.6	0	32.6	.81			.607	.116	5.23
20	100	82	1	1	1	1	12032.69	5792.69	.6	49.2	0	49.2	.79			.582	.11	5.38
21	110	73	1	1	1	1	13292.69	6428.69	.57	41.6	0	41.6	.77			.577	.104	5.54
22	120	24	1	1	1	1	14552.69	7064.69	.54	12.9	0	12.9	.74			.156	.099	1.57
23	130	29	1	1	1	1	15885.49	7773.49	.52	15	7	15.2	.72			.178	.093	1.91
24	140	61	1	1	1	1	17225.5	8489.5	.49	29.8	0	29.8	.71			.475	.088	5.39
25	150	71	1	1	1	1	18545.69	9185.69	.47	33.3	0	33.3	.69			.517	.083	6.22
26	160	56	1	1	1	1	19865.69	9881.69	.46	25.7	0	25.7	.68			.303	.079	3.83
27	170	82	1	1	1	1	21185.7	10577.69	.44	36	0	36	.66			.496	.077	6.42
28	180	96	1	1	1	1	22578.49	11346.49	.43	41.2	0	41.2	.65			.487	.075	6.49
29	190	82	1	1	1	1	23978.49	12122.49	.41	33.6	0	33.6	.64			.48	.073	6.57
30	201	81	1	1	1	1	25517.7	12975.29	.4	32.4	0	32.4	.63			.472	.07	6.74

Notes:  
 CSR analysis using SHAKE results.  
 CSR File: D:\0 WH PE\1425\WH100102\WH100102.cd  
 CRR using SPT Data and Seed et. al. Method in 1997 NCEEER Workshop.  
 Earthquake File for SHAKE Analysis: D:\WH\WH100102.ACC  
 Earthquake Magnitude for CRR Analysis: 6.4  
 Magnitude Scaling Factor (MSF): 1.5  
 Depth to Water Table for CRR Analysis (ft): 0  
 Depth to Water Table for Cn Calculation (ft): 0  
 Depth to Base Layer for CSR Analysis (ft): 205.9  
 MSF Option: L.M. Idriss (1987)  
 Cn Option: Liao & Whitman (1986)  
 Ksigma Option: L.F. Harder & R. Boulanger (1997)  
 SPT Energy Ratio: USA SafetyFactor: 1

**Table G.15** Liquefaction Analysis

Waite Ditch Site  
Ground Motion WD100105

SPT No.	Depth (ft)	N field	Energy Factor	Rod Factor	Sampler Factor	Borehole Factor	Total Stress (psf)	Effective Stress (psf)	Cn	(N1)60	Fines Content (%)	N1,60cs	Alpha	Ksigma	Kalpha	CRR	CSR	Safety Factor
1	20	58	1	1	1	1		47.6	2	116	91	144.2		1		.75	.301	2.49
2	21.5	51	1	1	1	1	1932.69	690.99	1.89	96.3	91	120.5		1		.75	.291	2.57
3	23	72	1	1	1	1	2072.09	636.89	1.82	131	91	162.2		1		.75	.277	2.7
4	24.5	63	1	1	1	1	2219.79	690.99	1.74	109.6	91	136.5		1		.75	.282	2.86
5	26	49	1	1	1	1	2420.79	798.39	1.62	79.3	91	100.1		1		.75	.246	3.04
6	27.5	46	1	1	1	1	2621.79	905.79	1.52	69.9	91	88.8		1		.75	.231	3.24
7	29	65	1	1	1	1	2822.79	1013.19	1.44	93.6	91	117.3		1		.75	.216	3.47
8	35	66	1	1	1	1	3626.79	1442.79	1.21	79.8	26	93.9		1		.75	.182	4.12
9	40	73	1	1	1	1	4291.4	1795.39	1.08	78.8	20	88.6		1		.75	.163	4.6
10	45	47	1	1	1	1	4951.4	2143.39	.99	46.5	8	47.3		.98		.735	.149	4.93
11	50	46	1	1	1	1	5613	2493	.92	42.3	0	42.3		.96		.719	.141	5.09
12	55	39	1	1	1	1	6278	2846	.86	33.5	0	33.5		.94		.705	.133	5.3
13	60	38	1	1	1	1	6942.99	3198.99	.81	30.7	0	30.7		.91		.682	.128	5.32
14	60	46	1	1	1	1	6942.99	3198.99	.81	37.2	0	37.2		.91		.682	.128	5.32
15	65	54	1	1	1	1	7607.99	3551.99	.77	41.5	8	42.3		.89		.667	.125	5.33
16	70	51	1	1	1	1	8252.69	3884.69	.73	37.2	0	37.2		.87		.652	.123	5.3
17	75	54	1	1	1	1	8882.69	4202.69	.7	37.8	0	37.8		.86		.645	.12	5.37
18	80	51	1	1	1	1	9512.69	4520.69	.68	34.6	0	34.6		.84		.63	.118	5.33
19	90	51	1	1	1	1	10772.69	5156.69	.64	32.6	0	32.6		.81		.607	.113	5.37
20	100	82	1	1	1	1	12032.69	5792.69	.6	49.2	0	49.2		.79		.592	.108	5.48
21	110	73	1	1	1	1	13292.69	6428.69	.57	41.6	0	41.6		.77		.577	.102	5.65
22	120	24	1	1	1	1	14552.69	7064.69	.54	12.9	0	12.9		.74		.156	.096	1.62
23	130	29	1	1	1	1	15885.49	7773.49	.52	15	7	15.2		.72		.178	.09	1.97
24	140	61	1	1	1	1	17225.5	8489.5	.49	29.8	0	29.8		.71		.475	.084	5.65
25	150	71	1	1	1	1	18545.69	9185.69	.47	33.3	0	33.3		.69		.517	.079	6.54
26	160	56	1	1	1	1	19865.69	9881.69	.46	25.7	0	25.7		.68		.303	.074	4.09
27	170	82	1	1	1	1	21185.7	10577.69	.44	36	0	36		.66		.495	.069	7.17
28	180	96	1	1	1	1	22578.49	11346.49	.43	41.2	0	41.2		.65		.487	.064	7.6
29	190	82	1	1	1	1	23978.49	12122.49	.41	33.6	0	33.6		.64		.48	.06	8
30	201	81	1	1	1	1	25517.7	12975.29	.4	32.4	0	32.4		.63		.472	.056	8.42

Notes:

CSR analysis using SHAKE results.  
 CSR File: D:\4-0 WA PE\1000\100105\100105.rpt  
 CRR using SPT Data and Seed et. al. Method in 1997 NCEEI Workshop.  
 Earthquake File for SHAKE Analysis: E:\W\100105.ACC  
 Earthquake Magnitude for CRR Analysis: 6.4  
 Magnitude Scaling Factor (MSF): 1.5  
 Depth to Water Table for CRR Analysis (ft): 0  
 Depth to Water Table for Cn Calculation (ft): 0  
 Depth to Base Layer for CSR Analysis (ft): 205.9  
 MSF Option: L.M. Idriss (1997)  
 Cn Option: Liao & Whitman (1986)  
 Ksigma Option: L.F. Harder & R. Boulanger (1997)  
 SPT Energy Ratio: USA\Safety\Roop: 1

**Table G.16 Liquefaction Analysis**

White Ditch Site  
Ground Motion WD100201

SPT No.	Depth (ft)	N field	Energy Factor	Rod Factor	Sampler Factor	Borehole Factor	Total Stress (psf)	Effective Stress (psf)	Cu	(N1)/60	Fines Content (%)	N1,60cs	Alpha	Ksigma	Kalpha	CRR	CSR	Safety Factor
1	20	58	1	1	1	1		47.6	2	116	91	144.2		1		.595	.405	1.46
2	21.5	51	1	1	1	1	1932.59	590.99	1.89	96.3	91	120.5		1		.595	.398	1.49
3	23	72	1	1	1	1	2072.09	636.89	1.82	131	91	162.2		1		.595	.384	1.54
4	24.5	63	1	1	1	1	2219.79	690.99	1.74	109.6	91	136.5		1		.595	.368	1.61
5	26	49	1	1	1	1	2420.79	798.39	1.62	79.3	91	100.1		1		.595	.351	1.69
6	27.5	46	1	1	1	1	2621.79	905.79	1.52	69.9	91	88.8		1		.595	.335	1.77
7	29	65	1	1	1	1	2822.79	1013.19	1.44	93.6	91	117.3		1		.595	.319	1.86
8	35	66	1	1	1	1	3626.79	1442.79	1.21	79.8	26	93.9		1		.595	.276	2.15
9	40	73	1	1	1	1	4291.4	1795.39	1.08	78.8	20	88.6		1		.595	.248	2.39
10	45	47	1	1	1	1	4951.4	2143.39	.99	48.5	8	47.3		.98		.583	.229	2.54
11	50	46	1	1	1	1	5613	2493	.92	42.3	0	42.3		.96		.571	.221	2.58
12	55	39	1	1	1	1	6278	2846	.86	33.5	0	33.5		.94		.559	.214	2.61
13	60	38	1	1	1	1	6942.99	3198.99	.81	30.7	0	30.7		.91		.541	.207	2.61
14	60	46	1	1	1	1	6942.99	3198.99	.81	37.2	0	37.2		.91		.541	.207	2.61
15	65	54	1	1	1	1	7607.99	3551.99	.77	41.5	8	42.3		.89		.529	.201	2.63
16	70	51	1	1	1	1	8252.69	3884.69	.73	37.2	0	37.2		.87		.517	.196	2.63
17	75	54	1	1	1	1	8882.69	4202.69	.7	37.8	0	37.8		.86		.511	.19	2.68
18	80	51	1	1	1	1	9512.69	4520.69	.68	34.6	0	34.6		.84		.499	.184	2.71
19	90	51	1	1	1	1	10772.69	5156.69	.64	32.8	0	32.6		.81		.481	.173	2.78
20	100	82	1	1	1	1	12032.69	5792.69	.6	49.2	0	49.2		.79		.47	.161	2.91
21	110	73	1	1	1	1	13292.69	6428.69	.57	41.6	0	41.6		.77		.458	.15	3.05
22	120	24	1	1	1	1	14552.69	7064.69	.54	12.9	0	12.9		.74		.123	.138	.89
23	130	29	1	1	1	1	15885.49	7773.49	.52	15	7	15.2		.72		.141	.126	1.11
24	140	61	1	1	1	1	17225.5	8489.5	.49	29.8	0	29.8		.71		.376	.119	3.15
25	150	71	1	1	1	1	18545.69	9185.69	.47	33.3	0	33.3		.69		.41	.112	3.66
26	160	56	1	1	1	1	19865.69	9881.69	.46	25.7	0	25.7		.68		.24	.106	2.26
27	170	82	1	1	1	1	21185.7	10577.69	.44	36	0	36		.66		.392	.101	3.88
28	180	96	1	1	1	1	22578.49	11346.49	.43	41.2	0	41.2		.65		.386	.096	4.02
29	190	82	1	1	1	1	23978.49	12122.49	.41	33.6	0	33.6		.64		.38	.09	4.22
30	201	81	1	1	1	1	25517.7	12975.29	.4	32.4	0	32.4		.63		.374	.084	4.45

Notes:

CSR analysis using SHAKE results.  
 CSR File: D:\1-0 WH PE\0508\WH100201\WH100201.grf  
 CRR using SPT Data and Seed et. al. Method in 1997 NCEER Workshop.  
 Earthquake File for SHAKE Analysis: D:\WH\WH100201.ACC  
 Earthquake Magnitude for CRR Analysis: 7  
 Magnitude Scaling Factor (MSF): 1.19  
 Depth to Water Table for CRR Analysis (ft): 0  
 Depth to Water Table for Cu Calculation (ft): 0  
 Depth to Base Layer for CSR Analysis (ft): 205.9  
 MSF Option: LM, Iriais (1997)  
 Cu Option: Liao & Whitman (1986)  
 Ksigma Option: L.F. Harder & R. Boulanger (1997)  
 SPT Energy Ratio: USA/SafetyFactor: 1

**Table G.17 Liquefaction Analysis**

White Ditch Site  
Ground Motion WD100202

SPT No.	Depth (ft)	N field	Energy Factor	Rod Factor	Sampler Factor	Borehole Factor	Total Stress (psf)	Effective Stress (psf)	Cn	(N1)60	Fines Content (%)	N1,60cs	Alpha	Ksigma	Kalpha	CRR	CSR	Safety Factor
1	20	58	1	1	1	1		47.6	2	116	91	144.2		1		.595	.353	1.68
2	21.5	51	1	1	1	1	1932.59	590.99	1.89	96.3	91	120.5		1		.595	.343	1.73
3	23	72	1	1	1	1	2072.09	636.89	1.82	131	91	162.2		1		.595	.329	1.8
4	24.5	63	1	1	1	1	2219.79	690.99	1.74	109.6	91	136.5		1		.595	.314	1.89
5	26	49	1	1	1	1	2420.79	796.39	1.62	79.3	91	100.1		1		.595	.299	1.96
6	27.5	46	1	1	1	1	2621.79	905.79	1.52	69.9	91	88.8		1		.595	.284	2.09
7	29	65	1	1	1	1	2822.79	1013.19	1.44	93.6	91	117.3		1		.595	.27	2.2
8	35	66	1	1	1	1	3626.79	1442.79	1.21	79.8	26	93.9		1		.595	.236	2.52
9	40	73	1	1	1	1	4291.4	1795.39	1.08	78.8	20	88.6		1		.595	.218	2.72
10	45	47	1	1	1	1	4951.4	2143.39	.99	46.5	8	47.3	.98			.583	.203	2.87
11	50	46	1	1	1	1	5613	2493	.92	42.3	0	42.3	.96			.571	.192	2.97
12	55	39	1	1	1	1	6278	2846	.86	33.5	0	33.5	.94			.559	.18	3.1
13	60	38	1	1	1	1	6942.99	3198.99	.81	30.7	0	30.7	.91			.541	.172	3.14
14	60	46	1	1	1	1	6942.99	3198.99	.81	37.2	0	37.2	.91			.541	.172	3.14
15	65	54	1	1	1	1	7607.99	3551.99	.77	41.5	8	42.3	.89			.529	.166	3.18
16	70	51	1	1	1	1	8252.69	3884.69	.73	37.2	0	37.2	.87			.517	.16	3.23
17	75	54	1	1	1	1	8882.69	4202.69	.7	37.8	0	37.8	.86			.511	.155	3.29
18	80	51	1	1	1	1	9512.69	4520.69	.68	34.6	0	34.6	.84			.499	.149	3.34
19	90	51	1	1	1	1	10772.69	5156.69	.64	32.6	0	32.6	.81			.481	.138	3.48
20	100	82	1	1	1	1	12032.69	5792.69	.6	49.2	0	49.2	.79			.47	.132	3.56
21	110	73	1	1	1	1	13292.69	6428.69	.57	41.6	0	41.6	.77			.458	.129	3.55
22	120	24	1	1	1	1	14552.69	7064.69	.54	12.9	0	12.9	.74			.423	.126	.97
23	130	29	1	1	1	1	15885.49	7773.49	.52	15	7	15.2	.72			.41	.124	1.13
24	140	61	1	1	1	1	17225.5	8489.5	.49	29.8	0	29.8	.71			.376	.119	3.15
25	150	71	1	1	1	1	18545.69	9185.69	.47	33.3	0	33.3	.69			.41	.114	3.59
26	160	56	1	1	1	1	19865.69	9881.69	.46	25.7	0	25.7	.68			.24	.109	2.2
27	170	82	1	1	1	1	21185.7	10577.69	.44	36	0	36	.66			.392	.103	3.8
28	180	96	1	1	1	1	22578.49	11346.49	.43	41.2	0	41.2	.65			.366	.098	3.93
29	190	82	1	1	1	1	23978.49	12122.49	.41	33.6	0	33.6	.64			.38	.093	4.08
30	201	81	1	1	1	1	25517.7	12975.29	.4	32.4	0	32.4	.63			.374	.088	4.25

**Notes:**

CSR analysis using SHAKE results.  
 CSR File: D:\10 WH PE10\SHAKE\100202\WH100202.plt  
 CRR using SPT Data and Seed et. al. Method in 1987 NCEER Workshop.  
 Earthquake File for SHAKE Analysis: D:\WH\WH100202.ACC  
 Earthquake Magnitude for CRR Analysis: 7  
 Magnitude Scaling Factor (MSF): 1.19  
 Depth to Water Table for CRR Analysis (ft): 0  
 Depth to Water Table for Cn Calculation (ft): 0  
 Depth to Base Layer for CSR Analysis (ft): 205.9  
 MSF Option: L.M. Idriss (1997)  
 Cn Option: Liao & Whitman (1986)  
 Ksigma Option: L.F. Harder & R. Boulanger (1997)  
 SPT Energy Ratio: USA SafetyFactor: 1

Table G.18 Liquefaction Analysis

Wahite Ditch Site  
Ground Motion WD100205

SPT No.	Depth (ft)	N field	Energy Factor	Rod Factor	Sampler Factor	Borehole Factor	Total Stress (psf)	Effective Stress (psf)	Cn	(N1)60	Fines Content (%)	N1,60cs	Alpha	Ksigma	Kalpha	CRR	CSR	Safety Factor
1	20	58	1	1	1	1		47.6	2	118	91	144.2		1		.595	.387	1.53
2	21.5	51	1	1	1	1	1932.59	590.99	1.89	96.3	91	120.5		1		.595	.38	1.56
3	23	72	1	1	1	1	2072.09	636.89	1.82	131	91	162.2		1		.595	.366	1.62
4	24.5	63	1	1	1	1	2219.79	690.99	1.74	109.6	91	136.5		1		.595	.35	1.7
5	26	49	1	1	1	1	2420.79	798.39	1.62	79.3	91	100.1		1		.595	.335	1.77
6	27.5	46	1	1	1	1	2621.79	905.79	1.52	69.9	91	88.8		1		.595	.319	1.86
7	29	65	1	1	1	1	2822.79	1013.19	1.44	93.8	91	117.3		1		.595	.303	1.96
8	35	66	1	1	1	1	3626.79	1442.79	1.21	79.8	26	93.9		1		.595	.264	2.25
9	40	73	1	1	1	1	4291.4	1795.39	1.08	78.8	20	88.6		1		.595	.24	2.47
10	45	47	1	1	1	1	4951.4	2143.39	.99	46.5	8	47.3	.98			.583	.223	2.61
11	50	46	1	1	1	1	5613	2493	.92	42.3	0	42.3	.96			.571	.215	2.65
12	55	39	1	1	1	1	6278	2846	.86	33.5	0	33.5	.94			.559	.207	2.7
13	60	38	1	1	1	1	6942.99	3198.99	.81	30.7	0	30.7	.91			.541	.201	2.69
14	60	46	1	1	1	1	6942.99	3198.99	.81	37.2	0	37.2	.91			.541	.201	2.69
15	65	54	1	1	1	1	7607.99	3551.99	.77	41.5	8	42.3	.89			.529	.196	2.69
16	70	51	1	1	1	1	8252.69	3884.69	.73	37.2	0	37.2	.87			.517	.191	2.7
17	75	54	1	1	1	1	8882.69	4202.69	.7	37.8	0	37.8	.86			.511	.186	2.74
18	80	51	1	1	1	1	9512.69	4520.69	.68	34.6	0	34.6	.84			.499	.181	2.75
19	90	51	1	1	1	1	10772.69	5156.69	.64	32.6	0	32.6	.81			.481	.171	2.81
20	100	82	1	1	1	1	12032.69	5792.69	.6	49.2	0	49.2	.79			.47	.161	2.91
21	110	73	1	1	1	1	13292.69	6428.69	.57	41.6	0	41.6	.77			.458	.152	3.01
22	120	24	1	1	1	1	14552.69	7064.69	.54	12.9	0	12.9	.74			.423	.144	.85
23	130	29	1	1	1	1	15885.49	7773.49	.52	15	7	15.2	.72			.41	.135	1.04
24	140	61	1	1	1	1	17225.5	8489.5	.49	29.8	0	29.8	.71			.376	.126	2.98
25	150	71	1	1	1	1	18545.69	9185.69	.47	33.3	0	33.3	.69			.41	.116	3.53
26	160	56	1	1	1	1	19865.69	9881.69	.46	25.7	0	25.7	.68			.24	.108	2.22
27	170	82	1	1	1	1	21185.7	10577.69	.44	36	0	36	.66			.392	.102	3.84
28	180	96	1	1	1	1	22578.49	11346.49	.43	41.2	0	41.2	.65			.386	.096	4.02
29	190	82	1	1	1	1	23978.49	12122.49	.41	33.6	0	33.6	.64			.38	.09	4.22
30	201	81	1	1	1	1	25517.7	12975.29	.4	32.4	0	32.4	.63			.374	.084	4.45

Notes:

CSR analysis using SHAKE results.  
 CSR File: D:\10\NH\PE\100205\100205\100205.gcf  
 CRR using SPT Data and Seed et. al. Method in 1987 NCEER Workshop.  
 Earthquake File for SHAKE Analysis: D:\NH\100205.ACC  
 Earthquake Magnitude for CRR Analysis: 7  
 Magnitude Scaling Factor (MSF): 1.19  
 Depth to Water Table for CRR Analysis (ft): 0  
 Depth to Water Table for Cn Calculation (ft): 0  
 Depth to Base Layer for CSR Analysis (ft): 205.0  
 NSF Option: LM. Ichna (1997)  
 Cn Option: Liao & Whitman (1986)  
 Ksigma Option: L.F. Harder & R. Boulanger (1987)  
 SPT Energy Ratio: USA Safety Rope: 1

**Table G.19 Liquefaction Analysis**

White Ditch Site  
Ground Motion W0020101

SPT No.	Depth (ft)	N field	Energy Factor	Rod Factor	Sampler Factor	Borehole Factor	Total Stress (psf)	Effective Stress (psf)	Cn	(N1)60	Fines Content (%)	N1,60cs	Alpha	Ksigma	Kalpha	CRR	CSR	Safety Factor
1	20	58	1	1	1	1		47.6	2	116	91	144.2		1		.45	.847	.53
2	21.5	51	1	1	1	1	1932.59	590.99	1.89	96.3	91	120.5		1		.45	.838	.53
3	23	72	1	1	1	1	2072.09	636.89	1.82	131	91	162.2		1		.45	.814	.55
4	24.5	63	1	1	1	1	2219.79	690.99	1.74	109.6	91	136.5		1		.45	.786	.57
5	26	49	1	1	1	1	2420.79	798.39	1.62	79.3	91	100.1		1		.45	.759	.59
6	27.5	46	1	1	1	1	2621.79	906.79	1.52	69.9	91	88.8		1		.45	.732	.61
7	29	65	1	1	1	1	2822.79	1013.19	1.44	93.6	91	117.3		1		.45	.704	.63
8	35	66	1	1	1	1	3626.79	1442.79	1.21	79.8	26	93.9		1		.45	.631	.71
9	40	73	1	1	1	1	4291.4	1735.39	1.08	78.8	20	88.6		1		.45	.584	.77
10	45	47	1	1	1	1	4951.4	2143.39	.99	46.5	8	47.3		.98		.441	.55	.8
11	50	46	1	1	1	1	5613	2493	.92	42.3	0	42.3		.96		.431	.535	.8
12	55	39	1	1	1	1	6278	2846	.86	33.5	0	33.5		.94		.422	.52	.81
13	60	38	1	1	1	1	6942.99	3198.99	.81	30.7	0	30.7		.91		.409	.508	.8
14	60	46	1	1	1	1	6942.99	3198.99	.81	37.2	0	37.2		.91		.409	.508	.8
15	65	54	1	1	1	1	7607.99	3551.99	.77	41.5	8	42.3		.89		.4	.501	.79
16	70	51	1	1	1	1	8252.69	3884.69	.73	37.2	0	37.2		.87		.391	.485	.78
17	75	54	1	1	1	1	8882.69	4202.69	.7	37.8	0	37.8		.86		.387	.488	.79
18	80	51	1	1	1	1	9512.69	4520.69	.68	34.6	0	34.6		.84		.378	.481	.78
19	90	51	1	1	1	1	10772.69	5156.69	.64	32.6	0	32.6		.81		.364	.467	.77
20	100	82	1	1	1	1	12032.69	5792.69	.6	49.2	0	49.2		.79		.355	.457	.77
21	110	73	1	1	1	1	13292.69	6428.69	.57	41.6	0	41.6		.77		.346	.45	.76
22	120	24	1	1	1	1	14552.69	7064.69	.54	12.9	0	12.9		.74		.093	.443	.2
23	130	29	1	1	1	1	15885.49	7773.49	.52	15	7	15.2		.72		.107	.436	.24
24	140	61	1	1	1	1	17225.5	8489.5	.49	29.8	0	29.8		.71		.285	.423	.67
25	150	71	1	1	1	1	18565.5	9205.5	.47	33.3	0	33.3		.69		.31	.411	.75
26	160	56	1	1	1	1	19904.1	9920.09	.46	25.7	0	25.7		.68		.181	.395	.45
27	170	82	1	1	1	1	21224.1	10616.1	.44	36	0	36		.66		.297	.379	.78
28	180	96	1	1	1	1	22544.1	11312.1	.43	41.2	0	41.2		.65		.292	.367	.79
29	190	82	1	1	1	1	23864.1	12006.1	.41	33.6	0	33.6		.64		.288	.359	.8
30	201	81	1	1	1	1	25403.3	12860.9	.4	32.4	0	32.4		.63		.283	.35	.8

**Notes:**

CSR analysis using SHAKE results.  
 CSR File: D:\4-0\WH PE 2309\W020101\W020101.gri  
 CRR using SPT Data and Seed et. al. Method in 1987 NCEER Workshop.  
 Earthquake File for SHAKE Analysis: C:\WWW\W020101.ACC  
 Earthquake Magnitude for CRR Analysis: 7.8  
 Magnitude Scaling Factor (MSF): .9  
 Depth to Water Table for CRR Analysis (ft): 0  
 Depth to Water Table for Cn Calculation (ft): 0  
 Depth to Base Layer for CSR Analysis (ft): 225.1  
 MSF Option: L.M. Idriss (1987)  
 Cn Option: Liao & Whitman (1988)  
 Ksigma Option: L.F. Harder & R. Boulanger (1987)  
 SPT Energy Ratio: USA/SafetyPopo: 1

**Table G.20 Liquefaction Analysis**

White Ditch Site  
Ground Motion WD100202

SPT No.	Depth (ft)	N field	Energy Factor	Rod Factor	Sampler Factor	Borehole Factor	Total Stress (psf)	Effective Stress (psf)	Cn	(N1)60	Fines Content (%)	N1,60cs	Alpha	Ksigma	Kalpha	CRR	CSR	Safety Factor
1	20	58	1	1	1	1		47.6	2	116	91	144.2		1		.595	.353	1.68
2	21.5	51	1	1	1	1	1932.59	590.99	1.89	96.3	91	120.5		1		.595	.343	1.73
3	23	72	1	1	1	1	2072.09	636.89	1.82	131	91	162.2		1		.595	.329	1.8
4	24.5	63	1	1	1	1	2219.79	690.99	1.74	109.6	91	136.5		1		.595	.314	1.89
5	26	49	1	1	1	1	2420.79	798.39	1.62	79.3	91	100.1		1		.595	.299	1.98
6	27.5	46	1	1	1	1	2621.79	905.79	1.52	69.9	91	88.8		1		.595	.284	2.09
7	29	65	1	1	1	1	2822.79	1013.19	1.44	93.6	91	117.3		1		.595	.27	2.2
8	35	66	1	1	1	1	3626.79	1442.79	1.21	79.8	26	93.9		1		.595	.236	2.52
9	40	73	1	1	1	1	4291.4	1795.39	1.08	78.8	20	88.6		1		.595	.218	2.72
10	45	47	1	1	1	1	4951.4	2143.39	.99	46.5	8	47.3	.98			.583	.203	2.87
11	50	46	1	1	1	1	5613	2493	.92	42.3	0	42.3	.96			.571	.192	2.97
12	55	39	1	1	1	1	6278	2846	.86	33.5	0	33.5	.94			.559	.18	3.1
13	60	38	1	1	1	1	6942.99	3198.99	.81	30.7	0	30.7	.91			.541	.172	3.14
14	60	46	1	1	1	1	6942.99	3198.99	.81	37.2	0	37.2	.91			.541	.172	3.14
15	65	54	1	1	1	1	7607.99	3551.99	.77	41.5	8	42.3	.89			.529	.166	3.18
16	70	51	1	1	1	1	8252.69	3884.69	.73	37.2	0	37.2	.87			.517	.16	3.23
17	75	54	1	1	1	1	8882.69	4202.69	.7	37.8	0	37.8	.86			.511	.155	3.29
18	80	51	1	1	1	1	9512.69	4520.69	.68	34.6	0	34.6	.84			.499	.149	3.34
19	90	51	1	1	1	1	10772.69	5156.69	.64	32.6	0	32.6	.81			.481	.138	3.48
20	100	82	1	1	1	1	12032.69	5792.69	.6	49.2	0	49.2	.79			.47	.132	3.56
21	110	73	1	1	1	1	13292.69	6428.69	.57	41.6	0	41.6	.77			.458	.129	3.55
22	120	24	1	1	1	1	14552.69	7064.69	.54	12.9	0	12.9	.74			.123	.126	.97
23	130	29	1	1	1	1	15885.49	7773.49	.52	15	7	15.2	.72			.141	.124	1.13
24	140	61	1	1	1	1	17225.5	8489.5	.49	29.8	0	29.8	.71			.376	.119	3.15
25	150	71	1	1	1	1	18545.69	9185.69	.47	33.3	0	33.3	.69			.41	.114	3.59
26	160	56	1	1	1	1	19865.69	9881.69	.46	25.7	0	25.7	.68			.24	.109	2.2
27	170	82	1	1	1	1	21185.7	10577.69	.44	36	0	36	.66			.392	.103	3.8
28	180	96	1	1	1	1	22578.49	11346.49	.43	41.2	0	41.2	.65			.386	.098	3.93
29	190	82	1	1	1	1	23978.49	12122.49	.41	33.6	0	33.6	.64			.38	.093	4.08
30	201	81	1	1	1	1	25517.7	12975.29	.4	32.4	0	32.4	.63			.374	.088	4.25

**Notes:**

CSR analysis using SHAKE results.  
 CSR File: D:\4-0 WH PE\NS00\100202\WH100202.rpt  
 CRR using SPT Data and Seed et. al. Method in 1987 NCEER Workshop.  
 Earthquake File for SHAKE Analysis: D:\WH\WH1\100202.ACC  
 Earthquake Magnitude for CRR Analysis: 7  
 Magnitude Scaling Factor (MSF): 1.19  
 Depth to Water Table for CRR Analysis (ft): 0  
 Depth to Water Table for Cn Calculation (ft): 0  
 Depth to Base Layer for CSR Analysis (ft): 205.9  
 MSF Option: Lk. Idrias (1987)  
 Cn Option: Liao & Whitman (1989)  
 Ksigma Option: L.F. Harder & R. Boulanger (1987)  
 SPT Energy Ratio: USA/SafetyFactor: 1

**Table G.21 Liquefaction Analysis**

White Ditch Site  
Ground Motion WDC20103

SPT No.	Depth (ft)	N field	Energy Factor	Rod Factor	Sampler Factor	Borehole Factor	Total Stress (psf)	Effective Stress (psf)	Cn	(N1)60	Fines Content (%)	N1,60cs	Alpha	Ksigma	Kalpha	CRR	CSR	Safety Factor
1	20	58	1	1	1	1		47.6	2	116	91	144.2		1		.45	1.021	.44
2	21.5	51	1	1	1	1	1932.59	590.99	1.89	96.3	91	120.5		1		.45	1.01	.44
3	23	72	1	1	1	1	2072.09	636.69	1.82	131	91	162.2		1		.45	.978	.46
4	24.5	63	1	1	1	1	2219.79	690.99	1.74	109.6	91	136.5		1		.45	.942	.47
5	26	49	1	1	1	1	2420.79	798.39	1.62	79.3	91	100.1		1		.45	.906	.49
6	27.5	46	1	1	1	1	2621.79	905.79	1.52	69.9	91	88.8		1		.45	.87	.51
7	29	65	1	1	1	1	2822.79	1013.19	1.44	93.6	91	117.3		1		.45	.833	.54
8	35	66	1	1	1	1	3626.79	1442.79	1.21	79.8	26	93.9		1		.45	.749	.6
9	40	73	1	1	1	1	4291.4	1795.39	1.06	78.8	20	88.6		1		.45	.701	.64
10	45	47	1	1	1	1	4951.4	2143.39	.99	46.5	8	47.3	.98			.441	.662	.66
11	50	46	1	1	1	1	5613	2493	.92	42.3	0	42.3	.96			.431	.635	.67
12	55	39	1	1	1	1	6278	2846	.86	33.5	0	33.5	.94			.422	.609	.69
13	60	38	1	1	1	1	6942.99	3198.99	.81	30.7	0	30.7	.91			.409	.586	.69
14	60	46	1	1	1	1	6942.99	3198.99	.81	37.2	0	37.2	.91			.408	.586	.69
15	65	54	1	1	1	1	7607.99	3551.99	.77	41.5	8	42.3	.89			.4	.568	.7
16	70	51	1	1	1	1	8252.69	3884.69	.73	37.2	0	37.2	.87			.391	.55	.71
17	75	54	1	1	1	1	8882.69	4202.69	.7	37.8	0	37.8	.86			.387	.532	.72
18	80	51	1	1	1	1	9512.69	4520.69	.68	34.8	0	34.8	.84			.378	.514	.73
19	90	51	1	1	1	1	10772.69	5156.69	.64	32.6	0	32.6	.81			.364	.478	.76
20	100	82	1	1	1	1	12032.69	5792.69	.6	49.2	0	49.2	.79			.355	.454	.78
21	110	73	1	1	1	1	13292.69	6428.69	.57	41.6	0	41.6	.77			.346	.437	.79
22	120	24	1	1	1	1	14552.69	7064.69	.54	12.9	0	12.9	.74			.093	.42	.22
23	130	29	1	1	1	1	15885.49	7773.49	.52	15	7	15.2	.72			.107	.403	.26
24	140	61	1	1	1	1	17225.5	8489.5	.49	29.8	0	29.8	.71			.285	.395	.72
25	150	71	1	1	1	1	18565.5	9205.5	.47	33.3	0	33.3	.69			.31	.388	.79
26	160	56	1	1	1	1	19904.1	9920.09	.46	25.7	0	25.7	.68			.181	.387	.46
27	170	82	1	1	1	1	21224.1	10616.1	.44	36	0	36	.66			.297	.387	.76
28	180	96	1	1	1	1	22544.1	11312.1	.43	41.2	0	41.2	.65			.292	.384	.76
29	190	82	1	1	1	1	23864.1	12008.1	.41	33.6	0	33.6	.64			.286	.379	.75
30	201	81	1	1	1	1	25403.3	12860.9	.4	32.4	0	32.4	.63			.283	.374	.75

**Notes:**

CSR analysis using SHAKE results.  
 CSR File: D:\V-O\WH PE 25\WH020103\WH020103.gnl  
 CRR using SPT Data and Seed et. al. Method in 1997 NCEEER Workshop.  
 Earthquake File for SHAKE Analysis: D:\WH020103\JACC  
 Earthquake Magnitude for CRR Analysis: 7.8  
 Magnitude Scaling Factor (MSF): .9  
 Depth to Water Table for CRR Analysis (ft): 0  
 Depth to Water Table for Cn Calculation (ft): 0  
 Depth to Base Layer for CSR Analysis (ft): 225.1  
 MSF Option: L.M. Idriss (1987)  
 Cn Option: Liao & Whitman (1989)  
 Ksigma Option: L.F. Harder & R. Boulanger (1987)  
 SPT Energy Ratio: USA/SafetyFactor: 1

**Table G.22 Liquefaction Analysis**

Wahite Ditch Site  
Ground Motion WD020202

SPT No.	Depth (ft)	N field	Energy Factor	Rod Factor	Sampler Factor	Borehole Factor	Total Stress (psf)	Effective Stress (psf)	Cn	(N1)60	Fines Content (%)	N1,60cs	Alpha	Ksigma	Kalpha	CRR	CSR	Safety Factor
1	20	58	1	1	1	1		47.6	2	116	91	144.2		1		.42	955	.43
2	21.5	51	1	1	1	1	1932.59	590.99	1.89	96.3	91	120.5		1		.42	945	.44
3	23	72	1	1	1	1	2072.09	636.89	1.82	131	91	162.2		1		.42	918	.45
4	24.5	63	1	1	1	1	2219.79	690.99	1.74	109.6	91	136.5		1		.42	887	.47
5	26	49	1	1	1	1	2420.79	798.39	1.62	79.3	91	100.1		1		.42	857	.49
6	27.5	46	1	1	1	1	2621.79	905.79	1.52	69.9	91	88.8		1		.42	826	.5
7	29	65	1	1	1	1	2822.79	1013.19	1.44	93.6	91	117.3		1		.42	796	.52
8	35	66	1	1	1	1	3626.79	1442.79	1.21	79.8	26	93.9		1		.42	704	.59
9	40	73	1	1	1	1	4291.4	1795.39	1.08	78.8	20	88.6		1		.42	639	.65
10	45	47	1	1	1	1	4951.4	2143.39	.99	46.5	8	47.3		.98		.411	.59	.69
11	50	46	1	1	1	1	5613	2493	.92	42.3	0	42.3		.96		.403	.564	.71
12	55	39	1	1	1	1	6278	2846	.86	33.5	0	33.5		.94		.394	.537	.73
13	60	38	1	1	1	1	6942.99	3198.99	.81	30.7	0	30.7		.91		.382	.519	.73
14	60	46	1	1	1	1	6942.99	3198.99	.81	37.2	0	37.2		.91		.382	.519	.73
15	65	54	1	1	1	1	7607.99	3551.99	.77	41.5	8	42.3		.89		.373	.511	.72
16	70	51	1	1	1	1	8252.69	3884.69	.73	37.2	0	37.2		.87		.365	.502	.72
17	75	54	1	1	1	1	8882.69	4202.69	.7	37.8	0	37.8		.86		.361	.494	.73
18	80	51	1	1	1	1	9512.69	4520.69	.68	34.6	0	34.6		.84		.352	.485	.72
19	90	51	1	1	1	1	10772.69	5156.69	.64	32.6	0	32.6		.81		.34	.468	.72
20	100	82	1	1	1	1	12032.69	5792.69	.6	49.2	0	49.2		.79		.331	.452	.73
21	110	73	1	1	1	1	13292.69	6428.69	.57	41.6	0	41.6		.77		.323	.437	.73
22	120	24	1	1	1	1	14552.69	7064.69	.54	12.9	0	12.9		.74		.087	.422	.2
23	130	29	1	1	1	1	15885.49	7773.49	.52	15	7	15.2		.72		.1	.407	.24
24	140	61	1	1	1	1	17225.5	8489.5	.49	29.8	0	29.8		.71		.266	.38	.7
25	150	71	1	1	1	1	18565.5	9205.5	.47	33.3	0	33.3		.69		.289	.353	.81
26	160	56	1	1	1	1	19904.1	9920.09	.46	25.7	0	25.7		.68		.169	.342	.49
27	170	82	1	1	1	1	21224.1	10616.1	.44	36	0	36		.66		.277	.332	.83
28	180	96	1	1	1	1	22544.1	11312.1	.43	41.2	0	41.2		.65		.272	.322	.84
29	190	82	1	1	1	1	23864.1	12008.1	.41	33.6	0	33.6		.64		.268	.313	.85
30	201	81	1	1	1	1	25403.3	12860.9	.4	32.4	0	32.4		.63		.264	.304	.86

Notes:  
 CSR analysis using SHAKE results.  
 CSR File: D:\KO\WH PE 2\WHD020202\WHD020202.gtl  
 CRR using SPT Data and Seed et. al. Method in 1997 NCEER Workshop.  
 Earthquake File for SHAKE Analysis: D:\WHD020202.ACC  
 Earthquake Magnitude for CRR Analysis: 8  
 Magnitude Scaling Factor (MSF): .04  
 Depth to Water Table for CRR Analysis (ft): 0  
 Depth to Water Table for Cn Calculation (ft): 0  
 Depth to Base Layer for CSR Analysis (ft): 225.1  
 MSF Option: L.M. Idriss (1997)  
 Cn Option: Luo & Whisman (1986)  
 Ksigma Option: L.F. Harder & R. Boulanger (1997)  
 SPT Energy Ratio: USA/Salemi/Poppe: 1

**Table G.23 Liquefaction Analysis**

White Ditch Site  
Ground Motion WD020203

SPT No.	Depth (ft)	N field	Energy Factor	Rod Factor	Sampler Factor	Borehole Factor	Total Stress (psf)	Effective Stress (psf)	Cn	(N1)60	Fines Content (%)	N1,60cs	Alpha	Ksigma	Kalpha	CRR	CSR	Safety Factor
1	20	58	1	1	1	1		47.6	2	116	91	144.2		1		.42	1.031	.4
2	21.5	51	1	1	1	1	1932.59	590.99	1.89	96.3	91	120.5		1		.42	1.02	.41
3	23	72	1	1	1	1	2072.09	636.89	1.82	131	91	162.2		1		.42	.986	.42
4	24.5	63	1	1	1	1	2219.79	690.99	1.74	109.6	91	136.5		1		.42	.949	.44
5	26	49	1	1	1	1	2420.79	796.99	1.62	79.3	91	100.1		1		.42	.911	.46
6	27.5	46	1	1	1	1	2621.79	905.79	1.52	69.9	91	88.8		1		.42	.873	.48
7	29	65	1	1	1	1	2822.79	1013.19	1.44	93.6	91	117.3		1		.42	.836	.5
8	35	66	1	1	1	1	3626.79	1442.79	1.21	79.8	26	93.9		1		.42	.746	.56
9	40	73	1	1	1	1	4291.4	1795.39	1.08	78.8	20	88.6		1		.42	.694	.6
10	45	47	1	1	1	1	4951.4	2143.39	.99	46.5	8	47.3	.98			.411	.652	.63
11	50	46	1	1	1	1	5613	2493	.92	42.3	0	42.3	.96			.403	.624	.64
12	55	39	1	1	1	1	6278	2846	.86	33.5	0	33.5	.94			.394	.597	.65
13	60	38	1	1	1	1	6942.99	3198.99	.81	30.7	0	30.7	.91			.382	.575	.66
14	60	46	1	1	1	1	6942.99	3198.99	.81	37.2	0	37.2	.91			.382	.575	.66
15	66	54	1	1	1	1	7607.99	3551.99	.77	41.5	8	42.3	.89			.373	.562	.66
16	70	51	1	1	1	1	8252.69	3884.69	.73	37.2	0	37.2	.87			.365	.549	.66
17	75	54	1	1	1	1	8882.69	4202.69	.7	37.8	0	37.8	.86			.361	.536	.67
18	80	51	1	1	1	1	9512.69	4520.69	.68	34.6	0	34.6	.84			.352	.522	.67
19	90	51	1	1	1	1	10772.69	5156.69	.64	32.6	0	32.6	.81			.34	.495	.68
20	100	82	1	1	1	1	12032.69	5792.69	.6	49.2	0	49.2	.79			.331	.47	.7
21	110	73	1	1	1	1	13292.69	6428.69	.57	41.6	0	41.6	.77			.323	.447	.72
22	120	24	1	1	1	1	14552.69	7064.69	.54	12.9	0	12.9	.74			.087	.424	.2
23	130	29	1	1	1	1	15885.49	7773.49	.52	15	7	15.2	.72			.1	.4	.25
24	140	61	1	1	1	1	17225.5	8489.5	.49	29.8	0	29.8	.71			.266	.372	.71
25	150	71	1	1	1	1	18565.5	9205.5	.47	33.3	0	33.3	.69			.289	.345	.83
26	160	56	1	1	1	1	19904.1	9920.99	.46	25.7	0	25.7	.68			.169	.348	.48
27	170	82	1	1	1	1	21224.1	10616.1	.44	36	0	36	.66			.277	.351	.78
28	180	98	1	1	1	1	22544.1	11312.1	.43	41.2	0	41.2	.65			.272	.35	.77
29	190	82	1	1	1	1	23864.1	12006.1	.41	33.6	0	33.6	.64			.268	.345	.77
30	201	81	1	1	1	1	25403.3	12860.9	.4	32.4	0	32.4	.63			.264	.339	.77

**Notes:**

CSR analysis using SHAKE results.  
 CSR File: D:\O WH PE 2\shd\020203\WH020203.sit  
 CRR using SPT Data and Seed et. al. Method in 1987 NCEER Workshop.  
 Earthquake File for SHAKE Analysis: D:\O WH PE 2\shd\020203\ACC  
 Earthquake Magnitude for CRR Analysis: 8  
 Magnitude Scaling Factor (MSF): .34  
 Depth to Water Table for CRR Analysis (ft): 0  
 Depth to Water Table for Cn Calculation (ft): 0  
 Depth to Base Layer for CSR Analysis (ft): 225.1  
 MSF Option: LM, Idriss (1987)  
 Cn Option: Liao & Whitman (1988)  
 Ksigma Option: L.F. Harder & R. Boulanger (1987)  
 SPT Energy Ratio: USA Safety Factor 1  
 \*Effective Stress column computed using Depth to Water Table for CRR Analysis

**Table G.24 Liquefaction Analysis**

White Ditch Site  
Ground Motion WD020205

SPT No.	Depth (ft)	N field	Energy Factor	Rod Factor	Sampler Factor	Borehole Factor	Total Stress (psf)	Effective Stress (psf)	Cn	(N1)60	Fines Content (%)	N1,60cs	Alpha	Ksigma	Kalpha	CRR	CSR	Safety Factor
1	20	58	1	1	1	1		47.6	2	116	91	144.2		1		.42	.88	.47
2	21.5	51	1	1	1	1	1932.59	590.99	1.89	96.3	91	120.5		1		.42	.869	.48
3	23	72	1	1	1	1	2072.09	636.89	1.82	131	91	162.2		1		.42	.84	.5
4	24.5	63	1	1	1	1	2219.79	690.99	1.74	109.6	91	136.5		1		.42	.808	.51
5	26	49	1	1	1	1	2420.79	798.39	1.62	79.3	91	100.1		1		.42	.776	.54
6	27.5	46	1	1	1	1	2621.79	905.79	1.52	69.9	91	88.8		1		.42	.744	.56
7	29	65	1	1	1	1	2822.79	1013.19	1.44	93.6	91	117.3		1		.42	.712	.58
8	35	66	1	1	1	1	3626.79	1442.79	1.21	79.8	26	93.9		1		.42	.632	.66
9	40	73	1	1	1	1	4291.4	1735.39	1.08	78.8	20	88.6		1		.42	.584	.71
10	45	47	1	1	1	1	4951.4	2143.39	.99	46.5	8	47.3		.96		.411	.547	.75
11	50	46	1	1	1	1	5613	2493	.92	42.3	0	42.3		.96		.403	.525	.76
12	55	39	1	1	1	1	6278	2846	.86	33.5	0	33.5		.94		.394	.503	.78
13	60	38	1	1	1	1	6942.99	3198.99	.81	30.7	0	30.7		.91		.382	.485	.78
14	60	46	1	1	1	1	6942.99	3198.99	.81	37.2	0	37.2		.91		.382	.485	.78
15	65	54	1	1	1	1	7607.99	3551.99	.77	41.5	8	42.3		.89		.373	.472	.79
16	70	51	1	1	1	1	8252.69	3884.69	.73	37.2	0	37.2		.87		.365	.459	.79
17	75	54	1	1	1	1	8882.69	4202.69	.7	37.8	0	37.8		.86		.361	.446	.8
18	80	51	1	1	1	1	9512.69	4520.69	.68	34.6	0	34.6		.84		.352	.433	.81
19	90	51	1	1	1	1	10772.69	5156.69	.64	32.6	0	32.6		.81		.34	.407	.83
20	100	82	1	1	1	1	12032.69	5792.69	.6	49.2	0	49.2		.79		.331	.389	.85
21	110	73	1	1	1	1	13292.69	6428.69	.57	41.6	0	41.6		.77		.323	.377	.85
22	120	24	1	1	1	1	14552.69	7064.69	.54	12.9	0	12.9		.74		.087	.365	.23
23	130	29	1	1	1	1	15885.49	7773.49	.52	15	7	15.2		.72		.1	.353	.28
24	140	61	1	1	1	1	17225.5	8489.5	.49	29.8	0	29.8		.71		.266	.344	.77
25	150	71	1	1	1	1	18565.5	9205.5	.47	33.3	0	33.3		.69		.289	.335	.86
26	160	56	1	1	1	1	19904.1	9920.09	.46	25.7	0	25.7		.68		.169	.335	.5
27	170	82	1	1	1	1	21224.1	10616.1	.44	36	0	36		.66		.277	.334	.82
28	180	96	1	1	1	1	22544.1	11312.1	.43	41.2	0	41.2		.65		.272	.333	.81
29	190	82	1	1	1	1	23864.1	12008.1	.41	33.6	0	33.6		.64		.268	.333	.8
30	201	81	1	1	1	1	25403.3	12860.9	.4	32.4	0	32.4		.63		.264	.332	.79

Notes:

CSR analysis using SHAKE results.  
 CSR File: D:\O WH\PE 250\NG220205\WH020205.gri  
 CRR using SPT Data and Seed et. al. Method in 1997 NCEER Workshop.  
 Earthquake File for SHAKE Analysis: D:\O WH\NG220205.ACC  
 Earthquake Magnitude for CRR Analysis: 8  
 Magnitude Scaling Factor (MSF): .14  
 Depth to Water Table for CRR Analysis (ft): 0  
 Depth to Water Table for Cn Calculation (ft): 0  
 Depth to Base Layer for CSR Analysis (ft): 225.1  
 MSF Option: L.M. Iwan (1997)  
 Cn Option: Liao & Whitman (1986)  
 Ksigma Option: L.F. Harder & R. Boulanger (1997)  
 SPT Energy Ratio: USA/SafetyRopc: 1

## H. STRUCTURAL ANALYSIS RESULTS

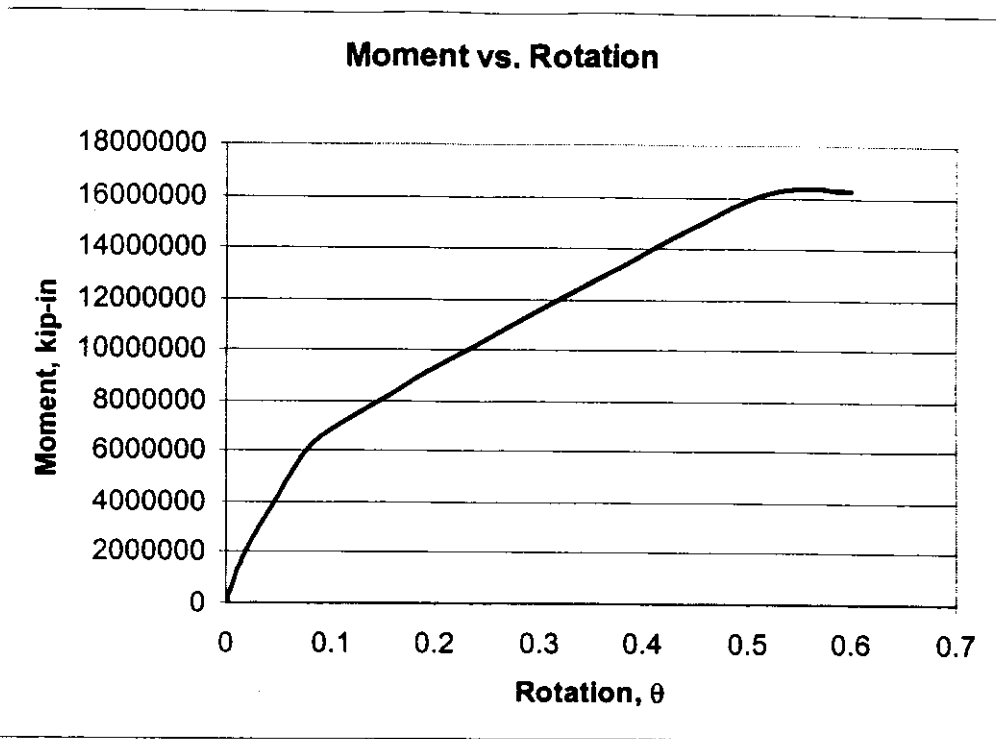


**Figure H.1** New St. Francis River Bridge Four Pile Footing

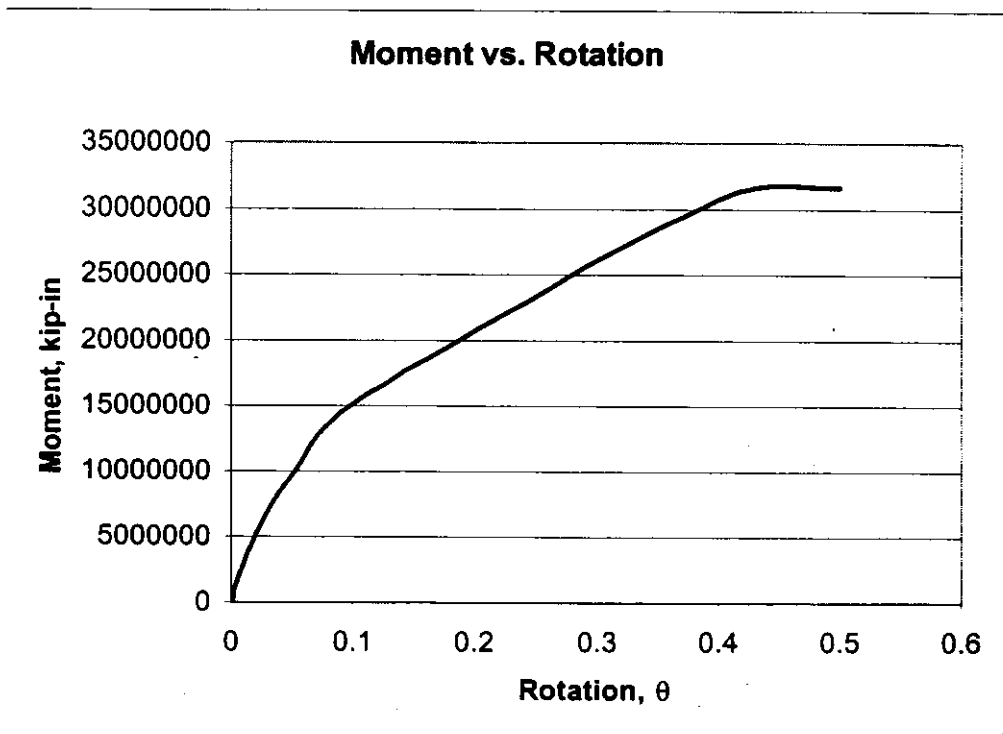


**Figure H.2** New St. Francis River Bridge Five Pile Footing

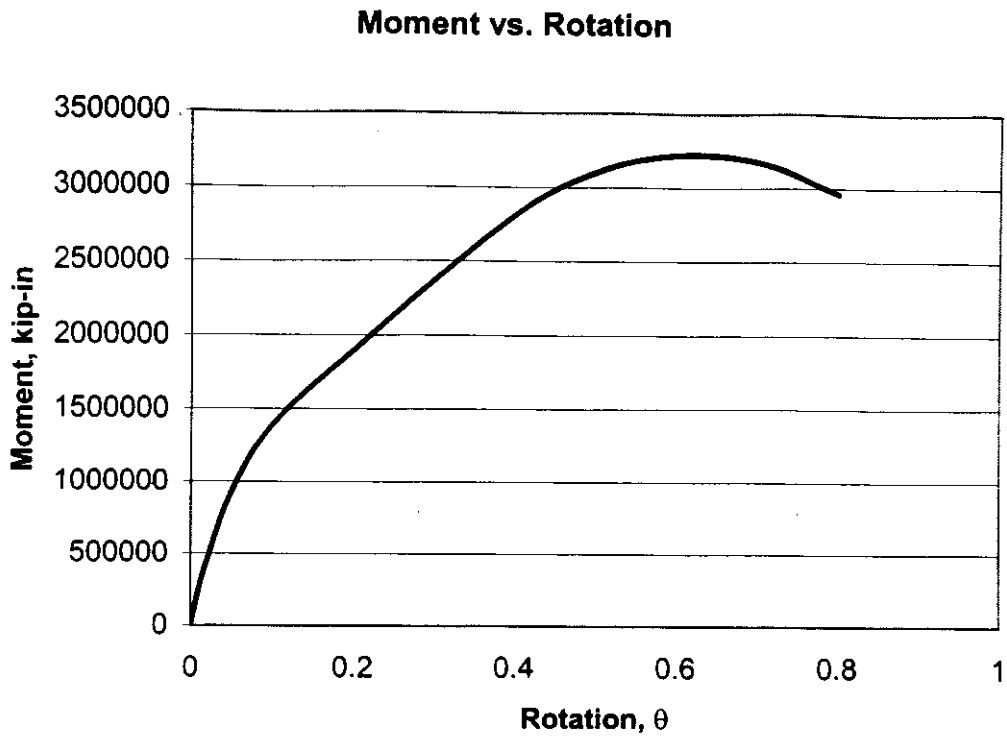


**Figure H.3** Old St. Francis River Bridge Three Pile Footing

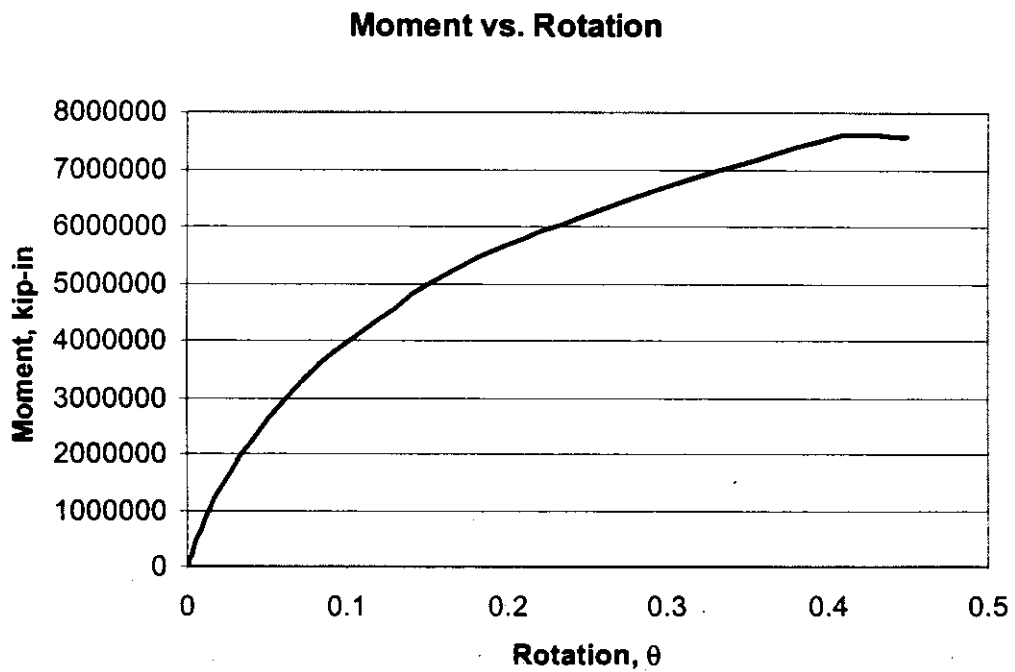


**Figure H.4** New Wahite Ditch Bridge Four Pile Footing

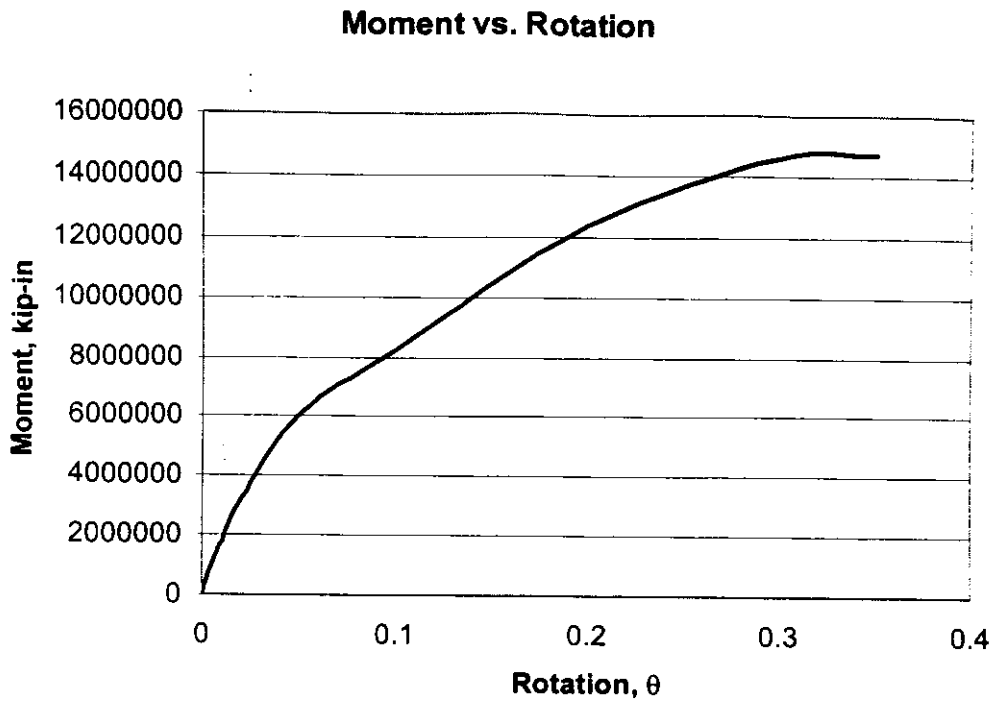


**Figure H.5** New Wahite Ditch Bridge Five Pile footing

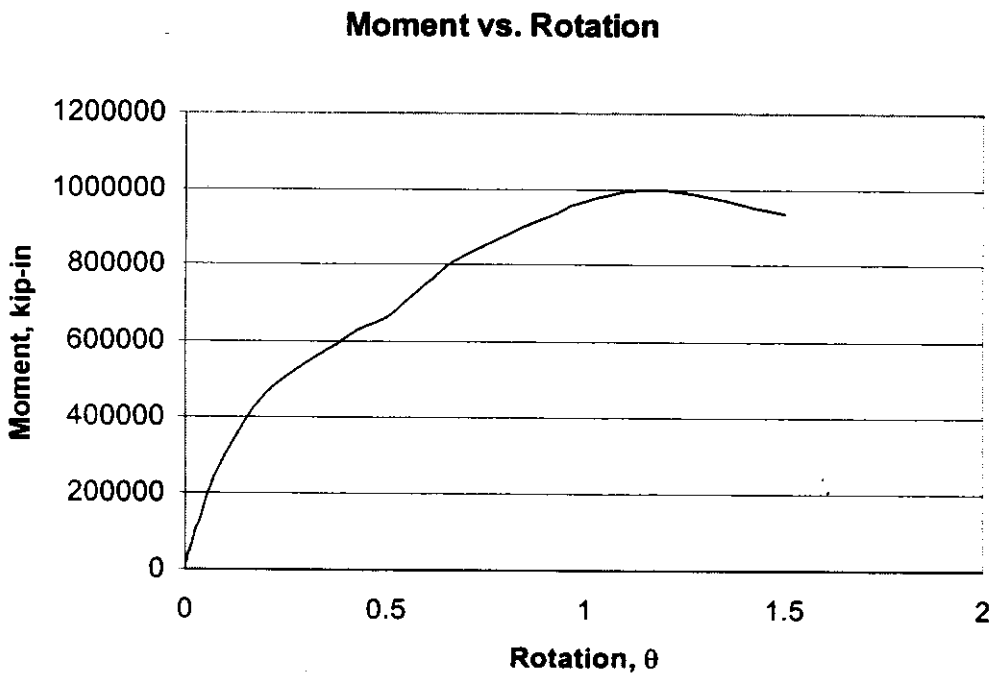


**Figure H.6** Old Wahite Ditch Bridge Two Pile Footing A

**Moment vs. Rotation**

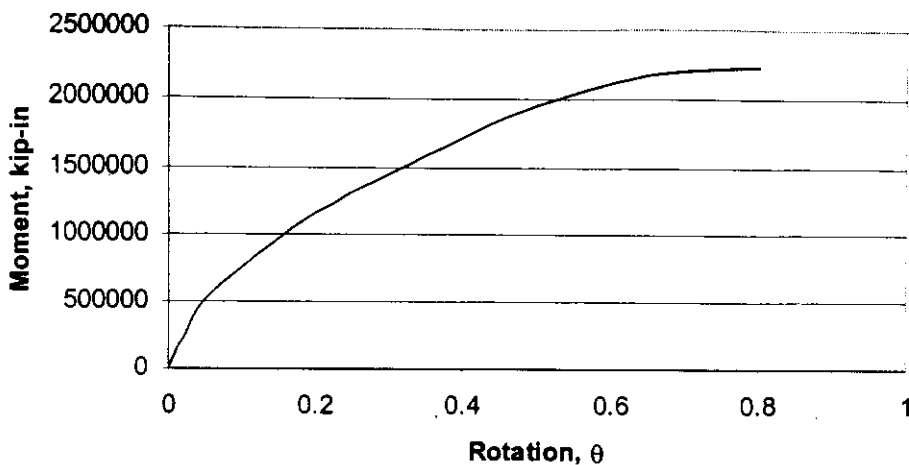


**Figure H.7 Old Wahite Ditch Bridge Three Pile Footing A**

**Moment vs. Rotation**

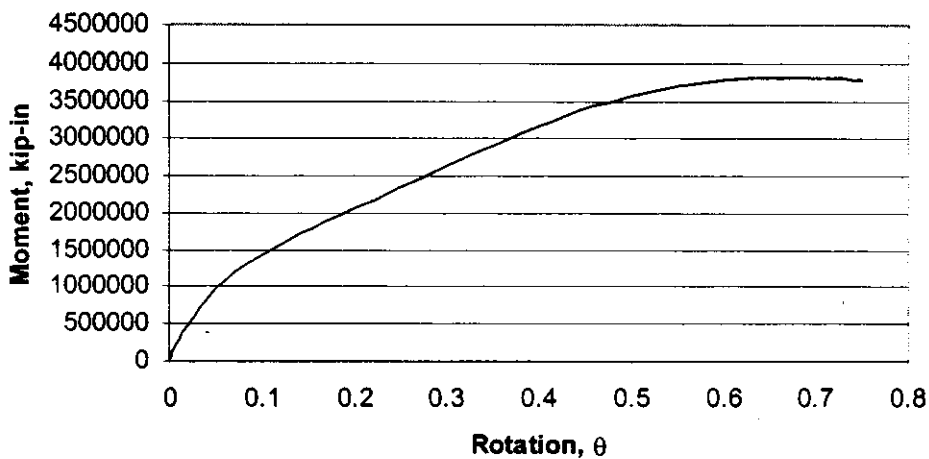


**Figure H.8 Old Wahite Ditch Bridge Three Pile Footing B**